DEVELOPING NEW SYNTHETIC METHODOLOGIES VIA DIRECT OXIDATIVE MANNER BY EMPLOYING ELECTROORGANIC CHEMISTRY

A Thesis Submitted

In Partial Fulfillment of the Requirements

for the Degree of

Doctor of Philosophy

by

"Rakesh Kumar"

(2019cyz0012)

DEPARTMENT OF CHEMISTRY

INDIAN INSTITUTE OF TECHNOLOGY ROPAR

May, 2024

DEDICATED

TO

My Beloved Parents

DECLARATION

I hereby declare that the work which is being presented in the thesis entitled "DEVELOPING NEW SYNTHETIC METHODOLOGIES VIA DIRECT OXIDATIVE MANNER BY EMPLOYING ELECTROORGANIC CHEMISTRY" has been solely authored by me. It presents the result of my own independent investigation/research conducted during the time from July, 2019 to May, 2024 under the supervision of Dr. Prabal Banerjee, Associate Professor, IIT Ropar. To the best of my knowledge, it is an original work, both in terms of research content and narrative, and has not been submitted or accepted elsewhere, in part or in full, for the award of any degree, diploma, fellowship, associateship, or similar title of any university or institution. Further, due credit has been attributed to the relevant state-of-the-art and collaborations with appropriate citations and acknowledgments, in line with established ethical norms and practices. I also declare that any idea/data/fact/source stated in my thesis has not been fabricated/ falsified/ misrepresented. All the principles of academic honesty and integrity have been followed. I fully understand that if the thesis is found to be unoriginal, fabricated, or plagiarized, the institute reserves the right to withdraw the thesis from its archive and revoke the associated degree conferred. Additionally, the institute also reserves the right to appraise all concerned sections of society of the matter for their information and necessary action. If accepted, I hereby consent for my thesis to be available online in the Institute's Open Access repository, inter-library loan, and the title & abstract to be made available to outside organizations.

Signature

Name: Rakesh Kumar

Entry Number: 2019cyz0012

Program: PhD

Department: Chemistry

Indian Institute of Technology Ropar

Rupnagar, Punjab 140001

Date: 21/08/2024

ACKNOWLEDGMENTS

At the outset, I would like to express my gratitude to the Indian Institute of Technology Ropar, Rupnagar, Punjab, India, and Department of Chemistry for providing me this opportunity to pursue PhD program. I would like to express my deep sense of gratitude and profound feeling of admiration to my thesis supervisor **Dr. Prabal Banerjee**, Associate Professor, Department of Chemistry, IIT Ropar for giving opportunity to carry my higher studies in his research group. His invaluable supervision with everlasting motivation was my biggest support for pursuing research in this new area of electroorganic synthesis. His trust in me and the freedom to work independently strengthened my self-confidence in developing the experimental skills that further led me to execute several independent projects and lead them. Moreover, the discussions with constructive criticism have always helped me to learn from my mistakes. While experiencing failures, his valuable inputs and morale boosts has helped me advance my scholarly skills with the much-needed scientific temperament to analyze a research problem and look for the solution. At this juncture, I must say, it was only because of his diligent guidance that this journey of research will be unforgettable for me. I express my sincere everlasting thankfulness to him.

I am indebted to **University Grant Commission (UGC)**, Government of India for my doctoral fellowship and IIT Ropar for research facility. I express my sincere thanks to **Prof. Rajeev Ahuja**, Director, IIT Ropar and **Prof. Sarit K. Das**, Ex-Director, IIT Ropar, **Dr. Navin Kumar** (Dean Research and Development), **Dr. Pushpendra P. Singh** (Associate Dean Research and Development), **Dr. Arun Kumar** (Associate Dean Student Affairs), **Dr. Dinesh K.S.** (Officiating Registrar) for providing all the required infrastructural facilities for carrying out my research work.

I would also like to thank my doctoral committee members **Dr. Debaprasad Mandal**, **Dr. Avijit Goswami**, **Dr. Srivastava Naidu** and chairperson **Dr. T. J. Dhilip Kumar** for their feedbacks and valuable suggestions during the presentations and other times. My sincere thanks to the present head of the department (HOD) **Dr. Tharamani C. N.** and all the other **faculty members** of Department of Chemistry for their sincere support and invaluable guidance.

I extend my thanks to all the supporting staff of the department of chemistry **Mr. Nagendra ji**, **Mr. Sushil ji**, **Mrs. Samita Saini**, **Ms. Hanspreet Kaur** for helping me out directly or indirectly in my dissertation work. My special thanks to **Mr. Manish Kumar** (for timely processing of NMR data), **Mr. Kamlesh Satpute** (for helping me to analyze single crystal data), **Mr. Nazre Heyat** and **Dr. Nilotpal** (for recording HRMS data), **Mrs. Poonam Kataria** (for always helping me in the administrative related issues).

I feel immensely grateful to all my seniors in the lab **Dr. Priyanka Singh**, **Dr. Rohit Varsanaya**, **Dr. Raghunath Dey**, **Dr. Pankaj Kumar, Dr. Irshad Majid Taily, Dr. Nilima Priyadarshni Mishra, Dr. Debarshi Saha, Dr. Navpreet Kaur** and **Dr. Sumit Rastogi** for exceptional guidance and motivation throughout this journey. All of them were the real motivation and the passion for the research which they carried was very contagious. I would like to extend my special thanks to my humble mentor **Pankaj sir** for providing all research training in my initial days and **Debarshi sir** for introducing the electroorganic chemistry and for being a great partner in setting up a new field in the laboratory and for planning all the trips we had together. I will miss those moments of togetherness we had.

I am extremely grateful to the other lab members **Arijit**, **Neeraj**, **Nakshatra, Shiv**, **Vikas**, **Rohan, Chandan, Neelam, and Umesh** for maintaining a supportive and cheerful environment in the laboratory. I would like to gratefully acknowledge the M.Sc. students of our lab **Sumitra**, **Kritika Singh**, **Naveen**, **Manish**, **Tanmay**, **Prince**, **Biswadeep**, **Kritika**, **Nidhi, Suman,** and summer intern **Arnab**.

This acknowledgement would be incomplete without giving a note of thanks to my all my batch mates and friends from other labs **Arijit, Sandeep, Priyank, Gulshan, Anoop, Ganesh, Vishal, Ritika, Akansha, Man Singh, Vatan, Shambhu, Sweta, Saurav, Rishikesh and Himanshu**. The journey of initial years of my research would not have been possible without them. Thank you, guys, for being the fantastic companion.

At this juncture, I would like to pay my regards to all the institution where I had my basic education, my school, **S.V. M. School**, Kotli, my graduation college Vallabh govt. college, **HPU**, my university, **Shoolini University**, my coaching institution **Bansal Academy**. I am proud to being a part of them. I would also like express my gratitude to my teachers **Dr. Sandeep**, **Dr. Vikas**, and **Dr. Kalpana Chauhan.**

As childhood friends, our path may change as life goes along, but the bond between us will remain forever. Thanks to my childhood buddies **Manish, Narender, Yadav, Vijay, Rahul, Jeet,** and **Jeewan** for all the support throughout this journey and my life. Thanks to my graduation and coaching friends **Manish, Harender, Narender, Shilpa, Taruna, Neha, Bharti, Ruma, Puneet, Arvind, Nirmal,** and **Manish** for always being there and maintaining a cheerful environment in my life.

Families are the compass that guides us. They are the inspiration to reach great heights. I cannot express enough thanks to my most loving family who were there all the time during all the ups and down in this journey. Whatever I am today is the result of the sacrifices made by my father **Mr. Uttam Chand** and my mother **Mrs. Prem Lata.** Without their love, affection, and moral support, I could not have accomplished this strenuous journey. Being a younger brother is always a blessing, thanks to my brother and sisters **Mr. Balbeer**, **Mrs. Deepa**, **Mrs. Geeta, Mrs. Urmila, Mrs. Manorama, and Mrs. Champa** for their incredible support, blessings, and love throughout the journey. Thanks, to my sister-in-law **Mrs. Neetu** and brother-in-law's **Mr. Thakar Dass, Mr. Surender, Mr. Gulab Singh, Mr. Sanjay Singh**, and **Mr. Khem Singh** for always being there for me and motivating me for my higher studies. Childrens are always a source of joy and happiness, thanks to my little nephews **Prikshit** and **Ayush** for always being alongside me whenever I was at home.

There are many more people to thank but it is not possible to name all of them. But at this moment, I remember each and every person who always stood beside me like a pillar and always supported me in this journey.

Finally, I express my heartfelt thanks to my God, who has made this journey the most exciting by bringing so many people into my life. Thanks a lot for the blessings showered during all the years of my life.

The work would not have been possible without these people and their countless blessings.

CERTIFICATE

This is to certify that the thesis entitled "**Developing New Synthetic Methodologies via Direct Oxidative Manner by Employing Electroorganic Chemistry**" submitted by **Rakesh Kumar (2019cyz0012)** for the award of the degree of "**Doctor of Philosophy**" of Indian Institute of Technology Ropar, is a record of bonafide research work carried out under my guidance and supervision. To the best of my knowledge and belief, the work presented in this thesis is original and has not been submitted, either in part or full, for the award of any other degree, diploma, fellowship, associateship or similar title of any university or institution. In my opinion, the thesis has reached the standard fulfilling the requirements of the regulations relating to the Degree.

Signature of the Supervisor
Dr. Prabal Banerjee
Department of Chemistry
Indian Institute of Technology Ropar
Rupnagar, Punjab 140001
Date: 21/08/2024

LAY SUMMARY

The continuous scarcity of natural resources is a growing concern in many parts of the world. Rapid growth in industrialization and increasing human population put a substantial pressure on our limited resources and leading to their depletion in many areas. The 21st century brings a lot of advancements in technological development such as utilization of renewable sources and building up more and more sustainable protocols to make processes greener and cheap. The scientific community has also been responded to these issues and contributing to the restricted use of fossil fuels. In this direction, organic chemists are also playing a huge role by incorporating greener and sustainable approaches in field of organic synthesis. Several sustainable methodologies have already been introduced like flow synthesis, mechanochemical chemistry and microwave assisted reactions etc. to overcome the traditional methods. However, in the past few decades electroorganic synthesis is rising in popularity due to effortlessness of scalability, evasion of stoichiometric oxidants or reductants, and adaptable reaction tunability. Several pioneers of science adopting this innate technology to design several remarkable methodologies. Inspired and motivated by incredible utility of electroorganic synthesis, we envisioned to utilize this greener and sustainable chemistry. With our continuous efforts, we could able to establish this chemistry in our laboratory and further, successfully documented several reports which are described in this thesis.

Chapter 1 describes the area of electroorganic chemistry in detail with several discoveries from beginning of 20th century up to present by the pioneers of science. Further, this chapter also discloses the electroorganic synthesis of various cyclic and acyclic scaffolds based on direct anodic oxidation of amines, phenols, and alkenes. Chapter 2 describes our initial efforts to establish electrosynthesis for the development of azomethine ylides from amine via iminium ion and their utilization for synthesis valuable five-membered cyclic derivatives. Chapter 3 discloses a novel protocol for site selective C-H functionalization of phenol. Several aromatic sulfoxide derivatives were synthesized via cross coupling reaction of phenols with sulfides. Chapter 4 of the thesis utilizes the alkene derived radical cation generated via SET from double bond to cleave the C-C bond of methylenecyclopropanes (MCPs). These protocols are environmentally benign and sustainable and in addition prevents the usage of harmful oxidants and reductants. Further, all the designed projects and their success are published in peer-reviewed international journals.

ABSTRACT

Chapter 1: Introduction to Electroorganic Chemistry and its Utilization via Direct Anodic Oxidation

The concept of electroorganic chemistry is discovered by Faraday and Kolbe with the introduction of Faraday's law of electrolysis and Kolbe's electrolysis in the 19th century. However, the field has not gained much attention till the mid of 20th century. After the discovery of potentiostat in 1942, several advancements have been achieved employing this sustainable approach and some notable transformations have been discovered. This chapter describes the basic concepts and requirements of electroorganic chemistry. A brief discussion of historical advancements from 1800 to end of 20th century have been documented. Moreover, remarkable achievements in the 21st century by the eminent organic chemists like Prof. Phil Baran, Prof. S.R. Waldvogel, Prof. Song Lin etc. have also been discussed. The development of diverse cyclic and acyclic scaffolds in a sustainable and step-economic manner has always been a subject of continual interest among the synthetic community. This thesis also describes the anodic oxidation-based synthesis of various cyclic and acyclic scaffolds from oxidation of amines, phenols, and alkenes. Their oxidation led to the generation of intermediate species like iminium ion, phenonium cation and alkene derived radical cation. This section of the thesis reviews the detailed study of these moieties and their accomplishments based on their oxidation in synthesizing several molecules. This comprehensive study of the electrosynthesis based on anodic oxidation encouraged us to engage ourselves towards the designing of the sustainable route for the synthesis of various carbo- and heterocycles. The aim of the thesis and the investigations carried out during the doctoral training are outlined in the form of different chapter as follows:

Chapter 2: Electrochemical Generation of a Nonstabilized Azomethine Ylide: Access to Substituted *N*-Heterocycles

The anodic oxidation of amines and amides led to the generation of *N*-centered radical cation which undergoes α-fragmentation to afford iminium ion. If a carbanion is present adjacent to iminium ion it refers to a 1,3 dipolar species which is azomethine ylide and they undergo 1,3-dipolar cycloaddition reaction with various dipolarophiles to afford cyclic *N*-heterocycles such as pyrrolidines, pyrrolines, and pyrroles. Based on substitution at the termini of the ylide, they can be classified as stabilized or nonstabilized ylide. Mostly, the azomethine ylides are generated *in-situ* and immediately reacted with dipolarophiles; however, in some case they can be isolated. Generation of the nonstabilized azomethine ylides and their 1,3-dipolar cycloaddition reactions with various dipolarophiles is a reliable and efficient protocol for the synthesis of *N*-heterocycles like pyrrolidines, oxazolidine and imidazolidines etc. Consequently, various traditional methods have been developed towards the construction of these *N*-heterocyclic ring system via generation of nonstabilized azomethine ylide. A few of the important methodologies include the fluoride ion initiated desilylation of cyanoamino silanes or trimethyl silyliminium salts and thermal ring opening of aziridines. However, most of these protocols rely on either metal-based activation or require high temperature. However, at the end of the 20th century, Pandey and coworkers reported a novel methodology for the generation of nonstabilized azomethine ylide from *N*-benzyl-1-(trimethylsilyl)-*N*-((trimethylsilyl)methyl) methanamine. In continuation with this endeavour, other groups, have also devised protocols for the generation of the nonstabilized azomethine ylide by employing visible-light, metal fluoride, and trifluoroacetic acid. However, all these conventional methods for the generation of nonstabilized azomethine ylides and their cycloaddition

necessitate external oxidants or photocatalyst towards the generation of 1,3-dipoles. Therefore, we have developed a metal and oxidant free protocol towards the *in-situ* generation of nonstabilized azomethine ylide under electrochemical conditions which undergoes 3+2 cycloaddition with ethyl acrylate as dipolarophile and the pyrrolidine product was obtained in 55% of yield after a comprehensive study of optimization. With this the substrate scope were evaluated w.r.t both the azomethine ylide precursors and dipolarophiles and a class of pyrrolidine derivatives were synthesised. Interestingly, the benzaldehyde derivatives as dipolarophiles were also found compatible with the protocol and afford oxazolidine derivatives in good yield. The protocol was also scalable to gram scale synthesis.

Chapter 3: Electrochemical sulfinylation of phenols with sulfides: a metal- and oxidant-free cross-coupling for the synthesis of aromatic sulfoxides

The C-H functionalization of arenes is an illustrious transformation in organic chemistry. It has been extensively exploited over the past few decades to manipulate the molecules to directly approach the target scaffolds. However, the analogous sulfinylation has largely remained unexplored despite having societal importance as medicines (antihypertensive, antibacterial, antifungal, antiulcer) and herbicide. These structures are also featured in a plethora of natural products. In addition, these sulfinates (existing in the S^{IV}-oxidation state) are well-established and reliable precursors or intermediates to diverse structurally and biologically significant functionalities existing in either the S^{IV} or S^{VI} oxidation states such as sulfones, sulfoximine, sulfinamides, sulfonate esters, sulfinate esters, sulfonyl halides, and others. In spite of the tremendous importance, there are only a few trivial strategies disclosed so far to construct aromatic sulfoxides. Though the direct mono-oxidation of diaryl sulfides has been a straightforward approach, the palladium-catalyzed cross-coupling of sulfenate anions by Poli and Madec, Walsh, Nolan, and Perrio has emerged as the promising gateway to these aryl sulfoxides. The other approaches include a nucleophilic substitution of sulfinyl precursors with organometallic reagents and the Lewis acid-mediated Friedel-Craft-type electrophilic aromatic substitutions of sulfinyl chlorides. The oxidation protocols suffer from employing hazardous peracid or hypervalent iodine oxidants in stoichiometric amounts, and the other requires metals and elevated temperatures to accomplish the transformation. Moreover, the over-oxidation of sulfide to sulfone is also encountered in most cases. Consequently, the development of a practically green, oxidant-free, and sustainable strategy for the selective synthesis of sulfoxides remains in high demand. In this direction, several groups have devised protocols towards the synthesis of various sulfoxide derivative via cross coupling reactions. In 2022, Baran and coworkers reported Ni-catalyzed electrochemical sulfinylation of aryl halides with SO_2. Motivated by our previous reports demonstrating the site-selective functionalization of phenol towards the direct synthesis of paracetamol and other arene oxidation-mediated functionalizations, we envisioned the direct synthesis of aryl sulfoxides via oxidative cross-coupling of phenols with sulfides and developed an electrochemical protocol towards the synthesis of aromatic sulfoxide via oxidative cross coupling of phenols and sulfides. The protocols afford 60% of yield after an extensive optimization studies. Further, the substrate scope w.r.t to both the phenols and sulfides have been tolerated well and procured the final compound up to 65% of the yield. Plausible mechanism is proposed after several control experiments. The practicality of the methodology was further demonstrated by gram scale synthesis and transformation of sulfoxide derivative to sulfone.

Chapter 4: Electrochemical Oxidative C-C Bond Cleavage of Methylenecyclopropanes with Alcohols

Cyclopropanes are the important building blocks, and their ring-opening via C-C bond cleavage driven by the release of ring strain has been widely applied in total synthesis. Methylenecyclopropanes (MCPs) are one of the important classes of small strained carbocycles which is having double bond directly attached to the cyclopropane ring. These are readily accessible and have been used very often in the construction of spiro-, hetero-, and polycyclic compounds. In general, the ring-opening reaction modes of MCPs are transition metal-catalyzed reactions, Lewis or Brønsted acid-catalyzed/mediated reactions, and thermal-induced cyclizations. At the same time, the MCPs have also been used as radical acceptors with a variety of radicals furnishing the ring-opening functionalized product. In 2019, Tang and coworkers reported silver-mediated oxidative C-C bond sulfonylation/ arylation of methylenecyclopropanes with sodium sulfinates initiated via radical addition. However, the reactivity of MCPs in other pathways, such as radical cation and singlet or triplet excited states, has rarely been explored. The first direct oxidation of MCPs by ozone was disclosed by Beck and coworkers in 2001 to afford cyclobutanone, peroxide, and ketone derivatives, illustrating the possibility of a single-electron oxidation pathway of MCPs. Later, direct photooxidation of MCPs to radical cationic species upon visible light irradiation has also been reported. However, all these conventional methods are concerned with the usage of stoichiometric oxidant, transition metal catalyst, or a photocatalyst towards the ring opening functionalization of MCPs. Organic electrochemistry has emerged as a sustainable alternative due to effortlessness of scalability, evasion of stoichiometric oxidants or reductants, and adaptable reaction tunability. The ring opening of MCPs via direct oxidation of double bonds followed by nucleophilic attack of has not been investigated so far. So, we developed an electricity-mediated C-C bond cleavage of MCPs towards the synthesis of methyl 4-methoxy-4-phenylbutanoate derivatives under oxidant and metal-free conditions via oxidation of double bond. After a comprehensive optimization, the carbon anode and nickel cathode in presence of tetrabutylammonium tetrafluoroborate as supporting at a constant current of 1 mA with methanol as solvent was found to be ideal condition for the transformation. The functional groups w.r.t methylenecyclopropanes were well tolerated and provide up to 80% of the yield. Different alcohol derivative was also used as nucleophiles to open the cyclopropane ring. Several mechanistic studies like radical scavenging experiment, D_2O experiment and cyclic voltammetry were carried out to prove the proposed reaction mechanism. The methodology was scalable up to gram scale synthesis. Next, the product was subjected to various post functionalizations such as reduction of ester, amidation of ester, and base hydrolysis.

LIST OF PUBLICATIONS

Journal papers

1. **Rakesh Kumar** and Prabal Banerjee, "Electrochemical Generation of a Nonstabilized Azomethine Ylide: Access to Substituted *N*-Heterocycles*" J. Org. Chem.,* **2021**, *86*, 16104-16113.

2. **Rakesh Kumar**, Irshad Maajid Taily, and Prabal Banerjee, "Electrochemical sulfinylation of phenols with sulfides: a metal- and oxidant-free cross-coupling for the synthesis of aromatic sulfoxides" *Chem. Commun.*, **2023**, *59*, 310-313.

3. **Rakesh Kumar**, Shiv Dutt, and Prabal Banerjee, "Electrochemical Oxidative C-C Bond Cleavage of Methylenecyclopropanes with Alcohols" *Chem. Commun.*, **2024,** *60*, 4246-4249.

4. **Rakesh Kumar,** Nakshatra Banerjee, Pankaj Kumar, and Prabal Banerjee, "Electrochemical Synthesis and Reactivity of Three-Membered Strained Carbo- and Heterocycles" *Chem. Eur. J.*, **2023**, e202301594. (**RK**, NB and PK contributed equally).

5. Debarshi Saha, Irshad Maajid Taily, **Rakesh Kumar,** and Prabal Banerjee, "Electrochemical rearrangement protocols towards the construction of diverse molecular frameworks" *Chem. Commun*., **2021**, *57*, 2464-2478. (DS, IMT and **RK** contributed equally).

6. Pankaj Kumar, **Rakesh Kumar** and Prabal Banerjee, "Accessing Dihydro-1,2-oxazine via Cloke–Wilson-Type Annulation of Cyclopropyl Carbonyls: Application toward the Diastereoselective Synthesis of Pyrrolo[1,2-*b*][1,2]oxazine" *J. Org. Chem.*, **2020**, *85*, 6535-6550.

7. Pankaj Kumar, Navpreet Kaur, **Rakesh Kumar** and Prabal Banerjee, "α,β-Unsaturated Carbonyls for One-Pot Transition-Metal-Free Access to 3,6-Dihydro-2H-pyrans" *J. Org. Chem*., **2022**, *87*, 7167-7178.

8. Shiv Dutt, **Rakesh Kumar**, Nakshatra Banerjee, Debarshi Saha, and Prabal Banerjee, "Electrochemical 1,3-Oxofluorination of Gem-Difluoro Cyclopropanes: Approach to α-CF_3-Substituted Carbonyl Compounds" *Adv. Synth. Catal.,* **2024**, *366*, 1-8.

9. Nakshatra Banerjee, **Rakesh Kumar**, Biswadeep Manna and Prabal Banerjee, "Strain-Released Hydrogenation of Donor-Acceptor Cyclopropane and Cyclobutane via Electrochemical Site Selective Carbonyl Reduction" *10.26434/chemrxiv-2023-1cz5j*.

Conferences

1. Recent Advances in Bioorganic and Medicinal Chemistry (RABMC - 2022)

Venue: NIPER Mohali, 19 November 2022.

Poster Presentation: Electrochemical Generation of a Nonstabilized Azomethine Ylide: Access to Substituted *N*-Heterocycles.

2. Chemical Science Symposium 2022: Sustainable Synthesis and Catalysis

Venue: London, UK. (Attended in online mode), 10-11 November 2022.

Poster Presentation: Electrochemical Generation of a Nonstabilized Azomethine Ylide: Access to Substituted *N*-Heterocycles.

3. Frontiers in Chemical Sciences-2022 (FICS-2022)

Venue: IIT Guwahati, 2-4 December 2022.

Poster Presentation: Electrochemical Generation of a Nonstabilized Azomethine Ylide: Access to Substituted *N*-Heterocycles.

4. Chemfest-2023

Venue: IIT Ropar, 9 March, 2023.

Poster Presentation: Electrochemical sulfinylation of phenols with sulfides: a metal- and oxidant-free cross-coupling for the synthesis of aromatic sulfoxides.

5. Fostering Catalysis for Societal Benefit (FSCB-2024)

Venue: University of Hyderabad, Hyderabad, India, January 15-17, 2024.

6. Attended Chemfest-2024.

Venue: IIT Ropar, 4 March, 2024.

Table of Contents

List of Figures

List of Schemes

List of Tables

Notations and Abbreviations

Acronym	Name
ACN (CH_3CN)	Acetonitrile
AC	Alternate current
Ar	Aryl
nBu	n-Butyl
Bn	Benzyl
BDD	Boron doped diamond
β	beta
br	Broad
BHT	Butylated hydroxytoluene
Bu_4NPF_6	Tetrabutylammonium hexafluorophosphate
Bu_4NBF_4	Tetrabutylammonium tertafluoroborate
CH_2Cl_2 /DCM	Dichloromethane
Cs_2CO_3	Cesium carbonate
CCl_4	Carbon tetrachloride
CF_3	Trifluoro methyl
^{13}C	Carbon NMR
CCDC	Cambridge crystallographic data centre
Cp_2Fe	Ferrocene
CCE	Constant current electrolysis
CPE	Constant potential electrolysis
$CDCl_3$	Chloroform-D
COSY	Correlation spectroscopy
°C	Degree Celsius
c.m.	Complex mixture
cm^{-1}	Centimetre
DABCO	1,4-Diazabicyclo[2.2.2]octane.
DBU	1,8-Diazabicyclo[5.4.0]undec-7-ene
DIPEA	*N*, *N*-Diisopropylethylamine
DMSO	Dimethyl sulphoxide
DMF	Dimethyl formamide
DCE	1,2-Dichloroethane
DCM	Dichloromethane
DMF	Dimethylformamide
DMSO	Dimethyl sulfoxide
DMA	Dimethylacetamide
d	Doublet
dd	Doublet of doublet
DC	Direct current
δ	Delta

DEPT	Distortionless enhancement by polarization transfer
E	Electrophile
EOS	Electroorganic Synthesis
EDG	Electron donating group
EWG	Electron withdrawing group
Et_4NPF_6	Tetraethylammonium hexafluorophosphate
Et_4NCl	Tetraethylammonium chloride
ee	Enantiomeric excess
etc.	Etcetera
e.g.	Exempli gratia
equiv.	Equivalent
et al.	Et alia
Et_2O	Diethyl Ether
EtOAc	Ethyl acetate
ESI	Electronspray ionization
Et	Ethyl
EtOH	Ethanol
F	Faraday
FG	Functional group
FTIR	Fourier Transform Infra-Red
g	Gram
gem	*Geminal*
GC	Gas Chromatography
h	Hour
H	Hydrogen
^1H	Proton NMR
Hz	Hertz
HRMS	High Resolution Mass Spectrometry
HFIP	Hexafluoroisopropanol
HI	Hydrogen iodide
HPLC	High-Performance Liquid Chromatography
H_2O	Water
I_2	Iodine
$InCl_3$	Indium (III) chloride
IPA	Isopropyl alcohol
KOH	Potassium hydroxide
LiCl	Lithium Chloride
$LiClO_4$	Lithium perchlorate
m	Multiplet
Me	Methyl
MS	Molecular Sieves

mA	Milliampere
mL	Millilitre
min	Minute
MHz	Mega Hertz
mg	Milligram
MeOH	Methanol
MgI_2	Magnesium (II) iodide
mp	Melting point
Nu	Nucleophile
nm	Nanometre
NMR	Nuclear Magnetic Resonance
NH_4OH	Ammonium hydroxide
n.r.	No product
N_2	Nitrogen
Ni	Nickel
Ag	Silver
AgCl	Silver chloride
Na_2CO_3	Sodium carbonate
NaH	Sodium hydride
NHPI	*N*-Hydroxyphthalimide
Na_2SO_4	Sodium sulphate
NOESY	Nuclear Overhauser effect spectroscopy
OMe	Methoxy
$Pd(OAc)_2$	palladium(II) acetate
Ph	Phenyl
Pt	Platinum
iPr	Isopropyl
PTSA	*p*-Toluene sulphonic acid
ppm	Part per million
PSU	Power supply unit
KBr	Potassium bromide
KCl	Potassium chloride
q	Quartet
R_f	Retention factor
RVC	Reticulated vitreous carbon
rac	Recemic
r.t	Room temperature
s	Singlet
SET	Single electron transfer
SHE	Standard hydrogen electrode
SN_1	Unimolecular Nucleophilic Substitution

SN_2	Bimolecular Nucleophilic Substitution
t	Triplet
TEA	Triethyl amine
TFE	Trifluoroethanol
TsCl	Tosyl chloride
THF	Tetrahydrofuran
THP	Tetrahydropyran
TEMPO	(2,2,6,6-tetramethylpiperidin-1-yl)oxidany
td	Triplet of doublet
TLC	Thin Layer Chromatography
TOF	Time-of-flight
TS	Transition State
UV	Ultra Violet
vic	*Vicinal*
V	Volt
v/v	Volume/Volume
XRD	X-Ray Diffraction

Chapter 1

Introduction to Electroorganic Chemistry and its Utilization in Direct Anodic Oxidation

1.1. Electroorganic Synthesis: Return of the sustainable methodology

Since the commencement of industrial revolution, for the first time in 21 st century the extreme energy consumption and energy sources became the major topics of social and political debates.[1] The limited fossil fuels escalates the movement in the direction of inception of sustainable synthesis techniques.[2] The usage of renewable energy sources and development of greener industrial processes is becoming more and more crucial which aims to reduce the massive amount of waste generation.[3] The scientific community has already been responded towards these issues and contributing to the restriction of greenhouse gases. In this direction, organic chemists are also playing a huge role by incorporating greener and sustainable approaches in field of organic synthesis. Several sustainable methodologies have already been introduced like flow synthesis, mechanochemical chemistry and microwave assisted reactions, and electroorganic synthesis etc. to overcome the traditional methods.

However, amongst all the electroorganic synthesis is appearing in popularity.[4-6] The wider use of electroorganic transformations is gaining more interest due to the supply of electricity from renewable resources like solar-, wind-, or hydropower.[7] Although, methodology was neglected for several decades, as mostly taught in physical chemistry, and focuses on interpretation of electric signals. This approach has also been used in some inorganic transformations like the chlor-alkali electrolysis and aluminium production by the Hall-Heroult process.[8] Moreover, the lack of knowledge and unavailability of proper standardized equipment has made this technique more inconvenient for the synthetic organic chemist. After being neglected for several decades, at present this inherent sustainable technology is remerged as a potential tool in the field of organic synthesis and becoming recognized chemistry with the development of tremendous electroorganic methodologies.[3-7]

1.2. Brief history of electroorganic synthesis

The door of electroorganic synthesis (EOS) was opened in 1800 by Alessandro Volta with the discovery of the voltaic pile.[9] As a first electric battery, it permit the movement of electrons throughout the circuit for the first time.[10] However, three decades later, the pioneering efforts of Faraday instigate the interest in utilising the current to develop several organic transformations.[11] The popular electrochemical terms such as electrolysis, anode, cathode, and development of Faraday's Law of Electrolysis (**eq. 1**) can all be accredited to Faraday's extensive studies.[12] The demonstration of the electrolysis of sodium acetate by Faraday later inspires the development of famous Kolbe's electrolysis of carboxylic acid to alkyl radicals in 1847 that subsequently undergoes dimerization.[13]

Faraday's law of electrolysis

$$n = \frac{Q}{zeN_A}$$

n = No. of moles of metal species
Q = Charged passed
z = Valency number of ions of the substrate
e = Elementary charge
N_A = Avogadro's number

(Eq. 1)

In 1907, a familiar cathodic reduction known as *Tafel rearrangement* was developed towards the synthesis of hydrocarbons.[14] By the end of 19th century, Haber's work on synthesis of aniline from reduction of nitrobenzene demonstrate another exceptional example of the potential of electroorganic synthesis.[15] This work illustrates the significance of applied potential in controlling the selectivity and outcome of reaction. Electrosynthesis in 19th

century solely depends on the constant current electrolysis where reactions were subjected to a constant steam of current, and potential rises over the time. However, in 1942, Hickling's invention of potentiostat unlock a new aspect where reactions could be carried out under constant potential, and current declines over the time.[16] The electrochemistry was further strengthen by the first demonstration of cyclic voltammetry in 1948 which is an essential technique for electrochemist's as it helps to find out the potential of unknown compounds.[17,18] Towards the end of 20th century, many major synthetic developments in electrochemistry were made and some of the notable examples includes Shono's oxidation (α-functionalisation of carbamates)[19], Yoshida's oxidation via use of S and Si electroauxillaries[20], Little (electroreductive cyclisation)[21] and Moeller (anodic olefin coupling) etc.[22] So, from the invention of the volta Pile in 1800 till the end of 20th century, various notable achievements have been accomplished. To sum up these achievements, a simplified timeline has been demonstrated which shows historical milestone with some of the well-known and representative works during this time of electrosynthesis (Figure 1.2.1).

These pioneering inventions in association with several advancements provides a route to many spectacular synthetic applications in the 21st century.[8] In 2002, Yoshida and coworkers revealed the fundamental concepts of cation pool and cation flow methods and exemplify their applications in organic synthesis.[23] Followed by this, Moeller, and coworkers in 2008 disclosed an intramolecular anodic oxidation based olefin coupling reaction towards the synthesis of cyclized product via generation of *N*-centered radical species that undergoes a radical-initiated intramolecular cyclization process with the olefin and renders the desired C-N coupled cyclized product.[24] The formation of C-C bonds in oxidative manner has been recognize as sustainable and scalable strategy as it avoids the formation of by-products obtained in the metal catalysed reactions. In this direction, Waldvogel *et al.*, in 2012 demonstrated an electrochemical protocol towards the synthesis of biaryl derivatives *via* radical cross coupling reaction of phenol.[25] With the continual research interest in this field, various research groups acquired this technology and several notable transformations in the direction of total synthesis have been achieved. In 2014, Baran and coworkers reported the total synthesis of Dixiamycin B via N-N bond formation utilizing electrochemical oxidation.[26] Followed by this, in 2015 Harran *et al*., also revealed an electrochemical pathway for the total synthesis of diazonamide drug DZ-2384.[27] In this manner, several notable bioactive molecules like Cyclosporine A,[28] Thebaine,[29] pyrrolophenanthridine alkaloids[30] and Dragocins A-C[31] etc. have been synthesised using this methodology. These achievements foster the field of electroorganic synthesis (EOS) and popularise electrochemistry as a strong field in modern organic synthesis.

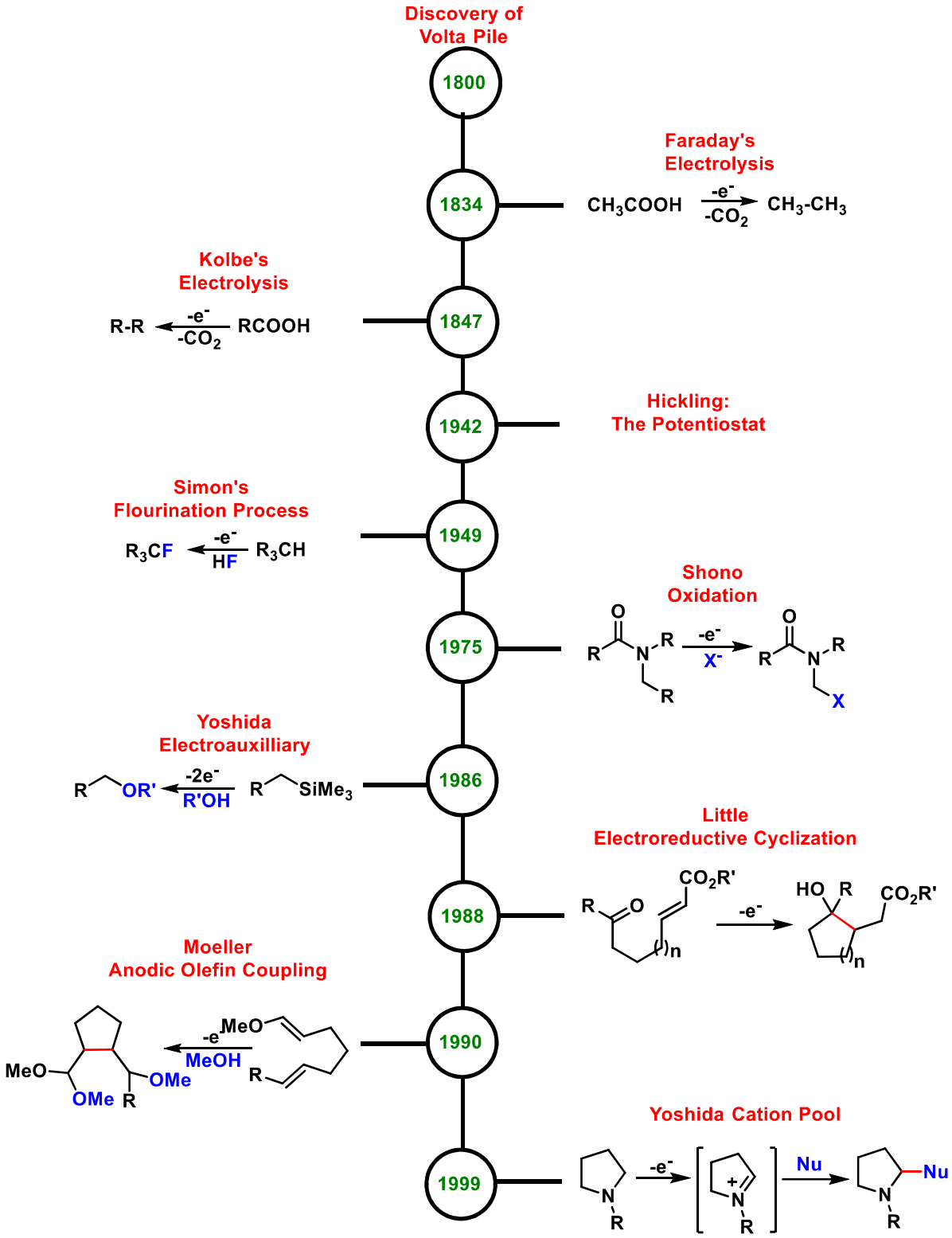

Figure 1.2.1. Historical development of electroorganic chemistry from 1800-2000.

1.3. Challenges in electroorganic synthesis

Regardless of great advantages of electroorganic synthesis, there are still many challenges restraining its broad endorsement in modern synthetic labs. There is lack of standardised electrochemical equipments as most of the set-ups for carrying out electrochemical reaction are 'homemade'. This leads to the lot of variations between research groups and lack of reproducibility of results. Moreover, only a restricted number of remarkable transformations have been discovered. However, the problem is slowly being addressed with the development of purposeful electrochemistry kits, e.g., Electrasyn 2.0 that can be used in synthetic laboratories,[17,32]. Although there are still so many challenges, however the significant advantages of widely using electrosynthesis method over traditional counterparts are encouraging us to take up and overcome these challenges. Electroorganic synthesis is now waiting for a resurgence.

1.4 . Basic requirements

The basic instrument to perform the electroorganic synthesis can start from very simple to a high-end apparatus. Although, the basic requirements to carry out electrolysis must be fulfilled. This section provides a brief outline of the components required in electroorganic synthesis.

1.4.1. The power supply Unit (PSU)[7,33,34]: Power supply is a device which supply the current to the reaction and thus movement of electrons takes place from anode to cathode. In other way, power supply is a source of electrons to the system. In simplest case, batteries can be used as source of current, however the output voltage and current cannot be controlled. Potentiostats or DC power supply can control either the current or the voltage. When the current is controlled, the mode is called constant current electrolysis (CCE) or galvanostatic mode and if the potential is controlled, the mode refers to constant potential mode (CPE) or potentiostatic mode. Reference electrode can also be used in case of potentiostatic mode. However, in the electrosynthesis, the power supply is sufficient without using the reference electrodes. The following pictures corresponds to the power supply systems in our laboratory.

DC Power Supply

Electrasyn 2.0

Figure 1.4.1 Power supply set up.

1.4.2. The electrodes[7,33,34]: Electrodes are one of the most important constituents of the electroorganic synthesis. Generally, any material which can conduct electricity be used as electrodes. It can be varied from a cheap graphite or aluminium foil up to an expensive boron doped diamond (BDD). The choice of electrode material affects the

outcome of the reaction because the transfer of electrons occurs at the surface of the electrodes. Therefore, electrodes having good surface area, corrosion stability and chemical inertness are found to be sustainable in electrosynthesis. Foams and meshes e.g. nickel foam, reticulated vitreous carbon (RVC) etc. having a high surface area and platinum, graphite and nickel etc. are corrosion and chemically inert. Electrodes like aluminium, zinc, tin, and magnesium etc. are also used and termed as sacrificial electrodes and mostly used in reduction processes.

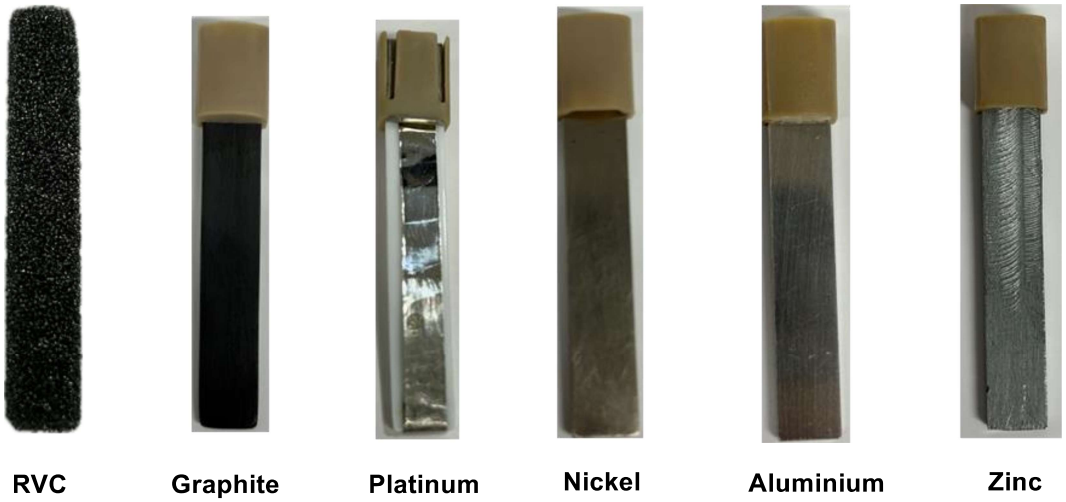

Figure 1.4.2. Common electrodes in electroorganic chemistry.

Sometimes, during reaction, deposition takes place on the surface of electrodes which is called electrode passivation that minimizes its activity. The passive layer formed due to oxidation of electron rich organic molecules, like alkenes and aromatic compounds. This problem can be solved by alternate current electrolysis where electrodes changed periodically from anode to cathode and vice-versa.

1.4.3. The electrolyte[7,33,34]: An electrolyte is used in most of the electrochemical reactions which helps to lower the potential of the system and thereby minimize the resistance. In electrolysis, mostly organic solvents like acetonitrile, dichloromethane, methanol and dichloroethane etc. are used having poor conductivity. Therefore, the addition of electrolytes improves the conductivity and thus lowers the cell resistance. Lowering of resistance depends on the amount of the electrolyte used in reaction as well as its nature. Most importantly, it should be soluble in solvent as well as unreactive under reaction conditions, so that it does not take part in any redox process. In electrochemical synthesis, mostly tetraalkylammonium and lithium salts are used owing to their good solubility in organic solvents. Some of the commonly used supporting electrolytes are tetrabutylammonium hexafluorophosphate (Bu_4NPF_6), tetraethylammonium chloride (Et_4NCl), tetrabutylammonium tetrafluoroborate (Bu_4NBF_4), tetraethylammonium hexafluorophosphate (Et_4NPF_6) and lithium perchlorate ($LiClO_4$) etc. The electrolyte coats the electrode surface area forming double layer affecting diffusion of the substrate which can influence reactivity.

Bu_4NClO_4 Bu_4NBF_4 Et_4NPF_6

Figure. 1.4.3. Common electrolytes in electroorganic chemistry.

1.4.4. The Solvent[7,34]: Like a conventional chemical reaction, the usage of solvent in an electrochemical reaction can have a pivotal role on outcome of the reaction. Organic solvents employed in electroorganic synthesis must dissolve the substrates, electrolyte, and be sufficiently stable under electrochemical conditions. Commonly, polar solvents are used owing to their low resistance property which led to high conductance. Some commonly used aprotic solvents are: CH_3CN, THF, DCM, DCE, DMF, DMA and DMSO and protic solvents are (fluorinated) alcohols, such as hexafluoroisopropanol (HFIP), trifluoroethanol (TFE), MeOH and EtOH. Protic solvents are generally used when oxidation is required as they serve as sacrificial substrate for reduction at the cathode.

1.4.5. The Additives[7,34]: Additives are used to boost the performance of electrochemical reactions. Either they help in completing the circuit by promoting the reactions at counter electrode or stabilise the radical intermediates. For oxidation reactions acid additives can often found beneficial as they act as a proton source which undergoes reduction at cathode and release hydrogen gas as a counter reaction. Fluorinated alcohols, such as HFIP or TFE, can also be employed as they stabilise radical intermediates.

1.5 Type of electrolytic cells

The electrolytic cells are used to carry out the electroorganic reactions and its design entirely depends on the type of the reactions. Generally, the electrochemical cell is formed of glass (quartz or Pyrex) material or sometimes it can be nylon or Teflon. The cell must be inert under electrochemical reaction and should not interfere in the course of sensitive measurements. In this section, basic type of electrochemical cell used to carry out electroorganic reactions will be described.

1.5.1. Undivided cell[33,34]: Undivided cell is the simplest designed cell to work in electroorganic synthesis. It is the most preferred cell as the setup is simpler. In an undivided cell the two electrodes are placed in a single chamber and dipped in the electrolytic solution and the distance between the two electrodes should be minimum but electrodes should not touch each other. To perform a reaction under inert atmosphere, cell could be sealed with a Teflon stopper. As there is no physical separation between the electrodes in an undivided cell, therefore the components of the electrolytic solution can hold both the electrodes. Hence, there is chances that the desired product formed can undergo further reaction at the counter electrode. This type of situation can be encountered by choosing an easy sacrificial reaction at counter electrode such as evolution of hydrogen gas from the reduction of protic solvents (MeOH, EtOH etc.) in case of anodic oxidation.

Figure. 1.5.1. Undivided cell setup. Left: schematic representation; Middle: home-made; Right: commercially available Electrasyn 2.0 from IKA.

1.5.2. Divided cell[33,34]: Sometimes it became necessary to separate the two electrodes physically to avoid the "chemical short-cut" or unwanted reactions at the counter electrodes. In such scenario, a divided cell is employed which is also known as H-type cell. In divided cell, two chambers are physically divided by a porous material or semipermeable membrane such as sintered glass or ceramics or nafion membranes. These membranes only allow the exchange of ions between the two chambers but avoid mixing of chemicals (substrates, reagents, product) between two compartments. Thus, it supresses the side reactions at counter electrode. However, the presence of frit or membrane increases the resistance and come up with an added degree of difficulty in setup.

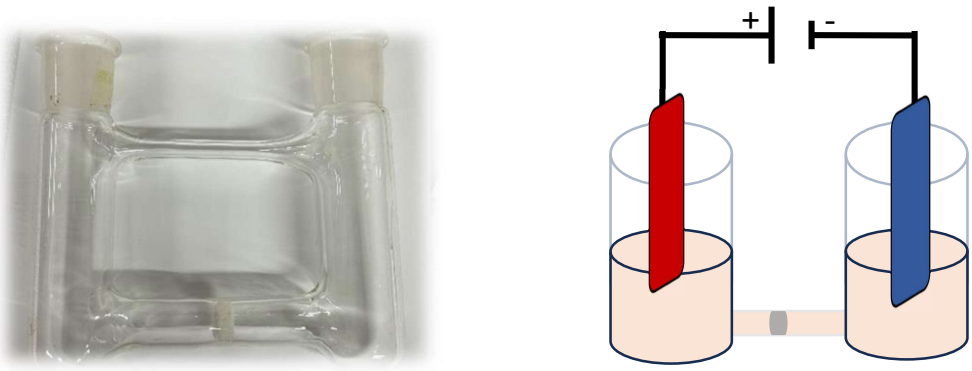

Figure. 1.5.2. Divided cell setup. Left: home-made; Right: schematic representation.

1.5.3. Quasi-divided cell[33]: Quasi-divided cell combines the features of divided and undivided cells. Usually, the cell design in such a way that working electrode has very large surface area and counter electrode has small surface area mostly a thin wire. The reactions are performed at low constant current, which subsequently causes

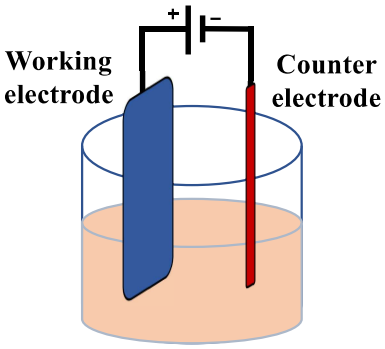

Figure. 1.5.3. Quasi-divided cell setup: schematic representation

low current density at working electrode. As a result, the substrate having low redox potential would get electrolyzed first. Ultimately, the current density is high at the thin wire counter electrode hence, the solvent gets electrolyzed due to the excess current. Therefore, quasi-divided cell brings forth the advantages of both divided and undivided cell.

1.5.4. Flow cells[35]: The electrochemical reactions under flow cell are carried by pumping the solution of reactant into a room of two electrodes having small gap between electrodes. The smaller the gap between the two electrodes lesser will be the cell resistance. Therefore, the reactions can be carried out without supporting electrolyte which avoids the generation of waste and make the process more sustainable. In addition, in flow electrolysis the the product is coming out continuously which lowers the chances of overoxidation of product. A simplified schematic representation of electrolysis under flow conditions is depicted in figure 1.5.4.

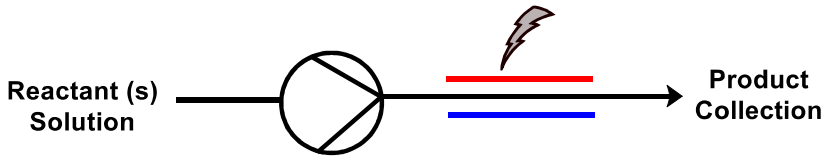

Figure 1.5.4. Schematic representation of electrochemical flow cell.

1.6 Setting up of a reaction in electroorganic synthesis

The following pictures represents the basic setup to carry out the electroorganic reactions in the laboratory (Figure 1.6.1). Initially, in the home-made reaction vessel or electrasyn 2.0 the substrates, supporting electrolytes, solvent, and additives (if needed) is added. The reaction solution is made homogeneous via sonication or stirring. Next, the electrodes setup is made as shown in figure 1.6.1 and electrodes are chosen according to the cell needed for electrolysis. The cell is fitted with electrodes and set up is connected to the DC power supply and the reaction is electrolyzed either at constant current or constant voltage conditions. The completion of the reaction is monitored by TLC. Further, the workup and purification processes are performed as per the protocols.

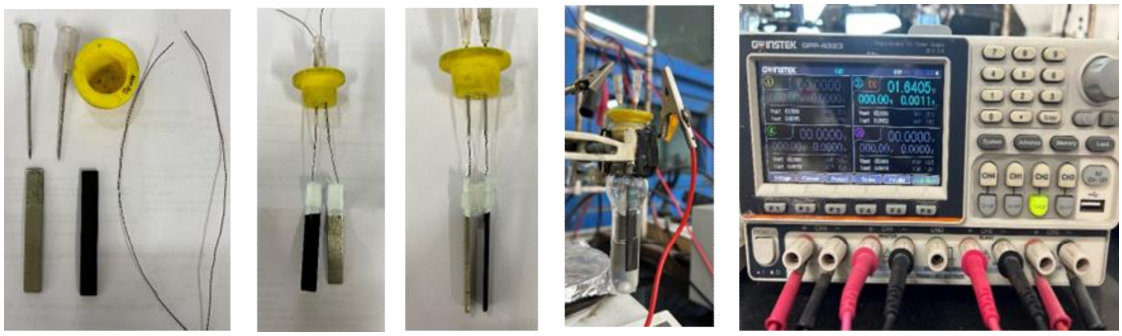

Figure 1.6.1 Various laboratory set up for electroorganic chemistry.

1.7 Modes of electrolysis

Electrochemical reactions can be controlled by the electrical parameter. Based on that electrolysis can be conducted at different modes as discussed below:

1.7.1. Galvanostatic electrolysis (control of the current)[7,33]: In this type of electrolysis, only two electrodes are required for the electrolysis and is the easiest mode to set up reaction. In this type of electrolysis constant current is supplied during the whole electrolysis time. The potential is not controlled in this type of electrolysis and keeps varying over the time. Therefore, the substrate having low redox potential undergoes electrochemical transformation at low current densities. However, the concentration of that substrate decreases with time and at some point, it becomes insufficient (Figure 1.7.1).

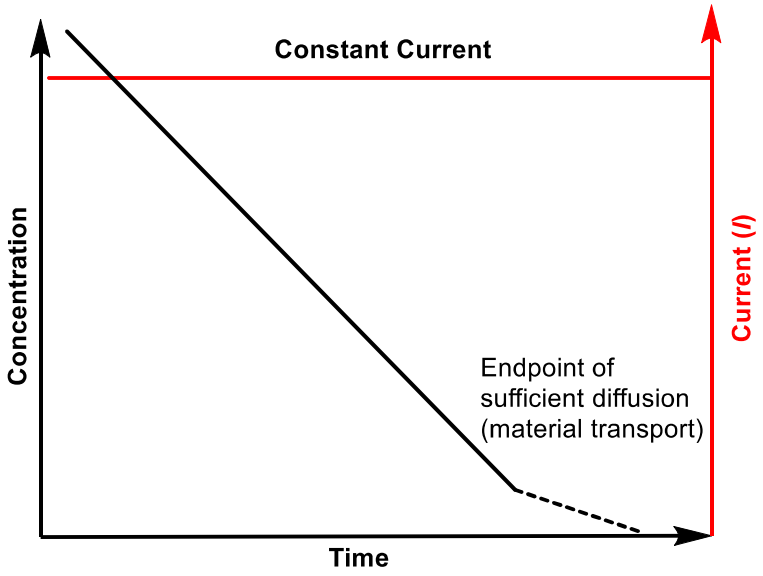

Figure 1.7.1. Concentration profile of galvanostatic electrolysis.

If the electrolysis goes beyond this point, the galvanostat increases the potential to maintain the current constant and thus the substrate with next lowest redox potential can be transformed. Sometimes, if this is product, over electrolysis takes place and side products formed.

1.7.2. Potentiostatic electrolysis (control of the potential)[7,33]: In this type of electrolysis, third electrode which is reference electrode is needed and it is more typical than the galvanostatic electrolysis. In this mode, a potentiostat is used as power source and a constant potential is applied throughout the reaction time. Since the potential has no natural fix point, therefore standard hydrogen electrode (SHE = 0 V) has been set as a fix point and sometimes other reference electrodes has been used e.g. Ag/AgCl and calomel electrodes are used. Generally, reference electrode is placed in a separate chamber and provides a constant reference potential as long as the concentrations in the chamber remain unchanged. For this, ceramic frits are used to avoid diffusion of organic solvents into reference electrode chamber. In this electrolysis, a potential of desired value is applied that matches the redox potential of a specific substrate in the reaction mixture. Therefore, the substrate must be of a known redox potential in the same solvent system which is used to carry the reaction. To achieve that cyclic voltammetry experiment of desired substrate is carried out before electrolysis.

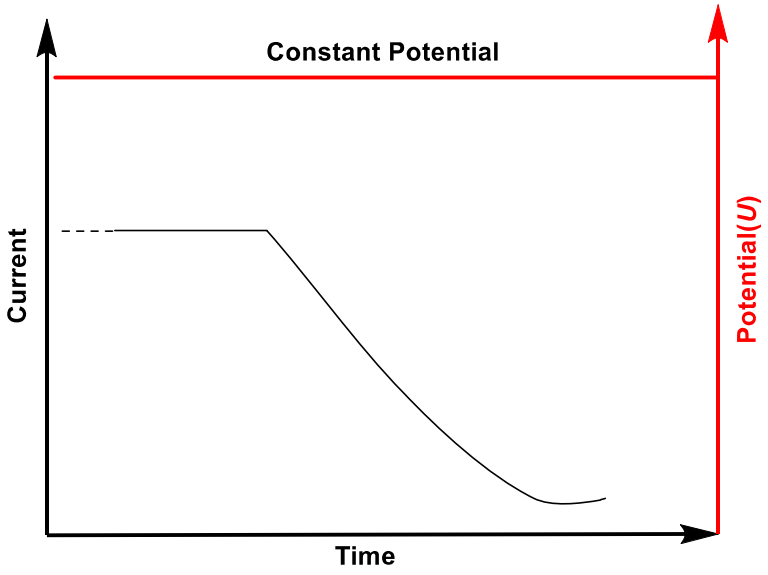

Figure 1.7.2. Current profile of potentiostatic electrolysis.

Under this mode of electrolysis, the concentration of substrate is high in the beginning of reaction, and the transfer of mass to electrode surface is sufficient and cell current remains constant to some extent. As the reaction proceeds, the concentration of reactant decreases and the transfer of mass becomes insufficient, therefore the cell current drops to the endpoint of the electrolysis (Figure 1.7.2).

1.7.3. Alternating current electrolysis[7,33]: The above two modes of electrolysis, depends on direct current where the polarity of the electrodes remains same throughout the reaction. However, one more way to perform electrolysis is alternating current (AC) electrolysis and has been applied in very few cases. If an electrochemical reaction causes deposition on the surface of electrodes, then polarisation of electrodes altered. The changes occur from anodic to cathodic conditions and *vice-versa* in a regular interval of time and eliminate the deposit from the surface of electrodes. Current flow diagram of an alternating current electrolysis is illustrated in figure 1.7.3.

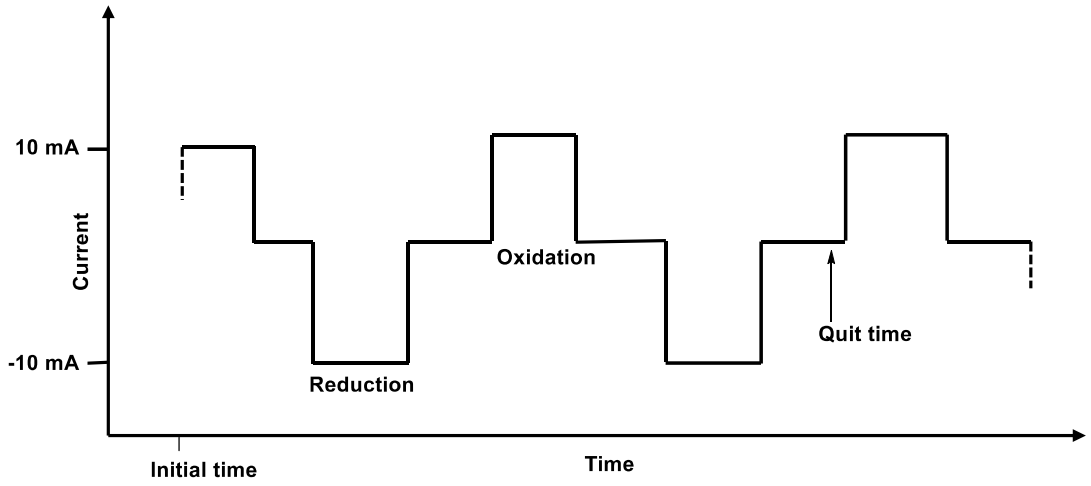

Figure 1.7.3. Current flow profile of an alternating current electrolysis.

1.8 Type of electrolysis

In electroorganic synthesis, the electron transfer occurs heterogeneously at the surface of electrodes. However, there are different types of electrolysis depending upon the mode of electron transfer between electrode surface and chemicals in the solution. Different modes of electrolysis will be discussed in the following section.

1.8.1. Direct electrolysis[33]: Direct electrolysis involves heterogeneous electron transfer between the electrode and adsorbed electroactive species. This heterogeneous electron transfer trigger the activation of substrate which go through the chemical transformations to afford the final product. Due to the continuous adsorption of substrate on the surface of electrode, the surface area of electrode decreases leading to the increase in potential of the system.

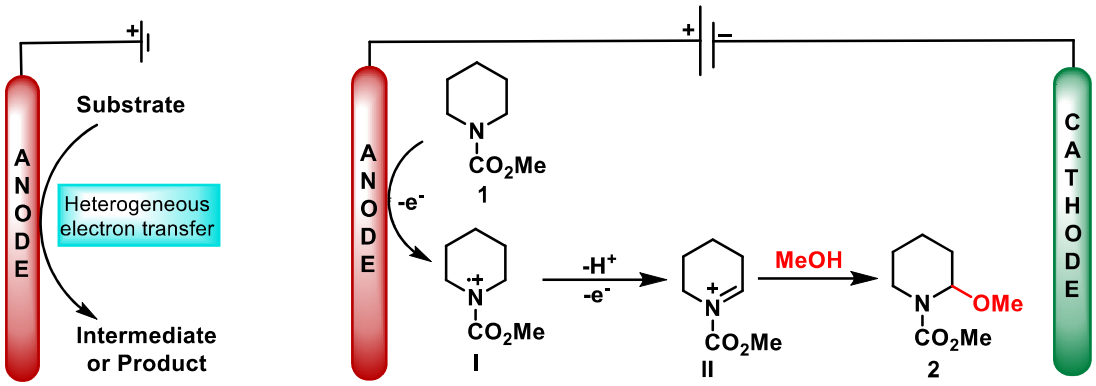

Figure 1.8.1. Schematic representation for direct electrolysis.

The electrochemical oxidation of dialkylcarbamate **1** in presence of methanol yielded the α-methoxylated product **2** is an example of direct electrolysis reported by Shono and coworkers in 1975[36]. The protocol was carried out at CCE in an undivided cell employing 50 mA of current in methanol as solvent and tetraethyl ammonium *p*-toulensulfonate as supporting electrolyte. Substrate **1** undergoes single electron transfer (SET) at anode to generate *N*-centered radical cationic species **I**, which undergoes loss of hydrogen atom followed by another oxidation

process to afford iminium cation **II**. The nucleophilic attack by methoxide ion on iminium cation rendered the final product **2**.[36]

1.8.2. Indirect electrolysis[33,37]: In some cases, the direct heterogeneous electron transfer between the substrate and the electrode is ineffective and sluggish. Sometimes, it could lead to the passivation of electrodes which minimizes the surface area of electrodes and affect the conductivity. In such cases, indirect electrolysis could be the alternate solution. In indirect electrolysis, a homogeneous redox reaction takes place in solution, which occurs between a redox mediator and the substrate. Firstly, the mediator gets activated at the surface of electrode followed by homogenous electron transfer with the substrate. Some commonly used redox mediators are triarylamines (Ar_3N), ferrocene (Cp_2Fe), TEMPO free radical (TEMPO), *N*-hydroxy phthalimides (NHPIs), transition metal ions, such as Fe(II/III), Co(II/III) etc.

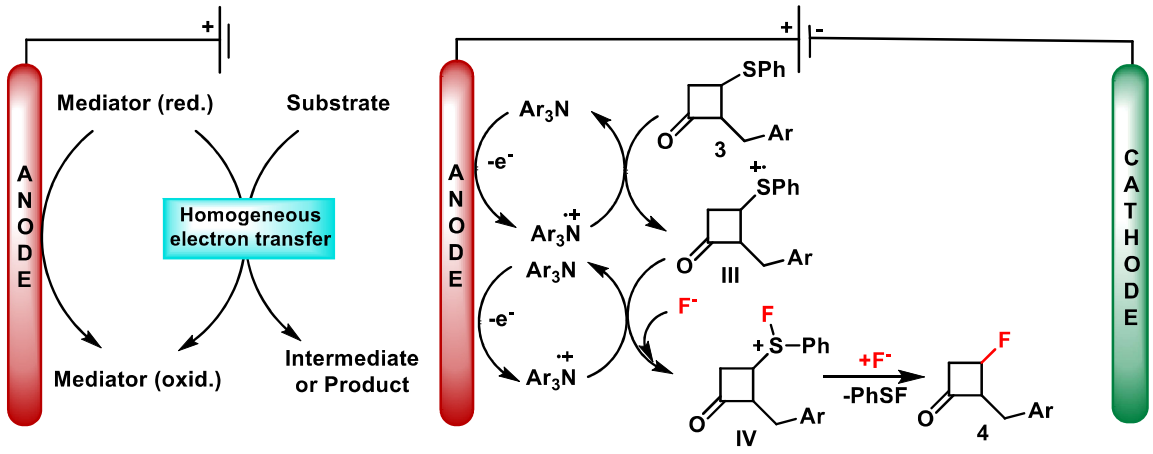

Figure 1.8.2. Schematic representation for indirect electrolysis.

However, mediators must fulfil some necessary conditions, such as, it should be stable at both oxidation states for longer period. Also, the heterogeneous electron transfer between electrode and mediator should not have high overpotentials and the homogeneous electron transfer from/to the substrate should not have high kinetic barriers. The electrolysis can be carried out at much lower potential if these pre-requisites are fulfilled. Indirect electrolysis has two different modes: in-cell and ex-cell. In the in-cell mode the substrate and the mediator remain in the electrochemical cell throughout the electrolysis. However, in the ex-cell mode the mediator is electrolysed firstly to generate reactive species then the substrate is added. For example, electrochemical flurodesulfurisation of *β*-phenylsulfenyl *β*-lactams **3** reported by Fuchigami and coworkers, depicted in figure 1.8.2 is an example of indirect electrolysis[38]. In this work, 10 mol% of triarylamine was used as redox mediator which accompanied the flurodesulfurisation of lactam derivatives towards the synthesis or fluorinated product **4**.[38]

1.8.3. Paired electrolysis[33]: In most of the electroorganic synthesis, only one-half cell reaction that is anodic oxidation or cathodic reduction is fruitful, and the other half reaction is sacrificial to complete the circuit. However, in paired electrolysis, both the half-cell reactions are productive to afford the products. This type of electrolysis is highly legitimate due to the effective usage of electricity and reduction of energy and chemical requirements. Paired electrolysis is categorised into five different types.

1.8.3.1. Parallel paired electrolysis: In this type of electrolysis, two different substrates are transformed into two different products at anode and cathode. In other words, both half-cell reactions are productive and simultaneously

generate two different products. This type of electrolysis can be carried out in both divided as well as undivided cell. The separation problem of unconsumed substrates and products is reduced when a divided cell is used.[33]

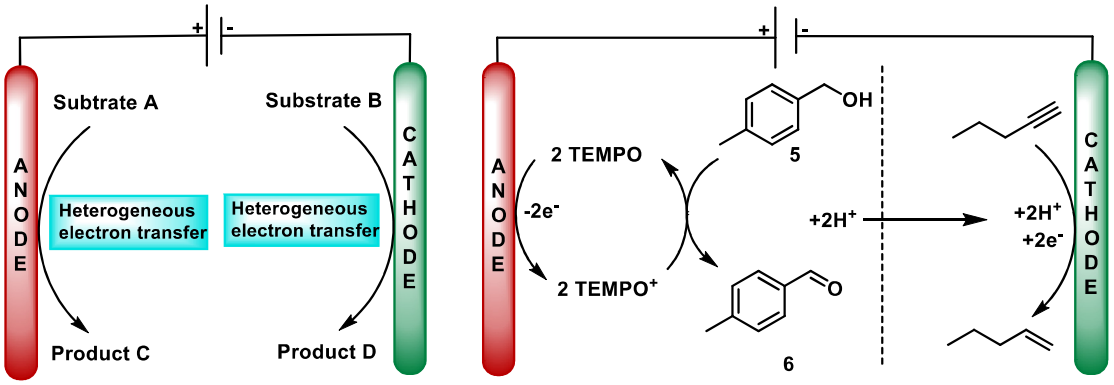

Figure 1.8.3. Schematic illustration for parallel paired electrolysis.

The above scheme describes a methodology that utilizes the concept of parallel paired electrolysis and is used by Berlinguette and coworkers towards the synthesis of benzaldehyde **6**. The process involves the TEMPO catalyzed oxidation of benzyl alcohol **5** to benzaldehyde **6** and the hydrogenation of alkyne to generate an alkene derivative (Figure 1.8.3)[39]. The evolution of the hydrogen gas takes place at the cathode which is utilized in hydrogenation process.

1.8.3.2. Divergent paired electrolysis[33]: In divergent paired electrolysis a single substrate undergoes simultaneous oxidation and reduction process providing two different products at each electrode (Figure 1.8.4). This type of electrolysis is limited to those substrates containing functional groups that can undergo both oxidation as well as reduction. Sometimes, the products can also react with each other to give undesired products.

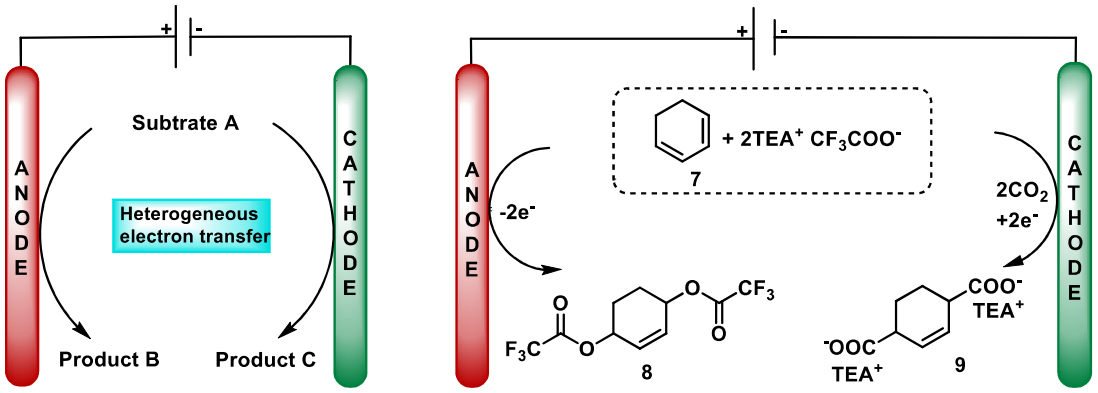

Figure 1.8.4. Schematic illustration for divergent paired electrolysis.

For example, conjugated diene **7** can undergoes simultaneous anodic acetoxylation and cathodic carboxylation to form 1,4-diol derivatives **8** and 1,4- dicarboxylates **9**, respectively (Figure 1.8.4).[40]

1.8.3.3. Convergent paired electrolysis[33]: In convergent paired electrolysis, a single product is obtained from two different intermediates generated via anodic oxidation and cathodic reduction of two different substrate. The intermediates generated are electrophilic and nucleophilic in nature. Buchwald and Jensen in 2020 reported an

example of convergent paired electrolysis for C-C bond formation via radical coupling of carbon-centred radicals generated simultaneously at the anode and the cathode (Figure 1.8.5).[41]

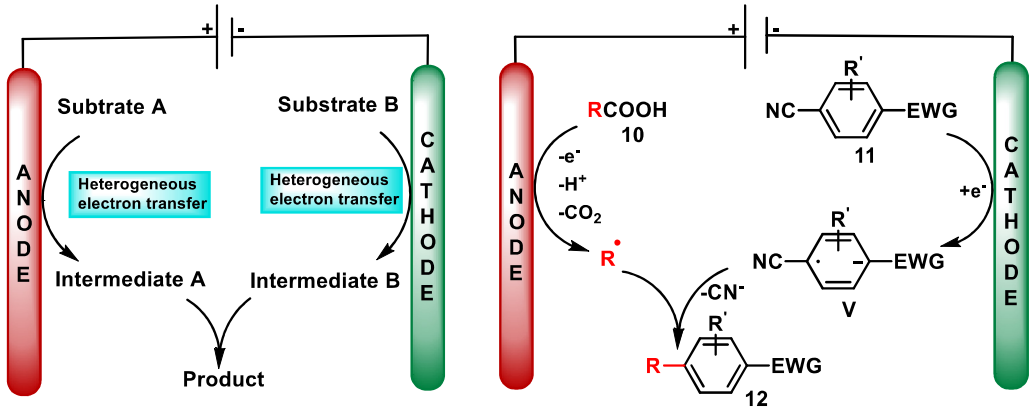

Figure 1.8.5. Schematic illustration for convergent paired electrolysis.

1.8.3.4. Sequential paired electrolysis (Domino paired electrolysis): In sequential paired electrolysis, the substrate experienced oxidation at anode followed by a reduction process to deliver desired product. Initially, substrate oxidizes at anode surface to generate an intermediate which further reduces at cathode to afford the final product. Waldvogel and coworkers in 2015, disclosed an electrochemical synthesis of nitriles **14** from aldoximes **13** via a Domino paired electrolysis. The methodology involves carbon anode and lead cathode at a constant current of 10 mA in acetonitrile solvent and led to the formation of the product **14** via intermediate **VI** in moderate yields (Figure 1.8.6).[42]

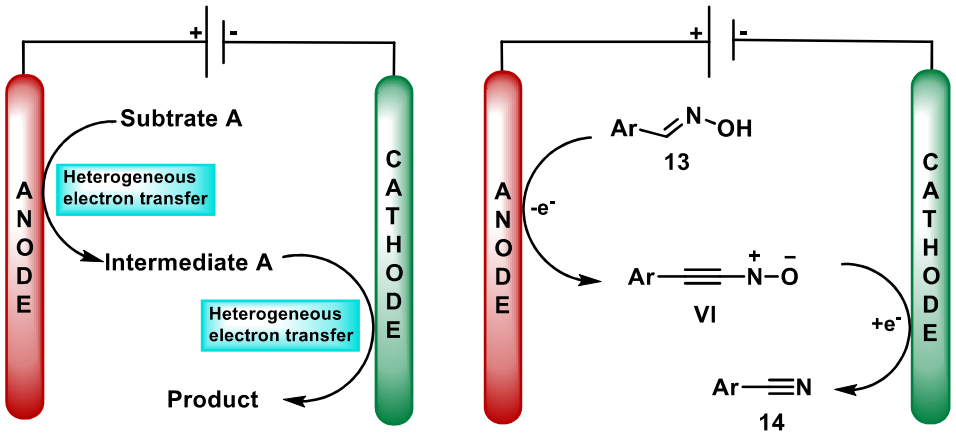

Figure 1.8.6. Schematic illustration for sequential paired electrolysis.

1.8.3.5. Linear paired electrolysis (200% current efficiency): Linear paired electrolysis is one of the most typical and interesting type of the electrolysis and it could achieve 200% efficiency. In this type of electrolysis, a single substrate oxidizes at anode as well as reduced at cathode to give a similar product. However, this type of electrolysis is impossible until a mediated process takes place to generate a strong oxidizing agent at the cathode or a strong reducing agent at the anode.[33] Recently, Hilt and coworkers reported an electrochemical bromination of cyclohexene **15** via linear paired electrolysis where bromine was generated from both the half-cell reactions, and added to alkenes giving the corresponding dibromo product **16** reaching up to 200% current yield (Figure 1.8.7).[43]

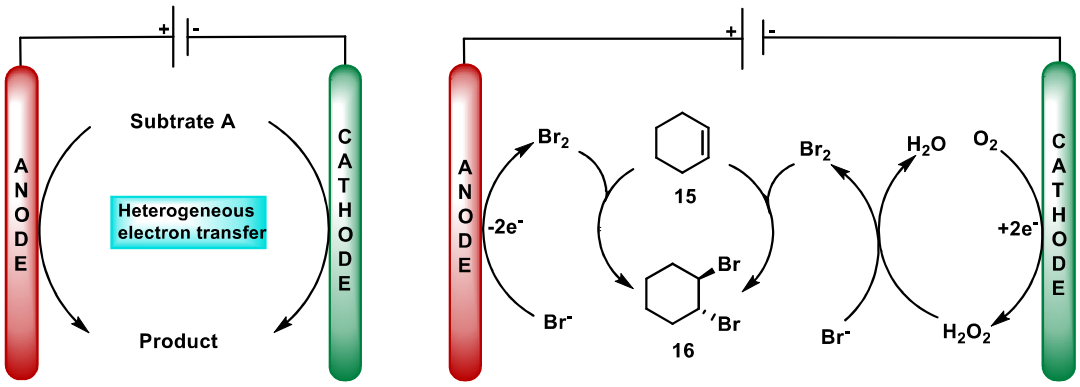

Figure 1.8.7. Schematic illustration for linear paired electrolysis.

1.9 Electrochemical direct anodic oxidation-based synthesis of various cyclic and acyclic scaffolds

1.9.1. Oxidation of amines and amides: Shono-type oxidation

Anodic oxidation provides an appropriate way to access *N*-centred radical cation from amines and amides. However, these intermediates undergo α-fragmentation to afford iminium ion (preferably *N*-acyl or *N*-carbamoyl iminium ion) which is referred to as Shono oxidation.[44,45] This iminium ion is primarily trapped by alcoholic solvent and provided a complimentary route to the α-C-H functionalisation of amines and amides. In this direction, Shono and coworkers disclosed the first electrochemical oxidation of amide **17** to generate a new carbon-carbon bond at α-methylene position via methoxylation step and Lewis acid promoted generation of an *N*-acyliminium ion intermediate **VIII**. A new carbon-carbon bond was formed at α-position of primary and secondary amines towards the synthesis of pyrrolidine, piperidine, and tropane alkaloids etc.[46]

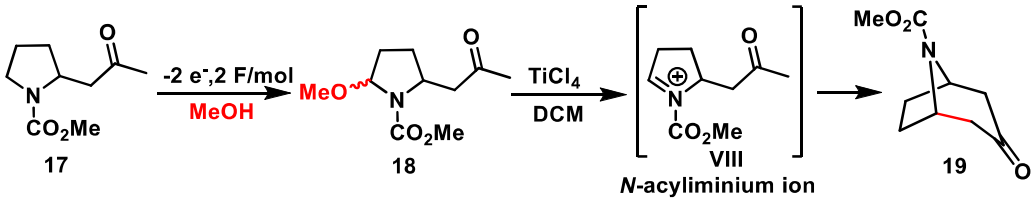

Scheme 1.9.1. Shono's C-C bond forming via anodic oxidation.

However, the anodic methoxylation takes place at the α-position of amines raised the question of regioselectivity, when it applies to the unsymmetrical amines. Generally, the oxidation occurs preferentially at less substituted position. However, Onomura efforts revealed that the regioselectivity was explained based on protecting group attached to nitrogen atom which affect and stabilise the *N*-acyliminium ion. In case of carbonyl and sulfonyl based protecting group the kinetic product **21** was solely formed, however on replacing the protecting group with cyano the thermodynamic product **22** was dominantly formed. Theoretical studies proposed that cyano group stabilised the more substituted iminium ion and favouring the methoxylation at more substituted position (Scheme 1.9.2).[47] In case of the bicyclic carbamates, the Shono oxidation occurs mainly at the ring junction (at more substituted position).[48]

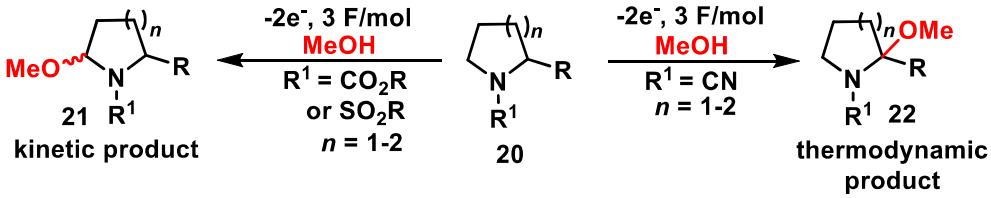

Scheme 1.9.2. The influence of the amino protecting group.

Despite of having low redox potential of amines, their anodic oxidation of is less explored than amides probably due to the unstable nature of imines and aminyl radical cations. The anodic oxidation of alkyl amines was reported by Gallardo and coworkers towards the synthesis of imidazolinium, tetrahydropyrimidinium,[49] and bulky alkyl diamines.[50] However, if a nucleophile is present inside the amine, the iminium intermediate can be trapped with nucleophile towards the intramolecular cyclization. In this direction, Okimoto and coworkers in 2007, reported cyclization of hydroquinolyl alcohols **23**, hydroquinolylamines, and dimethyl aminomalonates via oxidation of nitrogen.[51] The methodology was performed at a constant current of 300 mA by employing platinum anode and nickel cathode in presence of KI and NaOMe as mixture of supporting electrolyte and methanol solvent. Under these conditions, the cyclized product **24** was obtained in good to moderate yields (Scheme 1.9.3).

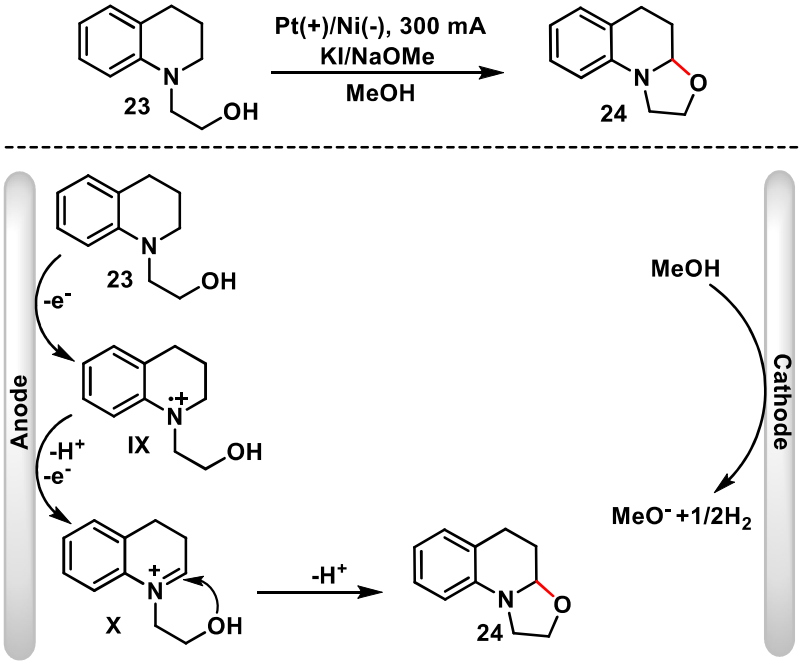

Scheme 1.9.3. Electrooxidative cyclization of hydroquinolyl alcohols.

Apart from the C-H bonds oxidation of α-carbon of amides and carbamates, the application of Shono oxidation can be extended to debenzylation and deallylation at the α-position. Onomura and coworkers reported an electrochemical oxidation of α-allylated cyclic amine **25** by using a carbon anode and platinum cathode and simply affords the corresponding α-methoxylated product **26** (Scheme 1.9.4).[52]

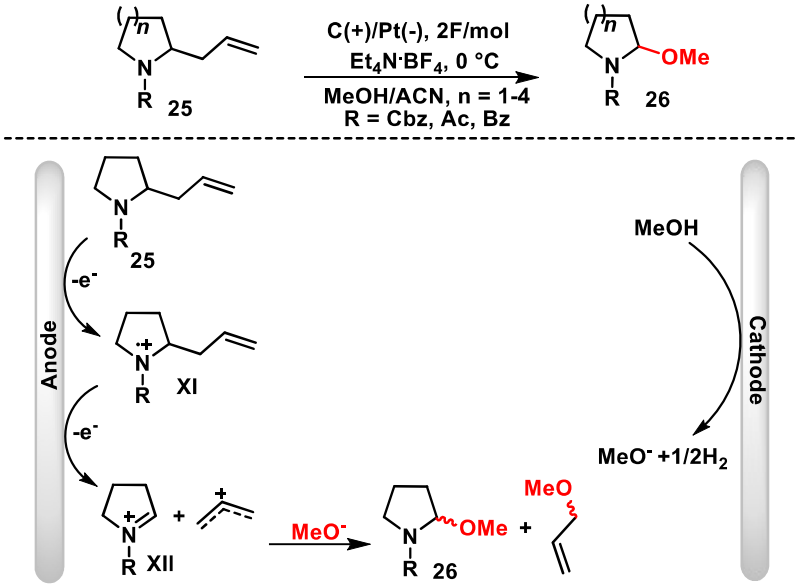

Scheme 1.9.4. Electrochemical deallylation of α-allyl cyclic amines.

The methodology was carried out at 0 °C in ACN/MeOH mixture of solvent in presence of tetraethyl ammonium tetrafluoroborate as supporting electrolyte. The α-methoxylated product **26** was obtained via formation of iminium cation X**II** through loss of two electrons and deallylation process which further capture via nucleophilic attack of methoxide ion to give side product. In a similar manner, debenzylation of cyclic amines can also takes place to afford the α-methoxylated product via Shono type oxidation.[52]

1.9.1.1. Variation of trapping nucleophiles: As discussed above, the alcohols are one of the ideal nucleophiles in Shono oxidation as they have high oxidation potentials compared to amines and amides. However, the trapping of iminium intermediate with carbon nucleophiles such as cyanide and enol ethers could be more complex. Alternatively, a two-step process is involved wherein an *N,O*-acetal generated in Shono oxidation is isolated and treated to further transformations. For example, the *N,O*-acetals **28** formed in Shono oxidations on treatment with triphenylphosphonium salts affords 1-(*N*-acylamino)alkyltriphenylphosphonium salts **29** wherein the alkoxy group is substituted by triphenylphosphine (Scheme 1.9.5).[53] These α-amidoalkylating agents **28** can also be transformed into amidosulfones[54] as well as into *N*-[1-(Benzotriazol-1-yl)alkyl]amides.[55]

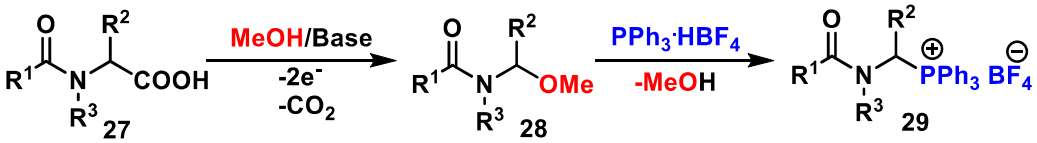

Scheme 1.9.5. Electrochemical transformation of *N*-acyl-α-amino acids into 1-(*N*-acylamino)alkyltriphenylphosphonium salts.

To overcome this, Tajima, and co-workers come up with a single-step α-cynation of amide **30** on the basis of principle of "site isolation." In this, the C-C bond formation happens directly via Shono oxidation in one step in presence of cyanide ion as nucleophile to afford product **31** (Scheme 1.9.6). Tetrabutylammonium tetrafluoroborate ($Bu_4N·BF_4$) and the cyanide salt of a solid-supported quaternary ammonium cation (PS-NMe_3·CN) were added at the same time into the reaction. Tetrabutylammonium tetrafluoroborate served as the supporting electrolyte while

the PS-NMe_3·CN reduced the concentration of cyanide in the solution and keeps the CN^- close to the polymer support and thus supressed the cyanide oxidation.[56]

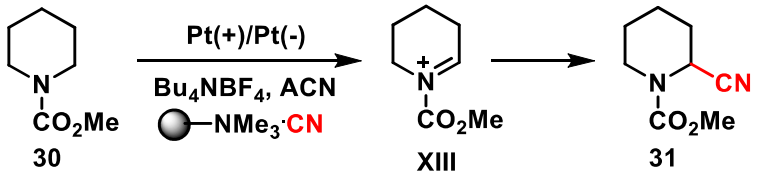

Scheme 1.9.6. Shono type oxidation via site isolation.

Using this method, several developments for the direct α-oxidation of amines or amides to form C-C bonds via iminium ion has been reported. For example, Atobe's direct Shono allylation using an ionic liquid (EMM·BF_4) and allyl-TMS as nucleophile,[57] and Tajima's alternative approach for one pot allylation of lactams.[58] Similarly, Onomura reported a single-step oxidative cyanation of amides/carbamates using TMSCN as nucleophile and methanesulfonic acid ($MeSO_3H$) as acid additive.[59]

Later, Luo *et al*., in 2017 come up with an idea of anodic oxidative coupling between tetrahydroisoquinoline derivatives **32** and alkyl ketones **33** via combining Shono-type oxidation and enamine catalysis to deliver the enantioselective product **34** (Scheme 1.9.7).[60]

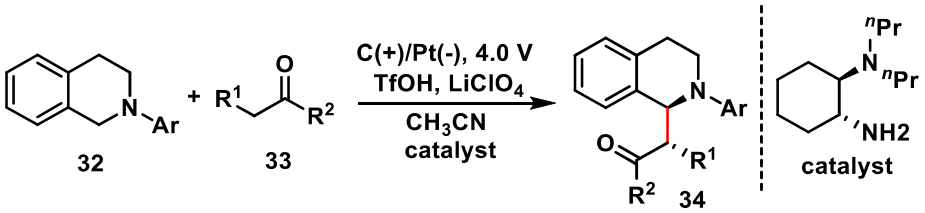

Scheme 1.9.7. Electrochemical α-aminoalkylation through enamine catalysis.

The protocol employs graphite as anode and platinum as cathode at constant voltage of 4.0 V in lithium perchlorate as supporting electrolyte in acetonitrile solvent where different types of primary amines are used as chiral amine catalyst. Simple ketones such as cyclopentanone, cyclohexanone, and cycloheptanone, as well as an acyclic ketone derivative, are also utilized and provides the synthesis of diverse, optically active tetrahydroisoquinoline derivatives.

1.9.1.2. The use of electroauxiliaries: Electroauxiliaries are the functional groups attached to lower the oxidation potential of the substrates.[61] This concept has proven beneficial for diversifying the scope of Shono-type oxidation of carbamates. Electroauxiliaries activate molecules towards electron transfer and controls the fate of the reactive intermediates and helps in the synthesis of the expected products. Mostly, silicon, tin and sulfur-based electroauxiliaries are used at α-position of carbamates and thereby helps in controlling the chemo- and regioselectivities of Shono oxidation. In 1997, Yoshida and coworkers, developed an anodic oxidation of carbamates using organithio group as electroaxiliaries.[62]

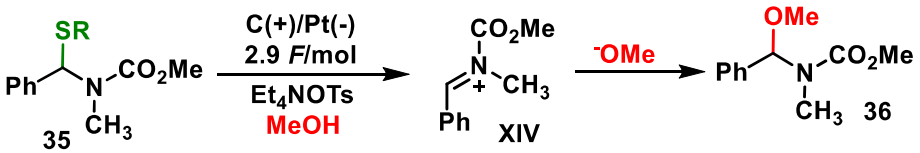

Scheme 1.9.8. Regioselective anodic oxidation using a thiophenyl electroauxiliary.

The reaction undergoes one electron oxidation of species **35** followed by selective cleavage of C-S bond to give iminium ion **XIV**, which undergoes nucleophilic attack by methoxy ion to deliver the α-methoxylated product **36** (Scheme 1.9.8). The strategy was used for both intermolecular as well as intramolecular carbon-carbon bond formation. In a similar manner, α-silyl carbamates can also undergo anodic oxidation at lower oxidation potential with complete regiocontrol due to the presence of silyl group at α-position of carbamates. In this direction, Moeller and coworkers used this strategy towards the chemoselective generation of iminium ion in a complex peptides under anodic oxidation. The reaction was carried out in carbon anode and platinum cathode employing tetrabutylammonium tetrafluoroborate as supporting electrolyte and methanol as solvent as well as nucleophile (Scheme 1.9.9).[63]

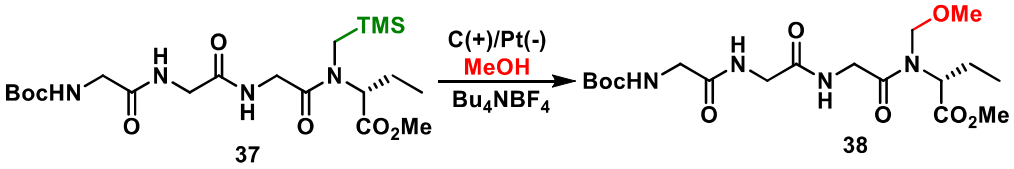

Scheme 1.9.9. Electrochemical peptide modification enabled by silyl electroauxiliary.

Later, Suga, Yoshida and co-workers synthesized a 2,2-disilylated and 2,5-disilylated pyrrolidine derivatives and upon sequential Shono type oxidation the different placements of silyl auxiliaries led to complementary regiochemical outcomes.[64,65]

1.9.1.3 Electrochemical generation of the acyl iminium cation pool: After the development of Shono oxidation, Yoshida and coworkers introduces the concept of "cation pool" method where the anodic oxidation takes place at low temperature and generates *N*-acyliminium ions which gets accumulated due to low temperature.[66] The accumulated intermediates can subsequently be captured with different nucleophiles. During the generation of *N*-acyliminium ions, there is no nucleophile present in reaction medium, so there is no concern about the oxidation of nucleophiles. For example, the pyrrolidine derivative **39** undergoes electrochemical oxidation in presence of carbon electrodes and tetrabutylammonium tetrafluoroborate as supporting electrolyte and dichloromethane solvent in a divided cell at -72 °C to afford the *N*-acyliminium ion **XV** which is characterized by spectroscopic techniques at low temperature. After that, allyltrimethylsilane is added to the reaction mixture and affords the corresponding allylated product **40** (Scheme 1.9.10).

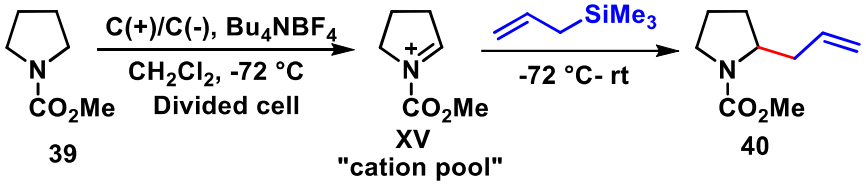

Scheme 1.9.10. Generation of *N*-acyliminium ion *via* cation pool method.

The *N*-acyliminium ions produced by the cation pool method can also encounter cycloaddition reactions to furnish the corresponding cycloadduct.[67] In this direction, Yoshida and coworkers reported a [4+2] cycloaddition reaction between *N*-acyliminium ion **XVI** and alkene /alkyne derivatives to deliver the corresponding cycloadduct **42** (Scheme 1.9.11).[68] However, in case of the reaction with the styrene derivatives the significant amount of byproducts formation takes place.

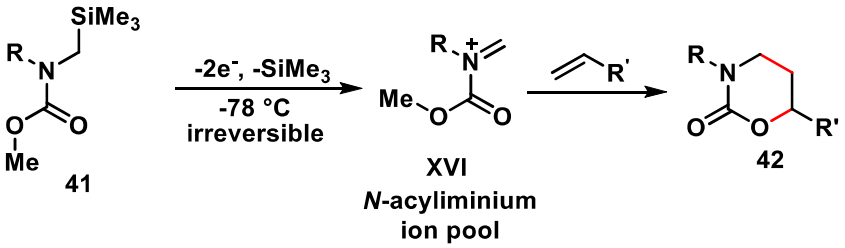

Scheme 1.9.11. [4+2] Cycloaddition of *N*-acyliminium ion and dienophile.

1.9.2 Oxidation of Phenols

Phenol and its derivatives belong to a broad class of biological active molecules and are widespread in many natural products like vitamins, hormones, amino acids, and antioxidants.[69] These derivatives contain a hydroxyl functional group (–OH) attached to an aromatic hydrocarbon group, having structure like that of benzene. These fascinating properties of phenol and its derivatives attracted the attention of many chemists from academia as well industry. Electrochemical oxidation of phenols has been a subject of continual research interest, and found many applications in the synthesis of diverse natural products.[70,71] The oxidation of phenols leads to the synthesis of complex and diverse scaffolds which are beneficial in the domain of synthetic organic chemistry. A common oxidation pathway for oxidation of phenol is shown in scheme 1.9.12.

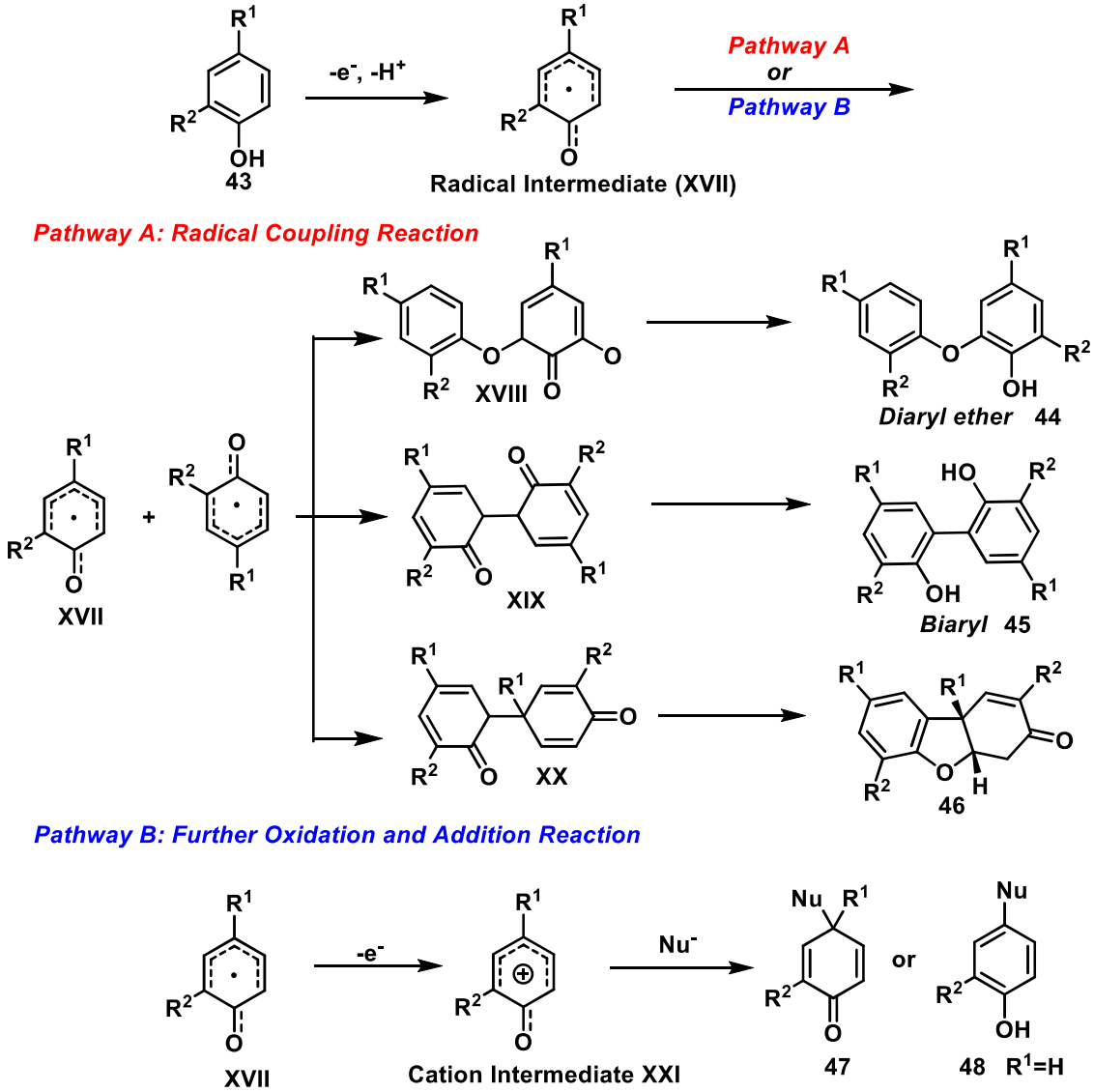

Scheme 1.9.12. Oxidation of phenol.

The first step is single electron transfer (SET) from substrate **43** at the surface of anode followed by loss of proton to provide radical intermediate **XVII**. This intermediate **XVII** proceeds via two pathways: radical coupling pathway (Pathway A, Scheme 1.9.12) and further oxidation and addition pathway (Pathway B, Scheme 1.9.12). In Pathway A, the intermediate **XVII** undergoes self-coupling to form diaryl ether **44**, biaryl **45**, or dienone frameworks **XX**, which could be further affords cyclized product **46** through nucleophilic addition or intramolecular cyclization to a cyclized product **46**. In Pathway B, the intermediate **XVII** undergoes further single electron oxidation to afford the cation intermediate **XXI** which is attacked by a nucleophile to form a dienone **47** or an aromatized product **48**. Following these two oxidation pathways, different strategies have been devised wherein phenols are converted into various functionalised scaffolds.

In this direction, Waldvogel and coworkers, in 2009 devised a protocol towards the C-C biaryl coupling via anodic oxidation of 2,4-dimethylphenol **49**.[72] The methodology was carried out in an undivided cell employing boron doped diamond (BDD) as anode and nickel as cathode at a constant current of 4.7 mA. Fluorinated solvents, like HFIP proved beneficial probably because it could stabilize the oxygen spin centres. The protocol was specifically

applicable with very electron-rich phenols as well as halogenated substrates. Later, based on these principles guaiacol derivatives has also been explored under electrochemical conditions towards cross coupling reaction.[73]

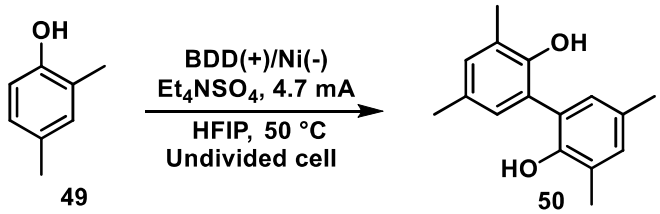

Scheme 1.9.13. Biaryl coupling of phenols.

This method could be further extended to accomplish cross-coupling of two different phenols.[74] Similar to the above methodology, solvents with good hydrogen-bonding abilities, such as HFIP are used. The phenol derivative having lower oxidation potential preferentially undergoes anodic oxidation and coupled with another partner to afford the cross coupled product.

The same group, in 2012, develop a new method to accomplish cross-coupling between phenol **51** and electron rich arene **52** to afford biaryl product **35**.[75] The process was performed with boron doped diamond (BDD) anode and nickel cathode by applying current density of 2.8 mA/cm^2 and Et_4NMeO_3SOMe as a supporting electrolyte in HFIP solvent to render the final product **53** in moderate to good yields. Addition of methanol or water to solvent found to be crucial to the phenomenon. Further, substrate scope variation disclosed that the designed protocol works better with the electron-rich arenes and deliver cross-coupled products **53** in good yields (scheme 1.9.14).[75]

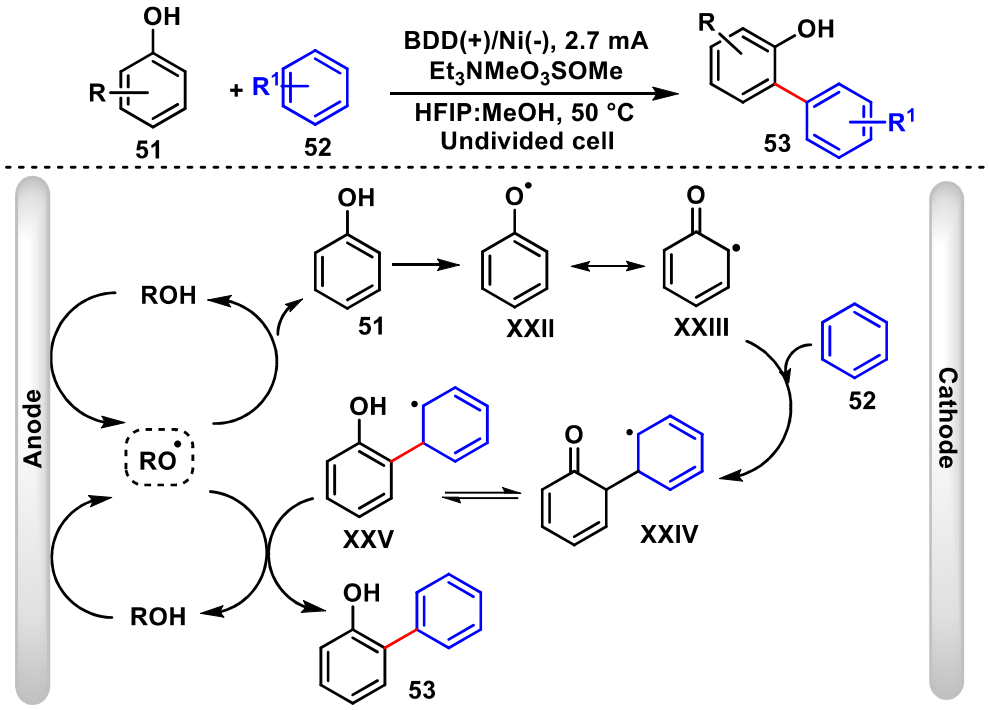

Scheme 1.9.14. Electrochemical phenol-arene coupling.

Like C-C bond coupling, the phenol oxidation can also utilize towards the synthesis of aryl ether via C-O bond formation. In this direction, Nishiyama and coworkers have performed extensive investigation of the anodic oxidation of *ortho*-halo phenols **55**.[70] The 2,5-dihalo substituted phenol derivatives **55** via anodic oxidation event

followed by dimerization and cathodic cleavage of a C-X bond led to the generation of diaryl ethers **56**.[8] The reaction was performed in an undivided cell equipped with platinum electrodes and methanol as solvent. The phenoxy radical **XXVI** undergoes C-O dimerization guided by one of the halogen atoms to afford regioselective product **XXVII**, which undergoes nucleophilic attack by methanol followed by C-X bond cleavage to afford intermediate **XXVIII**. This intermediate via cathodic reduction afford the desired product **56**. Further, this strategy was implemented towards the synthesis of natural product *O*-methylthalibrine **57** which is an alkaloid showing antimalarial and cytotoxic activities (Scheme 1.9.15).[76]

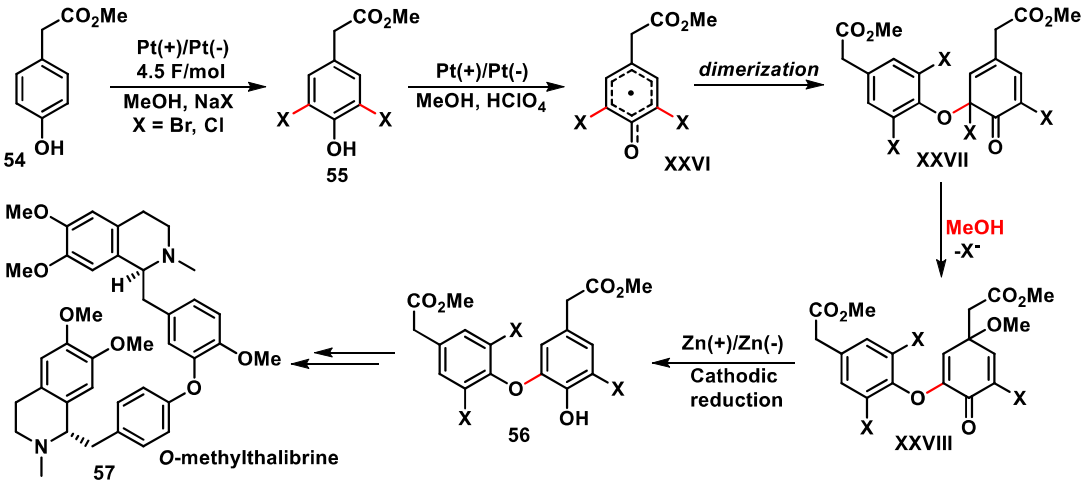

Scheme 1.9.15. Electrooxidative dimerization of ortho-dihalo phenols.

Later, the same group established the syntheses of various aryl ether-based drug molecules verbenachalcone[77] and isodityrosine[78] utilizing this strategy. They also explored the oxidation of isoeugenol **58** where the radical **XXIX** dimerized in a formal [3+2] cycloaddition manner into a cyclized product licarin **59**.[79] The methodology was performed in an undivided cell where BDD anode proved to be best for the transformation. Methanol was used as solvent and lithium perchlorate as supporting electrolyte. The reaction shows that methoxy radicals were produced by electrochemical oxidation of methanol in BDD anode (Scheme 1.9.16).

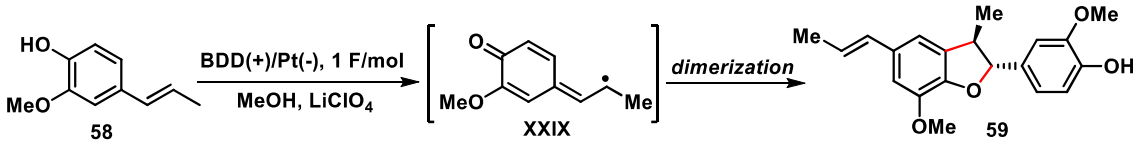

Scheme 1.9.16. Synthesis of licarin via electrooxidative phenol dimerization.

The above discussed methodologies developed were based on the radical radical homo coupling or cross coupling of phenoxy radical led to the generation of biaryls and biary ether. However, as discussed in scheme 1.9.12 there can be another pathway based on the two-electron oxidation of phenol to generate highly electrophilic species phenonium cation which can be trapped with various nucleophiles or can undergoes intramolecular cyclization.[80,81] Nishiyama's synthesis of aeroplysinin **63** is one of the examples of intramolecular cyclization onto a phenonium cation generated by two electron oxidation (Scheme 1.9.17).[82] The reaction was conducted in an undivided cell employing carbon as anode and platinum as cathode at a constant voltage of 1.6 V. Tetrabutylammonium perchlorate served as supporting electrolyte and acetonitrile as solvent. The reaction proceeds via formation of phenonium cation **XXXI** via sequential two electron oxidation of phenol moiety **60.** The phenonium cation **XXXI**

undergoes intramolecular nucleophilic attack by oxime oxygen to form the cyclized product **61** which further transformed into biological active molecule aeroplysinin **63** (Scheme 1.9.17).[82]

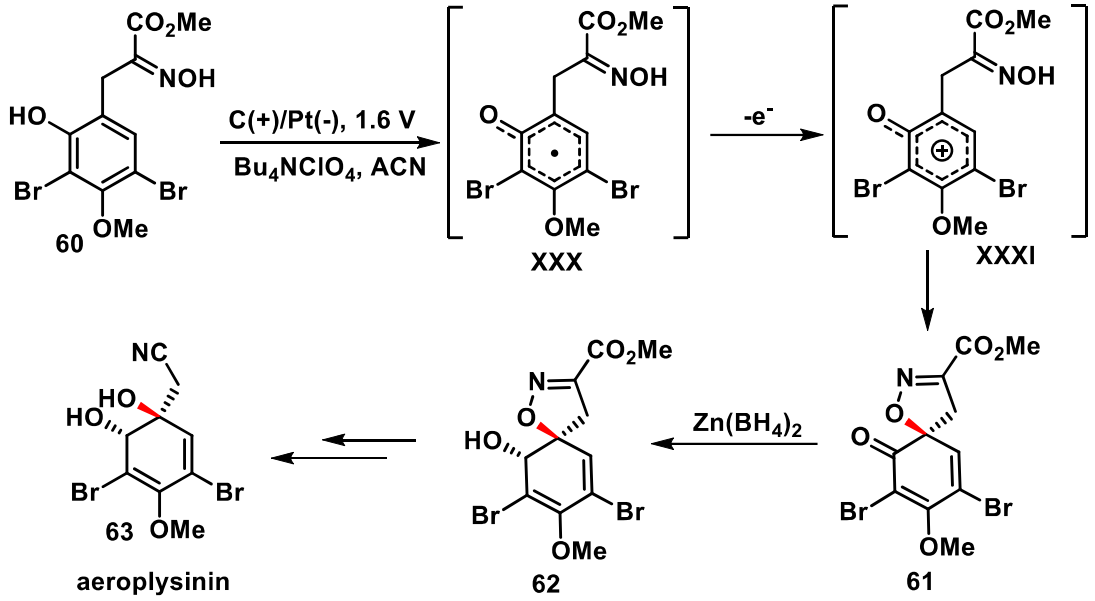

Scheme 1.9.17. Electrochemical synthesis of aeroplysinin.

Later, the same group utilized this chemistry towards the synthesis of spirodienone by cyclization of an alcohol with a phenonium cation, which was subjected to ring expansion by treatment with a Lewis acid towards the natural product heliannuol .[83] Alternatively, phenonium cations can also undergoes cycloaddition reactions with various types of electron rich olefins. In this direction, Chiba and co-workers disclosed a [3+2] cycloaddition reaction of phenols **64** and olefins **65** via generation of phenonium cation **XXXII** led to the generation of cycloadduct **66** (Scheme 1.9.18).[84,85] The reaction can be carried out in a multiphase solvent system where phenol remains in the polar nitromethane layer and cycloadduct accumulates in less polar thermomorphic layer of $MeNO_2$ and cyclohexane. The reaction was more favourable with electron rich multi substituted olefins than the monosubstituted olefins.

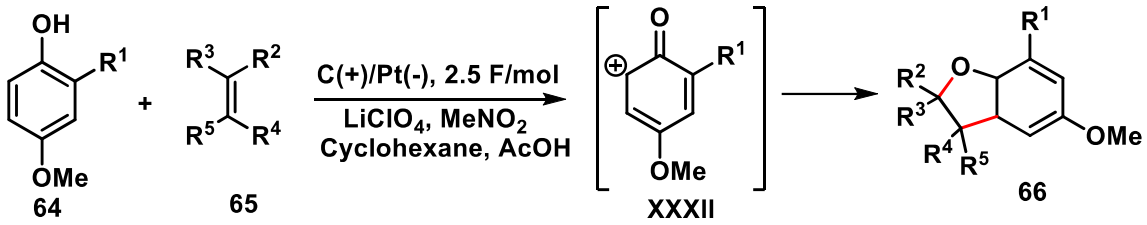

Scheme 1.9.18. Electrooxidative [3+2] cycloaddition between phenols and olefins.

The phenonium cation generated can also be trapped by an external nucleophile attack. In this direction, Banerjee, and co-workers in 2022 devised an electrochemical protocol towards the synthesis of paracetamol via Ritter-type C-H amination of phenol (Scheme 1.9.19).[86] The phenol **51** in acetonitrile was electrolysed in an undivided cell fitted with carbon electrodes in the presence of Bu_4NPF_6 as the supporting electrolyte at a constant current of 6 mA. The reaction starts off with two electron oxidations of phenol to generate phenonium carbocation **XXXVI**, which upon nucleophilic attack by acetonitrile followed by loss of hydrogen atom toe afford intermediate **XXXVIII.** The nucleophilic attack of hydroxide ion on intermediate **XXXVIII** and further rearrangement render

the amidation product **67**. The protocol can also be employed to several substituted phenols and tolerated various functionalities like aldehyde and ketones.

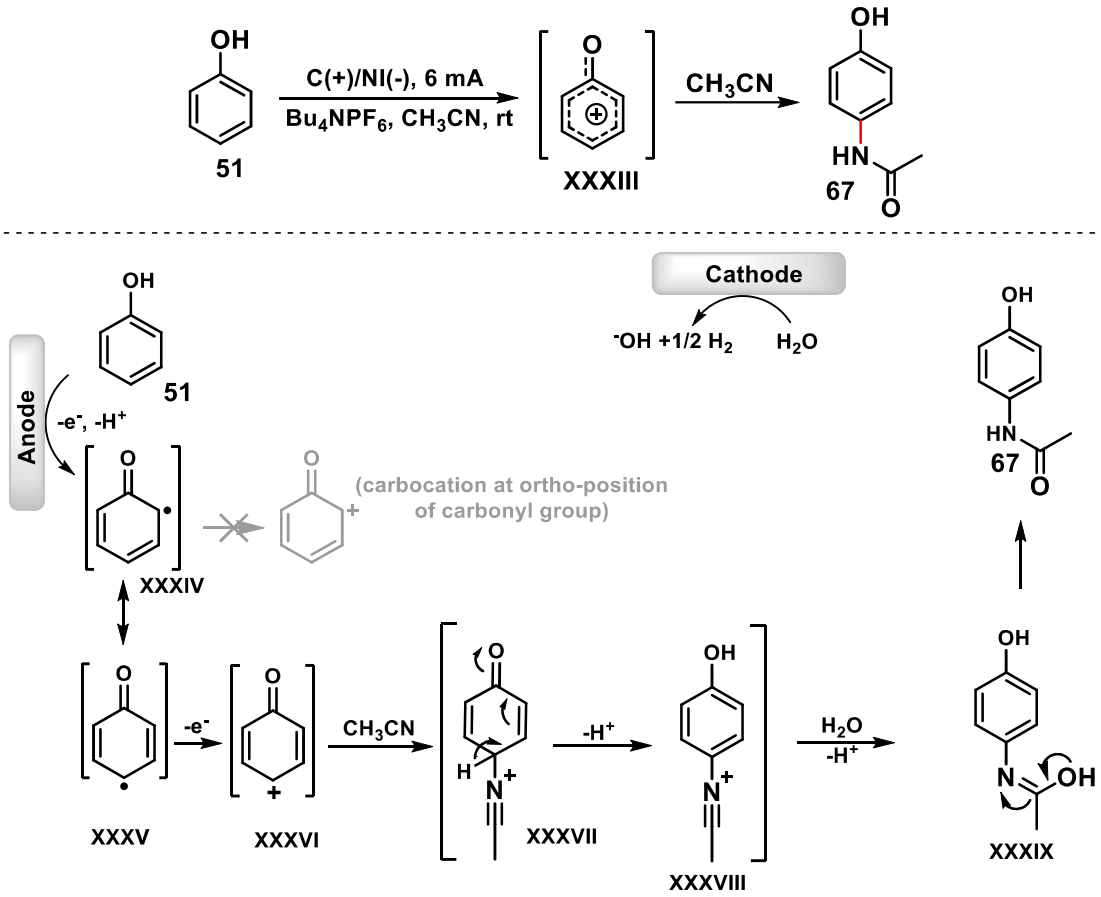

Scheme 1.9.19. Electrochemical synthesis of paracetamol.

1.9.3. Alkene oxidation

Alkenes are among the most attractive and accessible moieties in organic chemistry and exhibit widespread reactivity with a plethora of substrates to afford diverse range of organic compounds.[87] Radical-mediated transformations of alkenes can proceed via three different pathways; (i) alkenes acts as the radical acceptors (Scheme 1.9.20, Path I); (ii) reduction of alkenes to the radical anion intermediates (Scheme 1.9.20, Path II); and (iii) oxidation of alkene to radical cation (Scheme 1.9.20, Path III).

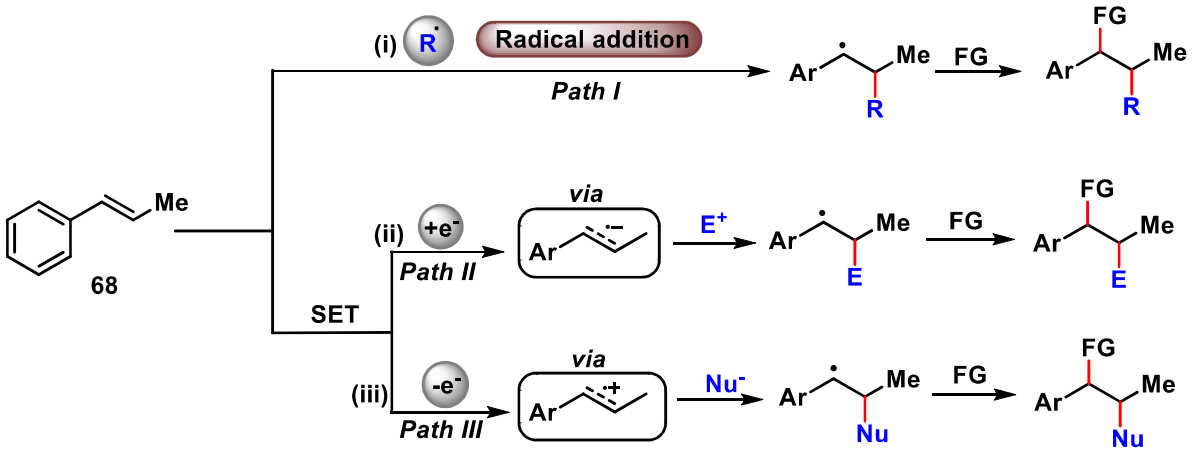

Scheme 1.9.20. Three possible radical pathways for alkene functionalization.

Among all these strategies, the alkene-derived radical cationic method (Path III) represents a peculiar transformation mode,[88,89] which enhances the other reaction substrates of the alkenes. These radical cations show dual reactivity due to the presence of a radical site and an electrophilic carbocation centre and have been broadly applied in the syntheses of various difunctionalized, hydro functionalized and cyclic systems via cycloaddition reactions.[90,91,92,93] Interestingly, the functionalization of alkenes using two nucleophiles can be done using this radical cationic strategy via sequential two electron oxidation. In this direction, Yoshida, and coworkers, in 2012 reported an electrochemical dihydroxylation of alkenes **69** via formation of bis-alkoxysolfonium intermediate **XLI**, which further hydrolyzed to produce 1,2-diol derivatives **70** in presence of aqueous NaOH solution.[94] The reaction was carried out in a divided cell at a constant current of 8 mA employing carbon as anode, platinum as anode and tetrabutylammonium tetrafluoroborate as supporting electrolyte in DMSO/DCM mixture of solvent.

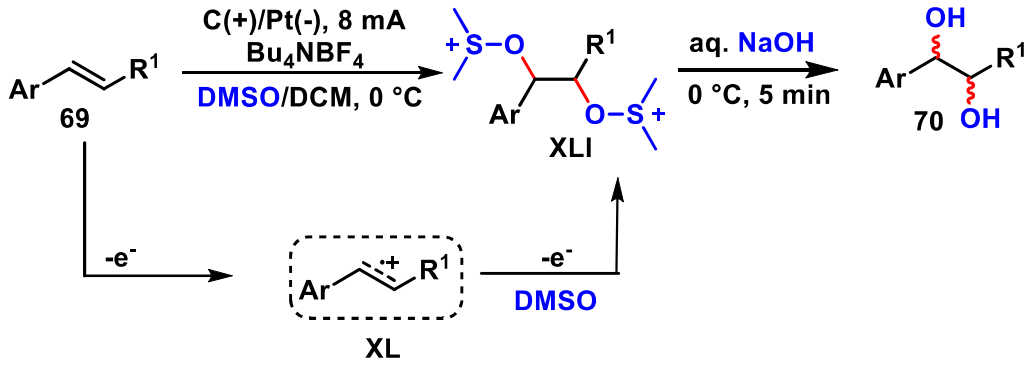

Scheme 1.9.21. Oxidative hydroxylation mediated by alkoxysulfonium ions.

The alkene derivative **69** undergoes one electron oxidation to generate radical cationic intermediate **XL,** which further oxidizes at anode and the cationic species trapped with the DMSO to give bis-alkoxysulfonium intermediate **XLI**, which on treatment with aqueous NaOH afford the desired dehydroxylated product **70** (Scheme 1.9.21).

Followed by this, in 2019, Xu *et al*., achieved an electrochemical dimethoxylation of olefins via generation of radical cation intermediate.[95] The reaction was electrolysed at constant current of 20 mA in an undivided cell fitted with platinum electrodes, tetrabutylammonium tetrafluoroborate as supporting electrolyte and anhydrous solvent

CH_3CN/MeOH as mixture under argon atmosphere at 60 °C. The protocol delivered the 1,2-dimethoxylation **72** or 1,1- dimethoxylation **73** products depending on nature of substituents on the alkenes (Scheme 1.9.22).[95]

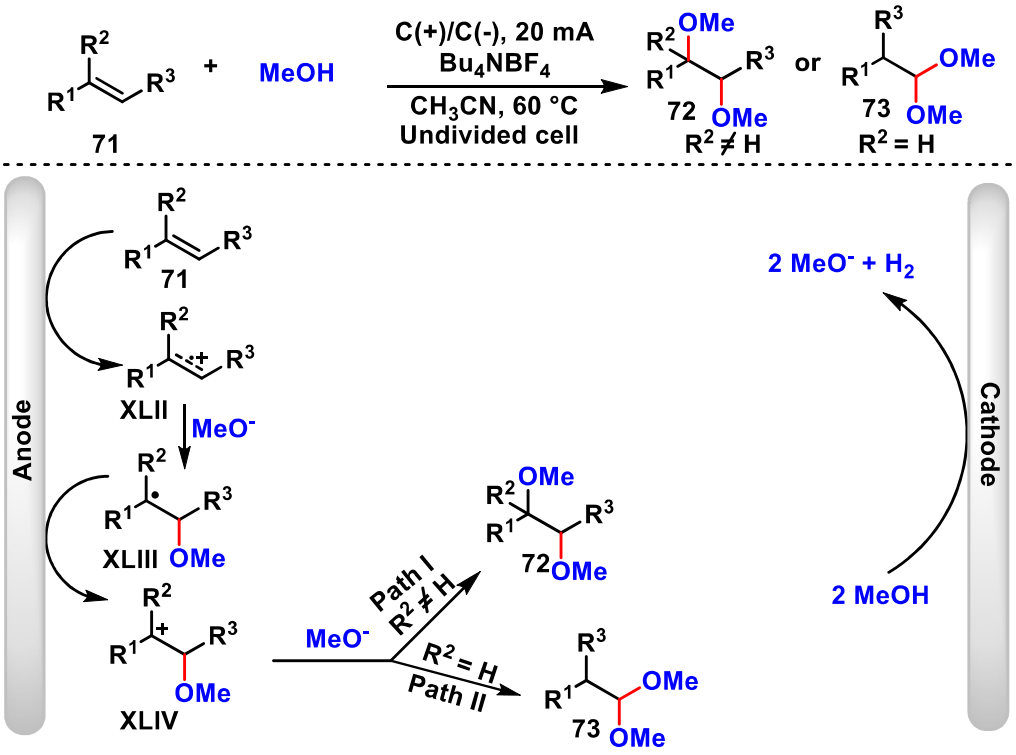

Scheme 1.9.22. Electrochemical dimethoxylation of alkenes.

Firstly, single electron transfer (SET) of alkene **71** generates a radical cation species **XLII**, followed by a nucleophilic attack by methoxy anion generated at the cathode affording the radical species **XLIII**. Further oxidation of transient radical **XLIII** generates the carbocation **XLIV**. Eventually, the carbocation **XLIV** can undergo two different pathways, based on the stability of **XLIV**. The more stable carbocation having multiple substituents undergoes direct nucleophilic attack (path I) to deliver product **72**, whereas the less stable proceeds via semipinacol rearrangement (path II) to deliver the acetal product **73** (Scheme 1.9.22).

Despite having remarkable development in the field of alkene dioxygenation, the stereoselective synthesis of 1,2-diol derivatives remains unexplored. In this direction, Kim, and coworkers in 2021 developed an electrochemical strategy towards the construction of *syn*-1,2-diol derivatives **75** from alkenes **74** using DMF as oxygen source.[96] The protocol was accomplished at constant current electrolysis by employing graphite as anode and platinum as cathode and tetrabutylammonium tetrafluoroborate as supporting electrolyte. Trifluoracetic acid (CF_3COOH) was used as acid additive (Scheme 1.9.23). The source of hydrogen atom and oxygen atom was confirmed by deuterium labelling experiment with DMF-d^6 and H_2O^{18}.

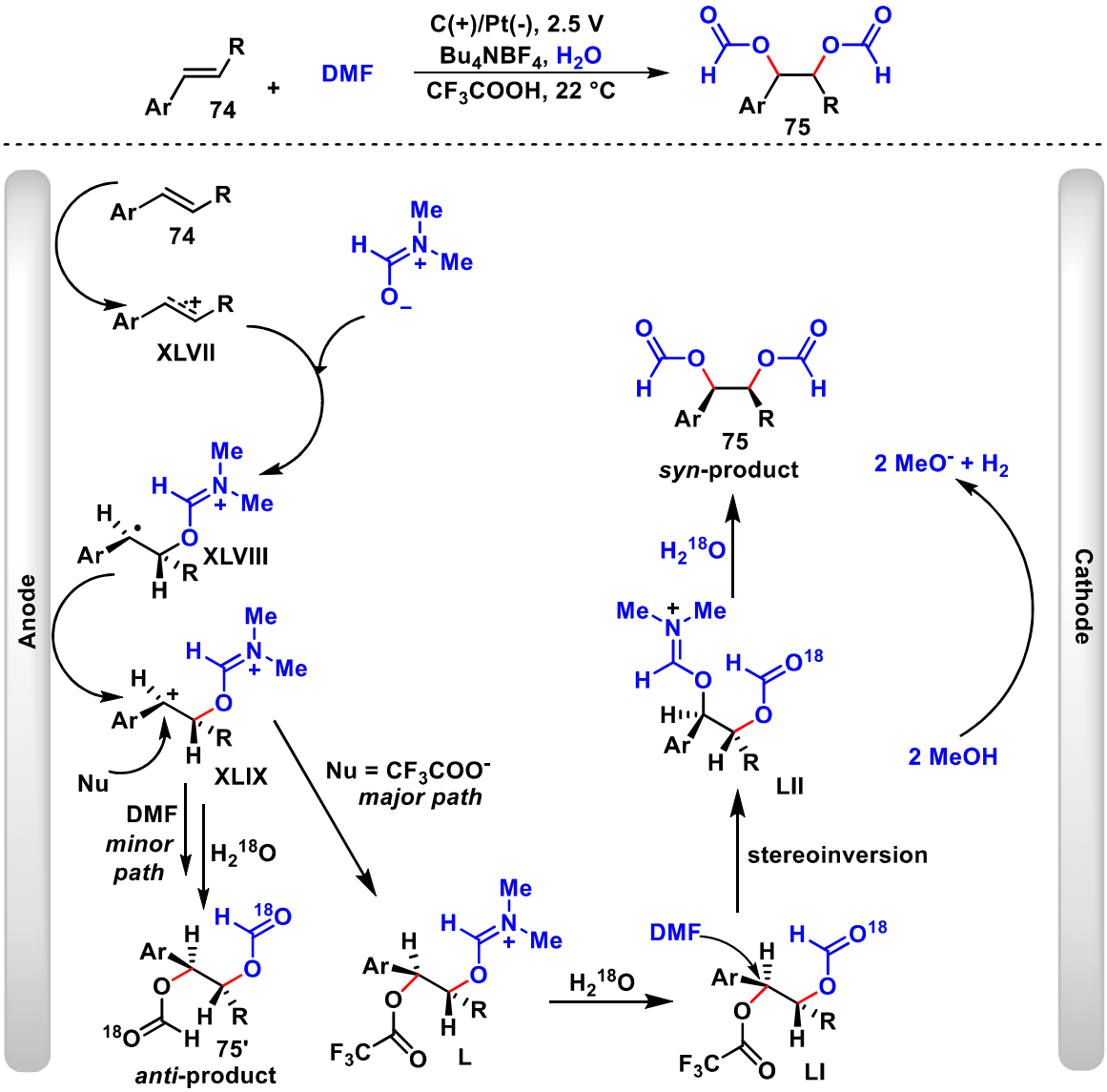

Scheme 1.9.23. Electrochemical synthesis of the protected syn-1,2-diol derivatives.

Initially, alkene **74** was first oxidized into radical cationic species **XLVII**, which subsequently captured by DMF to generate carbon-centered radical **XLVIII**. The radical species **XLVIII** was further oxidized at anode surface to afford dicationic species **XLIX**. Next, dication **XLIX** reacted with the DMF to furnish anti-diformyloxylated product **75'** which is minor pathway due to low yield of the product. Alternatively, dication **XLIX** was captured by a good nucleophile, trifluoroacetate, to afford intermediate **L**. Finally, nucleophilic replacement followed by hydrolysis processes led to the generation of syn-diformyloxylation product **75** with an excellent stereoselectivity (Scheme 1.9.23).[96]

Apart from the bifunctionalization of alkenes, the alkene derived radical cations can also react with unsaturated hydrocarbon to give diversified cyclic scaffolds, mainly four and six membered derivatives. The most common and efficient way towards the synthesis of functionalized cyclobutane is the [2+2] cyclization through combinations of two alkenes variant. In 2001, Chiba *et al*., disclosed that electron rich enol ethers can be used as radical cation precursors under electrochemical conditions which trigger the [2+2] cyclization reaction with other alkenes for the synthesis of substituted cyclobutane derivatives (Scheme 1.9.24).[97] The solution of enol ether **76** and alkene **77** was electrolyzed at 2.5 mA of current in the presence of nitromethane solvent and lithium perchlorate

as supporting electrolyte. However, the enol ethers bearing methoxyphenyl ring is needed for this transformation as the electron rich aryl group takes part in the synthesis of cyclobutane ring via intramolecular electron transfer between cyclobutane radical cation species **LIV** and phenyl ring to give radical cationic species **LV**, which via chain propagation step rendered the final product **78**. Later, the same group, in 2005, developed an electrochemical protocol leads to the cross metatheses between the anodically oxidized enol ethers and aliphatic alkenes.[98]

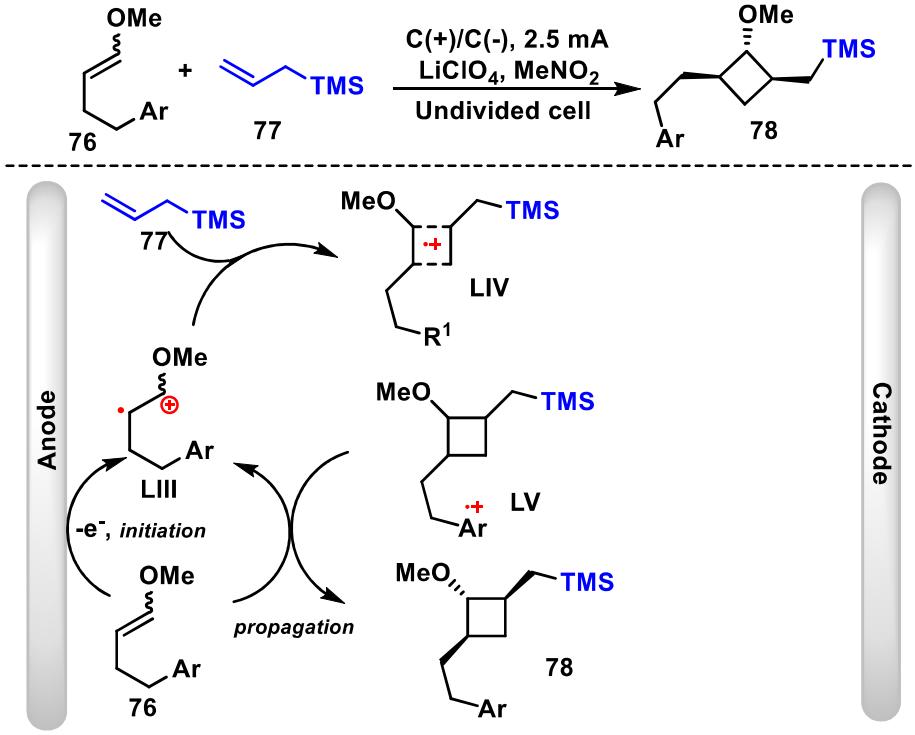

Scheme 1.9.24. Electrocatalytic intermolecular formal [2+2] cycloaddition between enol ethers and alkenes.

After the development of [2+2] cyclization of alkenes, the same group, in 2016, further explored electrochemical [4+2] cyclization between 1,3-diene and activated aryl alkenes initiated by the generation alkene radical cation.[99] Likewise [2+2] cyclization, the transfer of electron from cyclohexene radical cation to methoxyphenyl group is the crucial step in this [4+2] cyclization. It follows similar mechanism as discussed in above scheme. The speculation was further supported by DFT studies and cyclic voltammetry studies. However, the electron rich alkenes were found to be compatible in this methodology (Scheme 1.9.25).

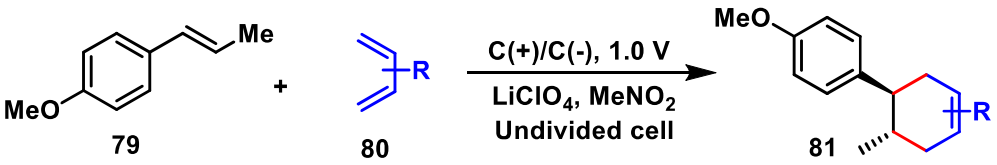

Scheme 1.9.25. Electrooxidative radical cation-initiated Diels-Alder reaction.

To enhance the restriction w.r.t alkenes, same group in 2019 disclosed that this radical cation mediated Diels-alder type reaction of non-conjugated alkenes with 1,3-diene can be carried out in an undivided cell. The stoichiometric amount of electricity or a catalytic amount of electricity plays crucial role to carry out this [4+2] annulation.[100]

The electroorganic synthesis has been witnessing a renaissance in the past decades, and brought remarkable growth and recognition to become mainstream in synthetic organic chemistry. Traceless electrons are used as redox agents

and participating in various SET processes to generate highly reactive intermediates, which can be further utilized in various organic transformations. In electroorganic synthesis, the electron transfer occurs between electrode and chemical species enabling the chemical transformations in the absence of exogenous metal oxidants, hence avoids the generation of chemical waste associated with conventional methods. So, electroorganic synthesis is considered as greener as compare to the traditional chemical methods and diminish the environmental burden of chemical processes. Henceforth, we believe that the adoption of this innate technology in synthesis laboratory can open several pathways associated with redox transformations. Moreover, various radical/ionic species like iminium ion, phenonium ion and alkene derived radical cation etc. generated via SET at anode surface discussed in this chapter are the prevalent intermediates in organic synthesis. These intermediates can be utilized in various cyclization, annulation, and functionalization reactions towards the synthesis of various cyclic and acyclic scaffolds.

1.10 Aim of thesis

This doctoral thesis aimed to develop the various synthetic methodologies via direct oxidation at anodic surface by employing electroorganic chemistry. The relevant experimental studies for the objective of this thesis are elaborated in the upcoming chapters as follows:

Chapter 2 discusses the electrochemical generation of a nonstabilized azomethine ylide: access to substituted *N*-heterocycles.

Chapter 3 elaborates the electrochemical sulfinylation of phenols with sulfides: a metal- and oxidant-free cross-coupling for the synthesis of aromatic sulfoxides.

Chapter 4 discloses electrochemical oxidative c–c bond cleavage of methylenecyclopropanes with alcohols.

1.11. References:

1. Olivier, J. G. J.; Janssens-Maenhout, G.; Muntean, M.; Peters, J. A. H. W. Trends in Global CO_2 Emissions: 2016 Report, The Hague, **2016**.
2. Cernansky, R. *Nature*, **2015**, *519*, 379-380.
3. Wiebe, A.; Gieshoff, T.; Mçhle, S.; Rodrigo, E.; Zirbes, M.; Waldvogel, S. R. *Angew. Chem. Int. Ed*., **2018**, *57*, 5594-5619.
4. Horn, E. J.; Rosen, B. R.; Baran, P. S. *ACS Cent. Sci*., **2016**, *2*, 302-308.
5. Karkas, M. D. *Chem. Soc. Rev.*, **2018**, *47*, 5786-5865.2020
6. Waldvogel, S. R.; Janza, B. *Angew. Chem., Int. Ed*., **2014**, *53*, 7122-7123.
7. Pollok, D.; Waldvogel, S. R. *Chem. Sci*., **2020**, *11*, 12386-12400.
8. Pletcher, D.; Walsh, F. Industrial Electrochemistry, Blackie Academic & Professional, London, New York, 2nd edn, **1993**.
9. Volta, A. Xvii. On the electricity excited by the mere contact of conducting substances of different kinds. In a letter from Mr. Alexander Volta, F. R. S. Professor of natural philosophy in the university of Pavia, to the Rt. Hon. Sir Joseph Banks, Bart. K.B. P. R. S. Philos. *Trans. R. Soc. Lond*. 90, 403431.
10. Volta, A. G. A. *Nat. Philos. Chem. Arts* **1800**, *4*, 179-187.
11. Faraday, M. *Ann. Phys. Leipzig* **1834**, *47*, 438-445.

12. Faraday, M. *Philos. Trans. R. Soc*., **1834**, *124*, 77-122.
13. Kolbe, H. J. *Prakt. Chem*. **1847**, *41*, 138.
14. Tafel, J.; Hahl, H. *Ber. Dtsch. Chem. Ges*. **1907**, *40*, 3312-3318.
15. Haber, F. Z.; Elektrochem. *Angew. Phys. Chem*., **1898**, *5*, 235.
16. Hickling, A. *Trans. Faraday Soc*., **1942**, *38*, 27-33.
17. Yan, M.; Kawamata, Y.; Baran. P. S. *Chem. Rev.* **2017**, *117*, 13230-13319.
18. Randles, J. E. B. *Trans. Faraday Soc.,* **1948**, *44*, 327-338.
19. Shono, T.; Hamaguchi, H.; Matsumura, Y. *J. Am. Chem. Soc*., **1975**, *97*, 4264-4268.
20. Yoshida, J.-I.; Murata, T.; Isoe, S. *Tetrahedron Lett*., **1986**, *27*, 3373-3376.
21. Little, R. D.; Fox, D. P.; Van Hijfte, L.; Dannecker, R.; Sowell, G.; Wolin, R. L.; Moens, L.; Baizer, M. M. *J. Org. Chem*., **1988**, *53*, 2287-2294.
22. Moeller, K. D. *Tetrahedron*, **2000**, *56*, 9527-9554.
23. Yoshida, J.-I.; Suga, S. *Chem. - Eur. J.,* **2002**, *8*, 2650-2658.
24. Xu, H.-C.; Moeller, K. D. *J. Am. Chem. Soc.,* **2008**, 130, 13542-13543.
25. Kirste, A.; Nieger, M.; Malkowsky, I. M.; Stecker, F.; Fischer, A.; Waldvogel, S. R. *Chem. -Eur. J.*, **2009**, *15*, 2273-2277.
26. Rosen, B. R.; Werner, E. W.; O'Brien, A. G.; Baran, P. S. *J. Am. Chem. Soc.* **2014**, *136*, 5571-5574.
27. Ding, H.; DeRoy, P. L.; Perreault, C.; Larivée, A.; Siddiqui, A.; Caldwell, C. G.; Harran, S.; Harran, P. G. *Angew. Chem., Int. Ed.* **2015**, *54*, 4818-4822.
28. Gütz, C.; Selt, M.; Bänziger, M.; Bucher, C.; Römelt, C.; Hecken, N.; Gallou, F.; Galvão, T. R.; Waldvogel, S. R. *Chem.-Eur. J.*, **2015**, *21*, 13878-13882.
29. Lipp, A.; Ferenc, D.; Gütz, C.; Geffe, M.; Vierengel, N.; Schollmeyer, D.; Schäfer, H. J.; Waldvogel, S. R.; Opatz, T. *Angew. Chem., Int. Ed*., **2018**, *57*, 11055-11059.
30. Okamoto, K.; Chiba, K. *Org. Lett*., **2020**, *22*, 3613-3617.
31. Smith, B. P.; Truax, N. J.; Pollatos, A. S.; Meanwell, M.; Bedekar, P.; Garrido-Castro, A. F.; Baran, P. S. *Angew. Chem. Int. Ed*., **2024**, e202401107.
32. Mahajan, V. A.; Shinde, P. D.; Gajare, A. S.; Karthikeyan, M.; Wakharkar, R. D. *Green Chem*., **2002**, *4*, 325-327.
33. Hilt, G. *ChemElectroChem*, **2020**, *7*, 395-405.
34. Kingston, C.; Palkowitz, M. D.; Takahira, Y.; Vantourout, J. C.; Peters, B. K.; Kawamata, Y.; Baran, P. S. *Acc. Chem. Res.* **2020**, *53*, 72-83.
35. Elsherbini, M.; Wirth, T. *Acc. Chem. Res.,* **2019**, *52*, 3287-3296.
36. Shono, T.; Hamaguchi, H.; Matsumura, Y. *J. Am. Chem. Soc.,* **1975**, *15*, 4264-4268.
37. Francke, R.; Little. R. D. *Chem. Soc. Rev*., **2014**, *43*, 2492-2521.
38. Fuchigami, T.; Tetsu, M.; Tajima, T.; Ishii, H. *Synlett,* **2001**, *8*, 1269-1271.
39. Sherbo, R. S.; Kurimoto, A.; Brown, C. M.; Berlinguette, C. P. *J. Am. Chem. Soc.* **2019**, *141*, 7815-7821.
40. Matthessen, R.; Fransaer, J.; Binnemans, K.; De Vos, D. E. *ChemElectroChem*, **2015**, *2*, 73-76.
41. Mo, Y.; Lu, Z.; Rughoobur, G.; Patil, P.; Gershenfeld, N.; Akinwande, A. I.; Buchwald, S. L.; Jensen, K. F. *Science*, **2020**, *368*, 1352-1357.
42. Hartmer, M. F.; Waldvogel, S. R. *Chem. Commun.*, **2015**, *51*, 16346-16348.
43. Strehl, J.; Abraham, M. L.; Hilt, G. *Angew. Chemie Int. Ed.,* **2021**, *60*, 9996-10000.

44. Jones, A. M.; Banks, C. E. *Beilstein J. Org. Chem.,* **2014**, *10*, 3056-3072.
45. Onomura, O. *Heterocycles* **2012**, *85*, 2111-2113.
46. Shono, T.; Matsumura, Y.; Tsubata, K.; *J. Am. Chem. Soc*., **1981**, *103*, 1172-1176.
47. Libendi, S. S.; Demizu, Y.; Matsumura, Y.; Onomura, O. *Tetrahedron* **2008**, *64*, 3935-3942.
48. Onomura, O.; Ishida, Y.; Maki, T.; Minato, D.; Demizu, Y.; Matsumura, Y. *Electrochemistry* **2006**, *74*, 645-648.
49. Gallardo, I.; Vila, N. *J. Org. Chem*. **2010**, *75*, 680-689.
50. Gallardo, I.; Vila, N. *J. Org. Chem.* **2008**, *73*, 6647-6656.
51. Okimoto, M.; Yoshida, T.; Hoshi, M.; Hattori, K.; Komata, M.; Numata, K.; Tomozawa, K. *Aust. J. Chem*. **2007**, *60*, 236-237.
52. Kirira, P. G.; Kuriyama, M.; Onomura, O. *Chem. - Eur. J*. **2010**, *16*, 3970-3982.
53. Mazurkiewicz, R.; Adamek, J.; Pazdzierniok-Holewa, A.; Zielińska, K.; Simka, W.; Gajos, A.; Szymura, K. *J. Org. Chem*. **2012**, *77*, 1952-1960.
54. Adamek, J.; Mazurkiewicz, R.; Pazdzierniok-Holewa, A.; Grymel,́ M.; Kuznik, A.; Zielinska, K. *J. Org. Chem*. **2014**, *79*, 2765-2770.
55. Adamek, J.; Mazurkiewicz, R.; Pazdzierniok-Holewa, A.; Kuźnik, A.; Grymel, M.; Zielińska, K.; Simka, W. *Tetrahedron* **2014**, *70*, 5725-5729.
56. Tajima, T.; Nakajima, A. *J. Am. Chem. Soc*. **2008**, *130*, 10496-10497.
57. Asami, R.; Fuchigami, T.; Atobe, M. *Chem. Commun*., **2008**, 244-246.
58. Tajima, T.; Kurihara, H.; Shimizu, S.; Tateno, H. *Electrochemistry* **2013**, *81*, 353-355.
59. Libendi, S. S.; Demizu, Y.; Onomura, O. *Org. Biomol. Chem*. **2009**, *7*, 351-356.
60. Fu, N.; Li, L.; Yang, Q.; Luo, S. *Org. Lett*. **2017**, *19*, 2122-2125.
61. Yoshida, J.-I.; Kataoka, K.; Horcajada, R.; Nagaki, A.; *Chem. Rev*. **2008**, 108, 2265-2299.
62. Sugawara, M.; Mori, K.; Yoshida, J.-I. *Eleerrochimica Acta*, **1997**, *42*, 1995-2003.
63. Sun, H.; Martin, C.; Kesselring, D.; Keller, R.; Moeller, K. D. *J. Am. Chem. Soc*. 2006, 128, 13761-13771.
64. Suga, S.; Watanabe, M.; Yoshida, J.-I. *J. Am. Chem. Soc*. **2002**, *124*, 14824-14825.
65. Suga, S.; Watanabe, M.; Song, C.-H.; Yoshida, J.-I. *Electrochemistry* **2006**, *74*, 672-679.
66. Yoshida, J.; Suga, S.; Suzuki, S.; Kinomura, N.; Yamamoto, A.; Fujiwara, K. *J. Am. Chem. Soc*. **1999**, *121*, 9546-9549.
67. Weinreb, S. M.; Scola, P. M. *Chem. Rev.* **1989**, *89*, 1525-1534.
68. Suga, S.; Nagaki, A.; Tsutsui, Y.; Yoshida, J. Org. Lett. 2003, 5, 945-947.
69. E. T. Denisov, I. B. Afanas'ev, Chemistry of Antioxidants in Oxidation and Antioxidants in Organic Chemistry and Biology, CRC Press, Taylor & Francis Group 6000 Broken Sound Parkway NW, 2005, pp. 488-500.
70. Yamamura, S.; Nishiyama, S. *Synlett* **2002**, *2002*, 533-543.
71. Quideau, S.; Pouysegu, L. *Curr. Org. Chem*. **2004**, *8*, 113-148.
72. Kirste, A.; Nieger, M.; Malkowsky, I. M.; Stecker, F.; Fischer, A.; Waldvogel, S. R. *Chem. - Eur. J*. **2009**, *15*, 2273-2277.
73. Kirste, A.; Schnakenburg, G.; Waldvogel, S. R. *Org. Lett.* **2011**, *13*, 3126-3129.

74. Elsler, B.; Schollmeyer, D.; Dyballa, K. M.; Franke, R.; Waldvogel, S. R. *Angew. Chem., Int. Ed*. **2014**, *53*, 5210-5213.
75. Kirste, A.; Elsler, B.; Schnakenburg, G.; Waldvogel, S. R. *J. Am. Chem. Soc*. **2012**, *134*, 3571-3576.
76. Kawabata, Y.; Naito, Y.; Saitoh, T.; Kawa, K.; Fuchigami, T.; Nishiyama, S. *Eur. J. Org. Chem.* **2014**, 99-104.
77. Tanabe, T.; Doi, F.; Ogamino, T.; Nishiyama, S. *Tetrahedron Lett*. **2004**, *45*, 3477-3480.
78. Uno, K.; Tanabe, T.; Nishiyama, S. *ECS Trans*. **2009**, 91-95.
79. Sumi, T.; Saitoh, T.; Natsui, K.; Yamamoto, T.; Atobe, M.; Einaga, Y.; Nishiyama, S. *Angew. Chem., Int. Ed*. **2012**, *51*, 5443-5446.
80. Mori, K.; Yamamura, S.; Nishiyama, S. *Tetrahedron* **2001**, *57*, 5533-5542.
81. Deffieux, D.; Fabre, I.; Titz, A.; Leger, J.-M.; Quideau, S. *J. Org. Chem*. **2004**, *69*, 8731-8738.
82. Ogamino, T.; Nishiyama, S. *Tetrahedron* **2003**, *59*, 9419-9423.
83. Doi, F.; Ogamino, T.; Sugai, T.; Nishiyama, S. *Synlett*, **2003**, 411-413.
84. Kim, S.; Hirose, K.; Uematsu, J.; Mikami, Y.; Chiba, K. *Chem. - Eur. J*. **2012**, *18*, 6284-6288.
85. Kim, S.; Noda, S.; Hayashi, K.; Chiba, K. *Org. Lett*. **2008**, *10*, 1827-1829.
86. Taily, I. M.; Saha, D.; Banerjee, P. *Org. Lett*. **2022**, *24*, 2310-2314.
87. Bary, G.; Jamil, M. I.; Arslan, M.; Ghani, L.; Ahmed, W.; Ahmad, H.; Zaman, G.; Ayub, K.; Sajid, M.; Ahmad, R.; Huang, D.; Liu, F.; Wang, Y. *Journal of Saudi Chemical Society*, **2021**, *25*, 101260.
88. Horner, J. H.; Newcomb, M. *J. Org. Chem*., **2007**, *72*, 1609-1616.
89. Romero, N. A.; Nicewicz, D. A. *J. Am. Chem. Soc*., **2014**, *136*, 17024-17035.
90. Moeller, K. D.; *Tetrahedron*, **2000**, *56*, 9527-9554.
91. Reddy, S. H. K.; Chiba, K.; Sun, Y. M.; Moeller, K. D. *Tetrahedron*, **2001**, *57*, 5183-5197.
92. Liu, B.; Duan, S.; Sutterer, A. C.; Moeller, K. D. *J. Am. Chem. Soc*., **2002**, *124*, 10101-10111.
93. Luo, M. J.; Xiao, Q.; Li, J. H. *Chem. Soc. Rev*., **2022**, *51*, 7206-7237.
94. Ashikari, Y.; Nokami, T.; Yoshida, J.-I. *Org. Lett*., **2012**, *14*, 938-941.
95. Zhang, S.; Li, L.; Wu, P.; Gong, P.; Liu, R.; Xu, K. *Adv. Synth. Catal*., **2019**, *361*, 485-489.
96. Chung, S.; Park, S. H.; Lee; S.-G.; Kim, H. *Chem. Sci*., **2021**, *12*, 5892-5897.
97. Chiba, K.; Miura, T.; Kim, S.; Kitano Y.; Tada, M.; *J. Am. Chem. Soc*., **2001**, *123*, 11314-11315.
98. Miura, T.; Kim, S.; Kitano, Y.; Tada, M.; Chiba, K.; *Angew. Chem., Int. Ed*., **2006**, *45*, 1461-1463.
99. Okada, Y.; Yamaguchi, Y.; Ozaki A.; Chiba, K. *Chem. Sci*., **2016**, *7*, 6387-6393.
100. Ozaki, A.; Yamaguchi, Y.; Okada, Y.; Chiba, K. *Chin. J. Chem*., **2019**, *37*, 561-564.

Chapter 2

Electrochemical Generation of Nonstabilized Azomethine Ylide: Access to Substituted N-Heterocycles

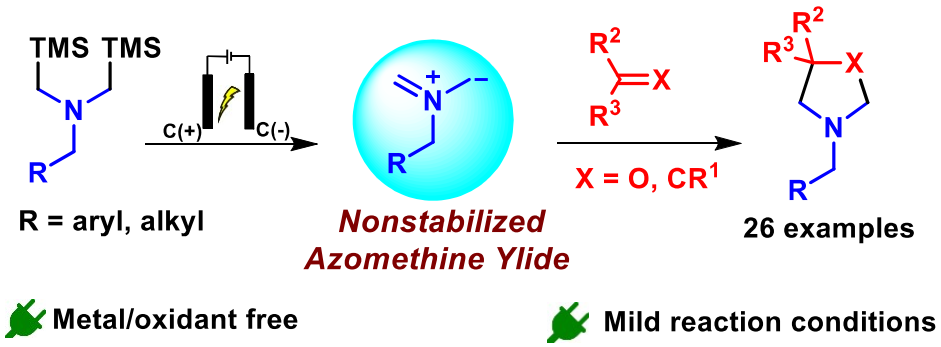

This work was published in *Journal of Organic Chemistry* (A journal of *American Chemical Society*). Please see citation "Kumar, R.; Banerjee, P. *J. Org. Chem*, **2021**, *86*, 16104-16113."

2.1. Introduction

Azomethine ylides are the nitrogen containing 1,3-dipoles having an iminium ion adjacent to carbanion, and they undergo 1,3-dipolar cycloaddition reaction with various dipolarophiles to afford cyclic *N*-heterocycles such as pyrrolidines, pyrrolines, and pyrroles.[1-3] Based on the electron-withdrawing or electron-donating groups at the termini of the ylide, they can be classified as stabilized or nonstabilized ylide.[4] Mostly, the azomethine ylides are generated *in-situ* and immediately reacted with dipolarophiles; however, stabilized ylides have been isolated in some cases.[5] Generation of the nonstabilized azomethine ylides and their 1,3-dipolar cycloaddition reactions with various dipolarophiles is a reliable and efficient protocol for the synthesis of pyrrolidine derivatives. Consequently, various traditional methods for the generation of nonstabilized azomethine ylide have been reported towards the construction of a pyrrolidine ring system.[6a] A few of the important methodologies include the fluoride ion initiated desilylation of cyanoamino silanes[6b] or trimethyl silyliminium salts[6c] and thermal ring opening of aziridines[6d]. However, most of these protocols rely on either metal-based activation or require high temperature. To address these issues, Rueping *et al*. and Itoh *et al*., in the last decade have disclosed the photocatalytic cycloaddition reactions highlighting the generation of stabilized azomethine ylides in the presence of ruthenium complexes[7], eosin Y (EY) or methylene blue[8] as photocatalyst. However, at the end of the 20th century, Pandey *et al*. reported a novel methodology for the generation of nonstabilized azomethine ylide from *N*-benzyl-1-(trimethylsilyl)-*N*-((trimethylsilyl)methyl)methanamine (Scheme 2.1.1).[9]

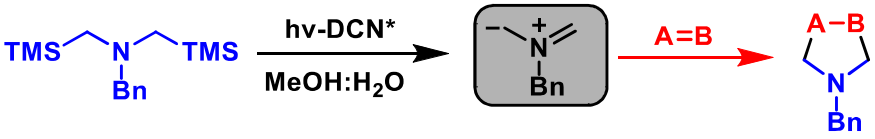

Scheme 2.1.1. Generation of nonstabilized azomethine ylide by PET initiation.

In continuation with this endeavor, other groups, have also devised protocols for the generation of the nonstabilized azomethine ylide by employing visible-light[10], metal fluoride[11], and trifluoroacetic acid (Scheme 2.1.2).[12] However, all these conventional methods for the generation of nonstabilized azomethine ylides and their cycloaddition necessitate external oxidants or photocatalyst towards the generation of 1,3-dipoles. Therefore, we believe that the development of a synthetic method without external oxidant and photocatalyst for the generation of nonstabilized azomethine ylide and its 1,3-dipolar cycloaddition reaction is quite appealing.

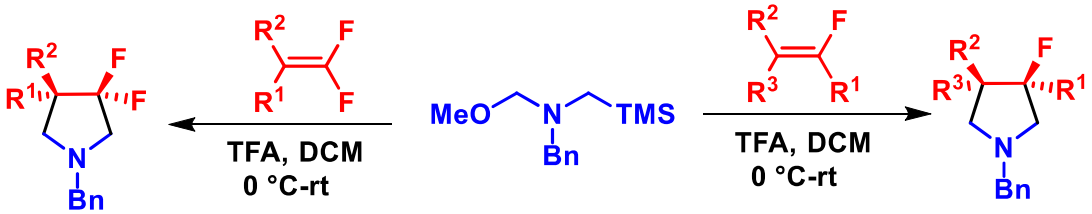

Scheme 2.1.2. Generation of non-stabilized azomethine ylide by TFA.

The history of electrochemical synthesis began in 20th century, where Shono *and* Yoshida works extensively in electroorganic oxidation of unfunctionalized amides *via* *N*-acyliminium ion.[13] Later, 21st century brings renaissance in the field of electrochemical synthesis due to its prime advantages of superior environment and economic acceptance over the traditional chemical and photochemical processes.[14-16] Electrochemical synthesis has been widely used in C-H bond functionalization[17], C-C[18,] and C-N[19] bond formation and diverse electrochemical rearrangement protocols[20]. Very recently, Li's group reported electrochemical generation of

stabilized azomethine ylide followed by cycloaddition towards the synthesis of polycyclic *N*-heterocycles[21]. Followed by this work, Masson *et al*. documented an electrochemical tandem radical trifluoromethylation of allylamines *via* 1,3-dipolar cycloaddition towards the construction of CF_3 containing imidazolines and oxazolidines[22]. However, the electrochemical generation of nonstabilized azomethine ylide remains unexplored. Herein, we report the development of an oxidant-free protocol for the electrochemical *in-situ* generation of nonstabilized azomethine ylide followed by 1,3-dipolar cycloaddition reaction. The notable aspect of this methodology is the use of electrons as the reagents. We envisioned that the anodic oxidation of *N*-benzyl-1-(trimethylsilyl)-*N*-((trimethylsilyl)methyl)methanamine **1a** would generate nonstabilized azomethine ylide *via a* double desilylation process. The azomethine ylide could then undergo (3+2) cycloaddition with dipolarophile **2a** and deliver the pyrrolidine derivatives (Scheme 2.1.3).

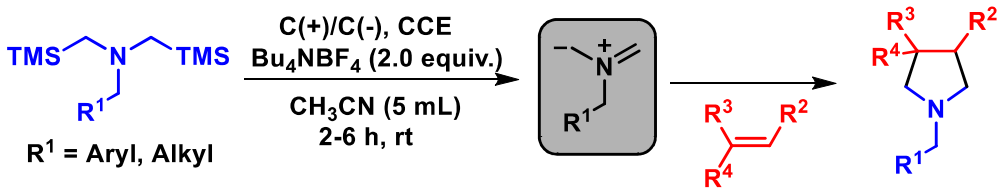

Scheme 2.1.3. Our idea of generating nonstabilized azomethine ylide under electrochemical conditions.

2.2. Results and Discussion

To test our hypothesis, **1a** and ethyl acrylate **2a** were chosen as the model substrates, Et_4NPF_6 (2.0 equiv.) as a supporting electrolyte in an undivided cell equipped with graphite electrodes. The mixture was electrolyzed in CH_3CN at a constant current of 3 mA at room temperature. Under these conditions, the expected pyrrolidine derivative **3aa** was obtained in 27% yield. Further, different supporting electrolytes were initially screened to optimize the reaction conditions (Table 2.2.1). Among these Bu_4NBF_4 served as a better electrolyte with a yield of 55% (Table 2.2.1, entry 1), and the use of other electrolytes such as Et_4NPF_6, Bu_4NPF_6, Bu_4NI, and Bu_4NBr resulted in lower yields (Table 2.2.1, entries 2-5). In contrast, the electrolytes $LiClO_4$ and Bu_4NOAc gave a complex mixture (Table 2.2.1, entry 6). Evaluation of the solvents disclosed that CH_3CN was ideal, while MeOH, DME, and DMF resulted in lower yields (Table 2.2.1, entries 7-9). Furthermore, replacement of CH_3CN with DCM and HFIP proved fatal (Table 2.2.1, entry 10). Amongst a different set of electrodes, graphite showed the best efficiency, while the replacement of graphite anode with platinum anode resulted in diminished yield (Table 2.2.1, entry 11). Furthermore, the usage of nickel as a cathode shows a falloff in yield (Table 2.2.1, entry 12). The role of electricity could be ascertained by the control experiment (Table 2.2.1, entry 13).

With the optimized reaction condition in hand, the scope of this electrochemical (3+2) cycloaddition reaction was examined. Initially, the azomethine ylide precursors bearing different substituents on the aryl ring were tested. The substrate bearing methyl group **1b** at *para*-position of aryl ring afforded **3ba** in 52% yield. Azomethine ylide precursors bearing halogen groups at *para*-position reacted with ethyl acrylate **2a**, to furnish the desired product **3ca** and **3da** in 47% and 48% yield, respectively. Furthermore, the substitution of a methoxy group at the *meta*-position of ylide precursor could render the pyrrolidine product **3ea** with a maximum yield of 63%. As the protocol emphasizes the *N*-benzyl azomethine ylides, we also explored the *N*-alkyl azomethine ylides. Delightfully, azomethine ylide precursors substituted with *N*-cyclohexylmethanamine **1f** undergoes cycloaddition with **2a** and *N*-phenylethanamine **1g** with **2b** and delivered the pyrrolidine product **3fa** and **3gb** in 40% and 47%, respectively. Next, the azomethine ylide precursor bearing methoxy group at *para*-position is tested with ethyl

cinnamate **2b** and delivered **3hb** in 61% yield. Also, the ylide precursor having pipernoyl group is reacted easily with **2b** to give the desired cycloadduct **3ib** in 63% yield (Scheme 2.2.1).

Table 2.2.1. Optimization of the reaction conditions.

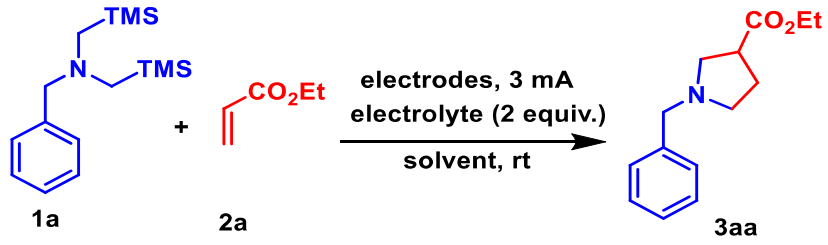

Entry	Variation from standard conditions[a]	Yield[b]
1	none	55
2	Et_4NPF_6 instead of Bu_4NBF_4	27
3	Bu_4NPF_6 instead of Bu_4NBF_4	32
4	Bu_4NI instead of Bu_4NBF_4	42
5	Bu_4NBr instead of Bu_4NBF_4	25
6	$LiClO_4$ and Bu_4NOAc instead of Bu_4NBF_4	c.m.
7	MeOH instead of CH_3CN	48
8	DME instead of CH_3CN	24
9	DMF instead of CH_3CN	18
10	DCM and HFIP instead of CH_3CN	n.r.
11	Pt anode instead of carbon	38
12	Ni cathode instead of carbon	45
13	Without electricity	n.r.

[a]Reaction conditions: **1a** (0.17 mmol), **2a** (0.17 mmol), Bu_4NBF_4 as the electrolyte (0.34 mmol), CH_3CN as the solvent (5 mL), 3 mA constant current, graphite electrodes, undivided cell, 25 °C. [b]Isolated yield, n.r. = no reaction. c.m. = complex mixture.

The substrate scope was further extended to dipolarophile component ethyl cinnamates, which all worked well with **1a** and afforded the desired cycloadducts in moderate to good yield. It was found that the cinnamates bearing electron-withdrawing groups **2c-2f** on the aryl ring conferred good yield as compared to those bearing electron-donating groups on the aryl ring **2g-2i**. Further replacement of aryl group with 2-napthyl **2j** and 2-furfural **2k** moiety afforded the desired product **3aj** and **3ak** in 47% and 42% yield, respectively.

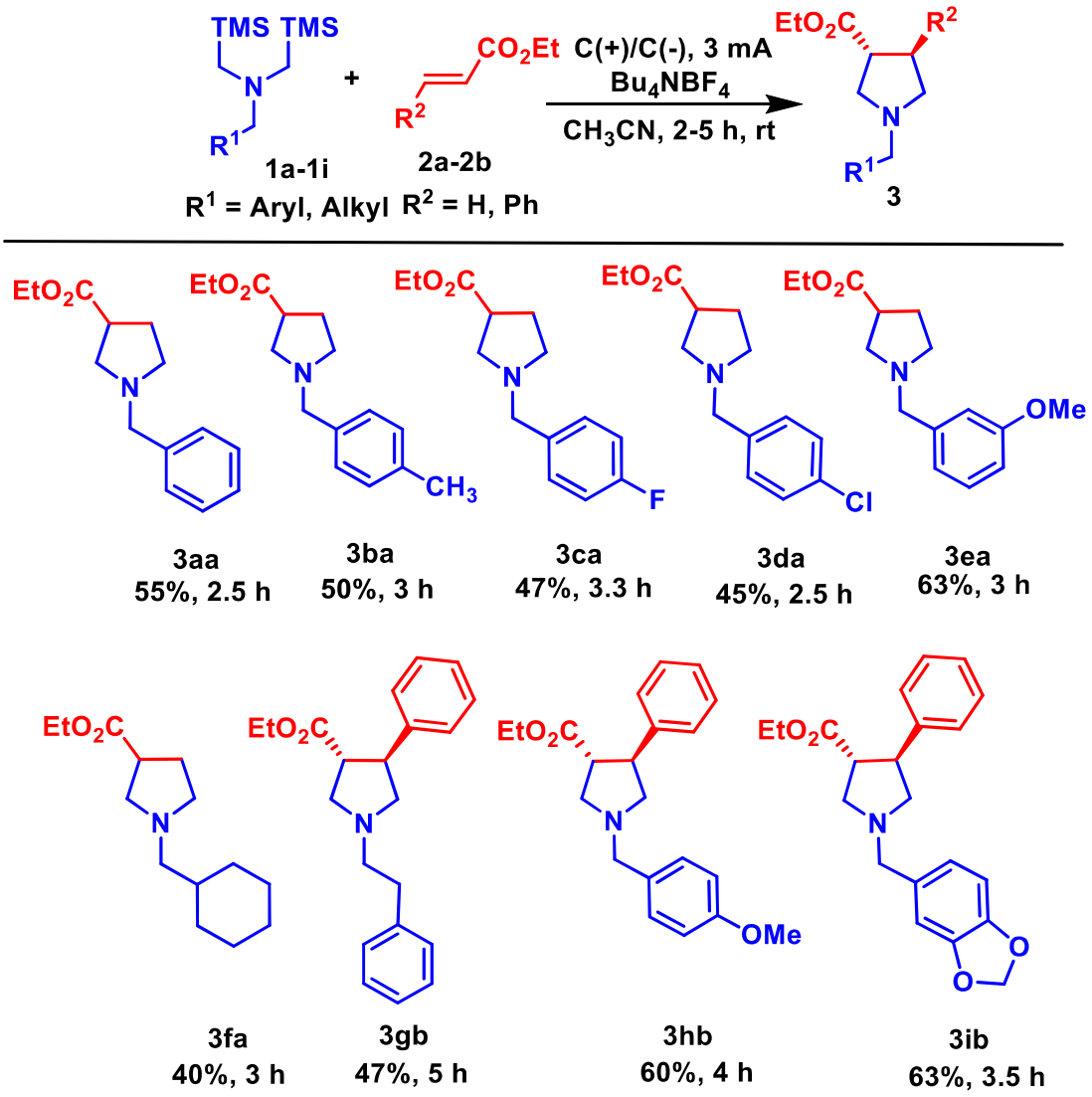

Scheme 2.2.1. Substrate scope w.r.t. azomethine ylides.

Apart from the ethyl cinnamates, the methodology has also been tested for methyl cinnamates, where it has been found that the **2l** with **1a** gave the desired product **3al** in 58% yield. Furthermore, diethyl 2-(4-fluorobenzylidene)malonate **2m** was also used as a dipolarophile which reacts smoothly with the dipole to furnish the cycloadduct **3am** in 48% yield. Benzyl methacrylate **2n** has also been tested as a dipolarophile which bestowed the desired product **3an** in 60% yield. The other dipolarophile β-nitrostyrene **2o** and dimethyl maleate **2p** were also compatible with the standard conditions and affords the corresponding products **3ao** and **3ap** in moderate yield. The methodology also works well with benzaldehyde **2q** and its derivative **2r** and provides an access to oxazolidine **3aq** and **3ar** with moderate yield (Scheme 2.2.2).

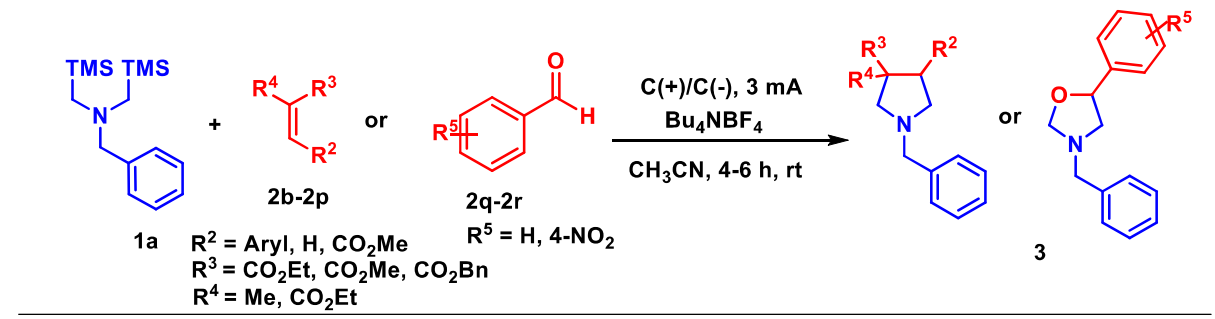

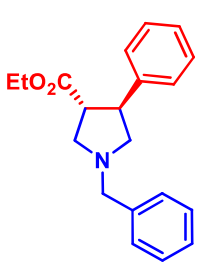
3ab
51%, 4 h

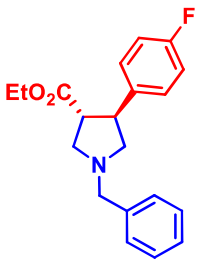
3ac
55%, 5 h

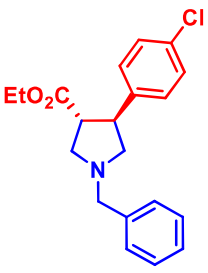
3ad
52%, 6 h

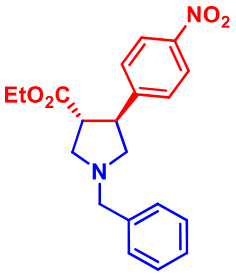
3ae
63%, 6 h

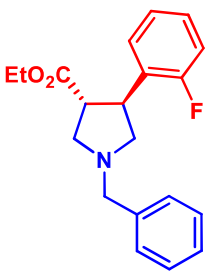
3af
62%, 5 h

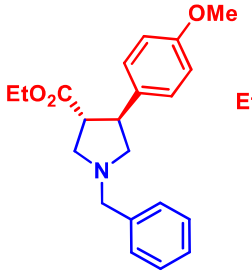
3ag
50%, 4 h

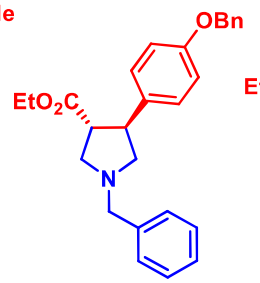
3ah
48%, 4.5 h

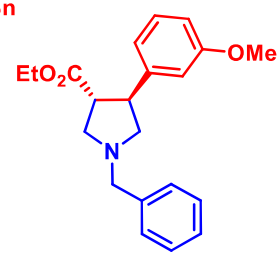
3ai
58%, 5.5 h

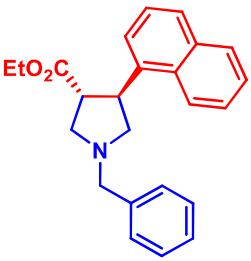
3aj
47%, 5 h

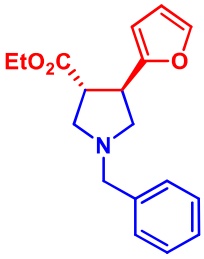
3ak
42%, 6 h

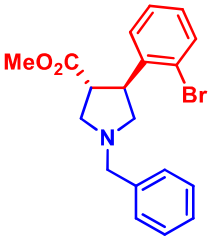
3al
55%, 5 h

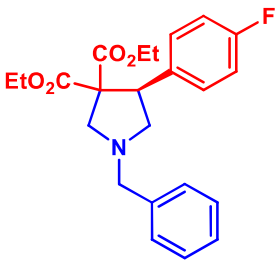
3am
48%, 4 h

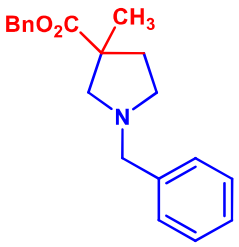
3an
60%, 4 h

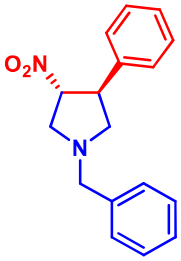
3ao
55%, 4 h

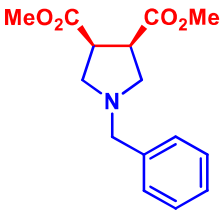
3ap
48%, 5 h

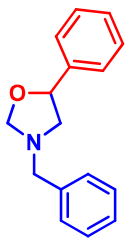
3aq
62%, 6 h

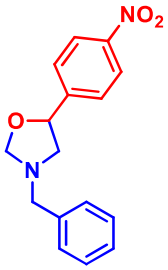
3ar
65%, 6 h

Scheme 2.2.2. Substrate scope of alkenes and aldehyde.

Next, to prove the mechanism, the redox behavior of reagents was studied by cyclic voltammetry experiments which revealed that the oxidation potential of **1a** is 0.75 V (Vs Ag/AgCl)[23] and no oxidation peak was observed for **2a** (Figure 2.2.1).

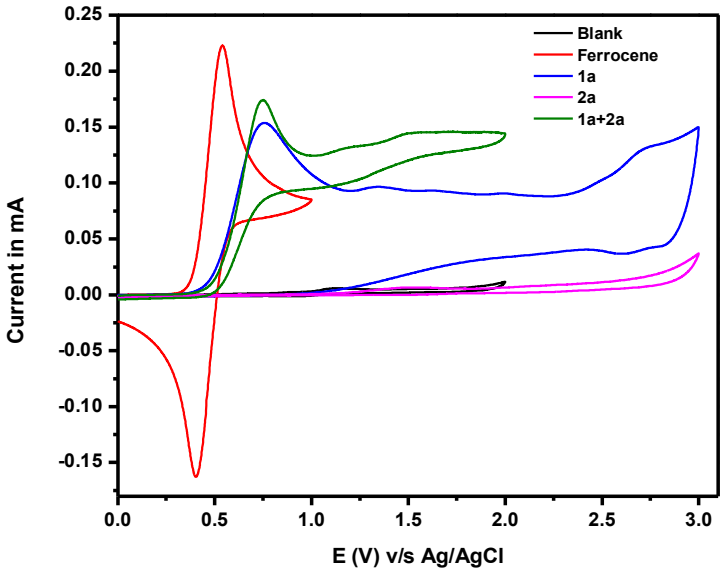

Figure 2.2.1. Cyclic voltammetry experiment.

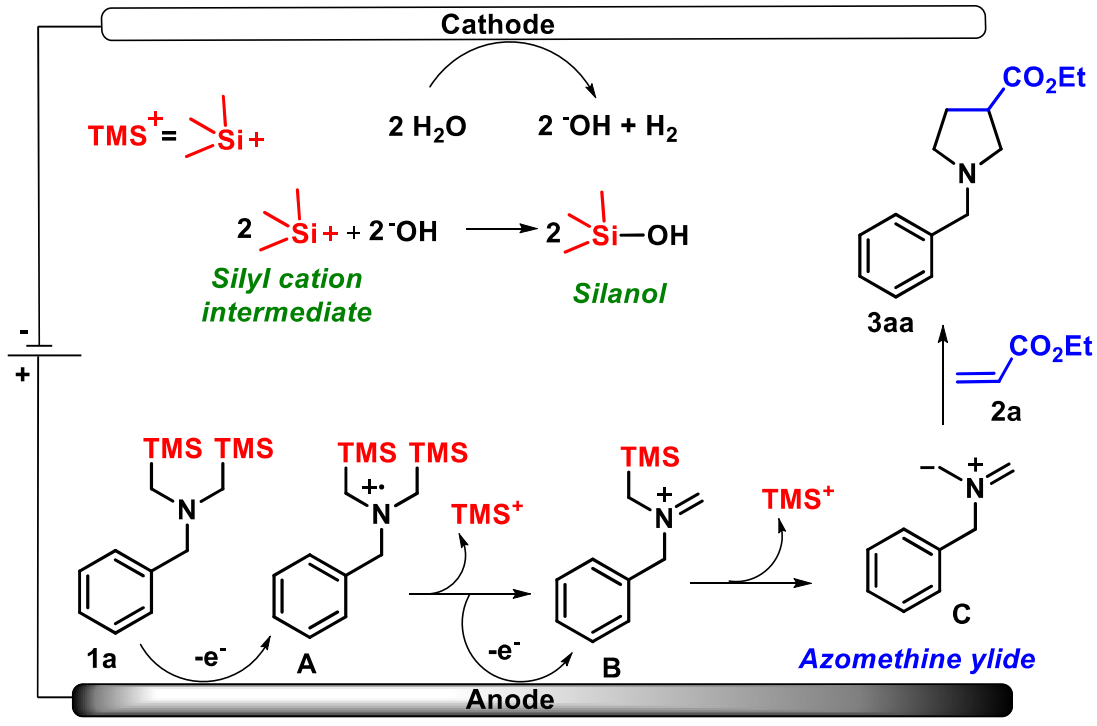

Scheme 2.2.3. Plausible mechanism.

Based on the cyclic voltammetry studies and literature precedents[9,10,18a, 24] a plausible mechanism for the electrochemical (3+2) cycloaddition reaction was proposed using **1a** and **2a** as a model substrate. Initially, **1a** undergoes anodic oxidation *via* single electron transfer (SET) to form radical cation species **A.** This radical cation

species undergoes desilylation followed by another single electron oxidation to form iminium cation **B**. Further desilylation of this iminium cation led to the formation of azomethine ylide **C,** which subsequently undergoes the expected (3+2) cycloaddition with **2a** to deliver the desired product **3aa.** Furthermore**,** trimethyl silyl cation generated could get quenched by the hydroxide ion obtained from the cathodic reduction of H_2O to give trimethyl silanol as the byproduct[24] (Scheme 2.2.3). Furthermore, to demonstrate the synthetic utility of the methodology, the electrochemical synthesis could be scaled up in grams; prolonging the reaction time to 38 h could render the desired cycloadduct in 70% yield (Scheme 2.2.4).

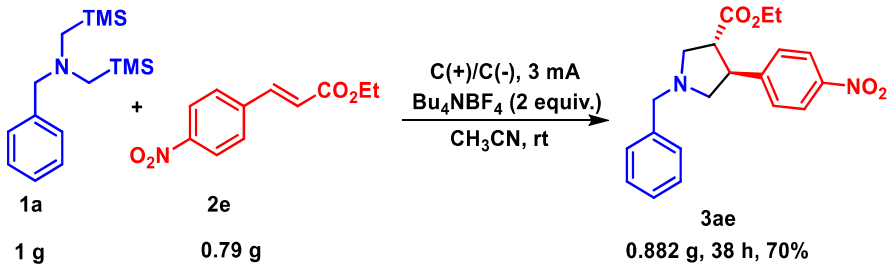

Scheme 2.2.4. Gram scale synthesis of **3ae**.

2.3. Conclusion

In summary, an electrochemical pathway for the *in-situ* generation of nonstabilized azomethine ylide under metal and external oxidant-free conditions have been demonstrated. The protocol led to the formation of 3- and 3,4-disubstituted five-membered *N*-heterocycles in a straightforward manner. The synthetic strategy implies the anodic oxidation followed by double desilylation to generate 1,3-dipole, which is then trapped with various alkenes as dipolarophiles to furnish the cycloadduct. The broad substrate scope, good functional group tolerance, and mild electrolytic conditions make the protocol fascinating and would encourage further exploration in the field of electrochemical generation of nonstabilized azomethine ylide.

2.4. Experimental Section

2.4.1. General Information

Unless noted otherwise, all reagents and solvents were purchased from commercial sources and used as received. All reactions were performed in oven dried round bottom flasks. Electrochemical reactions were performed at room temperature using ElectraSyn 2.0 and DC power supply of Keysight technologies. Electrodes were commercially available from IKA. Cyclic voltammetry analysis was carried out in CH instrument electrochemical analyzer (CHL1110C). Column chromatography was performed on silica gel mesh size 200-300. The proton (^{1}H) and carbon (^{13}C) NMR spectra were recorded using $CDCl_3$ in a 400 MHz spectrometer and are reported in δ units. Coupling constants (*J* Values) are reported in Hz. High-resolution mass spectra (HRMS) were obtained using the electron spray ionization (ESI) technique and TOF mass analyzer. IR spectra are reported in cm^{-1} units. Yields refer to isolated compounds, estimated to be less than 95% pure as determined by ^{1}HNMR. The description of the signals includes the following: s = singlet, d = doublet, dd = doublet of doublet, t = triplet, dt = doublet of triplet, q = quartet, br = broad and m = multiplet.

2.4.2. General procedure for the synthesis of azomethine ylide precursors[11a] (1a-1i)

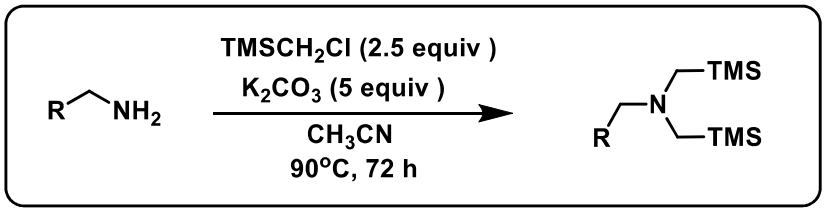

In an oven-dried two neck round bottom flask equipped with a magnetic bar, amines **1a-1i** (1 equiv.), chloromethyltrimethylsilane (2.5 equiv.) and powdered K_2CO_3 (5 equiv.) were taken. The reagents were purged twice with nitrogen. Under nitrogen atmosphere, anhydrous acetonitrile was added. The reaction mixture was refluxed at 90 °C for 72 h. Then, the reaction mixture was passed through a small Celite bed, and the bed was washed with ethyl acetate. The filtrate was concentrated under vacuum and purified by silica gel column chromatography with 100% hexane or 1% (ethyl acetate:hexane) as eluent.

2.4.2.1 Characterization data of starting material

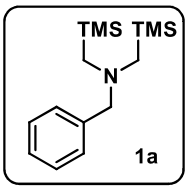

***N*-benzyl-1-(trimethylsilyl)-N-((trimethylsilyl)methyl)methanamine (1a)**

The title compound was purified by column chromatography (Hexane/ethyl acetate = 99:1), R_f = 0.8). Colorless liquid (410 mg, 81%). **^{1}H-NMR** (400 MHz): δ 7.32-7.14 (m, 5H), 3.35 (s, 2H), 1.84 (s, 4H), 0.002 (s, 18H).

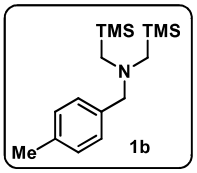

***N*-(4-methylbenzyl)-1-(trimethylsilyl)-N-((trimethylsilyl)methyl)methanamine (1b)**

The title compound was purified by column chromatography (Hexane/ethyl acetate = 99:1), R_f = 0.7). Colorless liquid (180 mg, 74%).**^{1}H-NMR** (400 MHz, $CDCl_3$): δ 7.20 (d, J = 7.9Hz, 2H), 7.10 (d, J = 7.8Hz, 2H), 3.35 (s, 2H), 2.32 (s, 3H), 1.87 (s, 4H), 0.0023(s, 18H).

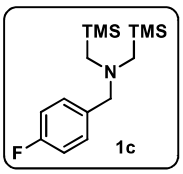

***N*-(4-fluorobenzyl)-1-(trimethylsilyl)-N-((trimethylsilyl)methyl)methanamine (1c)**

The title compound was purified by column chromatography (Hexane/ethyl acetate = 95:5), R_f = 0.5). Colorless liquid (193 mg, 84%).**^{1}H-NMR** (400 MHz, $CDCl_3$): δ 7.29-7.24 (m, 2H), 6.97 (t, J = 8.5Hz, 2H), 3.34 (s, 2H), 1.86 (s, 4H), 0.021(s, 18H).

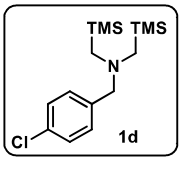

***N*-(4-chlorobenzyl)-1-(trimethylsilyl)-*N*-((trimethylsilyl)methyl)methanamine (1d)**

The title compound was purified by column chromatography (Hexane/ethyl acetate = 95:5), R_f = 0.5). Colorless liquid (172 mg, 78%).**^{1}H-NMR** (400 MHz, $CDCl_3$): δ 7.81 (d, J = 7.9Hz, 2H), 7.50 (d, J = 8.3Hz, 2H), 3.46 (s, 2H), 1.95 (s, 4H), 0.04(s, 18H)

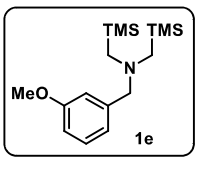

***N*-(3-methoxybenzyl)-1-(trimethylsilyl)-*N*-((trimethylsilyl)methyl)methanamine (1e).**The title compound was purified by column chromatography (Hexane/ethyl acetate = 9:1), R_f =0.5). Colorless liquid (154 mg, 68%).**^{1}H-NMR** (400 MHz, $CDCl_3$): δ 7.19-7.11

(m, 1H), 6.88 (s, 1H), 6.87 (d, J =7.3Hz, 1H), 6.76-6.68 (m, 1H), 3.75 (s, 3H), 3.34 (s, 2H), 1.86 (s, 4H), 0.03 (s, 18H).

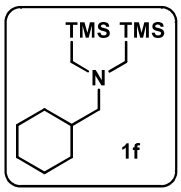

1-cyclohexyl-*N*,*N*-bis((trimethylsilyl)methyl)methanamine (1f)

The title compound was purified by column chromatography (Hexane/ethyl acetate = 9:1), R_f = 0.4). Colorless liquid (131 mg, 52%).**^{1}H-NMR** (400 MHz, $CDCl_3$): δ 2.82-2.30 (m, 3H), 2.04-1.43 (m, 8H), 1.27-0.62 (m, 6H), 0.009 (s, 18H).

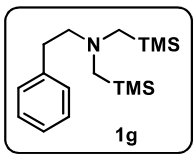

2-phenyl-*N*,*N*-bis((trimethylsilyl)methyl)ethanamine (1g)

The title compound was purified by column chromatography (Hexane/ethyl acetate = 95:5), R_f = 0.4). Colorless liquid (129 mg, 53%).**^{1}H-NMR** (400 MHz, $CDCl_3$): δ 7.28-7.23 (m, 2H), 7.20-7.14 (m, 3H), 2.74-2.67 (m, 2H), 2.61-2.54 (m, 2H), 1.98 (s, 4H), 0.03(s, 18H).

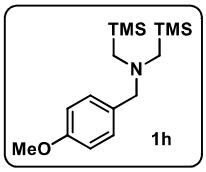

***N*-(4-methoxybenzyl)-1-(trimethylsilyl)-*N*-((trimethylsilyl)methyl)methanamine (1h)**

The title compound was purified by column chromatography (Hexane/ethyl acetate = 9:1), (R_f = 0.6). Colorless liquid (162 mg, 72%). **^{1}H-NMR** (400 MHz, $CDCl_3$): δ 7.22 (d, J = 8.3Hz, 2H), 6.84 (d, J = 8.3Hz, 2H), 3.80 (s, 3H), 3.32 (s, 2H), 1.86 (s, 4H), 0.02(s, 18H).

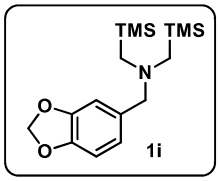

1-(benzo[d][1,3]dioxol-5-yl)-*N*,*N*-bis((trimethylsilyl)methyl)methanamine (1i)

The title compound was purified by column chromatography (Hexane/ethyl acetate = 95:5), (R_f = 0.5). Colorless liquid (139 mg, 65%).**^{1}H-NMR** (400 MHz, $CDCl_3$): δ 6.84 (s, 1H), 6.72 (s, 2H), 5.93 (s, 2H), 3.29 (s, 2H), 1.86 (s, 4H), 0.02(s, 18H).

2.4.3. General Procedure for the Synthesis of ethyl/methyl cinnamates[25a] (2b-2l)

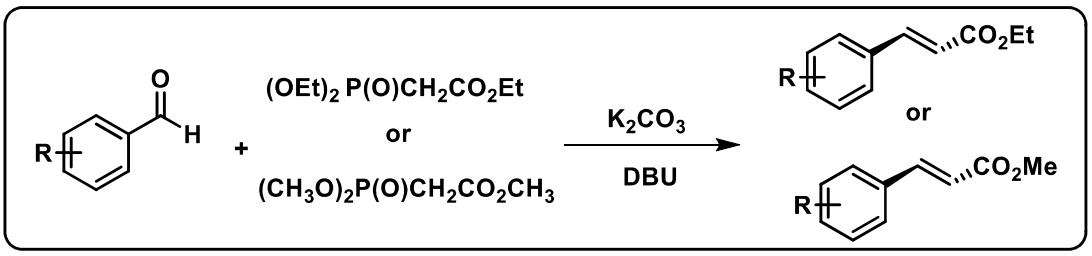

Triethyl phosphonoacetate (1.1 equiv.), DBU (0.035 equiv.), and finely powdered K_2CO_3 (2 equiv.) was taken in an oven dried round bottom flask and ArCHO (1 equiv.) was added. The resulting mixture was stirred using a magnetic stirrer for 4 h at room temperature under argon atmosphere. Ethyl acetate was added to the crude mixture and the solid was filtered off. The solid was washed with ethyl acetate and the combined filtrate was

concentrated. The resulting oil was distilled under reduced pressure using a bulb-to-bulb apparatus (10 mm Hg/240 °C) to give corresponding alkene (yield 84%) (E:Z= 99:1).

2.4.3.1 Characterization data of starting material

(E)-ethyl cinnamate (2b)

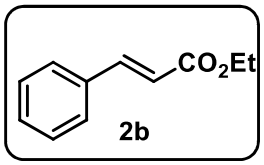

The title compound was purified by column chromatography (Hexane/ethyl acetate = 9:1); R_f = 0.5; Colorless liquid (745 mg, 90%); **^{1}H-NMR** (400 MHz, $CDCl_3$): δ 7.68 (d, *J* = 16.3Hz, 1H), 7.55-7.47 (m, 2H), 7.40-7.32 (m, 3H) 6.43 (d, J = 16.3Hz, 1H), 4.26 (q, *J* = 7.03Hz, 2H), 1.33 (t, *J* = 7.01Hz, 3H).

(E)-ethyl 3-(4-fluorophenyl)acrylate (2c)

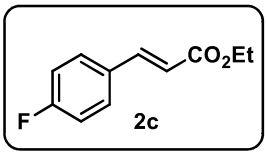

The title compound was purified by column chromatography (Hexane/ethyl acetate = 9:1), (R_f = 0.4). Colorless liquid (688 mg, 85%). **^{1}H-NMR** (400 MHz, $CDCl_3$): δ 7.65 (d, *J* = 16.2Hz, 1H), 7.53-7.47 (m, 2H), 7.10-7.03 (m, 2H), 6.35 (d, J = 16.2Hz, 1H), 4.25 (q, *J* = 7.2Hz 2H), 1.33 (t, *J* = 6.8Hz, 3H).

(E)-ethyl 3-(4-chlorophenyl)acrylate (2d)

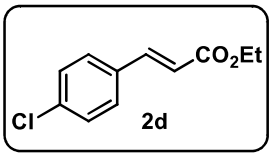

The title compound was purified by column chromatography (Hexane/ethyl acetate = 9:1); R_f = 0.4; Colorless liquid (594 mg, 82%); **^{1}H-NMR** (400 MHz, $CDCl_3$): δ 7.62 (d, *J* = 16.09Hz, 1H), 7.46-7.42 (m, 2H), 7.37- 7.32 (m, 2H), 6.40 (d, J = 16.0Hz, 1H), 4.25 (q, *J* = 7.2Hz, 2H), 1.33 (t, *J* = 6.9Hz, 3H).

(E)-ethyl 3-(4-nitrophenyl)acrylate (2e)

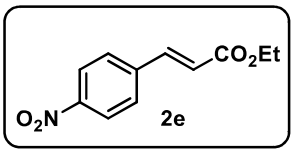

The title compound was purified by column chromatography (Hexane/ethyl acetate = 9:1), R_f = 0.4; yellow solid (586 mg, 80%); **^{1}H-NMR** (400 MHz, $CDCl_3$): δ 8.24 (d, *J* = 8.9Hz, 2H), 7.73-7.63 (m, 3H), 6.56 (d, J = 16.04Hz, 1H), 4.29 (q, *J* = 7.2Hz, 2H), 1.35 (t, *J* = 7.3Hz, 3H).

(E)-ethyl 3-(2-fluorophenyl)acrylate (2f)

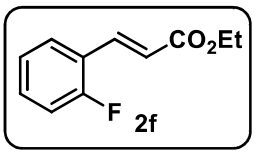

The title compound was purified by column chromatography (Hexane/ethyl acetate = 9:1); R_f = 0.6; Light yellow liquid (708 mg, 91%); **^{1}H-NMR** (400 MHz, $CDCl_3$): δ 7.73 (d, J = 16.4Hz, 1H), 7.48-7.39 (m, 1H), 7.30-7.21 (m, 1H), 7.10-6.97 (m, 2H), 6.45 (d, *J* = 16.1Hz, 1H), 4.19 (q, *J* = 6.9Hz, 2H), 1.25 (t, *J* = 7.3Hz, 3H).

(E)-ethyl 3-(4-methoxyphenyl)acrylate (2g)

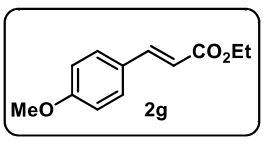

The title compound was purified by column chromatography (Hexane/ethyl acetate = 9:1); R_f = 0.3; White solid (699 mg, 92%); **^{1}H-NMR** (400 MHz, $CDCl_3$): δ 7.64 (d, *J* = 15.8Hz, 1H), 7.47(d, 8.7Hz, 2H), 6.90 (d, J = 8.7Hz, 2H), 6.31 (d, J

= 15.9Hz, 1H), 4.24 (q, *J* = 7.09Hz, 2H), 3.8 (s, 1H), 1.33 (t, *J* = 6.8Hz, 3H).

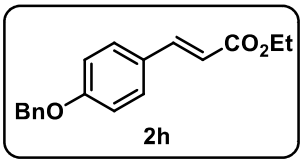

(E)-ethyl 3-(4-(benzyloxy)phenyl)acrylate (2h)

The title compound was purified by column chromatography (Hexane/ethyl acetate = 4:1); R_f = 0.5; White solid (513 mg, 78%); **^{1}H-NMR** (400 MHz, $CDCl_3$): δ 7.65 (d, *J* = 15.8Hz, 1H), 7.46 (d, *J* = 8.9Hz, 2H), 7.45-7.31 (m, 5H), 6.96 (d, *J* = 8.7Hz, 2H), 6.30 (d, J = 15.9Hz, 1H), 5.08 (s, 2H), 4.24 (q, *J* = 7.3Hz, 2H), 1.32 (t, *J* = 7.1Hz, 3H).

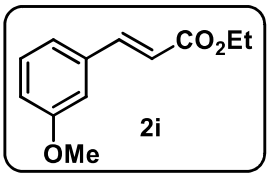

(E)-ethyl 3-(3-methoxyphenyl)acrylate (2i)

The title compound was purified by column chromatography (Hexane/ethyl acetate = 4:1); R_f = 0.6; Light yellow liquid (697 mg, 91%); **^{1}H-NMR** (400 MHz, $CDCl_3$): δ 7.61 (d, J = 16.08Hz, 1H), 7.24 (q, *J* = 8.1Hz, 1H), 7.08 (d, J = 7.6Hz, 1H), 7.02-6.97 (m, 1H), 6.91-6.85 (m, 1H), 6.38 (d, *J* = 15.7Hz, 1H), 4.22 (q, *J* = 7.3Hz, 2H), 3.78 (s, 3H), 1.30 (t, *J* = 7.2Hz, 3H).

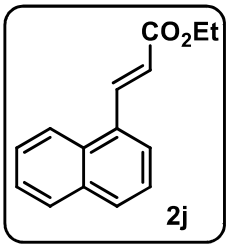

(E)-ethyl 3-(naphthalen-1-yl)acrylate (2j)

The title compound was purified by column chromatography (Hexane/ethyl acetate = 9:1); R_f = 0.5; Light yellow liquid (567 mg, 78%); **^{1}H-NMR** (400 MHz, $CDCl_3$): δ 8.52 (d, *J* = 15.7Hz, 1H), 8.18 (d, *J* = 8.59Hz, 1H), 7.87 (t, *J* = 2H), 7.73 (d, J = 7.36Hz, 1H) 7.59-7.42 (m, 3H), 6.52 (d, *J* = 15.8Hz, 1H), 4.30 (q, *J* = 6.9Hz, 2H), 1.37 (t, *J* = 6.9Hz, 3H).

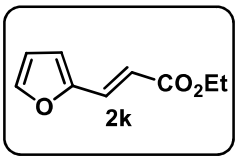

(E)-ethyl 3-(furan-2-yl)acrylate (2k)

The title compound was purified by column chromatography (Hexane/ethyl acetate = 9:1); R_f = 0.5; Orange liquid (784 mg, 90%); **^{1}H-NMR** (400 MHz, $CDCl_3$): δ 7.50-7.38 (m, 2H), 6.60 (s, 1H), 6.48-6.43 (m, 1H), 6.31 (d, *J* = 15.1Hz, 1H), 4.24 (q, *J* = 7.07Hz, 2H), 1.31 (t, *J* = 6.8Hz, 3H).

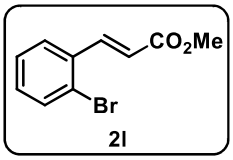

(E)-methyl 3-(2-bromophenyl)acrylate (2l)

The title compound was purified by column chromatography (Hexane/ethyl acetate = 9:1), R_f = 0.7; Light yellow liquid (515 mg, 79%). **^{1}H-NMR** (400 MHz, $CDCl_3$): δ 8.06 (d, J = 16.06Hz, 1H), 7.65-7.56 (m, 2H), 7.36-7.27 (m, 1H), 7.26-7.17 (m, 1H), 6.40 (d, *J* = 16.01Hz, 1H), 3.8 (s, 3H).

2.4.4. General procedure for the synthesis of diethyl 2-(4-fluorobenzylidene)malonate[25b] (2m)

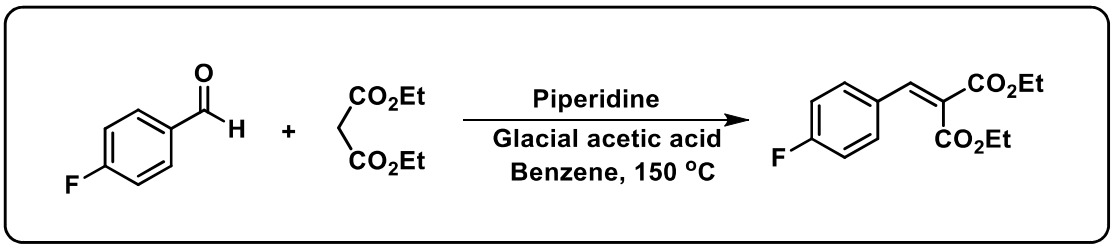

To a solution of diethylmalonate (1.0 equiv.) and piperidine (0.1 equiv.) in benzene (30 mL) was added aldehyde (1.0 equiv.) and glacial acetic acid (0.1 equiv.). The solution was refluxed under Dean-Stark conditions until water collection ceased. The reaction mixture was then sequentially washed with water, 5% aqueous HCl, saturated aqueous NaHCO3, and finally with brine. The organic layer was dried over anhydrous magnesium sulfate. The solvent was evaporated in vacuo and the crude sample on purification by flash silica gel column chromatography (Ethyl acetate-Hexane mixture) afforded the product in 78% yield.

2.4.4.1 Characterization data

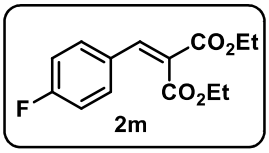

diethyl 2-(4-fluorobenzylidene)malonate (2m)

The title compound was purified by column chromatography (Hexane/ethyl acetate = 9:1); R_f = 0.4; Light brown liquid (830 mg, 78%). **^{1}H-NMR** (400 MHz, $CDCl_3$): δ 7.69 (s, 1H), 7.48-7.43 (m, 2H), 7.10-7.04 (m, 2H), 4.38-4.28 (m, 4H), 1.35-1.24 (m, 6H).

2.4.5. General procedure for the Synthesis of trans-β-nitrostyrene (2o)[25c]

A 50 mL round bottom flask was charged with aldehyde (5 mmol), nitro methane (6 mmol) and 25 mL methanol. The flask was kept at 0 °C on a mechanical stirrer. The aqueous solution of NaOH (5.5 mmol) was slow addded and then the reaction mixture was allowed to stir for 1h. After that the reaction mixture was poured into 6 M HCl (aq, 30 mL) and product was precipitated out immediately. The precipiate was filtered, washed with cold methanol and directly used for the next step.

2.4.5.1 Characterization data

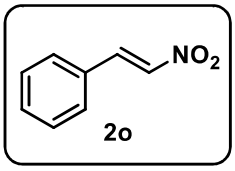

(E)-(2-nitrovinyl)benzene (2o)

The title compound was purified by column chromatography (Hexane/ethyl acetate = 9:1), R_f = 0.7); Yellow solid (477 mg, 78%); **^{1}H-NMR** (400 MHz, $CDCl_3$): δ 7.99 (d, *J* = 13.6 Hz, 1H), 7.61-7.38 (m, 6H).

2.4.6. General procedure for electrochemical reaction

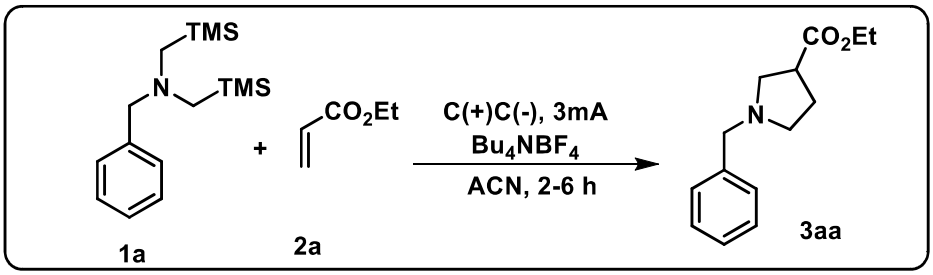

In an undivided cell equipped with magnetic bar and graphite as both anode and cathode, mixture of **1a-1i** (1.0 equiv.), **2a-2r** (1.0 equiv.), Bu_4NBF_4 (2.0 equiv.) and CH_3CN (5 mL) were added. The mixture was electrolyzed at a constant current of 3 mA at room temperature for 2-6 h in an electraSyn 2.0 and DC power supply. Upon completion, the solvent was removed under reduced pressure and the crude was purified by silica gel column chromatography (200-400mesh) to afford the desired product.

2.4.6.1 Characterization data of final compounds

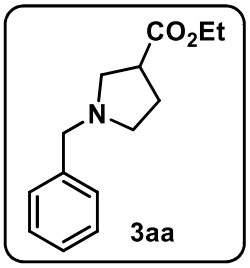

ethyl 1-benzylpyrrolidine-3-carboxylate (3aa)[25d]

The title compound was purified by column chromatography (Hexane/ethyl acetate = 1:4), R_f = 0.5; Colorless liquid (21 mg, 55%). **^{1}H-NMR** (400 MHz, $CDCl_3$): δ 7.34-7.27 (m, 5H), 4.13 (q, *J* = 7.2Hz, 2H), 3.64 (s, 2H), 3.08-2.98 (m, 1H), 2.94 (t, *J* = 8.9Hz, 1H), 2.78-2.69 (m, 1H), 2.66-2.59 (m, 1H), 2.52(q, *J* = 8.0Hz, 1H), 2.14-2.06 (m, 2H), 1.24 (t, *J* = 7.4Hz, 3H); **^{13}C{^{1}H} NMR** (100 MHz, $CDCl_3$): δ 175.2, 138.8, 128.8, 128.3, 127.1, 60.7, 60.1, 56.7, 53.8, 42.1, 27.7, 14.3; **IR (neat)**: 2923, 1730, 1452, 1371, 1175, 1028 cm^{-1}; **HRMS (ESI, Q-TOF)** *m/z*: [M + H] $^+$ Calculated for $C_{14}H_{20}NO_2$ 234.1494, found 234.1478

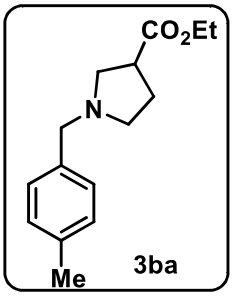

ethyl 1-(4-methylbenzyl)pyrrolidine-3-carboxylate (3ba)

The title compound was purified by column chromatography (Hexane/ethyl acetate = 9:1), R_f = 0.4; Light brown liquid (21 mg, 50%). **^{1}H-NMR** (400 MHz, $CDCl_3$): δ 7.22 (d, *J* = 7.8Hz, 2H), 7.13 (d, *J* = 7.9Hz, 2H), 4.13 (q, *J* = 7.09Hz, 2H), 3.61 (s, 2H), 3.07-2.99 (m, 1H), 2.95 (t, *J* = 9.06Hz, 1H), 2.78-2.73 (m, 1H), 2.64-2.59 (m, 1H), 2.50 (q, *J* = 8.01Hz, 1H), 2.33 (s, 3H), 2.12-2.07 (m, 2H), 1.25 (t, *J* = 7.3Hz, 3H); **^{13}C{^{1}H} NMR** (100 MHz, $CDCl_3$): δ 175.1, 136.6, 135.7, 129.0, 128.8, 60.6, 59.8, 56.7, 53.7, 42.1, 27.6, 21.2, 14.3; **IR (neat):** 2922, 1730, 1513, 1448, 1371, 1173, 1034 cm^{-1}; **HRMS (ESI, Q-TOF)** *m/z*: [M + H] $^+$ Calculated for $C_{15}H_{22}NO_2$ 248.1651, found 248.1665

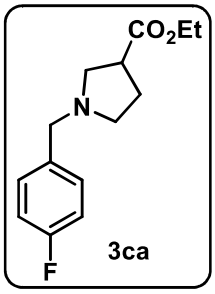

ethyl 1-(4-fluorobenzyl)pyrrolidine-3-carboxylate (3ca)

The title compound was purified by column chromatography (Hexane/ethyl acetate = 4:1), R_f = 0.7; Light brown liquid (18 mg, 47%). **^{1}H-NMR** (400 MHz, $CDCl_3$): δ 7.31-7.24 (m, 2H), 6.99 (t, *J* = 8.7Hz, 2H), 4.14 (q, *J* = 7.3Hz, 2H), 3.58 (d, *J* = 3.2Hz, 2H), 3.05-2.96 (m, 1H), 2.87 (t, *J* = 8.9Hz, 1H), 2.71-2.65 (m, 1H), 2.62-2.57 (m, 1H), 2.49 (q, *J* = 7.6Hz, 1H), 2.13-2.05 (m, 2H), 1.25 (q, *J* = 7.07Hz, 3H); **^{13}C{^{1}H} NMR** (100 MHz, $CDCl_3$): δ 175.0, 130.2, 130.1, 115.1, 114.9, 60.6, 59.2, 56.5, 53.6, 42.0, 27.6, 14.2; **IR (neat):** 2923, 1730, 1603, 1509, 1450, 1372, 1221 cm^{-1}; **HRMS (ESI, Q-TOF)** *m/z*: [M + H] $^+$ Calculated for $C_{14}H_{19}FNO_2$ 252.1400, found 252.1397

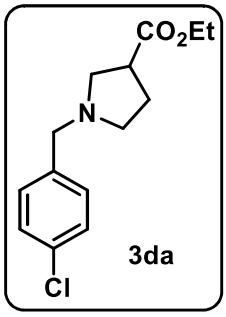

ethyl 1-(4-chlorobenzyl)pyrrolidine-3-carboxylate (3da)

The title compound was purified by column chromatography (Hexane/ethyl acetate = 9:1), R_f = 0.4; Light brown liquid (20 mg, 45%). **^{1}H-NMR** (400 MHz, $CDCl_3$): δ 7.23-7.15 (m, 4H), 4.06 (q, *J* = 7.2Hz, 2H), 3.52 (d, *J* = 3.7Hz, 2H), 3.00-2.90 (m, 1H), 2.81 (t, *J* = 8.3Hz, 1H), 2.65-2.51 (m, 2H), 2.44 (q, *J* = 8.1Hz, 1H), 2.06-1.98 (m, 2H), 1.17 (q, *J* = 7.3Hz, 3H); **^{13}C{^{1}H} NMR** (100 MHz, $CDCl_3$): δ 174.9, 137.3, 132.6, 130.0, 128.3, 60.6, 59.2, 56.5, 53.6, 42.0, 27.6, 14.1; **IR (neat):** 2925, 1729, 1490, 1186, 1087, 1014 cm^{-1}; **HRMS (ESI, Q-TOF)** *m/z*: [M + H] $^+$ Calculated for $C_{14}H_{19}ClNO_2$ 268.1104, found 268.1102

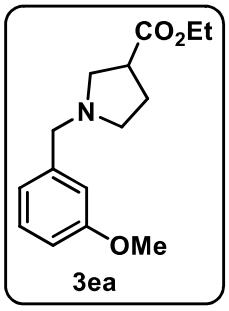

ethyl 1-(3-methoxybenzyl)pyrrolidine-3-carboxylate (3ea)

The title compound was purified by column chromatography (Hexane/ethyl acetate = 7:3), R_f = 0.5; Colorless liquid (26 mg, 63%). **^{1}H-NMR** (400 MHz, $CDCl_3$): δ 7.19-7.13 (m, 1H), 6.84-6.83 (m, 2H), 6.74-6.71 (m, 1H), 4.06 (q, *J* = 7.3Hz, 2H), 3.73 (s, 3H), 3.56 (s, 2H), 3.01-2.85 (m, 2H), 2.74-2.67 (m, 1H), 2.59-2.53 (m, 1H), 2.46 (q, *J* = 8.3Hz, 1H), 2.04 (q, *J* =7.7Hz, 2H), 1.17 (t, *J* = 7.13Hz, 3H); **^{13}C{^{1}H} NMR** (100 MHz, $CDCl_3$): δ 175.0, 159.7, 140.0, 129.3, 121.2, 114.3, 112.8, 60.7, 59.9, 56.5, 55.2, 53.7, 42.1, 27.6, 14.3; **IR (neat):** 2919, 1730, 1599, 1454, 1372, 1262, 1164, 1040 cm^{-1}; **HRMS (ESI, Q-TOF)** *m/z*: [M + H] $^+$ Calculated for $C_{15}H_{22}NO_3$ 264.1600, found 264.1597

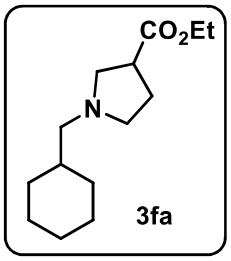

ethyl 1-(cyclohexylmethyl)pyrrolidine-3-carboxylate (3fa)

The title compound was purified by column chromatography (Hexane/ethyl acetate = 9:1), R_f = 0.4; Colorless liquid (16 mg, 40%). **^{1}H-NMR** (400 MHz, $CDCl_3$): δ 4.13 (q, *J* = 7.3Hz, 2H), 3.06-2.96 (m, 1H), 2.88 (t, *J* = 8.7Hz, 1H), 2.72-2.64 (m, 1H), 2.56-2.49 (m, 1H), 2.41 (q, *J* = 7.8Hz, 1H), 2.31-2.18 (m, 2H), 2.10-2.02 (m, 2H), 1.84-1.60 (m, 6H), 1.48-1.38 (m, 1H), 1.28-1.10 (m, 7H); **^{13}C{^{1}H}** NMR (100 MHz, $CDCl_3$): δ 175.1, 60.7, 56.9, 54.3, 42.1, 36.9, 31.9, 32.8, 29.7, 27.5, 26.7, 26.1, 14.3; **IR (neat):** 2922, 1731, 1451, 1176 cm^{-1}; **HRMS (ESI, Q-TOF)** *m/z*: [M + H] $^+$ Calculated for $C_{14}H_{26}NO_2$ 240.1964, found 240.1961

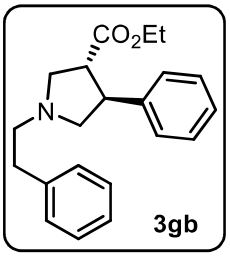

(3S,4R)-ethyl 1-phenethyl-4-phenylpyrrolidine-3-carboxylate and (3R,4S)-ethyl 1-phenethyl-4-phenylpyrrolidine-3-carboxylate (3gb)

The title compound was purified by column chromatography (Hexane/ethyl acetate = 9:1), R_f = 0.5; Colorless liquid (53 mg, 47%). **^{1}H-NMR** (400 MHz, $CDCl_3$): δ 7.34-7.18 (m, 10H), 4.19-4.07 (m, 2H), 3.67 (q, *J* = 7.2Hz, 1H), 3.12-2.96 (m, 4H), 2.88-2.76 (m, 4H), 2.74-2.64 (m, 1H), 1.22 (t, *J* = 7.2Hz, 3H); **^{13}C{^{1}H} NMR** (100 MHz, $CDCl_3$): δ 174.1, 143.8, 140.2, 128.6, 128.5, 128.3, 127.4, 126.5, 126.0, 61.9, 60.7, 57.7, 57.6, 51.5, 46.9, 35.3, 14.1; **IR (neat):** 2926, 1729, 1453, 1176, 1030 cm^{-1}; **HRMS (ESI, Q-TOF)** *m/z*: [M + Na]$^+$ Calculated for $C_{21}H_{25}NO_2$ 347.1817, found 347.1813

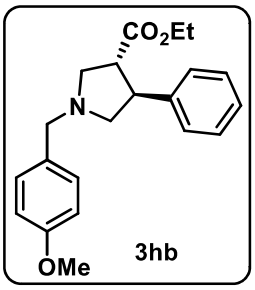

(3S,4R)-ethyl 1-(4-methoxybenzyl)-4-phenylpyrrolidine-3-carboxylate and (3R,4S)-ethyl 1-(4-methoxybenzyl)-4-phenylpyrrolidine-3-carboxylate (3hb)

The title compound was purified by column chromatography (Hexane/ethyl acetate = 9:1), R_f = 0.45; Colorless liquid (33 mg, 60%). **^{1}H-NMR** (400 MHz, $CDCl_3$): δ 7.34-7.26 (m, 6H), 7.23-7.16 (m, 1H), 6.85 (d, *J* = 8.7Hz, 2H), 4.16-4.06 (m, 2H), 3.79 (s, 3H), 3.69-3.55 (m, 3H), 3.10-2.96 (m, 3H), 2.88-2.83 (m, 1H), 2.76-2.70 (m, 1H), 1.20 (t, *J* = 7.05Hz, 3H); **^{13}C{^{1}H} NMR** (100 MHz, $CDCl_3$): δ 174.2, 158.5, 144.2, 129.7, 128.4, 127.4, 126.4, 113.5, 61.6, 60.6, 59.2, 57.2, 55.2, 51.7, 46.8, 14.1; **IR (neat)**: 2922, 1729, 1610, 1511, 1454, 1244, 1174, 1032 cm^{-1}; **HRMS (ESI, Q-TOF)** *m/z*: [M + H]$^+$ Calculated for $C_{21}H_{26}NO_3$ 340.1913, found 340.1900

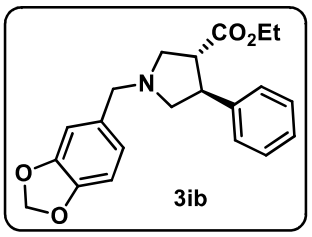

(3S,4R)-ethyl 1-(benzo[d][1,3]dioxol-5-ylmethyl)-4-phenylpyrrolidine-3-carboxylate and (3R,4S)-ethyl 1-(benzo[d][1,3]dioxol-5-ylmethyl)-4-phenylpyrrolidine-3-carboxylate (3ib)

The title compound was purified by column chromatography (Hexane/ethyl acetate = 4:1), R_f = 0.5; Colorless liquid (33 mg, 63%). **^{1}H-NMR** (400 MHz, $CDCl_3$): δ 7.33-7.27 (m, 4H), 7.22-7.17 (m, 1H), 6.90 (s, 1H), 6.79-6.71 (m, 2H), 5.94 (s, 1H), 4.16-4.06 (m, 2H), 3.69-3.60 (m, 1H), 3.58 (d, *J* = 3.3 Hz, 2H), 3.09-2.95 (m, 3H), 2.87-2.80 (m, 1H), 2.76-2.72 (m, 1H), 1.21 (t, *J* = 7.07Hz, 3H); **^{13}C{^{1}H} NMR** (100 MHz, $CDCl_3$): δ 174.2, 147.7, 146.6, 144.3, 132.8, 128.6, 127.5, 126.5, 121.7, 109.2, 107.9, 100.9, 61.7, 60.8, 59.7, 57.3, 51.8, 46.9, 14.2; **IR (neat)**: 2920, 1728, 1489, 1443, 1373, 1241, 1035 cm^{-1}; **HRMS (ESI, Q-TOF)** *m/z*: [M + H]$^+$ Calculated for $C_{21}H_{24}NO_4$ 354.1705 found 354.1707

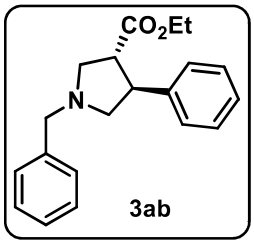

(3S,4R)-ethyl 1-benzyl-4-phenylpyrrolidine-3-carboxylate and (3R,4S)-ethyl 1-benzyl-4-phenylpyrrolidine-3-carboxylate (3ab)[25e]

The title compound was purified by column chromatography (Hexane/ethyl acetate = 4:1), R_f = 0.5; Colorless liquid (26 mg, 51%). **^{1}H-NMR** (400 MHz, $CDCl_3$): δ 7.39-7.17 (m, 10 H), 4.16-4.06 (m, 2H), 3.74-3.62 (m, 3H), 3.11-2.97 (m, 3H), 2.92-2.82 (m, 1H), 2.79-2.72 (m, 1H), 1.20 (t, *J* = 7.3 Hz, 3H); **^{13}C{^{1}H} NMR** (100 MHz, $CDCl_3$): δ 174.2, 140.5, 138.9, 133.9, 131.6, 128.9, 128.7, 128.4, 127.1, 126.0, 125.7, 125.5, 124.4, 123.9, 61.5, 60.8, 60.0, 57.9, 51.4, 42.5, 14.2; **IR (neat)**: 3735, 3446,

2364, 2024, 1730, 1174 cm^{-1}; **HRMS (ESI, Q-TOF)** *m/z*: [M + H] $^+$ Calculated for $C_{20}H_{24}NO_2$ 310.1807, found 310.1799

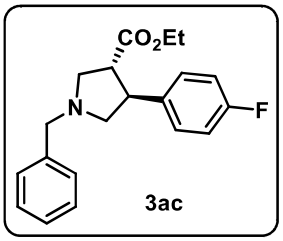

(3S,4R)-ethyl 1-benzyl-4-(4-fluorophenyl)pyrrolidine-3-carboxylate and (3R,4S)-ethyl 1-benzyl-4-(4-fluorophenyl)pyrrolidine-3-carboxylate (3ac)

The title compound was purified by column chromatography (Hexane/ethyl acetate = 9:1), R_f = 0.45; Colorless liquid (30 mg, 55%). ^{1}H-NMR (400 MHz, $CDCl_3$): δ 7.37-7.26 (m, 7H), 6.97 (t, *J* = 8.4Hz, 2H), 4.16-4.06 (m, 2H), 3.71-3.59 (m, 3H), 3.11-2.93 (m, 3H), 2.84-2.89 (m, 1H), 2.75-2.70 (m, 1H), 1.12 (t, *J* = 7.08 Hz, 3H); ^{13}C{^{1}H} NMR (100 MHz, $CDCl_3$): δ 173.9, 162.7, 160.3, 140.0, 138.7, 128.87, 128.8, 128.6, 128.2, 127.0, 115.3, 115.1, 61.7, 60.7, 59.8, 57.2, 52.0, 46.1, 14.1; **IR (neat)**: 2794, 1729, 1602, 1510, 1345, 1223, 1158, 1029 cm^{-1}; HRMS (ESI, Q-TOF) *m/z*: [M + H]$^+$ Calculated for $C_{20}H_{23}FNO_2$ 328.1713, found 328.1705

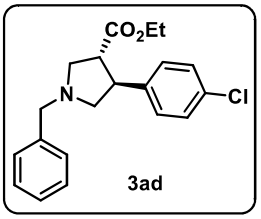

(3S,4R)-ethyl 1-benzyl-4-(4-chlorophenyl)pyrrolidine-3-carboxylate and (3R,4S)-ethyl 1-benzyl-4-(4-chlorophenyl)pyrrolidine-3-carboxylate (3ad)

The title compound was purified by column chromatography (Hexane/ethyl acetate = 9:1), R_f = 0.4; Colorless liquid (31 mg, 52%). **^{1}H-NMR** (400 MHz, $CDCl_3$): δ 7.29-7.15 (m, 9H), 4.08-4.00 (m, 2H), 3.59-3.51 (m, 3H), 3.04-2.85 (m, 3H), 2.78-2.72 (m, 1H), 2.67-2.63 (m, 1H), 1.13 (t, *J* = 7.29 Hz, 3H); **^{13}C{^{1}H} NMR** (100 MHz, $CDCl_3$): δ 174.0, 143.0, 138.7, 132.2, 128.9, 128.7, 128.4, 127.1, 61.6, 60.9, 59.9, 57.3, 52.0, 46.3, 42.8, 14.2; **IR (neat)**: 1729, 1264, 1171 cm^{-1}; **HRMS (ESI, Q-TOF)** *m/z*: [M + H] $^+$ Calculated for $C_{20}H_{23}ClNO_2$ 344.1417, found 344.1427

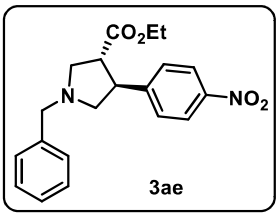

(3S,4R)-ethyl 1-benzyl-4-(4-nitrophenyl)pyrrolidine-3-carboxylate and (3R,4S)-ethyl 1-benzyl-4-(4-nitrophenyl)pyrrolidine-3-carboxylate (3ae)

The title compound was purified by column chromatography (Hexane/ethyl acetate = 4:1), R_f = 0.5; Orange liquid (37 mg, 63%). ^{1}H-NMR (400 MHz, $CDCl_3$): δ 8.15 (d, *J* = 9.06 Hz, 2H), 7.51 (d, *J* = 9.07 Hz, 2H), 7.38-7.23 (m, 5H), 4.18-4.09 (m, 2H), 3.78-3.63 (m, 3H), 3.20 (t, *J* = 8.6 Hz, 1H), 3.04 (q, *J* = 10.9 Hz, 1H), 2.93(t, *J* = 9.4 Hz, 1H), 2.86-2.74 (m, 2H), 1.22 (t, *J* = 7.3 Hz, 3H); ^{13}C{^{1}H} NMR (100 MHz, $CDCl_3$): δ 173.5, 152.6, 146.7, 138.5, 128.6, 128.4, 128.4, 127.3, 123.9, 61.1, 61.1, 59.7, 57.3, 52.0, 46.5, 14.2; IR (neat): 1728, 1599, 1517, 1343, 1179, 1028 cm^{-1}; HRMS (ESI, Q-TOF) *m/z*: [M + H] $^+$ Calculated for $C_{20}H_{23}N_2O_4$ 355.1658, found 355.1653

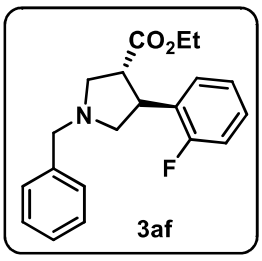

(3S,4R)-ethyl 1-benzyl-4-(2-fluorophenyl)pyrrolidine-3-carboxylate and (3R,4S)-ethyl 1-benzyl-4-(2-fluorophenyl)pyrrolidine-3-carboxylate (3af)

The title compound was purified by column chromatography (Hexane/ethyl acetate = 9:1), R_f = 0.4; Colorless liquid (34 mg, 62%). **^{1}H-NMR** (400 MHz, $CDCl_3$): δ 7.42-7.15 (m, 7H), 7.11-7.07 (m, 1H), 7.01-6.96 (m, 1H), 4.18-4.05 (m,

2H), 3.93 (q, *J* = 10.7 Hz, 1H), 3.72 (d, *J* = 13.1 Hz, 1H), 3.65 (d, *J* = 13.1 Hz, 1H), 3.14-2.99 (m, 3H), 2.94-2.90 (m,1H), 2.76-2.71 (m, 1H), 1.20 (t, *J* = 7.20 Hz, 3H); **$^{13}C\{^1H\}$ NMR** (100 MHz, $CDCl_3$): δ 174.1, 161.9, 159.5, 138.8, 130.6, 130.5, 129.1, 128.7, 128.3, 128.0, 127.1, 124.3, 115.5, 115.3, 60.8, 60.5, 59.9, 57.1, 50.4, 40.4, 14.2; **IR (neat)**: 1729, 1492, 1453, 1178, 1028 cm^{-1}; **HRMS (ESI, Q-TOF)** *m/z*: [M + H] $^+$ Calculated for $C_{20}H_{23}FNO_2$ 328.1713, found 328.1703.

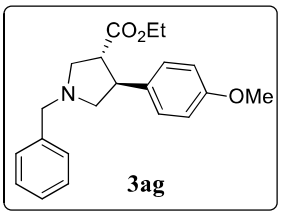

3ag

(3S,4R)-ethyl 1-benzyl-4-(4-methoxyphenyl)pyrrolidine-3-carboxylate and (3R,4S)-ethyl 1-benzyl-4-(4-methoxyphenyl)pyrrolidine-3-carboxylate (3ag)

The title compound was purified by column chromatography (Hexane/ethyl acetate = 9:1), R_f = 0.5; Colorless liquid (29 mg, 50%). **^{1}H-NMR** (400 MHz, $CDCl_3$): δ 7.38-7.21 (m, 7H), 6.83 (d, *J* = 8.8Hz, 2H), 4.16-4.04 (m, 2H), 3.78 (s, 1H), 3.72-3.57 (m, 3H), 3.07-2.95 (m, 3H), 2.91-2.82 (m,1H), 2.74-2.68 (m, 1H), 1.21 (t, *J* = 7.02 Hz, 3H); **$^{13}C\{^1H\}$ NMR** (100 MHz, $CDCl_3$): δ 174.3, 158.2, 138.9, 136.4, 128.7, 128.4, 128.3, 127.0, 113.9, 62.0, 60.7, 60.0, 57.4, 55.3, 52.0, 46.3, 14.3; **IR (neat)**: 2924, 1727, 1512, 1245, 1177, 1031 cm^{-1}; **HRMS (ESI, Q-TOF)** *m/z*: [M + H] $^+$ Calculated for $C_{21}H_{26}NO_3$ 340.1913, found 340.1937

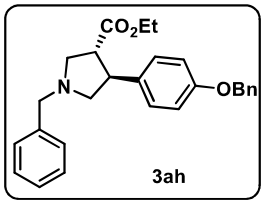

3ah

(3S,4R)-ethyl 1-benzyl-4-(4-(benzyloxy)phenyl)pyrrolidine-3-carboxylate and (3R,4S)-ethyl 1-benzyl-4-(4-(benzyloxy)phenyl)pyrrolidine-3-carboxylate (3ah)

The title compound was purified by column chromatography (Hexane/ethyl acetate = 4:1), R_f = 0.5; Colorless liquid (34 mg, 48%). **^{1}H-NMR** (400 MHz, $CDCl_3$): δ 7.38-7.20 (m, 9H), 7.19-7.11 (m, 3H), 6.82 (d, *J* = 8.7Hz, 2H), 4.95 (s, 2H), 4.08-3.97 (m, 2H), 3.63-3.49 (m, 3H), 2.97-2.88 (m, 3H), 2.81-2.75(m,1H), 2.65-2.61 (m, 1H), 1.12 (t, *J* = 7.2Hz, 3H); **$^{13}C\{^1H\}$ NMR** (100 MHz, $CDCl_3$): δ 174.3, 157.5, 138.9, 137.1, 136.6, 128.7, 128.6, 128.5 128.3, 128.0, 127.5, 114.8, 70.0, 61.9, 60.7, 60.0, 57.4, 52.0, 46.3, 14.3; **IR (neat)**: 2922, 1727, 1609, 1510, 1453, 1373, 1238, 1175 cm^{-1}; **HRMS (ESI, Q-TOF)** *m/z*: [M + H] $^+$ Calculated for $C_{27}H_{30}NO_3$ 416.2226, found 416.2224

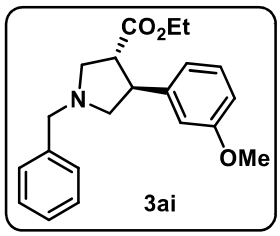

3ai

(3S,4R)-ethyl 1-benzyl-4-(3-methoxyphenyl)pyrrolidine-3-carboxylate and (3R,4S)-ethyl 1-benzyl-4-(3-methoxyphenyl)pyrrolidine-3-carboxylate (3ai)

The title compound was purified by column chromatography (Hexane/ethyl acetate = 4:1), R_f = 0.6; Colorless liquid (34 mg, 58%). ^{1}H-NMR (400 MHz, $CDCl_3$): δ 7.32-7.10 (m, 6H), 6.86-6.81 (m, 2H), 6.70-6.65(m, 1H), 4.10-4.00 (m, 2H), 3.71 (s, 3H), 3.66-3.53 (m, 3H), 3.04-2.95 (m, 2H), 2.92(t, *J* = 8.3Hz, 1H), 2.81-2.67(m, 2H), 1.14 (t, *J* = 7.1Hz, 3H); $^{13}C\{^1H\}$ NMR (100 MHz, $CDCl_3$): δ 174.1, 159.6, 146.0, 138.8, 129.4, 128.6, 128.2, 126.9, 119.7, 113.0, 111.7, 61.6, 60.7, 59.8, 57.4, 55.1, 51.7, 46.8, 14.1; IR (neat): 2922, 1729, 1601, 1453, 1258, 1159, 1029 cm^{-1}; HRMS (ESI, Q-TOF) *m/z*: [M + H] $^+$ Calculated for $C_{21}H_{26}NO_3$ 340.1913, found 340.1901

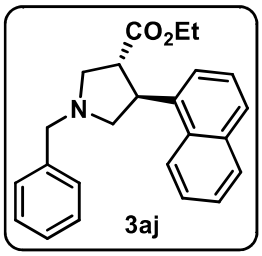

(3S,4R)-ethyl 1-benzyl-4-(naphthalen-1-yl)pyrrolidine-3-carboxylate and (3R,4S)-ethyl 1-benzyl-4-(naphthalen-1-yl)pyrrolidine-3-carboxylate (3aj)

The title compound was purified by column chromatography (Hexane/ethyl acetate = 9:1), R_f = 0.45; Light brown liquid (29 mg, 47%). **^{1}H-NMR** (400 MHz, $CDCl_3$): δ 8.34 (d, *J* = 8.2Hz, 1H), 7.83 (d, *J* = 8.1Hz, 1H), 7.73(d, *J* = 8.2Hz, 1H), 7.61(d, *J* = 7.3Hz, 1H), 7.52-7.39 (m, 5H), 7.34-7.31 (m, 2H), 7.26-7.23 (m, 1H), 4.51-4.45 (m, 1H), 4.08 (q, *J* = 7.2Hz, 2H), 3.77 (d, *J* = 12.8Hz, 1H), 3.70 (d, *J* = 13.0Hz, 1H), 3.33-3.25 (m, 2H), 3.09 (t, *J* = 9.2Hz, 1H), 3.04-2.98 (m, 1H), 2.86-2.79 (m, 1H), 1.14 (t, *J* = 7.2Hz, 3H); **^{13}C{^{1}H} NMR** (100 MHz, $CDCl_3$): δ 174.4, 140.5, 138.9, 133.9, 131.6, 128.9, 128.7, 128.4, 127.1, 126.0, 125.7, 125.5, 124.4, 123.9, 61.5, 60.8, 60.0, 57.9, 51.4, 42.5, 14.2; **IR (neat)**: 2794, 1727, 1452, 1177, 1027 cm^{-1}; **HRMS (ESI, Q-TOF)** *m/z*: [M + H] $^+$ Calculated for $C_{24}H_{26}NO_2$ 360.1964, found 360.1955

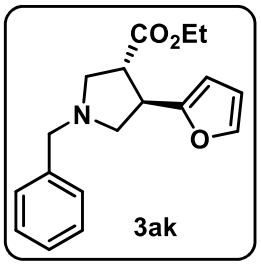

(3S,4S)-ethyl 1-benzyl-4-(furan-2-yl)pyrrolidine-3-carboxylate and (3S,4S)-ethyl 1-benzyl-4-(furan-2-yl)pyrrolidine-3-carboxylate (3ak)

The title compound was purified by column chromatography (Hexane/ethyl acetate = 4:1), R_f = 0.5; Light brown liquid (22 mg, 42%). **^{1}H-NMR** (400 MHz): δ 7.37-7.28 (m, 5H), 7.27-7.21 (m, 1H), 6.30-6.25 (m, 1H), 6.07 (d, *J* = 3.2Hz, 1H), 4.15 (q, *J* = 7.3Hz, 2H), 3.84-3.70 (m, 1H), 3.70 (d, *J* = 12.9Hz, 1H), 3.62 (d, *J* = 13.2Hz, 1H), 3.20-3.12 (m, 1H), 3.04 (t, *J* = 8.6Hz, 1H), 2.99-2.88 (m, 2H), 2.74-2.67 (m, 1H), 1.23 (t, *J* = 7.1Hz, 3H); **^{13}C{^{1}H} NMR** (100 MHz): δ 174.0, 156.1, 141.5, 138.6,128.7, 128.6, 128.3, 127.1, 125.6, 110.2, 105.1, 60.9, 59.7, 58.7, 56.8, 48.4, 40.3, 14.2; **IR (neat)**: 2923, 1730, 1452, 1176, 1028 cm^{-1}; **HRMS (ESI, Q-TOF)** *m/z*: [M + H] $^+$ Calculated for $C_{18}H_{22}NO_3$ 300.1600, found 300.1627

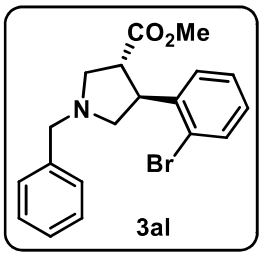

(3S,4R)-methyl 1-benzyl-4-(2-bromophenyl)pyrrolidine-3-carboxylate and (3R,4S)-methyl 1-benzyl-4-(2-bromophenyl)pyrrolidine-3-carboxylate (3al)

The title compound was purified by column chromatography (Hexane/ethyl acetate = 9:1), R_f = 0.5; Colorless liquid (35 mg, 55%). **^{1}H-NMR** (400 MHz, $CDCl_3$): δ 7.56-7.48 (m, 2H), 7.38-7.21 (m, 6H), 7.08-7.02 (m, 1H), 4.18-4.11 (m, 1H), 3.74-3.62 (m, 5H), 3.16 (t, *J* = 8.7Hz, 1H), 3.07 (q, *J* = 7.3Hz, 1H), 2.96 (t, *J* = 8.06Hz, 1H), 2.82-2.73 (m, 2H); **^{13}C{^{1}H} NMR** (100 MHz, $CDCl_3$): δ 174.4, 143.7, 138.6, 132.6, 128.6, 128.2, 127.9, 127.0, 124.3, 61.1, 59.8, 57.4, 52.0, 51.0, 45.8; **IR (neat)**: 2514, 2019, 1733, 1435, 1168, 1023 cm^{-1}; **HRMS (ESI, Q-TOF)** *m/z*: [M + Na]$^+$ Calculated for $C_{19}H_{21}BrNO_2$ 396.0575, found 396.0598

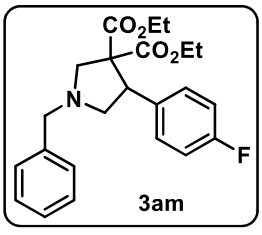

diethyl 1-(4-fluorobenzyl)-4-phenylpyrrolidine-3,3-dicarboxylate (3am)

The title compound was purified by column chromatography (Hexane/ethyl acetate = 9:1), R_f = 0.45; Colorless liquid (33 mg, 48%). **^{1}H-NMR** (400 MHz, $CDCl_3$): δ 7.40-7.22 (m, 7H), 6.92 (t, *J* = 8.8Hz, 2H), 4.31 (t, *J* = 7.03Hz, 1H), 4.27-4.16 (m, 2H),

3.74-3.65 (m, 3H), 3.54 (d, *J* = 10.2Hz, 1H), 3.49-3.40 (m, 1H), 3.09-3.05 (m, 1H), 3.03 (d, *J* = 10.1Hz, 1H), 2.83-2.78 (m, 1H), 1.22 (t, *J* = 7.2Hz, 3H), 0.78 (t, *J* = 7.3Hz, 3H); **^{13}C{^{1}H} NMR** (100 MHz, $CDCl_3$): δ 171.4, 169.2, 138.6, 135.9, 130.7, 128.6, 128.3, 127.1, 114.8, 114.6, 65.2, 61.8, 61.2, 60.6, 60.4, 59.5, 48.5, 14.0, 13.5; **IR (neat)**: 1728, 1510, 1260, 1222, 1096 cm^{-1}; **HRMS (ESI, Q-TOF)** *m/z*: [M + H] $^{+}$ Calculated for $C_{23}H_{27}FNO_4$ 400.1924, found 400.1915

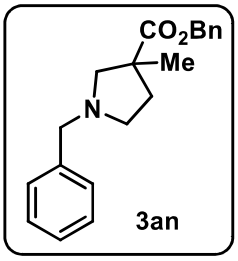

benzyl 1-benzyl-3-methylpyrrolidine-3-carboxylate (3an)

The title compound was purified by column chromatography (Hexane/ethyl acetate = 9:1), R_f = 0.4; Colorless liquid (32 mg, 60%). **^{1}H-NMR** (400 MHz, $CDCl_3$): δ 7.39-7.20 (m, 10H), 5.13 (s, 2H), 3.60 (d, *J* = 3.5Hz, 2H), 3.00 (d, *J* = 9.6Hz, 1H), 2.68-2.59 (m, 2H), 2.49-2.41 (m, 1H), 2.39 (d, *J* = 9.5Hz, 1H),1.71-1.62 (m, 1H), 1.36 (s, 3H); **^{13}C{^{1}H} NMR** (100 MHz, $CDCl_3$): δ 177.3, 139.1, 136.3, 128.67, 128.61, 128.3, 128.1, 127.8, 126.9, 66.4, 64.1, 60.0, 53.8, 48.5, 36.1, 25.4; **IR (neat)**: 2791, 1728, 1449, 1172, 1118, 1028 cm^{-1}; **HRMS (ESI, Q-TOF)** *m/z*: [M + H] $^{+}$ Calculated for $C_{20}H_{24}NO_2$ 310.1807, found 310.1802

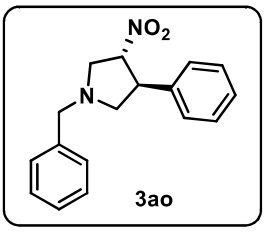

(3R,4S)-1-benzyl-3-nitro-4-phenylpyrrolidine and (3S,4R)-1-benzyl-3-nitro-4-phenylpyrrolidine (3ao)

The title compound was purified by column chromatography (Hexane/ethyl acetate = 94:1), R_f = 0.45 Colorless liquid (26 mg, 55%). **^{1}H-NMR** (400 MHz, $CDCl_3$): δ 7.39-7.24 (m, 10H), 4.97-4.90 (m, 1H), 4.05-3.98 (m, 1H), 3.70 (d, *J* = 9.1Hz, 2H), 3.42-3.38 (m, 1H), 3.31-3.27 (t, *J* = 8.7Hz 1H), 3.12-3.08 (m, 1H), 2.70-2.66 (m, 1H); **^{13}C{^{1}H} NMR** (100 MHz, $CDCl_3$): δ 140.7, 137.9, 129.0, 128.6, 128.5, 127.5, 91.2, 60.8, 59.3, 58.4, 49.3; **HRMS (ESI, Q-TOF)** *m/z*: [M + H] $^{+}$ Calculated for $C_{17}H_{19}N_2O_2$ 283.1447, found 283.1473.

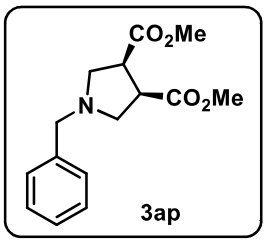

dimethyl (3R,4S)-1-benzylpyrrolidine-3,4-dicarboxylate (3ap)

The title compound was purified by column chromatography (Hexane/ethyl acetate = 9:1), R_f = 0.6; Colorless liquid (23 mg, 48%). **^{1}H-NMR** (400 MHz, $CDCl_3$): δ 7.34-7.17 (m, 5H), 3.69 (s, 1H), 3.68 (s, 1H), 3.64 (s, 6H), 3.35-3.25 (m, 2H), 3.17-3.09 (m, 2H), 2.75-2.65 (m, 2H); **^{13}C{^{1}H} NMR** (100 MHz, $CDCl_3$): δ 173.1, 138.5, 128.8, 128.4, 127.2, 59.9, 51.1, 52.0, 45.3; **HRMS (ESI, Q-TOF)** *m/z*: [M + H] $^{+}$ Calculated for $C_{15}H_{20}NO_4$ 278.1392, found 278.1383.

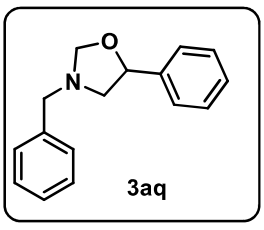

3-benzyl-5-phenyloxazolidine (3aq)

The title compound was purified by column chromatography (Hexane/ethyl acetate = 9:1), R_f = 0.6; Colorless liquid (25 mg, 62%). **^{1}H-NMR** (400 MHz, $CDCl_3$): δ 7.32-7.13 (m, 10H), 4.98 (t, *J* = 7.4Hz, 1H), 4.52 (s, 2H), 3.75 (s, 2H), 3.39-3.31 (dd, *J* = 11.3 and 6.5Hz, 1H), 2.79-2.71 (dd, *J* = 11.6 and 7.2Hz, 1H); **^{13}C{^{1}H}**

NMR (100 MHz, $CDCl_3$): δ 142.1, 138.6, 128.7, 128.4, 127.3, 127.2, 125.5, 87.5, 75.6, 60.6, 58.3; **HRMS (ESI, Q-TOF)** *m/z*: [M + H] $^+$ Calculated for $C_{18}H_{18}NO$ 240.1388, found 240.1400

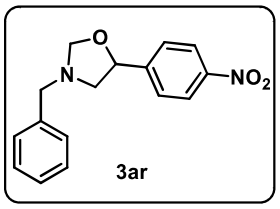

3-benzyl-5-(4-nitrophenyl)oxazolidine (3ar)

The title compound was purified by column chromatography (Hexane/ethyl acetate = 9:1), R_f = 0.4; Colorless liquid (32 mg, 65%). **^{1}H-NMR** (400 MHz, $CDCl_3$): δ 8.19 (d, *J* = 8.7Hz, 2H), 7.50 (d, *J* = 8.7Hz, 2H), 7.3-7.22 (m, 5H), 5.12 (t, *J* = 7.2Hz, 1H), 4.61 (s, 2H), 3.79 (s, 2H), 3.49-3.43 (dd, *J* = 11.6 and 6.7Hz, 1H), 2.80-2.73 (dd, *J* = 11.4 and 7.4Hz, 1H); **^{13}C{^{1}H} NMR** (100 MHz, $CDCl_3$): δ 150.1, 147.3, 138.2, 128.7, 128.6, 127.6, 126.2, 123.9, 87.9, 75.6, 60., 58.32; **HRMS (ESI, Q-TOF)** *m/z*: [M + H] $^+$ Calculated for $C_{16}H_{17}N_2O_3$ 285.1239, found 285.1275

2.4.7. Cyclic Voltammetry

Cyclic voltammetry analysis was carried out in CH instrument electrochemical analyzer (CHL1110C). Samples were prepared in 5 ml vial with 0.01 M of substrate (**1a**), 0.01 M of ferrocene, 0.01 M of ethyl acrylate (**2a**) and 0.1 M of Bu_4NBF_4 in acetonitrile. Measurements employed glassy carbon working electrode, platinum wire counter electrode and a 3M KCl silver-silver chloride reference electrode. The sweep rate applied was 50 mV/s. The oxidation potential obtained for compound (**1a)** was 0.75 V, while for **2a** no peak was observed up to 3V. All the CV experiments were carried out in Argon atmosphere and demonstrated as follow: (a) 0.1 M Bu_4NBF_4 (black) (b) 0.01 M Cp_2Fe (red) (c) 0.01 M **1a** (blue) (d) 0.01 M **2a** (pink) (e) 0.01 M **1a** and 0.01 M **2a** (green).

2.4.8. Procedure for electrochemical gram scale synthesis

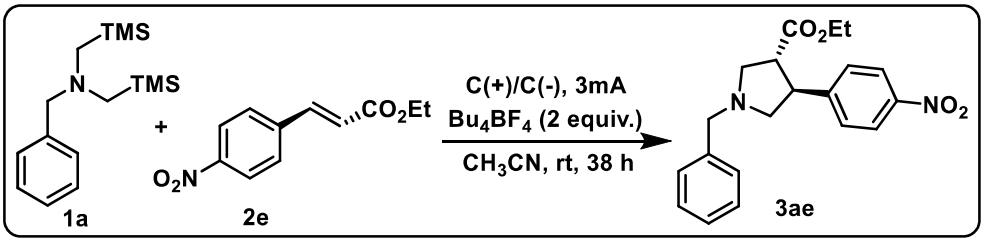

In an oven dried two neck round bottom flask (100 mL) equipped with magnetic bar and graphite as both anode and cathode, mixture of **1a** (3.57 mmol, 1.0 g), **2e** (3.57 mmol, 0.79 g), Bu_4NBF_4 (2 equiv.) and CH_3CN (30 ml) were added. The mixture was electrolyzed at a constant current of 3 mA at room temperature for 38 h in a DC power supply. Upon completion, the solvent was removed under reduced pressure and the crude was purified by silica gel column chromatography using 8-10 % ethyl acetate in hexane to afford the desired product in 70 % yield (0.882 g).

2.5. References

1. Iain, C.; Hufton, R. *Chem. Rev*. **2005**, *105*, 2765-2809.

2. Padwa, A.; Pearson, W. H.; Harwood, L. M.; Vickers, R. J. Azomethine Ylides. *Chemistry of Heterocyclic Compounds: A Series of Monographs*. **2003**, *59*, 169-252.

3. Marie, S. T. M.; Daniel, J. S. C.; Bruce, A. A. *Org. Lett*. **2010**, *12*, 4916-4919.

4. Pandey, G.; Banerjee, P.; Gadre, S. R. *Chem. Rev*. **2006**, *106*, 4484-4547.

5. (a) Huisgen, R.; Niklas, K. *Heterocycles*. **1984**, *22*, 22-26. (b) Song, G.; Chen, D.; Su, Y.; Han, K.; Pan, C. L.; Jia, A.; Li, X. *Angew. Chem., Int. Ed*. **2011**, *50*, 7791-7796.

6. (a) Pandey G.; Lakshmaiah, G. *Tetrahedron lett*. **1993**, *34*, 4861-4864. (b) Padwa, A.; Chen, Y. Y. *Tetrahedron Lett*. **1983**, *24*, 3447-3450. (c) Vedejs, E.; Martinez, G. R. *J. Am. Chem. Soc*. **1979**, *101*, 6452-6454. (d) Deshong, P.; Kell, D. A.; Sildler, D. R. *J. Org. Chem.* **1985**, *50*, 2309-2315.

7. Rueping, M.; Leonori, D.; Poisson, T. *Chem. Commun*. **2011**, *47*, 9615-9617.

8. Fujiya, A.; Tanaka, M.; Yamaguchi, E.; Tada, N.; Itoh, A. *J. Org. Chem*. **2016***, 81*, 7262-7270.

9. (a) Pandey G.; Lakshmaiah, G.; Kumaraswamy, G. *J. Chem. Soc., Chem. Commun.* **1992**, *18*, 1313-1314.

10. a) Thierry, T.; Lebargy, C.; Pfund, E.; Lequeux, T. *J. Org. Chem*. **2019**, *84*, 5877-5885. (b) Zou, Y. Q.; Lu, L. Q.; Fu, L.; Chang, N. J.; Rong, J.; Chen, J. R.; Xiao, W. J. *Angew Chem. Int. Ed.* **2012**, *50*, 7171-7175.

11. (a) Laha, J. K.; Jethava, K. P. *J. Org. Chem*. **2017**, *82*, 3597-3604. (b) Laha, J. K.; Jethava, K. P.; Tummalapalli, K. S. S.; Sharma, S. *Eur. J. Org. Chem*. **2017**, *31*, 4617-4624. (c) Cheng, X.; Cao, X.; Xuan, J.; Xiao, W. J. *Org. Lett.* **2018**, *20*, 52-55.

12. McAlpine, I.; Tran-Dube, M.; Wang, F.; Scales, S.; Matthews, J.; Collins, M. R.; Nair, S. K.; Nguyen, M.; Bian, J.; Alsina, L. M.; Sun, J.; Zhong, J.; Warmus, J. S.; O'Neil, B. T. *J. Org. Chem*. **2015**, *80*, 7266-7274.

13. (a) Shono, T.; Hamaguchi, H.; Matsumura, Y. *J. Am. Chem. Soc*. **1975**, *97*, 4264-4268. (b) Yoshida, J. I.; Isoe, S. *Tetrahedron Lett*. **1987**, *28*, 6621-6624.

14. (a) Yan, M.; Kawamata, Y.; Baran, P. S. *Chem. Rev.* **2017**, *117*, 13230-13319. (b) Pollok, D.; Waldvogel, S. R. *Chem. Sci*. **2020**, *11*, 12386-12400.

15. Yuan, Y.; Lei, A. *Nat. commun*. **2020**, *11*, 802.

16. (a) Jiang, Y.; Xu, K.; Zeng, C. *Chem. Rev*. **2018**, *118*, 4485-4540. (b) Nutting, J. E.; Rafiee, M.; Stahl, S. S. *Chem. Rev*. **2018**, *118*, 4834-4885. (c) Sauermann, N.; Meyer, T. H.; Qiu, Y.; Ackermann, L. *ACS Catal*. **2018**, *8*, 7086-7106.

17. (a) Zhao, H. B.; Liu, Z. J.; Song, J.; Xu, H. C. *Angew. Chem., Int. Ed.* **2017**, *56*, 12732-12735. (b) Wu, Z. J.; Li, S. R.; Long, H.; Xu, H. C. *Chem. Commun*. **2018**, *54*, 4601-4604. (c) Gao, X.; Wang, P.; Zeng, L.; Tang, S.; Lei, A. *J. Am. Chem. Soc*. **2018**, *140*, 4195-4199. (d) Yu, Y.; Yuan, Y.; Liu, H.; He, M.; Yang, M.; Liu, P.; Yu, B.; Dong, X.; Lei, A. *Chem. Commun*. **2019**, *55*, 1809-1812. (e) Yuan, Y.; Qiao, J.; Cao, Y.; Tang, J.; Wang, M.; Ke, G.; Lu, Y.; Liu, X.; Lei, A. *Chem. Commun.* **2019**, *55*, 4230-4233. (f) Yang, Q. L.; Li, Y. Q.; Ma, C.; Fang, P.; Zhang, X. J.; Mei, T. S. *J. Am. Chem. Soc*. **2017**, *139*, 3293-3298.

18. (a) Jones, A. M.; Banks, C. E. *Beilstein J. Org. Chem*. **2014**, *10*, 3056-3072. (b) Waldvogel, S. R.; Lips, S.; Selt, M.; Riehl, B.; Kampf, C. *J. Chem. Rev*. **2018**, *118*, 6706-6765.

19. (a) Saha, D.; Taily, I. M.; Naik, S.; Banerjee, P. *Chem. Commun*. **2021**, *57*, 631-634. (b) Karkas, M. D. *Chem. Soc. Rev*. **2018**, *47*, 5786-5865.

20. Saha, D.; Taily, I. M.; Kumar, R.; Banerjee, *Chem. Commun*. **2021**, *57*, 2464-2478.

21. Wang, Q.; Yuan, T.; Liu, Q.; Xu, Y.; Xie, G.; Lv, X.; Ding, S.; Wang, X.; Li, C. *Chem. Commun*. **2019**, *55*, 8398-8401.

22. Claraz, A.; Djian, A.; Masson, G. *Org. Chem. Front.* **2021**, *8*, 288-296.

23. Smith, J. R. L.; Masheder, D. *J. Chem. Soc., Perkin Trans. 2*, **1976**, *1*, 47-51.

24. Liang, H.; Wang, L. J.; Ji, Y. X.; Wang, H.; Zhang, B. *Angew. Chem. Int. Ed.* **2021**, *60*, 1839-1844.

25. (a) Ando, K.; Yamada, K. *Green Chem*., **2011**, *13*, 1143-1146. (b) John, J.; Hopf, H. *Eur. J. Org. Chem*. **2013**, *5*, 841-845. (c) Ni, Q.; Wang, X.; Zeng, D.; Wu, Q.; Song, X. *Org. Lett.* **2021**, *23*, 2273−2278. (d) Srihari, P.; Yaragorla, S.R.; Basu, D.; Chandrasekhar, S. *Synthesis*. **2006**, *16*, 646-2648. (e) Pandiancherri, S.; Ryan, S. J.; Lupton, D. W. *Org. Biomol. Chem.*, **2012**, *10*, 7903-7911.

2.6. NMR spectra of starting materials

^{1}H NMR (400 MHz, $CDCl_3$) of 1a

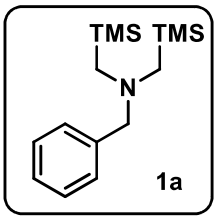

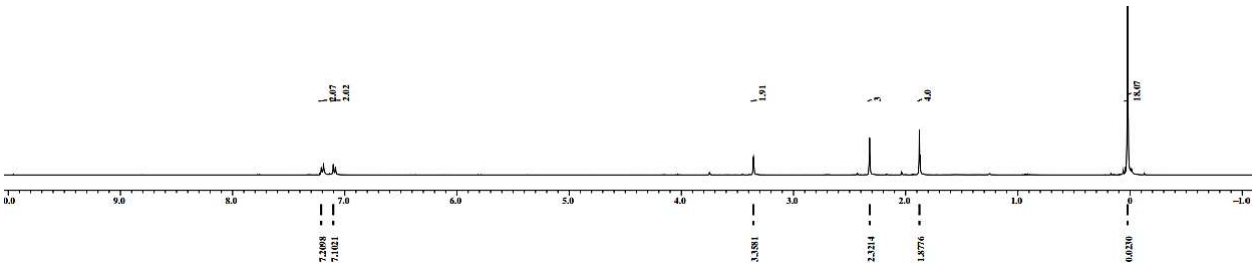

^{1}H NMR (400 MHz, $CDCl_3$) of 1b

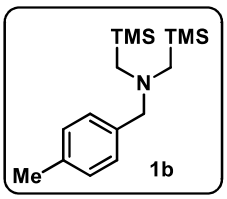

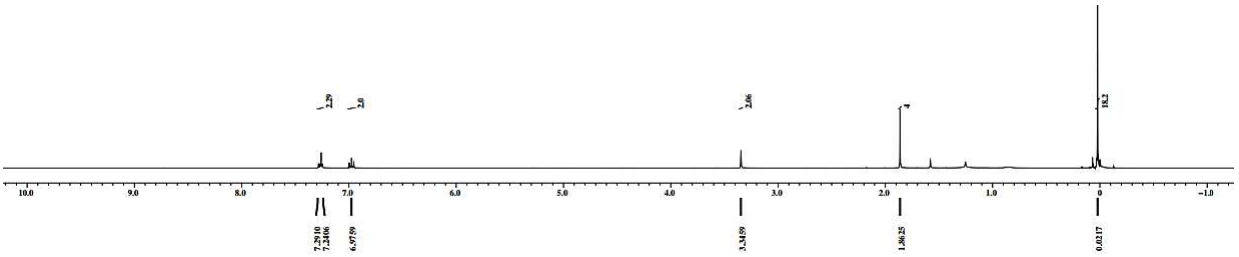

^{1}H NMR (400 MHz, $CDCl_3$) of 1c

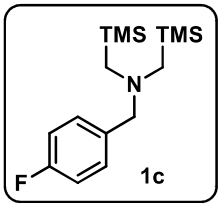

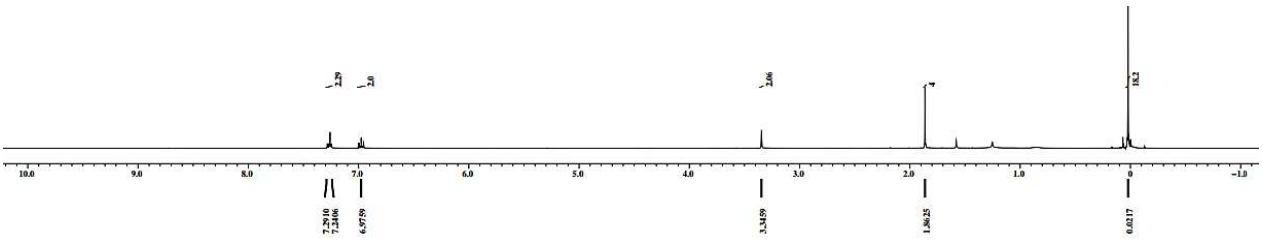

^{1}H NMR (400 MHz, $CDCl_3$) of 1d

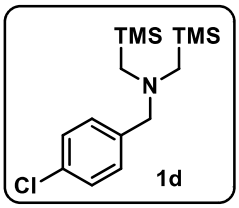

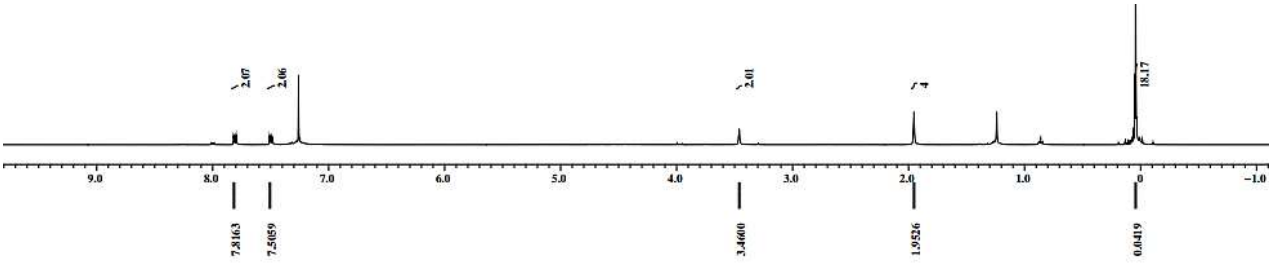

^{1}H NMR (400 MHz, $CDCl_3$) of 1e

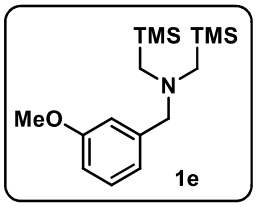

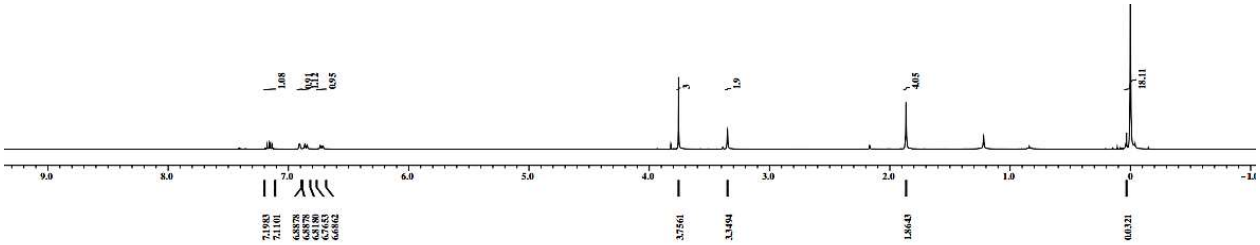

^{1}H NMR (400 MHz, $CDCl_3$) of 1f

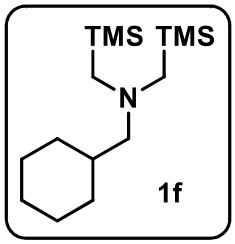

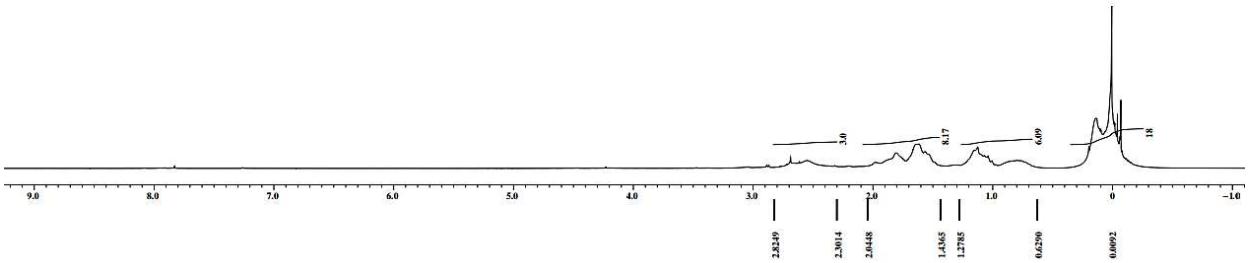

^{1}H NMR (400 MHz, $CDCl_3$) of 1g

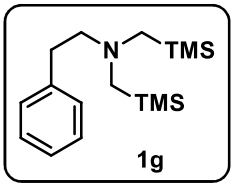

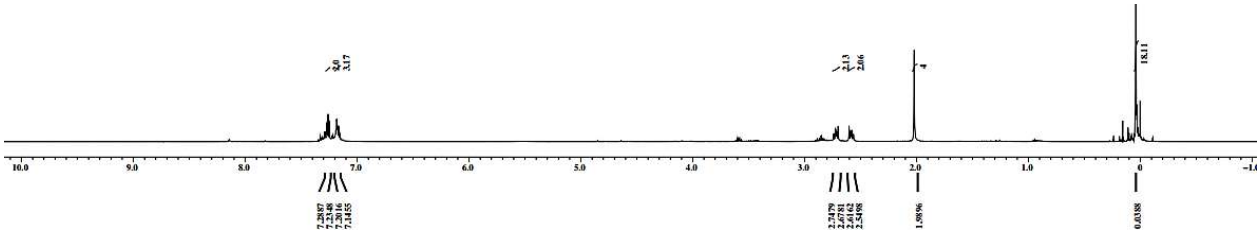

^{1}H NMR (400 MHz, $CDCl_3$) of 1h

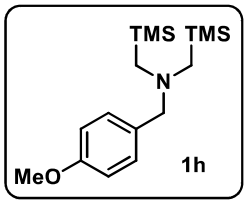

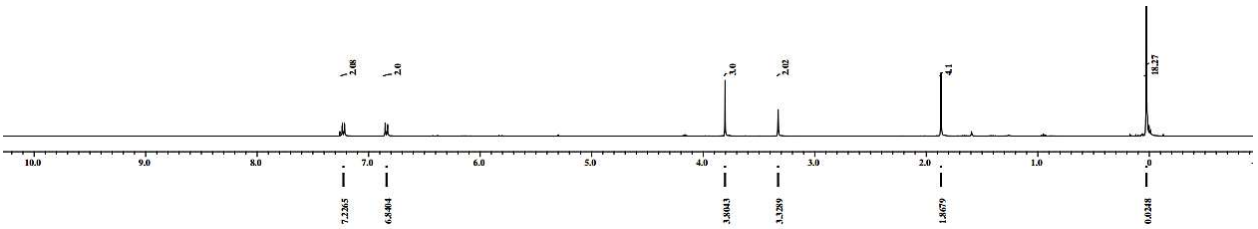

^{1}H NMR (400 MHz, $CDCl_3$) of 1i

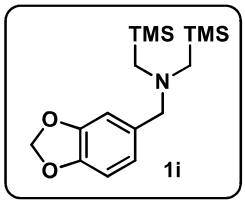

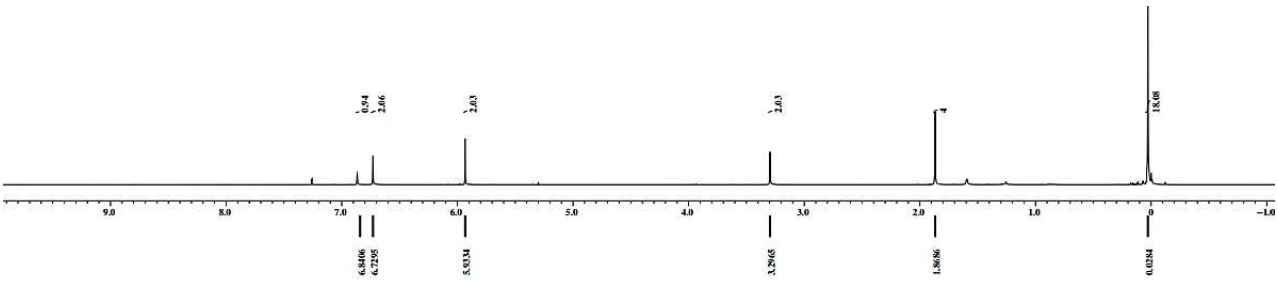

^{1}H NMR (400 MHz, $CDCl_3$) of 2b

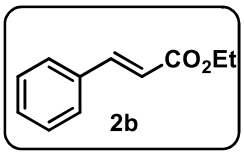

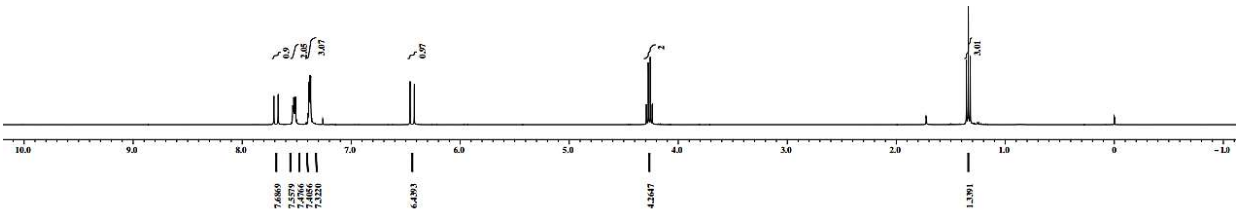

^{1}H NMR (400 MHz, $CDCl_3$) of 2c

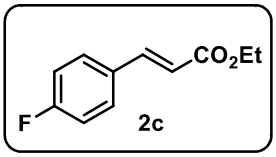

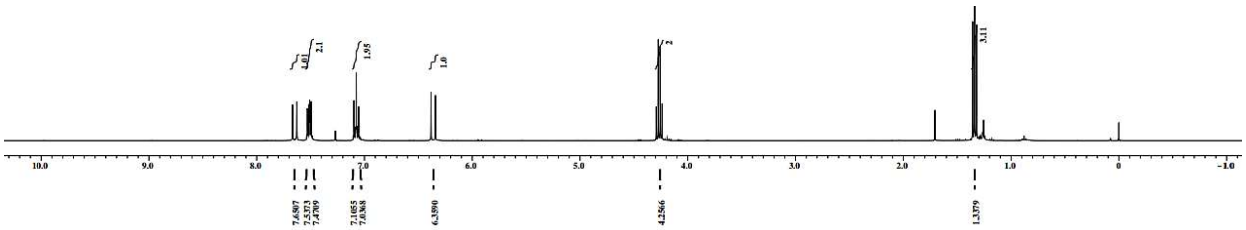

^{1}H NMR (400 MHz, $CDCl_3$) of 2d

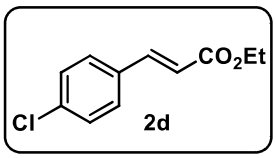

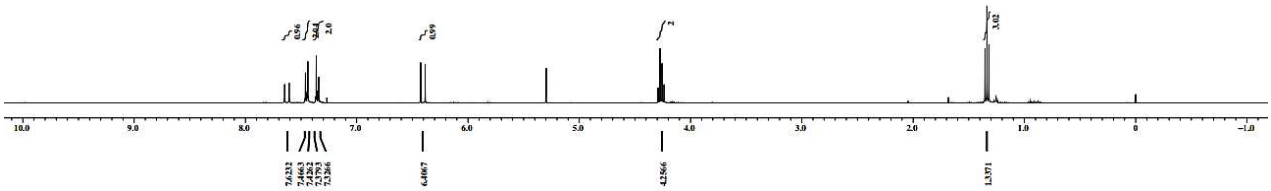

^{1}H NMR (400 MHz, $CDCl_3$) of 2e

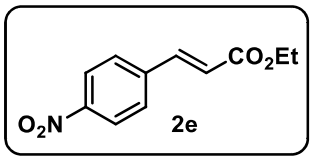

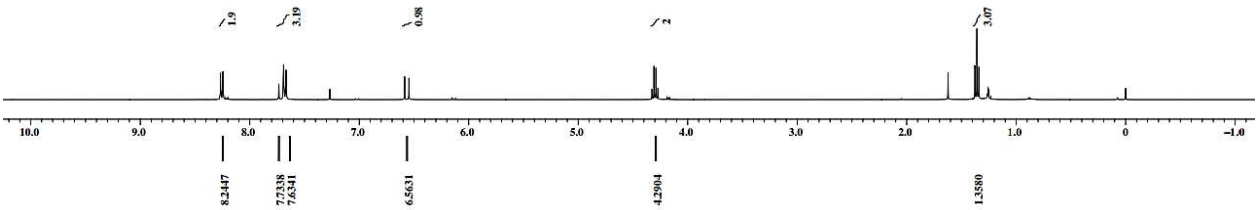

^{1}H NMR (400 MHz, $CDCl_3$) of 2f

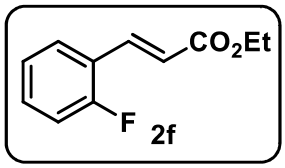

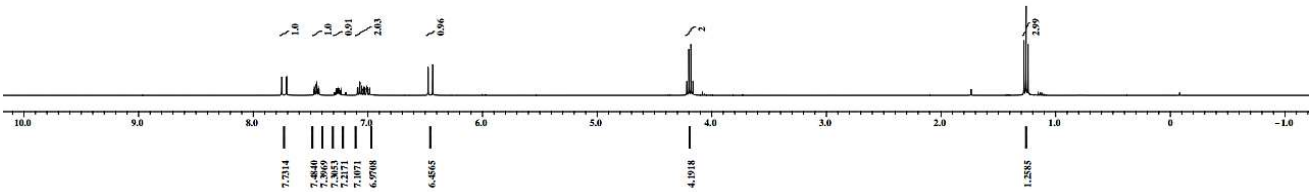

^{1}H NMR (400 MHz, $CDCl_3$) of 2g

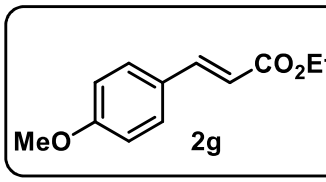

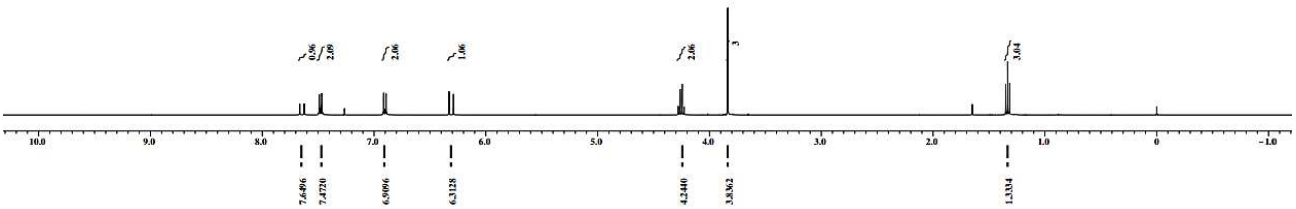

^{1}H NMR (400 MHz, $CDCl_3$) of 2h

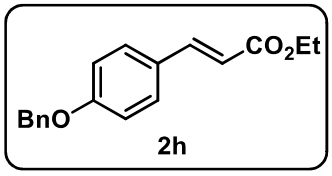

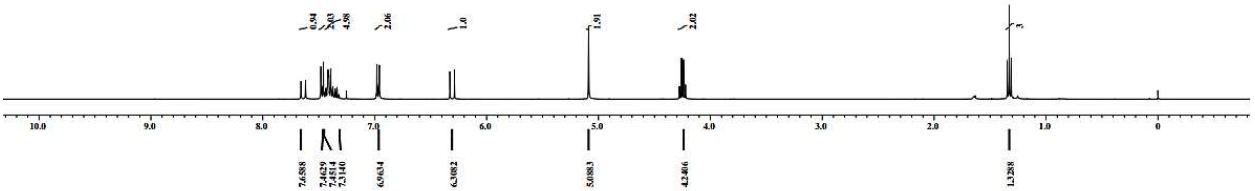

^{1}H NMR (400 MHz, $CDCl_3$) of 2i

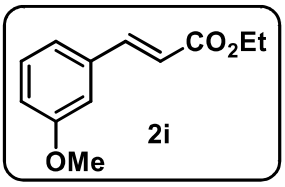

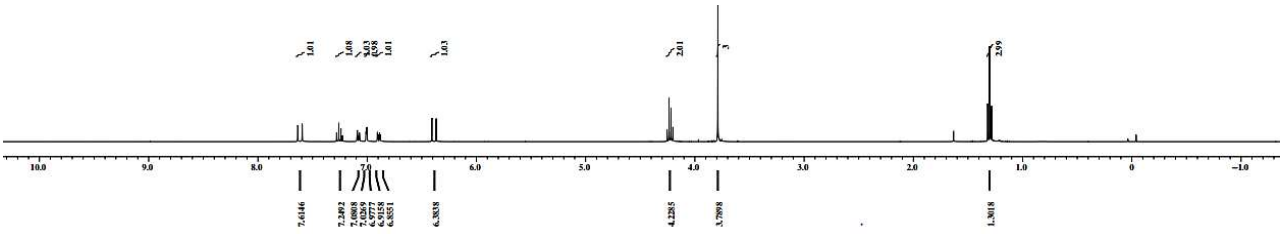

^{1}H NMR (400 MHz, $CDCl_3$) of 2j

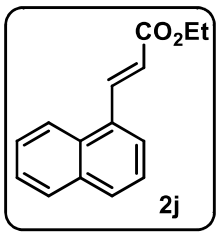

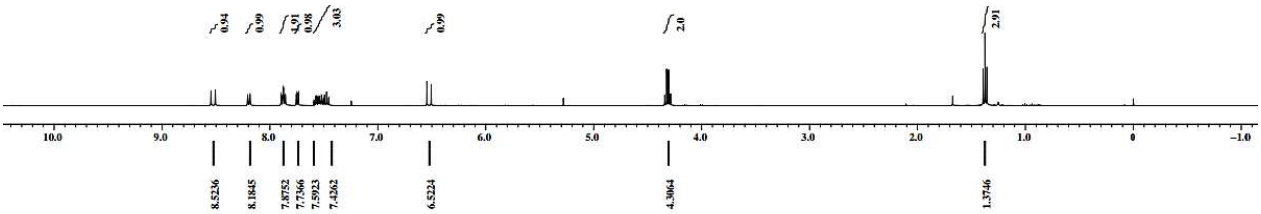

^{1}H NMR (400 MHz, $CDCl_3$) of 2k

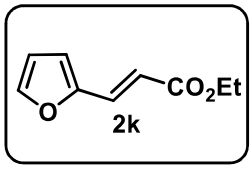

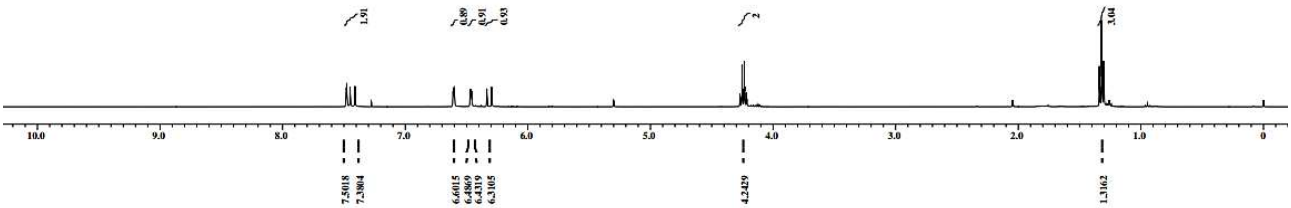

^{1}H NMR (400 MHz, $CDCl_3$) of 2l

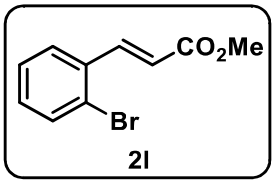

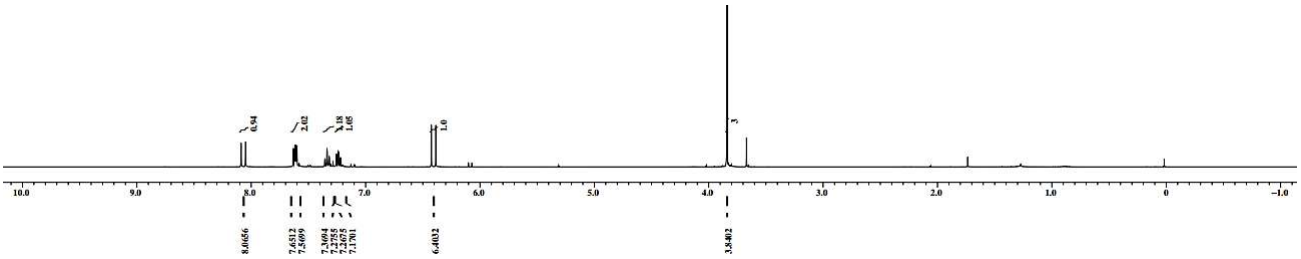

^{1}H NMR (400 MHz, $CDCl_3$) of 2m

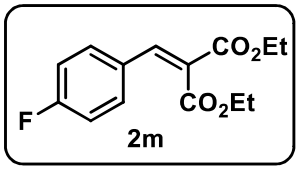

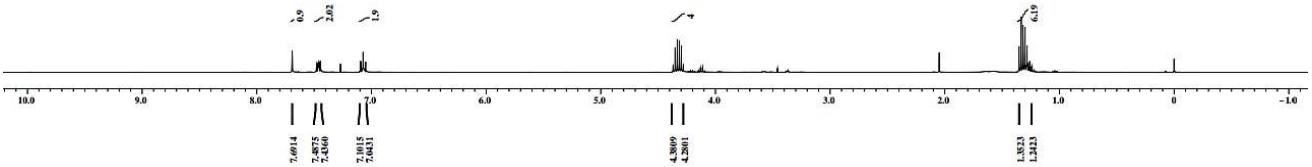

^{1}H NMR (400 MHz, $CDCl_3$) of 2o

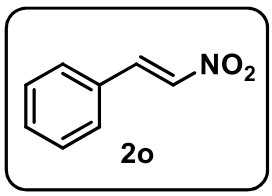

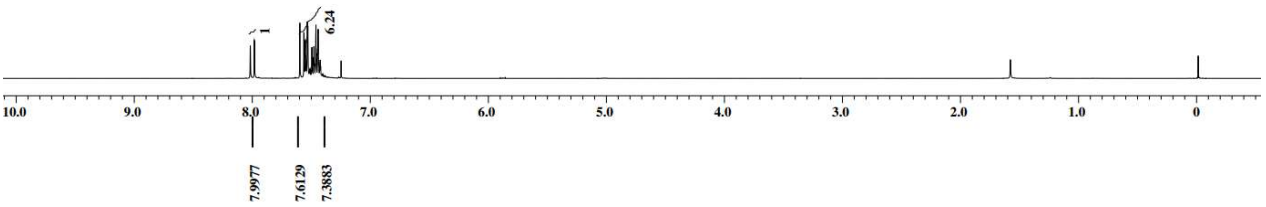

2.7. NMR spectra of final products

^{1}H NMR (400 MHz, $CDCl_3$) of 3aa

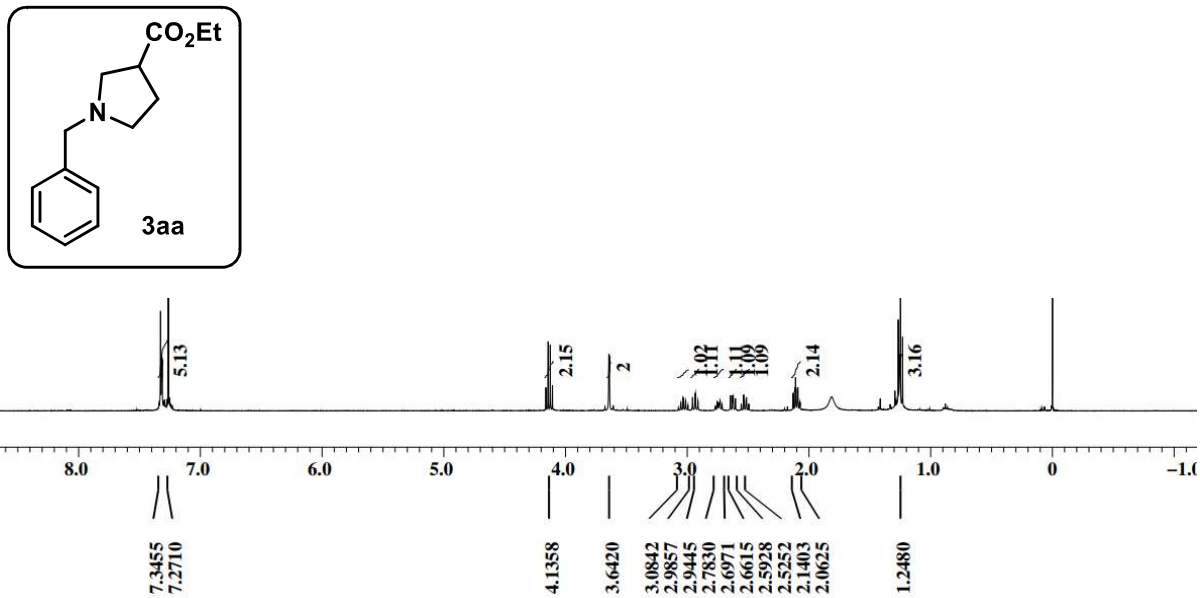

^{13}C {^{1}H} NMR (100 MHz, $CDCl_3$) of 3aa

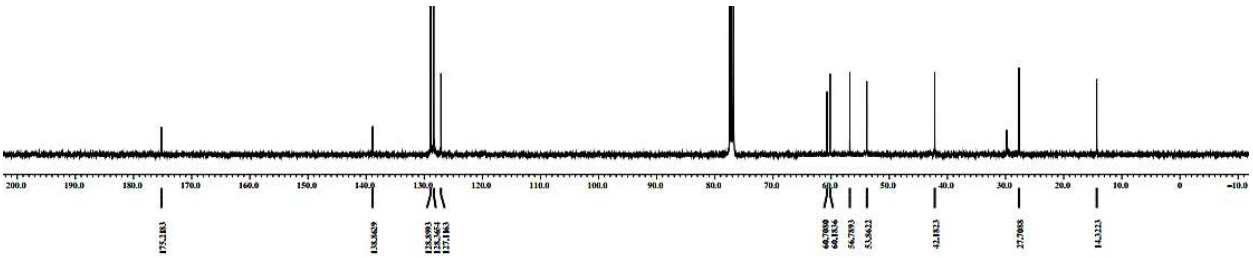

FTIR of 3aa

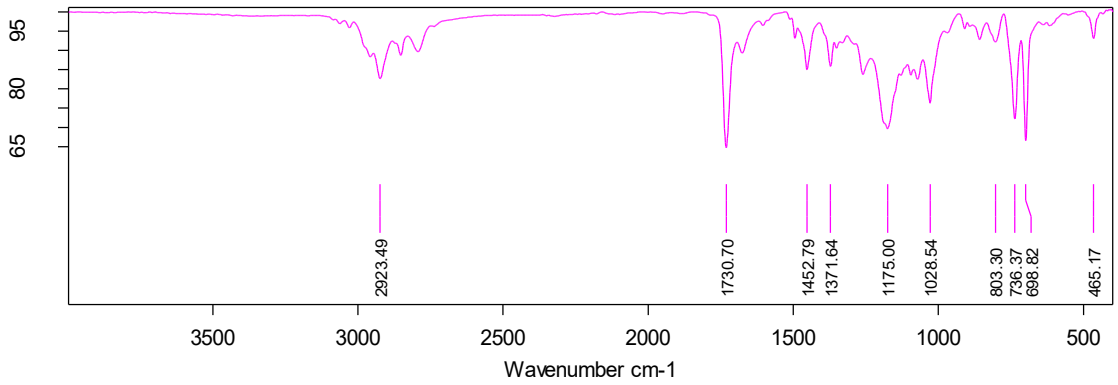

D:\FTIR DATA\DR. PRABAL\Rakesh\TPA.17	TPA	45	2/26/2021

^{1}H NMR (400 MHz, $CDCl_3$) of 3ba

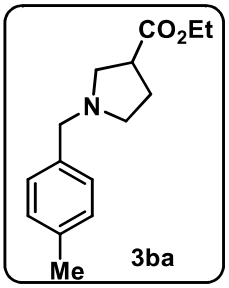

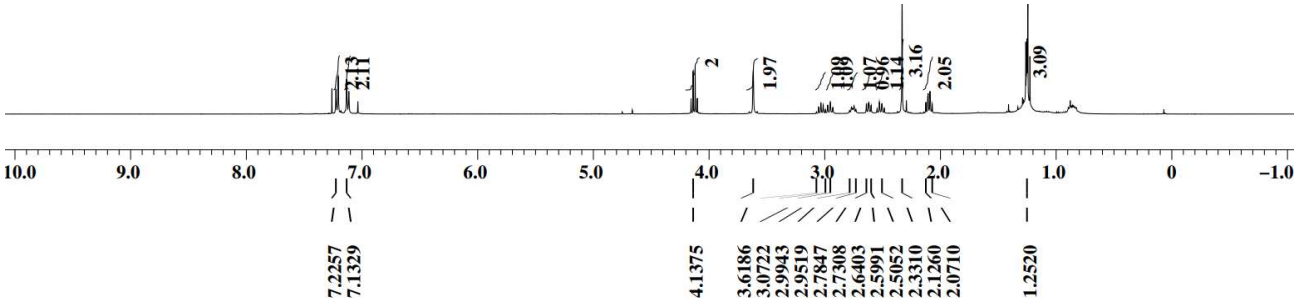

^{13}C {^{1}H} NMR (100 MHz, $CDCl_3$) of 3ba

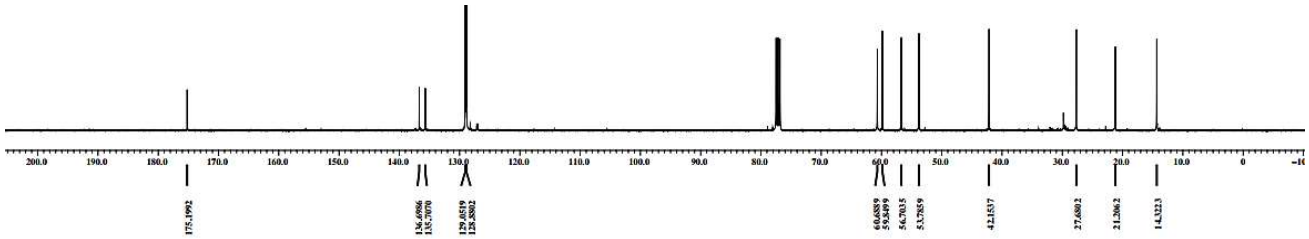

FTIR of 3ba

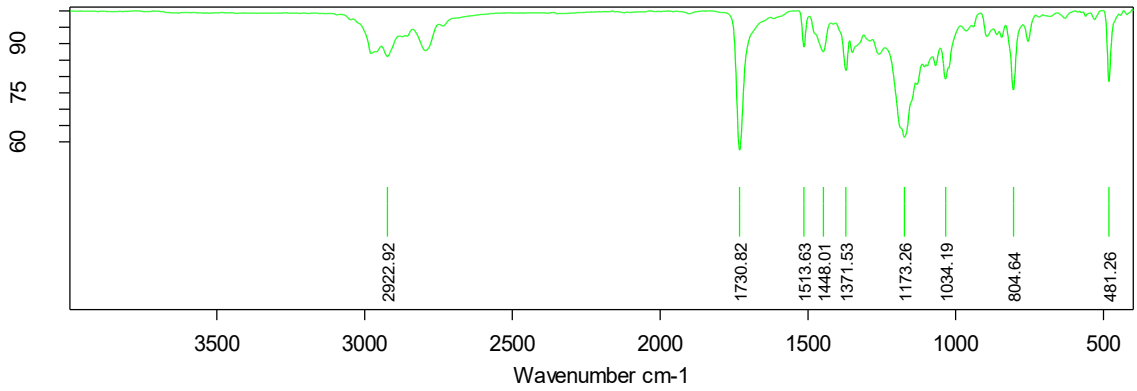

D:\FTIR DATA\DR. PRABAL\Rakesh\TPA.33	TPA	228	2/26/2021

^{1}H NMR (400 MHz, $CDCl_3$) of 3ca

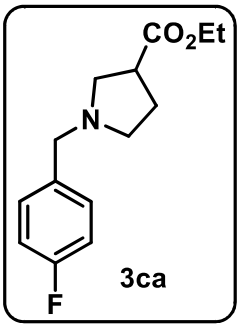

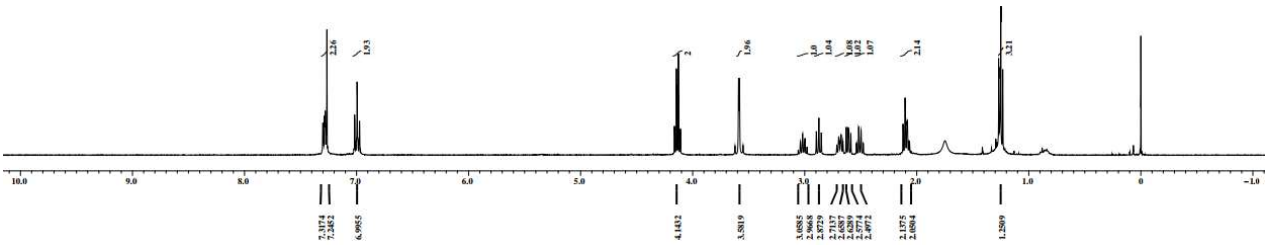

^{13}C {^{1}H} NMR (100 MHz, $CDCl_3$) of 3ca

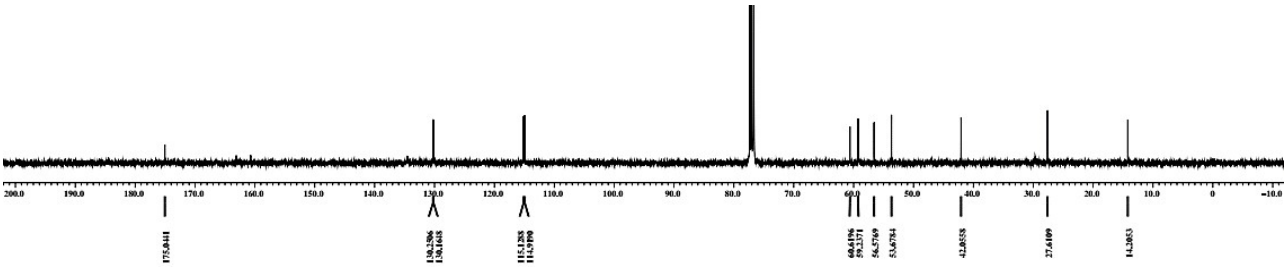

FTIR of 3ca

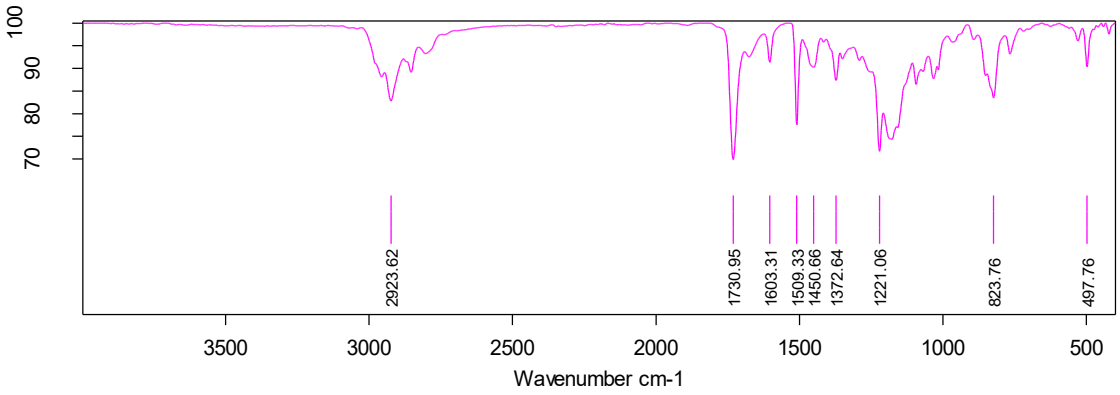

D:\FTIR DATA\DR. PRABAL\Rakesh\TPA.32	TPA	125	2/26/2021

^{1}H NMR (400 MHz, $CDCl_3$) of 3da

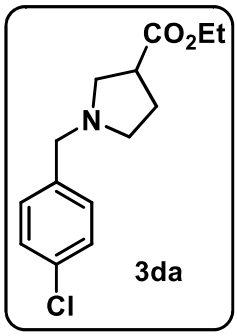

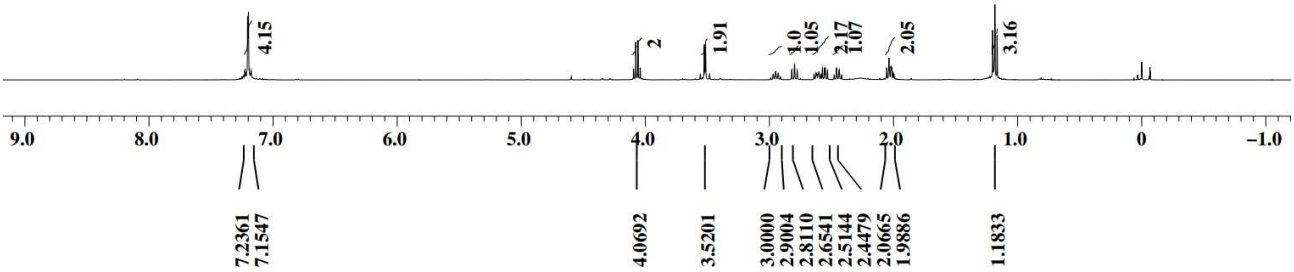

^{13}C {^{1}H} NMR (100 MHz, $CDCl_3$) of 3da

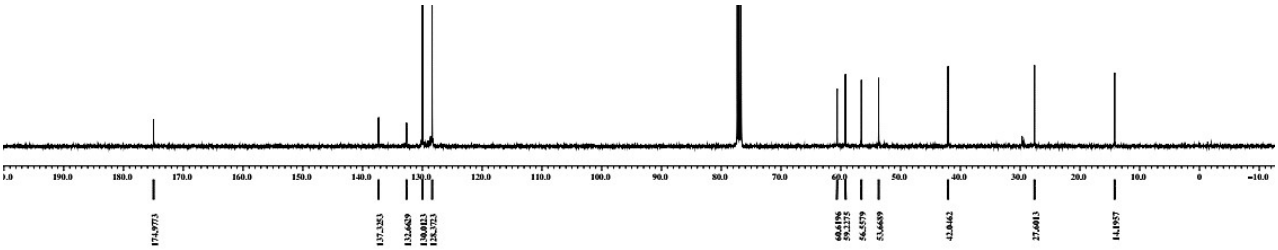

FTIR of 3da

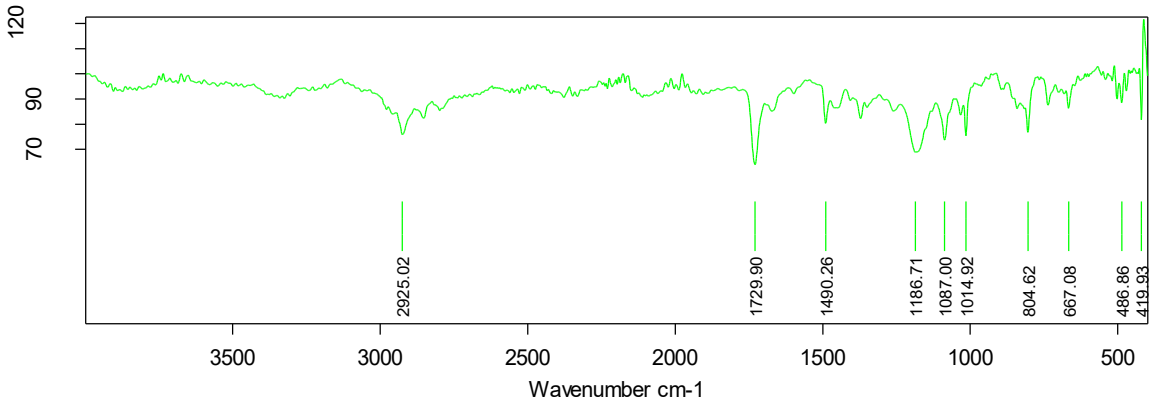

D:\FTIR DATA\DR. PRABAL\Rakesh\.3	126	LIQUID	3/12/2021

^{1}H NMR (400 MHz, $CDCl_3$) of 3ea

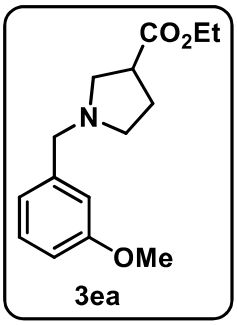

3ea

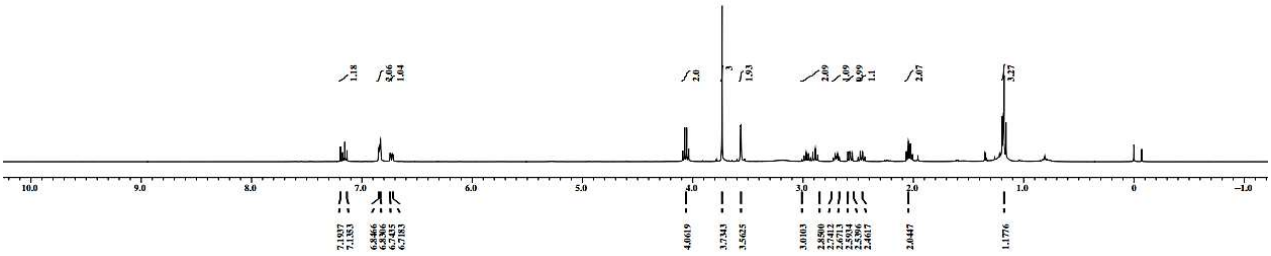

^{13}C {^{1}H} NMR (100 MHz, $CDCl_3$) of 3ea

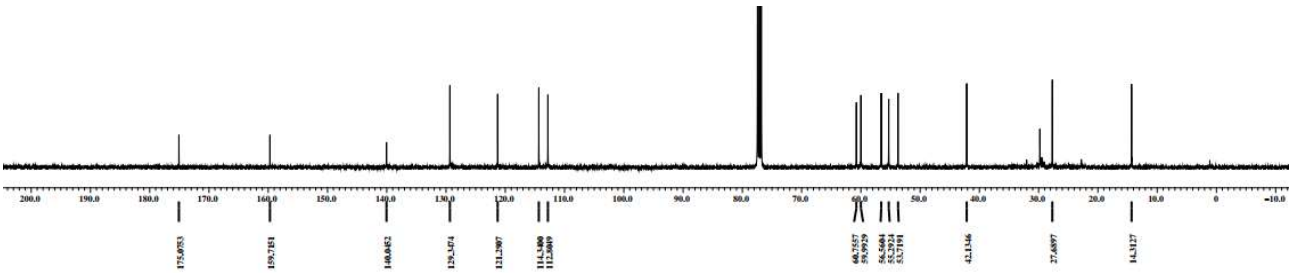

FTIR of 3ea

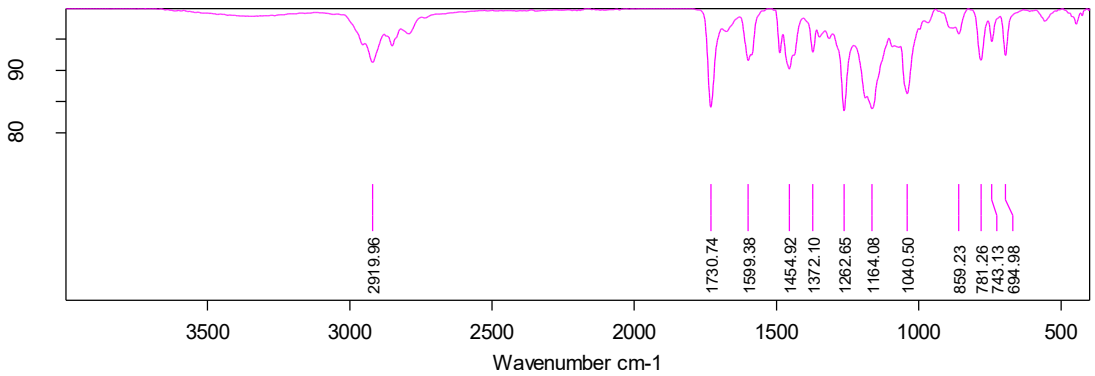

D:\FTIR DATA\DR. PRABAL\Rakesh\TPA.2	TPA	132 (1)	2/26/2021

^{1}H NMR (400 MHz, $CDCl_3$) of 3fa

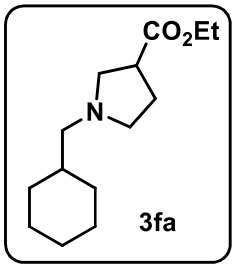

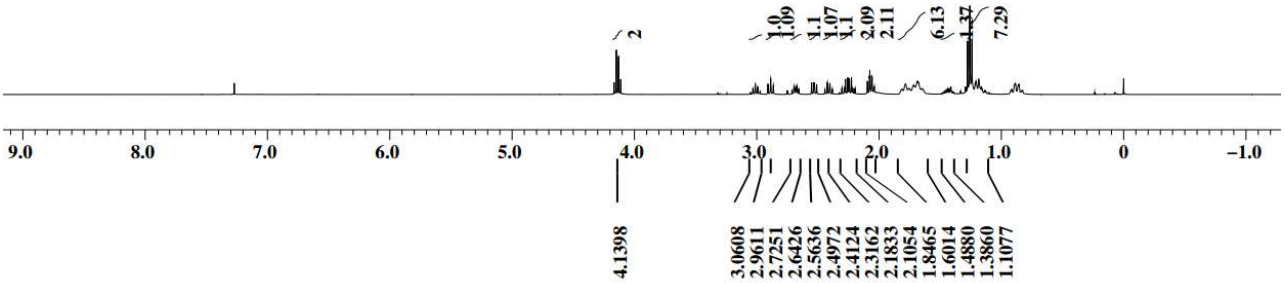

^{13}C {^{1}H} NMR (100 MHz, $CDCl_3$) of 3fa

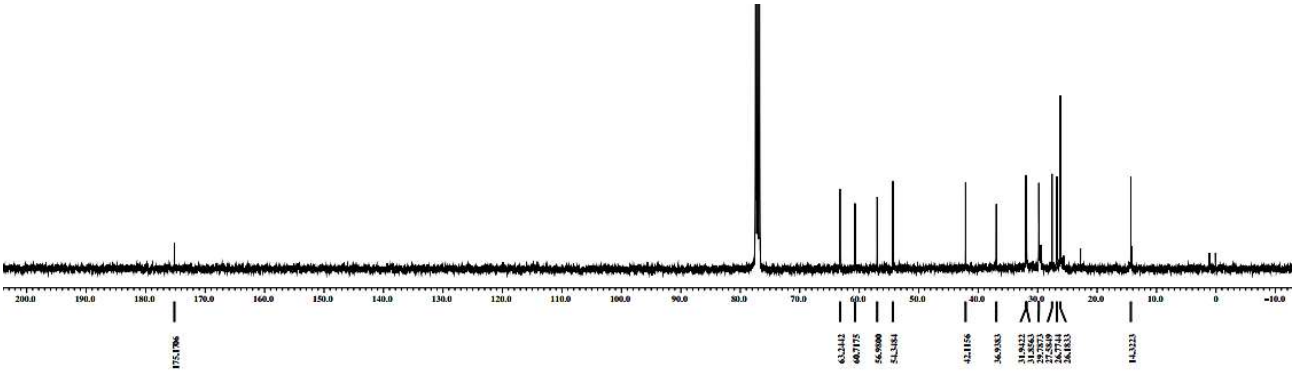

FTIR of 3fa

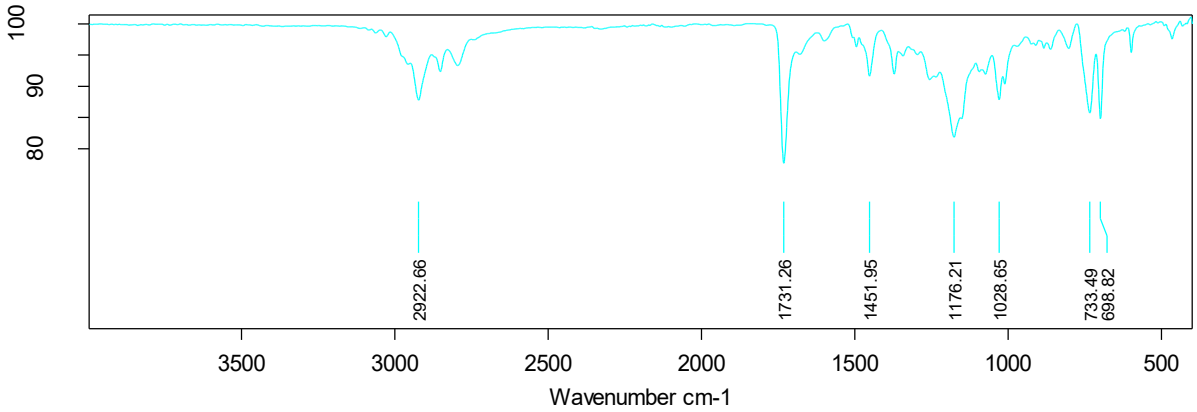

D:\FTIR DATA\DR. PRABAL\Rakesh\TPA.19	TPA	170-2	2/26/2021

^{1}H NMR (400 MHz, $CDCl_3$) of 3gb

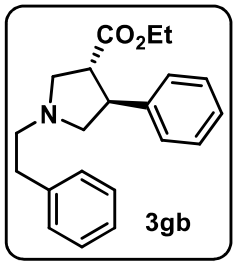

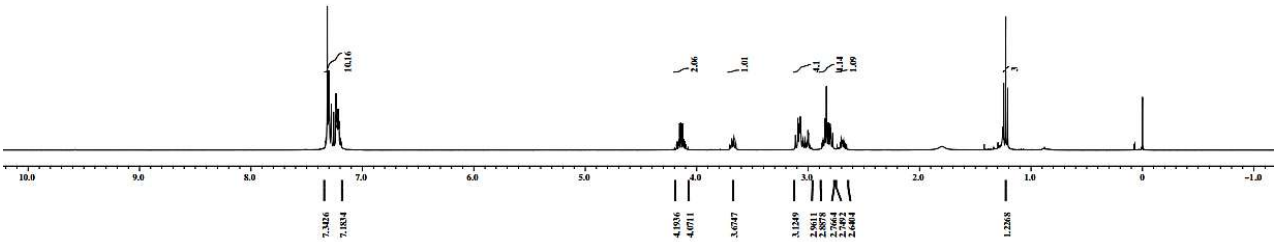

^{13}C {^{1}H} NMR (100 MHz, $CDCl_3$) of 3gb

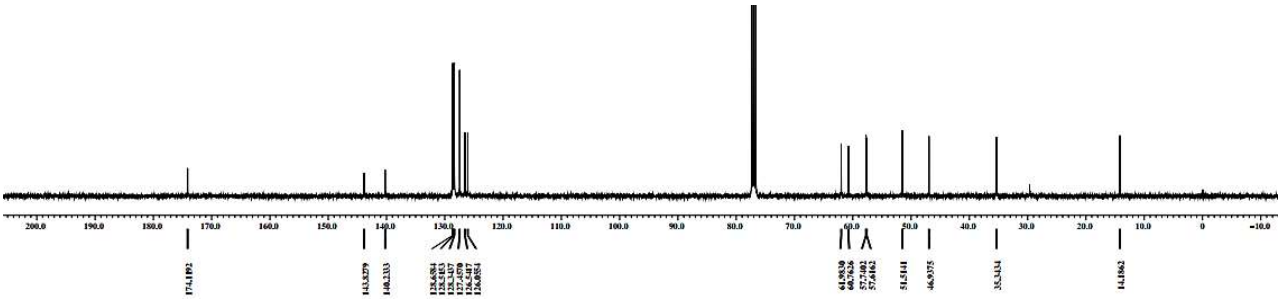

FTIR of 3gb

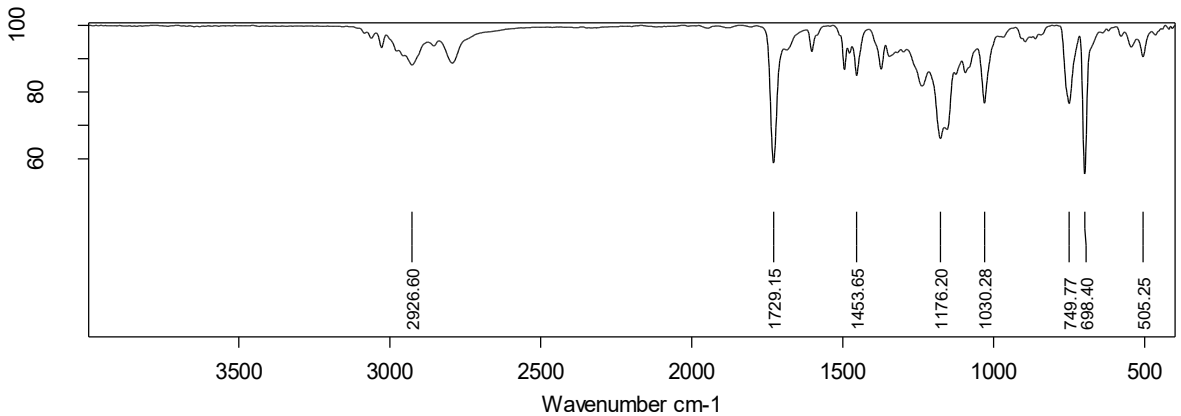

D:\FTIR DATA\DR. PRABAL\Rakesh\TPA.28	TPA	233	2/26/2021

^{1}H NMR (400 MHz, $CDCl_3$) of 3hb

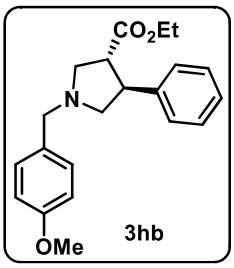

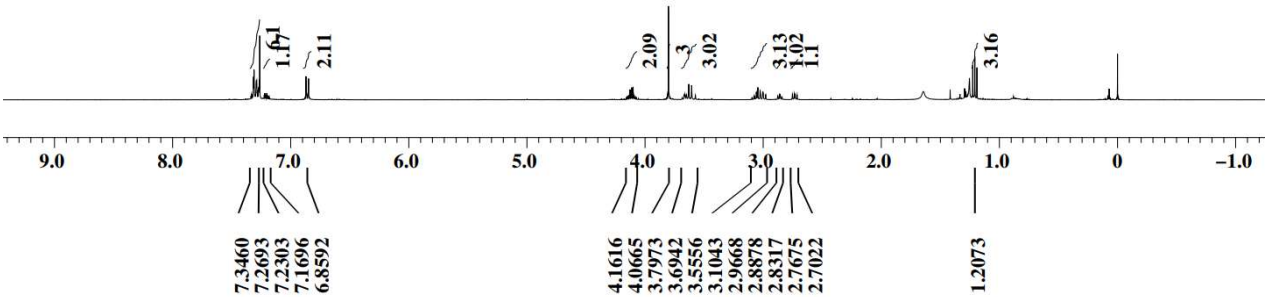

^{13}C {^{1}H} NMR (100 MHz, $CDCl_3$) of 3hb

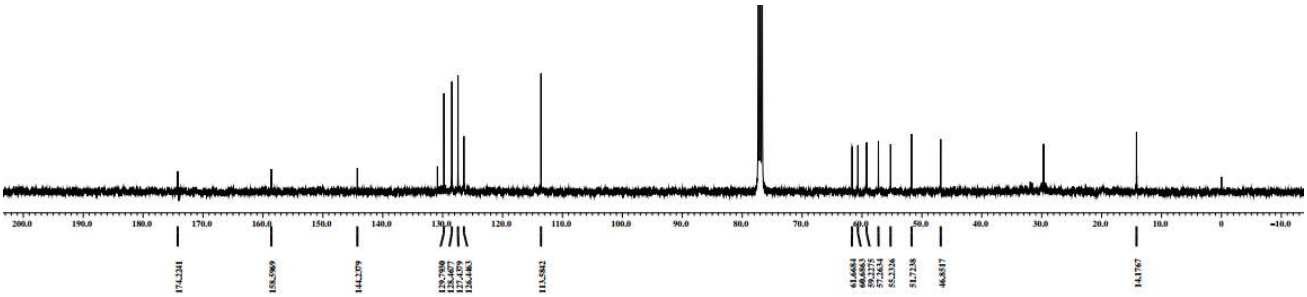

FTIR of 3hb

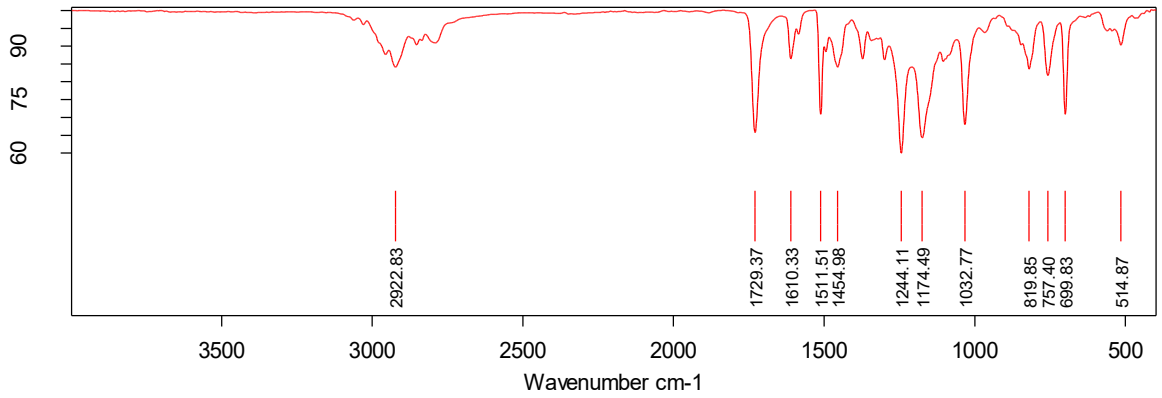

D:\FTIR DATA\DR. PRABAL\Rakesh\TPA.31	TPA	226	2/26/2021

^{1}H NMR (400 MHz, $CDCl_3$) of 3ib

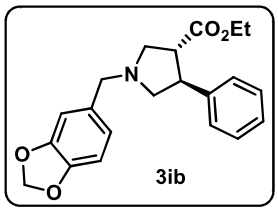

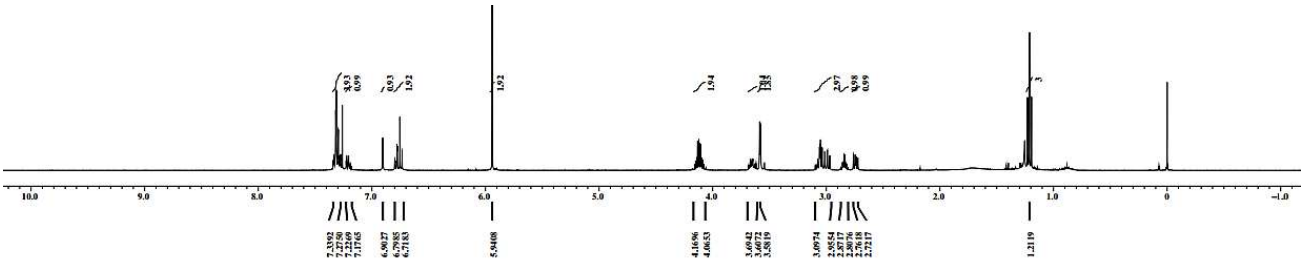

^{13}C {^{1}H} NMR (100 MHz, $CDCl_3$) of 3ib

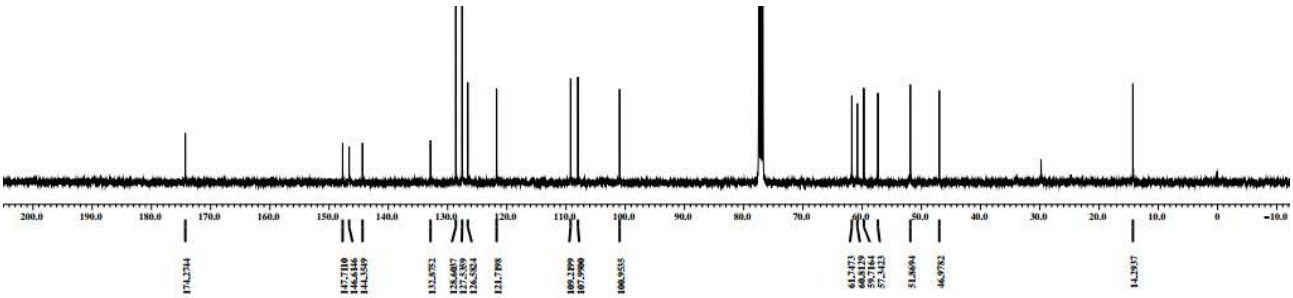

FTIR of 3ib

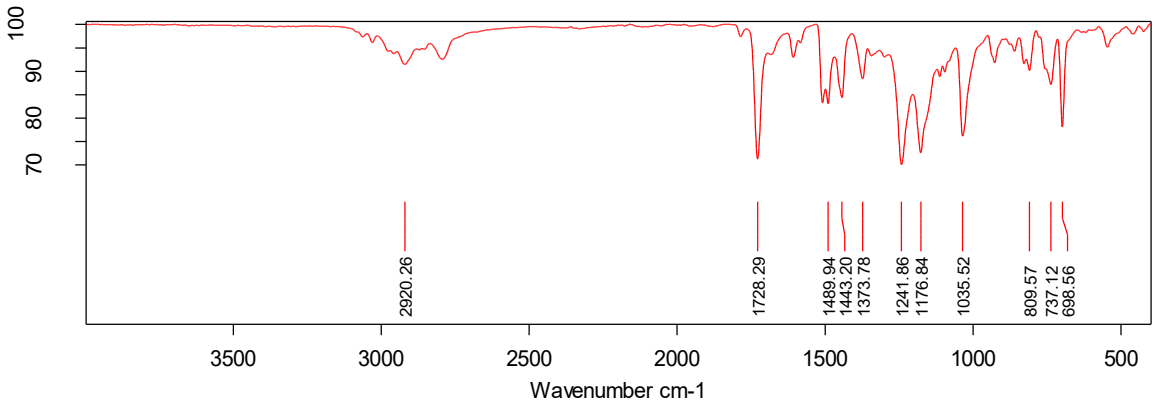

D:\FTIR DATA\DR. PRABAL\Rakesh\TPA.16	TPA	213	2/26/2021

^{1}H NMR (400 MHz, $CDCl_3$) of 3ab

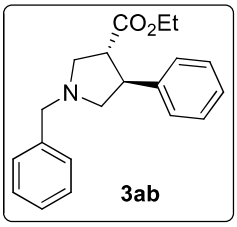

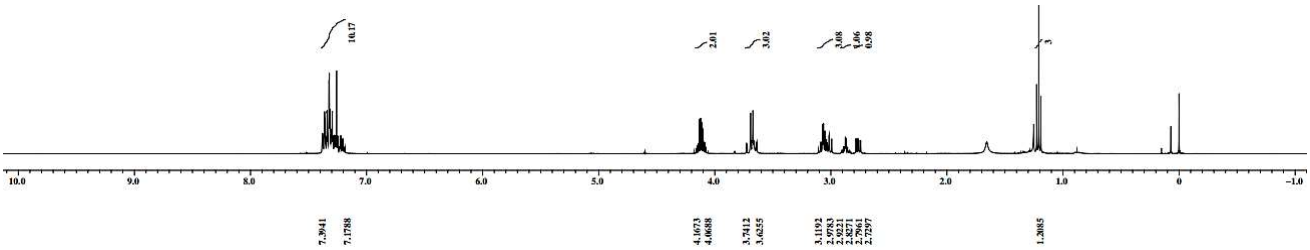

$^{13}C\{^1H\}$ NMR (100 MHz, $CDCl_3$) of 3ab

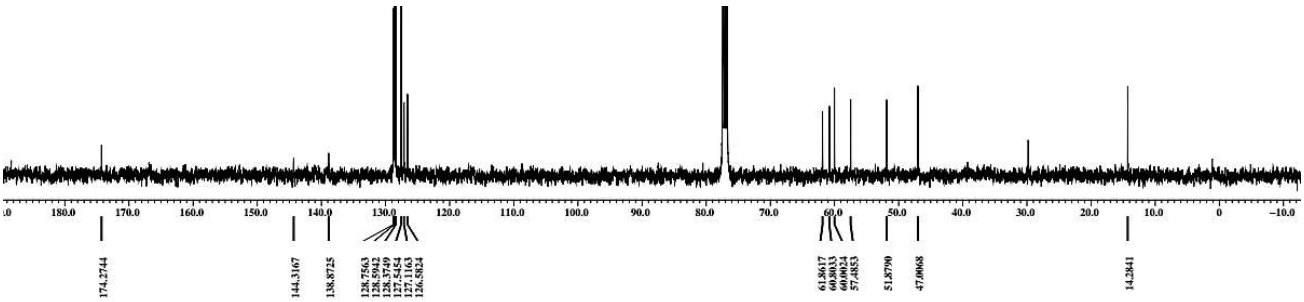

FTIR of 3ab

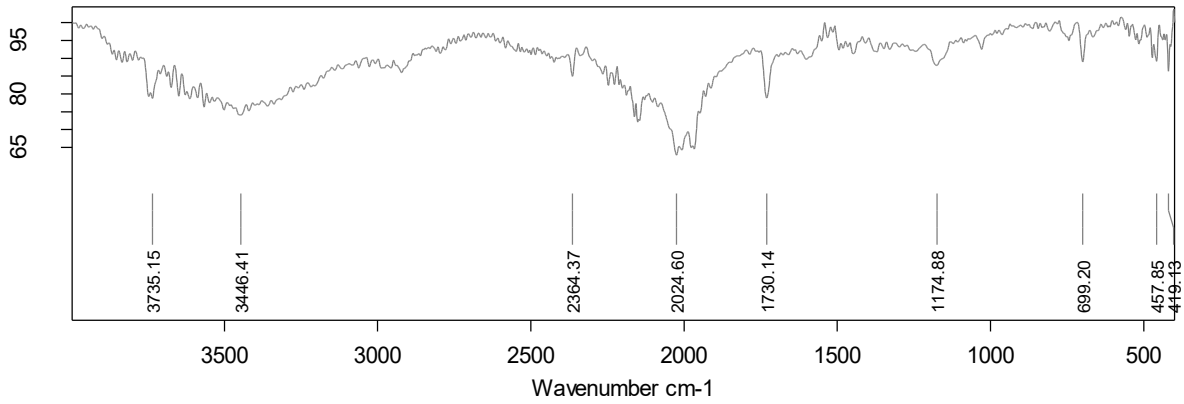

D:\FTIR DATA\DR. PRABAL\Rakesh\.7	180	LIQUID	3/12/2021

^{1}H NMR (400 MHz, $CDCl_3$) of 3ac

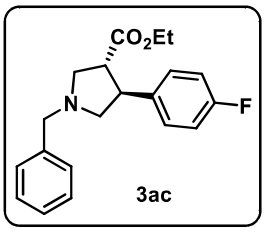

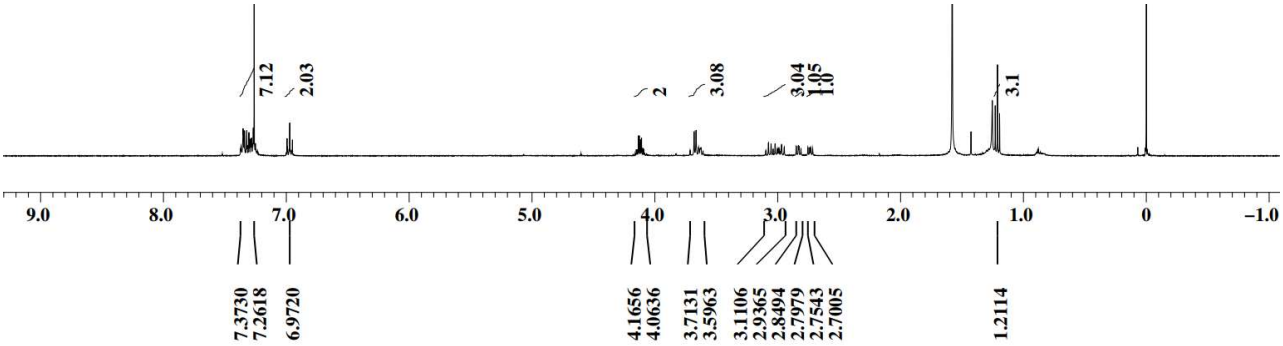

$^{13}C\{^1H\}$ NMR (100 MHz, $CDCl_3$) of 3ac

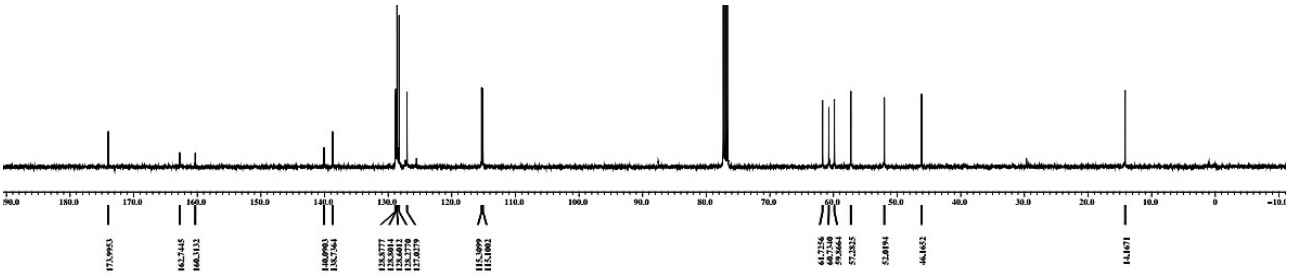

FTIR of 3ac

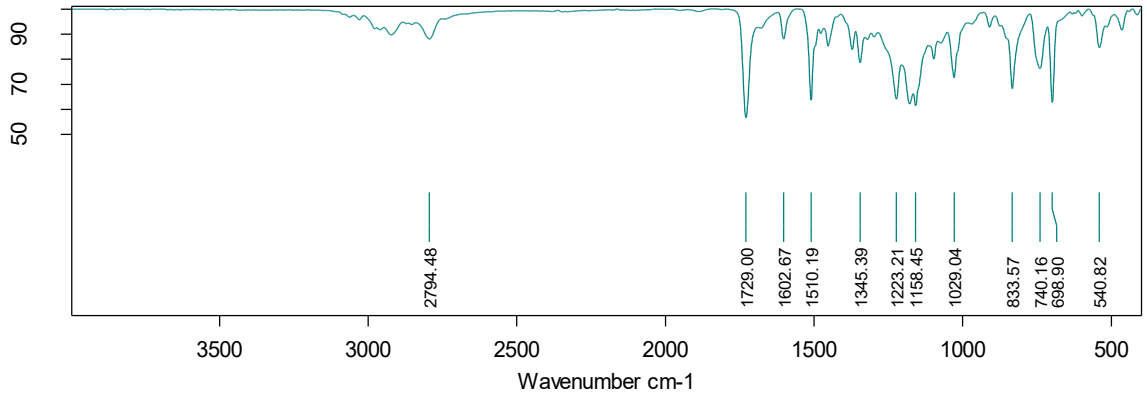

D:\FTIR DATA\DR. PRABAL\Rakesh\TPA.27	TPA	196	2/26/2021

^{1}H NMR (400 MHz, $CDCl_3$) of 3ad

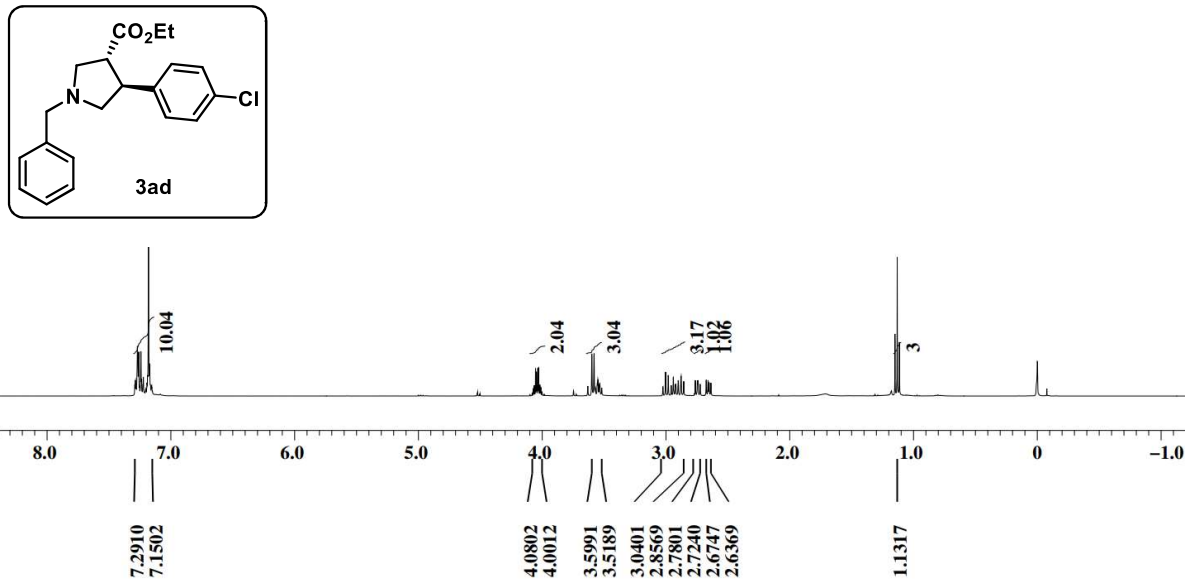

$^{13}C\{^1H\}$ NMR (100 MHz, $CDCl_3$) of 3ad

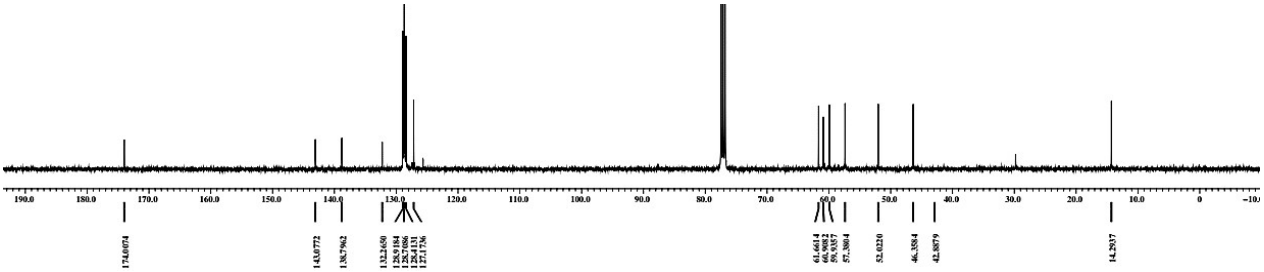

FTIR of 3ad

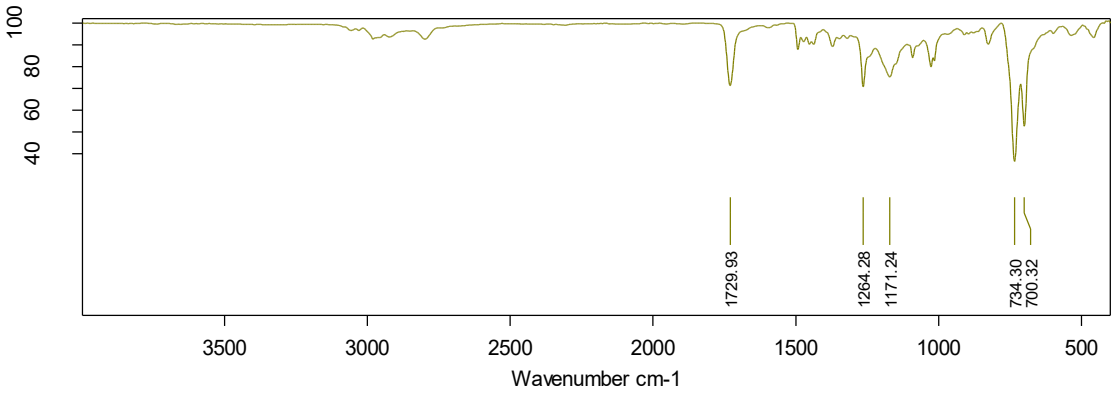

D:\FTIR DATA\DR. PRABAL\Rakesh\TPA.36	TPA	197	2/26/2021

^{1}H NMR (400 MHz, $CDCl_3$) of 3ae

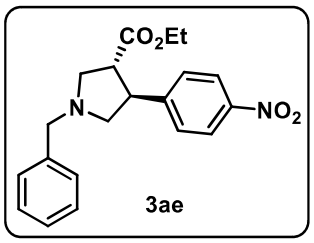

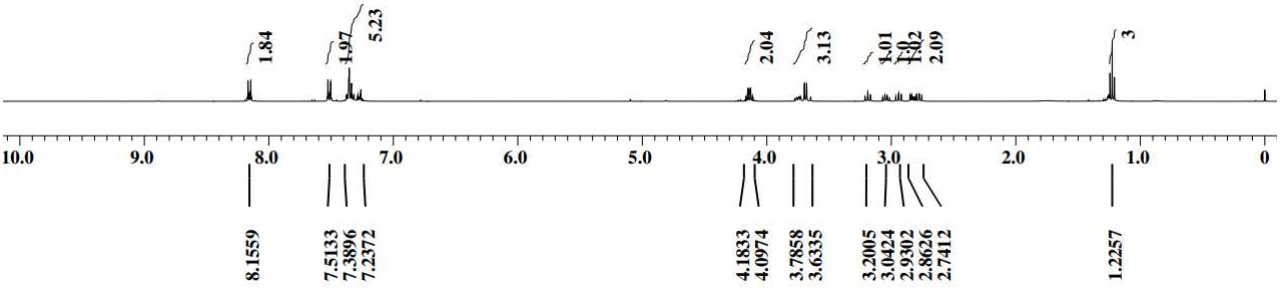

$^{13}C\{^1H\}$ NMR (100 MHz, $CDCl_3$) of 3ae

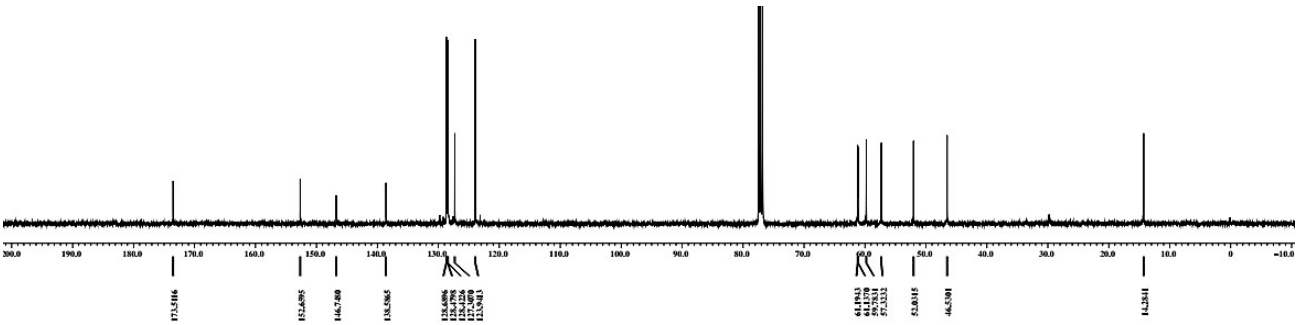

FTIR of 3ae

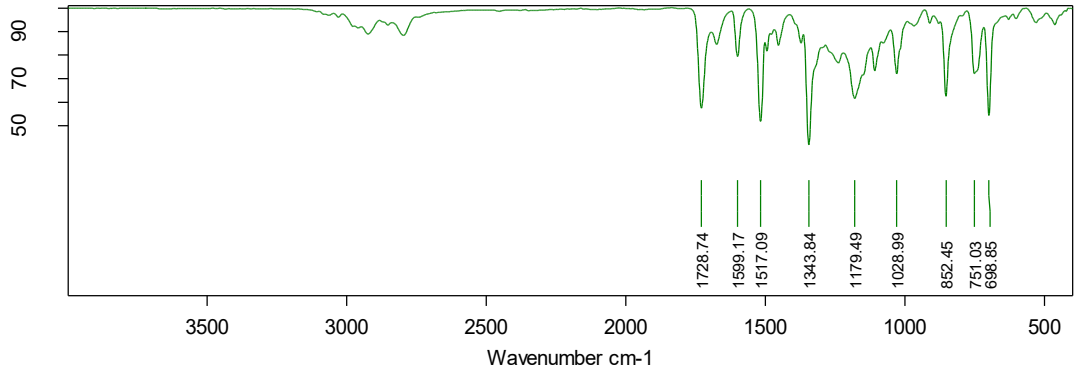

D:\FTIR DATA\DR. PRABAL\Rakesh\TPA.26	TPA	194	2/26/2021

^{1}H NMR (400 MHz, $CDCl_3$) of 3af

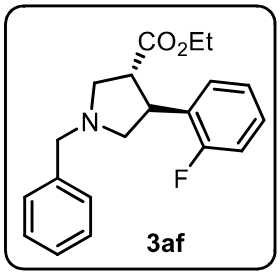

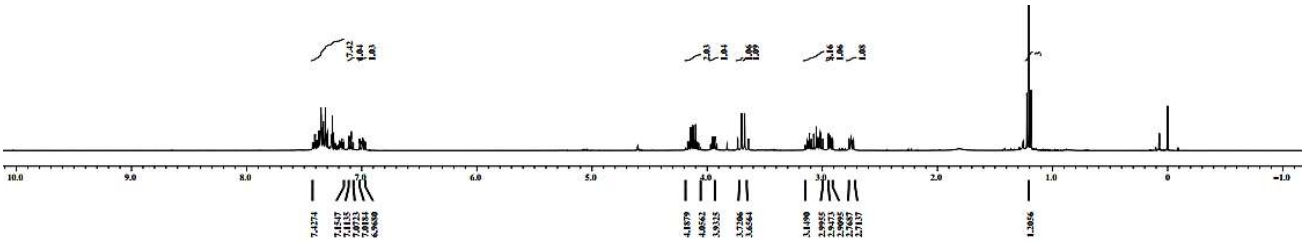

$^{13}C\{^{1}H\}$ NMR (100 MHz, $CDCl_3$) of 3af

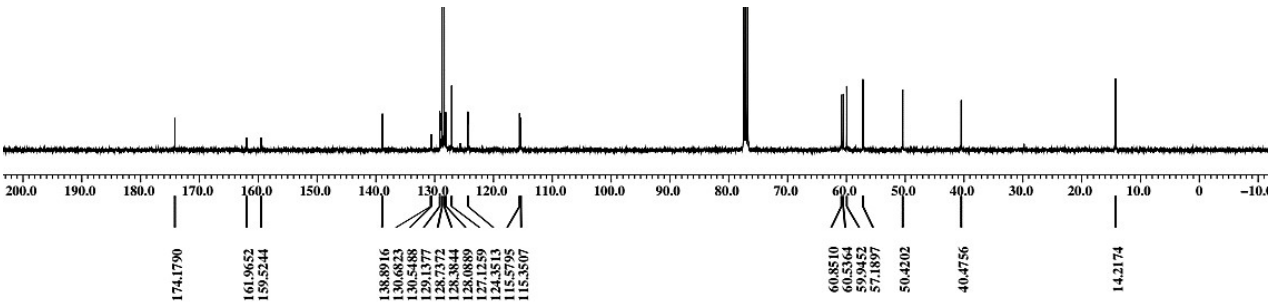

FTIR of 3af

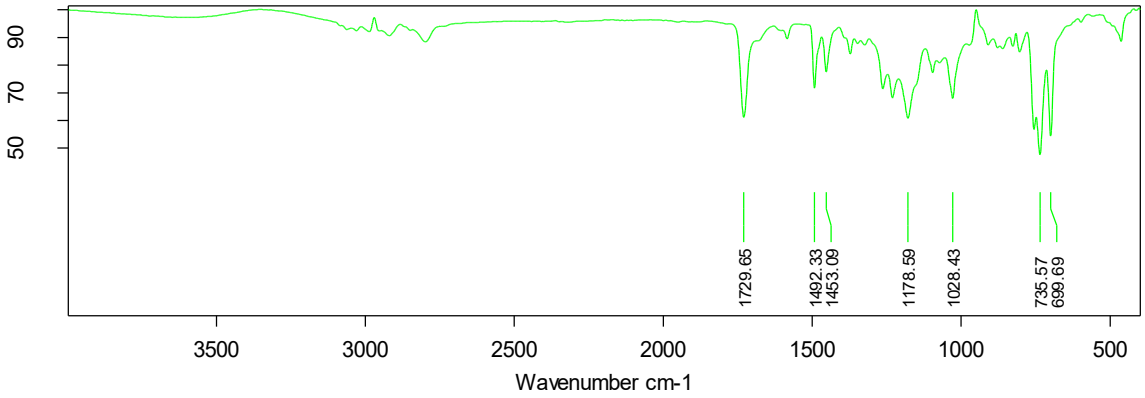

D:\FTIR DATA\DR. PRABAL\Rakesh\TPA.3	TPA	241	2/26/2021

^{1}H NMR (400 MHz, $CDCl_3$) of 3ag

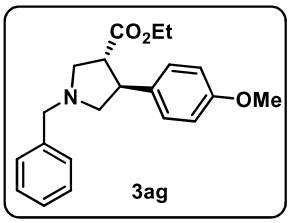

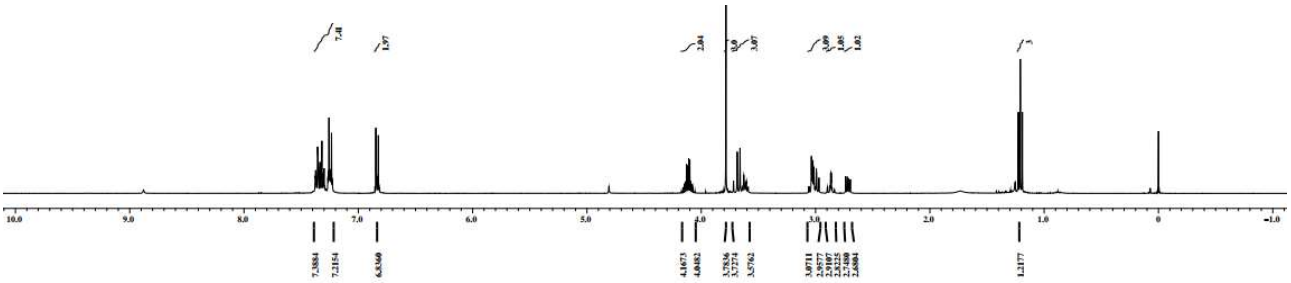

$^{13}C\{^1H\}$ NMR (100 MHz, $CDCl_3$) of 3ag

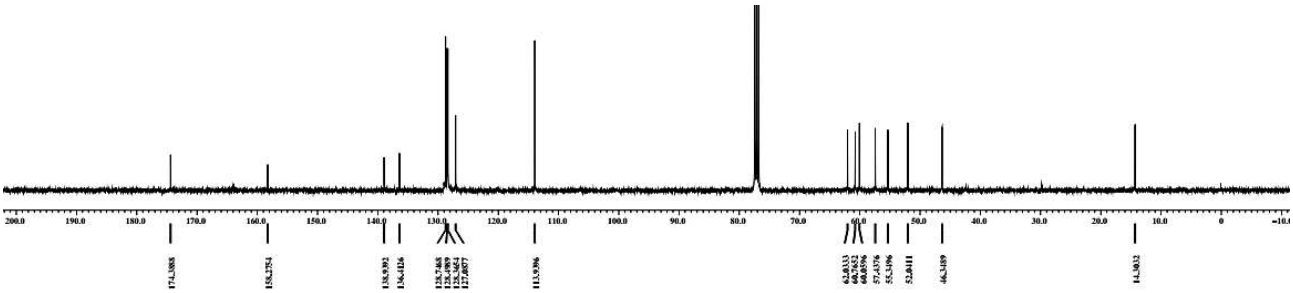

FTIR of 3ag

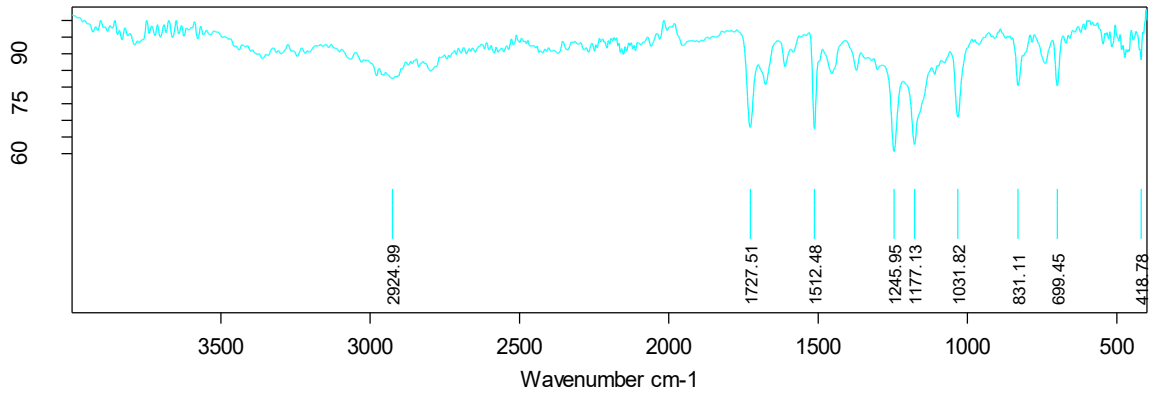

D:\FTIR DATA\DR. PRABAL\Rakesh\.4	217	LIQUID	3/12/2021

^{1}H NMR (400 MHz, $CDCl_3$) of 3ah

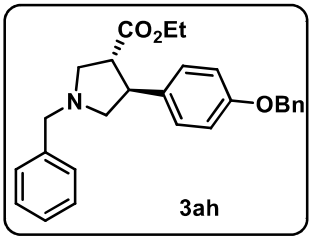

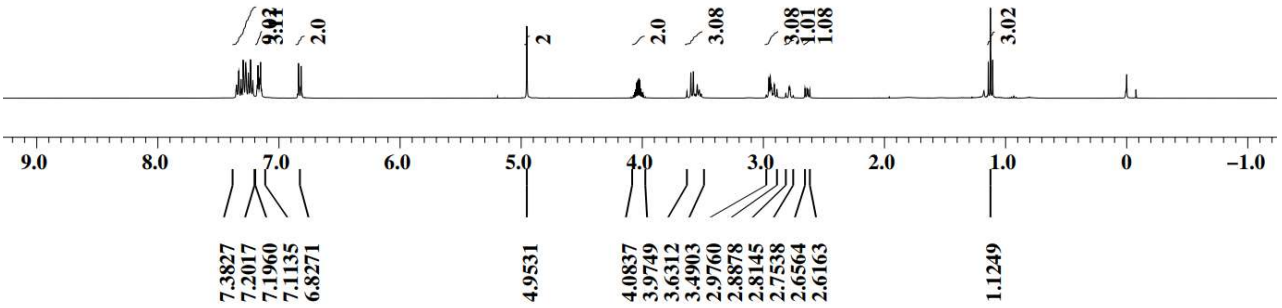

$^{13}C\{^1H\}$ NMR (100 MHz, $CDCl_3$) of 3ah

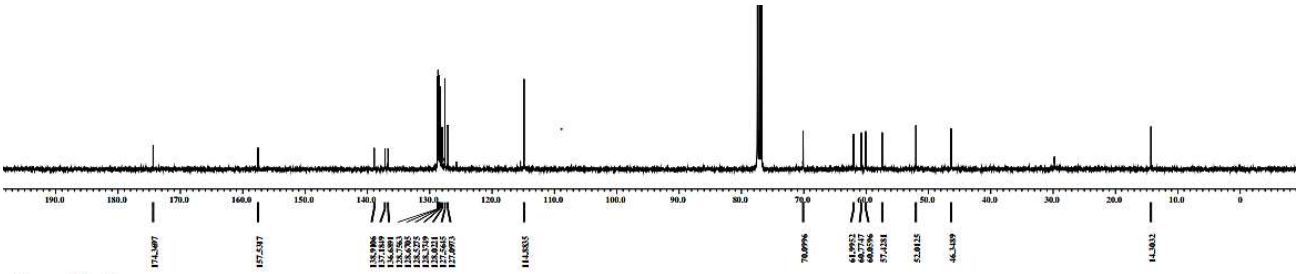

FTIR of 3ah

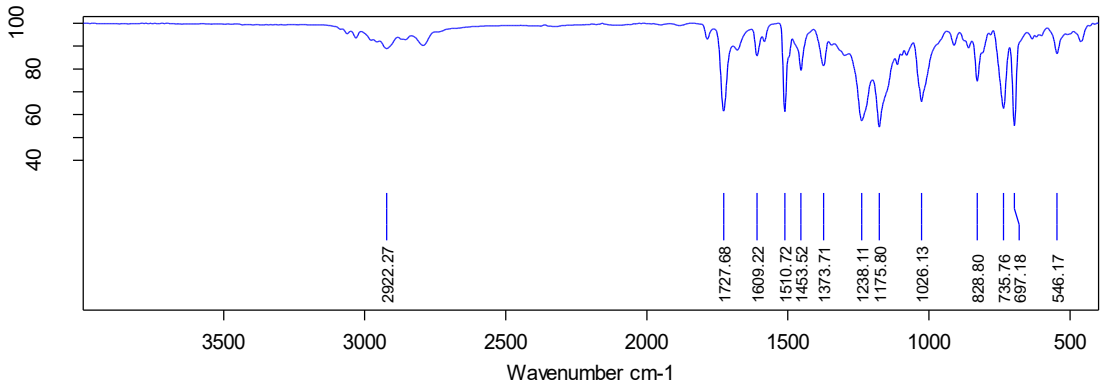

D:\FTIR DATA\DR. PRABAL\Rakesh\TPA.15	TPA	216	2/26/2021

^{1}H NMR (400 MHz, $CDCl_3$) of 3ai

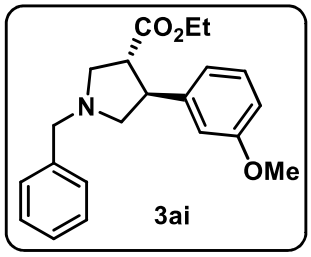

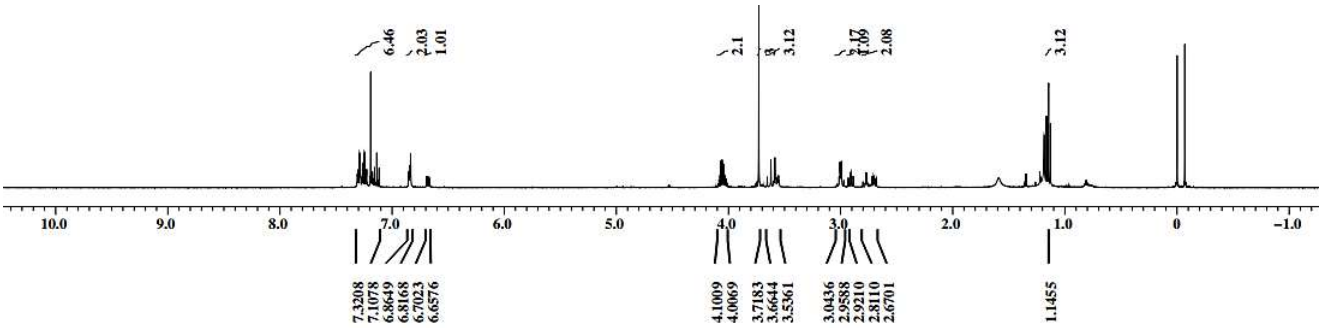

$^{13}C\{^1H\}$ NMR (100 MHz, $CDCl_3$) of 3ai

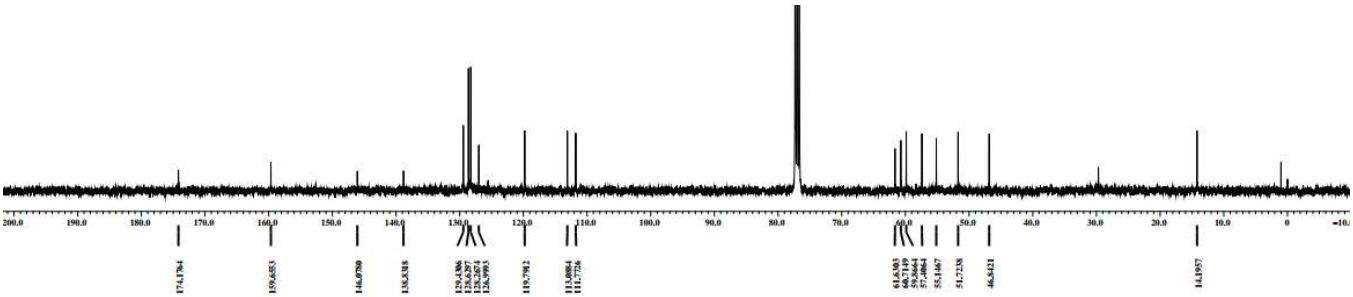

FTIR of 3ai

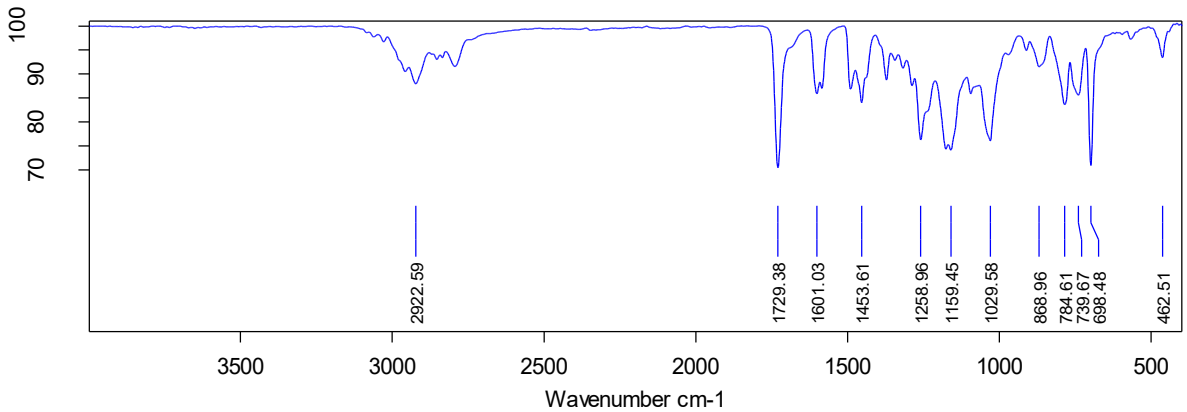

D:\FTIR DATA\DR. PRABAL\Rakesh\TPA.30	TPA	245	2/26/2021

^{1}H NMR (400 MHz, $CDCl_3$) of 3aj

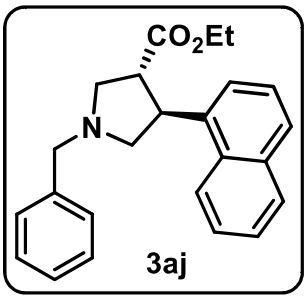

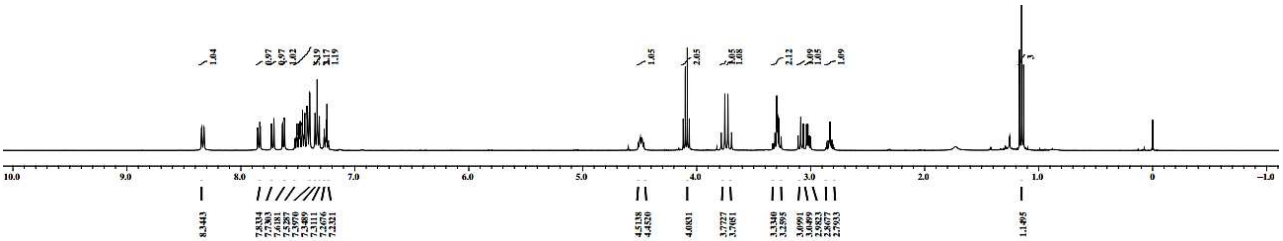

$^{13}C\{^1H\}$ NMR (100 MHz, $CDCl_3$) of 3aj

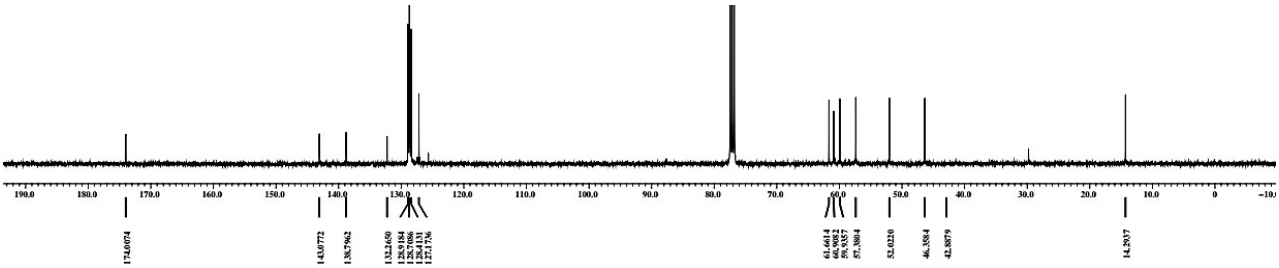

FTIR of 3aj

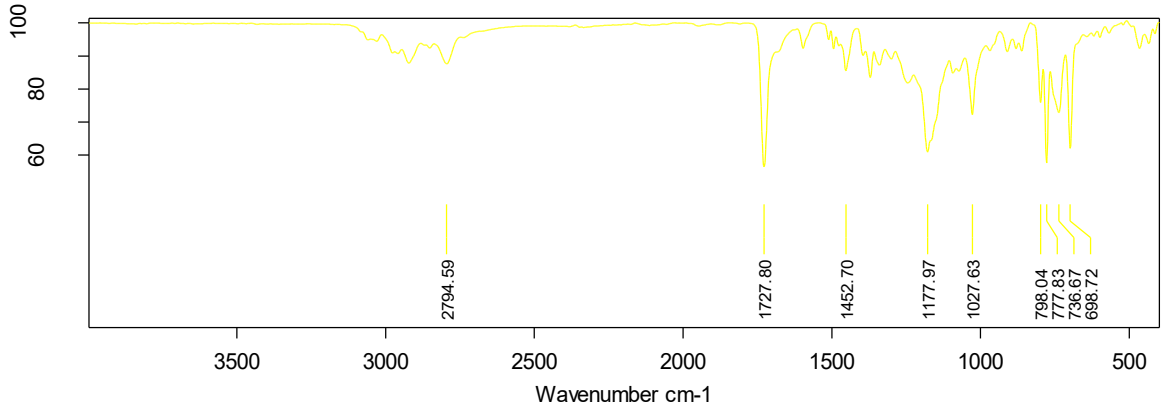

D:\FTIR DATA\DR. PRABAL\Rakesh\TPA.20	TPA	201-1	2/26/2021

^{1}H NMR (400 MHz, $CDCl_3$) of 3ak

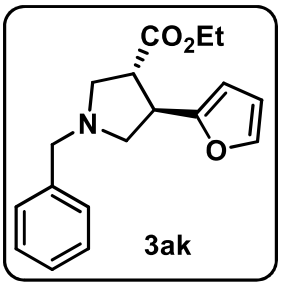

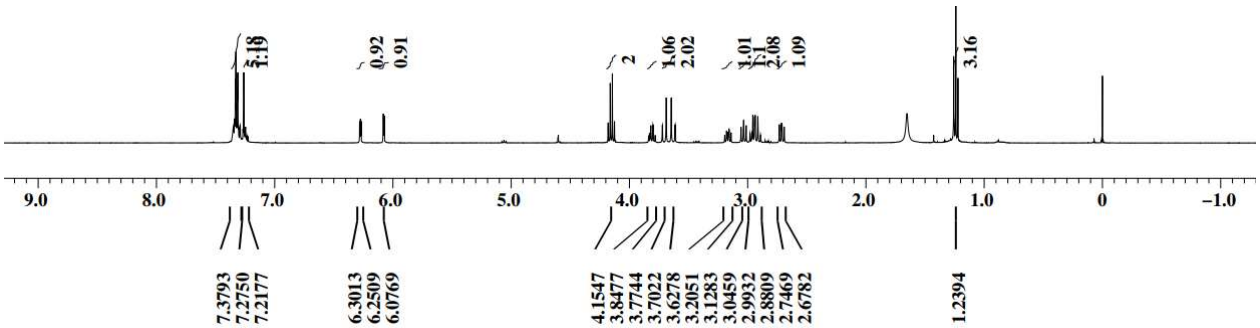

$^{13}C\{^1H\}$ NMR (100 MHz, $CDCl_3$) of 3ak

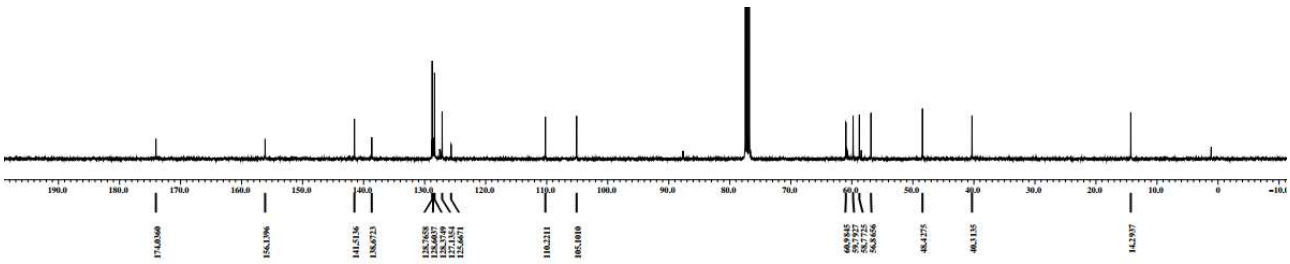

FTIR of 3ak

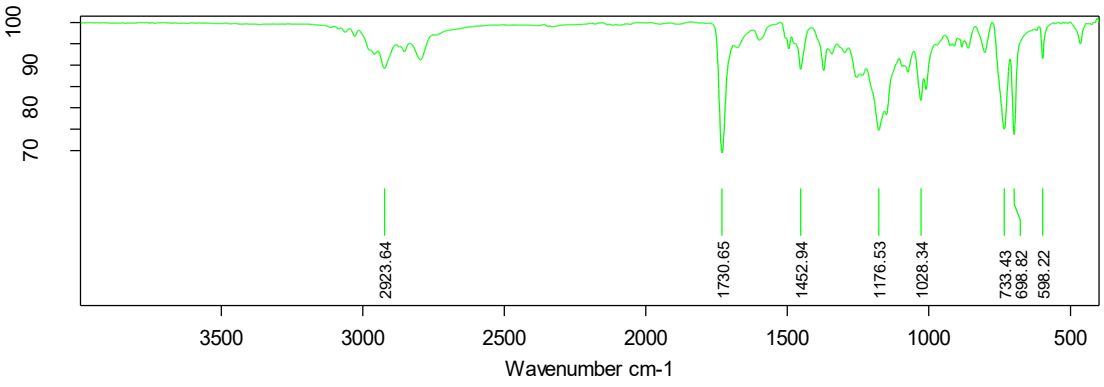

D:\FTIR DATA\DR. PRABAL\Rakesh\TPA.18	TPA	202	2/26/2021

^{1}H NMR (400 MHz, $CDCl_3$) of 3al

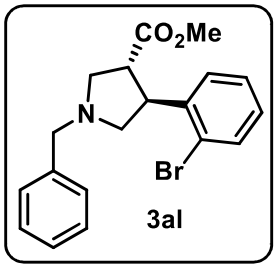

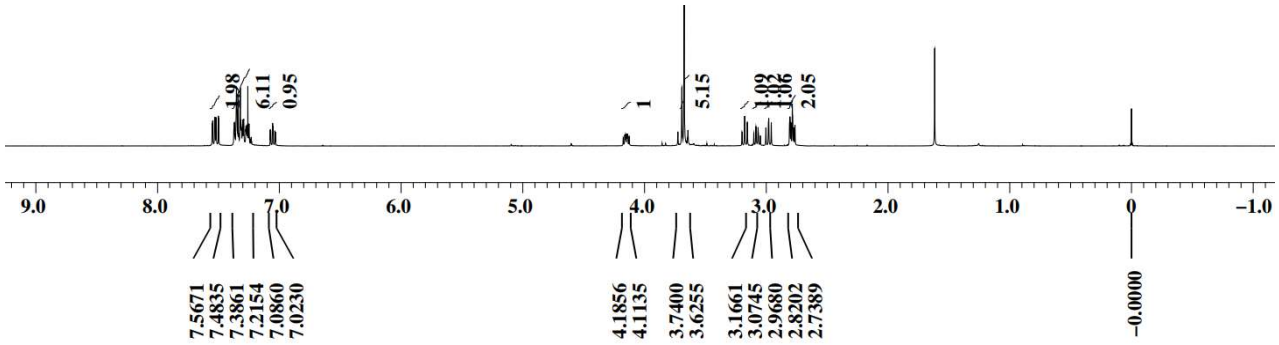

$^{13}C\{^1H\}$ NMR (100 MHz, $CDCl_3$) of 3al

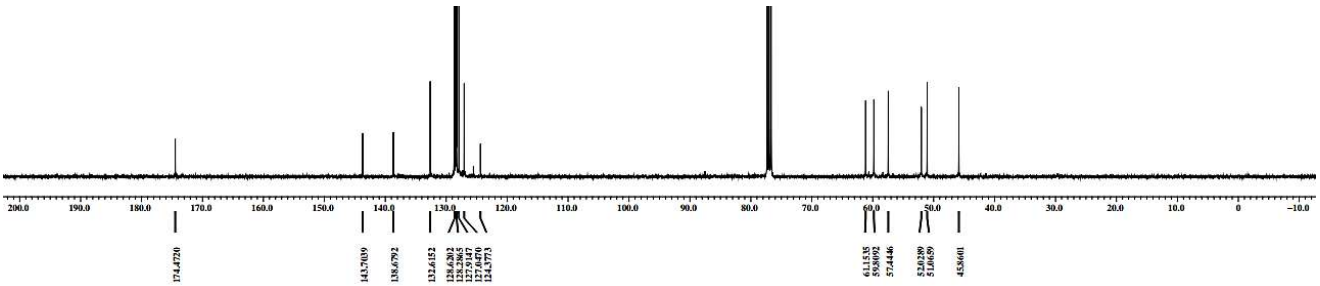

FTIR of 3al

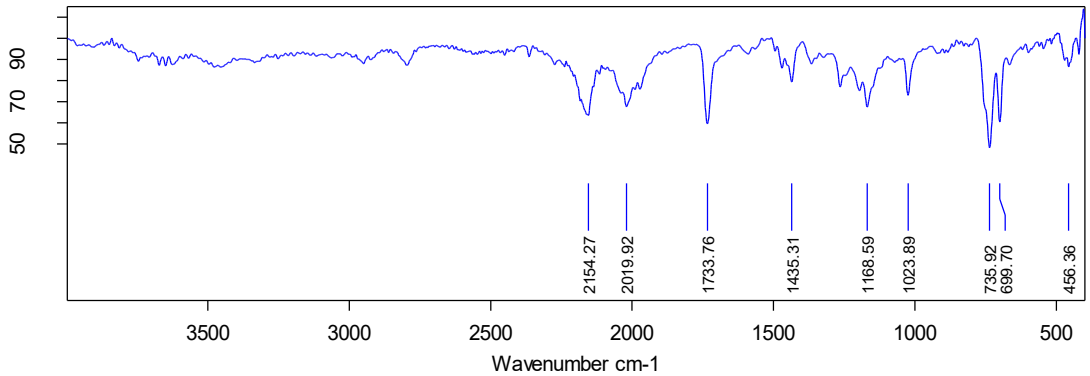

D:\FTIR DATA\DR. PRABAL\Rakesh\.0	248	LIQUID	3/12/2021

^{1}H NMR (400 MHz, $CDCl_3$) of 3am

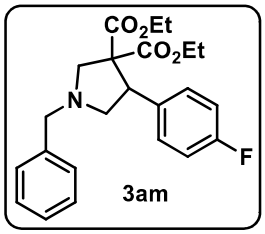

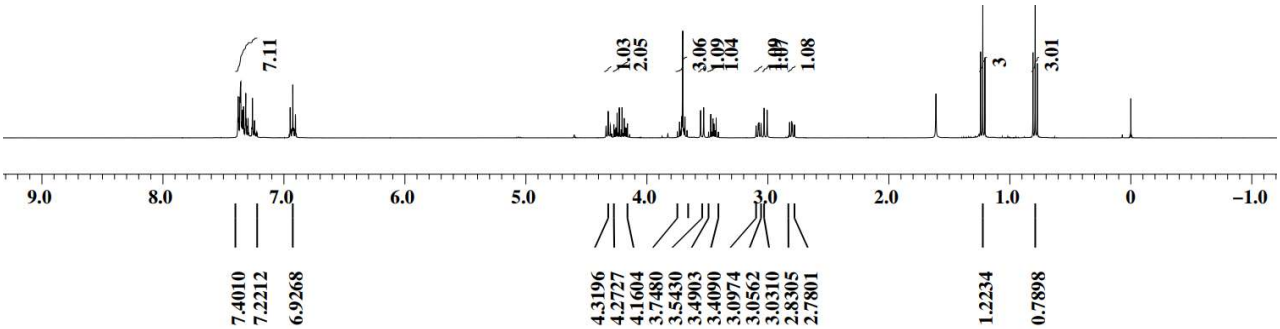

$^{13}C\{^1H\}$ NMR (100 MHz, $CDCl_3$) of 3am

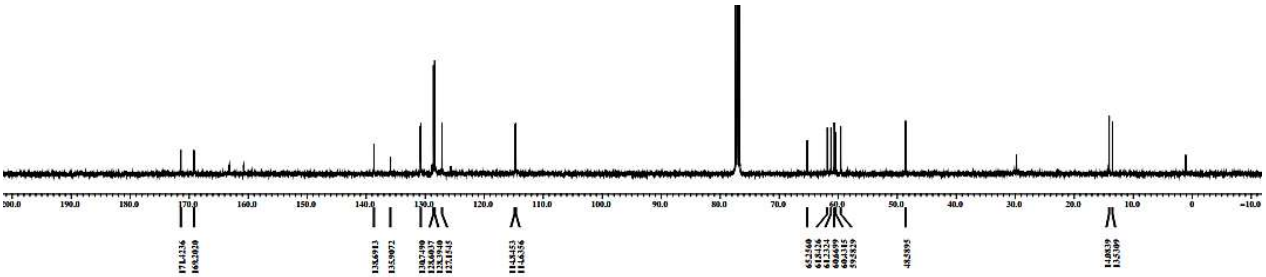

FTIR of 3am

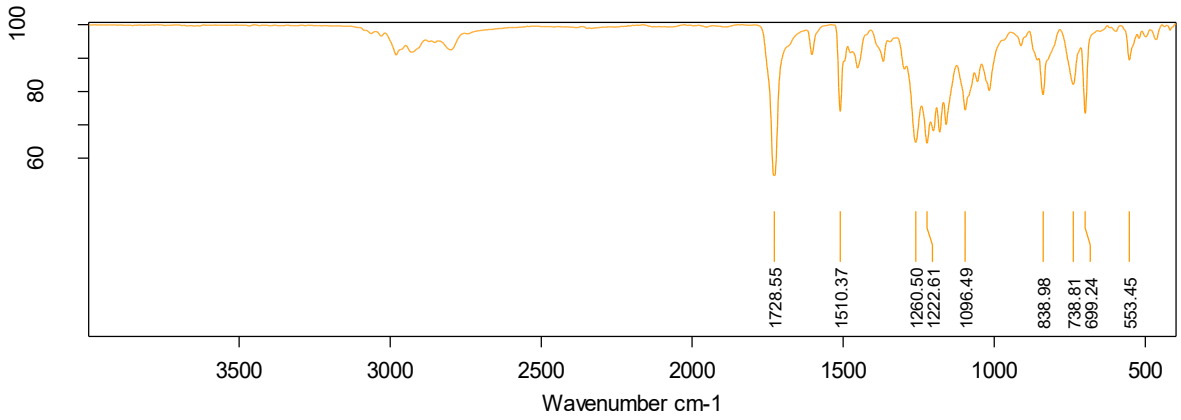

D:\FTIR DATA\DR. PRABAL\Rakesh\TPA.29	TPA	214	2/26/2021

^{1}H NMR (400 MHz, $CDCl_3$) of 3an

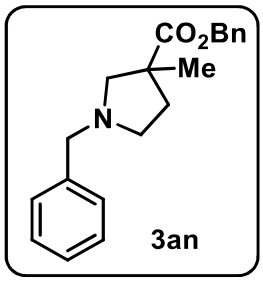

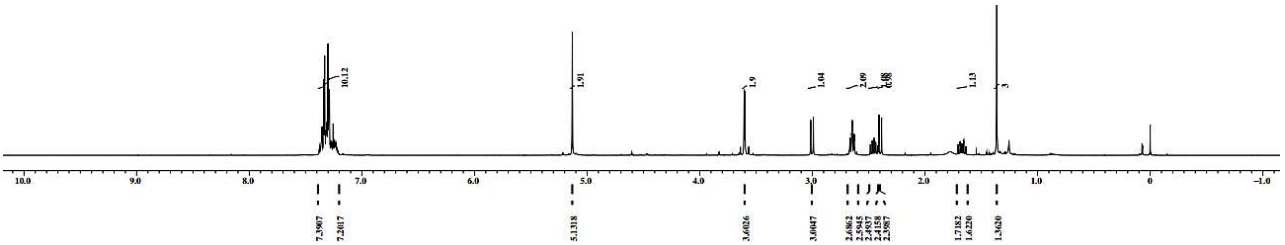

$^{13}C\{^1H\}$ NMR (100 MHz, $CDCl_3$) of 3an

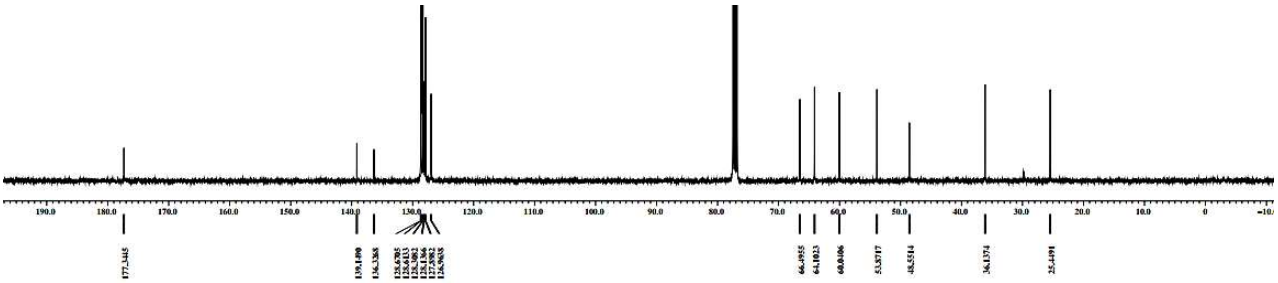

FTIR of 3an

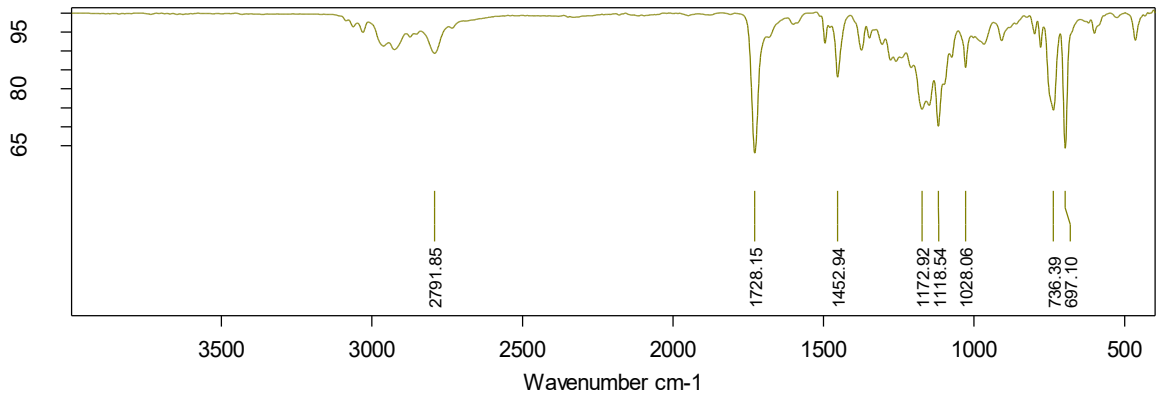

D:\FTIR DATA\DR. PRABAL\Rakesh\TPA.21	TPA	230-1	2/26/2021

^{1}H NMR (400 MHz, $CDCl_3$) of 3ao

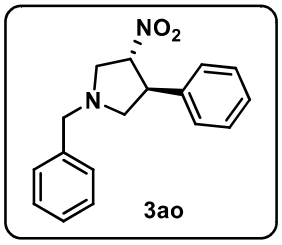

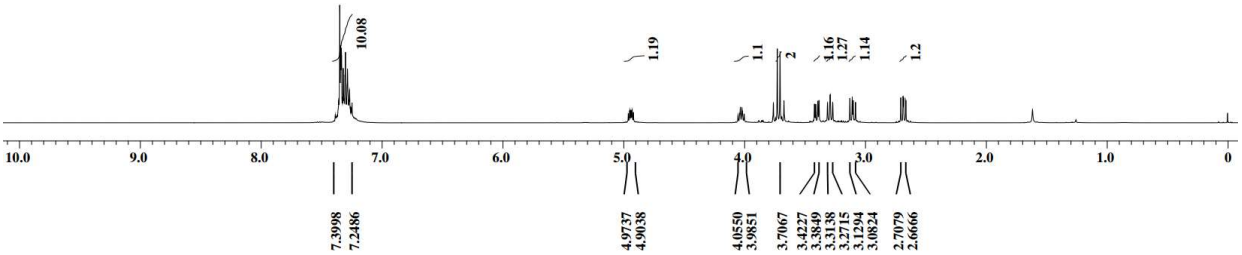

$^{13}C\{^1H\}$ NMR (100 MHz, $CDCl_3$) of 3ao

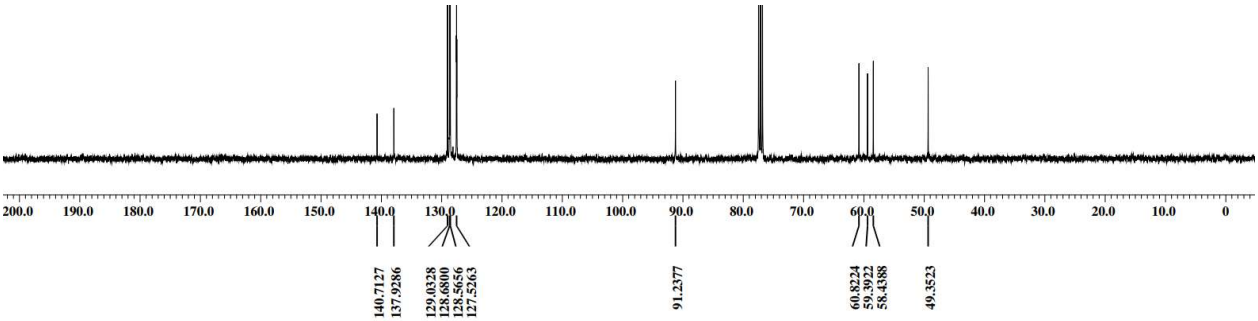

^{1}H NMR (400 MHz, $CDCl_3$) of 3ap

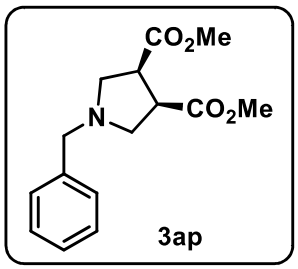

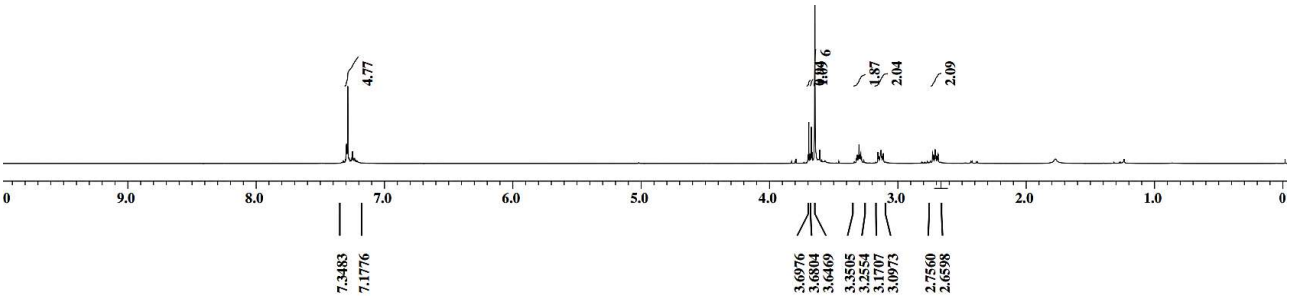

$^{13}C\{^{1}H\}$ NMR (100 MHz, $CDCl_3$) of 3ap

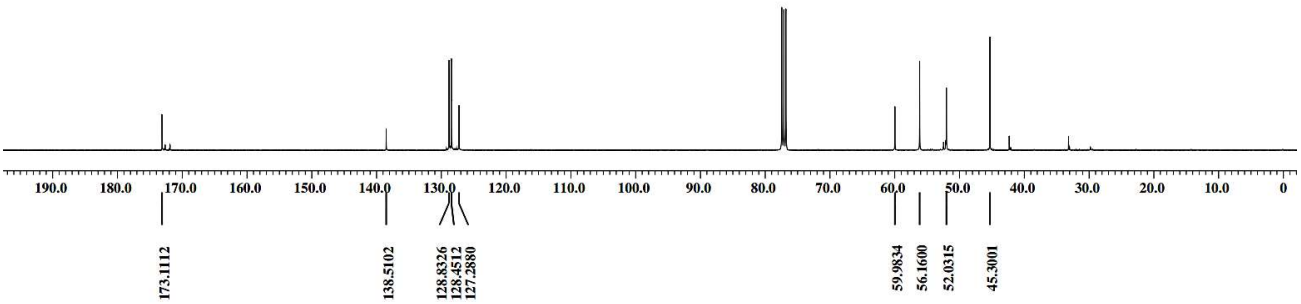

^{1}H NMR (400 MHz, $CDCl_3$) of 3aq

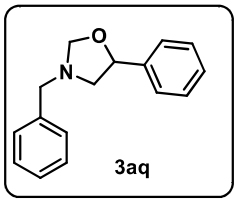

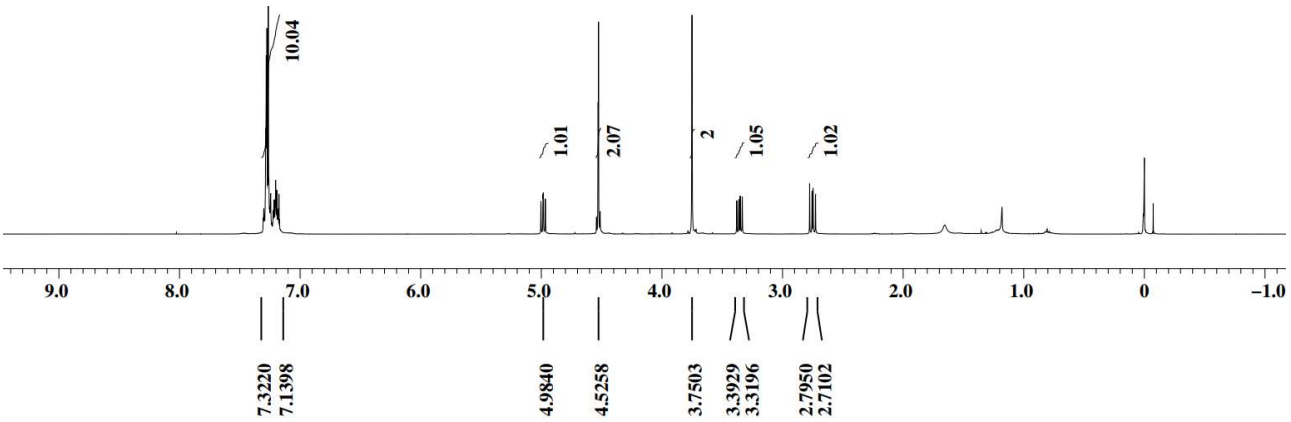

$^{13}C\{^{1}H\}$ NMR (100 MHz, $CDCl_3$) of 3aq

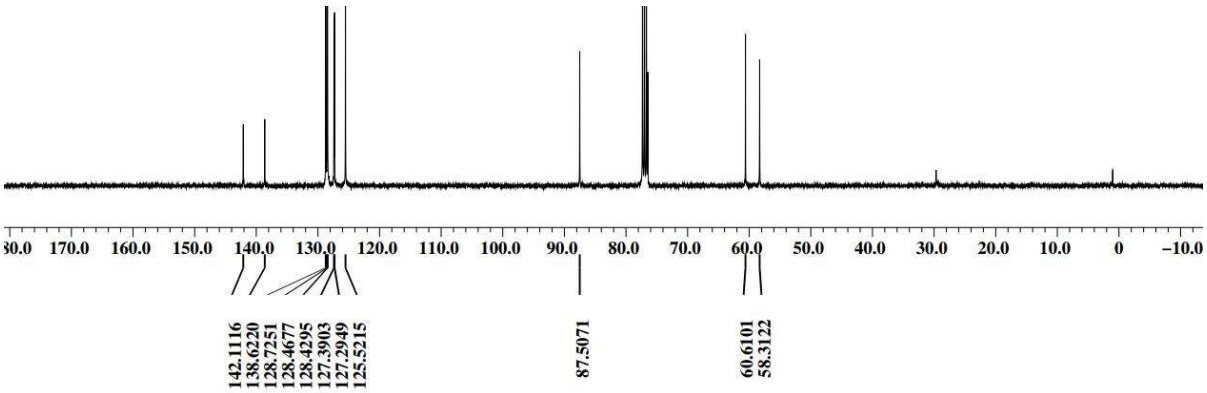

^{1}H NMR (400 MHz, $CDCl_3$) of 3ar

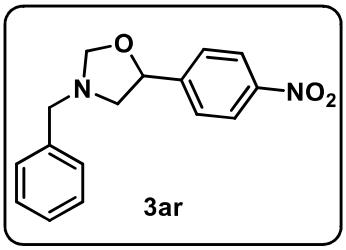

3ar

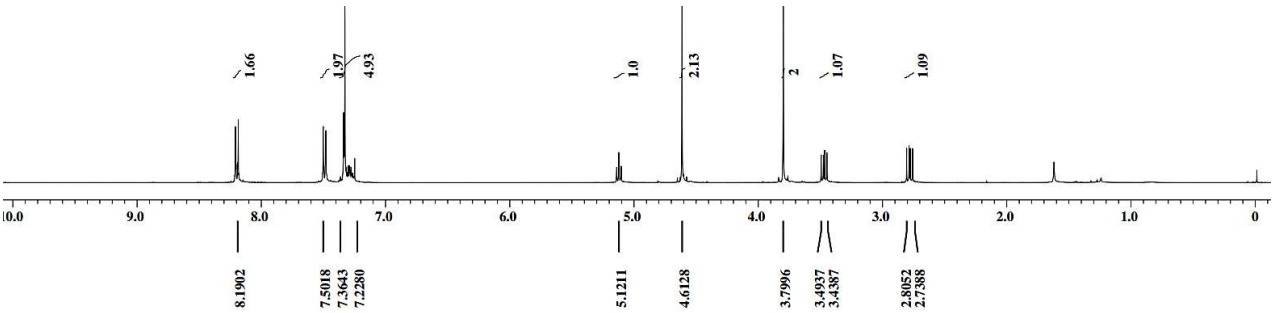

$^{13}C\{^1H\}$ NMR (100 MHz, $CDCl_3$) of 3ar

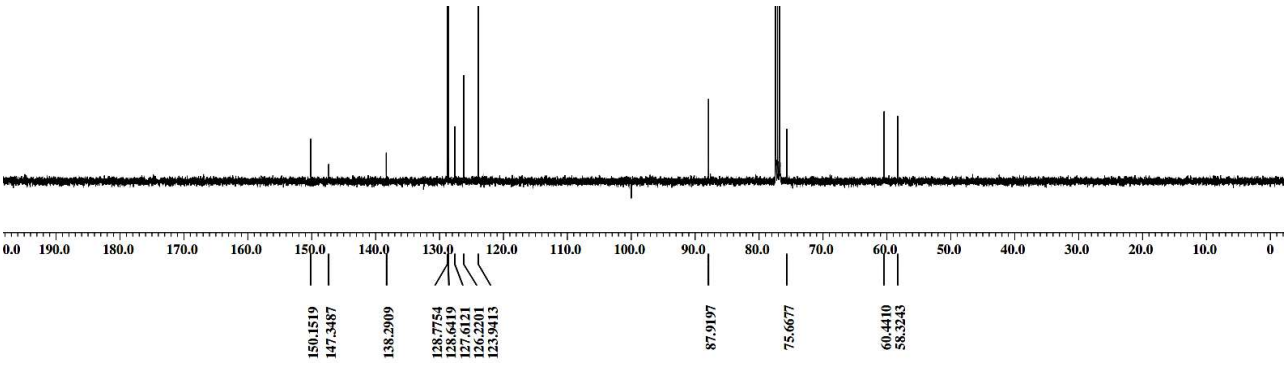

Chapter 3

Electrochemical Sulfinylation of Phenols with Sulfides: A Metal- and Oxidant-free Cross-Coupling for the Synthesis of Aromatic Sulfoxides

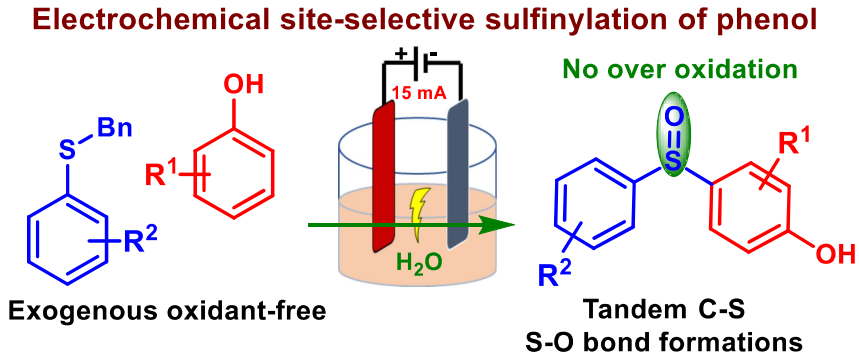

This work was published in *Chemical Communications* (A journal of *The Royal Society of Chemistry*). Please see citation "Kumar, R.; Taily, I. M.; Banerjee, P. *Chem. Commun.,* **2023***, 59,* 310-313.

3.1. Introduction

The C-H functionalization of arenes is an illustrious transformation in organic chemistry.[1] It has been extensively exploited over the past few decades to manipulate the molecules in order to directly approach the target scaffolds. However, the analogous sulfinylation has largely remained unexplored despite having societal importance as medicines (antihypertensive, antibacterial, antifungal, antiulcer) and herbicide.[2, 3] These structures are also featured in a plethora of natural products.[4] In addition, these sulfinates (existing in the S^{IV}-oxidation state) are well-established and reliable precursors or intermediates to diverse structurally and biologically significant functionalities existing in either the S^{IV} or S^{VI} oxidation states such as sulfones, sulfoximine, sulfinamides, sulfonate esters, sulfinate esters, sulfonyl halides, and others.[5] In spite of the tremendous importance, there are only a few trivial strategies disclosed so far to construct aromatic sulfoxides. Though the direct mono-oxidation of diaryl sulfides has been a straightforward approach,[6] the palladium-catalyzed cross-coupling of sulfenate anions by Poli and Madec[7], Walsh[8], Nolan[9], and Perrio[10] has emerged as the promising gateway to these aryl sulfoxides. The other approaches include a nucleophilic substitution of sulfinyl precursors with organometallic reagents and the Lewis acid-mediated Friedel-Craft-type electrophilic aromatic substitutions of sulfinyl chlorides.[11] The oxidation protocols suffer from employing hazardous peracid or hypervalent iodine oxidants in stoichiometric amounts, and the other requires metals and elevated temperatures to accomplish the transformation. Moreover, the over-oxidation of sulfide to sulfone is also encountered in the majority of cases. Consequently, the development of a practically green, oxidant-free, and sustainable strategy for the selective synthesis of sulfoxides still remains in high demand. In 2017, the König group demonstrated the visible light-mediated cross-coupling of sulfinamides and peroxodisulfates toward the synthesis of aryl sulfoxides [Scheme 3.1.1(a)].[2] Followed by this, the Lee[12] and Wei groups[13] independently disclosed the cross-coupling of thiols and aryldiazo derivatives for their construction of sulfoxides in 2018 and 2019, respectively [Scheme 3.1.1(b-c)]. Very recently, in 2022, Baran *et al.* reported Ni-catalyzed electrochemical sulfinylation of aryl halides with SO_2.[13b]

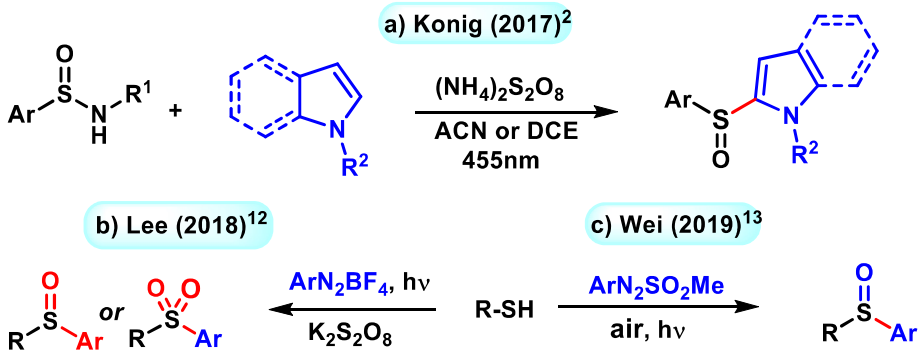

Scheme 3.1.1. Photoinduced cross coupling reactions to access aryl sulfoxides.

The renewed interest in incorporating sustainability to promote various challenging bond-making and breaking transformations has directed organic chemists toward the implementation of environmentally benign alternative tools. In recent years, organic electrochemistry has emerged as a promising sustainable alternative from this perspective.[14] Substantial attainments have been realized in this field by various research groups via anodic oxidation[14], and a handful of protocols for sulfoxide formation exploiting the

same strategy have also been demonstrated. In 2021, Wirth and co-workers developed the flow electrosynthesis of sulfoxides and sulfones by oxidizing sulfides.[15] Very recently, Zhang group also established scalable selective oxidation of sulfides to sulfoxides using NaCl as a supporting electrolyte as well as a redox mediator.[16] Although both the Wirth and Zhang methodologies involved the anodic oxidation of pre-constructed aryl sulfides. However, to the best of our knowledge, the direct electrochemical synthesis of aryl sufoxides via intermolecular cross-coupling of arenes and sulfides has not been revealed yet. Motivated by our recent reports demonstrating the site-selective functionalization of phenol towards the direct synthesis of paracetamol[17a] and other arene oxidation-mediated functionalizations[17b], we envisioned the direct synthesis of aryl sulfoxides via oxidative cross-coupling of phenols with sulfides (Scheme 3.1.2).

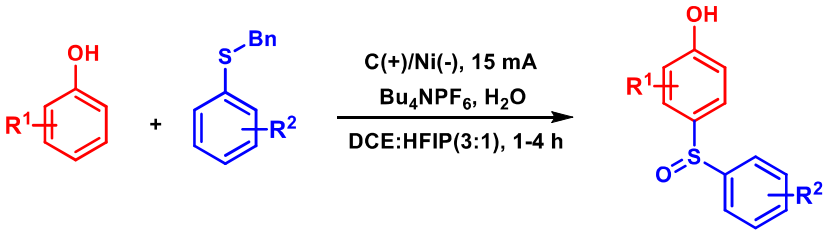

Scheme 3.1.2. Our idea for electrochemical sulfinylation of phenols.

3.2 Result and Discussion

Initially, our study commenced with the reaction of 2-ethylphenol **1a** and thiophenol under electrochemical conditions employing Bu_4NBF_4 as a supporting electrolyte in an undivided cell equipped with graphite anode and nickel cathode. The mixture was electrolyzed in DCE at a constant current of 3 mA. Under these conditions, the expected sulfoxide product was not obtained; however, the dimer of the thiophenol was encountered (Table 3.2.1, entry 2). Further, the application of higher currents (5, 10 mAs) rendered the same dimer. Next, several attempts with various disulfides were made instead of thiols as the sulfur source. Among them, diphenyl disulfide failed to render the desired product (Table 3.2.1, entry 3). Interestingly, 1,2-bis(4-methoxyphenyl)disulfane successfully furnished the expected product, albeit in low yield (Table 3.2.1, entry 4). Next, we tried other reaction parameters, current, supporting electrolytes, etc., but all the variations failed to provide any promising results. So, we envisaged that the replacement of disulfides with alkyl-protected thiols could probably address the problem. Henceforth, we attempted the reaction with methyl(phenyl)sulfane. Unfortunately, a complex mixture was obtained in this case (Table 3.2.1, entry 5). Further, we investigated the role of protecting group and anticipated that the installation of a good leaving group would be a potential choice. To test the hypothesis, the methyl group was replaced with the benzyl group and gratifyingly the desired product **3a** could be delivered in 40% yield with a high para-regioselectivity. However, an increase in the resistance of the reaction was observed with time (potential was rising to 6-7 V). Delightfully, the problem of the high resistance was rectified by employing a mixture of DCE and HFIP in the ratio of 3:1. With this setup, the screening of various supporting electrolytes was carried out, and Bu_4NPF_6 served as a better electrolyte with a 60% yield (Table 3.2.1, entry 1). Next, other supporting electrolytes such as Bu_4NBF_4 and Et_4NPF_6 resulted in diminished yield (Table 3.2.1, entries 6-7). The use of electrolytes like Bu_4NBr, Bu_4NI, and Bu_4NCl having halogen counter anion delivered the complex mixtures (Table 3.2.1, entry 8). Next, the effect of various solvents was also checked and different solvents or a mixture of solvents like DCE and MeOH resulted in lower

Table 3.2.1. Optimization of the reaction conditions

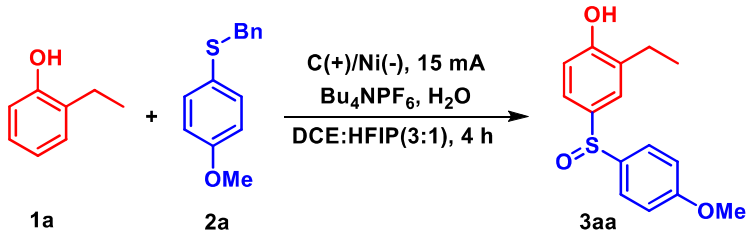

1a 2a 3aa

entry	Variation from standard conditions[a]	Yield[b]
1	none	60
2	Thiophenol instead of **2a**	30[d]
3	PhSSPh instead of **2a**	n.r
4	(*p*-OMe)PhSSPh(*p*-OMe) instead of **2a**	35
5	Me instead of Bn as protecting group	c.m
6	Bu_4NBF_4 instead of Bu_4NPF_6	40
7	Et_4NPF_6 instead of Bu_4NPF_6	46
8	Bu_4NBr, Bu_4NI, Bu_4NCl, instead of Bu_4NPF_6	c.m.
9	DCE instead of DCE: HFIP	48
10	MeOH instead of DCE: HFIP	35
11	THF and DCM: HFIP instead of DCE: HFIP	n.r.
12	Graphite as both electrodes	45
13	10 mA instead of 15 mA	40
14	Without electricity	n.r.

[a]Reaction conditions: **1a** (0.25 mmol), **2a** (0.25 mmol), Bu_4NPF_6 as an electrolyte (0.49 mmol), DCE: HFIP (3:1) as the solvent (4 mL), 15 mA constant current, graphite anode, nickel cathode, undivided cell, rt. [b]Isolated yield, [c] 0.5 mL of H_2O was added, [d]dimer of thiol formed, n.r. = no reaction. c.m. = complex mixture.

yields (Table 3.2.1, entries 9-10). Furthermore, employing THF and DCM: HFIP (3:1) proved detrimental to the transformation (Table 3.2.1, entry 11). Amongst a set of electrodes, graphite as anode and nickel as cathode was found to be the best combination, while the replacement of nickel cathode with graphite resulted in a compromised yield (Table 3.2.1, entry 12). Furthermore, diminished yields were also obtained when the current was decreased from 15 mA (Table 3.2.1, entry 13). The role of electricity was ascertained by the control experiment (Table 3.2.1, entry 14).

With the optimal reaction conditions in hand, the generality of the protocol was next evaluated, and a series of phenol and sulfide derivatives were screened, as depicted in schemes 3.2.1 and 3.2.2. Initially, the *ortho*-substituted phenols bearing electron-donating groups like methyl, ethyl, isopropyl, *tert*-butyl, and benzyl were tested. Delightfully, all the precursors furnished the desired aryl sulfoxide product **3aa**-**3fa** in moderate yields.

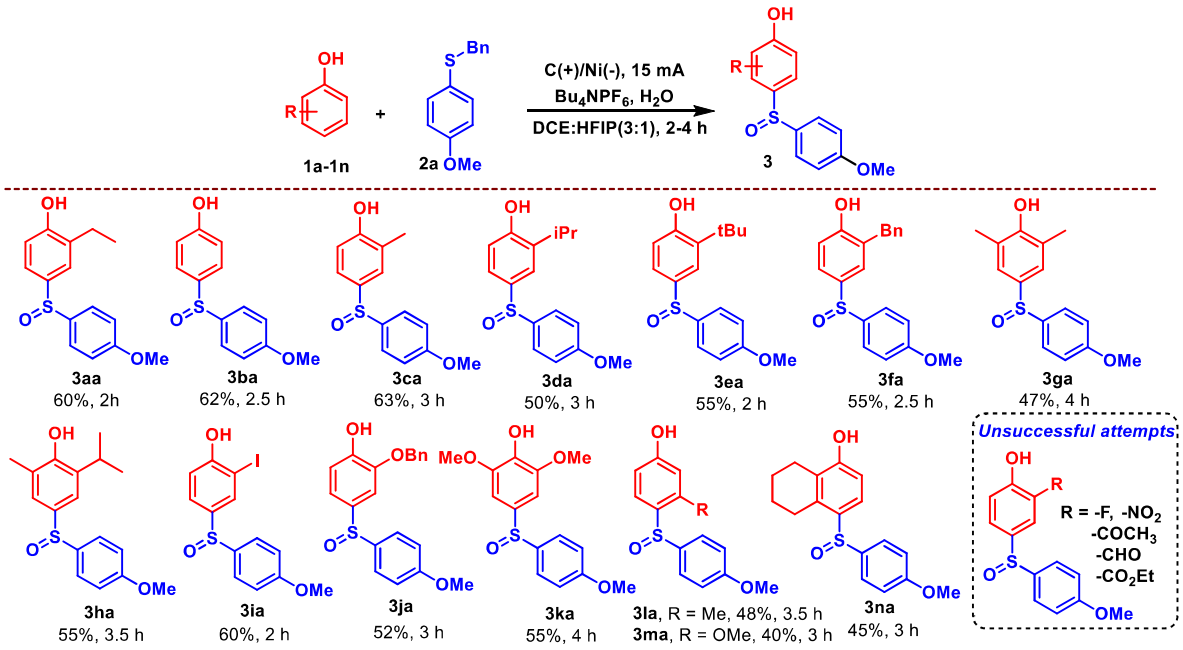

Scheme 3.2.1. Substrate scope for phenols.

Furthermore, substitution on both the *ortho* positions, such as 2,6- dimethylphenol and 2-isopropyl-6-methyl phenol, also render the products **3ga** and **3ha** in 47% and 55%, respectively. Halogen substituted phenol was also found compatible with the methodology, and the desired product **3ia** was isolated in 60% yield. Next, the alkyloxy (methoxy and benzyloxy) substituents at the *ortho* position of phenol furnished the anticipated sulfoxide derivatives **3ja** and **3ka** in 52% and 55% yield, respectively. However, electron withdrawing groups like fluoro, nitro, -CHO at *ortho*-positon of phenol failed to deliver the desired products. Subsequently, the substitution on *meta*-position of phenol was screened. Pleasingly, it was observed that methyl, and methoxy groups on *meta*-position were well tolerated and successfully delivered the desired products **3la** and **3ma** in 48% and 40%, respectively. Further, the phenol derivative 5,6,7,8-tetrahydronaphthalen-1-ol also responded positively to the transformation and procured the respective product **3na** in 45% yield (Scheme 3.2.1). Unfortunately, the phenol ring bearing electron withdrawing groups failed to deliver the desired product.

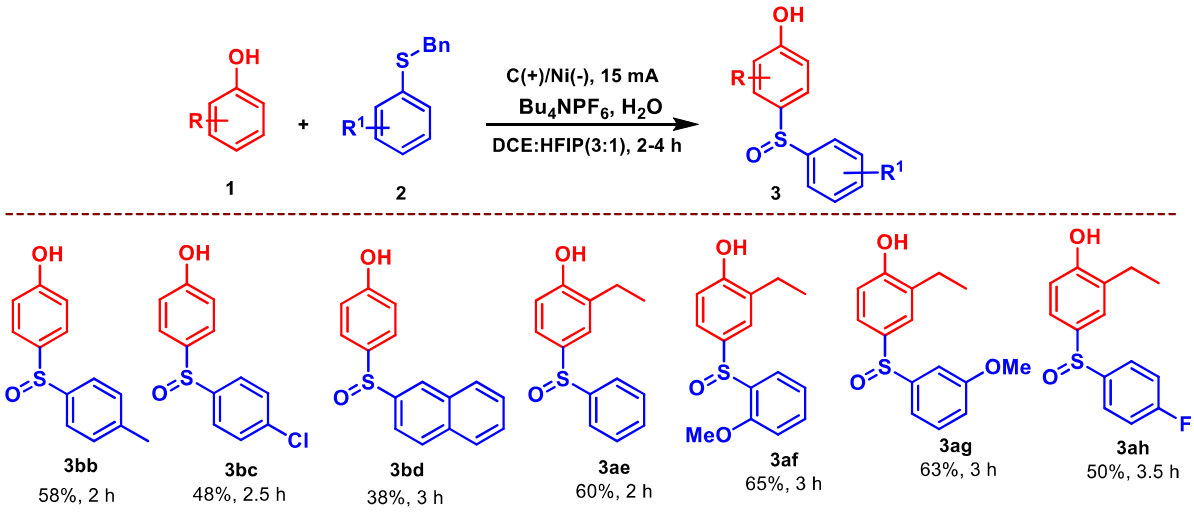

Scheme 3.2.2. Substrate scope for sulfides.

After phenol derivatives, the substrate scope was further extended with respect to the sulfide precursor (Scheme 3.2.2). The electron-donating groups like methyl and methoxy at different positions of the aryl ring of sulfide (**2b, 2f,** and **2g**) bestowed the anticipated product **3bb**, **3af,** and **3ag** in 58%, 65%and 63% yield, respectively. Also, the electron-withdrawing groups like *chloro* and *fluoro* at *para* position conferred the desired product **3bc** and **3ah** in 48% and 50%, respectively. Besides the aryl ring, the naphthyl ring substituted sulfide **2d** was also found viable for transformation and afforded the corresponding sulfoxide **3bd** in 38% yield. Even the phenyl substituted sulfide furnished the desired product **3ae** in 60% yield. Further, the substituents on *ortho*, *meta* and *para* position of aryl ring of sulfides also deliver the corresponding sulfoxide product **3af-3ah** in moderate yields (Scheme 3.2.2).

Next, to gain further insight into the reaction mechanism, a series of control experiments were performed (Scheme 3.2.3). The oxidation of phenol at the anode was verified by divided cell experiments [Scheme 3.2.3(a)]. The transformation was successfully executed when the reaction mixture was placed in the anodic chamber; however, a drop in yield and an increase in the reaction time was observed in comparison to the standard conditions [Scheme 3.2.3(ai)]. Failure of the reaction in the cathodic chamber further accentuates the anodic oxidation as the key step for the transformation [Scheme 3.2.3(aii)]. The possibility of chain propagation in the reaction, which could involve the oxidation of phenol by the sulfide radical cation instead of anodic oxidation, was excluded on the basis of a time-based electrolysis experiment [Scheme 3.2.3(b)]. A trace amount of product formation on performing the reaction for 30 minutes and no further conversion in the absence of electricity was observed, indicating that a chain propagation mechanism is absent. Further, the LC-MS and GC-MS studies confirmed the presence of benzyl alcohol as one of the side products of the protocol [Scheme 3.2.3(c)]. Further, making intermediate **V** and performing the reaction of **V** under standard conditions provides the desired product **3ba**, which confirms the formation of intermediate **V** in the reaction [Scheme 3.2.3(c)].

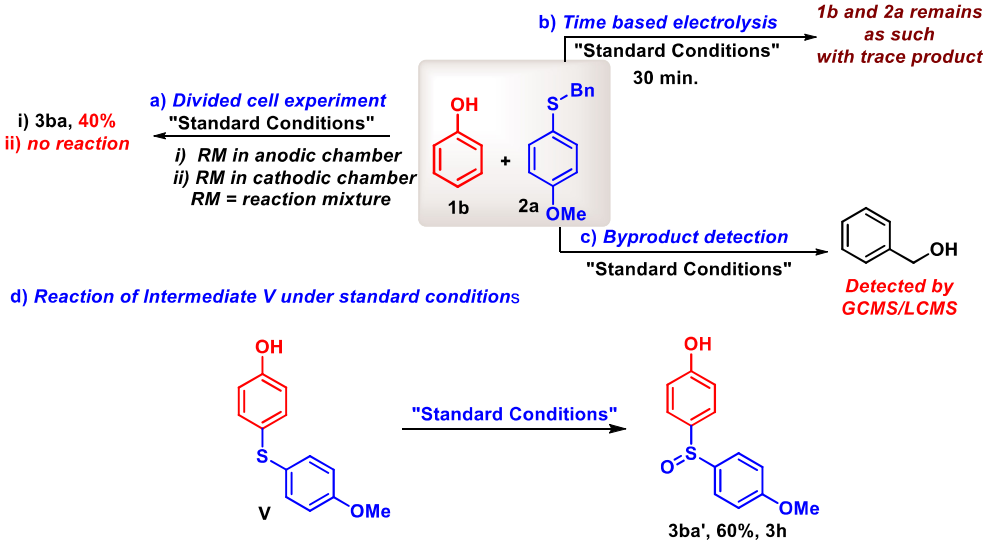

Scheme 3.2.3. Mechanistic studies.

Further, cyclic voltammetry (CV) experiment was carried out to study the redox behavior of the reagents. The oxidation potential of **1b** was observed to be 1.10 V (vs. Ag/AgCl), and 1.5 V (vs. Ag/AgCl) for **2a,** indicating that the phenol (**1b**) oxidizes before **2a**. However, on adding both the reagents together, a slight shift in the oxidation potential of both **1b** and **2a** to 1.37 V and 1.89 V, respectively, was observed with a remarkable improvement in

the catalytic current (electrocatalytic effect). This observation suggests that the reaction becomes more feasible and efficiently renders the desired product (Figure 3.2.1).

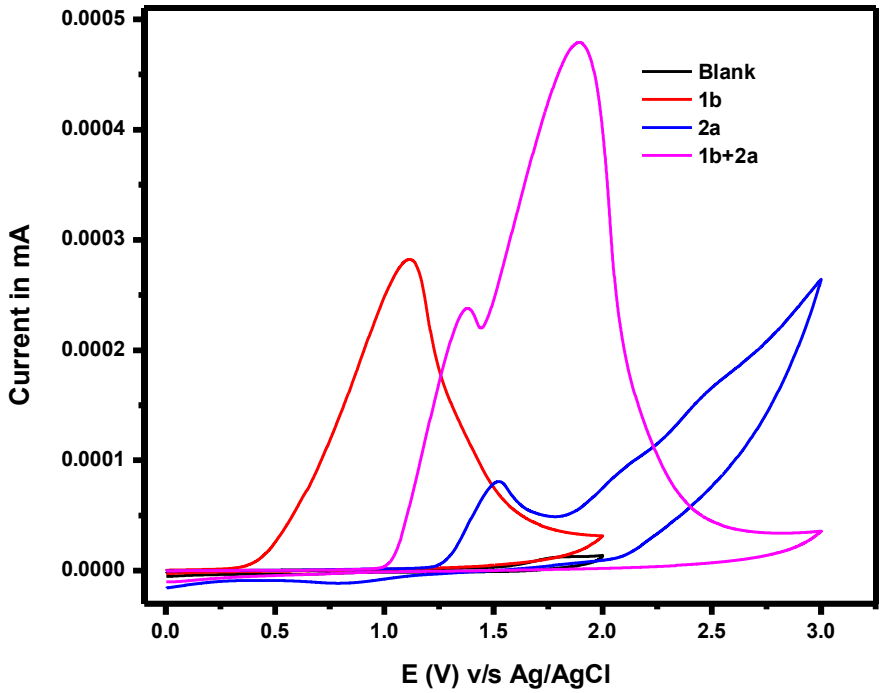

Figure 3.2.1. Cyclic voltammetry experiment.

Based on the control experiments and literature reports,[18, 19a,19b,] a plausible mechanism is proposed (Scheme 3.2.4). The reaction gets initiated with the single-electron oxidation (SET) of phenol **1b** to generate the radical species **II**, which further undergoes anodic oxidation leading to carbocation **III**. The nucleophilic attack of sulfide **2a** on carbocation **III** generates sulfonium cation intermediate **IV**. The active benzylic position of intermediate **IV** undergoes nucleophilic attack by hydroxide ion, which is formed by the cathodic reduction of water (moisture) and affords the species **V** with benzyl alcohol as a side product (detected by GC-MS and LC-MS). Species **V** further undergoes one-electron oxidation followed by the attack of water and another anodic oxidation to deliver the sulfoxide **3ba** (Scheme 3.2.4).

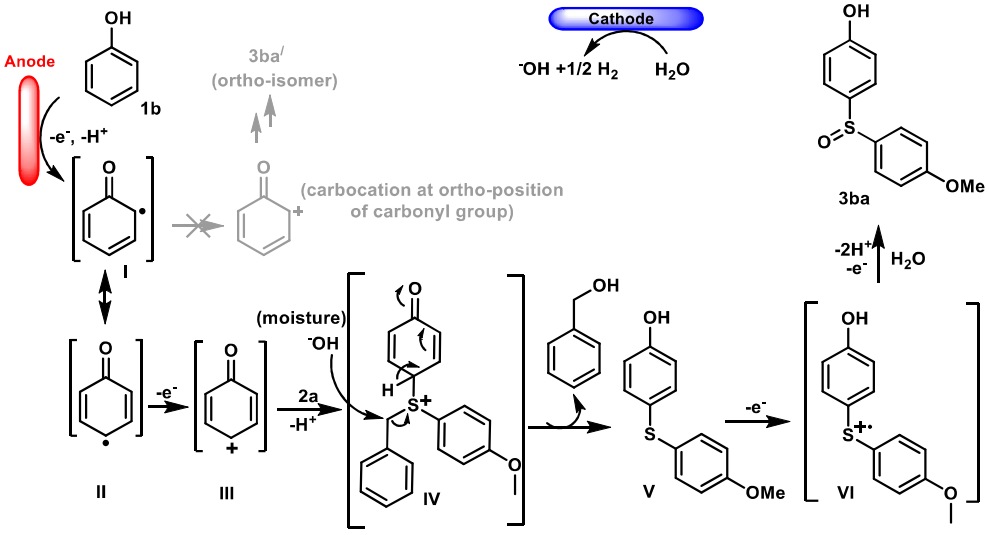

Scheme 3.2.4. Plausible mechanism.

However, the radical-radical coupling of Intermediate **II** with sulfide radical cation **2a**' cannot be ruled out. So, based on this hypothesis, another pathway for a plausible mechanism is proposed (see section 3.4.6). The scalability of transformation was further demonstrated by the successful execution of the reaction at a gram scale [Scheme 3.2.5(a)]. The desired current could be obtained even by reducing the supporting electrolyte to 1.0 equivalent. Further, on subjecting **3ga** to H_2O_2 oxidation, the sulfone product **4ga** was delivered in 70% yield [Scheme 3.2.5(b)]. [19c]

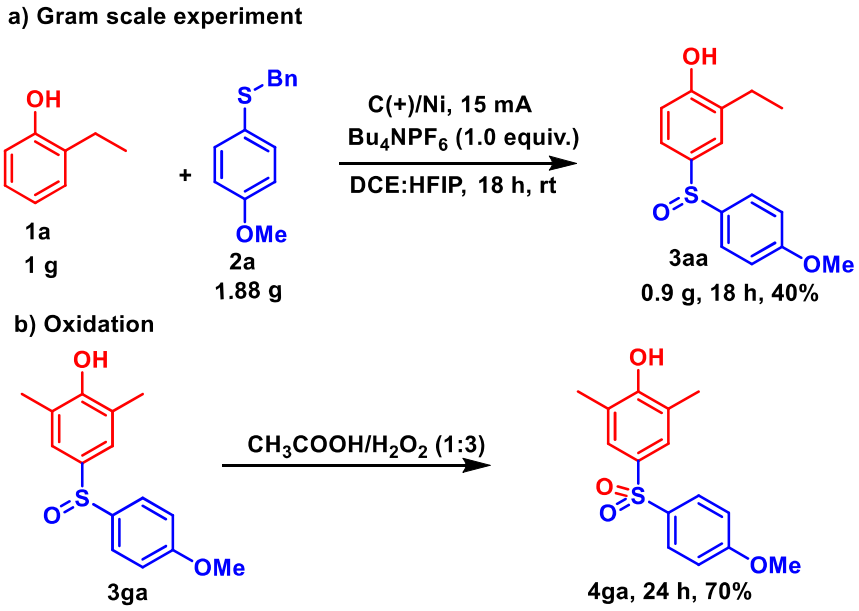

Scheme 3.2.5. Synthetic utility.

3.3. Conclusion

In summary, we have established a facile oxidant-free and regioselective sulfinylation *via* electrochemical oxidative cross-coupling of phenols with sulfides at room temperature. A class of structurally diverse sulfoxides was synthesized from readily available phenol derivatives. The formation of over-oxidized sulfone products was not observed in the developed transformation. It exhibited wide substrate scope and good functional group tolerance and furnished the products with moderate yields. Furthermore, the synthetic utility was demonstrated by a gram-scale experiment and the derivatization to sulfones.

3.4. Experimental section

3.4.1. General Information

Unless noted otherwise, all reagents and solvents were purchased from commercial sources and used as received. All reactions were performed in oven dried round bottom flasks. Electrochemical reactions were performed at room temperature using DC power supply of Keysight technologies (25 V, 5A) and GW INSTEK GPP-4323 (32 V, 3 A). Electrodes were commercially available from IKA. Cyclic voltammetry analysis was carried out in CH

instrument electrochemical analyzer (CHL1110C). The developed chromatogram was analyzed by UV lamp (254 nm) or p-anisaldehyde solution. Column chromatography was performed on silica gel mesh size 200-300. The proton (^{1}H) and carbon ^{13}C{^{1}H} NMR spectra were recorded in 400 MHz JEOL JNM ECS400 spectrometer in the $CDCl_3$ solvent (unless otherwise mentioned) and are reported in δ units. Chemical shifts of NMR spectra are expressed in parts per million (ppm). Coupling constants (*J* Values) are reported in Hz. High-resolution mass spectra (HRMS) were obtained using the electron spray ionization (ESI) technique and TOF mass analyzer. Yields refer to isolated compounds, estimated to be less than 95% pure as determined by ^{1}HNMR. The description of the signals includes the following: s = singlet, d = doublet, dd = doublet of doublet, t = triplet, dt = doublet of triplet, q = quartet, br = broad and m = multiplet

3.4.2. General procedure for the synthesis of $ArCH_2SAr'$[20]

In an oven dried 100 mL round-bottomed flask equipped with a magnetic bar, benzyl bromides (1 equiv.), thiophenols (1 equiv.) and powered K_2CO_3 (1.1 equiv.) in DMF were taken. The reaction was allowed to stir for 4 h and completion was monitored by TLC. After completion, water was added to the reaction mixture and extracted with ethyl acetate three times. The resulting organic layer was further washed with brine solution and dried over anhydrous sodium sulfate. The solvent was removed on a rotavap under reduced pressure, the residue was subjected to flash column chromatography to obtain the desired products.

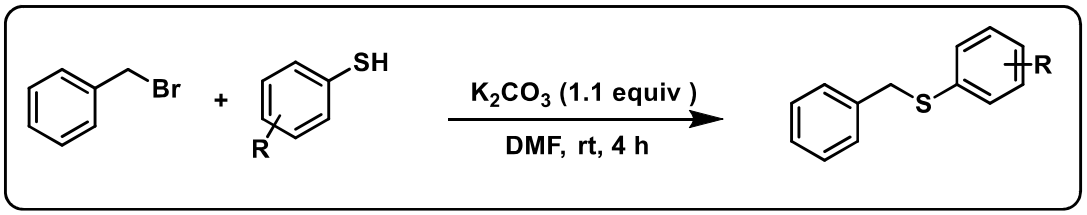

3.4.2.1 Characterization data of starting material

Benzyl(4-methoxyphenyl)sulfane(2a)

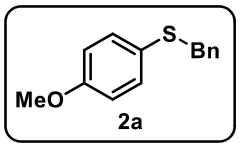

Overall yield: 90%, 0.438 g; **Nature:** White solid; ^{1}H NMR (400 MHz, CHLOROFORM-D): δ 7.27-7.20 (m, 5H), 7.19-7.17 (m, 2H), 6.80-6.76 (m, 2H), 3.97 (s, 2H), 3.77 (s, 3H).

Benzyl(p-tolyl)sulfane(2b)

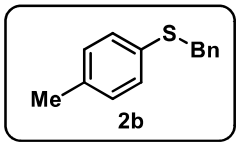

Overall yield: 88%, 0.467 g; **Nature:** White solid; **^{1}H-NMR** (400 MHz, CHLOROFORM-D): δ 7.28-7.20 (m, 7H), 7.06 (d, J = 8.1 Hz, 1H), 4.07 (s, 2H), 2.31 (s, 3H).

Benzyl(4-chlorophenyl)sulfane(2c)

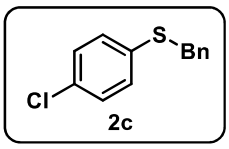

Overall yield: 92%, 0.450 g; **Nature:** White solid, **^{1}H-NMR** (400 MHz, CHLOROFORM-D): δ 7.30-7.22 (m, 5H), 7.20 (s, 4H), 4.07 (s, 2H).

Benzyl(naphthalen-2-yl)sulfane(2d)

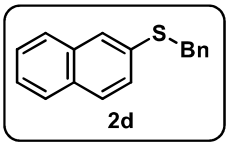

Overall yield: 85%, 0.402 g; **Nature:** White solid, **^{1}H-NMR** (400 MHz, CHLOROFORM-D): δ 7.79-7.70 (m, 4H), 7.48-7.40 (m, 3H), 7.35-7.23 (m, 5H), 4.23 (s, 2H).

Benzyl(phenyl)sulfane(2e)

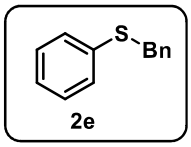

Overall yield: 95%, 0.515 g; **Nature:** White solid; **^{1}H NMR** (400 MHz, CHLOROFORM-D): δ 7.33-7.20 (m, 4H), 7.20-7.15 (m, 1H), 4.11 (s, 1H).

benzyl(2-methoxyphenyl)sulfane(2f)

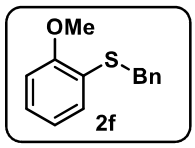

Overall yield: 87%, 0.430 g; **Nature:** White solid; **^{1}H NMR** (400 MHz, CHLOROFORM-D): δ 7.31-7.16 (m, 7H), 6.86 (m, 2H), 4.09 (s, 2H), 3.88 (s, 1H).

benzyl(3-methoxyphenyl)sulfane (2g)

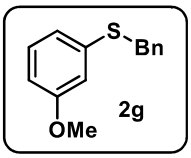

Overall yield: 81%, 0.4 g; **Nature:** Transparent liquid; **^{1}H NMR** (400 MHz, CHLOROFORM-D): δ 7.33-7.21 (m, 5H), 7.19-7.14 (m, 1H), 6.91-6.88 (m, 1H), 6.82-6.81 (m, 1H), 6.73-6.70 (m, 1H), 4.12 (s, 2H), 3.73 (s, 3H).

benzyl(4-fluorophenyl)sulfane (2h)

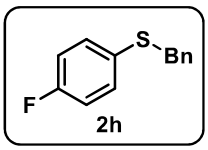

Overall yield: 68%, 0.350 g; **Nature:** Transparent liquid; **^{1}H NMR** (400 MHz, CHLOROFORM-D): δ 7.29-7.19 (m, 7H), 6.96-6.91 (m, 2H), 4.02 (s, 2H).

3.4.3. General procedure for synthesis of intermediate V[21]

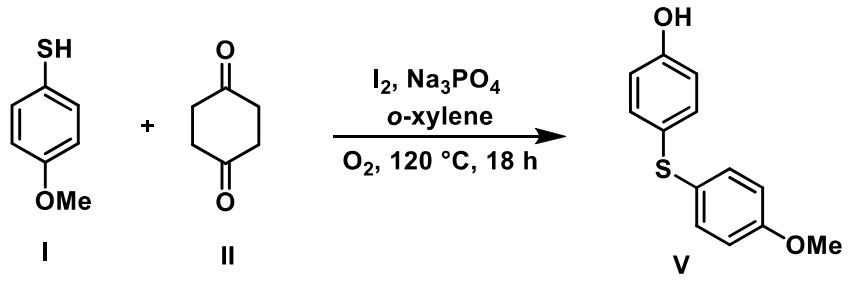

In an oven-dried reaction vessel charged with cyclohexanones (0.5 mmol), thiophenols (0.3 mmol), I_2 (0.2 mmol), Na_3PO_4 (0.2 mmol), and o-xylene (1.5 mL). The reaction vessel was purged with oxygen three times and stirred at 120 °C for 18 h. After cooling to room temperature, the reaction mixture was diluted with EtOAc and filtered. The filtrate was then concentrated in vacuo, and the resulting residue was purified by column chromatography on silica gel to afford the corresponding product.

3.4.3.1 Characterization data

4-((4-methoxyphenyl)thio)phenol(V)

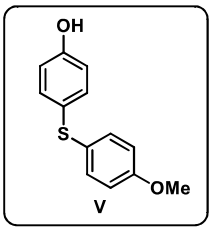

Overall yield: 65%, 0.540 g; **Nature:** yellow liquid; **^{1}H NMR** (400 MHz, CHLOROFORM-D): δ 7.81 (d, *J* = 9.0 Hz, 2H), 7.75 (d, *J* = 6.8 Hz, 2H), 6.93 (d, *J* = 8.9 Hz, 2H), 6.88 (d, *J* = 8.7 Hz, 2H), 3.82 (s, 3H).

3.4.4. General procedure for electrochemical reaction

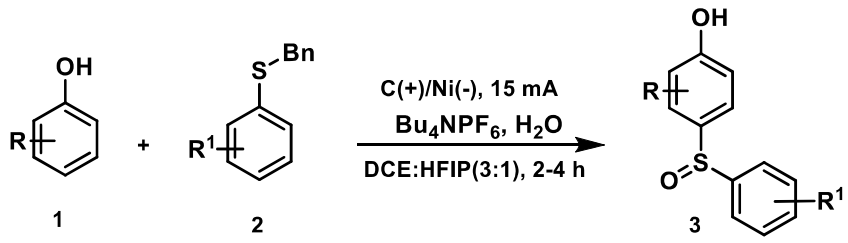

In an undivided cell equipped with magnetic bar and graphite as anode and nickel as cathode, mixture of **1a-1n** (1.0 equiv.), **2a-2e** (1.0 equiv.), Bu_4NPF_6 (2.0 equiv.) and DCE: HFIP (3:1) 4 mL were added. The mixture was electrolyzed at a constant current of 15 mA at room temperature for 2-6 h in a DC power supply. Upon completion, the solvent was removed under reduced pressure and the crude was subjected to silica gel column chromatography (200-400 mesh) to afford the desired product.

3.4.4.1 Characterization data of final compounds

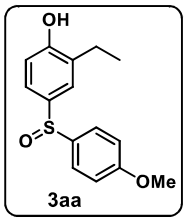

2-ethyl-4-((4-methoxyphenyl)sulfinyl)phenol(3aa)

Overall yield: 60%, 41 mg; **Nature:** Brown liquid; **R_f** = 0.4 (Hexane/ethyl acetate = 9:1); **^{1}H-NMR** (400 MHz, CHLOROFORM-D): ^{1}H NMR (400 MHz, CHLOROFORM-D); δ 7.27-7.23 (m, 2H), 7.16 (d, *J* = 2.3 Hz, 1H), 7.04 (dd, *J* = 8.3, 2.3 Hz, 1H), 6.85-6.80 (m, 1H), 6.68 (d, *J* = 8.3 Hz, 1H), 4.80 (s, 1H), 3.78 (s, 3H), 2.57 (q, *J* = 7.5 Hz, 1H), 1.19 (t, *J* = 7.6 Hz, 1H);**^{13}C{^{1}H} NMR** (101 MHz, CHLOROFORM-D): δ 158.9, 153.0, 132.8, 132.5, 131.1, 130.5, 127.8, 127.2, 116.1, 114.8, 55.4, 22.9, 13.9; **HRMS** (ESI, Q-TOF) m/z $[M + H]^+$ Calcd for $C_{15}H_{17}O_3S$ 277.0898, found 277.0894.

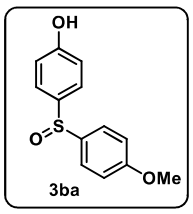

4-((4-methoxyphenyl)sulfinyl)phenol(3ba)

Overall yield: 62%, 49 mg; **Nature:** Brown semisolid; **R_f** = 0.5 (Hexane/ethyl acetate = 9:1); **^{1}H-NMR** (400 MHz, CHLOROFORM-D): δ 7.28-7.26 (m, 2H), 7.22-7.19 (m, 2H), 6.84-6.81 (m, 2H), 6.76-6.71 (m, 2H), 4.87 (s, 1H), 3.78 (s, 3H); **^{13}C{^{1}H} NMR** (101 MHz, CHLOROFORM-D): δ 159.1, 154.1, 132.9, 127.8, 127.3, 116.3, 114.8, 55.4; **HRMS** (ESI, Q-TOF) m/z $[M + H]^+$ Calcd for $C_{13}H_{13}O_3S$ 249.0585, found 249.580.

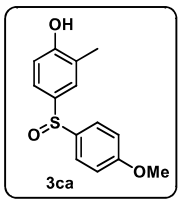

4-((4-methoxyphenyl)sulfinyl)-2-methylphenol(3ca)

Overall yield: 63%, 49 mg; **Nature:** Brown liquid; **R_f** = 0.4 (Hexane/ethyl acetate = 9:1); **^{1}H-NMR** (400 MHz, CHLOROFORM-D): ^{1}H NMR (400 MHz, CHLOROFORM-D) δ 7.27-7.24 (m, 2H), 7.13 (d, *J* = 2.1 Hz, 1H), 7.06 (dd, *J* = 8.2, 2.3 Hz, 1H), 6.84-6.80 (m, 2H), 6.69 (d, *J* = 8.3 Hz, 1H), 4.83 (s, 1H), 3.78 (s, 3H), 2.19 (s, 3H); **^{13}C{^{1}H} NMR** (101 MHz, CHLOROFORM-D): δ 158.9, 153.4, 134.3, 132.6, 130.6, 127.7, 127.1, 124.9, 115.7, 114.8, 55.4, 15.8; **HRMS** (ESI, Q-TOF) m/z [M + H]+ Calcd for $C_{14}H_{15}O_3S$ 263.0742, found 263.0743.

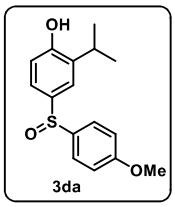

2-isopropyl-4-((4-methoxyphenyl)sulfinyl)phenol(3da)

Overall yield: 50%, 32 mg; **Nature:** light brown liquid; **R_f** = 0.4 (Hexane/ethyl acetate = 9:1); **^{1}H-NMR** (400 MHz, CHLOROFORM-D): ^{1}H NMR (400 MHz, CHLOROFORM-D) δ 7.26-7.22 (m, 3H), 7.01 (dd, *J* = 8.3, 2.3 Hz, 1H), 6.84-6.80 (m, 1H), 6.66 (d, *J* = 8.3 Hz, 1H), 4.81 (s, 1H), 3.78 (s, 1H), 3.14 (dt, *J* = 13.8, 6.9 Hz, 1H), 1.21 (d, *J* = 6.9 Hz, 6H); **^{13}C{^{1}H} NMR** (101 MHz, CHLOROFORM-D): δ 158.9, 152.3, 135.5, 132.4, 130.1, 127.7, 127.3, 116.2, 114.8, 55.4, 27.2, 22.6; **HRMS** (ESI, Q-TOF) m/z $[M + H]^+$ Calcd for $C_{16}H_{19}O_3S$ 291.1055, found 291.1051.

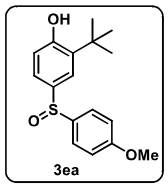

2-(tert-butyl)-4-((4-methoxyphenyl)sulfinyl)phenol(3ea)

Overall yield: 55%, 34 mg; **Nature:** light brown liquid; **R_f** = 0.4 (Hexane/ethyl acetate = 9:1); **^{1}H-NMR** (400 MHz, CHLOROFORM-D): δ 7.29 – 7.25 (m, 3H), 7.00 (dd, *J* = 8.1, 2.3 Hz, 1H), 6.82 (d, *J* = 9.0 Hz, 2H), 6.58 (d, *J* = 8.1 Hz, 1H), 4.90 (s, 1H), 3.78 (s, 3H),

1.35 (s, 9H); **^{13}C{^{1}H} NMR** (101 MHz, CHLOROFORM-D): δ 158.9, 153.8, 137.1, 132.6, 130.7, 130.1, 127.6, 126.9, 117.5, 114.8, 55.4, 34.8, 29.5; ; **HRMS** (ESI, Q-TOF) m/z [M + H]+ Calcd for $C_{17}H_{21}O_3S$ 305.1211, found 305.1212.

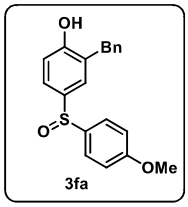

2-benzyl-4-((4-methoxyphenyl)sulfinyl)phenol(3fa)

Overall yield: 55%, 31 mg; **Nature:** Brown liquid; **R$_f$** = 0.4 (Hexane/ethyl acetate = 9:1); **^{1}H-NMR** (400 MHz, CHLOROFORM-D): δ 7.29-7.25 (m, 4H), 7.22-7.17 (m, 3H), 7.13 (d, *J* = 2.3 Hz, 1H), 7.07 (dd, *J* = 8.3, 2.3 Hz, 1H), 6.83-6.81 (m, 2H), 6.70 (d, *J* = 8.3 Hz, 1H), 4.74 (s, 1H), 3.92 (s, 2H), 3.78 (s, 3H); **^{13}C{^{1}H} NMR** (101 MHz, CHLOROFORM-D): 159.0, 153.2, 139.4, 133.9, 132.9, 130.9, 128.7, 128.0, 127.8, 127.3, 126.6, 116.7, 114.8, 55.4, 36.4; **HRMS** (ESI, Q-TOF) m/z [M + H]+ Calcd for $C_{20}H_{19}O_3S$ 339.1055, found 339.1050.

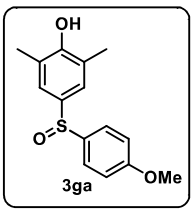

4-((4-methoxyphenyl)sulfinyl)-2,6-dimethylphenol(3ga)

Overall yield: 47%, 32 mg; **Nature:** light brown liquid, **R$_f$** = 0.5 (Hexane/ethyl acetate = 85:15); **^{1}H-NMR** (400 MHz, CHLOROFORM-D): δ 7.27-7.23 (m, 2H), 7.00 (s, 2H), 6.84-6.80 (m, 2H), 4.63 (s, 1H), 3.78 (s, 3H), 2.18 (s, 6H); **^{13}C{^{1}H} NMR** (101 MHz, CHLOROFORM-D): δ 158.8, 151.9, 132.4, 132.1, 127.9, 126.2, 124.1, 114.8, 55.4, 15.9; **HRMS** (ESI, Q-TOF) m/z [M + H]+ Calcd for $C_{15}H_{17}O_3S$ 277.0898, found 277.0895.

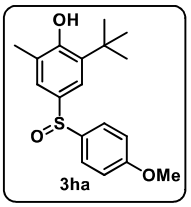

2-(tert-butyl)-4-((4-methoxyphenyl)sulfinyl)-6-methylphenol(3ha)

Overall yield: 55%, 31 mg; **Nature:** Brown liquid; **R$_f$** = 0.5 (Hexane/ethyl acetate = 95:5); **^{1}H-NMR** (400 MHz, CHLOROFORM-D): δ 7.26-7.24 (m,2H), 7.18 (d, *J* = 2.3 Hz, 1H), 6.97 (d, *J* = 2.3 Hz, 1H), 6.84-6.81 (m, 2H), 4.77 (s, 1H), 3.78 (s, 1H), 2.18 (s, 1H), 1.36 (s, 9H); **^{13}C{^{1}H} NMR** (101 MHz, CHLOROFORM-D): δ 158.8, 152.4, 136.7, 132.3, 131.8, 128.9, 127.9, 125.9, 124.2, 114.7, 55.4, 34.7, 29.7, 16.0; **HRMS** (ESI, Q-TOF) m/z [M + H]+ Calcd for $C_{18}H_{23}O_3S$ 319.1368, found 319.1365.

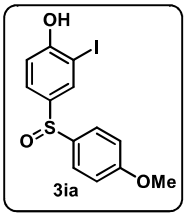

2-iodo-4-((4-methoxyphenyl)sulfinyl)phenol(3ia)

Overall yield: 60%, 26 mg; **Nature:** Brown liquid; **R$_f$** = 0.4 (Hexane/ethyl acetate = 85:15); **^{1}H-NMR** (400 MHz, CHLOROFORM-D): δ 7.59 (d, *J* = 2.2 Hz, 1H), 7.32-7.28 (m, 2H), 7.17 (dd, J = 8.4, 2.2 Hz, 1H), 6.87 (dd, J = 13.9, 8.7 Hz, 3H), 5.27 (s, 1H), 3.79 (s, 3H); **^{13}C{^{1}H} NMR** (101 MHz, CHLOROFORM-D): δ 159.5, 154.0, 139.8, 133.5, 132.8, 129.0, 128.3, 115.0, 114.6, 55.4; **HRMS** (ESI, Q-TOF) m/z [M + H]+ Calcd for $C_{13}H_{12}O_3SI$ 374.9552, found 374.9554.

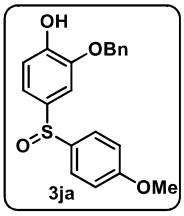

2-(benzyloxy)-4-((4-methoxyphenyl)sulfinyl)phenol(3ja)

Overall yield: 52%, 28 mg; **Nature:** light brown liquid; $\mathbf{R_f}$ = 0.5 (Hexane/ethyl acetate = 85:15); **^{1}H-NMR** (400 MHz, CHLOROFORM-D): δ 7.38-7.34 (m, 5H), 7.24 (dd, *J* = 6.7, 2.2 Hz, 3H), 6.93-6.86 (m, 2H), 6.83-6.80 (m, 2H), 5.65 (s, 1H), 5.01 (s, 2H), 3.79 (s, 3H); **^{13}C{^{1}H} NMR** (101 MHz, CHLOROFORM-D): δ 159.4, 146.0, 144.7, 136.2, 133.5, 128.7, 127.8, 124.4, 122.3, 120.1, 114.9, 112.3, 71.4, 55.4. ; **HRMS** (ESI, Q-TOF) m/z $[M + H]^+$ Calcd for $C_{20}H_{19}O_4S$ 355.1004, found 355.0997.

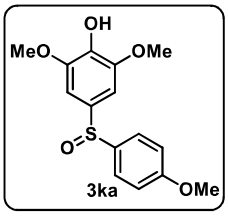

2,6-dimethoxy-4-((4-methoxyphenyl)sulfinyl)phenol(3ka)

Overall yield: 55%, 33 mg; **Nature:** Brown liquid; $\mathbf{R_f}$ = 0.5 (Hexane/ethyl acetate = 85:15); **^{1}H-NMR** (400 MHz, CHLOROFORM-D): δ 7.32-7.28 (m, 2H), 6.86-6.82 (m, 2H), 6.57 (q, *J* = 8.7 Hz, 2H), 5.62 (s, 1H), 3.89 (s, 3H), 3.84 (s, 3H), 3.78 (s, 3H); **^{13}C{^{1}H} NMR** (101 MHz, CHLOROFORM-D): δ 159.2, 147.3, 145.6, 139.1, 133.6, 125.7, 122.7, 121.9, 114.9, 107.2, 60.8, 56.4, 55.4; **HRMS** (ESI, Q-TOF) m/z $[M + H]^+$ Calcd for $C_{15}H_{17}O_5S$ 309.0797, found 309.0793.

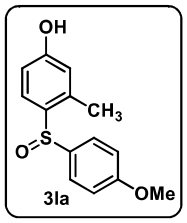

4-((4-methoxyphenyl)sulfinyl)-3-methylphenol(3la)

Overall yield: 48%, 35 mg; **Nature:** light brown liquid; $\mathbf{R_f}$ = 0.5 (Hexane/ethyl acetate = 85:15); **^{1}H-NMR** (400 MHz, CHLOROFORM-D): δ 7.19 (d, *J* = 8.4 Hz, 1H), 7.14-7.10 (m, 2H), 6.82-6.78 (m, 2H), 6.72 (d, *J* = 2.8 Hz, 1H), 6.61 (dd, *J* = 8.4, 2.8 Hz, 1H), 4.91 (s, 1H), 3.77 (s, 3H), 2.31 (s, 3H); **^{13}C{^{1}H} NMR** (101 MHz, CHLOROFORM-D): δ 158.5, 155.5, 142.2, 135.1, 131.2, 127.7, 125.7, 117.6, 114.8, 113.8, 55.5, 20.8; **HRMS** (ESI, Q-TOF) m/z $[M + H]^+$ Calcd for $C_{14}H_{15}O_3S$ 263.0742, found 263.0741.

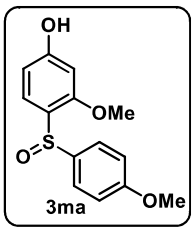

3-methoxy-4-((4-methoxyphenyl)sulfinyl)phenol(3ma)

Overall yield: 40%, 27 mg; **Nature:** light brown liquid; $\mathbf{R_f}$ = 0.4 (Hexane/ethyl acetate = 85:15); **^{1}H-NMR** (400 MHz, CHLOROFORM-D): δ 7.24 (d, *J* = 4.5 Hz, 1H), 6.99 (d, *J* = 8.3 Hz, 1H), 6.84-6.80 (m, 2H), 6.43 (d, *J* = 2.5 Hz, 1H), 6.33 (dd, *J* = 8.3, 2.6 Hz, 1H), 5.07 (s, 1H), 3.80 (s, 3H), 3.78 (s, 3H); **^{13}C{^{1}H} NMR** (101 MHz, CHLOROFORM-D): δ 158.9, 158.9, 156.7, 133.6, 132.8, 126.2, 115.6, 114.8, 107.9, 99.6, 77.4, 77.1, 76.8, 56.0, 55.4; **HRMS** (ESI, Q-TOF) m/z $[M + H]^+$ Calcd for $C_{14}H_{15}O_4S$ 279.0691, found 279.0692.

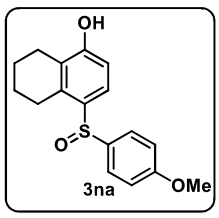

4-((4-methoxyphenyl)sulfinyl)-5,6,7,8-tetrahydronaphthalen-1-ol(3na)

Overall yield: 45%, 28 mg; **Nature:** light brown liquid; $\mathbf{R_f}$ = 0.5 (Hexane/ethyl acetate = 9:1); **^{1}H-NMR** (400 MHz, CHLOROFORM-D): δ 7.15-7.12 (m, 2H), 7.04 (d, *J* = 8.4 Hz, 1H), 6.83-6.79 (m, 2H), 6.58 (d, *J* = 8.3 Hz, 1H), 4.86 (s, 1H), 3.77 (s, 3H), 2.75 (t, *J* = 5.7 Hz, 2H), 2.62 (t, *J* = 5.8 Hz, 2H), 1.79-1.71 (m, 4H); **^{13}C{^{1}H} NMR** (101 MHz, CHLOROFORM-D): δ 158.5, 153.6, 140.5, 131.4, 131.4, 127.5, 125.8, 124.8, 114.8, 112.6, 55.4, 28.07, 23.4, 22.7, 22.1; **HRMS** (ESI, Q-TOF) m/z $[M + H]^+$ Calcd for $C_{17}H_{19}O_3S$ 303.1055, found 303.1045

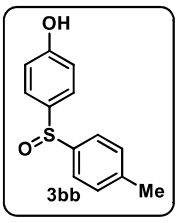

4-(p-tolylsulfinyl)phenol(3bb)

Overall yield: 58%, 43 mg; **Nature:** light brown liquid; $\mathbf{R_f}$ = 0.5 (Hexane/ethyl acetate = 9:1); **^{1}H-NMR** (400 MHz, CHLOROFORM-D): δ 7.32-7.28 (m, 2H), 7.13-7.11 (m, 2H), 7.05 (d, *J* = 8.1 Hz, 2H), 6.83-6.77 (m, 2H), 4.96 (s, 1H), 2.29 (s, 3H);); **^{13}C{^{1}H} NMR** (101 MHz, CHLOROFORM-D): δ 155.5, 136.3, 134.6, 129.9, 129.5, 125.9, 116.4, 21.1; **HRMS** (ESI, Q-TOF) m/z $[M + H]^+$ Calcd for $C_{13}H_{13}O_2S$ 233.0636, found 233.0628.

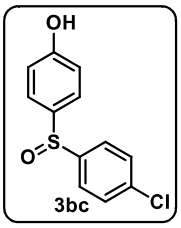

4-((4-chlorophenyl)sulfinyl)phenol(3bc)

Overall yield: 48%, 39 mg; **Nature:** light brown liquid; $\mathbf{R_f}$ = 0.5 (Hexane/ethyl acetate = 9:1); **^{1}H-NMR** (400 MHz, CHLOROFORM-D): δ 7.36 – 7.33 (m, 1H), 7.20 – 7.17 (m, 1H), 7.08 – 7.05 (m, 1H), 6.84 – 6.81 (m, 1H), 4.98 (s, 1H); **^{13}C{^{1}H} NMR** (101 MHz, CHLOROFORM-D): δ 156.2, 135.8, 130.1, 129.3, 129.1, 128.5, 116.7, 115.3; **HRMS** (ESI, Q-TOF) m/z $[M + H]^+$ Calcd for $C_{12}H_{10}O_2SCl$ 253.0090, found 253.0082.

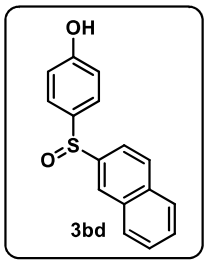

4-(naphthalen-2-ylsulfinyl)phenol(3bd)

Overall yield: 38%, 32 mg; **Nature:** light brown semisolid; $\mathbf{R_f}$ = 0.5 (Hexane/ethyl acetate = 9:1); **^{1}H-NMR** (400 MHz, CHLOROFORM-D): δ 7.75 (d, *J* = 7.2 Hz, 1H), 7.68 (dd, *J* = 17.9, 8.0 Hz, 2H), 7.59 (s, 1H), 7.45-7.38 (m, 4H), 7.28 (dd, *J* = 8.6, 1.8 Hz, 1H), 6.84 (d, *J* = 8.6 Hz, 2H), 4.96 (s, 1H); **^{13}C{^{1}H} NMR** (101 MHz, CHLOROFORM-D): δ 155.9, 135.8, 135.5, 133.8, 131.81, 128.6, 127.8, 127.2, 126.8, 126.6, 125.8, 124.8, 116.6; **HRMS** (ESI, Q-TOF) m/z $[M + H]^+$ Calcd for $C_{16}H_{13}O_2S$ 269.0636, found 269.0627.

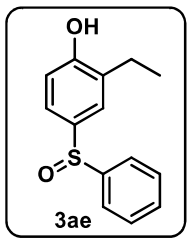

2-ethyl-4-(phenylsulfinyl)phenol(3ae)

Overall yield: 60%, 36 mg; **Nature:** Brown liquid; $\mathbf{R_f}$ = 0.5 (Hexane/ethyl acetate = 9:1); **^{1}H-NMR** (400 MHz, CHLOROFORM-D): δ 7.28 (d, *J* = 2.2 Hz, 1H), 7.24-7.19 (m, 3H), 7.17-7.10 (m, 3H), 6.74 (t, *J* = 6.7 Hz, 1H), 4.93 (s, 1H), 2.60 (q, *J* = 7.6 Hz, 2H), 1.21 (t, *J* = 7.6 Hz, 3H); **^{13}C{^{1}H} NMR** (101 MHz, CHLOROFORM-D): δ 153.9, 138.8, 135.3, 133.2, 131.3, 128.9, 128.1, 125.7, 124.2, 116.3, 22.9, 13.8; **HRMS** (ESI, Q-TOF) m/z $[M + H]^+$ Calcd for $C_{14}H_{15}O_2S$ 247.0793, found 247.0793.

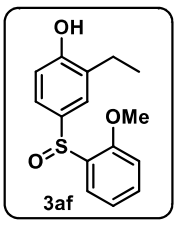

2-ethyl-4-((2-methoxyphenyl)sulfinyl)phenol (3af)

Overall yield: 65%, 44 mg; **Nature:** Brown liquid; $\mathbf{R_f}$ = 0.5 (Hexane/ethyl acetate = 9:1); **^{1}H-NMR** (400 MHz, CHLOROFORM-D): δ 7.30 (d, *J* = 2.2 Hz, 1H), 7.22 (dd, *J* = 8.2, 2.3 Hz, 1H), 7.13-7.08 (m, 1H), 6.85-6.81 (m, 1H), 6.79-6.74 (m, 3H), 4.95 (s, 1H), 3.90 (s, 3H), 2.61 (q, *J* = 7.5 Hz, 2H), 1.21 (t, *J* = 7.5 Hz, 3H); **^{13}C{^{1}H} NMR** (101 MHz, CHLOROFORM-D): δ 155.5, 154.1, 131.4, 127.8, 126.4, 122.6, 121.3, 116.3, 110.3, 55.9, 22.9, 13.8; **HRMS** (ESI, Q-TOF) m/z $[M + H]^+$ Calcd for $C_{15}H_{17}O_3S$ 277.0898, found 277.0894.

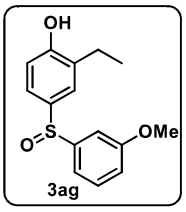

2-ethyl-4-((3-methoxyphenyl)sulfinyl)phenol (3ag)

Overall yield: 63%, 43 mg; **Nature:** Brown liquid; $\mathbf{R_f}$ = 0.5 (Hexane/ethyl acetate = 9:1); **^{1}H-NMR** (400 MHz, CHLOROFORM-D): δ 7.30-7.28 (m, 2H), 7.23-7.20 (m, 1H), 7.15-7.11 (m, 1H), 6.75 (d, *J* = 8.3 Hz, 1H), 6.73-6.70 (m, 1H), 6.67-6.64 (m, 1H), 4.87 (s, 1H), 3.72 (s, 3H), 2.61 (q, *J* = 7.5 Hz, 2H), 1.21 (t, *J* = 7.6 Hz, 3H); **^{13}C{^{1}H} NMR** (101 MHz, CHLOROFORM-D): δ 160.0, 154.0, 140.4, 135.6, 133.4, 129.8, 123.7, 120.0, 116.2, 113.1, 111.2, 55.2, 22.9, 13.8; **HRMS** (ESI, Q-TOF) m/z [M + H]$^+$ Calcd for $C_{15}H_{17}O_3S$ 277.0898, found 277.0894.

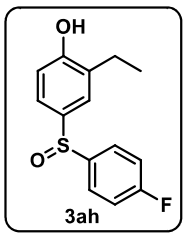

2-ethyl-4-((4-fluorophenyl)sulfinyl)phenol (3ah)

Overall yield: 50%, 32 mg; **Nature:** Brown liquid; $\mathbf{R_f}$ = 0.5 (Hexane/ethyl acetate = 9:1); **^{1}H-NMR** (400 MHz, CHLOROFORM-D): δ 7.22 (d, *J* = 2.3 Hz, 1H), 7.20-7.12 (m, 3H), 6.97-6.92 (m, 2H), 6.73 (d, *J* = 8.3 Hz, 1H), 4.82 (s, 1H), 2.59 (q, *J* = 7.5 Hz, 2H), 1.20 (t, *J* = 7.5 Hz, 3H); **^{13}C{^{1}H} NMR** (101 MHz, CHLOROFORM-D): δ 162.8, 160.4, 153.7, 134.4, 132.2, 131.4, 130.9, 130.9, 125.2, 116.3, 116.2, 116.0, 22.9, 13.8; **HRMS** (ESI, Q-TOF) m/z [M + H]$^+$ Calcd for $C_{14}H_{14}O_2FS$ 265.0699, found 265.0674.

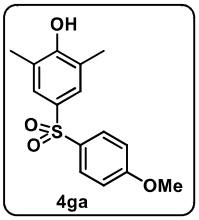

4-((4-methoxyphenyl)sulfonyl)-2,6-dimethylphenol (4ga)

Overall yield: 70%, 15 mg; **Nature:** Transparent liquid; $\mathbf{R_f}$ = 0.5 (Hexane/ethyl acetate = 70:); **^{1}H-NMR** (400 MHz, CHLOROFORM-D): δ = 7.54 -7.49 (m, 2H), 7.19 (s, 2H), 6.97-6.91 (m, 2H), 5.32 (s, 1H), 3.81 (s, 3H), 2.21 (s, 6H); **^{13}C{^{1}H} NMR** (101 MHz, CHLOROFORM-D): δ = 161.7, 155.0, 136.8, 135.8, 126.9, 125.7, 124.5, 114.7, 55.5, 16.1; **HRMS** (ESI, Q-TOF) m/z [M + H]$^+$ Calcd for $C_{15}H_{17}O_4S$ 293.0848, found 293.0846.

3.4.5. Mechanistic studies

3.4.5.1. Divided cell experiment

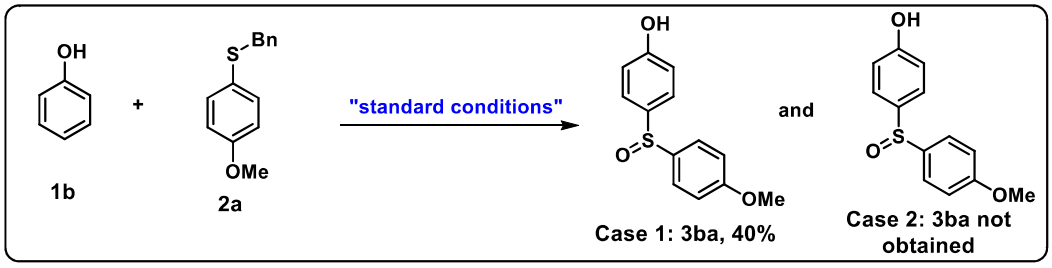

Case 1: In anodic chamber: A divided cell was equipped with two magnetic stir bars in anodic and cathodic chamber respectively. Further, the anodic chamber was filled with corresponding Phenol **1b** (1.0 equiv.), benzyl(4-methoxyphenyl)sulfane **2a** (1.0 equiv.), tetrabutylammonium hexafluorophosphate (Bu_4NPF_6) (2.0 equiv.), in DCE:HFIP (3:1) solvent. The cathodic chamber was filled only with supporting electrolyte solution and the solution was electrolyzed with carbon anode (in anodic chamber) and nickel cathode (in cathodic chamber) at a

constant current of 15 mA for 10 h at room temperature (25-30 °C). However, there is a slight decrease in yield as the desired product was obtained in 40 % yield.

Case 2: In cathodic chamber: A divided cell was equipped with two magnetic stir bars in anodic and cathodic chamber respectively. Further, the cathodic chamber was filled with corresponding Phenol **1b** (1.0 equiv.), benzyl(4-methoxyphenyl)sulfane **2a** (1.0 equiv.), tetrabutylammonium hexafluorophosphate (Bu_4NPF_6) (2.0 equiv.) in DCE:HFIP (3:1) solvent. The anodic chamber was filled with supporting electrolyte solution and the solution was electrolyzed with carbon anode (in anodic chamber) and nickel cathode (in cathodic chamber) at a constant current of 15 mA for 10 h at room temperature. The progress of the reaction was monitored by TLC, which shows that starting material remain unconsumed. This infers that the reaction takes place by the anodic oxidation.

3.4.5.2. Time based electrolysis

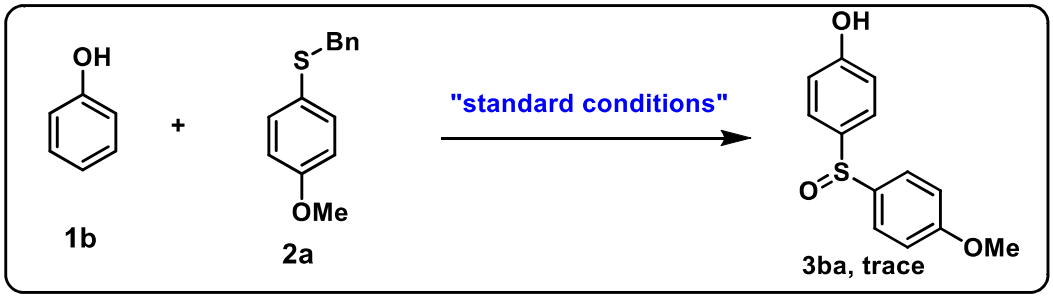

A test tube was equipped with a magnetic stir bar and was added corresponding Phenol **1b** (1.0 equiv.), benzyl(4-methoxyphenyl)sulfane **2a** (1.0 equiv.), tetrabutylammonium hexafluorophosphate (Bu_4NPF_6) (2.0 equiv.) in DCE:HFIP (3:1) solvent. Further, the solution was electrolyzed with carbon anode and nickel cathode at a constant current of 15 mA for 1 h at room temperature. The progress of the reaction was monitored by TLC, which shows that starting material remain unconsumed with trace amount of product formation. After, that the reaction was stirred overnight without electricity. Again, the progress of the reaction was monitored by TLC, which indicated that a similar TLC was observed. Further, the reaction mixture was purified through column chromatography and approx. 70% of the starting material was recovered. This indicates that the chain propagation step is absent in this case.

3.4.5.3. Reaction of intermediate V under standard conditions

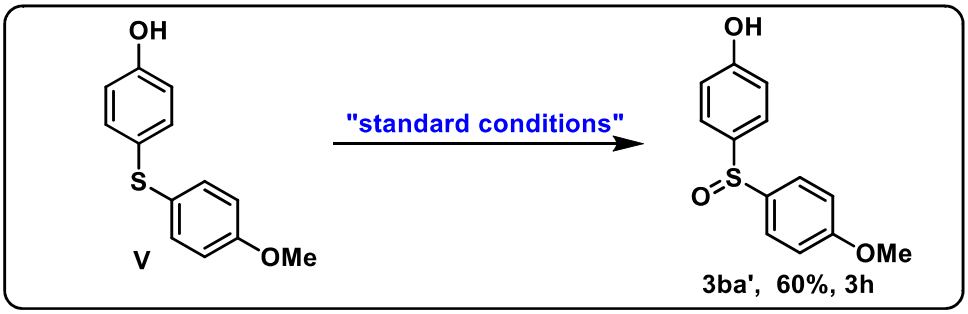

In an undivided cell equipped with magnetic bar and graphite as anode and nickel as cathode, mixture of **V** (1.0 equiv., 0.10 mmol), Bu_4NPF_6 (2.0 equiv., .21 mmol) and DCE: HFIP (3:1) 4 mL were added. The mixture was electrolyzed at a constant current of 15 mA at room temperature for 3 h in a DC power supply. Upon completion, the solvent was removed under reduced pressure and the crude was subjected to silica gel column chromatography (200-400 mesh) to afford the desired product.

3.4.5.4. Cyclic voltammetry

Cyclic voltammetry analysis was carried out in CH instrument electrochemical analyzer (CHL1110C). Samples were prepared in 5 ml vial with 0.01 M of substrate (**1b**), 0.01 M of benzyl(4-methoxyphenyl)sulfane (**2a**) and 0.1 M of Bu_4NPF_6 in DCE:HFIP (3:1) 4 mL. Measurements employed glassy carbon working electrode, platinum wire counter electrode and a 3M KCl silver-silver chloride reference electrode. The sweep rate applied was 50 mV/s. The oxidation potential of **1b** was observed to be 1.10 V (vs Ag/AgCl), and 1.5 V (vs Ag/AgCl) for **2a**. However, on adding both the reagents together, a slight shift in the oxidation potential of both **1b** and **2a** to 1.37 V and 1.89 V respectively was observed (Figure 1). All the CV experiments were carried out in Argon atmosphere and demonstrated as follow: (a) 0.1 M Bu_4NBF_4 (black (b) 0.01 M **1b** (red) (d) 0.01 M **2a** (blue) (e) 0.01 M **1a** and 0.01 M **2a** (pink).

3.4.5.5. Plausible mechanism

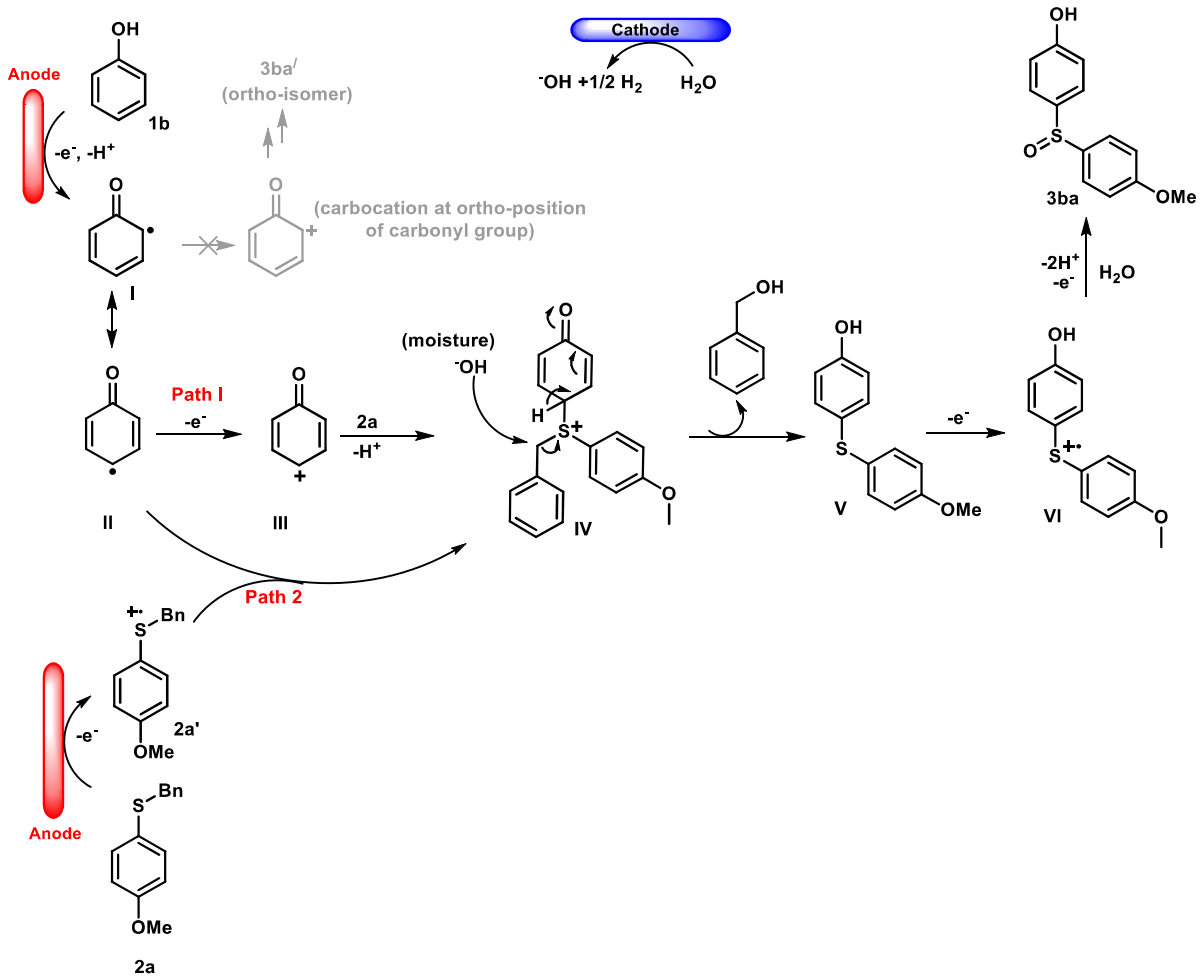

Path 1: The reaction gets initiated with the single-electron oxidation (SET) of phenol **1b** to generate the radical species **II**, which further undergoes anodic oxidation leading to carbocation **III**. Nucleophilic attack of sulfide **2a** on carbocation **III** generates sulfonium cation intermediate **IV**. The active benzylic position of intermediate **IV** undergoes nucleophilic attack by hydroxide ion, which is formed by the cathodic reduction of water (moisture) and afford the species **V** with benzyl alcohol as a side product (detected by GC-MS and LC-MS). Species **V** further undergoes one-electron oxidation followed by the attack of water and another anodic oxidation to deliver the sulfoxide **3ba**.

Path 2: Like path 1, The reaction gets initiated with the single-electron oxidation (SET) of phenol **1b** to generate the radical species **II.** At the same time the sulfide **2a** undergoes one electron oxidation leading to radical cation **2a'**. The radical-radical coupling of intermediate **II** and **2a'** generates the intermediate **IV.** Further, The active benzylic position of intermediate **IV** undergoes nucleophilic attack by hydroxide ion, which is formed by the cathodic reduction of water (moisture) and afford the species **V** with benzyl alcohol as a side product (detected by GC-MS and LC-MS). Species **V** further undergoes one-electron oxidation followed by the attack of water and another anodic oxidation to deliver the sulfoxide **3ba**.

3.4.6. General procedure for electrochemical gram scale synthesis

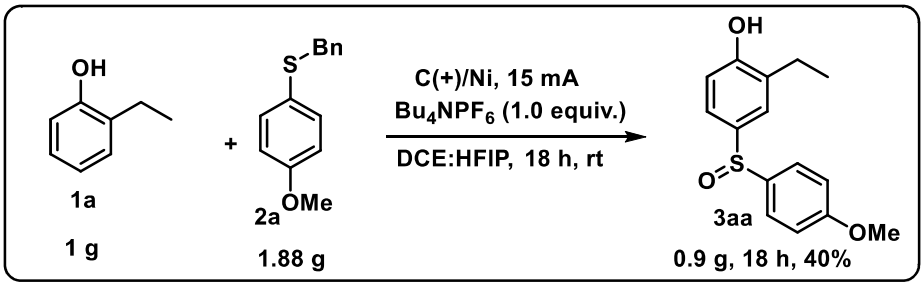

In an oven-dried two-neck round-bottom flask (100 mL) equipped with a magnetic bar and graphite as both the anode and cathode, **1a** (8.18 mmol, 1.0 g), **2a** (8.18 mmol, 1.88 g), Bu_4NPF_6 (1 equiv.), and DCE: HFIP (3:1) (24 mL) were added. The mixture was electrolyzed at a constant current of 15 mA at room temperature for 18 h in a DC power supply. After 18 h, the solvent was removed under reduced pressure, and the crude was purified by silica gel column chromatography using 6-8% ethyl acetate in hexane to afford the desired product in 40% yield (0.9 g).

3.5. References

1. (a) Prabagar, B.; Yang, Y.; Shi, Z. *Chem. Soc. Rev.*, **2021**, *50*, 11249-11269; (b) Saha, D.; Das, P.; Biswas, P.; Guin, J. *Chem. Asian J.* **2019**, *14*, 4534-4548.
2. Meyer, A. U.; Wimmer, A.; Konig, B. *Angew. Chem. Int. Ed*. **2017**, *56*, 409-412.
3. a) Legros, J.; Dehli, J. R.; Bolm, C. *Adv. Synth. Catal*. **2005**, *347*,19-31; (b) Bentley, R. *Chem. Soc. Rev.* **2005**, *34*, 609-624.
4. a) Suwanborirux, K.; Charupant, K.; Amnuoypol, S.; Pummangura, S.; Kubo, A.; Saito, N. *J. Nat. Prod*. **2002**, *65*, 935-937; (b) Kim, S.; Kubec, R.; Musah, R. A. *J. Ethnopharmacol*. **2006**, *104*, 188-192.
5. Lou, T. S. B.; Kawamata, Y.; Ewing, T.; Correa-Otero, G. A.; Collins, M. R.; Baran, P. S. *Angew. Chem. Int. Ed*. **2022**, e202208080.

6. a) Bolm, C. *Coord. Chem. Rev*. **2003**, *237*, 245-256; (b) Wojaczynska, E.; Wojaczynski, J. *Chem. Rev.* **2010**, *110*, 4303-4356; (c) Dornan, P. M.; Leung, P. L.; Dong, V. M. *Tetrahedron,* **2011**, *67*, 4378-4384.
7. a) Maitro, G.; Vogel, S.; Prestat, G.; Madec, D.; Poli, G. *Org. Lett*. **2006**, *8*, 5951-5954; (b) Maitro, G.; Vogel, S.; Sadaoui, M.; Prestat, G.; Madec, D.; Poli, G. *Org. Lett.* **2007**, *9*, 5493-5496; (c) Bernoud, E.; Duc, G. L.; Bantreil, X.; Prestat, G.; Madec, D.; Poli, G. *Org. Lett*. **2010**, *12*, 320-323.
8. a) Jia, T.; Bellomo, A.; Baina, K. E.; Dreher, S. D.; Walsh, P. J. *J. Am. Chem. Soc.* **2013**, *135*, 3740-3743; (b) Jia, T.; Bellomo, A.; Montel, S.; Zhang, M.; Baina, K. E.; Zheng, B.; Walsh, P. J. *Angew. Chem. Int. Ed*. **2014**, *53*, 260-264; (c) Jia, T.; Zhang, M.; Jiang, H.; Wang, C. Y.; Walsh, P. J. *J. Am. Chem. Soc.* **2015**, *137*, 13887-13893.
9. Izquierdo, F.; Chartoire, A.; Nolan, S. P. *ACS Catal*. **2013**, *3*, 2190-2193.
10. Gelat, F.; Lohier, J. F.; Gaumont, A. C.; Perrio, S. *Adv. Synth. Catal*. **2015**, *357*, 2011-2016.
11. (a) Olah, G. A.; Nishimura, J. *J. Org. Chem*. **1974**, *39*, 1203-1205; (b) Yuste, F.; Linares, A. H.; Mastranzo, V. M.; Ortiz, B.; Obrego´n, R. S.; Fraile, A.; Ruano, J. L. G. *J. Org. Chem*. **2011**, *76*, 4635-4644.
12. Kim, D. H.; Lee, J.; Lee, A. *Org. Lett*. **2018**, *20*, 764-767.
13. Liu, Q.; Wang, L.; Yue, H.; Li, J. S.; Luod, Z.; Wei, W. *Green Chem*. **2019**, *21*, 1609-1613; (b) Lou, T. S. B.; Kawamata, Y.; Ewing, T.; Correa-Otero, G. A.; Collins, M. R.; Baran, P. S. *Angew. Chem.* **2022**, *134*, e202208080.
14. (a) Yan, M.; Kawamata, Y.; Baran, P. S. *Chem. Rev*. **2017**, *117*, 13230-13319; (b) Yuan, Y.; Lei, A. *Nat. Commun*. **2020**, *11*, 802; (c) Gnaim, S.; Takahira, Y.; Wilke, H. R.; Yao, Z.; Li, J.; Delbrayelle, D.; Echeverria, P.; Vantourout, J.; Baran, P. S. *Nat. Chem*. **2021**, *13*, 367-372; (d) Wang, Y.; Oliveira, J. C. A.; Lin, Z.; Ackermann, L. *Angew. Chem. Int. Ed*. **2021**, *60*, 6419-6424; (e) Jiang, Y.; Xu, K.; Zeng, C. *Chem. Rev.* **2018**, *118*, 4485-4540; (f) Sauermann, N.; Meyer, T. H.; Qiu, Y.; Ackermann, L. *ACS Catal*. **2018**, *8*, 7086-7106.
15. Amri, N.; Wirth, T. *J. Org. Chem*. **2021**, *86*, 15961-15972.
16. Fu, Z. H.; Tian, H. D.; Ni, S. F.; Wright, J. S.; Li, M.; Wen, L. R.; Zhang, L. B. *Green Chem*. **2022**, *24*, 4772-4777.
17. (a) Taily, I. M.; Saha, D.; Banerjee, P. *Org. Lett*. **2022**, *24*, 2310-2314; (b) Saha, D.; Taily, I. M.; Banerjee, P. *Euro. J. Org. Chem.* **2021**, 5053-5057.
18. (a) Enache, T. A.; Oliveira-Brett, A. M. J. *Electroanal. Chem.* **2011**, *655*, 9-16; (b) Ferg, E. E.; Gouws, S.; S. Pongoma, B. *Afr. J. Chem.* **2012**, *65*, 165-173.
19. (a) Zhou, P.; Niu, K.; Song, H.; Liu, Y.; Wang, Q. *Green chem*. **2022**, *24*, 5760-5763; (b) Li, F.; Pei, C. Koenigs, R. M. *Org. Lett*. **2020**, *22*, 6816-6821; (c) Ibrahim, M.; Latif, A.; Ahmad, M.; Ahmad, S.; Ali, A.; Siddique, A. B.; Saadiq, M.; Akbar, N.; Farooq, U.; Khan, A.; Al-Harrasi, A.; Ali, M. *J. Mol. Struct.* **2022**, *1252*, 13215.
20. Yu, M.; Xie, Y.; Xie, C.; Zhang, Y. *Org. Lett.* **2012**, *14*, 2164-2167.
21. Xiao, F.; Tang, M.; Huang, H.; Guo-Jun Deng, G. J. *J. Org. Chem*., **2022**, *87*, 512-523.

3.6. NMR spectra of starting materials

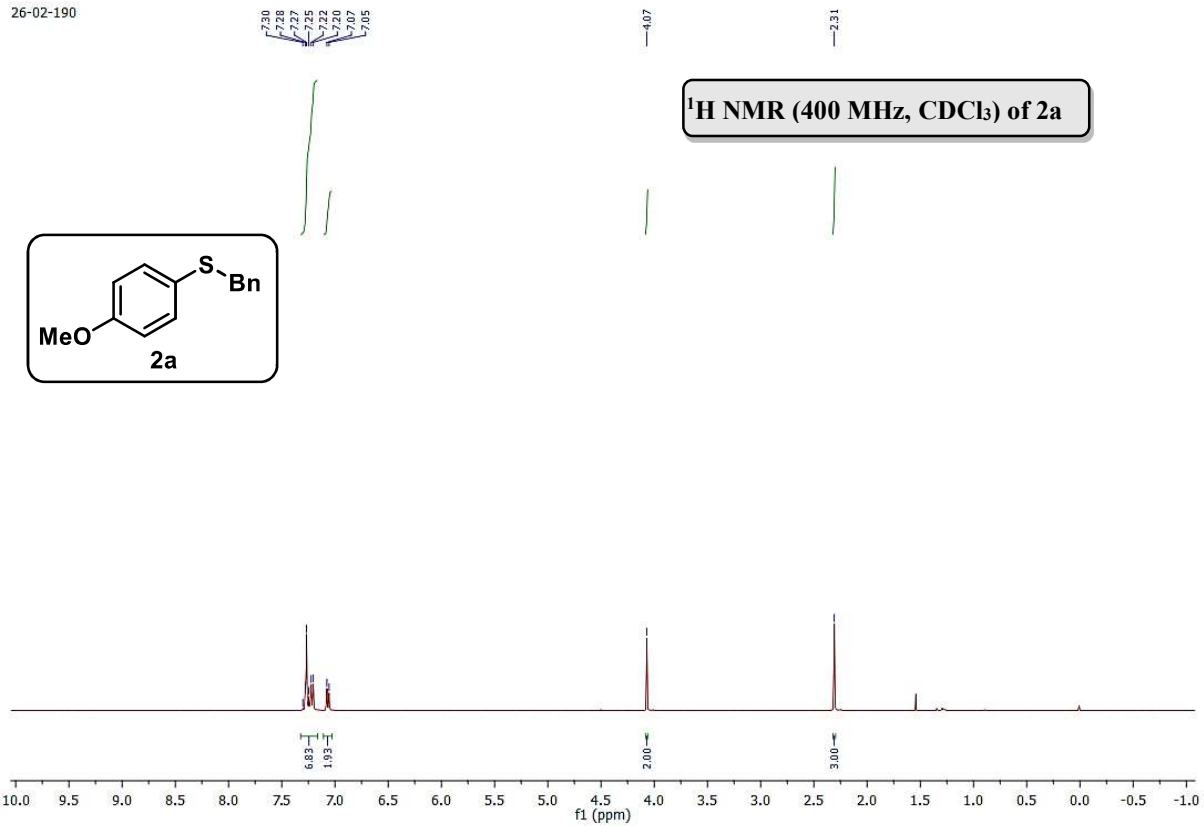

^{1}H NMR (400 MHz, $CDCl_3$) of 2a

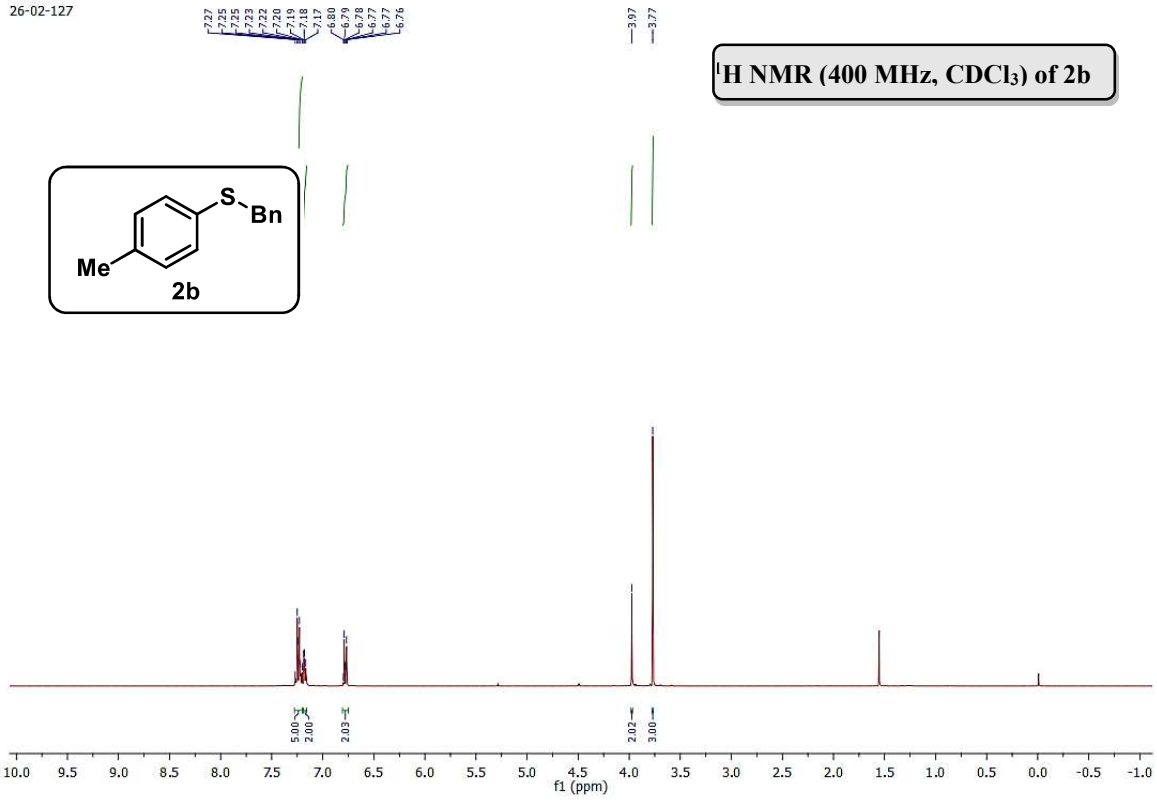

^{1}H NMR (400 MHz, $CDCl_3$) of 2b

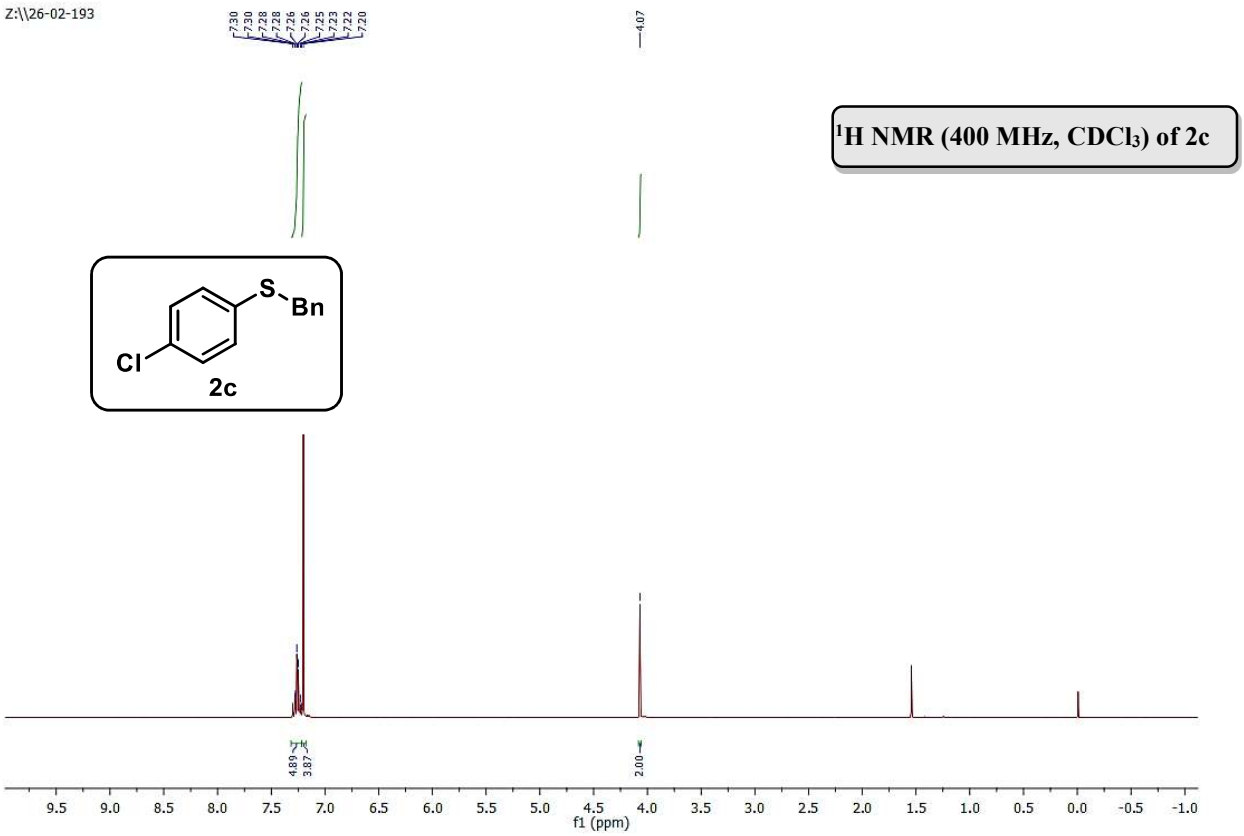

^{1}H NMR (400 MHz, $CDCl_3$) of 2c

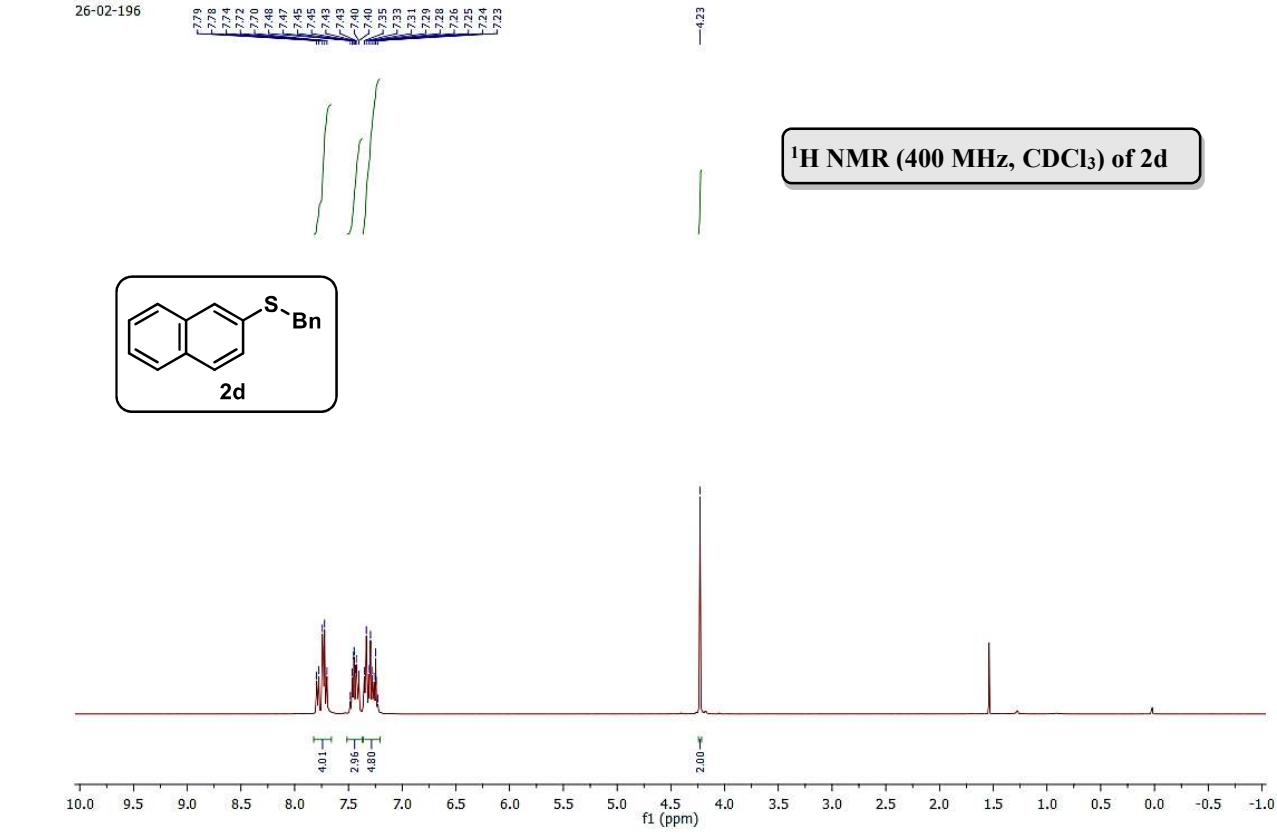

^{1}H NMR (400 MHz, $CDCl_3$) of 2d

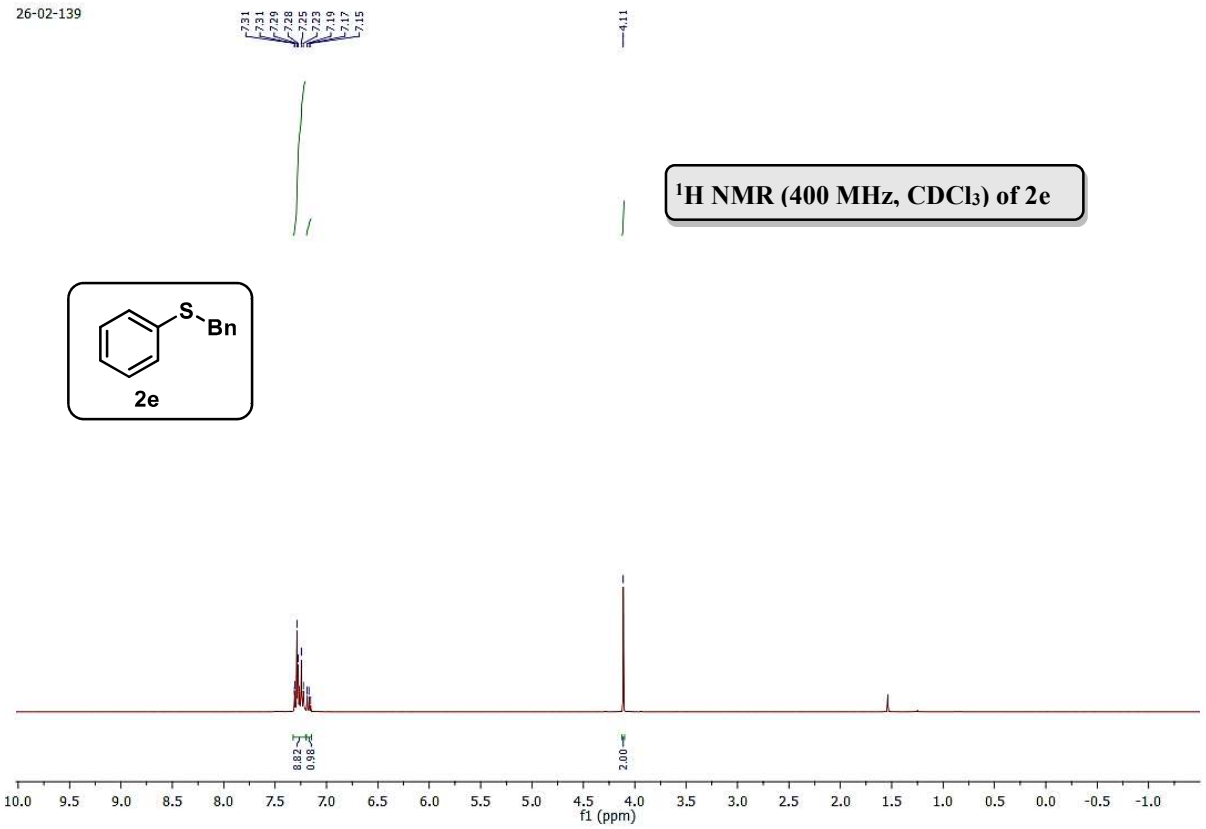

^{1}H NMR (400 MHz, $CDCl_3$) of 2e

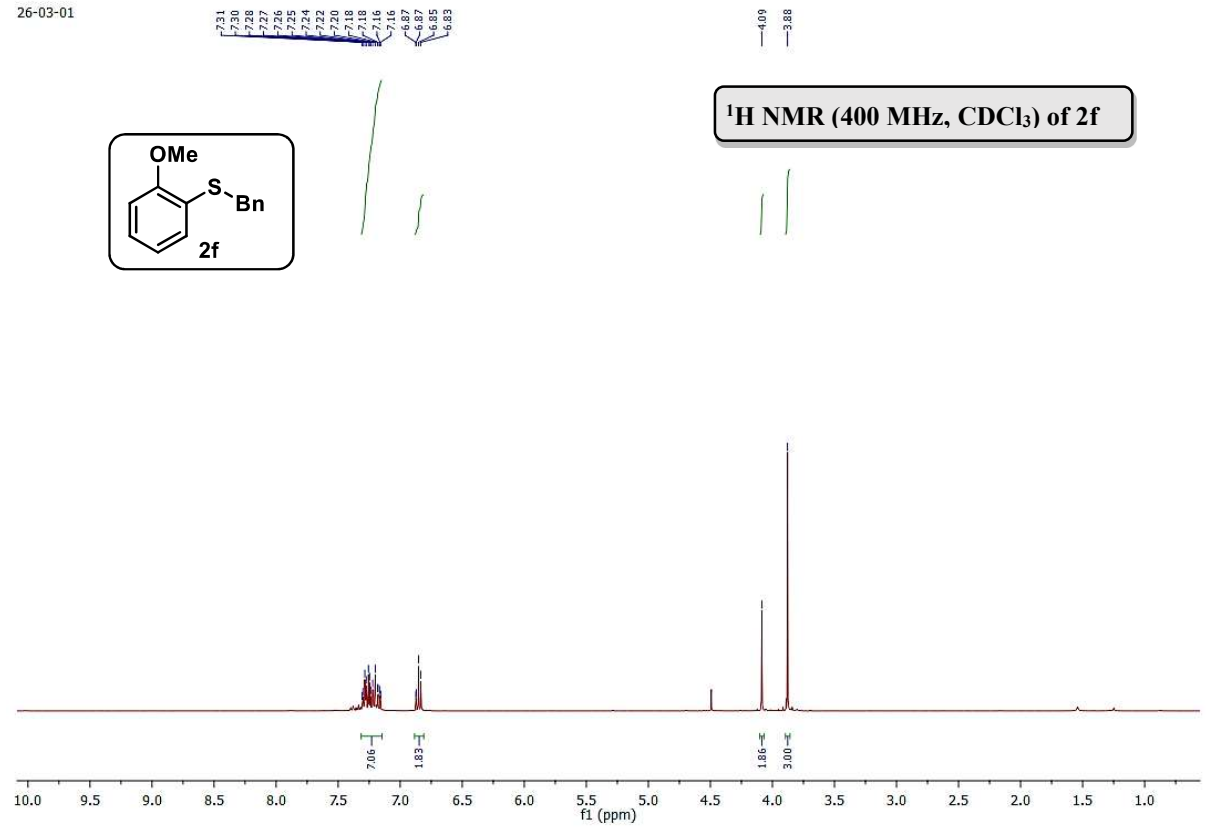

^{1}H NMR (400 MHz, $CDCl_3$) of 2f

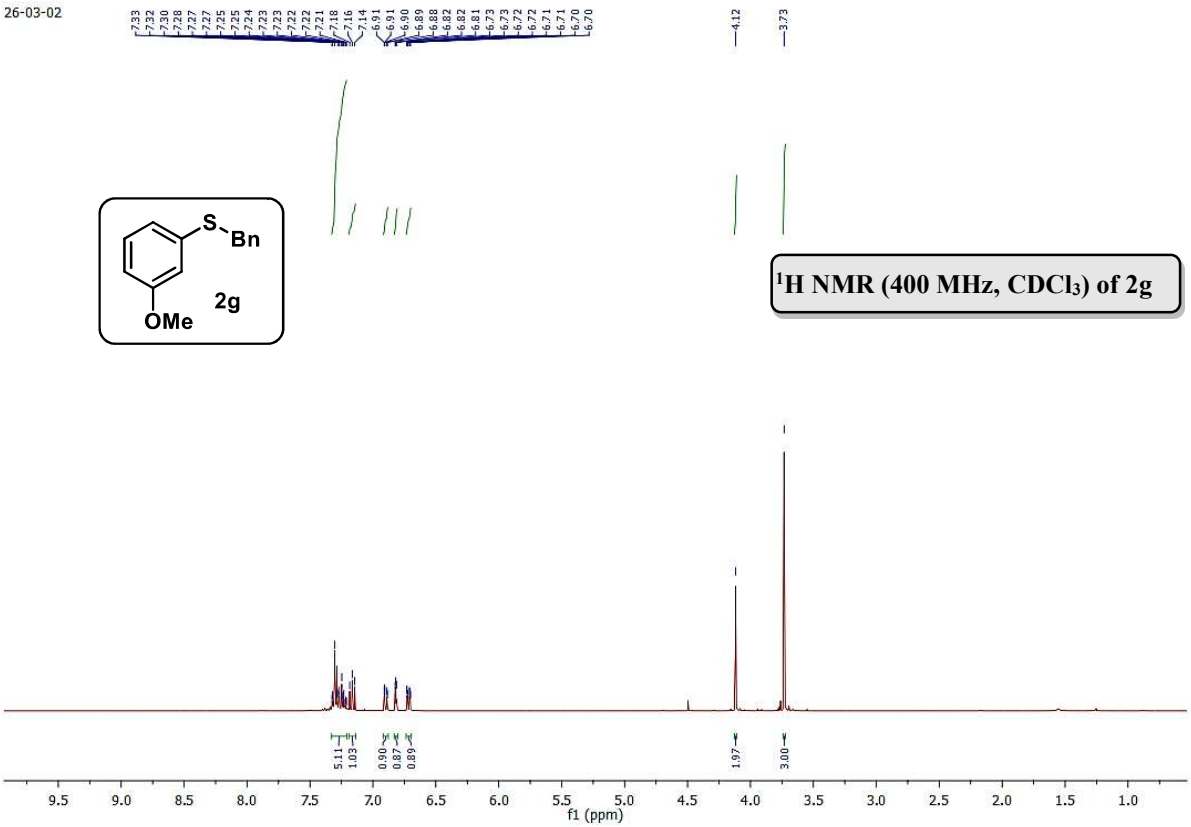

^{1}H NMR (400 MHz, $CDCl_3$) of 2g

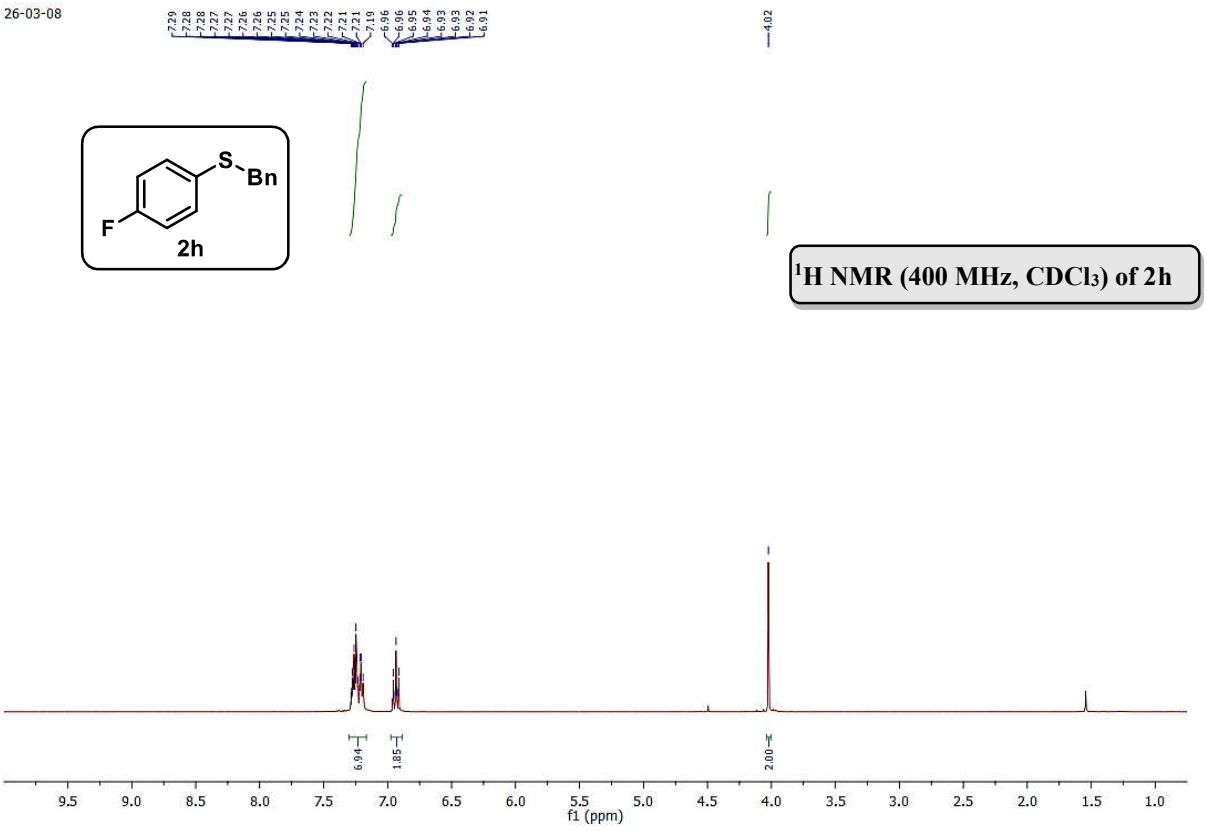

^{1}H NMR (400 MHz, $CDCl_3$) of 2h

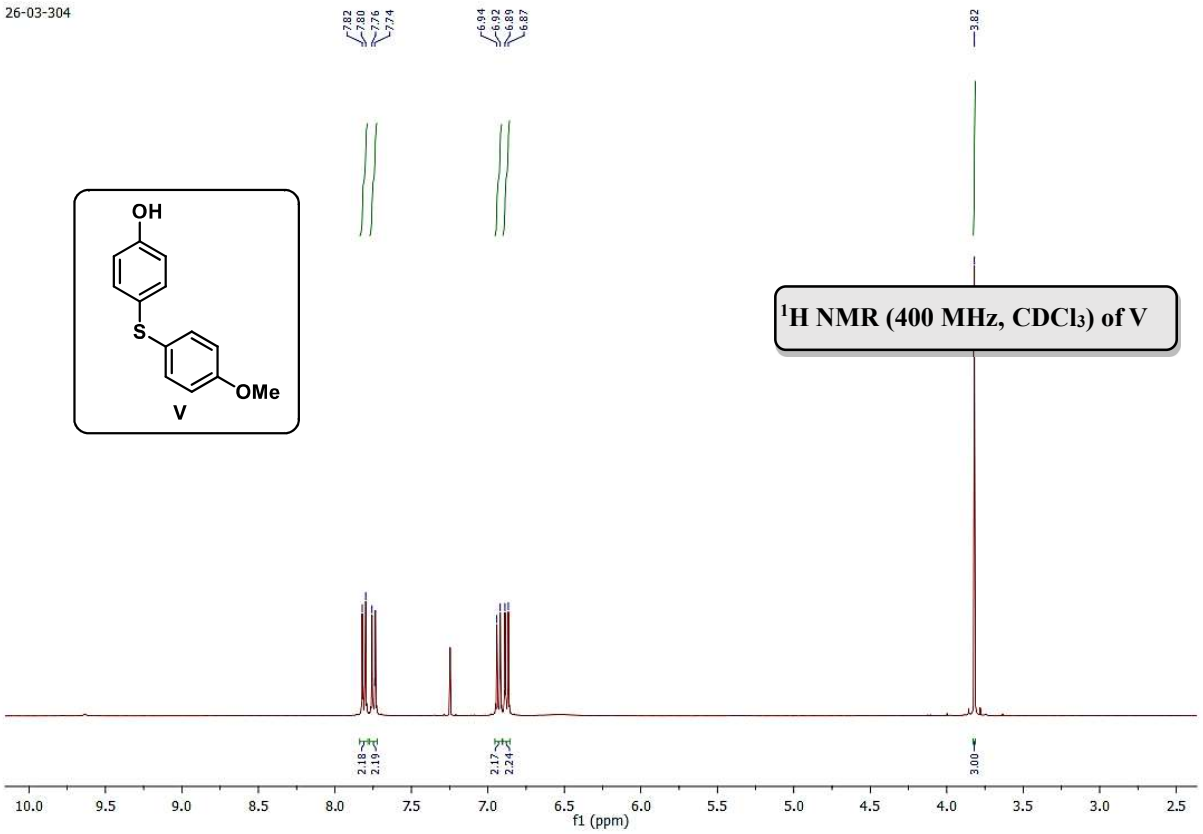

3.7. NMR spectra of final products

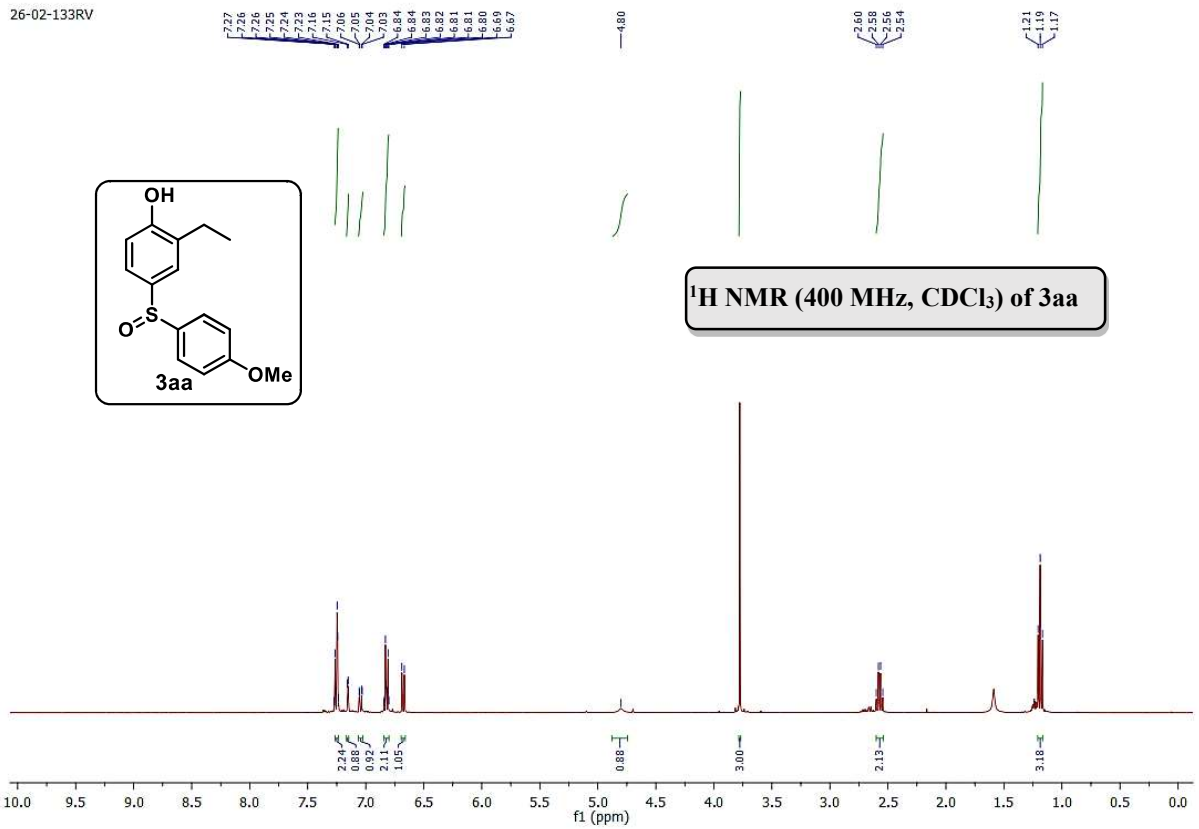

^{1}H NMR (400 MHz, $CDCl_3$) of 3aa

$^{13}C\{^{1}H\}$ NMR (101 MHz, $CDCl_3$) of 3aa

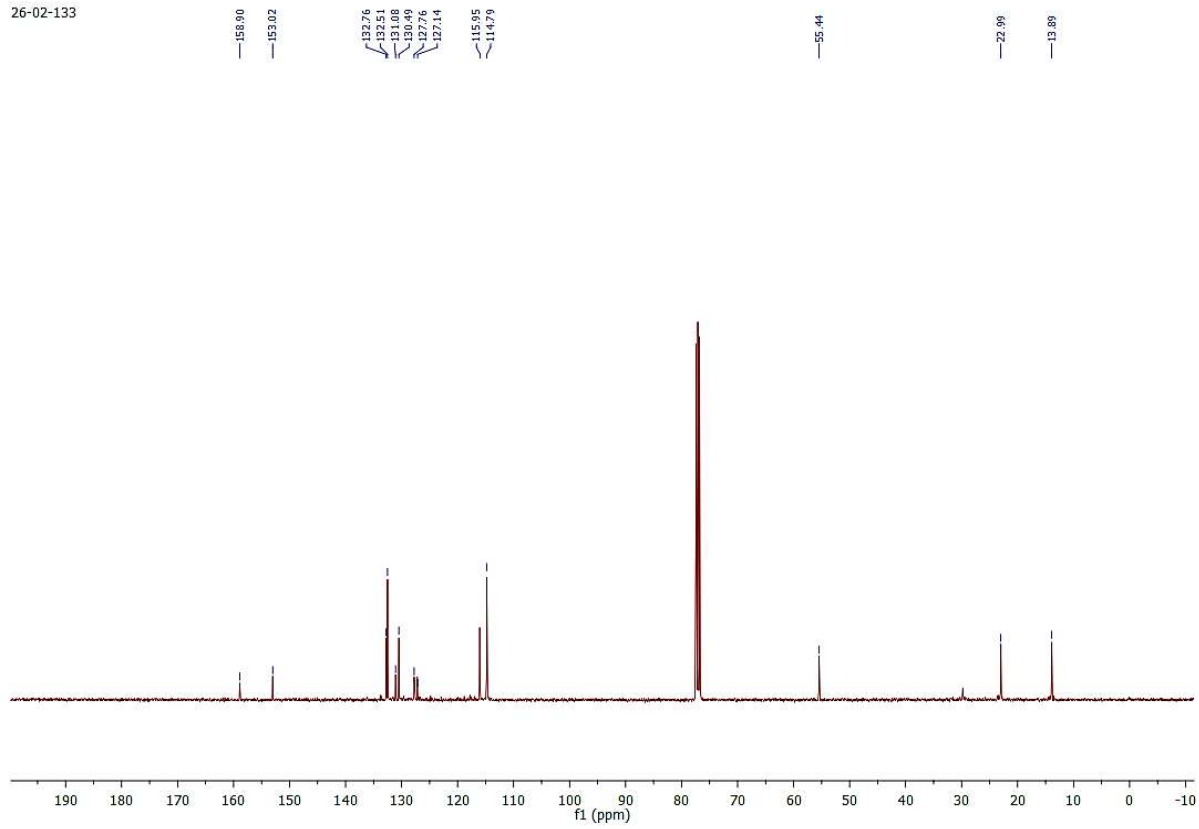

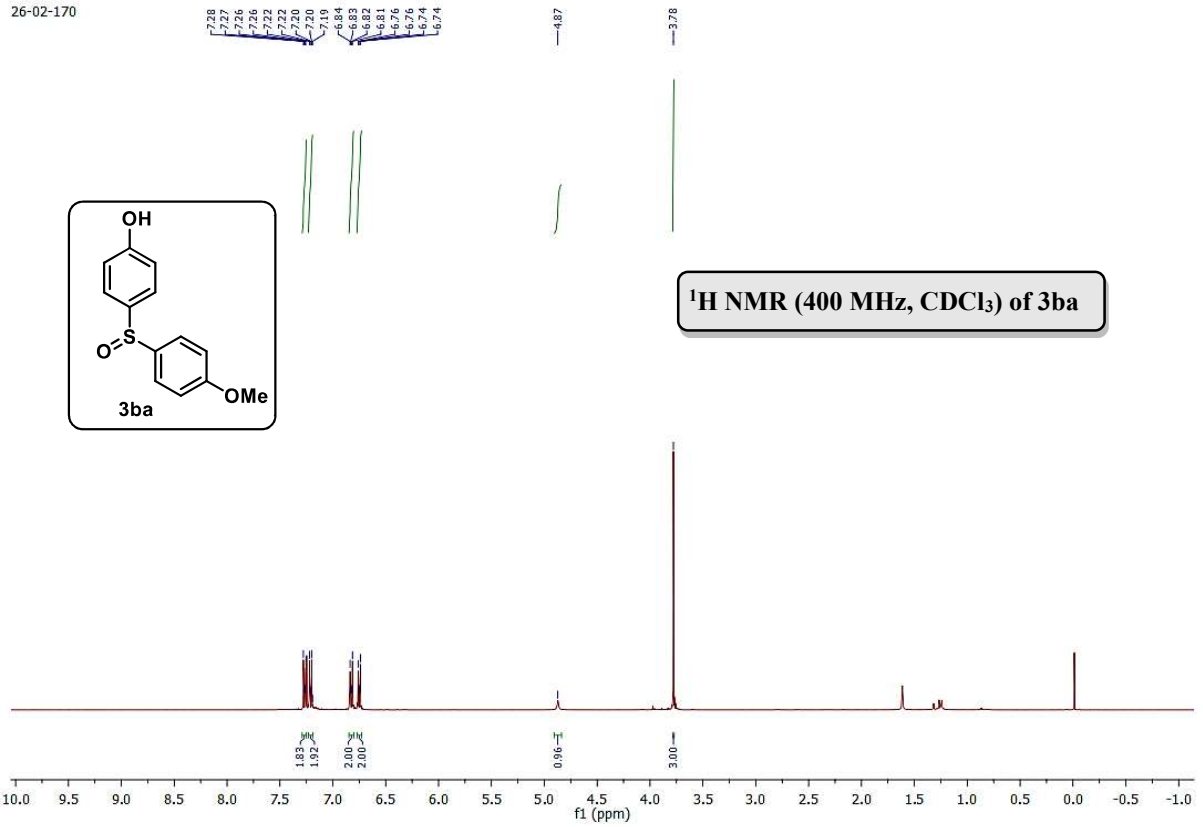

^{1}H NMR (400 MHz, $CDCl_3$) of 3ba

$^{13}C\{^{1}H\}$ NMR (101 MHz, $CDCl_3$) of 3ba

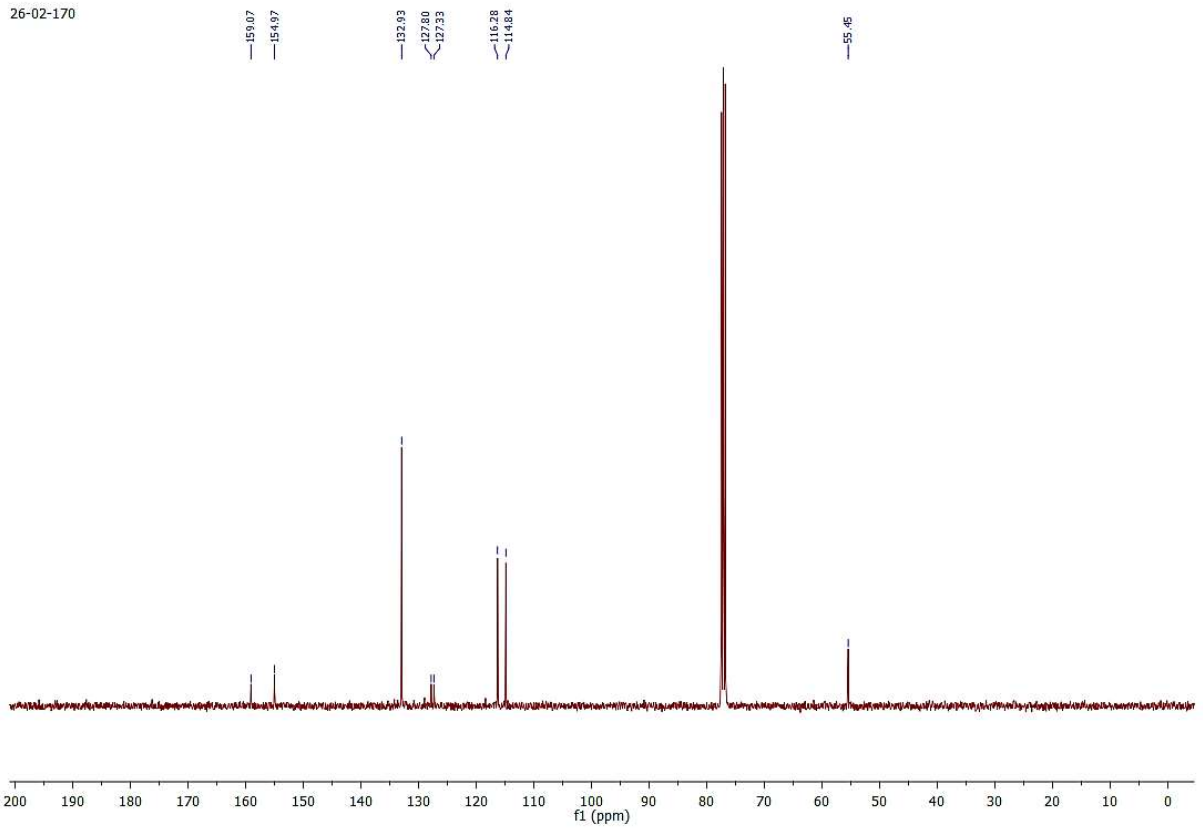

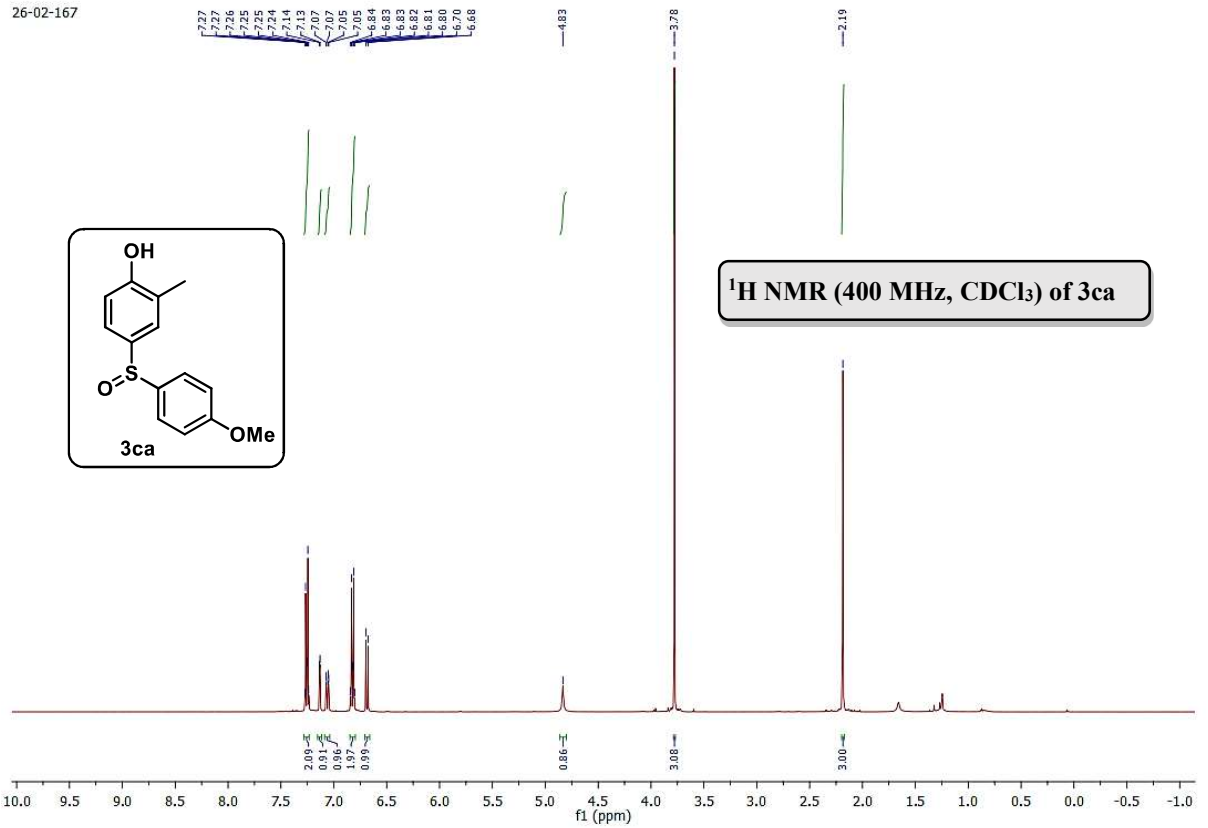

^{1}H NMR (400 MHz, $CDCl_3$) of 3ca

^{13}C{^{1}H} NMR (101 MHz, $CDCl_3$) of 3ca

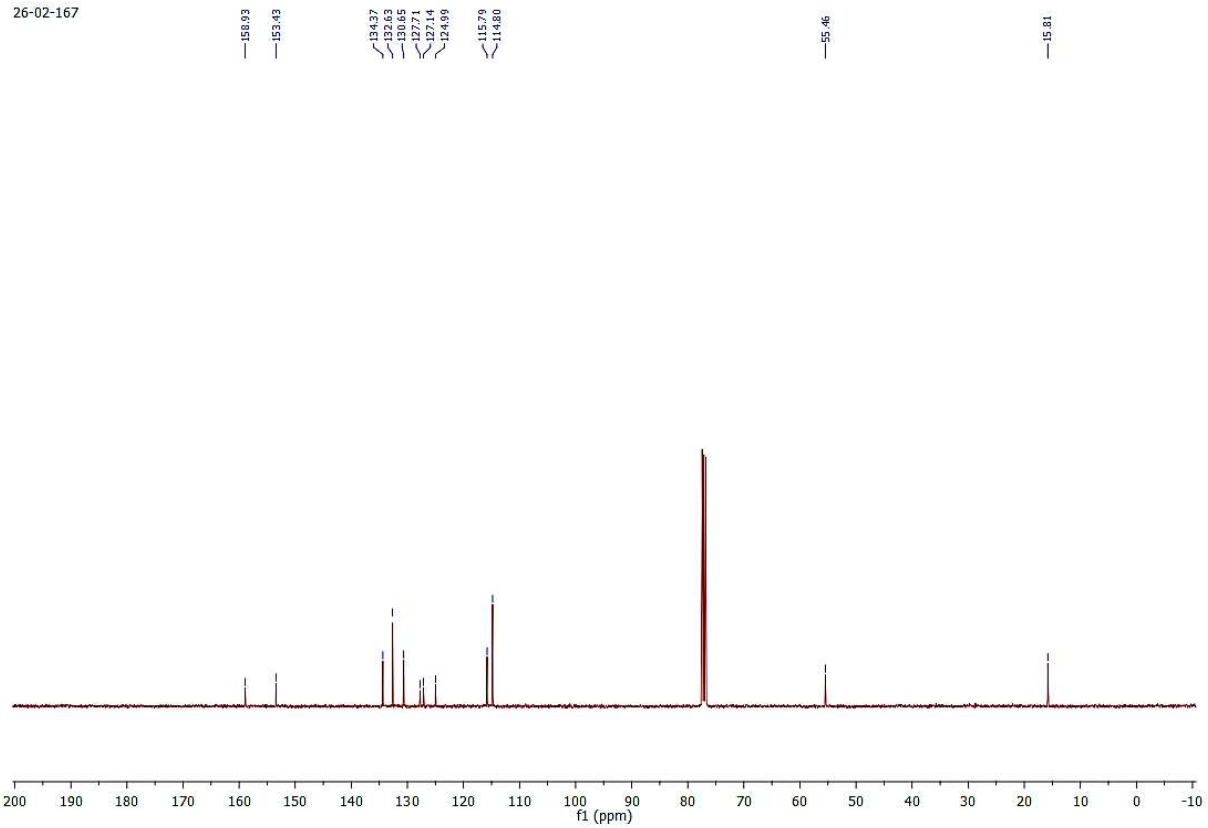

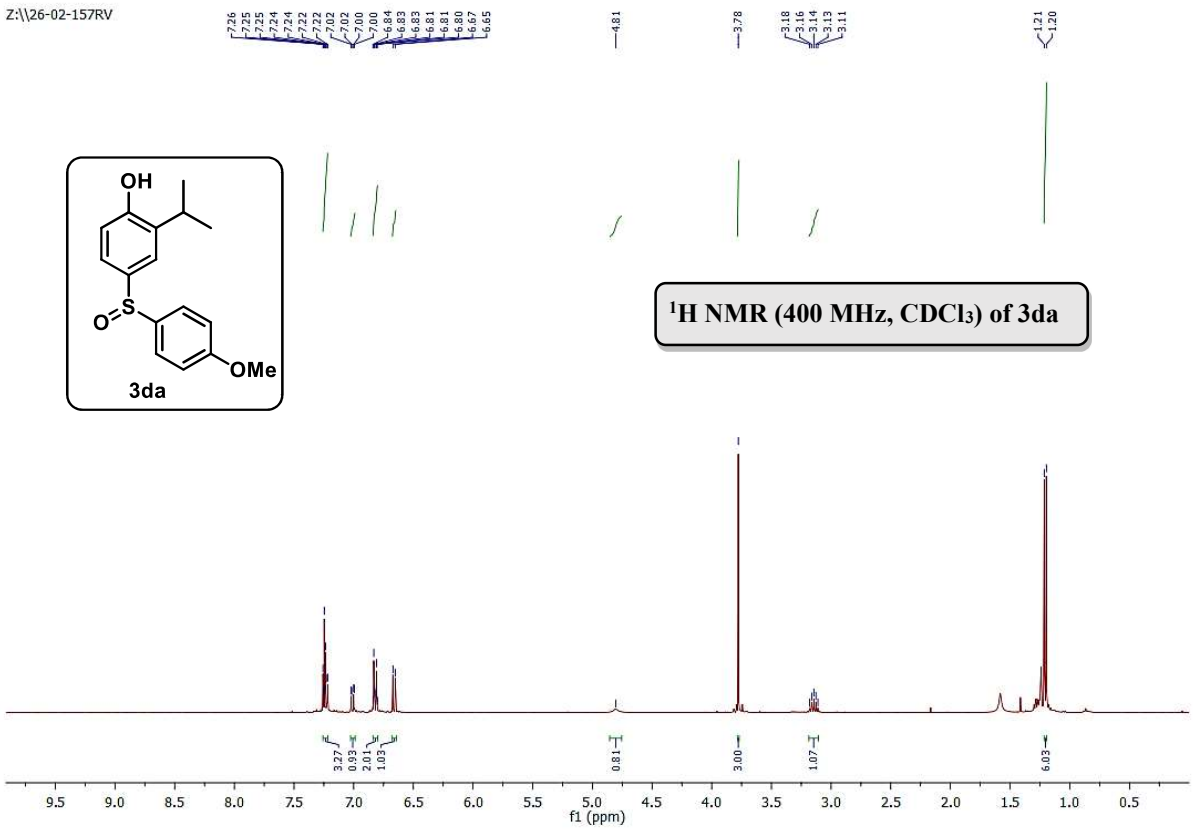

^{1}H NMR (400 MHz, $CDCl_3$) of 3da

$^{13}C\{^{1}H\}$ NMR (101 MHz, $CDCl_3$) of 3da

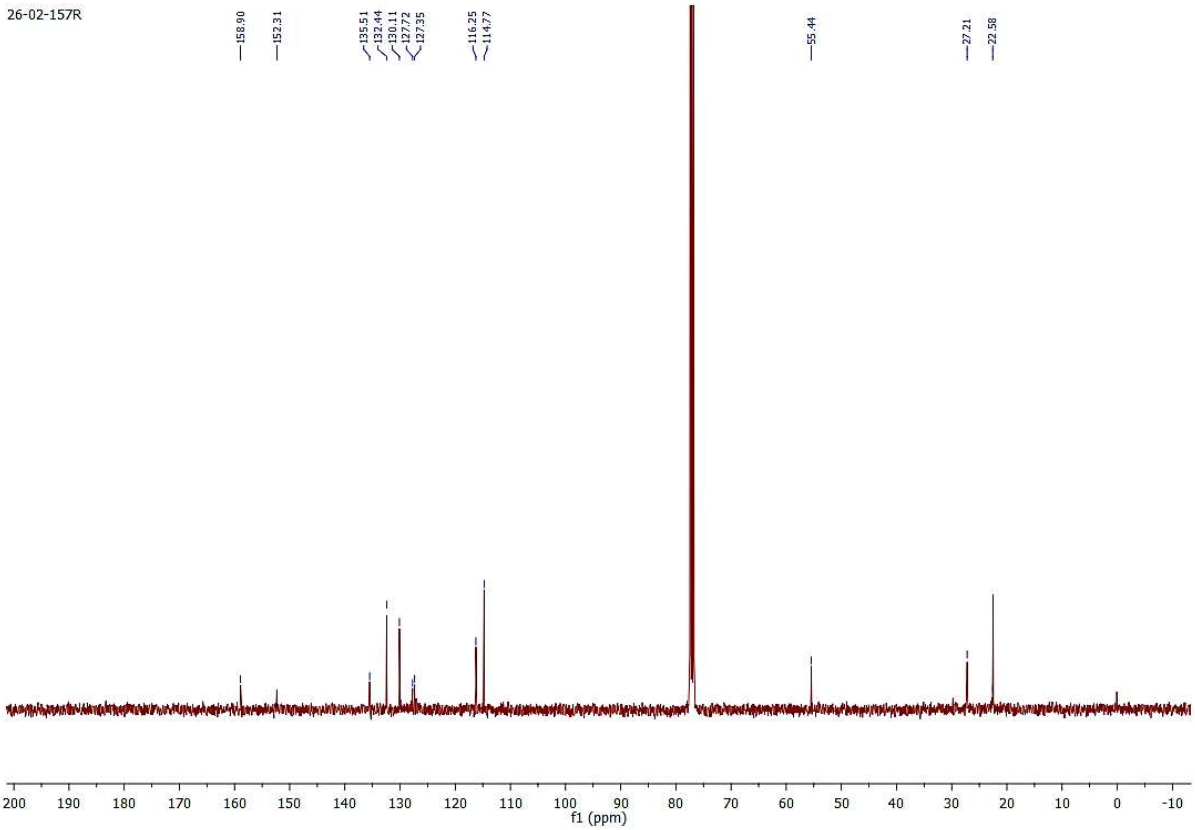

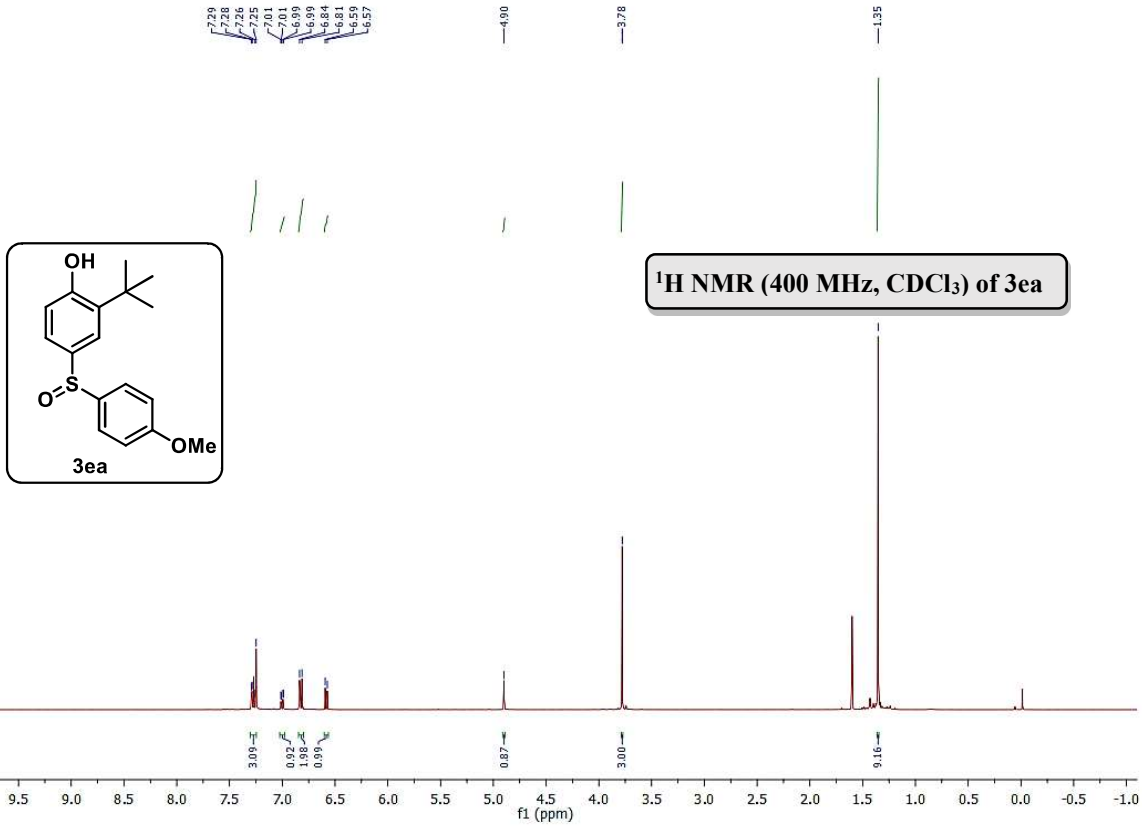

^{1}H NMR (400 MHz, $CDCl_3$) of 3ea

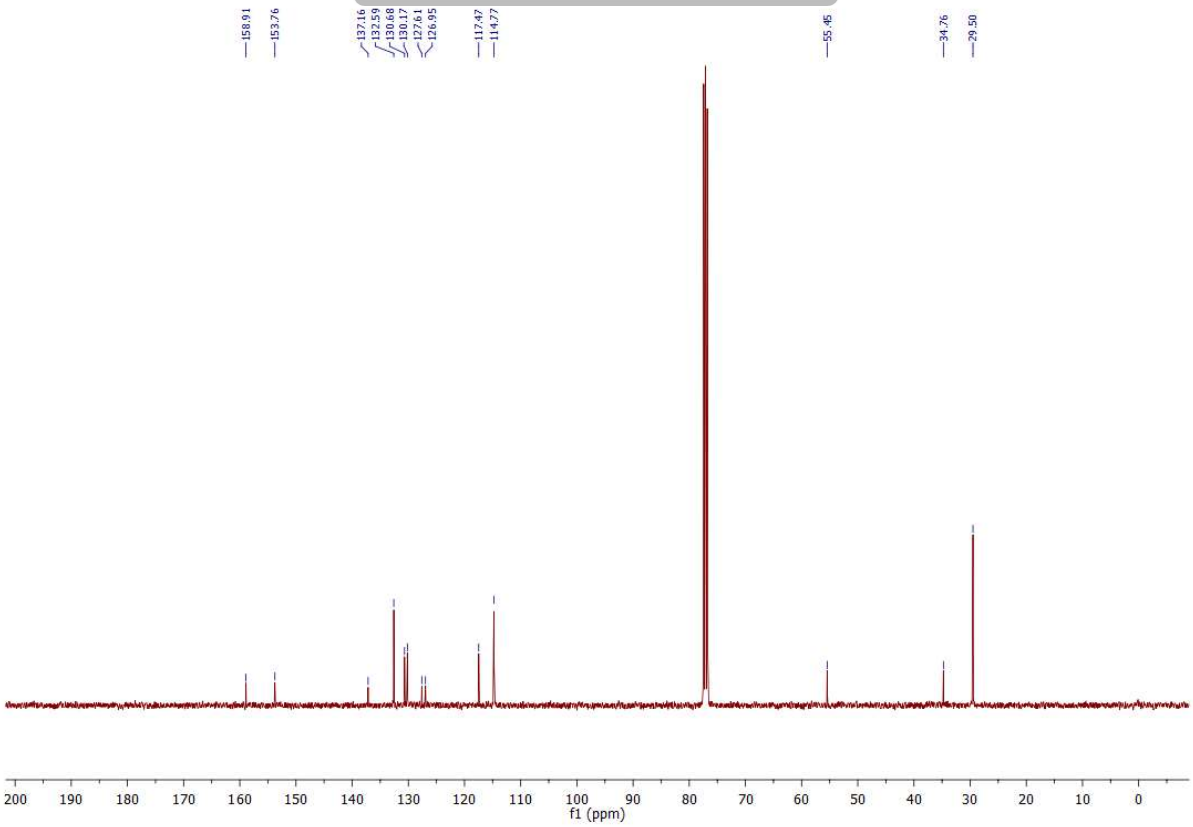

^{13}C{^{1}H} NMR (101 MHz, $CDCl_3$) of 3ea

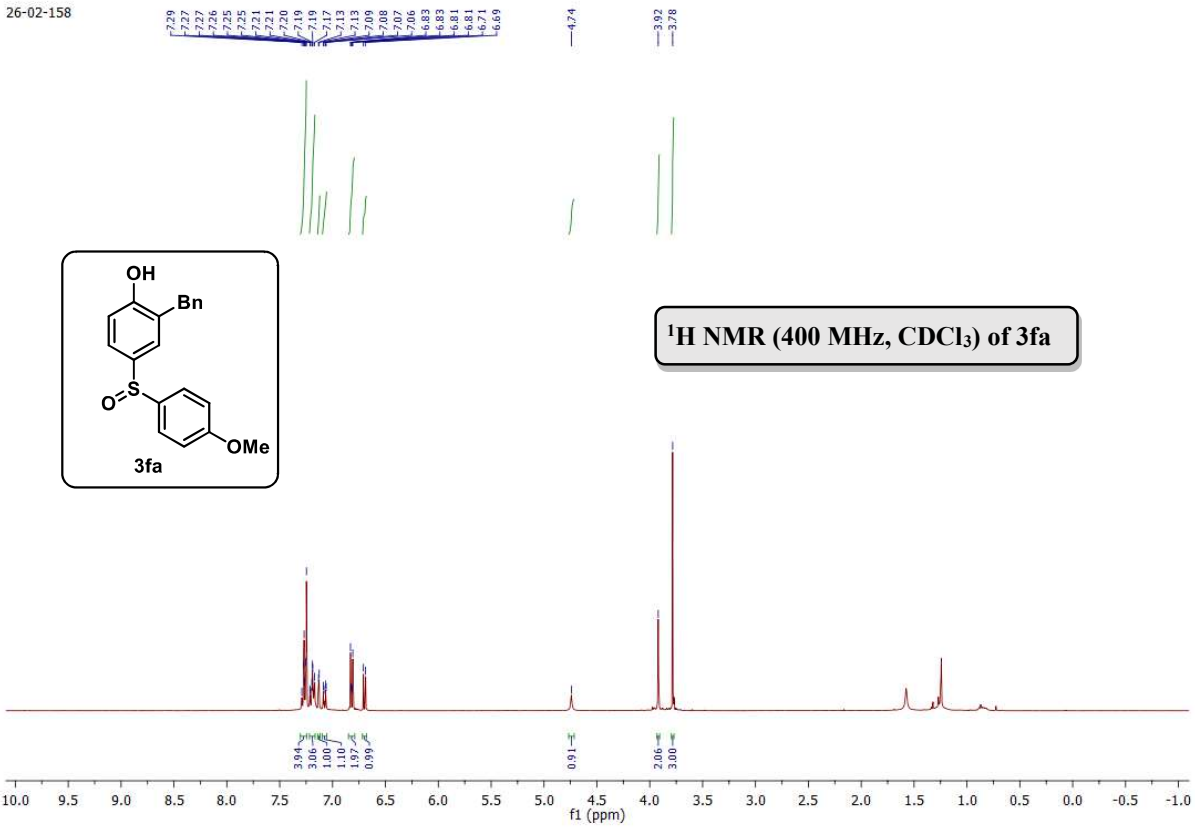

^{1}H NMR (400 MHz, $CDCl_3$) of 3fa

$^{13}C\{^{1}H\}$ NMR (101 MHz, $CDCl_3$) of 3fa

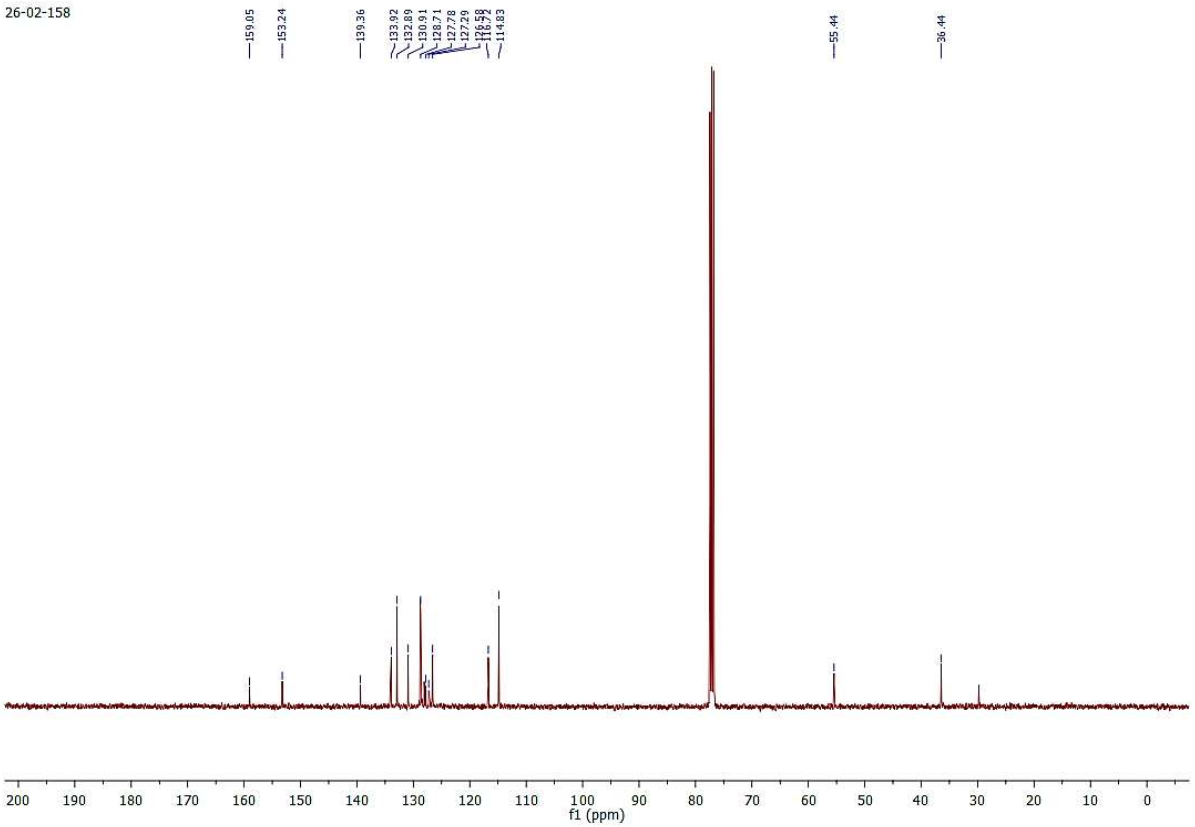

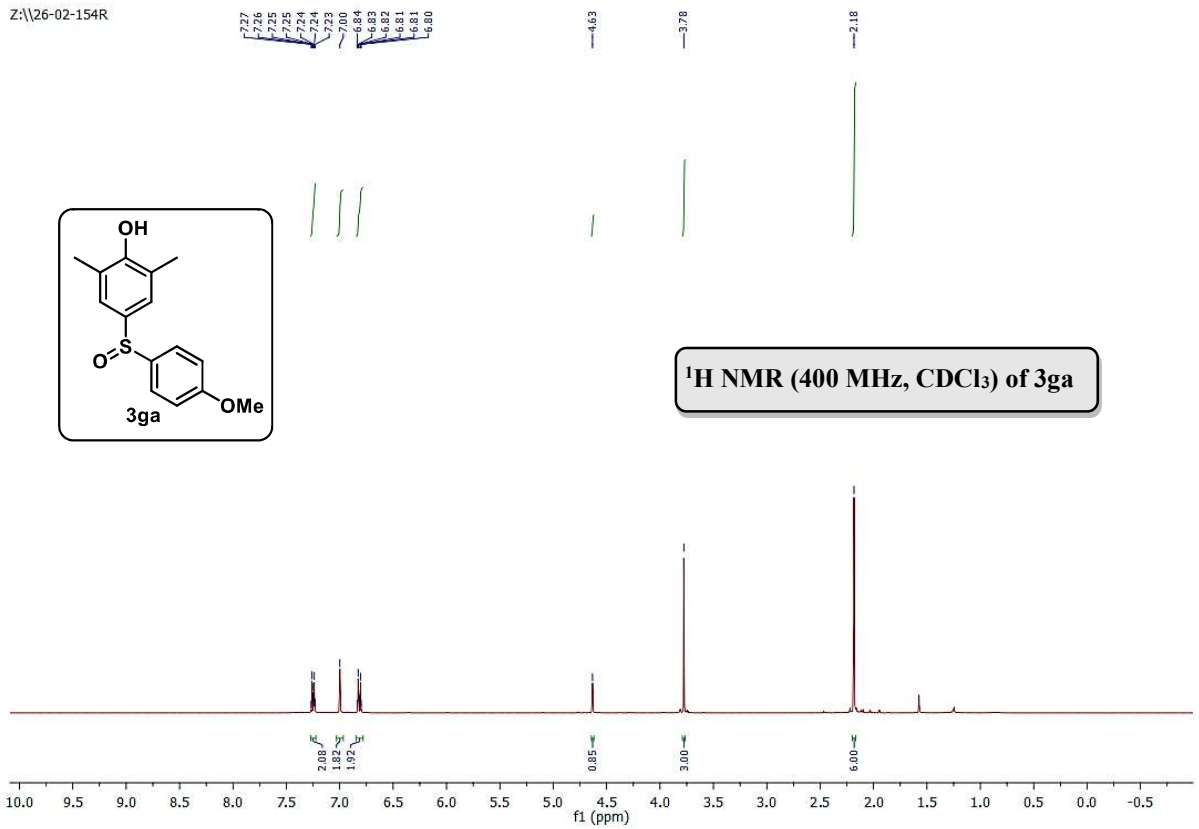

^{1}H NMR (400 MHz, $CDCl_3$) of 3ga

$^{13}C\{^{1}H\}$ NMR (101 MHz, $CDCl_3$) of 3ga

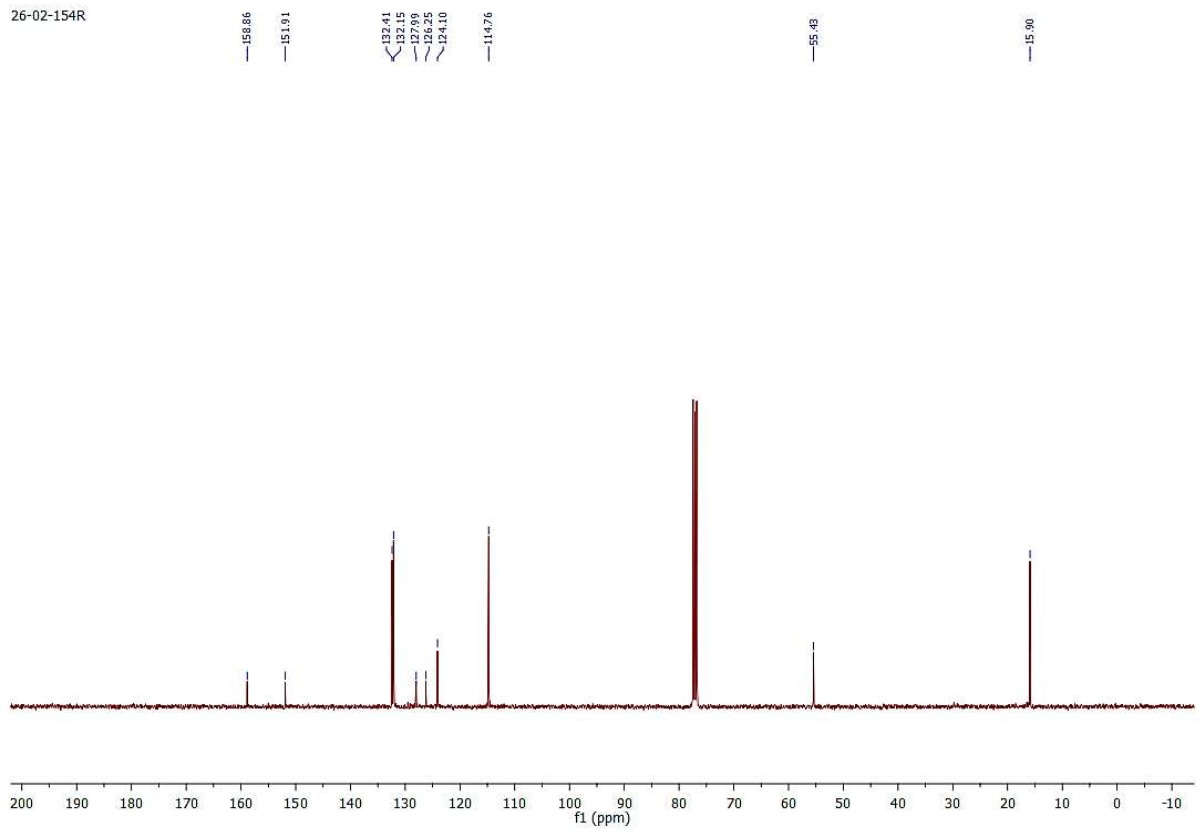

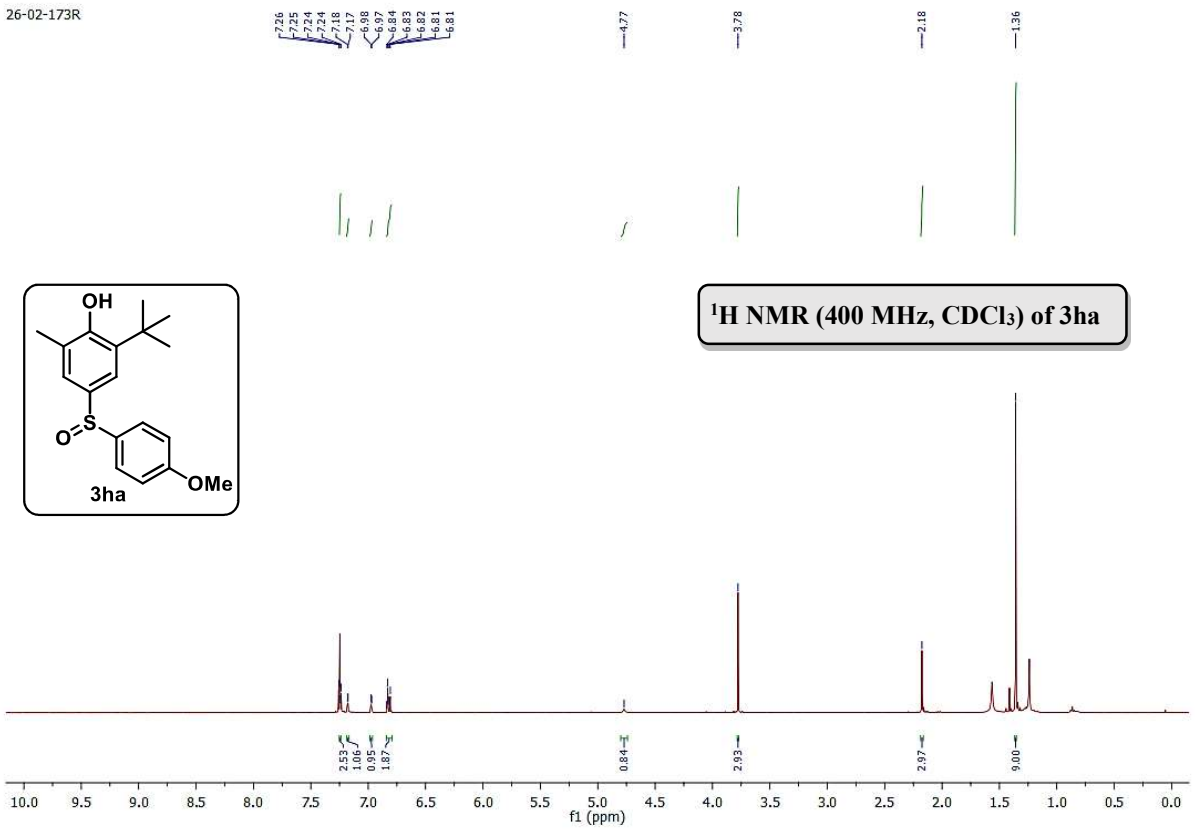

^{1}H NMR (400 MHz, $CDCl_3$) of 3ha

$^{13}C\{^{1}H\}$ NMR (101 MHz, $CDCl_3$) of 3ha

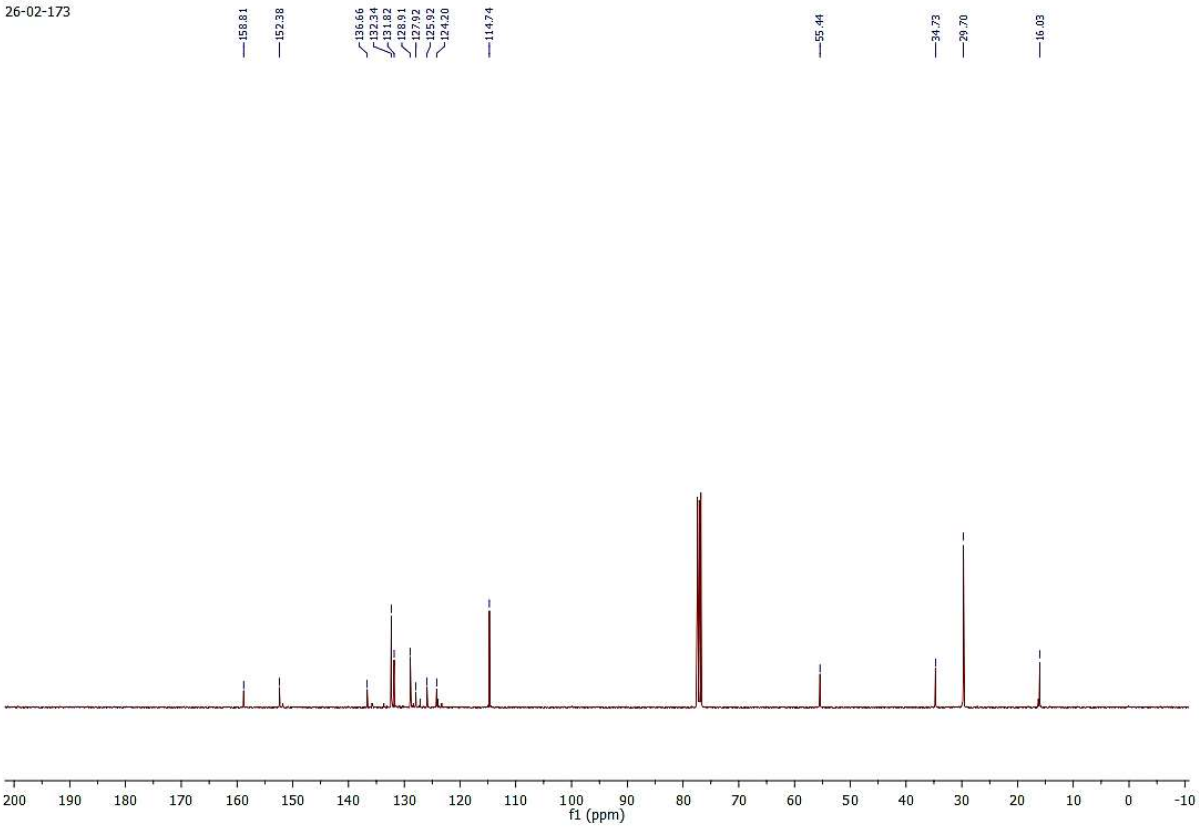

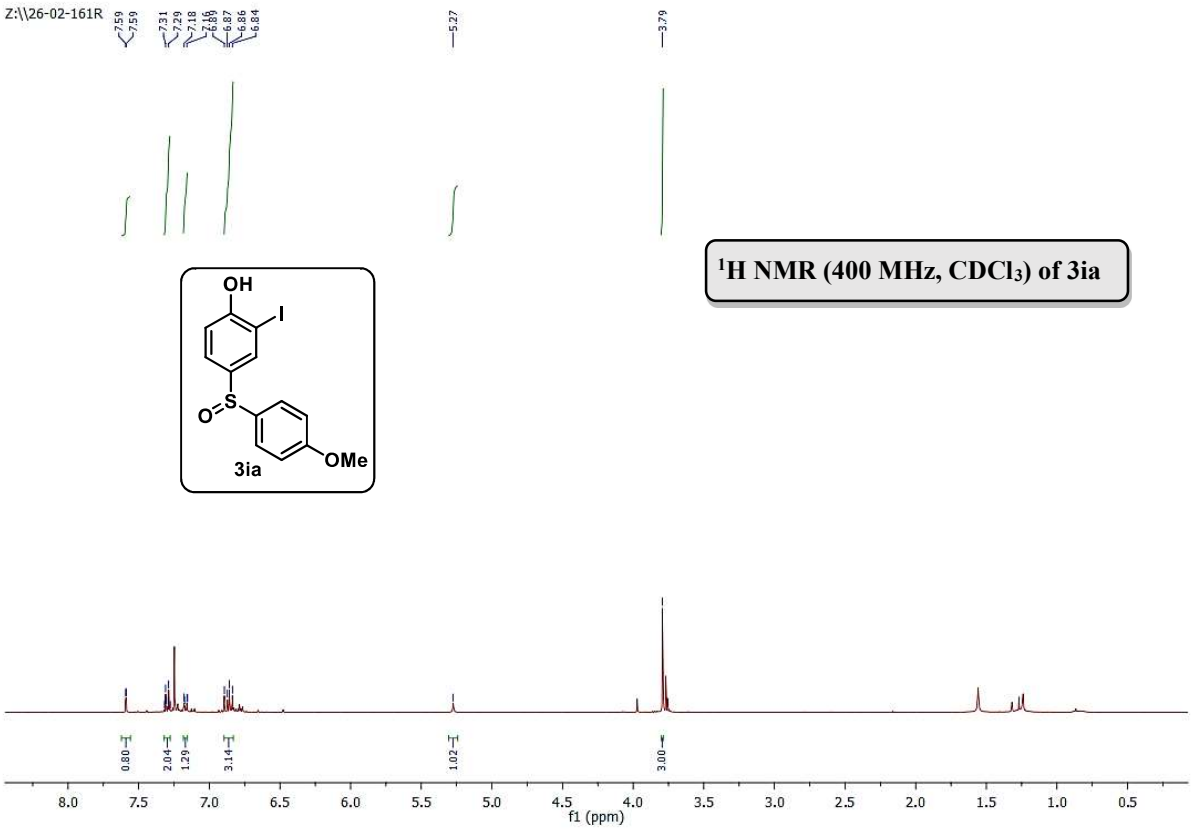

^{1}H NMR (400 MHz, $CDCl_3$) of 3ia

$^{13}C\{^{1}H\}$ NMR (101 MHz, $CDCl_3$) of 3ia

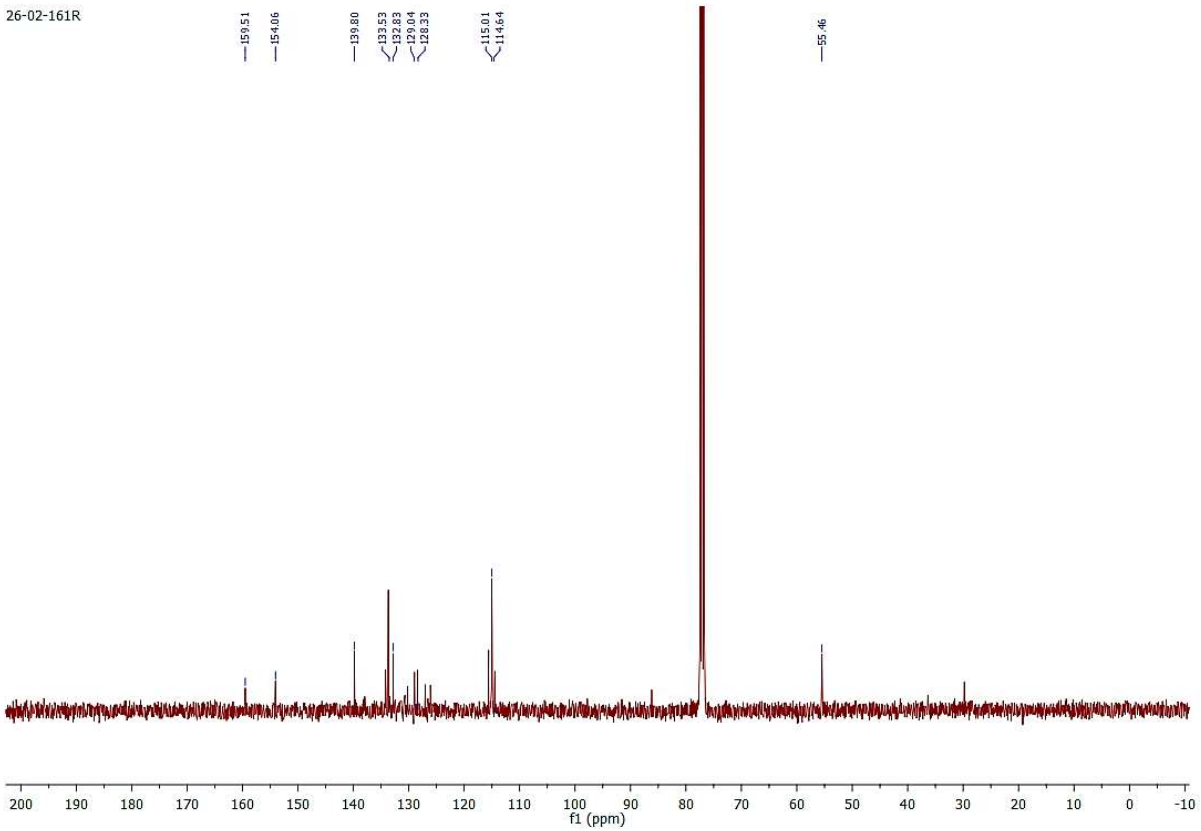

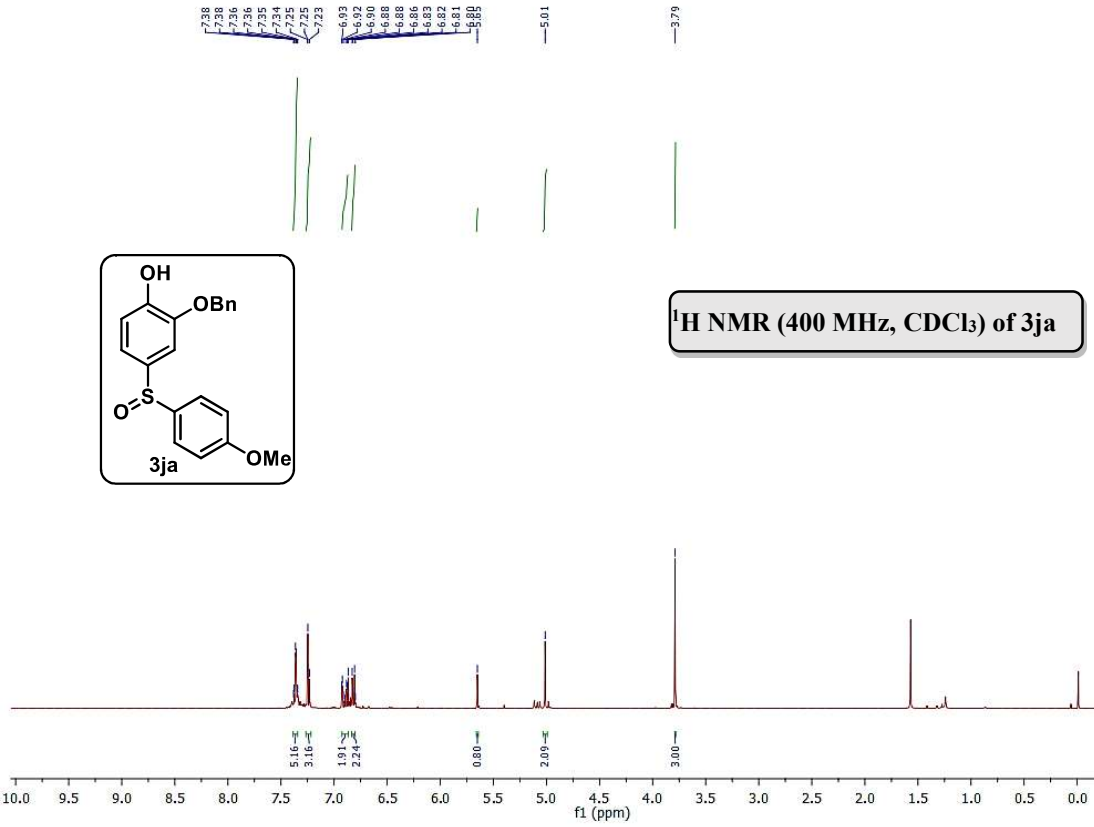

^{1}H NMR (400 MHz, $CDCl_3$) of 3ja

^{13}C {^{1}H} NMR (101 MHz, $CDCl_3$) of 3ja

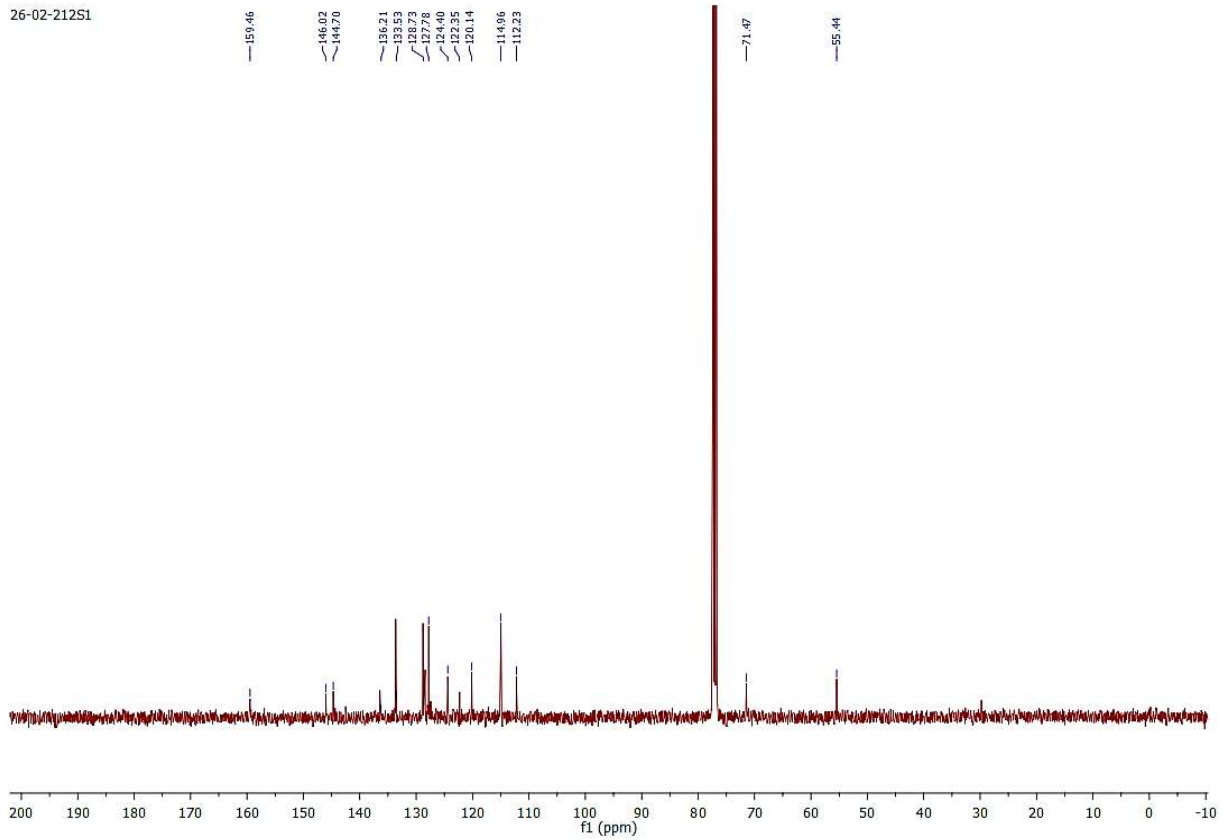

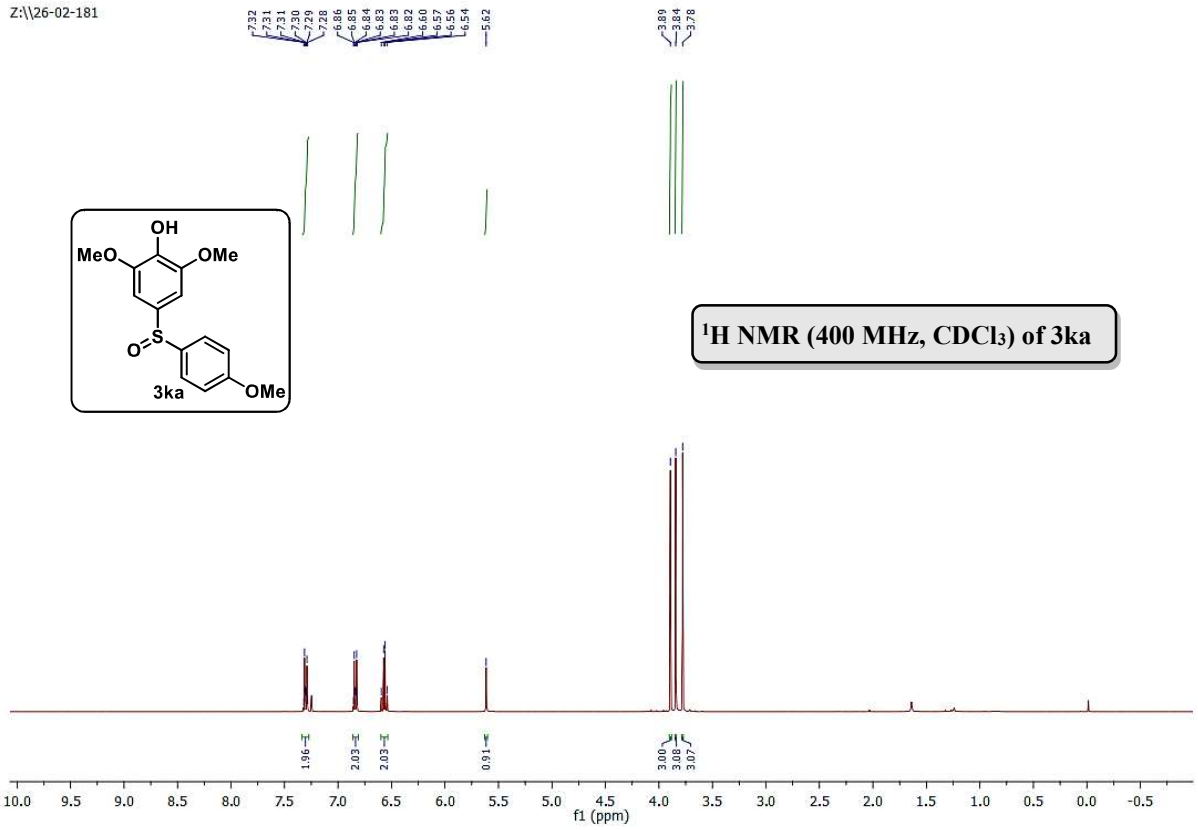

^{1}H NMR (400 MHz, $CDCl_3$) of 3ka

$^{13}C\{^{1}H\}$ NMR (101 MHz, $CDCl_3$) of 3ka

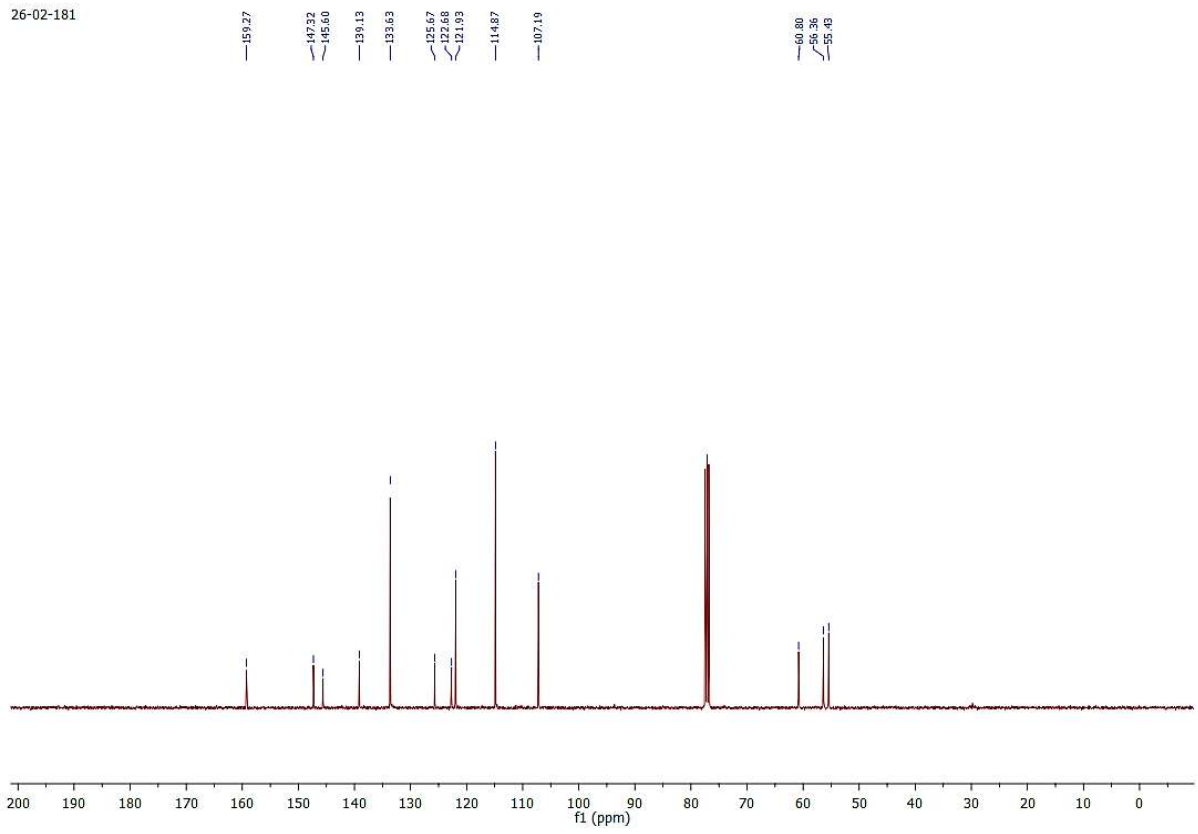

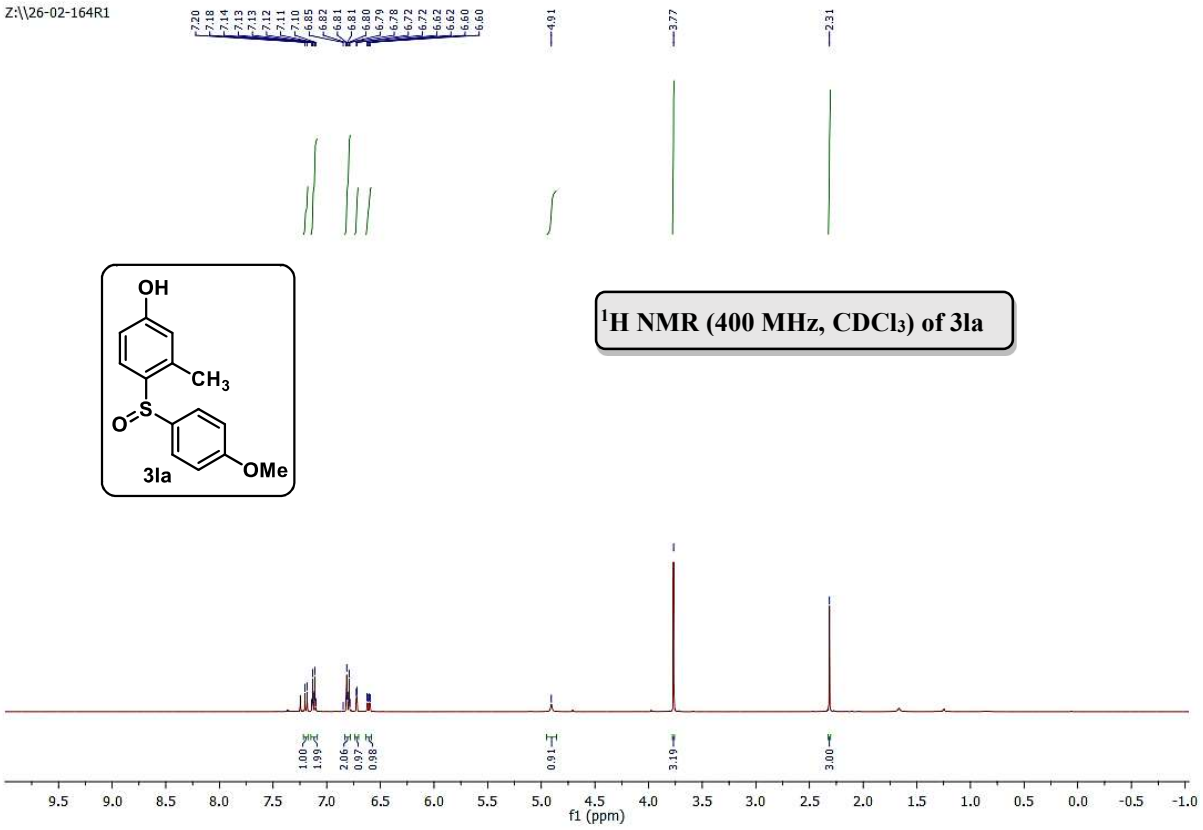

^{1}H NMR (400 MHz, $CDCl_3$) of 3la

$^{13}C\{^{1}H\}$ NMR (101 MHz, $CDCl_3$) of 3la

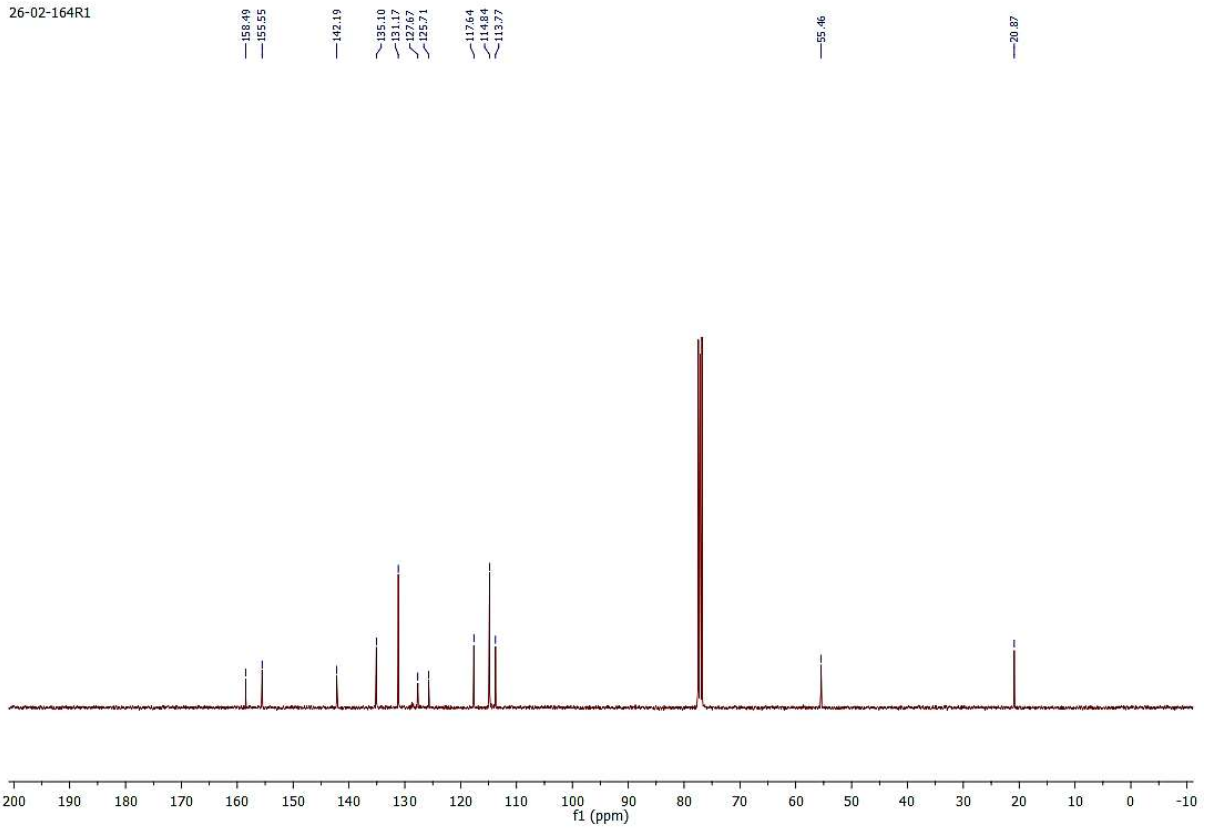

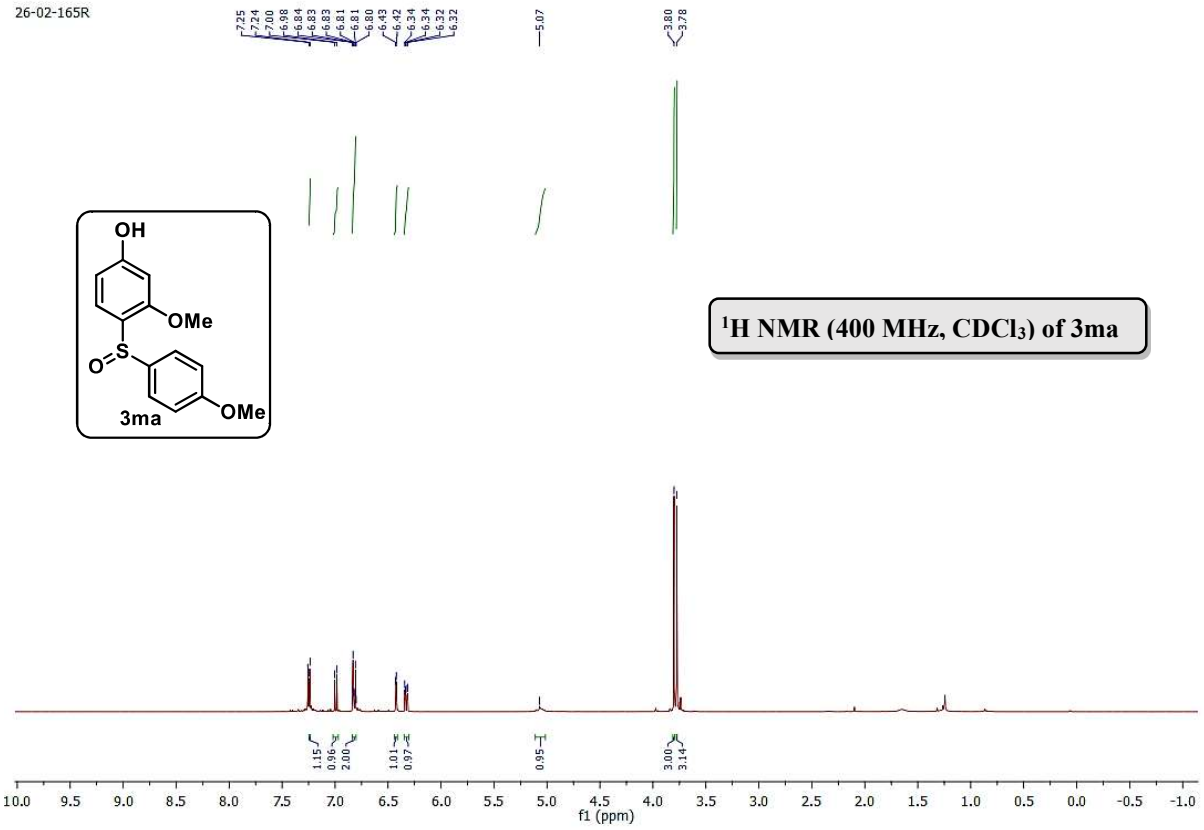

^{1}H NMR (400 MHz, $CDCl_3$) of 3ma

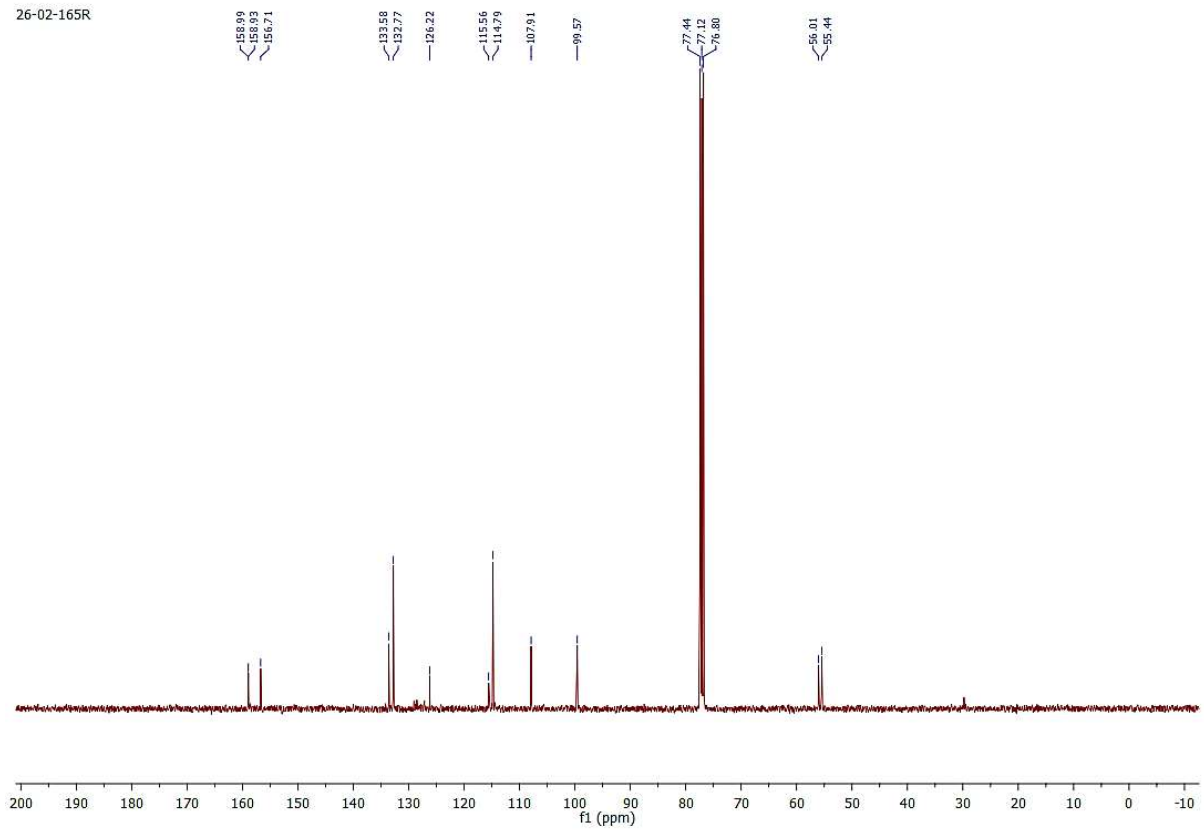

$^{13}C\{^{1}H\}$ NMR (101 MHz, $CDCl_3$) of 3ma

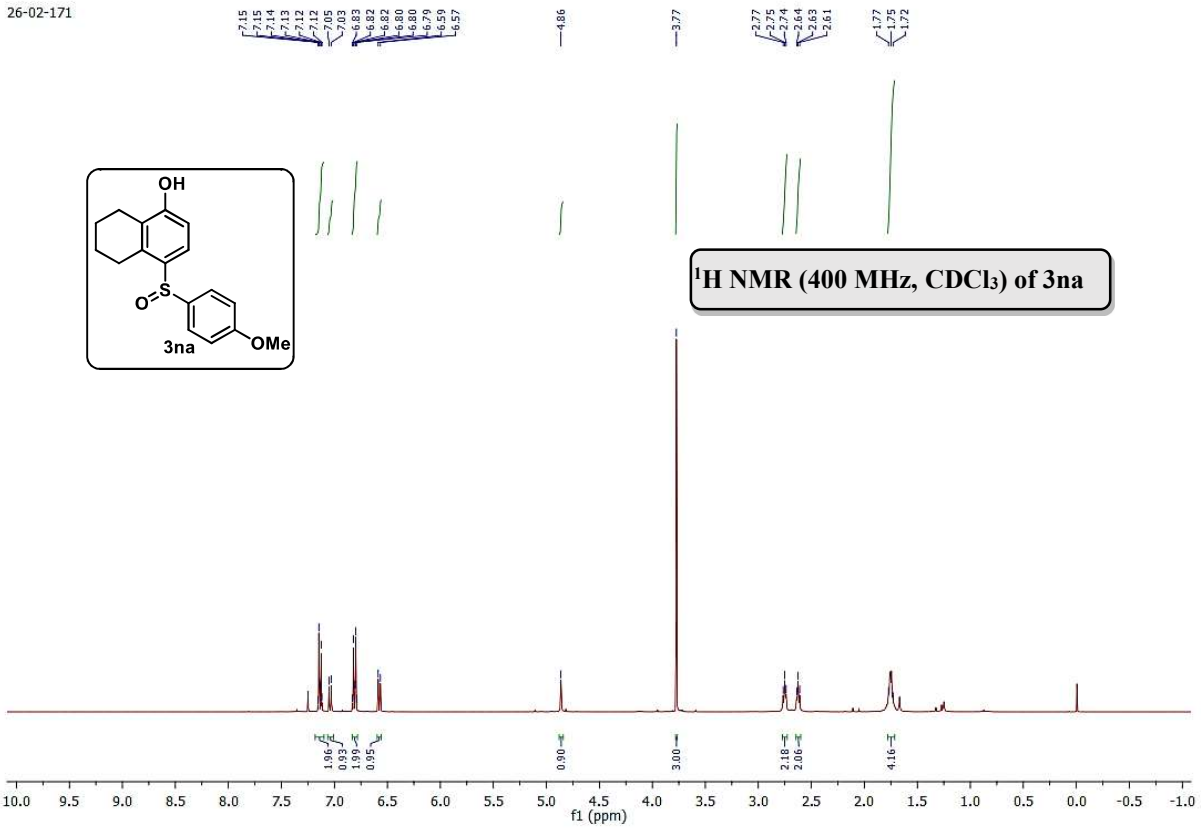

^{1}H NMR (400 MHz, $CDCl_3$) of 3na

$^{13}C\{^{1}H\}$ NMR (101 MHz, $CDCl_3$) of 3na

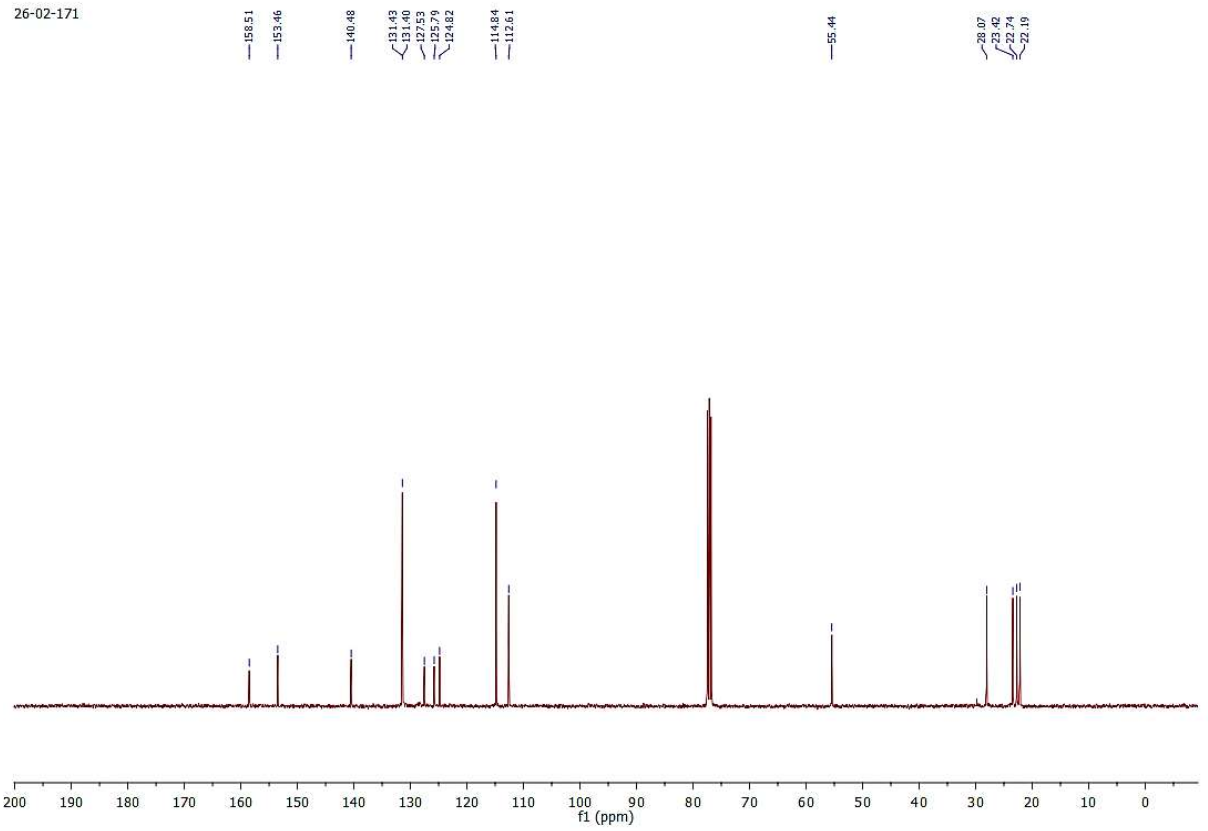

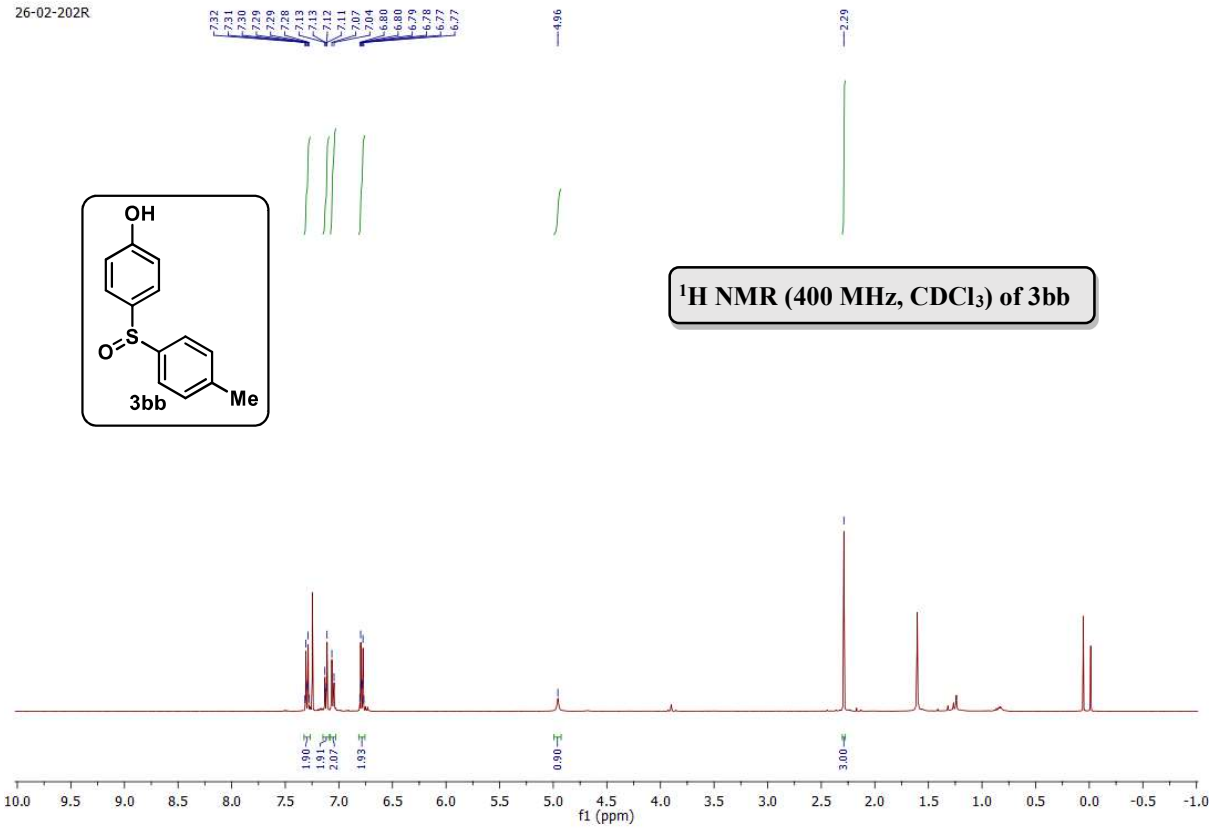

^{1}H NMR (400 MHz, $CDCl_3$) of 3bb

$^{13}C\{^{1}H\}$ NMR (101 MHz, $CDCl_3$) of 3bb

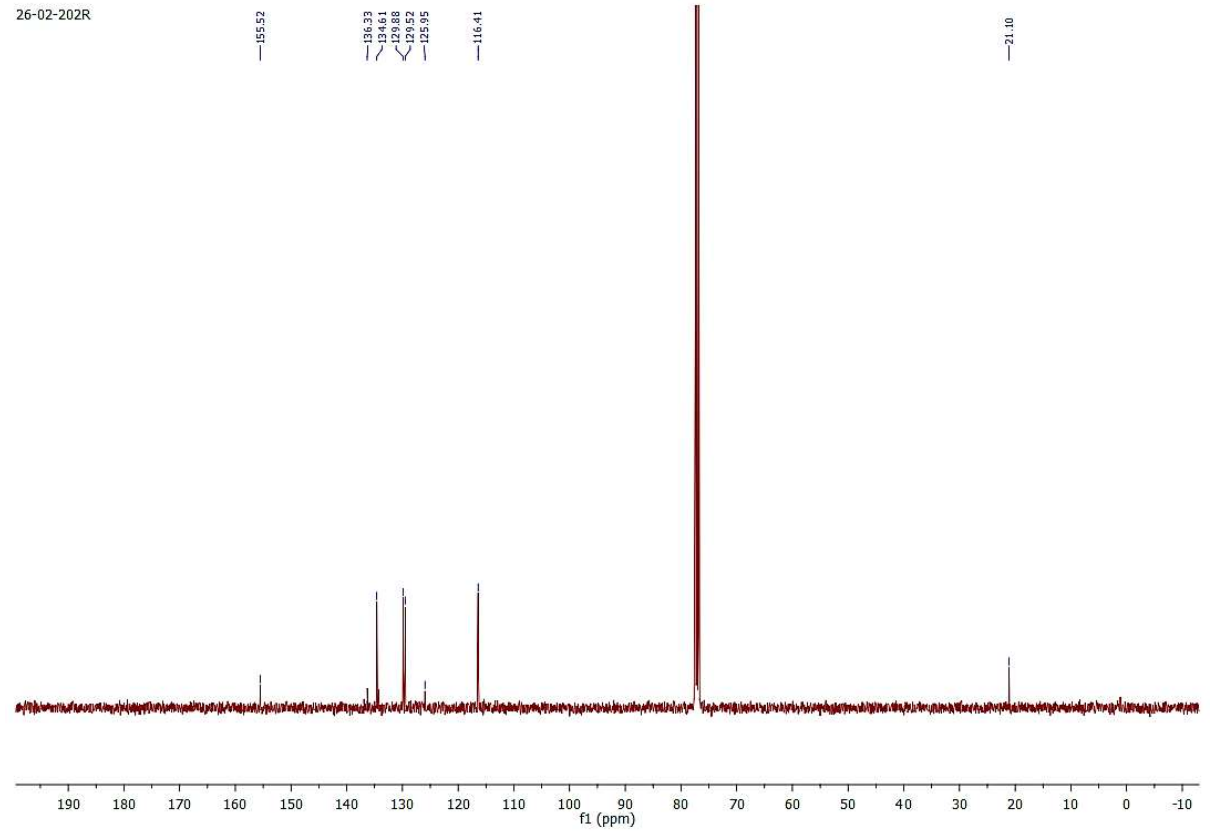

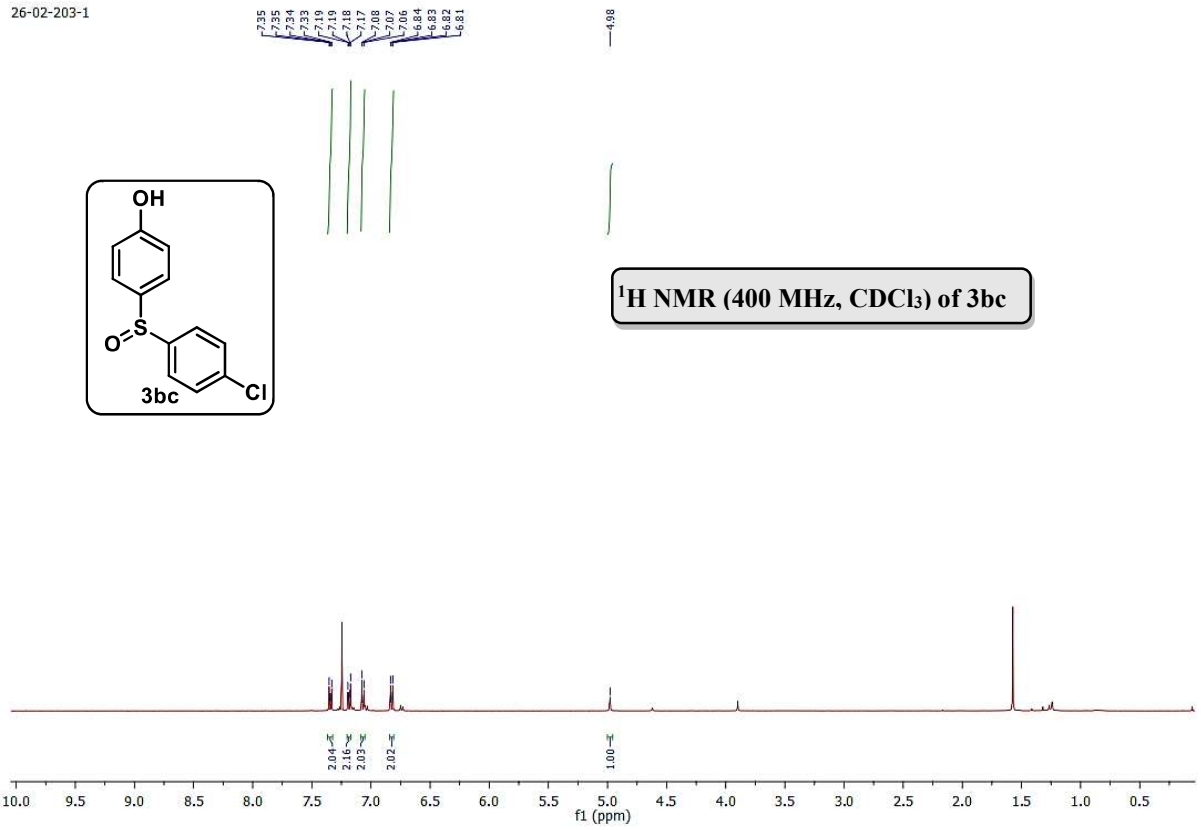

^{1}H NMR (400 MHz, $CDCl_3$) of 3bc

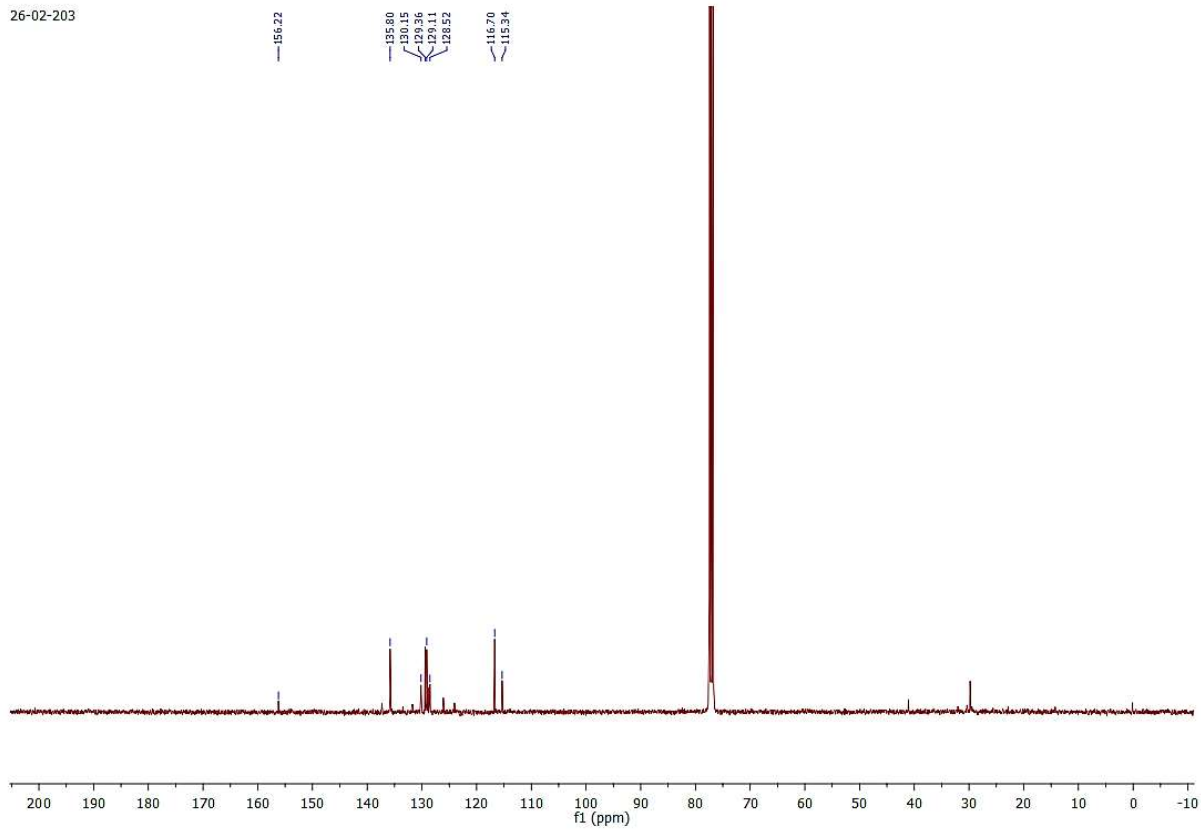

^{13}C{^{1}H} NMR (101 MHz, $CDCl_3$) of 3bc

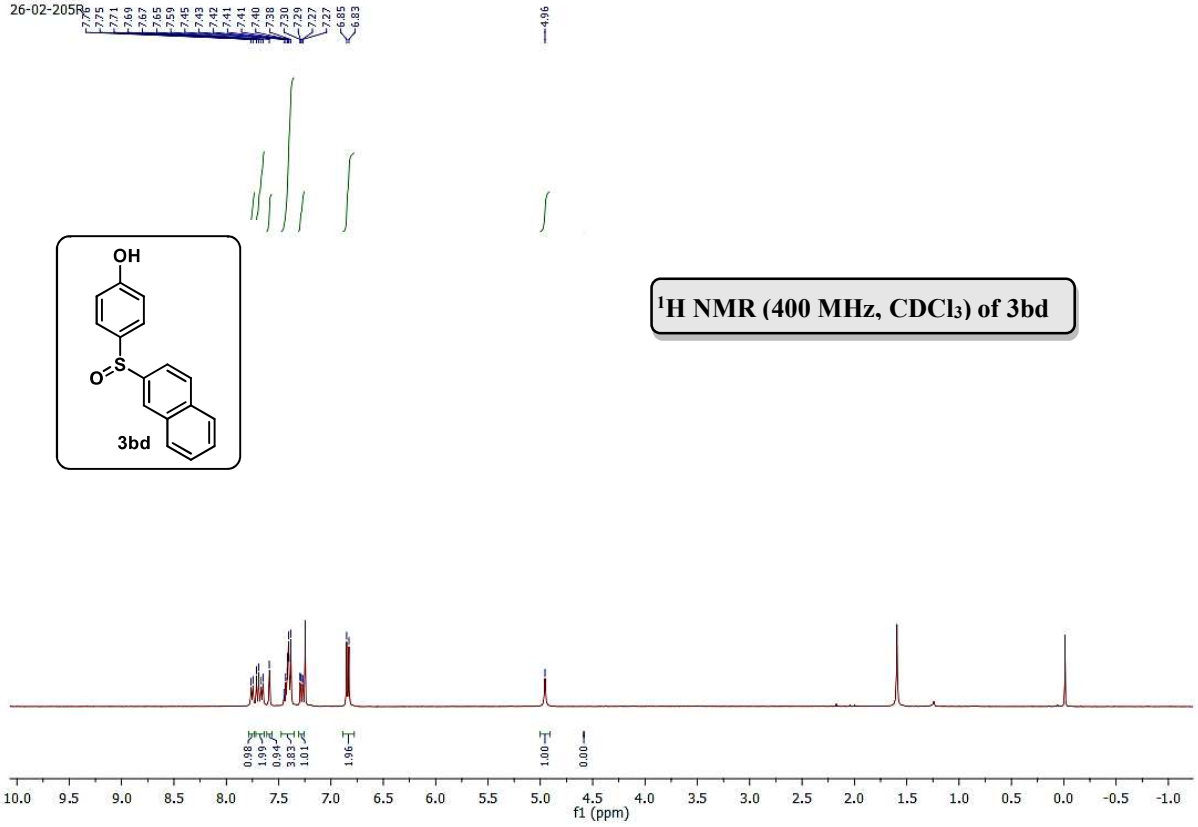

^{1}H NMR (400 MHz, $CDCl_3$) of 3bd

$^{13}C\{^{1}H\}$ NMR (101 MHz, $CDCl_3$) of 3bd

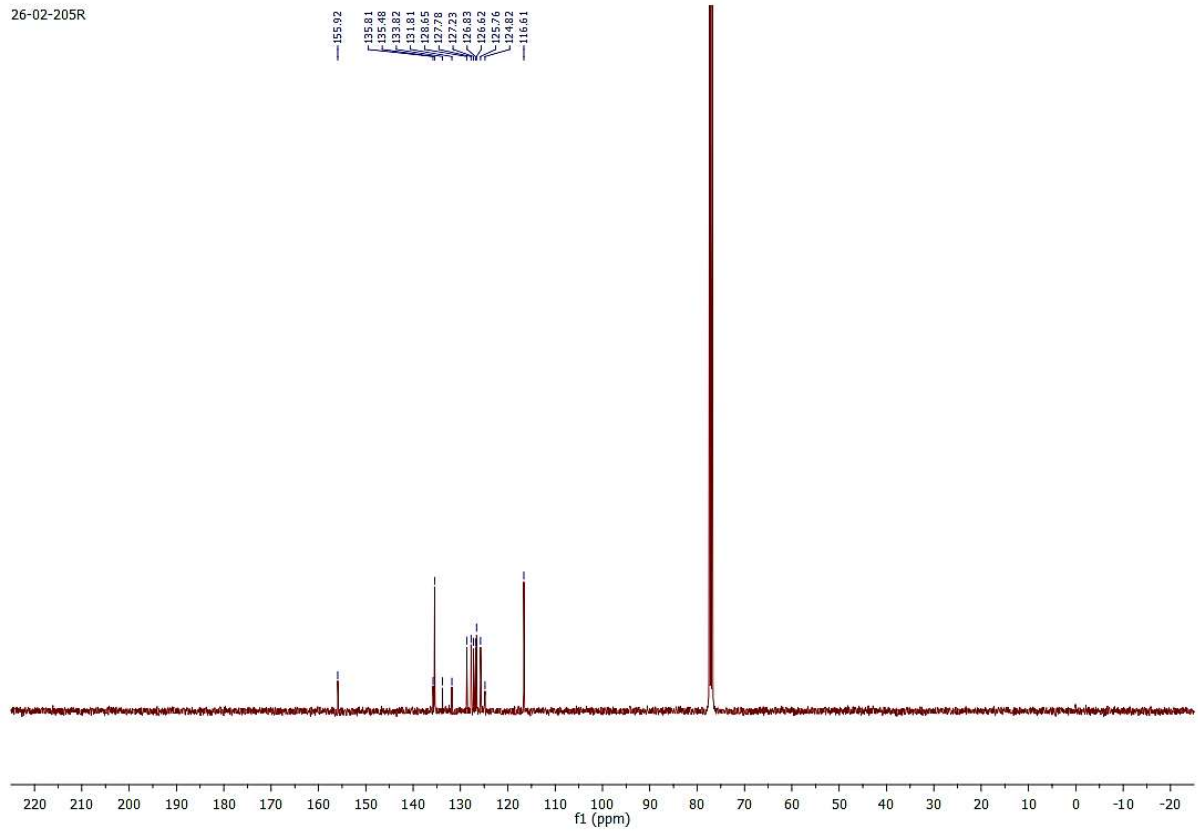

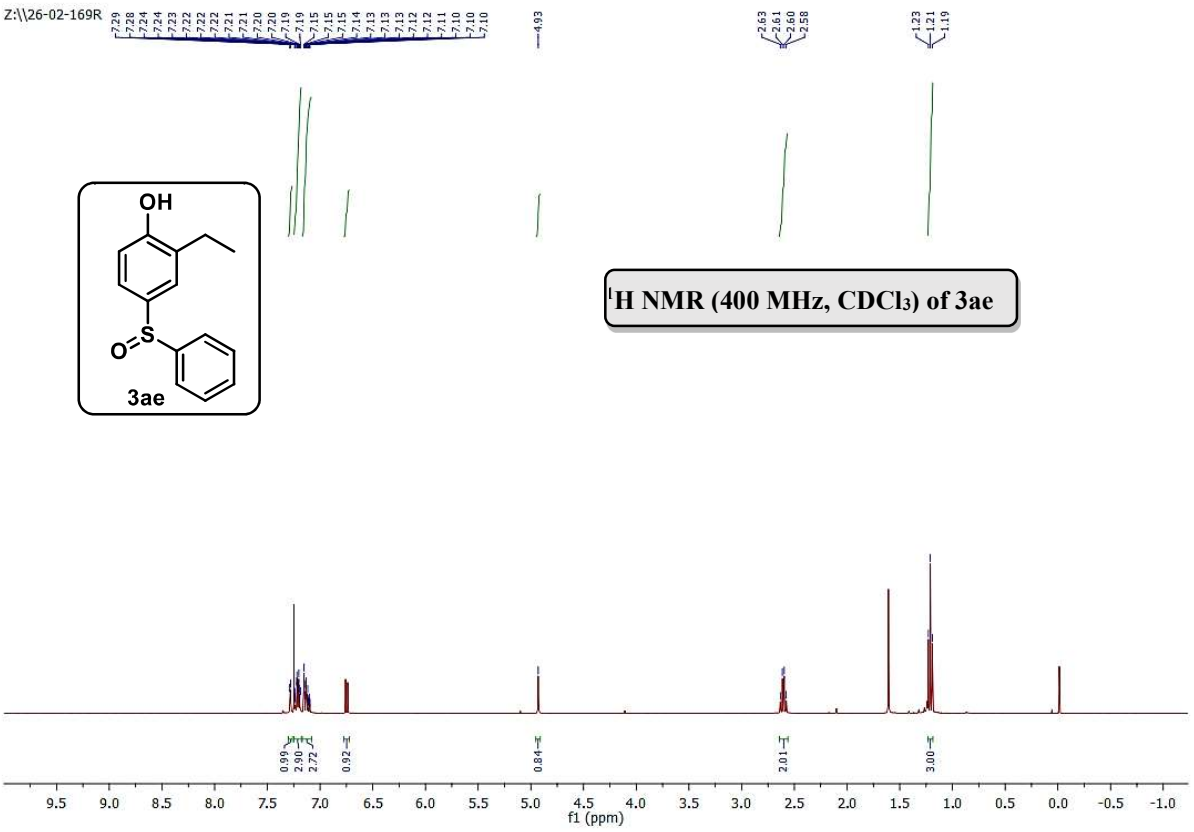

^{1}H NMR (400 MHz, $CDCl_3$) of 3ae

$^{13}C\{^{1}H\}$ NMR (101 MHz, $CDCl_3$) of 3ae

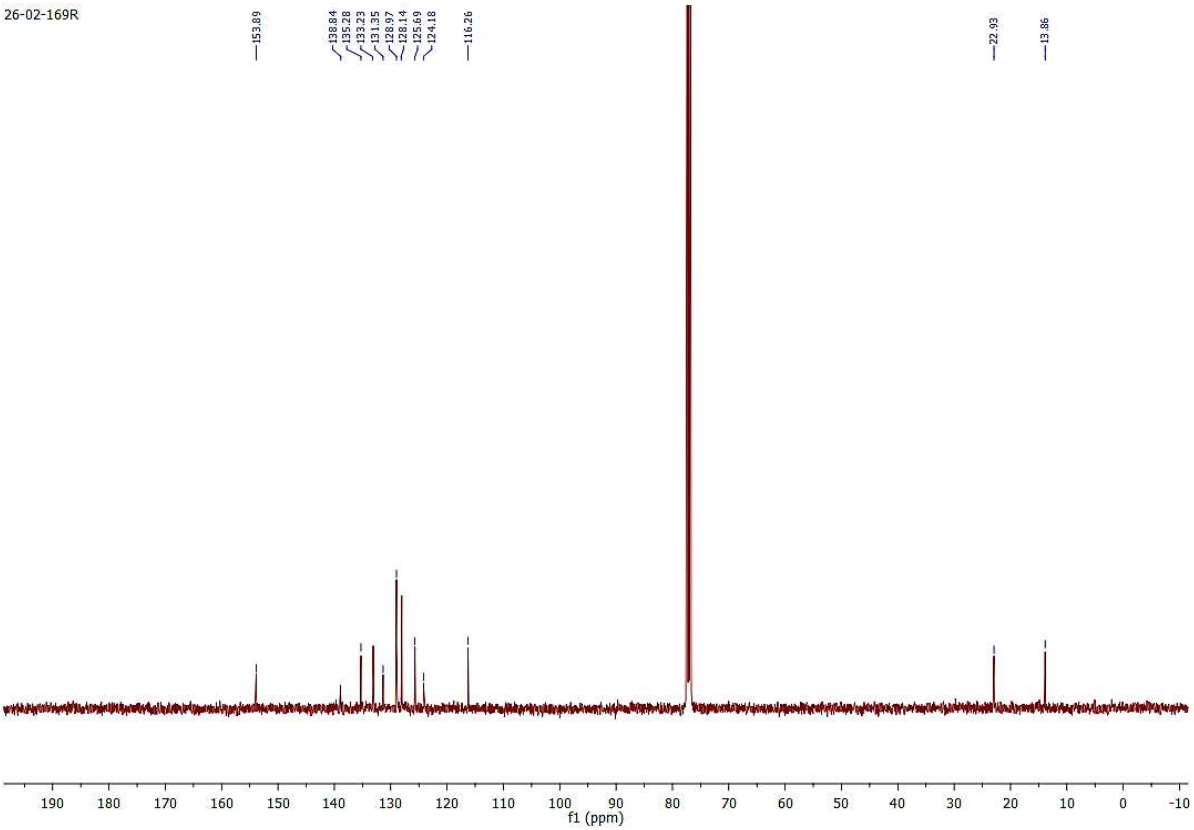

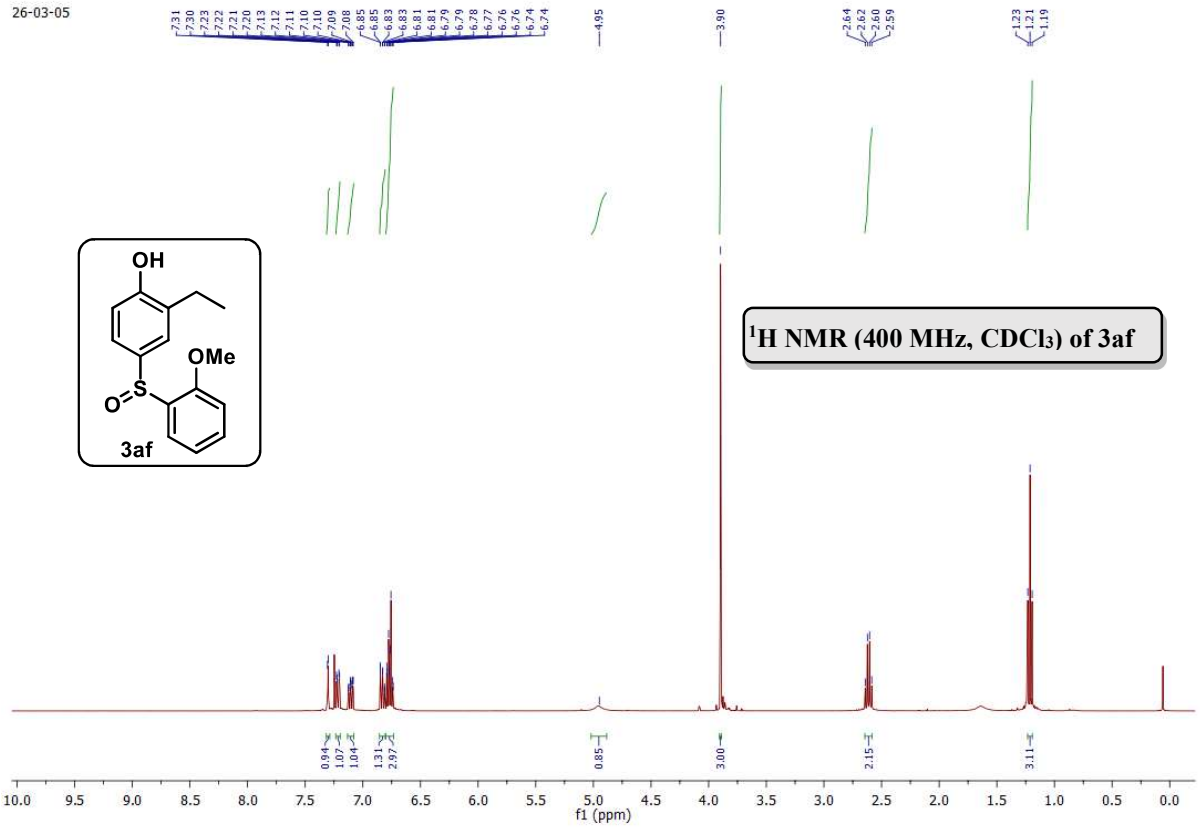

^{1}H NMR (400 MHz, $CDCl_3$) of 3af

$^{13}C\{^{1}H\}$ NMR (101 MHz, $CDCl_3$) of 3af

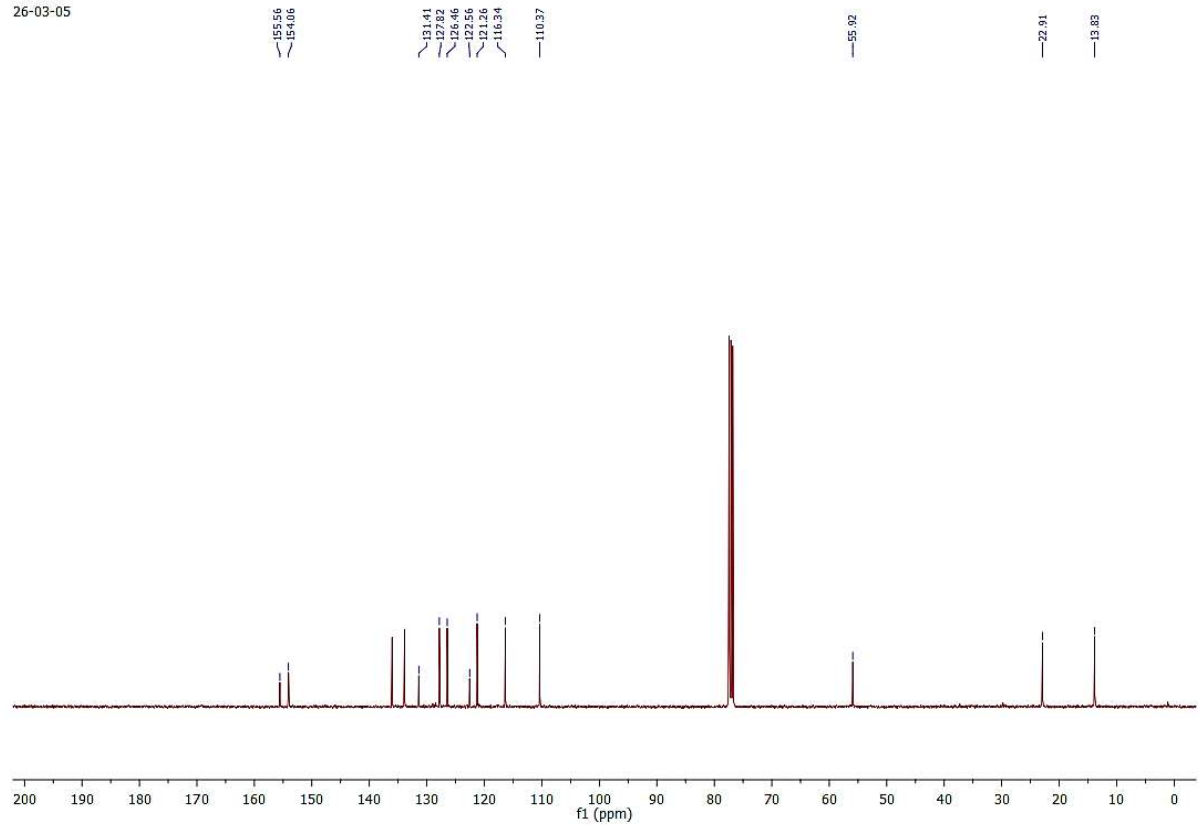

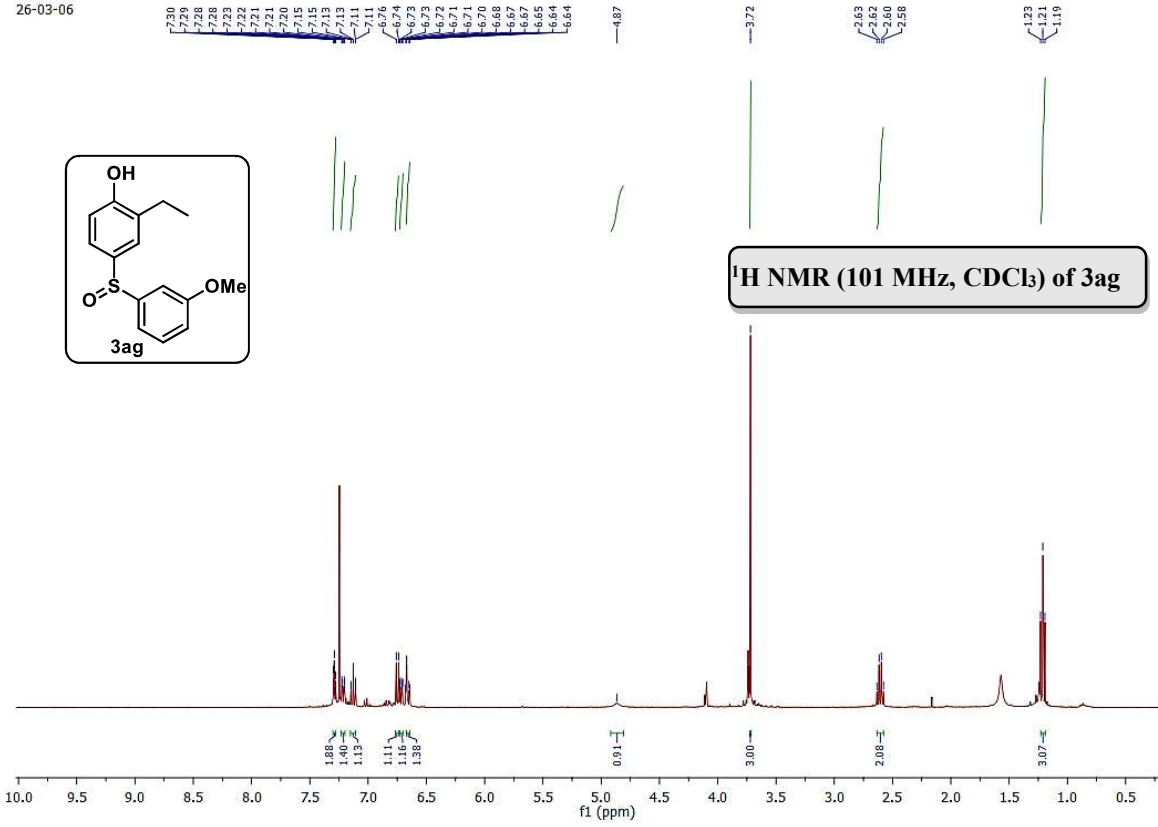

^{1}H NMR (101 MHz, $CDCl_3$) of 3ag

^{13}C{^{1}H} NMR (101 MHz, $CDCl_3$) of 3ag

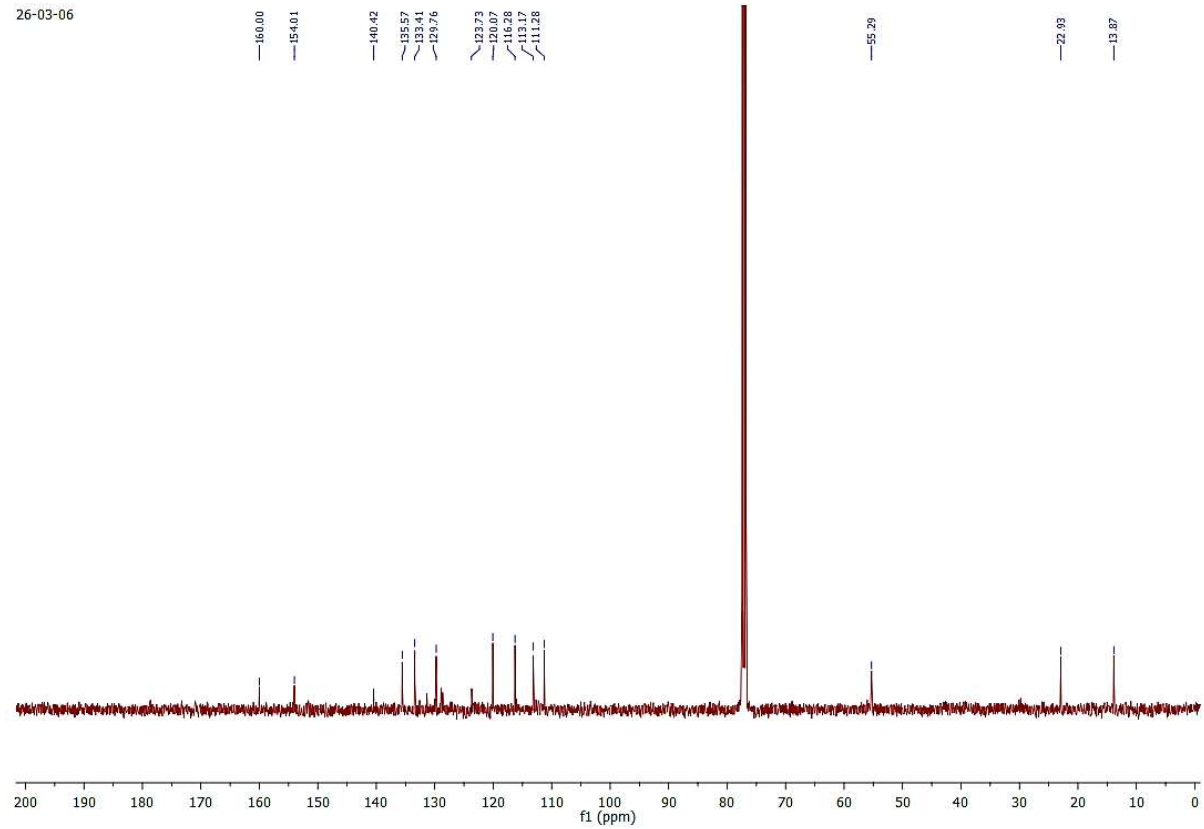

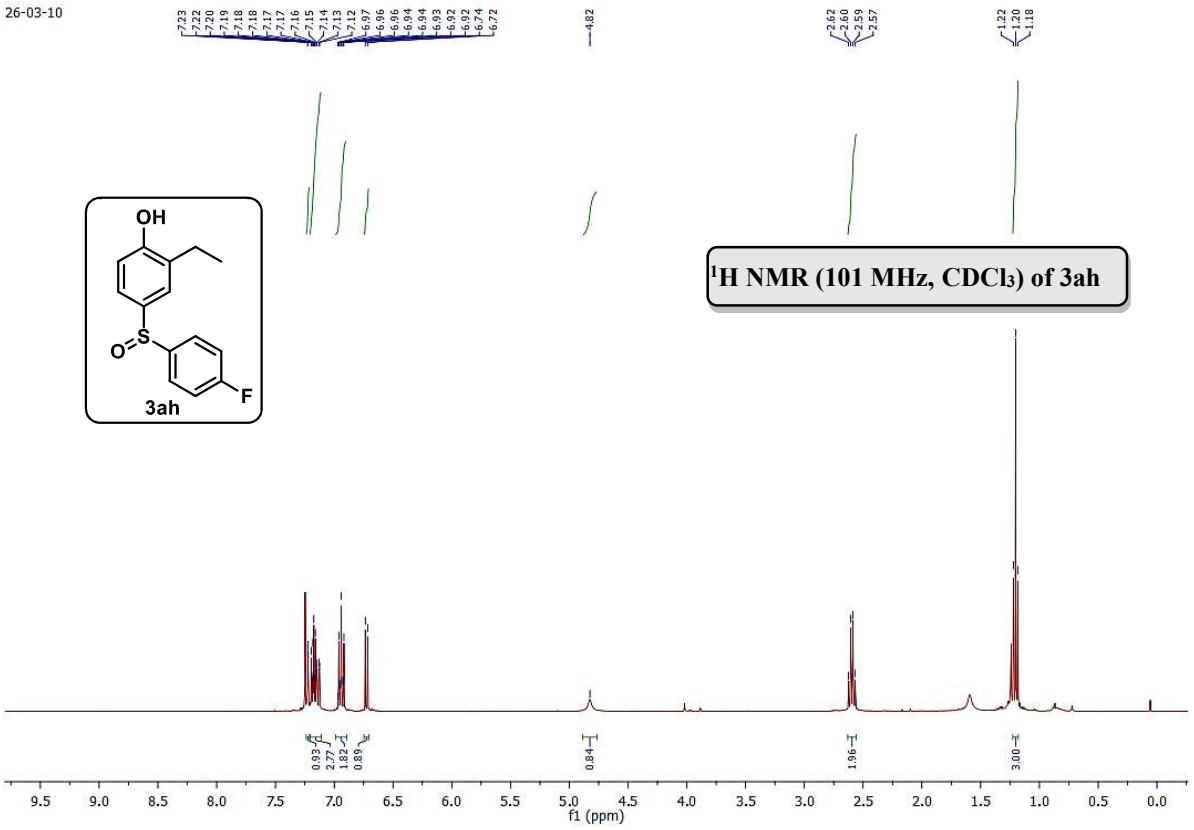

^{1}H NMR (101 MHz, $CDCl_3$) of 3ah

^{13}C{^{1}H} NMR (101 MHz, $CDCl_3$) of 3ah

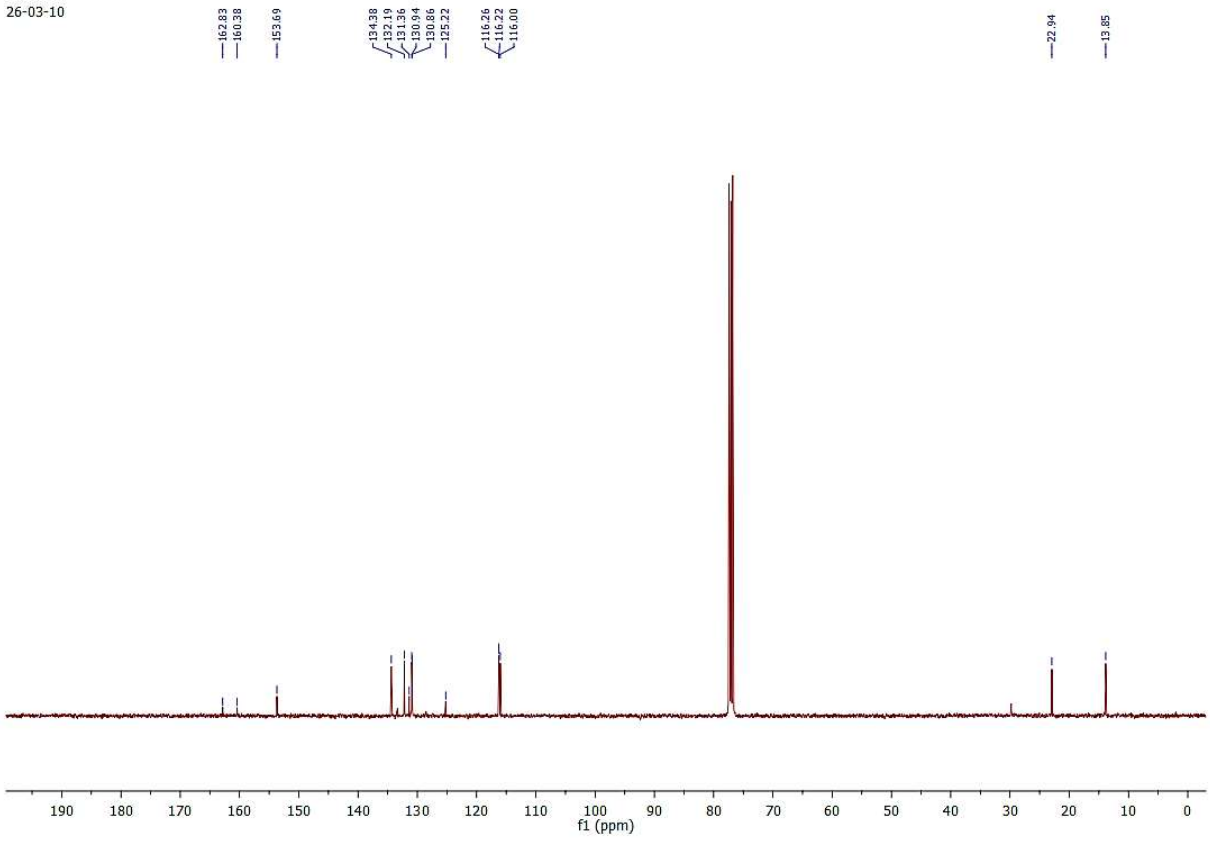

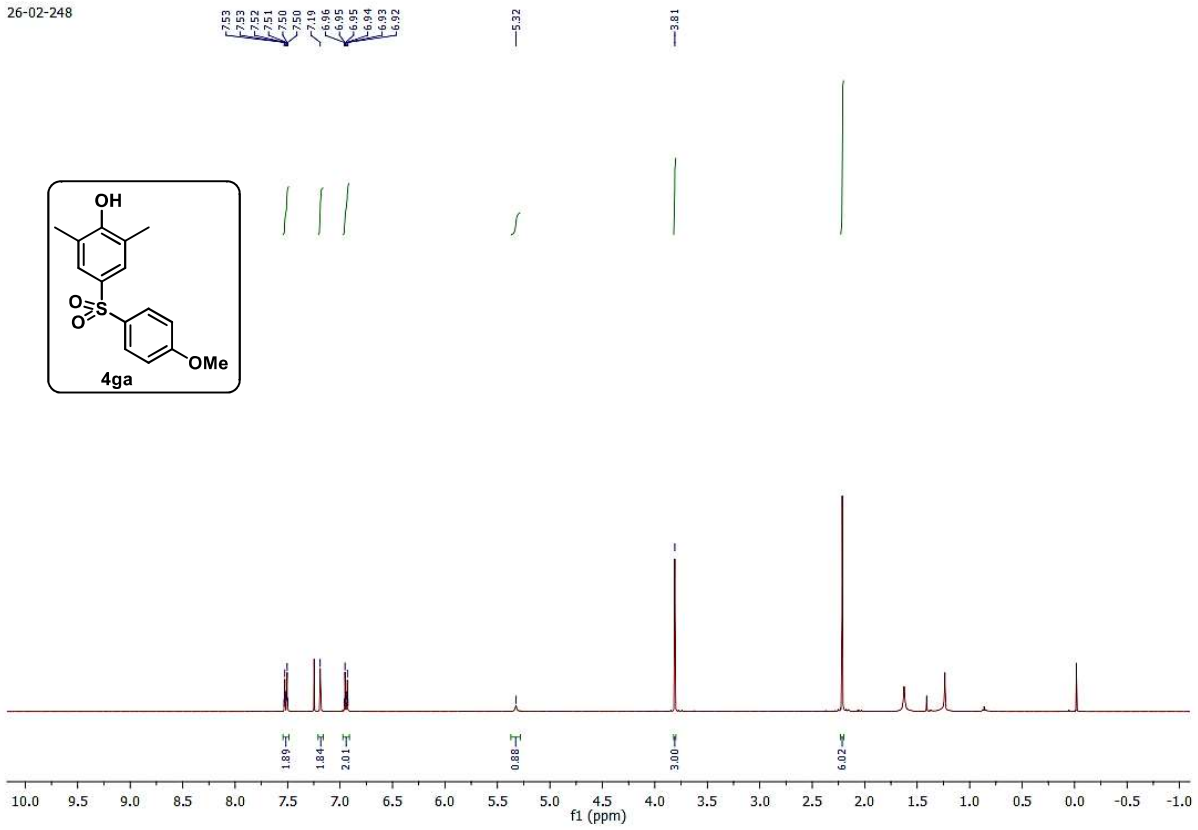

$^{13}C\{^{1}H\}$ NMR (101 MHz, $CDCl_3$) of 4ga

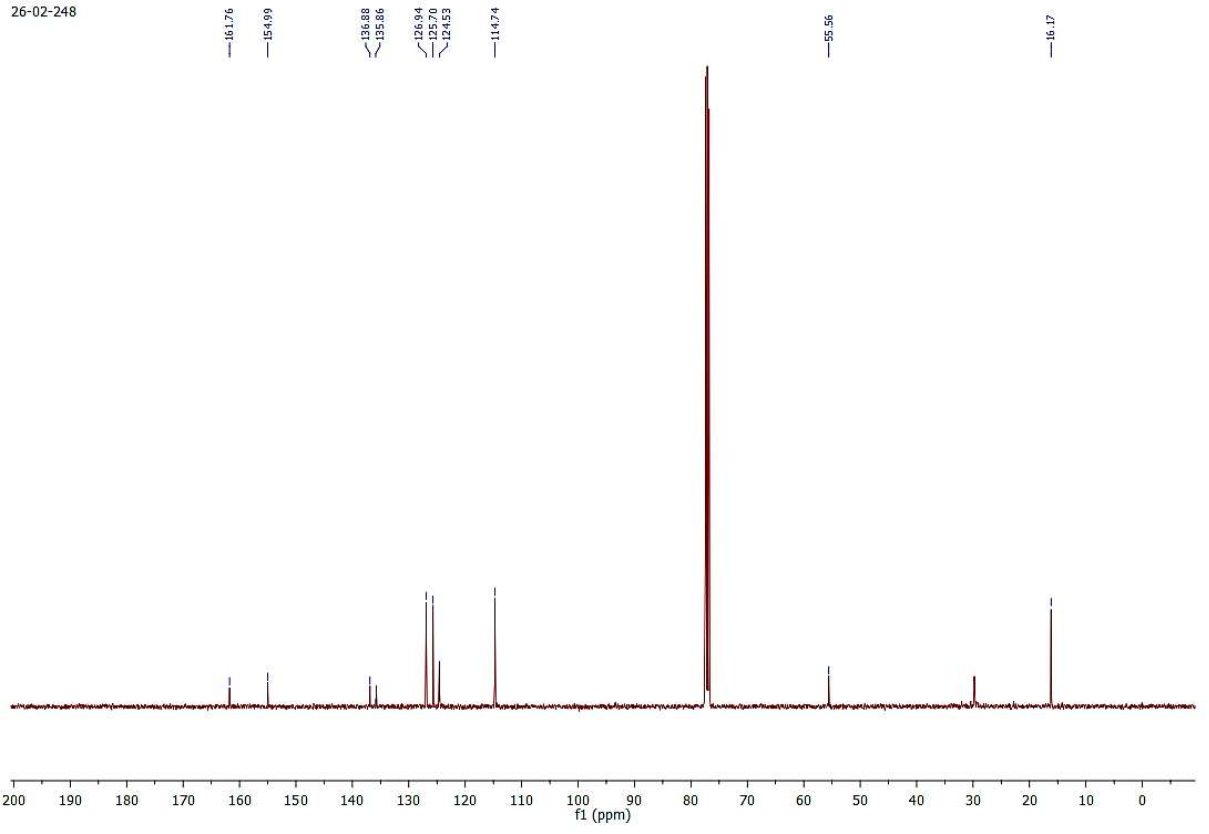

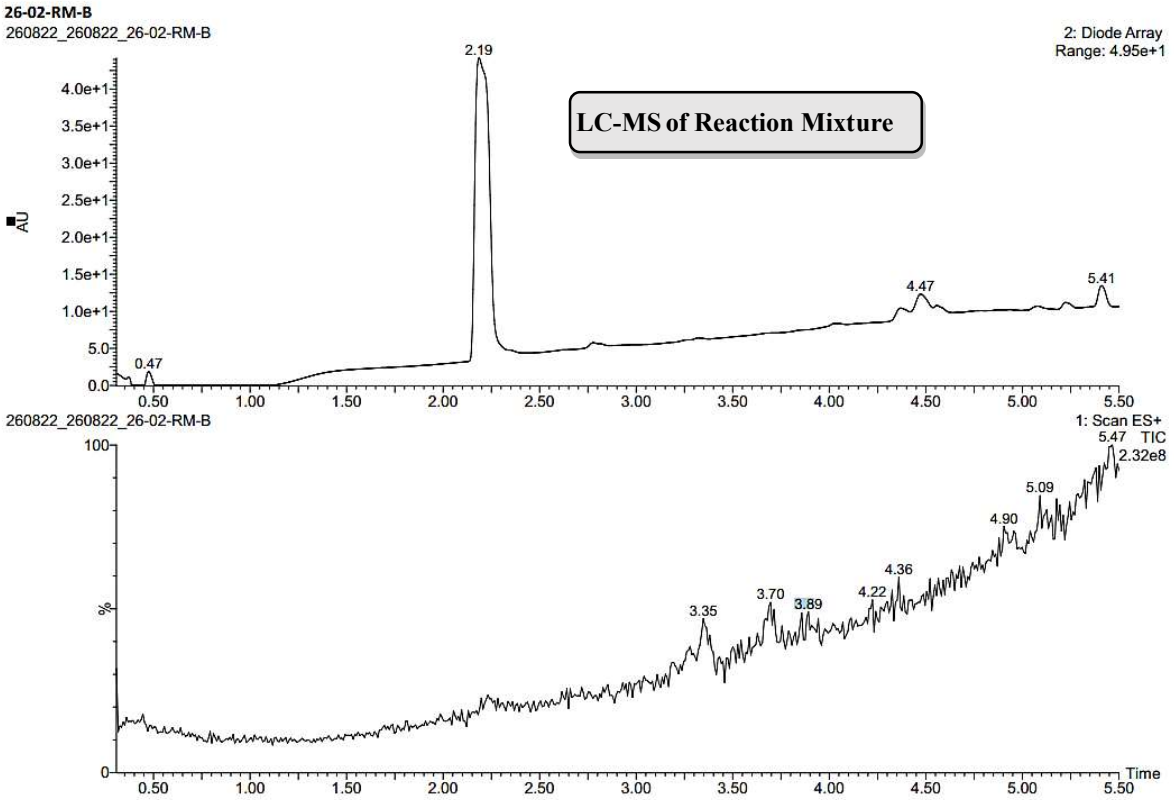

LC-MS Spectra of Reaction Mixture

[M+Na] = 131.90 for Benzyl alcohol

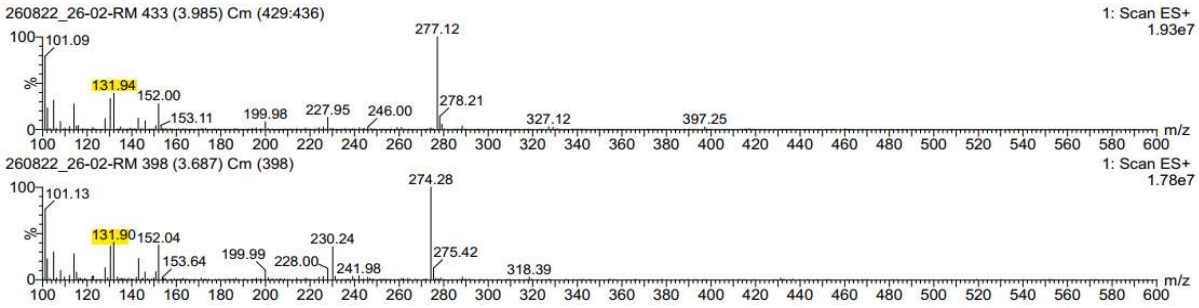

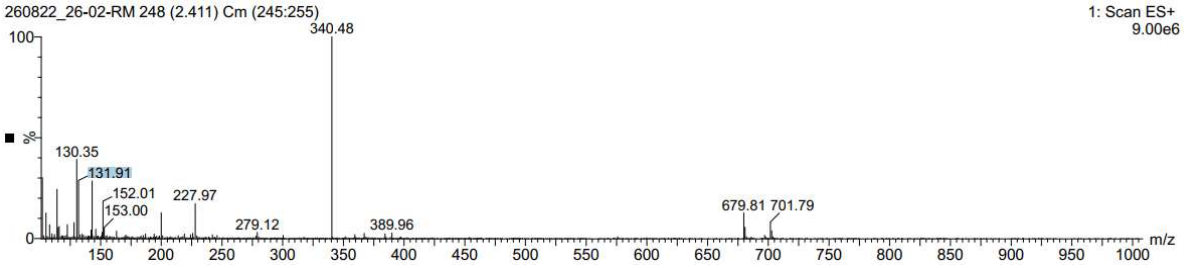

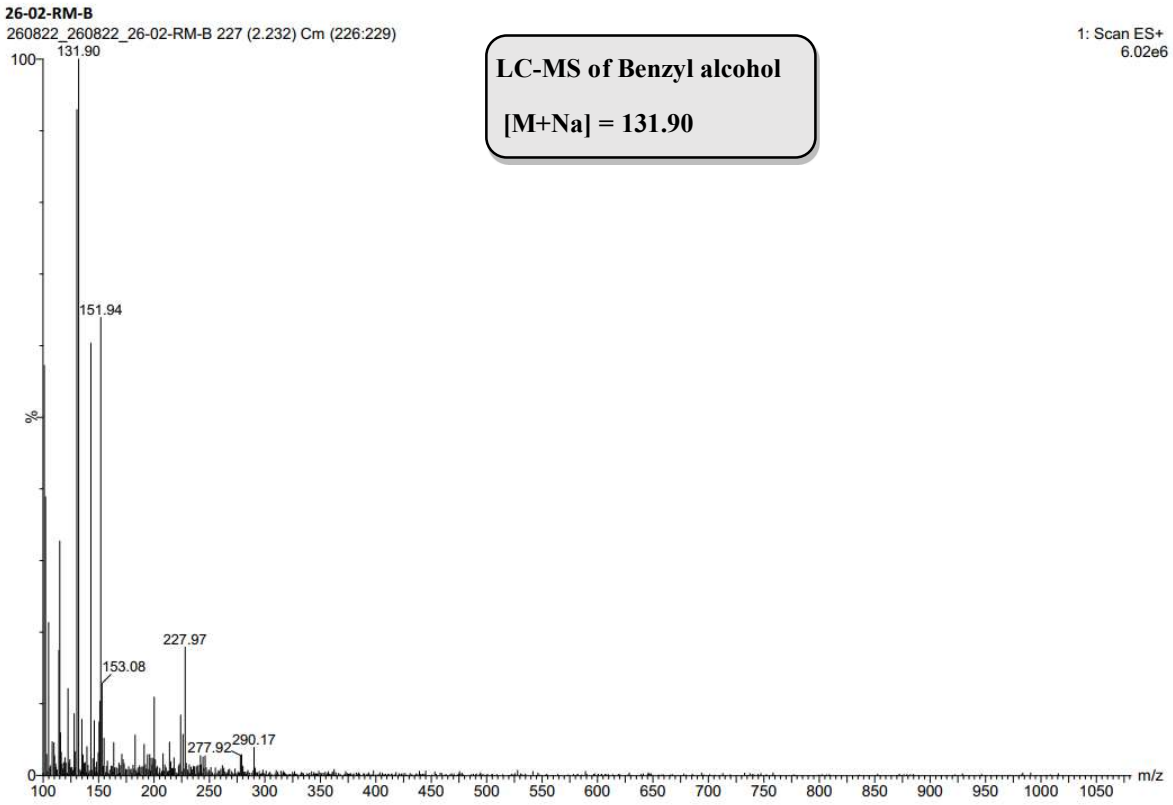

LC-MS of Benzyl alcohol

[M+Na] = 131.90

GC-MS of Benzyl alcohol

Base peak- 108

<< Target >>
Line#:1 R.Time:9.350(Scan#:1671) MassPeaks:463
RawMode:Single 9.350(1671) BasePeak:108.10(10000)
BG Mode:None Group 1 - Event 1 Scan

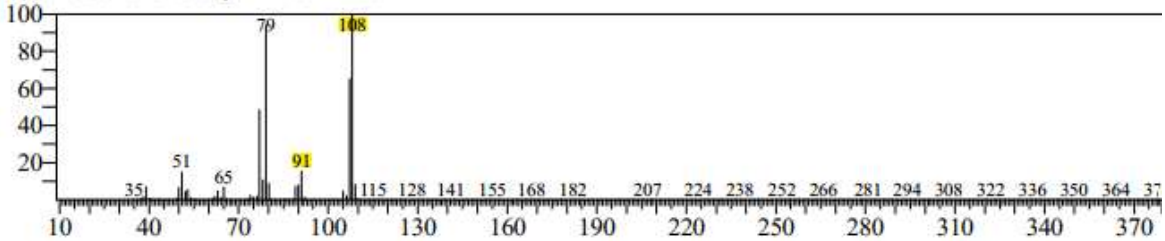

Hit#:1 Entry:5979 Library:NIST17.lib
SI:98 Formula:C7H8O CAS:100-51-6 MolWeight:108 RetIndex:1036
CompName:Benzyl alcohol

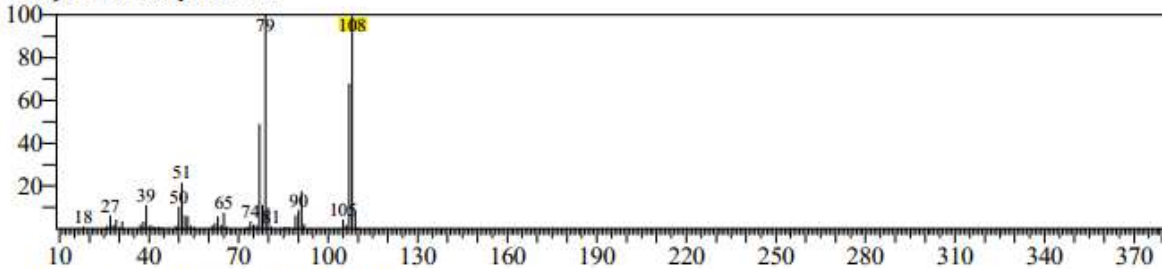

Hit#:2 Entry:5969 Library:NIST17.lib

GC-MS of Reaction mixture

Base peak- 108

<< Target >>
Line#:1 R.Time:24.655(Scan#:4732) MassPeaks:465
RawMode:Single 24.655(4732) BasePeak:108.10(10000)
BG Mode:None Group 1 - Event 1 Scan

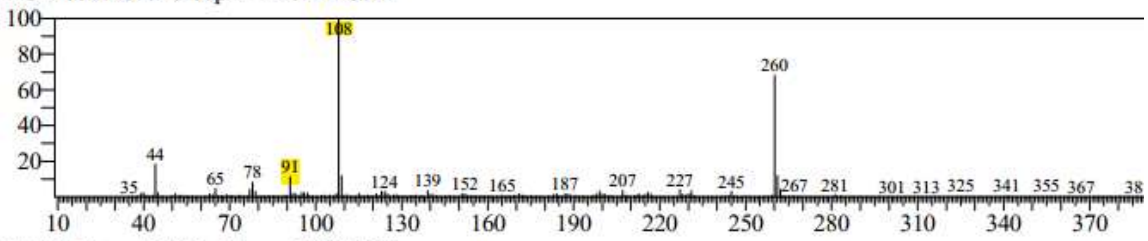

Hit#:1 Entry:133422 Library:NIST17.lib
SI:65 Formula:C16H20O3 CAS:0-00-0 MolWeight:260 RetIndex:1971
CompName:Sericenine

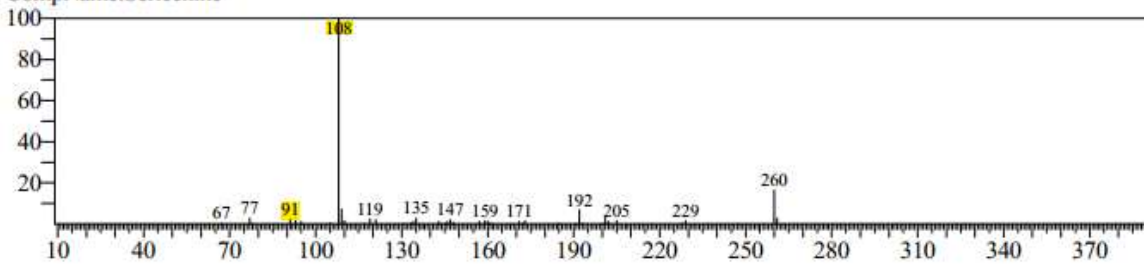

Chapter 4

Electrochemical Oxidative C-C Bond Cleavage of Methylenecyclopropanes with Alcohols

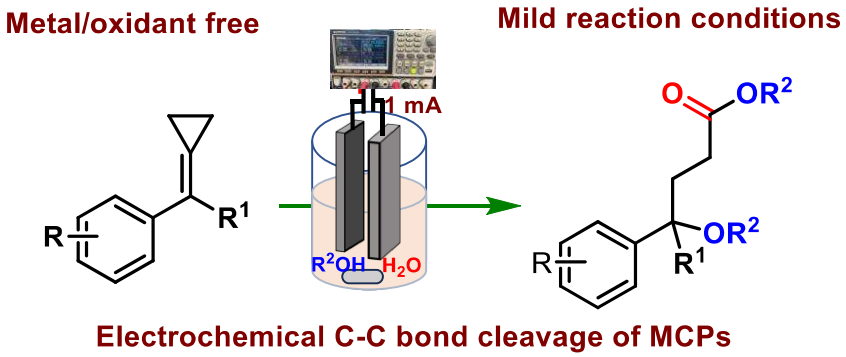

This work was published in *Chemical Communications* (A journal of *The Royal Society of Chemistry*). Please see citation "Kumar, R.; Dutt, S.; Banerjee, P. *Chem. Commun.*, **2024**, *60*, 4246-4249.

4.1. Introduction

Cyclopropanes are the important building blocks, and their ring-opening via C-C bond cleavage driven by the release of ring strain has been widely applied in total synthesis.[1,2] Methylenecyclopropanes (MCPs) are one of the important classes of small strained carbocycles that are readily accessible and have been used very often in the construction of spiro-[3,4], hetero-[5], and polycyclic[6] compounds. In general, the ring-opening reaction modes of MCPs are transition metal-catalyzed reactions,[7] Lewis or Brønsted acid-catalyzed/mediated reactions,[8] and thermal-induced cyclizations.[9] At the same time, the MCPs have also been used as radical acceptors with a variety of radicals furnishing the ring-opening functionalized product.[10] In 2019, Tang and coworkers reported silver-mediated oxidative C-C bond sulfonylation/ arylation of methylenecyclopropanes with sodium sulfinates initiated via radical addition [Scheme 4.1.1(a)].[11] However, the reactivity of MCPs in other pathways, such as radical cation and singlet or triplet excited states, has rarely been explored. The first direct oxidation of MCPs by ozone was disclosed by Beck et al. in 2001 to afford cyclobutanone, peroxide, and ketone derivatives, illustrating the possibility of a single-electron oxidation pathway of MCPs.[12] Another single electron oxidation of MCPs by the usage of selectflour was reported by Min Shi and group towards the synthesis of fluorinated cyclobuta[b]indoline derivatives.[13] The same group in 2021, reported a new synthetic method for the preparation of 4-aryl-1,2-dihydronaphthalene derivatives through the direct photooxidation of MCPs to radical cationic species upon visible light irradiation [Scheme 4.1.1(b)].[14]

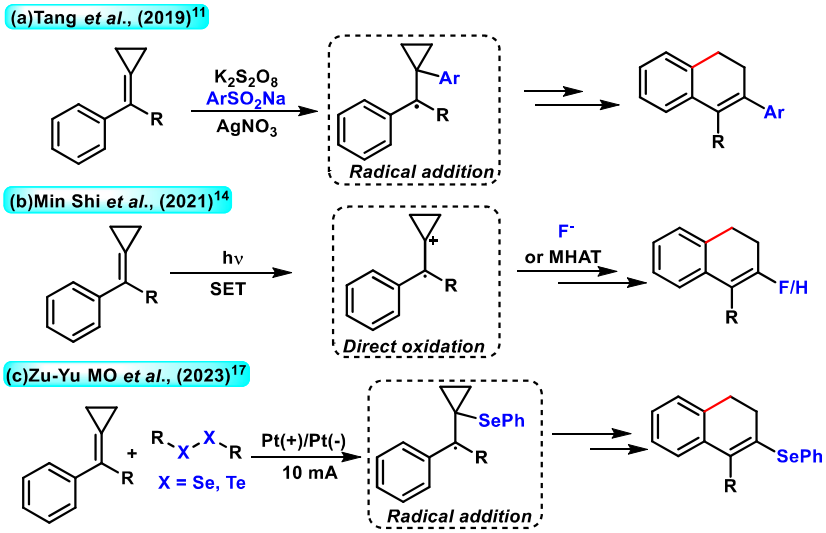

Scheme 4.1.1. Traditional reaction modes of methylenecyclopropanes.

However, all these conventional methods are concerned with the usage of stoichiometric oxidant, transition metal catalyst, or a photocatalyst towards the ring opening functionalization of MCPs. Therefore, we believe that the development of a new synthetic method without an external oxidant and photocatalyst for the ring opening of MCPs is quite appealing. Organic electrochemistry has emerged as a sustainable alternative due to effortlessness of scalability, evasion of stoichiometric oxidants or reductants, and adaptable reaction tunability.[15] Various redox processes such as C-H functionalization, oxidative coupling, and C-C bond forming and cleavage have been developed.[16] However, electrooxidative C-C bond cleavage/functionalization of MCPs is rarely explored due to the inertness and weak electronic bias of C-C binds. In 2023, the first report of electrooxidation opening of MCPs in the presence of diselenides/ditellurides was developed by Zu-Yu Mo and group towards the synthesis of 3-selenide/telluride-1,2-dihydronaphthalenes [Scheme 4.1.1(c)].[17] However, the ring opening has been initiated by

the addition of seleno radical or selenium cation to the double bond of MCPs. To the best of our knowledge, the ring opening of MCPs via direct oxidation of double bonds followed by nucleophilic attack of alcohols has not been investigated so far. In this work, we report an electricity-mediated C-C bond cleavage of MCPs towards the synthesis of methyl 4-methoxy-4-phenylbutanoate derivatives under oxidant and metal-free conditions (Scheme 4.1.2).

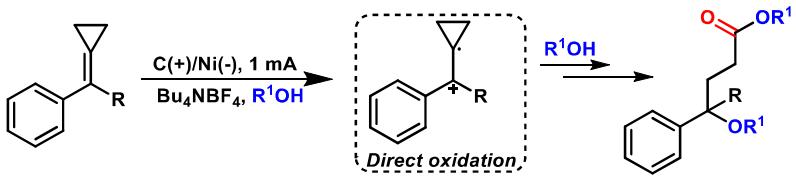

Scheme 4.1.2. Our approach for ring opening of methylenecyclopropanes.

4.2. Result and Discussion

We began our investigation with the electrolysis of 1-(cyclopropylidenemethyl)-4-methoxybenzene **1b** as model substrate at a constant current of 1 mA in the presence of Bu_4NBF_4 as supporting electrolyte, graphite electrodes, and MeOH as solvent (Table 4.2.1, entry 2).

Table 4.2.1. Optimization of reaction conditions.

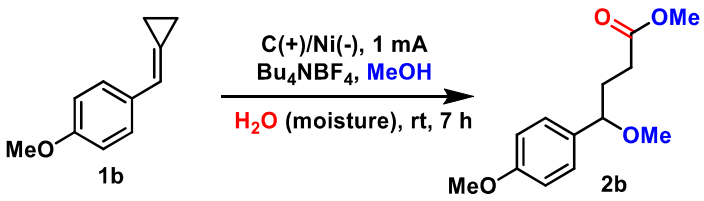

entry	Variation from standard conditions[a]	Yield[b]
1	none	76
2	Bu_4NPF_6 instead of Bu_4NBF_4	55
3	Bu_4NOAc instead of Bu_4NBF_4	50
4	ET_4NOTf instead of Bu_4NBF_4	48
5	NH_4OAc, NaOAc, and NaI instead of Bu_4NBF_4	c. m.
6	ACN: MeOH (3.5:0.5 ml) instead of MeOH	50
7	MeOH: H_2O (3.5:0.5 ml) instead of MeOH	60
8	Carbon as cathode instead of nickel	65
9	Platinum cathode instead of nickel	55
10	Platinum as anode and cathode	c. m.
11	3 mA of current instead of 1 mA	60
12	$MeNH_2$, $Et_3N{\cdot}3HF$ and 1*H*-Pyrazole (2 equiv.) instead of methanol	n. r.
13	Without electricity	n.r.

[a]Reaction conditions: **1b** (0.187 mmol), Bu_4NBF_4 as the electrolyte (0.37 mmol), methanol as the solvent (4 mL), 1 mA constant current, graphite anode, nickel cathode, dimensions (W×H×D) 8×52.5×2 mm, distance between two electrodes is 5 mm and dipped 20 mm in solution, undivided cell, 25 °C. [b]Isolated yield, c. m. = complex mixture, n.r. = no reaction.

To our delight, the desired product **2b** was obtained in a moderate yield of 55% after electrolyzing the mixture for 7 hours at room temperature. To further improve the yield, various supporting electrolytes were initially screened (Table 4.2.1). Among all, Bu_4NBF_4 served as better electrolyte with a maximum yield of 76% (entry 1), and the usage of other electrolyte like Bu_4NPF_6, Bu_4NOAc, Et_4NOTf (entries 2-4). In contrast, the electrolyte NH_4OAc, NaOAc, and NaI gave a complex mixture (entry 5). Next, screening of a mixture of solvents such as CH_3CN: MeOH and MeOH: H_2O resulted in the lowering of the yield (entries 6-7). Among the different sets of electrodes, graphite as anode and nickel as cathode were optimal for the reaction, while the replacement of nickel cathode with graphite and platinum resulted in diminished yield (entries 8-9). Further, the usage of platinum as an anode and cathode provides the complex mixture (entry 10). Moreover, the diminished yield was obtained when the current was increased to 3 mA along with the increased reaction potential (entry 11). Apart from alcoholic solvents, other nucleophiles like $MeNH_2$, $Et_3N{\cdot}3HF$, and 1*H*-Pyrazole failed to deliver the desired product (entry 12). The role of electricity was ascertained by the control experiment (entry 13). Consequently, the optimal conditions for this transformation involve graphite anode and nickel cathode at a constant current of 1 mA in methanol as solvent and Bu_4NBF_4 as a supporting electrolyte.

With the optimal reaction conditions in hand, the generality of the protocol was next evaluated using a variety of MCPs **1a-1w** (Scheme 4.2.1). Initially, the electron donating groups on the various positions of the aryl ring of MCPs were tested. The aryl ring without any substituents **2a** and electron-donating substituents like methoxy, methyl, isopropyl, and phenoxy at the *para*-position of the aryl ring furnished the desired product **2b-2e** in good to moderate yield. Furthermore, the cyclopropyl methoxy and allyloxy group at *para*-position were also well tolerated and afforded the desired product **2f** and **2g** in 80% and 78% yield, respectively. The electron-donating substituents at *ortho*-position, like methoxy **2h** and benzyloxy **2i,** also rendered the final product in good yields. Subsequently, when the *meta*-position of the aryl ring is substituted, the sole product **2j** could be obtained in 55% of the yield. The 2,4,6-trimethyl substituted ring also affords the desired product **2k** in 65% with a little prolonged time up to 10 h. Further, moving towards the halogen substituents (Cl, Br, F) at *para* and *ortho*-position of the aryl ring also conferred the desired product **2l** and **2m** and **2n** in 78%, 75% and 58%, respectively. In the case of a disubstituted aromatic ring having electron-donating and electron-withdrawing groups, the corresponding products **2o**, **2p** and **2q** were obtained in 80%, 76% and 75% respectively. Replacement of the aryl ring with the naphthyl ring was also found viable for the transformation and afforded the desired product **2r** in 55% yield. Further, the replacement of R^1 group with an alkyl group also conferred the expected product **2s** and **2t** was delivered in 60% and 65% yields, respectively. Interestingly, when R^1 group is substituted with a cyclopropyl group, even then, the desired product **2u** was obtained in 75% yield. Replacing the alkyl group with a phenyl ring also affords the product **2v** in 65% yield. Moreover, a pharmaceutical such as Eugenol has also been used for substitution on cyclopropane which affords the product **2w** in 60% yield. Unfortunately, *N,N*-dimethyl group at *para* position of aryl ring could not able to deliver the desired product.

The substrate scope was further evaluated concerning the alcoholic nucleophile. A diverse set of primary alcohols was employed, showing that ethanol (**2a'**), 1-propanol (**2b'**), and 1-butanol (**2c'**) were compatible with the

methodology. The secondary alcohol (**2d'**) also delivered the desired product in moderate yield (Scheme 4.2.1). Unfortunately, *tert*-butanol, fluorinated alcohols, and other substituted alcohols failed to deliver the expected product.

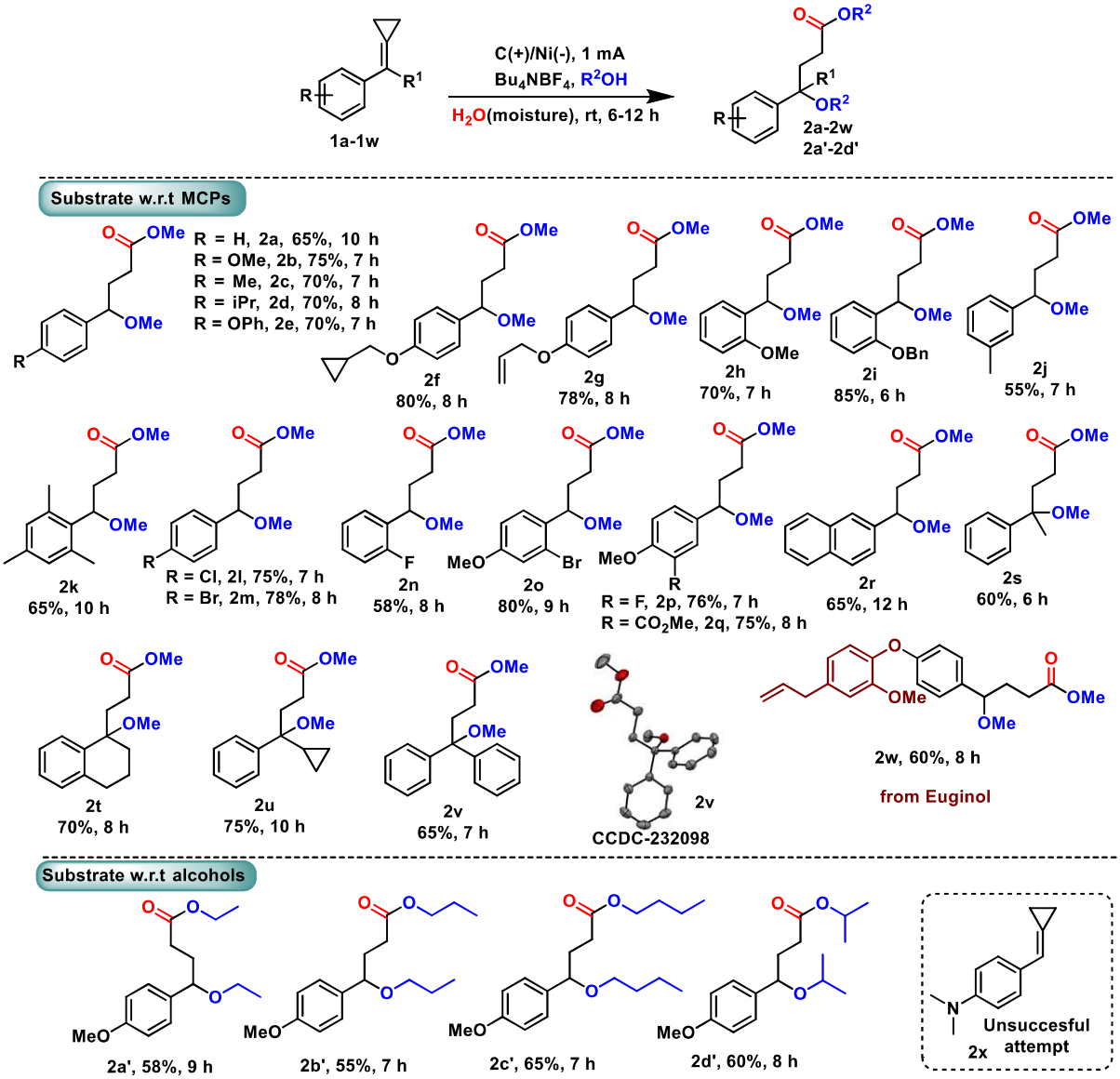

Scheme 4.2.1. Substrate scope.

Preliminary mechanistic experiments were performed to get insights into the reaction mechanism (Scheme 4.2.2). The reaction was completely stopped when radical scavenger like 2,2,6,6-tetramethyl-1-piperidinyloxy (TEMPO) was added, and a trace amount of product **2b** was observed along with the formation of butylated hydroxytoluene (BHT) adduct **2b'** when BHT was added (Scheme 4.2.2 a(i) and a(ii)). This implies that the reaction follows a radical pathway. Further, the oxidation of MCP at the anode was verified by a divided cell experiment (Scheme 4.2.2 b). The desired product was successfully formed when the reaction mixture was placed in the anodic chamber; however, a drop in the yield and an increase in the reaction time were observed in comparison to the standard conditions (Scheme 4.2.2 b(i)). Failure of the reaction in the cathodic chamber further proves that anodic oxidation is the key step for the transformation (Scheme 4.2.2 b(ii)). The failure of the reaction with **1y** under standard conditions proves that the reaction was initiated via the oxidation of a double bond (Scheme 4.2.2 c). Further, the role of the aryl ring was also confirmed by the reaction of **1z** under standard conditions (Scheme 4.2.2 d). Both the

experiments confirm that the aryl ring and double bond are necessary for the transformation as the aryl ring makes the double bond active towards the oxidation. The formation of product **2u** also proves that the cyclopropyl ring opens via double bond activation, as the other cyclopropyl ring remains intact in the product (Scheme 4.2.1). Further, making intermediate **III** and performing its reaction under standard conditions provides the desired product **2b**, which confirms the formation of intermediate **III** in the reaction (Section 4.4.9.5). To confirm the role of H_2O the reaction was carried out in methanol: D_2O and intermediate **III'** was confirmed by GC-MS analysis (see experimental section). Moreover, the electricity on/off experiment confirms that current is needed throughout the reaction time ((Section 4.4.9.5).

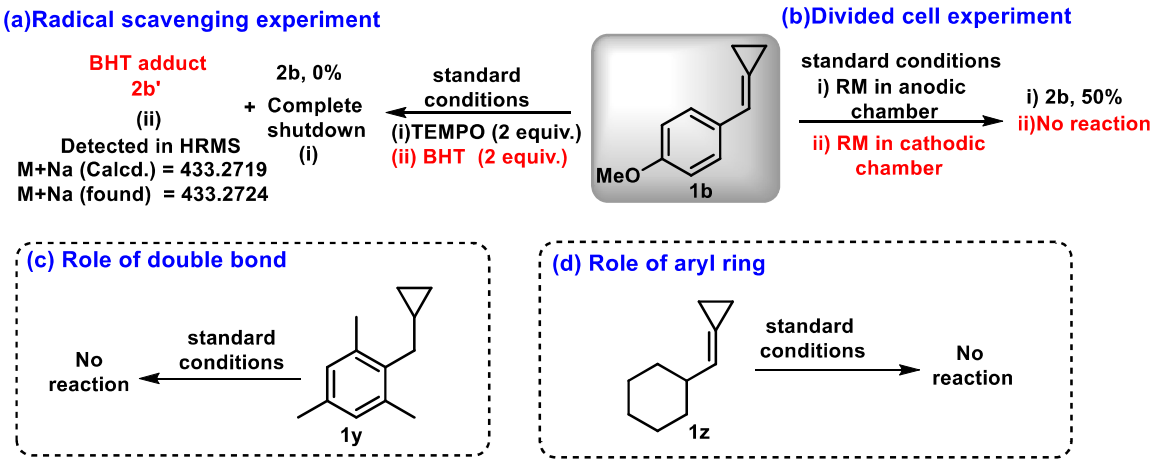

Scheme 4.2.2. Control experiments.

Further, a cyclic voltammetry (CV) experiment was carried out to study the redox behavior of the reagents (Figure 4.2.1). The oxidation potential of **1b** was observed to be 1.55 V (vs. Ag/AgCl).[17] However, the oxidation potential of **1v** having no double bond was found to be 2.2 V (vs. Ag/AgCl), which belongs to the aryl ring and therefore confirms that the lower oxidation potential 1.55 V, in the case of **1b** corresponds to the double bond.

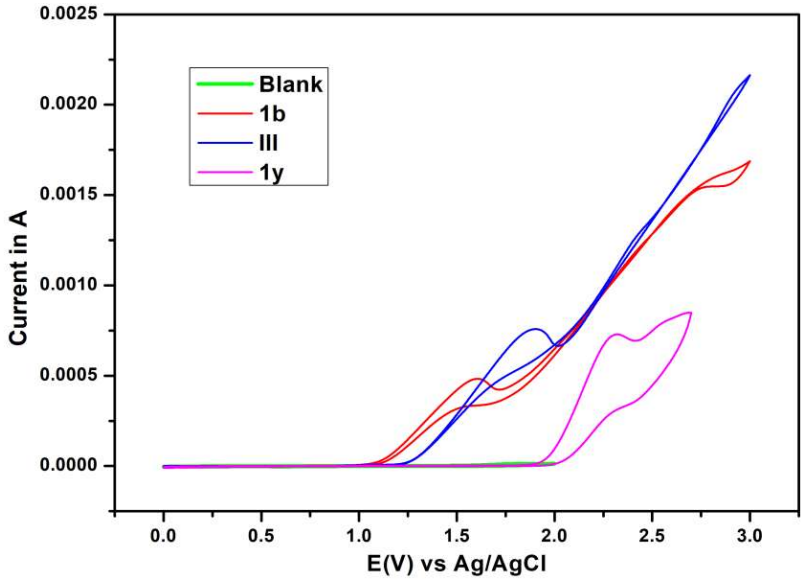

Figure 4.2.1. Cyclic voltammetry.

Based on the control experiments, cyclic voltammetry, and literature reports[17,18] a plausible mechanism is proposed in two different pathways. In pathway I, the reaction gets initiated by single-electron oxidation of **1b** to generate radical cationic species **I**, which undergoes nucleophilic attack of methoxide generated at the cathode followed by another oxidation leading to carbocation **II**. Carbocation **II** probably exists as a resonating structure **II'** due to the β-methoxy group as like carbocation is stabilized by a β-silyl group.[19] Further, the nucleophilic attack of hydroxide ion on carbocation **II'** led to the ring opening product **III**. Intermediate **III** undergoes sequential two-electron oxidation and loss of two water molecules to afford aldehyde intermediate **IV**.[18a] Single electron oxidation of aldehyde **IV** followed by loss of hydrogen atom led to the formation of stable acylium cation **V**, which on further nucleophilic addition of methoxide delivered the desired product **2b** (Scheme 4.2.3).[18b] However, there can be another pathway for ring opening after formation of intermediate **I** (see experimental section).

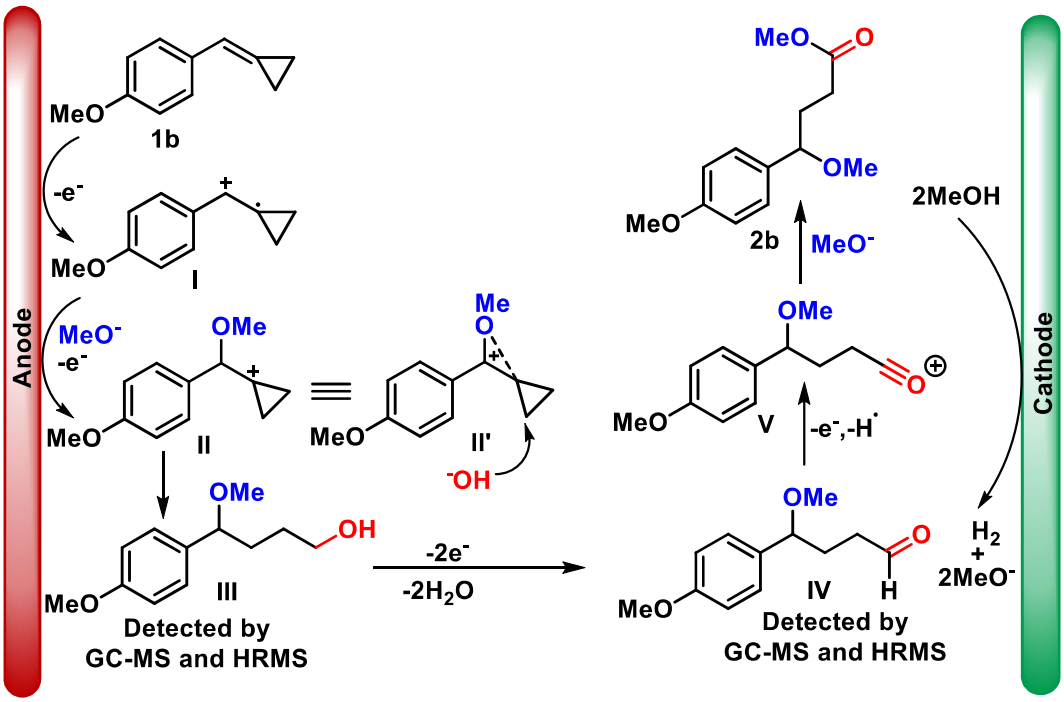

Scheme 4.2.3. Plausible mechanism.

Furthermore, to demonstrate the synthetic utility of the methodology, the electrochemical synthesis was successfully executed on a gram scale (Scheme 4.2.4a). Next, the product was subject to various post functionalizations such as reduction of ester (Scheme 4.2.4b), amidation of ester (Scheme 4.2.4c), and base hydrolysis (Scheme 4.2.4d). The hydrolyzed product **3c** was further transformed into a scaffold containing a biological active menthol ring (Scheme 4.2.4d).

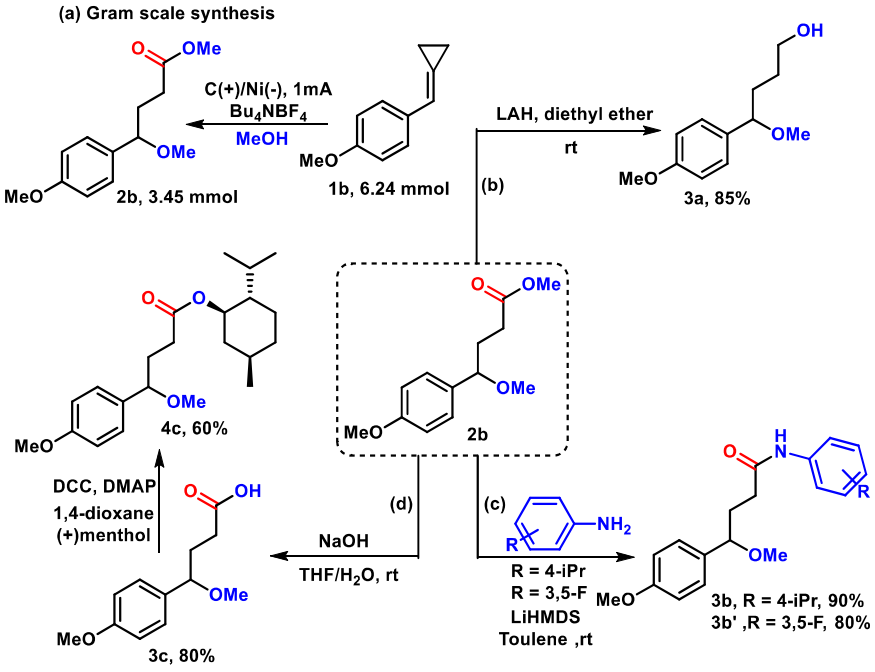

Scheme 4.2.4. Synthetic utility.

4.3. Conclusion

In conclusion, we have developed the first direct electrochemical oxidative ring opening functionalization of MCPs via C-C bond cleavage in the presence of water followed by alcohols as nucleophiles towards the synthesis of alkyl 4-alkoxy-4-phenylbutanoate derivatives. Neither an additional oxidant nor metal catalyst was needed in this transformation. The mechanistic studies suggest that the reaction proceeds via direct oxidation of the C=C bond of MCPs followed by ring opening to form the desired product**.**

4.4. Experimental section

4.4.1. General Information

Unless noted otherwise, all reagents and solvents were purchased from commercial sources and used as received. All reactions were performed in oven dried round bottom flasks. Electrochemical reactions were performed at room temperature using DC power supply of Keysight technologies (25 V, 5A) and GW INSTEK GPP-4323 (32 V, 3 A). Electrodes were commercially available from IKA. Cyclic voltammetry analysis was carried out in CH instrument electrochemical analyzer (CHI1210C). The developed chromatogram was analyzed by UV lamp (254 nm) or p-anisaldehyde solution. Column chromatography was performed on silica gel mesh size 200-300. The proton (^{1}H) and carbon ^{13}C{^{1}H} and ^{19}F NMR spectra were recorded in 400 MHz JEOL JNM ECS400 spectrometer in the $CDCl_3$ solvent (unless otherwise mentioned) and are reported in δ units. Chemical shifts of NMR spectra are expressed in parts per million (ppm). Coupling constants (*J* Values) are reported in Hz. High-resolution mass spectra (HRMS) were obtained using the electron spray ionization (ESI) technique and TOF mass analyzer. Yields refer to isolated compounds, estimated to be less than 95% pure as determined by ^{1}HNMR. The description of the signals includes the following: s = singlet, d = doublet, dd = doublet of doublet, ddd = doublet of doublet of doublets, ddt = doublet of doublet of Triplets, dtd = doublet of triplet of doublets, tdd = triplet of doublet of doublets, t = triplet, dt = doublet of triplet, q = quartet, br = broad and m = multiplet.

4.4.2. General Procedure for synthesis of Alkylidene cyclopropane

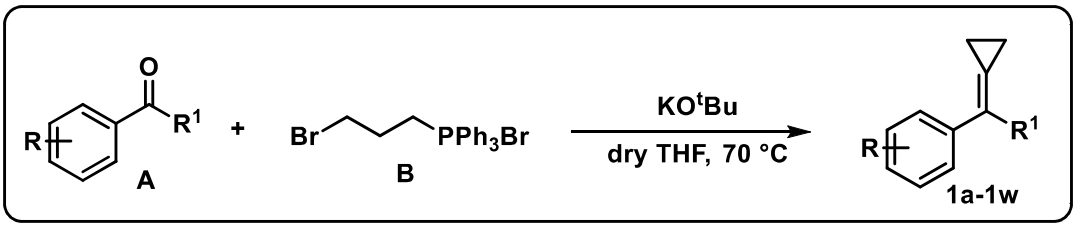

Following a slightly modified a procedure a solution of KO^{t}Bu (1.23 g, 3.00 equiv., 11.01 mmol) in THF (9 mL, 1.3 M) was gradually added to a solution of (3- bromopropyl)triphenylphosphonium bromide (2.56 g, 1.5 equiv., 5.50 mmol) in dry THF (11 mL, 0.5 M) and stirred at 70 °C for 30-60 minutes. Next, a solution of benzaldehyde (0.5g, 1.00 equiv., 3.67 mmol) in THF (1.83 mL, 2.0 M) was added dropwise and the mixture was refluxed or heated for 3-4 h and reaction completion was monitored by TLC. After cooling to the room temperature, the suspension was filtered, and the solvent was removed under vacuum to obtain the crude product. The crude product was purified by silica gel column chromatography 100 % hexane or 99:1 (hexane: ethyl acetate).

4.4.2.1 Characterization data of starting material

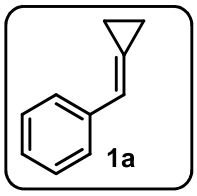

(cyclopropylidenemethyl)benzene (1a)

Overall yield: 55%, 0.337 g; **Nature**: oily liquid; **^{1}H NMR** (400 MHz, CHLOROFORM-D); δ 7.57 – 7.52 (m, 1H), 7.34 (dd, *J* = 10.4, 4.8 Hz, 2H), 7.22 (dd, *J* = 13.6, 6.2 Hz, 2H), 6.78 – 6.74 (m, 1H), 1.46 – 1.40 (m, 2H), 1.21 – 1.16 (m, 2H).

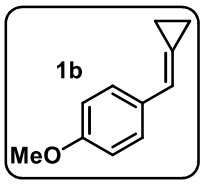

1-(cyclopropylidenemethyl)-4-methoxybenzene (1b)

Overall yield: 60%, 0.352 g; **Nature:** yellow oil; **^{1}H NMR** (400 MHz, CHLOROFORM-D); δ 7.46 (d, *J* = 8.7 Hz, 2H), 6.89 – 6.84 (m, 2H), 6.71 – 6.67 (m, 1H), 3.80 (s, 3H), 1.37 (ddd, *J* = 7.7, 6.2, 2.2 Hz, 2H), 1.17 – 1.12 (m, 2H).

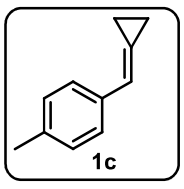

1-(cyclopropylidenemethyl)-4-methylbenzene (1c)

Overall yield: 40%, 0.239 g; **Nature:** yellow oil; **^{1}H NMR** (400 MHz, CHLOROFORM-D); δ 7.44 (d, *J* = 8.0 Hz, 2H), 7.14 (d, *J* = 8.0 Hz, 2H), 6.74 – 6.71 (m, 1H), 2.35 (s, 3H), 1.43 – 1.38 (m, 2H), 1.19 – 1.14 (m, 2H).

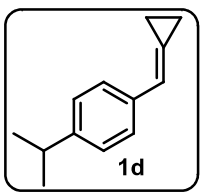

1-(cyclopropylidenemethyl)-4-isopropylbenzene (1d)

Overall yield: 45%, 0.260 g; **Nature:** yellow oil; **^{1}H NMR** (400 MHz, CHLOROFORM-D); δ 7.52 (d, *J* = 7.2 Hz, 2H), 7.24 (t, *J* = 6.2 Hz, 2H), 6.78 (s, 1H), 2.95 (dt, *J* = 13.8, 6.9 Hz, 1H), 1.48 – 1.42 (m, 2H), 1.30 (dd, *J* = 6.9, 1.2 Hz, 6H), 1.24 – 1.18 (m, 2H).

1-(cyclopropylidenemethyl)-4-phenoxybenzene (1e)

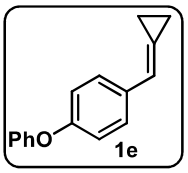

Overall yield: 60%, 0.335 g; **Nature:** yellow viscous liquid; **^{1}H NMR** (400 MHz, CHLOROFORM-D); δ 7.53 (d, *J* = 8.5 Hz, 2H), 7.35 (t, *J* = 7.9 Hz, 2H), 7.12 (dd, *J* = 11.5, 4.2 Hz, 1H), 7.06 – 6.99 (m, 4H), 6.75 (s, 1H), 1.44 – 1.39 (m, 2H), 1.22 – 1.17 (m, 2H).

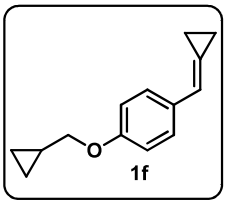

1-(cyclopropylidenemethyl)-4-(cyclopropylmethoxy)benzene (1f)

Overall yield: 50%, 0.282 g; **Nature:** white solid; **^{1}H NMR** (400 MHz, CHLOROFORM-D); δ 7.48 – 7.42 (m, 2H), 6.90 – 6.84 (m, 2H), 6.68 (t, *J* = 2.9 Hz, 1H), 3.80 (d, *J* = 6.9 Hz, 2H), 1.41 – 1.36 (m, 2H), 1.30 – 1.25 (m, 1H), 1.17 – 1.12 (m, 2H), 0.67 – 0.61 (m, 2H), 0.38 – 0.32 (m, 2H).

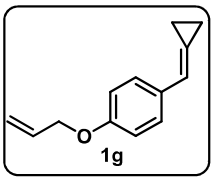

1-(allyloxy)-4-(cyclopropylidenemethyl)benzene (1g)

Overall yield: 55%, 0.314 g; **Nature:** white solid; **^{1}H NMR** (400 MHz, CHLOROFORM-D); δ 7.48 – 7.42 (m, 2H), 6.91 – 6.85 (m, 2H), 6.7-.6.67 (m, 1H), 6.06 (ddt, *J* = 17.2, 10.5, 5.3 Hz, 1H), 5.41 (dq, *J* = 17.4, 1.7 Hz, 1H), 5.29 (dt, *J* = 10.5, 1.4 Hz, 1H), 4.54 (dt, *J* = 5.2, 1.4 Hz, 2H), 1.40 – 1.35 (m, 2H), 1.17 – 1.12 (m, 2H).

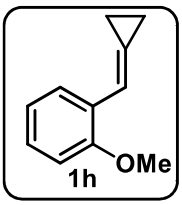

1-(cyclopropylidenemethyl)-2-methoxybenzene (1h)

Overall yield: 60%, 0.352 g; **Nature:** yellow oil; **^{1}H NMR** (400 MHz, CHLOROFORM-D); δ 7.76 (dd, *J* = 7.7, 1.7 Hz, 1H), 7.23 – 7.18 (m, 1H), 7.17 – 7.13 (m, 1H), 6.95 (t, *J* = 7.5 Hz, 1H), 6.89 (d, J = 8.4 Hz, 1H), 3.86 (s, 3H), 1.42 – 1.37 (m, 2H), 1.20 – 1.15 (m, 2H).

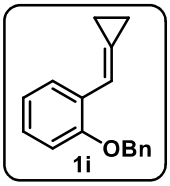

1-(benzyloxy)-2-(cyclopropylidenemethyl)benzene (1i)

Overall yield: 70%, 0.387 g; **Nature:** white solid; **^{1}H NMR** (400 MHz, CHLOROFORM-D); δ 7.79 (dd, *J* = 7.6, 1.5 Hz, 1H), 7.46 (d, *J* = 7.1 Hz, 2H), 7.42 – 7.36 (m, 2H), 7.35 – 7.29 (m, 1H), 7.22 (dd, *J* = 4.0, 2.0 Hz, 1H), 7.16 (td, *J* = 7.8, 1.6 Hz, 1H), 6.95 (t, *J* = 8.4 Hz, 2H), 5.10 (s, 2H), 1.41 – 1.36 (m, 2H), 1.18 – 1.13 (m, 2H).

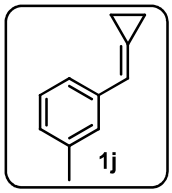

1-(cyclopropylidenemethyl)-3-methylbenzene (1j)

Overall yield: 40%, 0.239 g; **Nature:** colourless liquid; **^{1}H NMR** (400 MHz, CHLOROFORM-D); δ 7.38 (d, *J* = 8.1 Hz, 2H), 7.25 (t, *J* = 7.4 Hz, 1H), 7.06 (d, *J* = 7.4 Hz, 1H), 6.75 (s, 1H), 2.39 (s, 3H), 1.48 – 1.42 (m, 2H), 1.22 – 1.17 (m, 2H).

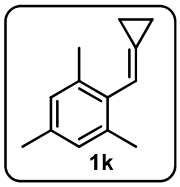

2-(cyclopropylidenemethyl)-1,3,5-trimethylbenzene (1k)

Overall yield: 45%, 0.260 g; **Nature:** colourless liquid; **^{1}H NMR** (400 MHz, CHLOROFORM-D); δ 6.98 (s, 2H), 6.89 (s, 1H), 2.39 (s, 3H), 2.35 (s, 6H), 1.38 – 1.33 (m, 2H), 1.20 (ddd, *J* = 6.9, 4.1, 2.2 Hz, 2H).

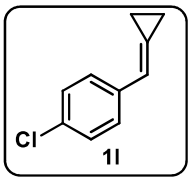

1-chloro-4-(cyclopropylidenemethyl)benzene (1l)

Overall yield: 50%, 0.293 g; **Nature:** white solid; **^{1}H NMR** (400 MHz, CHLOROFORM-D); δ 7.46 – 7.41 (m, 2H), 7.29 – 7.25 (m, 2H), 6.70 – 6.68 (m, 1H), 1.40 (ddd, *J* = 9.8, 5.8, 2.2 Hz, 2H), 1.20 – 1.15 (m, 2H).

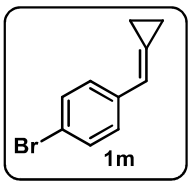

1-bromo-4-(cyclopropylidenemethyl)benzene (1m)

Overall yield: 55%, 0.309 g; **Nature:** yellow solid; **^{1}H NMR** (400 MHz, CHLOROFORM-D); δ 7.44 – 7.36 (m, 4H), 6.68 (dd, *J* = 3.9, 1.9 Hz, 1H), 1.42 – 1.36 (m, 2H), 1.19 – 1.14 (m, 2H).

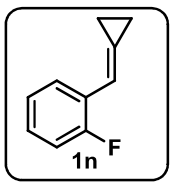

1-(cyclopropylidene(phenyl)methyl)-2-fluorobenzene (1n)

Overall yield: 45%, 0.266 g; **Nature:** yellow oil; **^{1}H NMR** (400 MHz, CHLOROFORM-D); δ 7.75 (td, *J* = 7.7, 1.8 Hz, 1H), 7.29 – 7.22 (m, 1H), 7.13 – 7.06 (m, 2H), 7.00 – 6.96 (m, 1H), 1.44 – 1.38 (m, 2H), 1.22 – 1.16 (m, 2H).

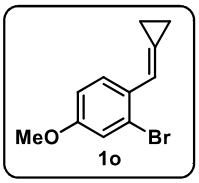

2-bromo-1-(cyclopropylidenemethyl)-4-methoxybenzene (1o)

Overall yield: 65%, 0.358 g; **Nature:** white solid; **^{1}H NMR** (400 MHz, CHLOROFORM-D); δ 7.73 (d, *J* = 8.7 Hz, 1H), 7.09 (d, *J* = 2.7 Hz, 1H), 7.07 – 7.04 (m, 1H), 6.84 (dd, *J* = 8.7, 2.6 Hz, 1H), 3.78 (s, 3H), 1.40 – 1.35 (m, 2H), 1.21 – 1.16 (m, 2H).

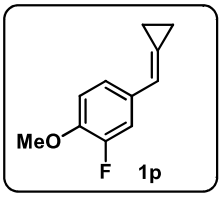

4-(cyclopropylidenemethyl)-2-fluoro-1-methoxybenzene (1p)

Overall yield: 60%, 0.345 g; **Nature:** yellow solid; **^{1}H NMR** (400 MHz, CHLOROFORM-D); δ 7.32 (dd, *J* = 12.8, 2.1 Hz, 1H), 7.15 (d, *J* = 8.4 Hz, 1H), 6.89 (t, *J* = 8.6 Hz, 1H), 6.64 (s, 1H), 3.87 (s, 3H), 1.40 – 1.35 (m, 2H), 1.18 – 1.13 (m, 2H).

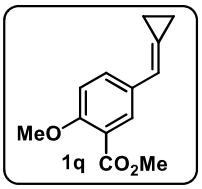

methyl 5-(cyclopropylidenemethyl)-2-methoxybenzoate (1q)

Overall yield: 60%, 0.250 g; **Nature:** yellow liquid; **^{1}H NMR** (400 MHz, CHLOROFORM-D); δ 7.91 (d, *J* = 2.3 Hz, 1H), 7.64 (dd, *J* = 8.6, 2.4 Hz, 1H), 6.93 (d, *J* = 8.7 Hz, 1H), 6.69 – 6.64 (m, 1H), 3.89 (s, 6H), 1.42 – 1.37 (m, 2H), 1.18 – 1.13 (m, 2H).

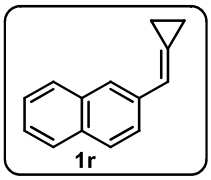

2-(cyclopropylidenemethyl)naphthalene (1r)

Overall yield: 30%, 0.173 g; **Nature:** Colourless liquid; **^{1}H NMR** (400 MHz, CHLOROFORM-D); δ 7.76 (m, 5H), 7.43 (m, 2H), 6.93 – 6.90 (m, 1H), 1.54 – 1.48 (m, 2H), 1.25 – 1.19 (m, 2H).

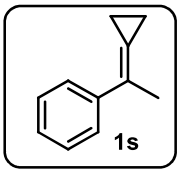

(1-cyclopropylideneethyl)benzene (1s)

Overall yield: 50%, 0.299 g; **Nature:** white solid; **^{1}H NMR** (400 MHz, CHLOROFORM-D); δ 7.73 – 7.59 (m, 2H), 7.40 – 7.29 (m, 2H), 7.23 (ddd, *J* = 7.3, 6.3, 1.3 Hz, 1H), 2.26 – 2.23 (m, 3H), 1.46 (tdd, *J* = 7.1, 3.7, 1.9 Hz, 2H), 1.15 – 1.09 (m, 2H).

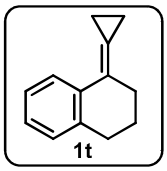

1-cyclopropylidene-1,2,3,4-tetrahydronaphthalene (1t)

Overall yield: 50%, 0.291 g; **Nature:** colourless liquid; **^{1}H NMR** (400 MHz, CHLOROFORM-D); δ 7.93 (d, *J* = 7.4 Hz, 1H), 7.19 – 7.13 (m, 2H), 7.12 (dd, *J* = 5.1, 1.2 Hz, 2H), 2.85 (t, *J* = 6.2 Hz, 2H), 2.68 – 2.63 (m, 2H), 1.92 – 1.86 (m, 2H), 1.49 – 1.43 (m, 2H), 1.10 – 1.05 (m, 2H).

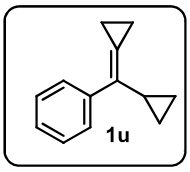

(cyclopropyl(cyclopropylidene)methyl)benzene(1u)

Overall yield: 60%, 0.340 g; **Nature:** colourless liquid; **^{1}H NMR** (400 MHz, CHLOROFORM-D); δ 7.82 (d, *J* = 7.5 Hz, 2H), 7.36 (t, *J* = 7.2 Hz, 2H), 7.25 (dd, *J* = 8.0, 6.7 Hz, 1H), 1.82 – 1.73 (m, 1H), 1.30 – 1.21 (m, 4H), 0.88 – 0.81 (m, 2H), 0.77 – 0.72 (m, 2H).

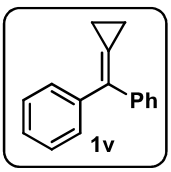

(cyclopropylidenemethylene)dibenzene (1v)

Overall yield: 65%, 0.367 g; **Nature:** white solid; **^{1}H NMR** (400 MHz, CHLOROFORM-D); δ 7.49 – 7.40 (m, 4H), 7.38 – 7.31 (m, 4H), 7.30 – 7.24 (m, 2H), 1.42 (s, 4H).

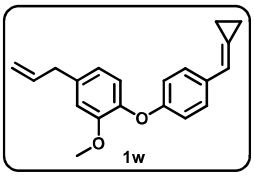

4-allyl-1-(4-(cyclopropylidenemethyl)phenoxy)-2-methoxybenzene (1w)

Overall yield: 40%, 0.217 g; **Nature:** colourless liquid; **^{1}H NMR** (400 MHz, CHLOROFORM-D); δ 7.44 (d, *J* = 8.7 Hz, 2H), 6.88 (ddd, *J* = 7.1, 5.1, 3.2 Hz, 3H), 6.81 (d, *J* = 1.9 Hz, 1H), 6.73 (dd, *J* = 8.2, 1.8 Hz, 1H), 6.69 (d, *J* = 1.8 Hz, 1H), 6.03 – 5.93 (m, 1H), 5.14 – 5.07 (m, 2H), 3.81 (s, 3H), 3.38 (d, *J* = 6.7 Hz, 2H), 1.39 – 1.34 (m, 2H), 1.17 – 1.12 (m, 2H).

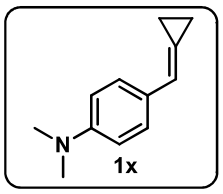

4-(cyclopropylidenemethyl)-N,N-dimethylaniline (1x)

Overall yield: 60%, 0.289 g; **Nature:** white solid; **^{1}H NMR** (400 MHz, CHLOROFORM-D); δ 7.46 – 7.39 (m, 2H), 6.74 – 6.69 (m, 2H), 6.67 – 6.63 (m, 1H), 2.95 (s, 6H), 1.36 (ddd, *J* = 9.3, 5.3, 2.2 Hz, 2H), 1.15 – 1.10 (m, 2H).

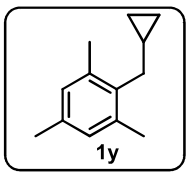

2-(cyclopropylmethyl)-1,3,5-trimethylbenzene (1y)

Overall yield: 60%, 0.413 g; **Nature:** colourless liquid; **^{1}H NMR** (400 MHz, CHLOROFORM-D); δ 6.88 (s, 1H), 6.84 (s, 1H), 2.66 (d, *J* = 6.0 Hz, 2H), 2.35 (s, 36), 2.31 (s, 3H), 0.95 – 0.85 (m, 1H), 0.50 – 0.43 (m, 2H), 0.22 – 0.16 (m, 2H)

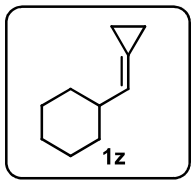

(cyclopropylidenemethyl)cyclohexane (1z)

Overall yield: 70%, 0.423g; **Nature:** colourless liquid; **^{1}H NMR** (400 MHz, CHLOROFORM-D); δ 5.70 – 5.65 (m, 1H), 2.18 – 2.10 (m, 1H), 1.80 – 1.60 (m, 6H), 1.26 (ddd, *J* = 9.2, 8.7, 2.7 Hz, 6H), 1.17 (dd, *J* = 17.6, 6.7 Hz, 2H), 1.08 – 1.02 (m, 2H), 0.97 – 0.92 (m, 2H).

4.4.3. General Procedure for electrochemical reaction

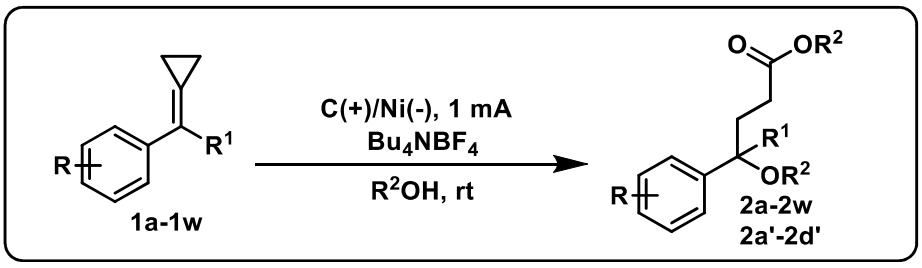

In a homemade undivided cell equipped with magnetic bar and graphite as anode and nickel as cathode having dimensions (W×H×D) 8×52.5×2 mm, mixture of **1a-1w** (1.0 equiv., 0.187 mmol), Bu_4NBF_4 (0.374 mmol, 2.0 equiv.) and methanol (4 ml) were added. The distance between the electrodes is 5 mm and dipped 20 mm in solution. The mixture was electrolyzed at a constant current of 1 mA at room temperature for 7-12 h in a DC power

supply. Upon completion, the solvent was removed under reduced pressure and the crude was subjected to silica gel column chromatography (200-400 mesh) to afford the desired product.

4.4.3.1. Characterization data of final products

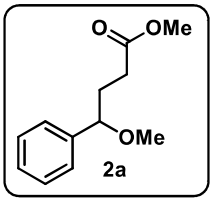

methyl 4-methoxy-4-phenylbutanoate (2a)

Overall yield: 65%, 31 mg; **Nature:** yellow oil; R_f = 0.5 (Hexane/ethyl acetate = 95:5); **^{1}H NMR** (400 MHz, CHLOROFORM-D); δ 7.36 – 7.31 (m, 2H), 7.29 – 7.24 (m, 3H), 4.14 (dd, *J* = 7.9, 5.3 Hz, 1H), 3.64 (s, 3H), 3.19 (s, 3H), 2.38 (t, *J* = 7.5 Hz, 2H), 2.11 – 1.91 (m, 2H); **^{13}C{^{1}H} NMR** (101 MHz, CHLOROFORM-D); δ 174.0, 141.5, 128.5, 127.8, 126.6, 82.8, 56.8, 51.6, 33.1, 30.4; **HRMS** (ESI, Q-TOF) m/z [M + H]$^+$ Calcd for $C_{12}H_{16}NaO_3$ 231.0997, found [M+Na]$^+$ 231.0997.

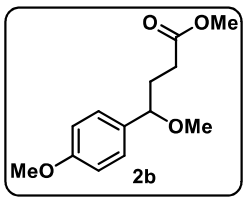

methyl 4-methoxy-4-(4-methoxyphenyl)butanoate (2b)

Overall yield: 75%, 33 mg; **Nature:** yellow oil; R_f = 0.5 (Hexane/ethyl acetate = 95:5); **^{1}H NMR** (400 MHz, CHLOROFORM-D); δ 7.18 (d, *J* = 8.6 Hz, 2H), 6.89 – 6.84 (m, 2H), 4.08 (dd, *J* = 7.8, 5.5 Hz, 1H), 3.79 (s, 3H), 3.63 (s, 3H), 3.16 (s, 3H), 2.35 (t, *J* = 7.4 Hz, 2H), 2.06 (dq, *J* = 14.9, 7.5 Hz, 2H), 1.97 – 1.88 (m, 1H); **^{13}C{^{1}H} NMR** (101 MHz, CHLOROFORM-D); δ 174.0, 159.2, 133.5, 127.9, 113.8, 111.9, 82.3, 56.5, 55.3, 51.6, 33.1, 30.5; **HRMS** (ESI, Q-TOF) m/z [M + Na]$^+$ Calcd for $C_{13}H_{18}NaO_4$ 261.1103, found [M+Na]$^+$ 261.1104.

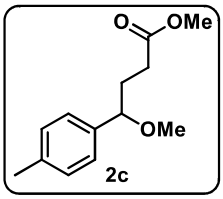

methyl 4-methoxy-4-(p-tolyl)butanoate (2c)

Overall yield: 70%, 22 mg; **Nature: yellow oil**; R_f = 0.5 (Hexane/ethyl acetate = 95:5); **^{1}H NMR** (400 MHz, CHLOROFORM-D); δ 7.15 (s, 4H), 4.10 (dd, *J* = 7.9, 5.3 Hz, 1H), 3.64 (s, 3H), 3.18 (s, 3H), 2.36 (t, *J* = 7.5 Hz, 2H), 2.33 (s, 3H), 2.05 (td, *J* = 14.8, 7.4 Hz, 2H), 1.98 – 1.89 (m, 1H); **^{13}C{^{1}H} NMR** (101 MHz, CHLOROFORM-D); δ 174.0, 138.4, 137.4, 129.2, 82.6, 56.7, 51.6, 33.1, 30.5, 21.2; **HRMS** (ESI, Q-TOF) m/z [M + Na]$^+$ Calcd for $C_{13}H_{18}NaO_3$ 245.1154, found [M+Na]$^+$ 245.1144.

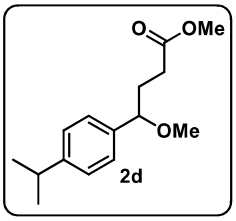

methyl 4-(4-isopropyl-2-methoxyphenyl)-4-methoxybutanoate (2d)

Overall yield: 70%, 30 mg; **Nature: yellow oil**; R_f = 0.5 (Hexane/ethyl acetate = 97:3); **^{1}H NMR** (400 MHz, CHLOROFORM-D); δ 7.18 (s, 4H), 4.10 (dd, *J* = 7.9, 5.3 Hz, 1H), 3.63 (s, 3H), 3.19 (s, 3H), 2.88 (dt, *J* = 13.8, 6.9 Hz, 1H), 2.37 (t, *J* = 7.5 Hz, 2H), 2.11 – 1.90 (m, 2H), 1.23 (d, *J* = 7.0 Hz, 2H); **^{13}C{^{1}H} NMR** (101 MHz, CHLOROFORM-D); δ 174.1, 148.3, 138.8, 126.6, 126.5, 82.6, 56.7, 51.6, 33.8, 33.1, 30.5, 24.0; **HRMS** (ESI, Q-TOF) m/z [M + Na]$^+$ Calcd for $C_{15}H_{22}NaO_3$ 273.1467, found [M+Na]$^+$ 273.1477.

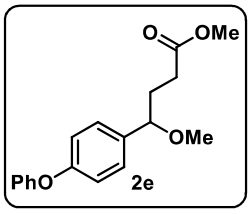

methyl 4-methoxy-4-(4-phenoxyphenyl)butanoate (2e)

Overall yield: 72%, 28 mg; **Nature:** yellow oil; R_f = 0.5 (Hexane/ethyl acetate = 97:3); **^{1}H NMR** (400 MHz, CHLOROFORM-D); δ 7.36 – 7.30 (m, 2H), 7.25 – 7.21 (m, 2H), 7.12 – 7.07 (m, 1H), 7.02 – 6.96 (m, 4H), 4.12 (dd, *J* = 7.9, 5.3 Hz, 1H), 3.65 (s, 3H), 3.20 (s, 3H), 2.38 (t, *J* = 7.5 Hz, 2H), 2.11 – 2.02 (m, 1H), 2.00 – 1.92 (m, 1H); **^{13}C{^{1}H} NMR** (101 MHz, CHLOROFORM-D); δ 174.0, 156.9, 136.3, 129.8, 128.0, 123., 119.05, 118.7, 82.3, 56.7, 51.6, 33.1, 30.4; **HRMS** (ESI, Q-TOF) m/z [M + Na]$^+$ Calcd for $C_{18}H_{20}NaO_4$ 323.1259, found [M+Na]$^+$ 323.1259.

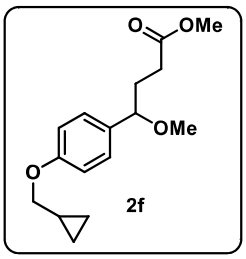

methyl 4-(4-(cyclopropylmethoxy)phenyl)-4-methoxybutanoate (2f)

Overall yield: 80%, 33 mg; **Nature: yellow oil**; R_f = 0.5 (Hexane/ethyl acetate = 93:7); **^{1}H NMR** (400 MHz, CHLOROFORM-D); δ 7.19 – 7.15 (m, 2H), 6.88 – 6.84 (m, 2H), 4.07 (dd, *J* = 7.8, 5.5 Hz, 1H), 3.77 (d, *J* = 6.9 Hz, 2H), 3.63 (s, 3H), 3.15 (s, 3H), 2.34 (t, *J* = 7.5 Hz, 2H), 2.10 – 2.01 (m, 1H), 1.96 – 1.87 (m, 1H), 1.31 – 1.25 (m, 1H), 0.66 – 0.60 (m, 2H), 0.35 – 0.31 (m, 2H); **^{13}C{^{1}H} NMR** (101 MHz, CHLOROFORM-D); δ 174.0, 158.6, 133.4, 127.8, 114.5, 82.4, 72.8, 56.5, 51.6, 33.1, 30.5, 10.3, 3.28; **HRMS** (ESI, Q-TOF) m/z [M + Na]$^+$ Calcd for $C_{16}H_{22}NaO_4$ 301.1416, found [M+Na]$^+$ 301.1417.

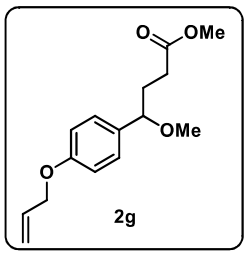

methyl 4-(4-(allyloxy)phenyl)-4-methoxybutanoate (2g)

Overall yield: 78%, 33 mg; **Nature:** yellow oil; R_f = 0.5 (Hexane/ethyl acetate = 95:5); **^{1}H NMR** (400 MHz, CHLOROFORM-D); δ 7.20 – 7.15 (m, 2H), 6.90 – 6.86 (m, 2H), 6.05 (ddt, *J* = 17.2, 10.5, 5.3 Hz, 1H), 5.40 (dq, *J* = 17.3, 1.7 Hz, 1H), 5.28 (dq, *J* = 10.5, 1.4 Hz, 1H), 4.52 (dt, *J* = 5.2, 1.4 Hz, 2H), 4.07 (dd, *J* = 7.8, 5.5 Hz, 1H), 3.63 (s, 3H), 3.16 (s, 3H), 2.35 (t, *J* = 7.5 Hz, 2H), 2.10 – 2.01 (m, 1H), 1.97 – 1.88 (m, 1H); **^{13}C{^{1}H} NMR** (101 MHz, CHLOROFORM-D); δ 174.0, 158.2, 133.6, 133.3, 127.8, 117.8, 114.6, 82.3, 68.9, 56.6, 51.6, 33.1, 30.5; **HRMS** (ESI, Q-TOF) m/z [M + Na]$^+$ Calcd for $C_{15}H_{20}NaO_4$ 287.1259, found [M+Na]$^+$ 287.1263.

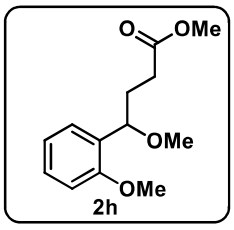

methyl 4-methoxy-4-(2-methoxyphenyl)butanoate (2h)

Overall yield: 70%, 22 mg; **Nature:** yellow oil; R_f = 0.5 (Hexane/ethyl acetate = 93:7); **^{1}H NMR** (400 MHz, CHLOROFORM-D); δ 7.32 (dd, *J* = 7.5, 1.7 Hz, 1H), 7.25 – 7.19 (m, 1H), 6.99 – 6.93 (m, 1H), 6.85 (d, *J* = 7.7 Hz, 1H), 4.62 (t, *J* = 6.2 Hz, 1H), 3.79 (s, 3H), 3.62 (s, 3H), 3.22 (s, 3H), 2.43 - 2.36 (m, 2H), 2.01 - 1.96 (m, 2H); **^{13}C{^{1}H} NMR** (101 MHz, CHLOROFORM-D); δ 174.3, 157.0, 129.6, 128.3, 126.5, 120.7, 110.2, 76.37, 56.9, 55.3, 51.5, 31.7, 30.4; **HRMS** (ESI, Q-TOF) m/z [M + Na]$^+$ Calcd for $C_{13}H_{18}NaO_4$ 261.1103, found [M+Na]$^+$ 261.1145.

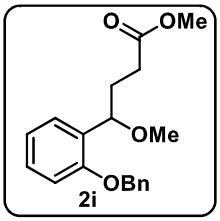

methyl 4-(2-(benzyloxy)phenyl)-4-methoxybutanoate (2i)

Overall yield: 85%, 33 mg; **Nature:** yellow oil; R_f = 0.5 (Hexane/ethyl acetate = 93:7); **^{1}H NMR** (400 MHz, CHLOROFORM-D); δ 7.43 – 7.36 (m, 5H), 7.35 – 7.30 (m, 1H), 7.22 (td, *J* = 8.2, 1.7 Hz, 1H), 6.99 (t, *J* = 7.4 Hz, 1H), 6.92 (d, *J* = 8.2 Hz, 1H), 5.08 (d, *J* = 3.5 Hz, 2H), 4.72 (t, *J* = 6.1 Hz, 1H), 3.57 (s, 3H), 3.23 (s, 3H), 2.42 – 2.36 (m, 2H), 2.07 – 2.01 (m, 2H); **^{13}C{^{1}H} NMR** (101 MHz, CHLOROFORM-D); δ 174.1, 156.1, 137.2, 130.0, 128.6, 128.3, 127.9, 127.2, 126.6, 121.1, 111.8, 76.2, 70.0, 57.0, 51.5, 31.8, 30.4; **HRMS** (ESI, Q-TOF) m/z [M + Na]$^+$ Calcd for $C_{19}H_{22}NaO_4$ 337.1416, found [M+Na]$^+$ 337.1417.

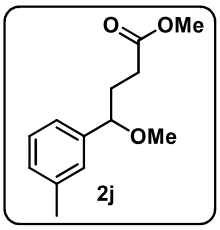

methyl 4-methoxy-4-(m-tolyl)butanoate (2j)

Overall yield: 55%, 25 mg; **Nature:** yellow oil; R_f = 0.5 (Hexane/ethyl acetate = 97:3); **^{1}H NMR** (400 MHz, CHLOROFORM-D); δ 7.24 – 7.20 (m, 1H), 7.10 – 7.04 (m, 3H), 4.09 (dd, *J* = 7.9, 5.3 Hz, 1H), 3.64 (s, 3H), 3.19 (s, 3H), 2.37 (t, *J* = 7.5 Hz, 2H), 2.34 (s, 3H), 2.10 – 2.00 (m, 1H), 1.99 – 1.91 (m, 1H); **^{13}C{^{1}H} NMR** (101 MHz, CHLOROFORM-D); δ 174.0, 141.5, 138.1, 128.5, 128.4, 127.2, 123.7, 82.8, 56.8, 51.6, 33.1, 30.5, 21.5; **HRMS** (ESI, Q-TOF) m/z [M + Na]$^+$ Calcd for $C_{13}H_{18}NaO_3$ 245.1154, found [M+Na]$^+$ 245.1156.

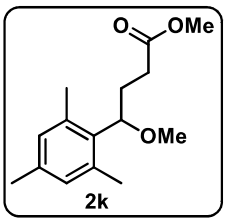

methyl 4-mesityl-4-methoxybutanoate (2k)

Overall yield: 65%, 28 mg; **Nature:** yellow oil; R_f = 0.5 (Hexane/ethyl acetate = 95:5); **^{1}H NMR** (400 MHz, CHLOROFORM-D); δ 6.81 (s, 2H), 4.62 (dd, *J* = 9.8, 4.6 Hz, 1H), 3.66 (s, 3H), 3.14 (s, 3H), 2.52 – 2.45 (m, 2H), 2.35 (s, 6H), 2.24 (s, 3H), 2.23 – 2.16 (m, 1H), 1.98 – 1.89 (m, 1H); **^{13}C{^{1}H} NMR** (101 MHz, CHLOROFORM-D); δ 174.1, 136.7, 136.6, 133.5, 130.0, 79.5, 56.3, 51.6, 30.9, 29.9, 20.8, 20.4; **HRMS** (ESI, Q-TOF) m/z [M + Na]$^+$ Calcd for $C_{15}H_{22}NaO_3$ 273.1467, found [M+Na]$^+$ 273.1476.

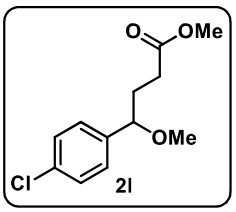

methyl 4-(4-chlorophenyl)-4-methoxybutanoate (2l)

Overall yield: 75%, 33 mg; **Nature:** yellow oil; R_f = 0.5 (Hexane/ethyl acetate = 93:7); **^{1}H NMR** (400 MHz, CHLOROFORM-D); δ 7.33 – 7.28 (m, 2H), 7.22 – 7.19 (m, 2H), 4.12 (dd, *J* = 8.0, 5.2 Hz, 1H), 3.64 (s, 3H), 3.18 (s, 3H), 2.39 – 2.33 (m, 2H), 2.05 – 1.88 (m, 2H).; **^{13}C{^{1}H} NMR** (101 MHz, CHLOROFORM-D); δ 173.8, 140.2, 133.4, 128.7, 128.0, 82.1, 56.8, 51.6, 33.1, 30.2; **HRMS** (ESI, Q-TOF) m/z [M + Na]$^+$ Calcd for $C_{12}H_{15}ClNaO_3$ 265.0607, found [M+Na]$^+$ 265.0605

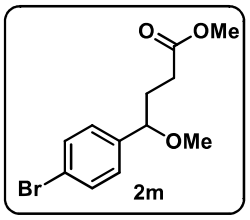

methyl 4-(4-bromophenyl)-4-methoxybutanoate (2m)

Overall yield: 78%, 31 mg; **Nature:** yellow oil; R_f = 0.5 (Hexane/ethyl acetate = 93:7); **^{1}H NMR** (400 MHz, CHLOROFORM-D); δ 7.48 – 7.44 (m, 2H), 7.17 – 7.13 (m, 2H), 4.11 (dd, *J* = 8.0, 5.2 Hz, 1H), 3.64 (s, 3H), 3.18 (s, 3H), 2.38 – 2.34 (m, 2H), 2.05 – 1.98 (m, 1H), 1.96 – 1.87 (m, 1H); **^{13}C{^{1}H} NMR** (101 MHz, CHLOROFORM-D); δ 173.8, 140.7, 131.7, 128.3, 121.5, 82.17, 56.9, 51.7, 33.0, 30.2; **HRMS** (ESI, Q-TOF) m/z [M + Na]$^+$ Calcd for $C_{12}H_{15}BrNaO_3$ 309.0102, found [M+Na]$^+$ 309.0107.

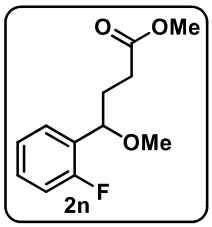

methyl 4-(2-fluorophenyl)-4-methoxybutanoate (2n)

Overall yield: 58%, 26 mg; **Nature:** yellow oil; R_f = 0.5 (Hexane/ethyl acetate = 95:5); **^{1}H NMR** (400 MHz, CHLOROFORM-D); δ 7.37 (td, *J* = 7.5, 1.8 Hz, 1H), 7.24 (tdd, *J* = 7.2, 5.2, 1.9 Hz, 1H), 7.14 (td, *J* = 7.4, 1.0 Hz, 1H), 7.04 – 6.98 (m, 1H), 4.54 (dd, *J* = 7.7, 5.2 Hz, 1H), 3.63 (s, 3H), 3.22 (s, 3H), 2.43 – 2.37 (m, 2H), 2.10 – 1.98 (m, 2H); **^{13}C{^{1}H} NMR** (101 MHz, CHLOROFORM-D); δ 173.8, 161.8, 159.4, 129.1, 129.0, 127.5, 124.4, 124.4, 115.5, 115.3, 75.8, 57.1, 51.6, 31.9, 30.3; **^{19}F NMR** (376 MHz, CHLOROFORM-D) δ -119.79; **HRMS** (ESI, Q-TOF) m/z [M + Na]$^+$ Calcd for $C_{12}H_{15}FNaO_3$ 249.0903, found [M+Na]$^+$ 249.0903.

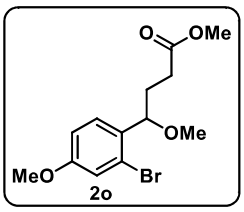

methyl 4-(2-bromo-4-methoxyphenyl)-4-methoxybutanoate (2o)

Overall yield: 80%, 31 mg; **Nature:** yellow oil; R_f = 0.5 (Hexane/ethyl acetate = 93:7); **^{1}H NMR** (400 MHz, CHLOROFORM-D); δ 7.30 (d, *J* = 8.7 Hz, 1H), 7.05 (d, *J* = 2.6 Hz, 1H), 6.88 (dd, *J* = 8.6, 2.6 Hz, 1H), 4.53 (dd, *J* = 7.8, 4.9 Hz, 1H), 3.78 (s, 3H), 3.64 (s, 3H), 3.18 (s, 3H), 2.48 – 2.34 (m, 2H), 2.02 – 1.89 (m, 2H); **^{13}C{^{1}H} NMR** (101 MHz, CHLOROFORM-D); δ 173.9, 159.3, 132.5, 128.1, 123.4, 117.7, 114.2, 80.7, 56.9, 55.6, 51.6, 32.1, 30.4; **HRMS** (ESI, Q-TOF) m/z [M + Na]$^+$ Calcd for $C_{13}H_{17}BrNaO_4$ 339.0208, found [M+Na]$^+$ 339.0206.

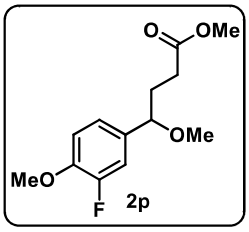

methyl 4-(3-fluoro-4-methoxyphenyl)-4-methoxybutanoate (2p)

Overall yield: 76%, 32 mg; **Nature:** yellow oil; R_f = 0.5 (Hexane/ethyl acetate = 97:3); **^{1}H NMR** (400 MHz, CHLOROFORM-D); δ 7.01 (dd, *J* = 12.0, 2.0 Hz, 1H), 6.96 (dd, *J* = 8.5, 2.0 Hz, 1H), 6.91 (t, *J* = 8.2 Hz, 1H), 4.06 (dd, *J* = 7.9, 5.4 Hz, 1H), 3.86 (s, 3H), 3.63 (s, 3H), 3.16 (s, 3H), 2.34 (t, *J* = 7.4 Hz, 2H), 2.04 – 1.96 (m, 1H), 1.95 – 1.85 (m, 1H); **^{13}C{^{1}H} NMR** (101 MHz, CHLOROFORM-D); δ 173.9, 153.7, 151.3, 147.1, 147.0, 134.6, 122.5, 114.2, 114.0, 113.2, 81.9, 56.7, 56.3, 51.6, 33.0, 30.3; **^{19}F NMR** (376 MHz, CHLOROFORM-D) δ -134.95; **HRMS** (ESI, Q-TOF) m/z [M + Na]$^+$ Calcd for $C_{13}H_{17}BFNaO_4$ 279.1009, found [M+Na]$^+$ 279.1024.

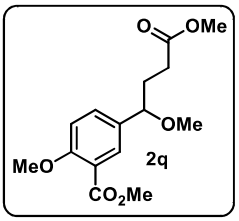

methyl 5-(1,4-dimethoxy-4-oxobutyl)-2-methoxybenzoate (2q)

Overall yield: 75%, 30 mg; **Nature:** yellow oil; R_f = 0.5 (Hexane/ethyl acetate = 85:15); **^{1}H NMR** (400 MHz, CHLOROFORM-D); δ 7.69 (d, *J* = 2.3 Hz, 1H), 7.39 (dd, *J* = 8.6, 2.3 Hz, 1H), 6.96 (d, *J* = 8.6 Hz, 1H), 4.11 (dd, *J* = 8.0, 5.2 Hz, 1H), 3.89 (s, 3H), 3.88 (s, 3H), 3.64 (s, 3H), 3.17 (s, 3H), 2.36 (t, *J* = 7.4 Hz, 2H), 2.05 (dt, *J* = 15.2, 7.3 Hz, 1H), 1.93 (ddd, *J* = 19.4, 10.7, 6.4 Hz, 1H); **^{13}C{^{1}H} NMR** (101 MHz, CHLOROFORM-D); δ 173.9, 166.6, 158.8, 133.2, 131.7, 130.1, 119.9, 112.2, 81.9, 56.7, 56.2, 52.1, 51.6, 33.0, 30.4; **^{19}F NMR** (376 MHz, CHLOROFORM-D) δ -134.95; **HRMS** (ESI, Q-TOF) m/z [M + Na]$^+$ Calcd for $C_{15}H_{20}NaO_6$ 319.1158, found [M+Na]$^+$ 319.1158.

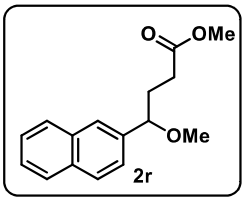

methyl 4-methoxy-4-(naphthalen-2-yl)butanoate (2r)

Overall yield: 65%, 26 mg; **Nature:** yellow oil; R_f = 0.5 (Hexane/ethyl acetate = 95:5); **^{1}H NMR** (400 MHz, CHLOROFORM-D); δ 7.83 (dd, *J* = 8.6, 5.7 Hz, 3H), 7.72 (s, 1H), 7.49 – 7.45 (m, 2H), 7.43 (dd, *J* = 8.5, 1.6 Hz, 1H), 4.32 (dd, *J* = 7.8, 5.4 Hz, 1H), 3.64 (s, 3H), 3.24 (s, 3H), 2.41 (t, *J* = 7.4 Hz, 2H), 2.21 – 2.12 (m, 1H), 2.09 – 2.01 (m, 1H); **^{13}C{^{1}H} NMR** (101 MHz, CHLOROFORM-D); δ 174.0, 138.9, 133.2, 133.2, 128.5, 127.9, 127.8, 126.2, 125.9, 125.9, 124.3, 82.9, 56.9, 51.6, 33.0, 30.4; **HRMS** (ESI, Q-TOF) m/z [M + H]$^+$ Calcd for $C_{16}H_{19}O_3$ 259.1334, found [M+H]$^+$ 259.1256.

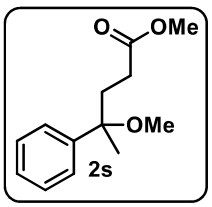

methyl 4-methoxy-4-phenylpentanoate (2s)

Overall yield: 60%, 27 mg; **Nature:** yellow oil; R_f = 0.5 (Hexane/ethyl acetate = 97:3); **^{1}H NMR** (400 MHz, CHLOROFORM-D); δ 7.36 – 7.31 (m, 4H), 7.26 – 7.22 (m, 1H), 3.59 (s, 3H), 3.09 (s, 3H), 2.30 – 2.21 (m, 2H), 2.12 – 2.05 (m, 2H), 1.52 (s, 3H); **^{13}C{^{1}H} NMR** (101 MHz, CHLOROFORM-D); δ 174.3, 144.4, 128.3, 127.0, 126.1, 78.2, 51.6, 50.4, 37.1, 29.0, 23.4; **HRMS** (ESI, Q-TOF) m/z [M + Na]$^+$ Calcd for $C_{13}H_{18}NaO_3$ 245.1154, found [M+Na]$^+$ 245.1160.

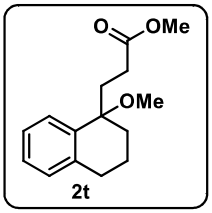

methyl 3-(1-methoxy-1,2,3,4-tetrahydronaphthalen-1-yl)propanoate (2t)

Overall yield: 70%, 30 mg; **Nature:** yellow oil; R_f = 0.5 (Hexane/ethyl acetate = 97:3); **^{1}H NMR** (400 MHz, CHLOROFORM-D); δ 7.39 (dd, *J* = 7.5, 1.6 Hz, 1H), 7.17 (ddd, *J* = 13.4, 6.9, 1.6 Hz, 2H), 7.07 (dd, *J* = 6.7, 1.9 Hz, 1H), 3.62 (s, 3H), 3.02 (s, 3H), 2.82 – 2.68 (m, 2H), 2.48 – 2.34 (m, 2H), 2.13 – 2.02 (m, 4H), 1.91 – 1.81 (m, 2H); **^{13}C{^{1}H} NMR** (101 MHz, CHLOROFORM-D); δ 174.5, 138.8, 138.4, 128., 127.14, 126.9, 125.9, 77.0, 51.6, 50.2, 37.2, 29.7, 29.6, 29.0, 20.5; **HRMS** (ESI, Q-TOF) m/z [M + Na]$^+$ Calcd for $C_{15}H_{20}BrNaO_3$ 271.1310, found [M+Na]$^+$ 271.1316.

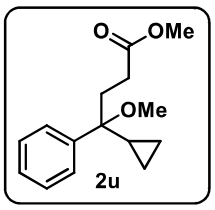

methyl 4-cyclopropyl-4-methoxy-4-phenylbutanoate (2u)

Overall yield: 75%, 32 mg; **Nature:** colorless liquid; R_f = 0.5 (Hexane/ethyl acetate = 97:3); **^{1}H NMR** (400 MHz, CHLOROFORM-D); δ 7.39 (dt, *J* = 3.1, 1.9 Hz, 2H), 7.34 – 7.30 (m, 2H), 7.25 – 7.21 (m, 1H), 3.62 (s, 3H), 3.19 (s, 3H), 2.53 – 2.44 (m, 1H), 2.24 – 2.15 (m, 2H), 2.03 – 1.96 (m, 1H), 1.09 (ddd, *J* = 11.7, 7.0, 4.2 Hz, 1H), 0.54 – 0.47 (m, 2H), 0.42 – 0.34 (m, 2H); **^{13}C{^{1}H} NMR** (101 MHz, CHLOROFORM-D); δ 174.69, 143.28, 128.00, 126.96, 126.83, 79.28, 51.68, 50.20, 30.11, 28.41, 19.60, 2.69, 0.96. **HRMS** (ESI, Q-TOF) m/z [M + Na]$^+$ Calcd for $C_{15}H_{20}BrNaO_3$ 271.1310, found [M+Na]$^+$ 271.1311.

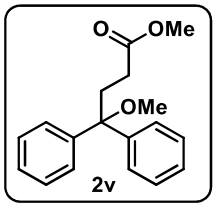

methyl 4-methoxy-4,4-diphenylbutanoate (2v)

Overall yield: 65%, 26 mg; **Nature:** yellow oil; R_f = 0.5 (Hexane/ethyl acetate = 95:5); **^{1}H NMR** (400 MHz, CHLOROFORM-D); δ 7.36 – 7.33 (m, 4H), 7.30 – 7.24 (m, 4H), 7.22 – 7.17 (m, 2H), 3.61 (s, 3H), 3.04 (s, 3H), 2.69 – 2.64 (m, 2H), 2.19 – 2.14 (m, 2H); **^{13}C{^{1}H} NMR** (101 MHz, CHLOROFORM-D); δ 174.4, 144.7, 128.1, 126.9, 81.7, 51.6, 50.1, 30.0, 28.2; **HRMS** (ESI, Q-TOF) m/z [M + Na]$^+$ Calcd for $C_{18}H_{20}BrNaO_3$ 307.1310, found [M+Na]$^+$ 307.1316.

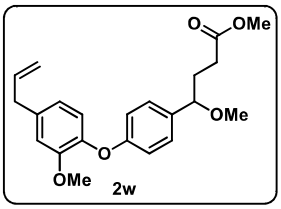

methyl 4-(4-(4-allyl-2-methoxyphenoxy)phenyl)-4-methoxybutanoate (2w)

Overall yield: 60%, 22 mg; **Nature:** yellow oil; R_f = 0.5 (Hexane/ethyl acetate = 93:7); **^{1}H NMR** (400 MHz, CHLOROFORM-D); δ 7.19 – 7.14 (m, 2H), 6.92 – 6.87 (m, 3H), 6.81 (d, *J* = 1.9 Hz, 1H), 6.74 (dd, *J* = 8.0, 2.0 Hz, 1H), 5.98 (ddt, *J* = 16.9, 10.1, 6.8 Hz, 1H), 5.14 – 5.07 (m, 2H), 4.09 (dd, *J* = 7.8, 5.4 Hz, 1H), 3.81 (s, 3H), 3.64 (s, 3H), 3.38 (d, *J* = 6.8 Hz, 2H), 3.17 (s, 3H), 2.36 (d, *J* = 15.0 Hz, 2H), 2.10 – 2.00 (m, 1H), 1.98 – 1.89 (m, 1H); **^{13}C{^{1}H} NMR** (101 MHz, CHLOROFORM-D); δ 174.0, 157.9, 151.4, 143.0, 137.3, 137.17, 135.2, 127.8, 121.3, 121.0, 116.9, 116.1, 113.0, 82.3, 56.6, 56.0, 51.65, 40.1, 33.1, 30.5; **HRMS** (ESI, Q-TOF) m/z [M + Na]$^+$ Calcd for $C_{22}H_{26}NaO_4$ 393.1678, found [M+Na]$^+$ 393.1679.

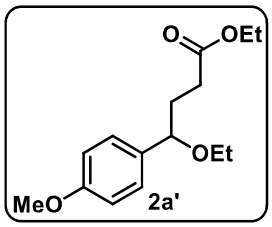

ethyl 4-ethoxy-4-(4-methoxyphenyl)butanoate (2a')

Overall yield: 58%, 28 mg; **Nature:** yellow oil; R_f = 0.5 (Hexane/ethyl acetate = 95:5); **^{1}H NMR** (400 MHz, CHLOROFORM-D); δ 7.19 (d, *J* = 8.2 Hz, 2H), 6.86 (d, *J* = 7.3 Hz, 2H), 4.21 – 4.16 (m, 1H), 4.12 – 4.05 (m, 2H), 3.78 (s, 3H), 3.38 – 3.30 (m, 2H), 3.37 – 3.22 (m, 2H), 2.35 (t, *J* = 7.4 Hz, 2H), 2.04 (td, *J* = 14.2, 6.9 Hz, 1H), 1.91 (td, *J* = 13.7, 6.9 Hz, 1H), 1.22 (td, *J* = 6.9, 1.2 Hz, 3H), 1.13 (td, *J* = 6.9, 1.3 Hz, 3H); **^{13}C{^{1}H} NMR** (101 MHz, CHLOROFORM-D); δ 173.6, 159.0, 134.3, 127.7, 113.8, 80.4,

64.0, 60.3, 55.3, 33.3, 30.9, 15.3, 14.3; **HRMS** (ESI, Q-TOF) m/z [M + Na]$^+$ Calcd for $C_{15}H_{22}NaO_4$ 289.1416, found [M+Na]$^+$ 289.1456.

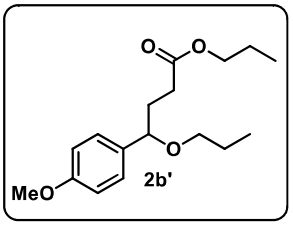

propyl 4-(4-methoxyphenyl)-4-propoxybutanoate (2b')

Overall yield: 55%, 30 mg; **Nature:** yellow oil; R_f = 0.5 (Hexane/ethyl acetate = 97:3); **^{1}H NMR** (400 MHz, CHLOROFORM-D); δ 7.21 – 7.17 (m, 2H), 6.88 – 6.84 (m, 2H), 4.17 (dd, *J* = 8.1, 5.2 Hz, 1H), 4.00 (t, *J* = 6.7 Hz, 2H), 3.79 (s, 3H), 3.24 (dt, *J* = 9.1, 6.7 Hz, 1H), 3.15 (dt, *J* = 9.1, 6.6 Hz, 1H), 2.38 (dd, *J* = 11.4, 4.0 Hz, 2H), 2.09 – 1.99 (m, 1H), 1.97 – 1.87 (m, 1H), 1.62 (dd, *J* = 14.4, 7.1 Hz, 2H), 1.52 (dt, *J* = 14.1, 7.1 Hz, 2H), 0.92 (t, *J* = 7.5 Hz, 3H), 0.87 (t, *J* = 7.4 Hz, 3H); **^{13}C{^{1}H} NMR** (101 MHz, CHLOROFORM-D); δ 173.7, 159.1, 134.4, 127.7, 113.8, 80.6, 70.5, 66.0, 55.3, 33.4, 30.9, 23.1, 22.0, 10.7, 10.5; **HRMS** (ESI, Q-TOF) m/z [M + Na]$^+$ Calcd for $C_{17}H_{26}NaO_4$ 317.1729, found [M+Na]$^+$ 317.1730.

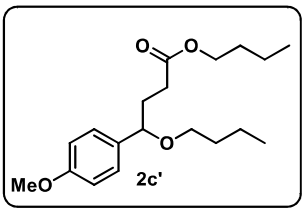

butyl 4-butoxy-4-(4-methoxyphenyl)butanoate (2c')

Overall yield: 70%, 41 mg; **Nature:** yellow oil; R_f = 0.5 (Hexane/ethyl acetate = 97:3); **^{1}H NMR** (400 MHz, CHLOROFORM-D); δ 7.21 – 7.17 (m, 2H), 6.88 – 6.83 (m, 2H), 4.16 (dd, *J* = 8.1, 5.2 Hz, 1H), 4.04 (t, *J* = 6.7 Hz, 2H), 3.79 (s, 3H), 3.27 (dt, *J* = 9.2, 6.6 Hz, 1H), 3.18 (dt, *J* = 9.2, 6.5 Hz, 1H), 2.36 (t, *J* = 7.8 Hz, 2H), 2.07 – 1.98 (m, 1H), 1.95 – 1.86 (m, 1H), 1.60 – 1.47 (m, 4H), 1.38 – 1.29 (m, 4H), 0.91 (t, *J* = 7.4 Hz, 3H), 0.86 (t, *J* = 7.3 Hz, 3H); **^{13}C{^{1}H} NMR** (101 MHz, CHLOROFORM-D); δ 173.8, 159.0, 134.4, 127.7, 113.8, 80.6, 68.5, 64.2, 55.3, 33.4, 32.0, 30.9, 30.7, 19.4, 19.2, 14.0, 13.8; **HRMS** (ESI, Q-TOF) m/z [M + Na]$^+$ Calcd for $C_{19}H_{30}NaO_4$ 345.2042, found [M+Na]$^+$ 345.2047.

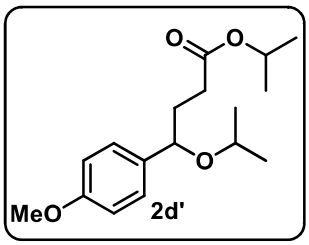

isopropyl 4-isopropoxy-4-(4-methoxyphenyl)butanoate (2d')

Overall yield: 60%, 32 mg; **Nature:** yellow oil; R_f = 0.5 (Hexane/ethyl acetate = 97:3); **^{1}H NMR** (400 MHz, CHLOROFORM-D); δ 7.23 – 7.19 (m, 2H), 6.87 – 6.83 (m, 2H), 4.98 (dt, *J* = 12.6, 6.2 Hz, 1H), 4.30 (dd, *J* = 8.4, 5.1 Hz, 1H), 3.79 (s, 3H), 3.43 (dt, *J* = 12.1, 6.1 Hz, 1H), 2.34 (td, *J* = 7.1, 1.5 Hz, 2H), 2.00 – 1.83 (m, 2H), 1.20 (d, *J* = 6.3 Hz, 6H), 1.10 (d, *J* = 6.0 Hz, 2H), 1.04 (d, *J* = 6.2 Hz, 2H); **^{13}C{^{1}H} NMR** (101 MHz, DMS-*d*^{6}); δ 172.6, 159.0, 135.4, 127.9, 114.2, 77.0, 68.3, 67.4, 55.5, 33.9, 31.0, 23.8, 22.1, 21.5; **HRMS** (ESI, Q-TOF) m/z [M + Na]$^+$ Calcd for $C_{17}H_{26}NaO_4$ 317.1729, found [M+Na]$^+$ 317.1736.

4.4.4. General Procedure for electrochemical gram-scale synthesis

In an electrasyn 2.0 vial (20 ml) equipped with a magnetic bar and graphite as anode and nickel as cathode, 1b (1 equiv., 6.24 mmol, 1.0 g), Bu_4NBF_4 (2 equiv., 12.48 mmol), and methanol (12 mL) were added. The mixture was

electrolyzed at a constant current of 1 mA at room temperature for 40 h in a DC power supply. After 40 h, the solvent was removed under reduced pressure, and the crude was purified by silica gel column chromatography using 4-5 % ethyl acetate in hexane to afford the desired product in 55% yield (0.822 g).

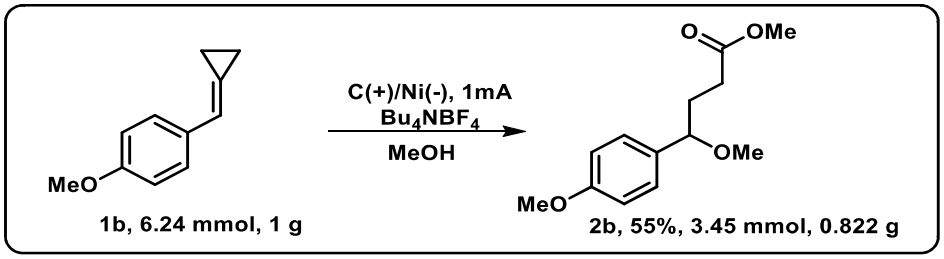

4.4.5. General Procedure for synthesis of 4-methoxy-4-(4-methoxyphenyl)butan-1-ol (3a)

To a stirred solution of LAH (1.5 equiv., 0.376 mmol) in diethyl ether was added dropwise a solution of methyl 4-methoxy-4-(4-methoxyphenyl)butanoate **2b** (1 equiv., 0.251 mmol) in of diethyl ether under a N_2 atmosphere. After addition was completed, the reaction mixture was stirred at room temperature for another 2-6 h. Upon completion (monitored by TLC), the excess LAH was destroyed by ice-cold water. H_2SO_4 (10%) and ether were added, and the aqueous layer was extracted several times with diethyl ether. The combined organic layer was washed with water and 5% $NaHCO_3$, dried over $MgSO_4$, and concentrated in a rotary evaporator. The crude material was purified by silica gel chromatography 75:25 (Hexane: ethyl acetate) and desired product was obtained in 85% yield.

4.4.5.1. Characterization data of 3a

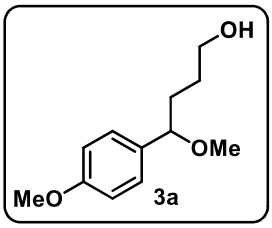

4-methoxy-4-(4-methoxyphenyl)butan-1-ol (3a)

Overall yield: 85%, 44 mg; **Nature:** yellow oil; R_f = 0.5 (Hexane/ethyl acetate = 70:30); **^{1}H NMR** (400 MHz, CHLOROFORM-D); δ 7.21 – 7.16 (m, 2H), 6.89 – 6.85 (m, 2H), 4.07 (dd, *J* = 7.8, 5.0 Hz, 1H), 3.79 (s, 3H), 3.62 (t, *J* = 6.2 Hz, 2H), 3.17 (s, 3H), 1.87 – 1.79 (m, 1H), 1.77 – 1.69 (m, 1H), 1.66 – 1.57 (m, 2H); **^{13}C{^{1}H} NMR** (101 MHz, CHLOROFORM-D); δ 13C NMR (101 MHz, CHLOROFORM-D) δ 159.1, 134.0, 127.7, 114.0, 83.6, 62.9, 56.4, 55.3, 35.1, 29.5; **HRMS** (ESI, Q-TOF) m/z $[M + Na]^+$ Calcd for $C_{12}H_{18}NaO_3$ 233.1154, found $[M+H]^+$ 233.1164.

4.4.6. General Procedure for synthesis of amide 3b and 3b'

An oven-dried round bottom flask equipped with a stir bar was charged with methyl 4-methoxy-4-(4-methoxyphenyl)butanoate **2b** (1.0 equiv., 0.167 mmol), aniline (1.2 equiv., 0.20 mmol), placed under a positive pressure of argon, and subjected to three evacuation/backfilling cycles. Toluene and LiHMDS (1.0 M in THF, 2.0 equiv.) were sequentially added with vigorous stirring at room temperature and the reaction mixture was stirred for 15 h at room temperature. On completion (monitored by TLC), the reaction mixture was quenched with NH_4Cl,

extracted with EtOAc (3x) and the organic layers were combined, washed with HCl, water, brine and dried over Na_2SO_4 and concentrated. Purification by chromatography on silica gel (EtOAc/hexanes 30:70) afforded the title product.

4.4.6.1. Characterization data of 3b and 3b'

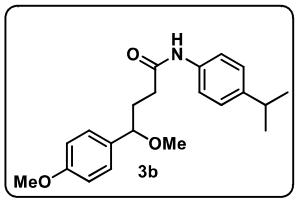

***N*-(4-isopropylphenyl)-4-methoxy-4-(4-methoxyphenyl)butanamide (3b)**

Overall yield: 90%, 51 mg; **Nature:** yellow oil; R_f = 0.5 (Hexane/ethyl acetate = 75:25); **^{1}H NMR** (400 MHz, CHLOROFORM-D); δ 7.40 (d, *J* = 8.5 Hz, 2H), 7.18 (dd, *J* = 18.8, 8.5 Hz, 4H), 6.88 (d, *J* = 8.6 Hz, 2H), 4.17 (dd, *J* = 8.1, 5.2 Hz, 1H), 3.79 (s, 3H), 3.21 (s, 3H), 2.86 (dt, *J* = 13.8, 6.9 Hz, 1H), 2.47 – 2.37 (m, 2H), 2.14 – 2.04 (m, 2H), 1.21 (d, *J* = 6.9 Hz, 6H); **^{13}C{^{1}H} NMR** (101 MHz, CHLOROFORM-D); δ 170.9, 159.3, 144.8, 135.7, 133.3, 127.8, 126.9, 119.9, 113.9, 82.7, 56.5, 55.3, 34.2, 33.6, 24.1; **HRMS** (ESI, Q-TOF) m/z $[M + Na]^+$ Calcd for $C_{21}H_{27}NNaO_3$ 364.1889, found $[M+H]^+$ 364.1891.

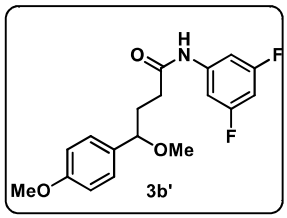

***N*-(3,5-difluorophenyl)-4-methoxy-4-(4-methoxyphenyl)butanamide (3b')**

Overall yield: 80%, 33 mg; **Nature:** yellow oil; R_f = 0.5 (Hexane/ethyl acetate = 75:25); **^{1}H NMR** (400 MHz, CHLOROFORM-D); δ 8.31 (s, 1H), 7.21 – 7.16 (m, 2H), 7.11 (dd, *J* = 8.9, 2.0 Hz, 2H), 6.89 – 6.85 (m, 2H), 6.51 (tt, *J* = 8.8, 2.3 Hz, 1H), 4.17 (dd, *J* = 8.2, 4.9 Hz, 1H), 3.78 (s, 3H), 3.22 (s, 3H), 2.48 – 2.42 (m, 2H), 2.12 – 2.03 (m, 2H); **^{13}C{^{1}H} NMR** (101 MHz, CHLOROFORM-D); δ 13C NMR (101 MHz, CHLOROFORM-D) δ 171.7, 164.5, 164.3, 162.0, 161.9, 159.4, 140.5, 140.4, 140.2, 132.9, 127.8, 114.0, 102.7, 102.4, 99.4, 99.2, 98.9, 82.9, 56.6, 55.3, 34.5, 33.4; **^{19}F NMR** (376 MHz, CHLOROFORM-D) δ -109.02; **HRMS** (ESI, Q-TOF) m/z $[M + Na]^+$ Calcd for $C_{18}H_{19}F_2NNaO_3$ 358.1231, found $[M+H]^+$ 358.1230.

4.4.7. General Procedure for synthesis of 3c

Methyl 4-methoxy-4-(4-methoxyphenyl)butanoate 2b (1 equiv., 0.083 mmol) was dissolved in a THF/H_2O mixture (1:1, 2 mL) in a round bottom flask and NaOH (3 equiv., 0.249 mmol) was added and the slurry was stirred at room temperature for 18 hours. The mixture was quenched and acidified with 1 M HCl and the aqueous phase was extracted with EtOAc (3x). The organic phase was washed with water (1x), brine (1x), dried over Na_2SO_4 and concentrated in vacuo. The crude was purified by silica gel chromatography 60:40 (Hexane: ethyl acetate).

4.4.7.1. Characterization data of 3c

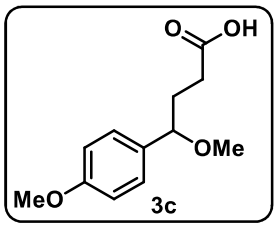

4-methoxy-4-(4-methoxyphenyl)butanoic acid (3c)

Overall yield: 80%, 15 mg; **Nature:** yellow oil; R_f = 0.5 (Hexane/ethyl acetate = 60:40); **^{1}H NMR** (400 MHz, CHLOROFORM-D); δ 7.21 – 7.16 (m, 2H), 6.90 – 6.85 (m, 2H), 4.11 (dd, *J* = 8.0, 5.3 Hz, 1H), 3.79 (s, 3H), 3.18 (s, 3H), 2.41 (t, *J* = 7.3 Hz, 2H), 2.07 (dt, *J* = 15.0, 7.3 Hz, 1H), 1.98 – 1.88 (m, 1H); **^{13}C{^{1}H} NMR** (101 MHz, CHLOROFORM-D); δ 179.2, 159.2, 133.2, 127.9, 113.9, 82.4, 56.5, 55.3, 32.8, 30.6; **HRMS** (ESI, Q-TOF) m/z [M + Na]$^+$ Calcd for $C_{12}H_{17}O_4$ 225.1127, found [M+H]$^+$ 225.1137.

4.4.8. General Procedure for synthesis of 4c

In a round bottom flask, (1R,2S,5R)-2-Isopropyl-5-methylcyclohexanol (1 equiv., 0.096 mmol) was dissolved in dry 1,4-dioxane. Acid (2.5 equiv., 0.24 mmol) was gradually added to ensure complete solubility. The reaction mixture was stirred for 5 minutes after adding 4-dimethylaminopyridine (1 equiv., 0.096 mmol). It was followed by the addition of *N,N*-dicyclohexylcarbodiimide (2.5 equiv., 0.24 mmol), and the resultant mixture was stirred for 8–12 hours under a nitrogen atmosphere. The reaction progress was monitored using TLC. DCC was filtered off after the reaction was completed. The filtrate was mixed with DCM and subjected to an aqueous workup (3×). The organic layer was separated, passed through anhydrous Na_2SO_4, and concentrated. Further, the product was purified by silica gel chromatography.

4.4.8.1. Characterization data of 4c

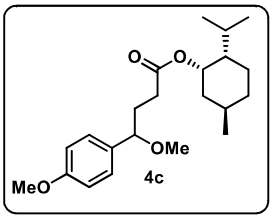

(*1S,2S,5R*)-2-isopropyl-5-methylcyclohexyl 4-methoxy-4-(4-methoxyphenyl)butanoate (4c)

Overall yield: 60%, 38 mg; Nature: yellow oil; R_f = 0.5 (Hexane/ethyl acetate = 90:10); ^{1}H NMR (400 MHz, CHLOROFORM-D); δ 7.18 (dd, *J* = 8.6, 0.9 Hz, 2H), 6.89 – 6.84 (m, 2H), 4.66 (td, *J* = 10.9, 4.4 Hz, 1H), 4.10 – 4.04 (m, 1H), 3.79 (s, 3H), 3.16 (s, 3H), 2.32 (ddd, *J* = 9.6, 5.8, 2.7 Hz, 2H), 2.06 (dt, *J* = 15.0, 7.4 Hz, 1H), 1.98 – 1.77 (m, 4H), 1.70 – 1.60 (m, 3H), 1.38 – 1.29 (m, 1H), 1.05 – 0.96 (m, 1H), 0.87 (dd, *J* = 6.7, 3.9 Hz, 6H), 0.73 (d, *J* = 7.0 Hz, 3H); ^{13}C{^{1}H} NMR (101 MHz, CHLOROFORM-D); δ 173.0, 159.2, 133.6, 127.9, 113.8, 82.4, 74.0, 56.5, 55.3, 41.0, 34.3, 33.2, 31.4, 31.1, 26.2, 23.4, 22.1, 20.8, 16.3; HRMS (ESI, Q-TOF) m/z [M + Na]$^+$ Calcd for $C_{22}H_{23}NaO_4$ 385.2355, found [M+H]$^+$ 385.2353.

4.4.9. Mechanistic studies

4.4.9.1 Radical scavenging experiment

(a) With 2,2,6,6-tetramethyl-1-piperidinyloxy radical (TEMPO)

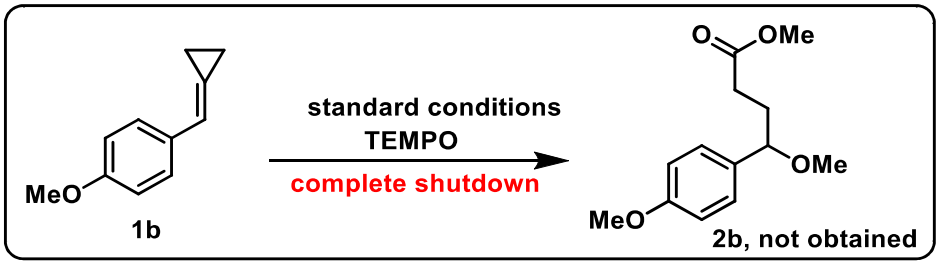

In an undivided cell equipped with magnetic bar and graphite as anode and nickel as cathode, 1b (1.0 equiv., 0.187 mmol,), Bu_4NBF_4 (2.0 equiv., 0.344 mmol), TEMPO (2 equiv., 0.344 mmol) and methanol (4 ml) were added. The mixture was electrolyzed at a constant current of 1 mA at room temperature for 7-8 h in a DC power supply. The progress of the reaction was monitored by TLC, which shows that starting material remain unconsumed. This infers that employing TEMPO completely shut down the reaction indicating the possibility of a radical path for the reaction.

(a) With butylated hydroxytoluene (BHT)

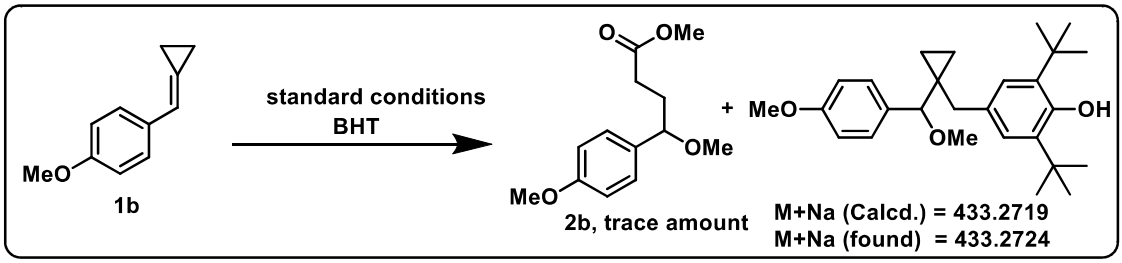

In an undivided cell equipped with magnetic bar and graphite as anode and nickel as cathode, 1b (1.0 equiv., 0.187 mmol,), Bu_4NBF_4 (2.0 equiv., 0.344 mmol), BHT (2 equiv., 0.344 mmol) and methanol (4 ml) were added. The mixture was electrolyzed at a constant current of 1 mA at room temperature for 7-8 h in a DC power supply. The progress of the reaction was monitored by TLC, which shows that starting material consumed and complex reaction mixture was observed. The BHT adduct with the first methanol attack was found in HRMS which confirms that the reaction was initiated by oxidation of double to radical cation.

4.4.9.2 Divided cell experiment

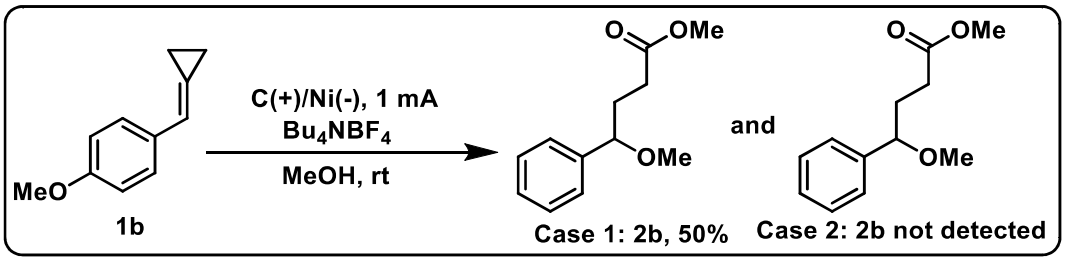

Case 1: In anodic chamber: A divided cell was equipped with two magnetic stir bars in anodic and cathodic chamber respectively. Further, the anodic chamber was filled with corresponding cyclopropane **1b** (1.0 equiv., 0.187 mmol), tetrabutylammonium hexafluorophosphate (Bu_4NBF_4) (3.0 equiv., 0.562 mmol), in methanol solvent. The cathodic chamber was filled only with supporting electrolyte solution and the solution was electrolyzed with carbon anode (in anodic chamber) and nickel cathode (in cathodic chamber) at a constant current of 1 mA for 10 h at room temperature (25-30 °C). However, there is a slight decrease in yield as the desired product was obtained in 50% yield.

Case 2: In cathodic chamber: A divided cell was equipped with two magnetic stir bars in anodic and cathodic chamber respectively. Further, the cathodic chamber was filled with corresponding cyclopropane **1b** (1.0 equiv., 0.187 mmol), tetrabutylammonium hexafluorophosphate (Bu_4NBF_4) (3.0 equiv., 0.562 mmol), in methanol solvent. The anodic chamber was filled with supporting electrolyte solution and the solution was electrolyzed with carbon anode (in anodic chamber) and nickel cathode (in cathodic chamber) at a constant current of 1 mA for 10 h at room temperature. The progress of the reaction was monitored by TLC, which shows that starting material remain unconsumed. This infers that the reaction takes place by the anodic oxidation.

4.4.9.3 Electrochemical reaction of 2-(cyclopropylmethyl)-1,3,5-trimethylbenzene (1y)

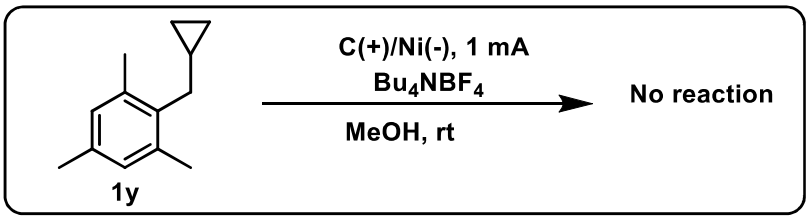

In an undivided cell equipped with magnetic bar and graphite as anode and nickel as cathode, **1y** (1.0 equiv., 0.172 mmol), Bu_4NBF_4 (2.0 equiv., 0.344 mmol) and methanol (4 ml) were added. The mixture was electrolyzed at a constant current of 1 mA at room temperature for 12 h in a DC power supply. After 12 hours, there was no formation of desired product, which confirms that double bond is necessary for the ring opening of the cyclopropane.

4.4.9.4. Electrochemical reaction of (cyclopropylidenemethyl)cyclohexane (1w)

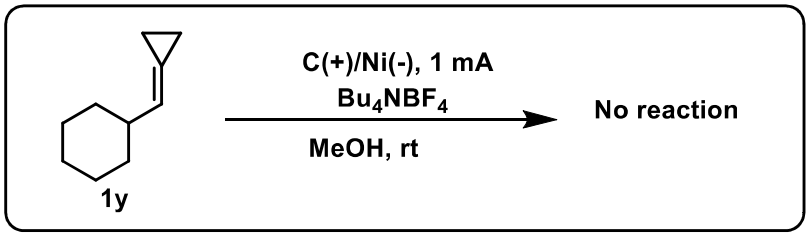

In an undivided cell equipped with magnetic bar and graphite as anode and nickel as cathode, **1y** (1.0 equiv., 0.220 mmol), Bu_4NBF_4 (2.0 equiv., 0.44 mmol) and methanol (4 ml) were added. The mixture was electrolyzed at a constant current of 1 mA at room temperature for 12 h in a DC power supply. After 12 hours, there was no formation of desired product, which confirms that aryl ring is also necessary for the ring opening of the cyclopropane.

4.4.9.5. Reaction of intermediate III under standard conditions

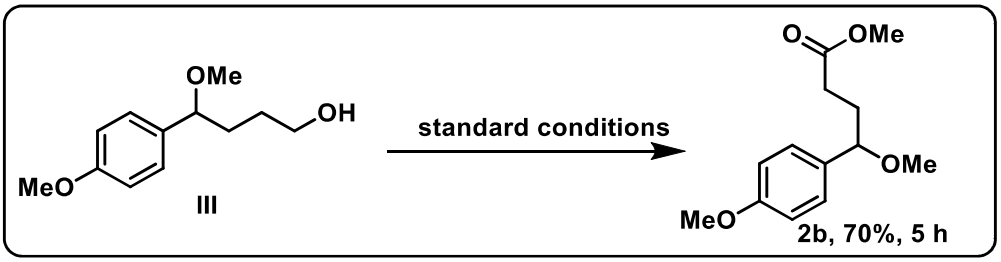

4-methoxy-4-(4-methoxyphenyl)butan-1-ol **III** (1.0 equiv., 0.142 mmol), electrolyte (2.0 equiv., 0.284 mmol) and solvent (4 ml) were taken in an undivided cell equipped with stir bar and graphite anode and nickel cathode. The

mixture was electrolyzed at a constant current of 1 mA at room temperature for 5 h. After the completion of reaction, the mixture was evaporated in vacuo and the crude was purified by silica gel column chromatography using 4 % ethyl acetate in hexane to get the methyl 4-methoxy-4-(4-methoxyphenyl)butanoate **(2b)** in 70% isolated yield.

4.4.9.6. D_2O Experiment

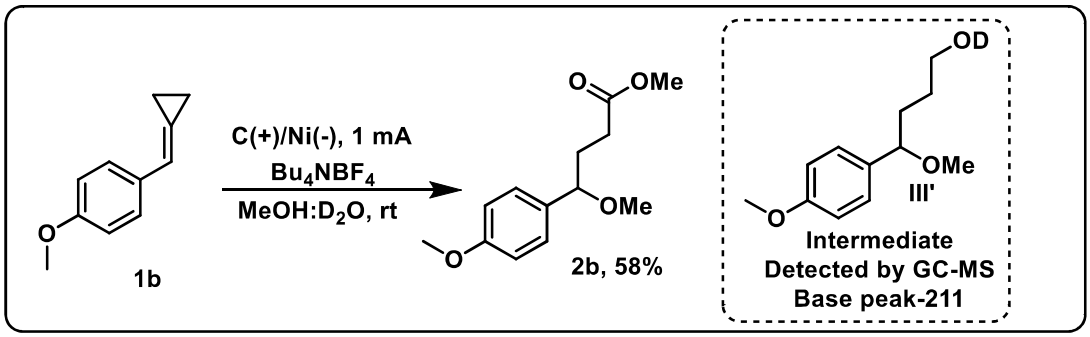

1-(cyclopropylidenemethyl)-4-methoxybenzene (**1b**, 1 equiv., 0.187 mmol), electrolyte (2.0 equiv., 0.374 mmol) and methanol: D_2O (3.5:0.5 ml) were taken in an undivided cell equipped with stir bar and graphite anode and nickel cathode. The mixture was electrolyzed at a constant current of 1 mA at room temperature for 7 h. After the completion of reaction, the mixture was evaporated in vacuo and the crude was purified by silica gel column chromatography using 3% ethyl acetate in hexane to get the methyl 4-methoxy-4-(4-methoxyphenyl)butanoate **(2b)** in 58% isolated yield. The intermediate **III'** was detected by GC-MS analysis which confirms that the ring opening of cyclopropane takes place by hydroxide ion (OD^-) from D_2O.

4.4.9.7. Electricity on/off experiment

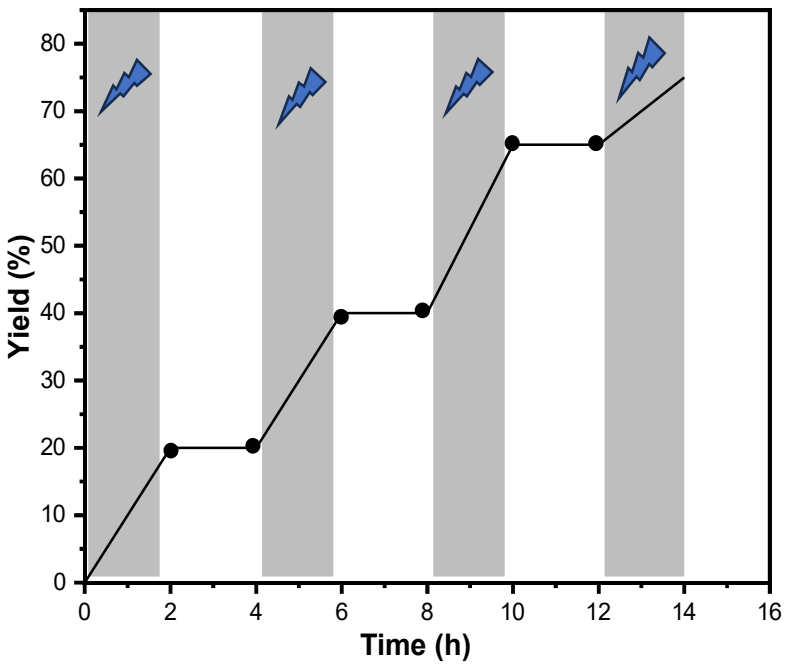

4.4.9.8. Cyclic voltammetry experiment

Cyclic voltammetry analysis was carried out in CH instrument electrochemical analyzer (CHI1210C). Samples were prepared in 5 ml vial with 0.01 M of substrate (1b), 0.01 M of (1y) and 0.1 M of Bu_4BF_4 in methanol (4ml). Measurements employed glassy carbon working electrode (Disk electrode), platinum wire counter electrode and a silver-silver chloride(non-aqueous) reference electrode. The sweep rate applied was 50 mV/s ranging from 0 to 3V. The oxidation potential of 1b was observed to be 1.55 V (vs Ag/AgCl), and 2.2 V (vs Ag/AgCl) for 1y. All the CV experiments were carried out in argon atmosphere in positive or oxidative direction and demonstrated as follow: (a) 0.1 M Bu_4NBF_4 (green) (b) 0.01 M 1b (red) (d) 0.01 M 1v (blue). Cyclic voltagrams are according to the IUPAC convention.

4.4.9.9. Calculation of Faradaic efficiency

The faradaic efficiency of the reaction was calculated using the following formula:

$$n = \frac{Q_{theo}}{Q_{exp}} * 100\%$$

$$Q_{theo} = Zp \cdot Np \cdot F = Z \cdot N \cdot Y \cdot F$$

$$Q_{exp} = I \cdot t = Z \cdot N \cdot F \cdot equiv.$$

$$n = \frac{Z \cdot N \cdot Y \cdot F}{Z \cdot N \cdot F \cdot equiv.} = \frac{Y}{equiv.}$$

n: Faradaic efficiency in percent [%], Q_{theo}: theoretical charge in Coulomb [C], Q_{exp}: experimental charge in Coulomb [C], equiv.: electron equivalents (F mol^{-1} or equiv.), z_P: Number of electrons per product [−], N_P: Number of mols of the product [mol], Y: yield in percent [%].

Here, Y = 76 % yield, equiv.= 2.5 F mol^{-1}

$$n = \frac{76}{2.09} = 30.4\%$$

4.4.9.10. Plausible mechanism (Pathway 2)

Like path 1, the reaction gets initiated by single-electron oxidation of **1b** to generate radical cationic species **I**, which undergoes nucleophilic attack of methoxide generated at cathode leading to the radical species **II**. Radical species **II** release the strain of cyclopropyl ring via homolytic cleavage of C-C bond to afford radical anionic species **III**. The anion was stabilized by hydrogen atom and the radical further undergoes one electron oxidation followed by nucleophilic attack of hydroxide ion to generate intermediate **IV** (detected by GC-MS and HRMS). After that, like pathway-1, intermediate **IV** undergoes sequential two-electron oxidation and loss of two water molecules to afford aldehyde intermediate **V**. Single electron oxidation of aldehyde **V** followed by loss of hydrogen atom led to the formation of stable acylium cation **VI**, which on further nucleophilic addition of methoxide delivered the desired product **2b**.

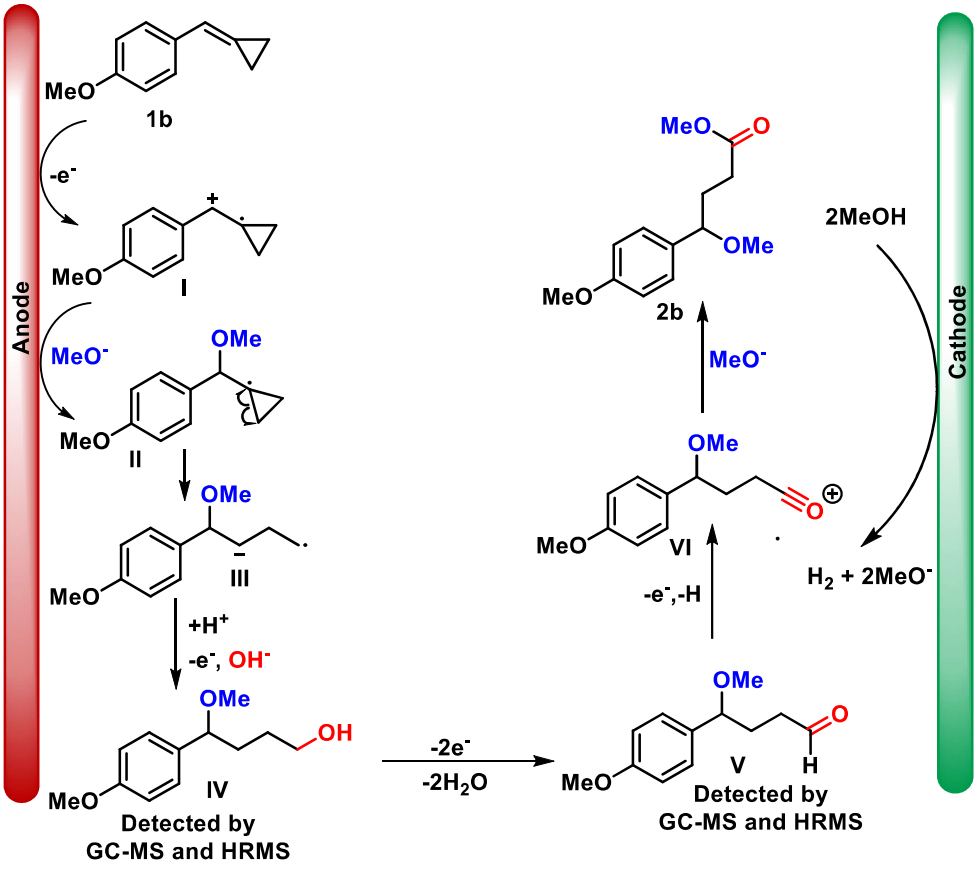

4.5. References

1. Salaun, J. *Chem. Rev*., **1989**, *89*, 1247-1270.

2. Wong, H. N. C.; Hon, M. Y.; Tse, C. W.; Yip, Y. C.; Tanko, J.; Hudlicky, T. *Chem. Rev.*, **1989**, 89, 165-198.

3. For reviews: (a) Liu, J.; Liu, R.; Wei, Y.; Shi, M. *Trends in Chemistry*, **2019**, *1*, 779-793; (b) Zhang, D.-H.; Tang, X.-Y.; Shi, M. *Acc. Chem. Res*., **2013**, *47*, 913-924; (c) Masarwa, A.; Marek, I. *Chem. Eur. J*., **2010**, *16*, 9712-9721; (d Lautens, M.; Klute, W.; Tam, W. *Chem. Rev*., **1996**, *96*, 49-92.

4. (a) Verdugo, F.; Villarino, L.; Durán, J.; Gulías, M.; Mascareñas, J. L.; López, F. *ACS Catal*., **2018**, *8*, 6100-6105; (b) Cui, S.; Zhang, Y.; Wu, Q. *Chem. Sci*., **2013**, *4*, 3421-3426; (c) Zhang, X.-Y.; Yang, S.; Wei, Y.; Shi, M. *Org. Biomol. Chem.,* **2018**, *16*, 6399-6404; (d) Liu, J.; Li, Q.; Wei, Y.; Shi, M. *Org. Lett*., **2020**, *22*, 2494-2499.

5. (a) Mazumder, S.; Shang, D.; Negru, D. E.; Baik, M.-H.; Evans, P. A. *J. Am. Chem. Soc*.,**2012**, *134*, 20569-20572; (b) Evans, P. A.; Burnie, A. J.; Negru, D. E. *Org. Lett*., **2014**, *16*, 4356-4359; (c) Kim, S.; Chung, Y. K. *Org. Lett*., **2014**, *16*, 4352-4355.

6. (a) Chen, K.; Tang, X.-Y.; Shi, M. *Chem. Commun*., **2016**, *52*, 1967-1970; (b) Bai, D.; Xu, T.; Ma, C.; Zheng, X.; Liu, B.; Xie, F.; Li, X. *ACS Catal*., **2018**, *8*, 4194-4200; (c) He, X.; Tang, Y.; Wang, Y.; Chen, J-B.; Xu, S.; Dou, J.; Li, Y. *Angew. Chem. Int. Ed*., **2019**, *58*, 10698-10702.

7. (a) Tsukada, N.; Shibuya, A.; Nakamura, I.; Yamamoto, Y. *J. Am. Chem. Soc*., **1997**, *119*, 8123-8124; (b) Shi, M.; Liu, L.-P.; Tang, J. *J. Am. Chem. Soc*., **2006**, *128*, 7430-7431; (c) Aïssa, C.; Fürstner, A. *J. Am. Chem. Soc*., **2007**, *129*, 14836-14837.

8. (a) Shi, M.; Xu, B. *Org. Lett*., **2002**, *4*, 2145-2148; (b) Shi, M.; Xu, B.; Huang, J.-W. *Org. Lett.*, **2004**, *6*, 1175-1178; (e) Scott, M. E.; Bethuel, Y.; Lautens, M. *J. Am. Chem. Soc*., **2007**, *129*, 1482-1483.

9. (a) Nakamura, I.; Nemoto, T.; Yamamoto, Y.; de Meijere, A. *Angew. Chem. Int. Ed*., **2006**, *45*, 5176-5179; (b) Tang, X.-Y.; Shi, M. *J. Org. Chem*., **2009**, *74*, 5983-5986; (c) Chen, K.; Sun, R.; Xu, Q.; Wei, Y.; Shi, M. *Org. Biomol. Chem.,* **2013**, *11*, 3949-3953.

10. For examples of radical initiated reactions of MCPs, see: (a) Xu, B.; Chen, Y.; Shi, M. *Tetrahedron Lett.* **2002**, *43*, 2781-2784; (b) Liu, L.-P.; Shi, M. *Chem. Commun.*, **2004**, *24*, 2878-2879; (c) Huang, J.-W.; Shi, M. *J. Org. Chem*., **2005**, *70*, 3859-3863.

11. Liu, Y.; Wang, Q.-L.; Chen, Z.; Zhou, Q.; Zhou, C.-S.; Xiong, B.-Q.; Zhang, P.-L.; Yang, C.-A.; Tang, K.-W. *Org. Biomol. Chem*., **2019**, *17*, 1365-1369.

12. Langler, R. F.; Raheja, R. K.; Schank, K.; Beck, H. *Helv. Chim. Acta*, **2001**, *84*, 1943-1951.

13. Fan, X.; Wang, Q.; Wei, Y.; Shi, M. *Chem. Commun.*, **2018**, *54*, 10503-10506.

14. Liu, J.; Wei, Y.; Shi, M. *Org. Chem. Front*., **2021**, *8*, 94-100.

15. Yan, M.; Kawamata, Y.; Baran, P. S. *Chem. Rev*., **2017**, *117*,13230-13319; (b) Jiang, Y.; Xu, K.; Zeng, C. *Chem. Rev*., **2018**, *118*, 4485-4540; (c) Sauermann, N.; Meyer, T. H.; Qiu, Y.; Ackermann, L. *ACS Catal*., **2018**, *8*, 7086-7106; (d) Yuan, Y.; Lei, A. *Nat. Commun*., **2020**, *11*, 802.

16. (a) Taily, I. M.; Saha, D.; Banerjee, P. *Org. Lett*., **2022**, *24*, 2310-2314; (b) Kumar, R.; Taily, I. M.; Banerjee, P. *Chem. Commun*., **2023**, *59*, 310-313; (c) Gao, X.; Wang, P.; Zeng, L.; Tang, S.; Lei, A. *J. Am. Chem. Soc.*, **2018**, *140*, 4195-4199; (d) Saha, D.; Taily, I. M.; Banerjee, N.; Banerjee, P. *Chem. Commun*., **2022**, *58*, 5459-5462;

17. Zhan, L.; Gao, L.; Pan, Y.; He, M.; Ma, X.; Mo, Z. *Adv. Synth. Catal*. **2023**, *365*, 3295-3300.

18. (a) Wang, D.; Wang, P.; Wang, S.; Chen, Y.-H.; Zhang, H.; Lei, A. *Nat. Commun*., **2019**, *10*, 1-8; (b) Smeyne, D.; Verboom, K.; Bryan, M.; LoBue, J.; Shaikh, A. *Tetrahedron Lett*., **2021**, *68*, 152898-152903.

19. Dabbagh, H. A.; Zamani, M.; Fakhraee, S. *Res Chem Intermed*, **2013**, 39, 2011-2033.

4.6. Spectra of starting materials

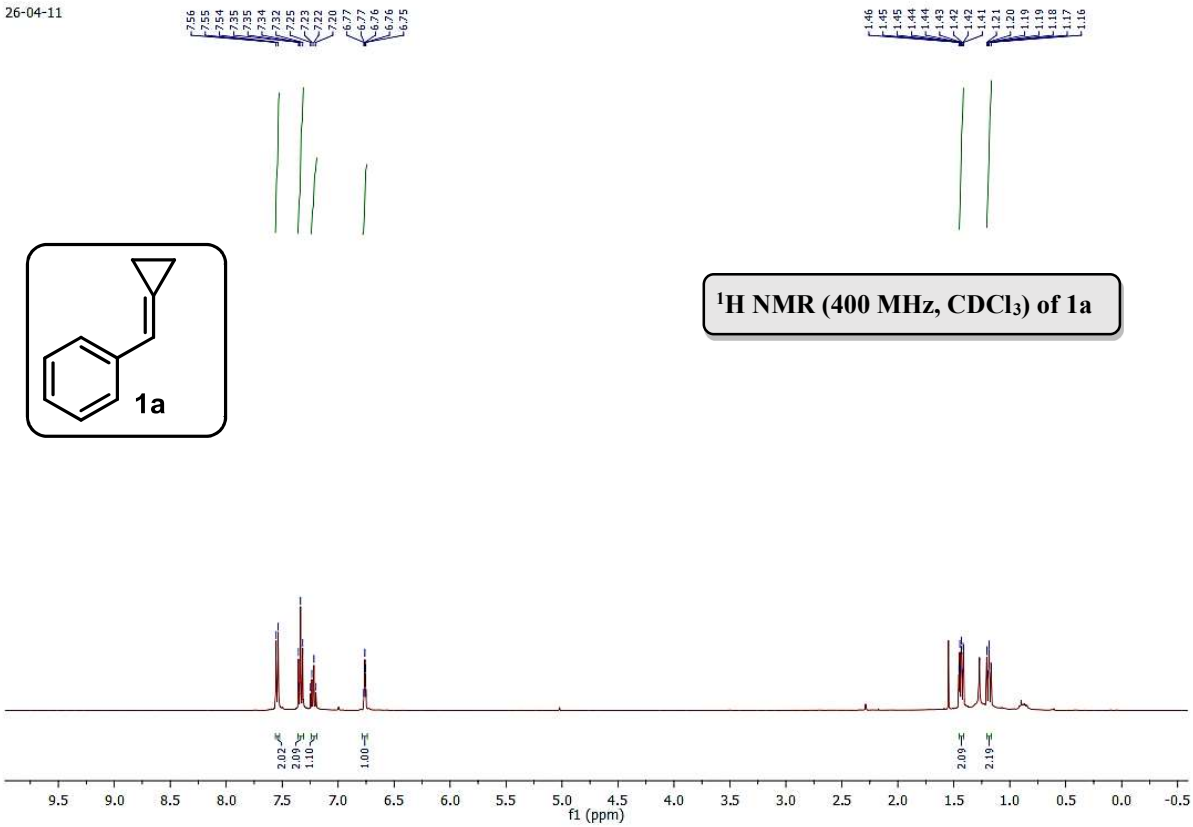

^{1}H NMR (400 MHz, $CDCl_3$) of 1a

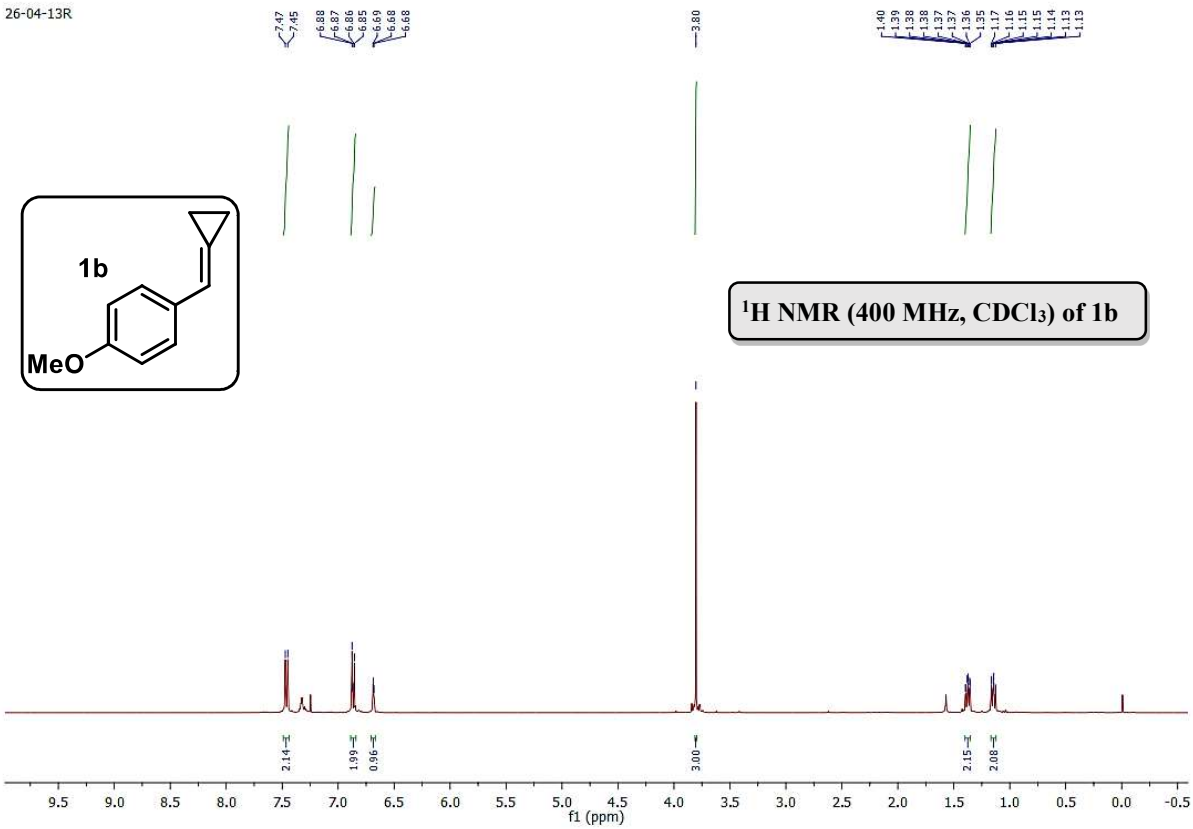

^{1}H NMR (400 MHz, $CDCl_3$) of 1b

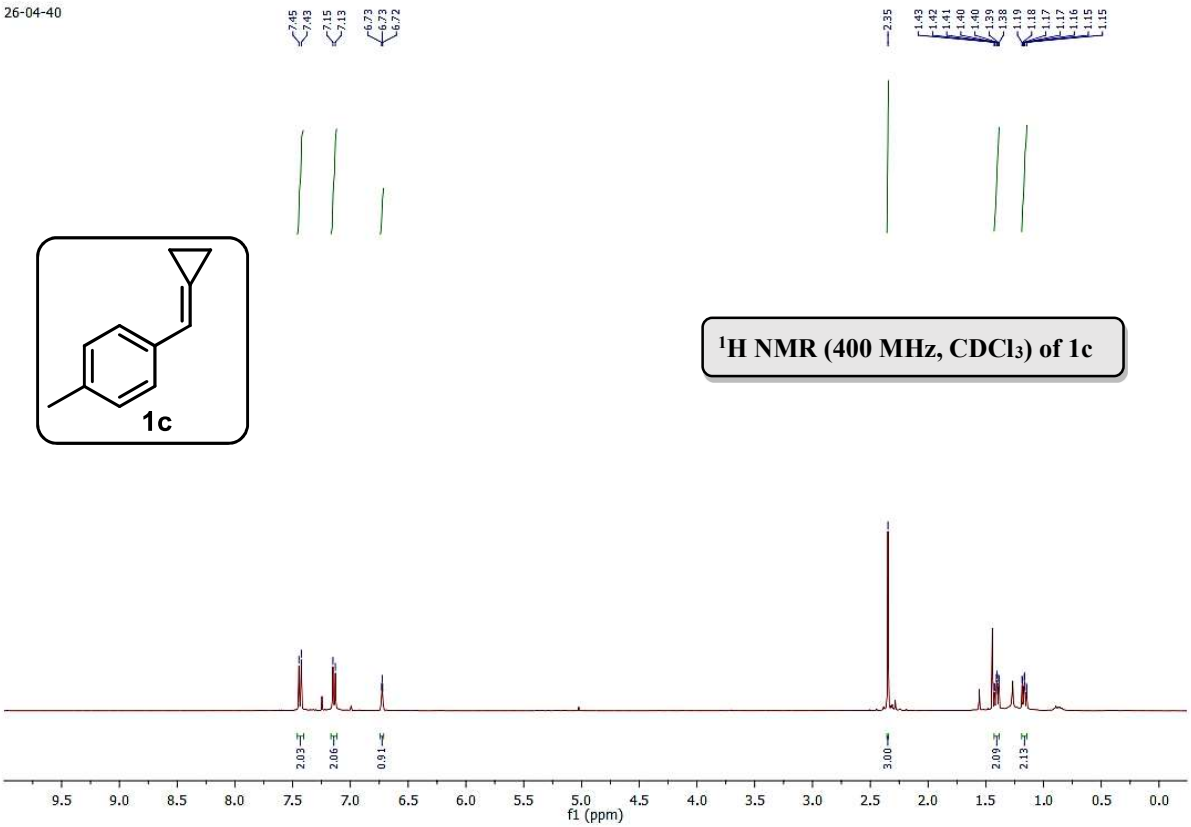

^{1}H NMR (400 MHz, $CDCl_3$) of 1c

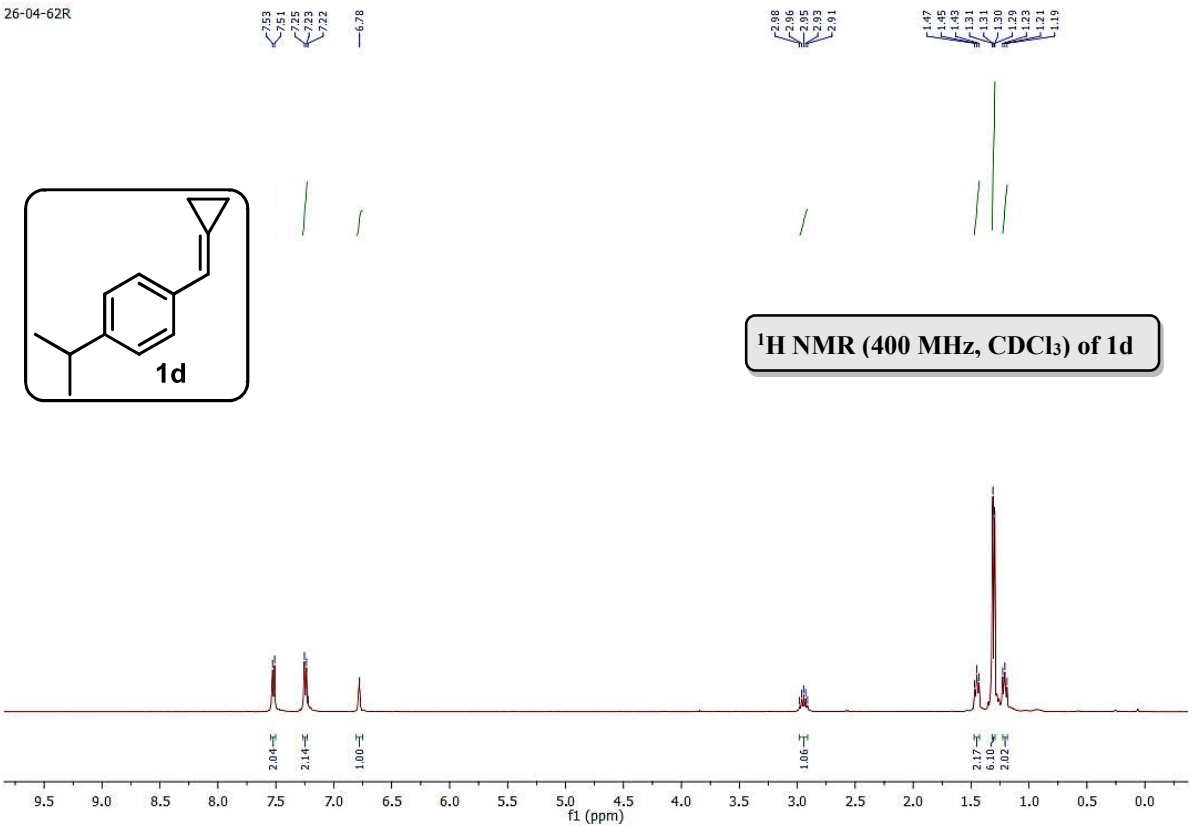

^{1}H NMR (400 MHz, $CDCl_3$) of 1d

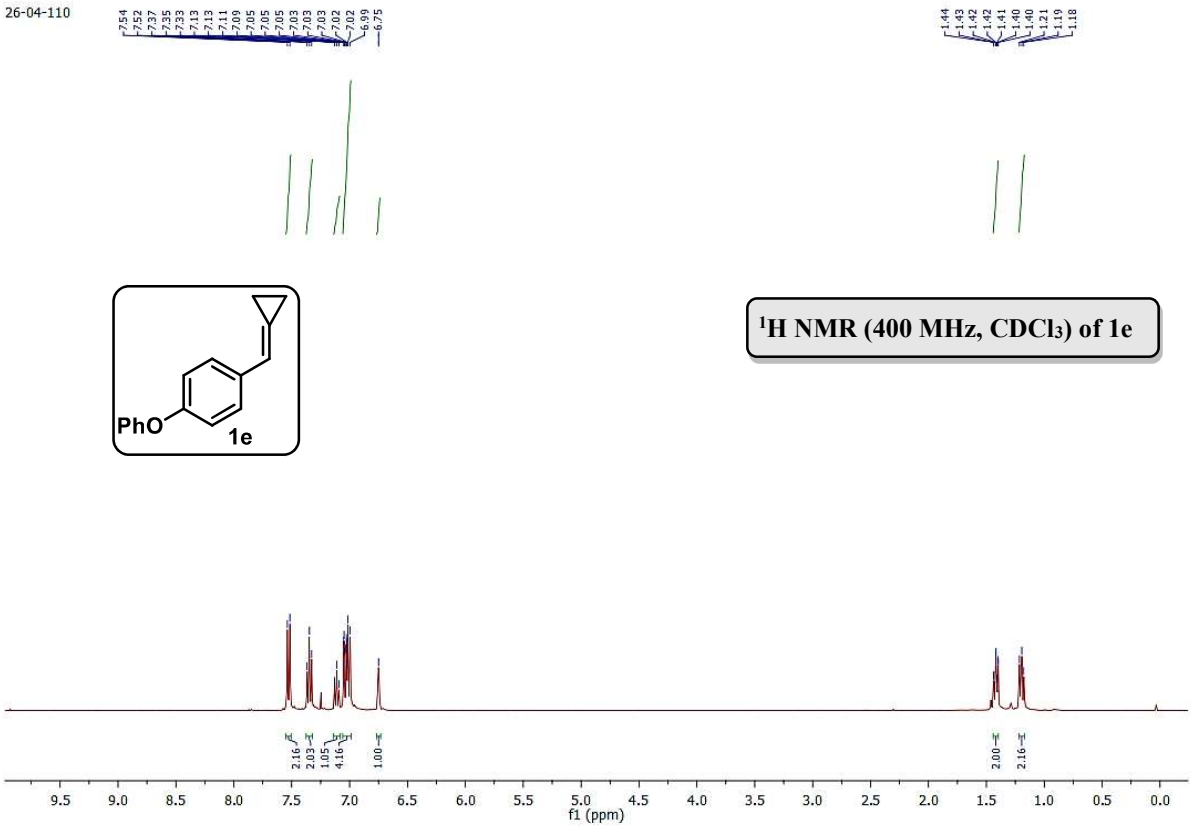

^{1}H NMR (400 MHz, $CDCl_3$) of 1e

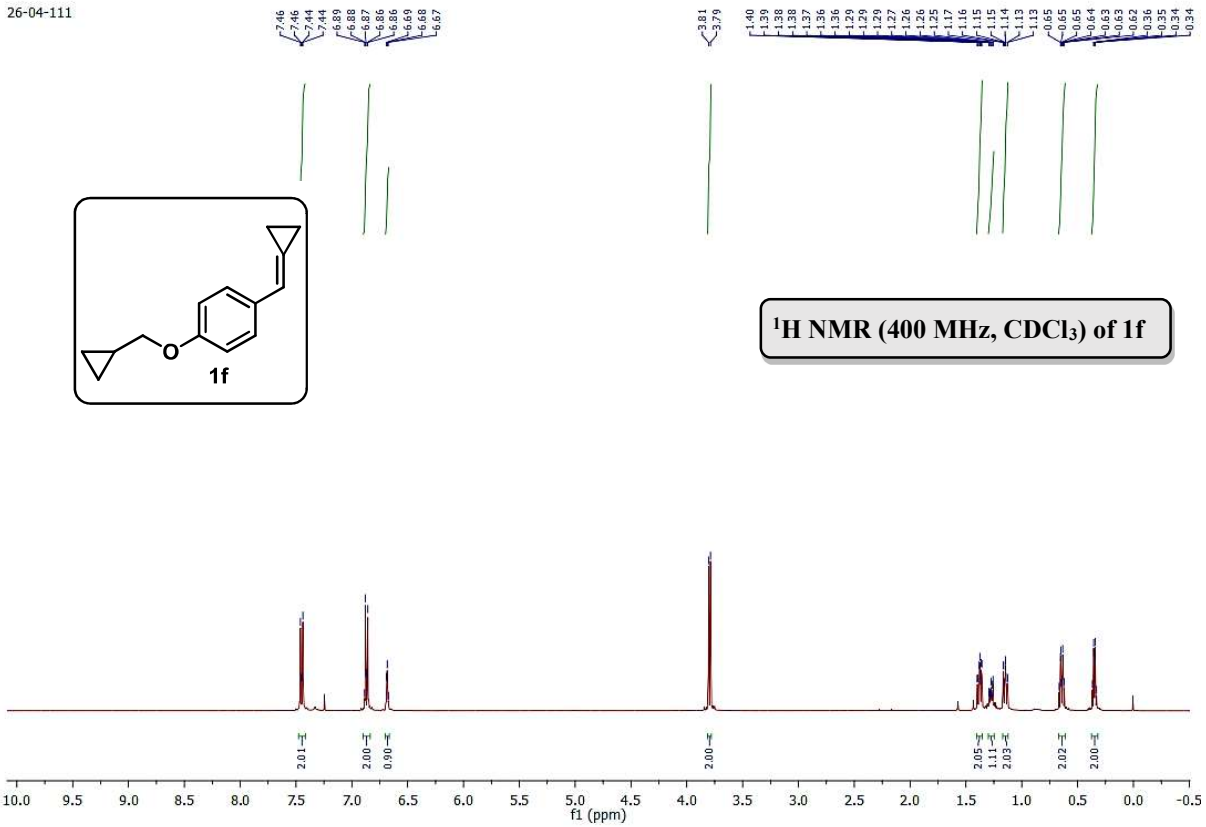

^{1}H NMR (400 MHz, $CDCl_3$) of 1f

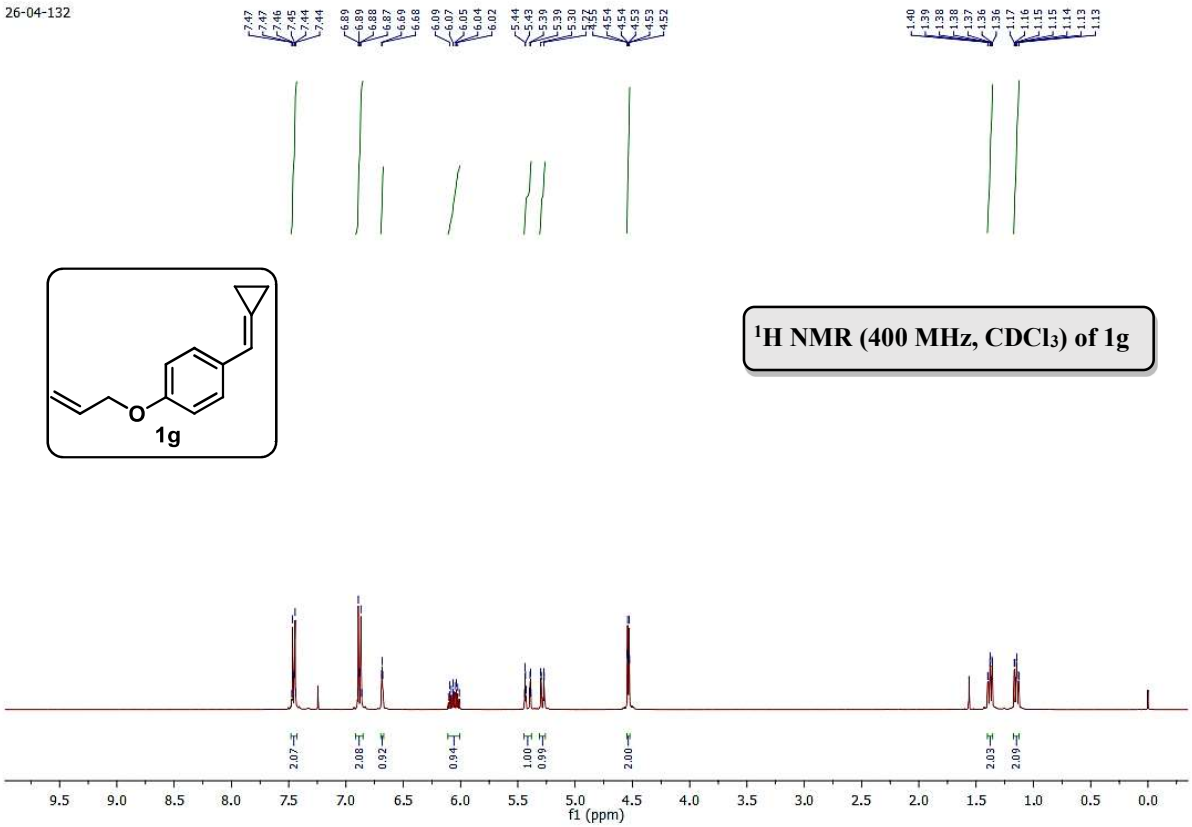

^{1}H NMR (400 MHz, $CDCl_3$) of 1g

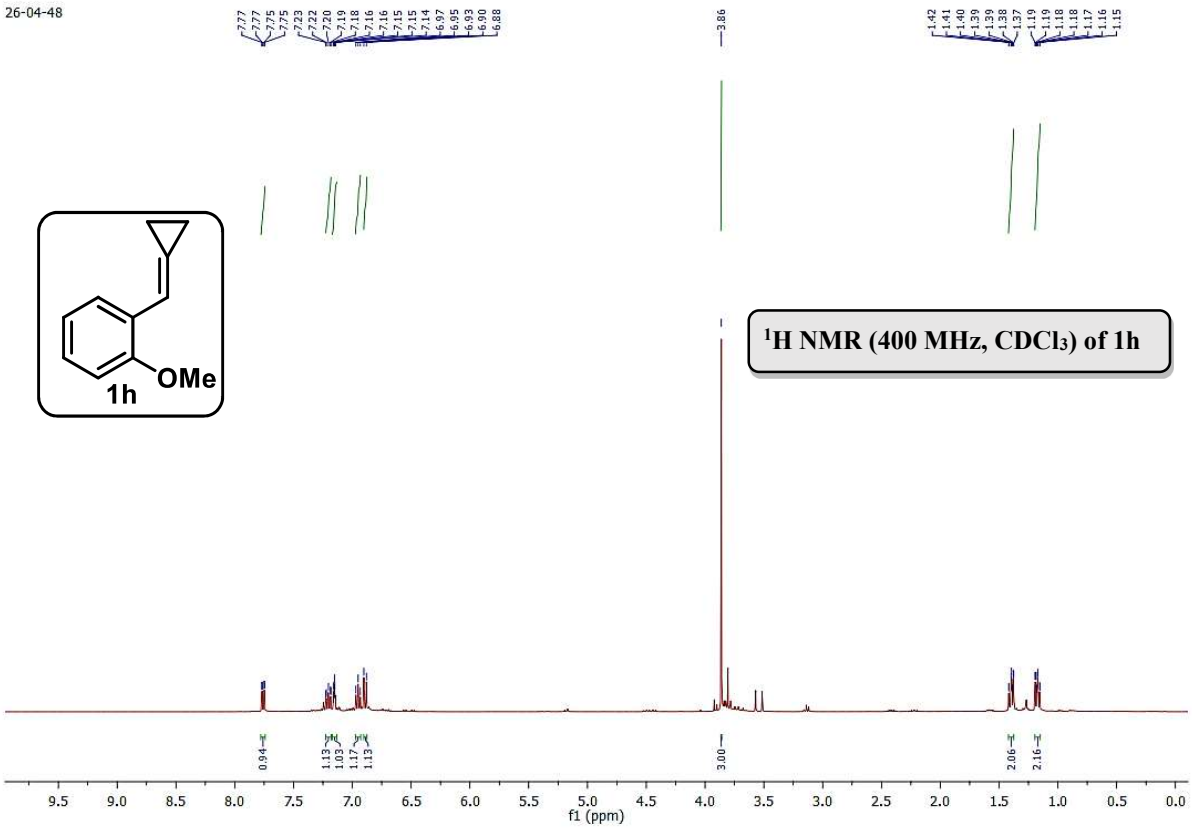

^{1}H NMR (400 MHz, $CDCl_3$) of 1h

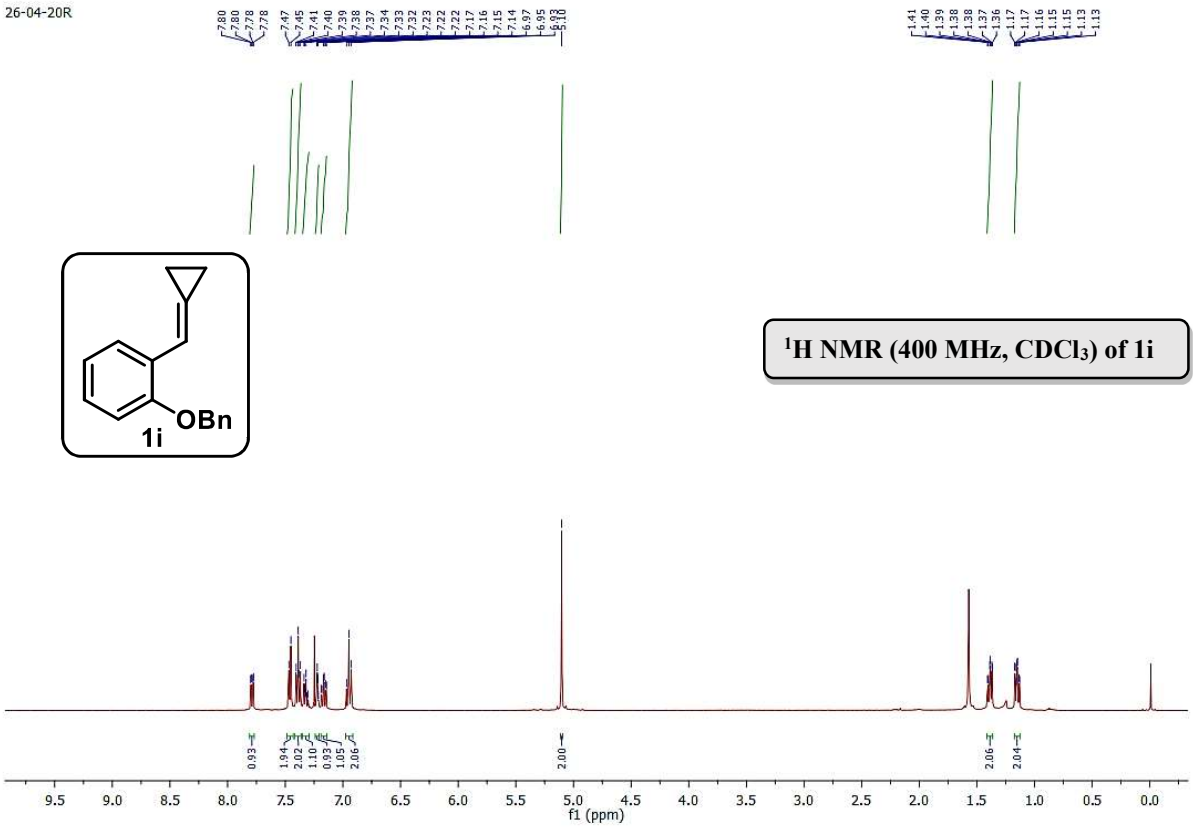

^{1}H NMR (400 MHz, $CDCl_3$) of 1i

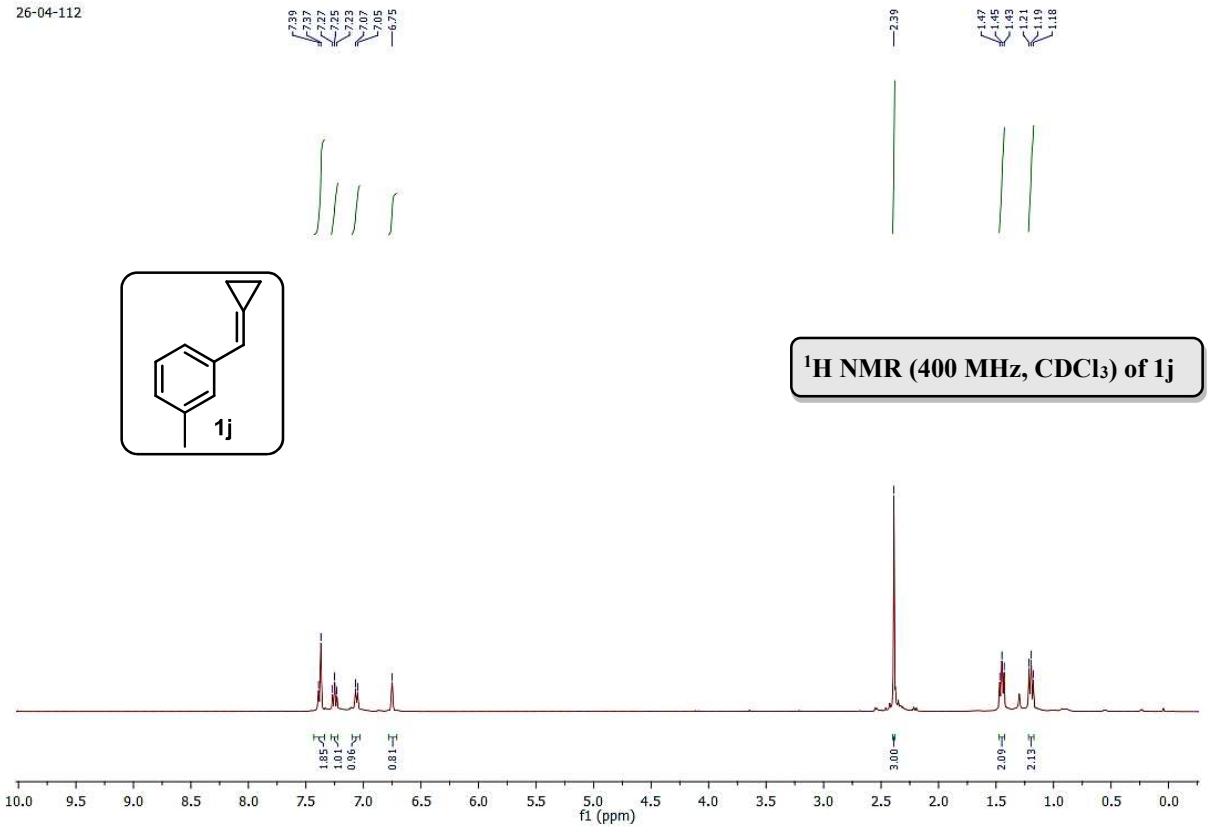

^{1}H NMR (400 MHz, $CDCl_3$) of 1j

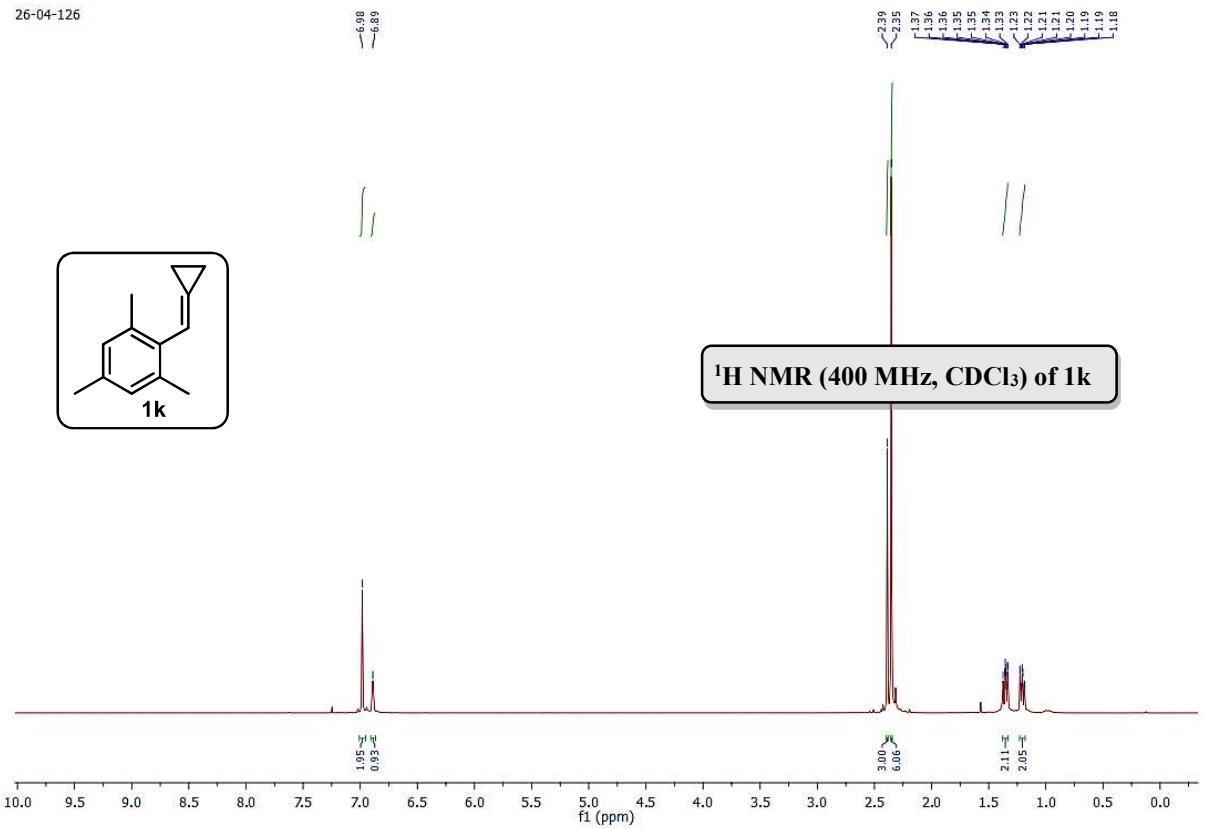

^{1}H NMR (400 MHz, $CDCl_3$) of 1k

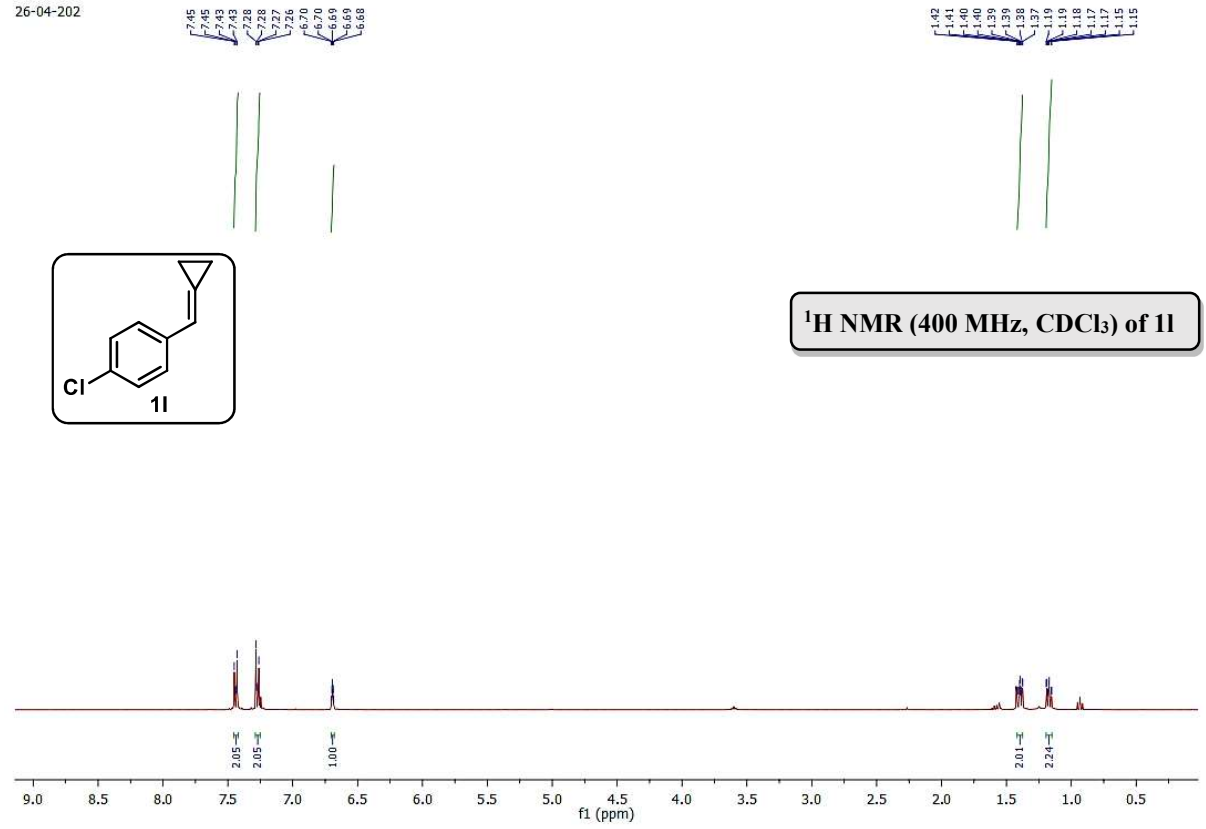

^{1}H NMR (400 MHz, $CDCl_3$) of 1l

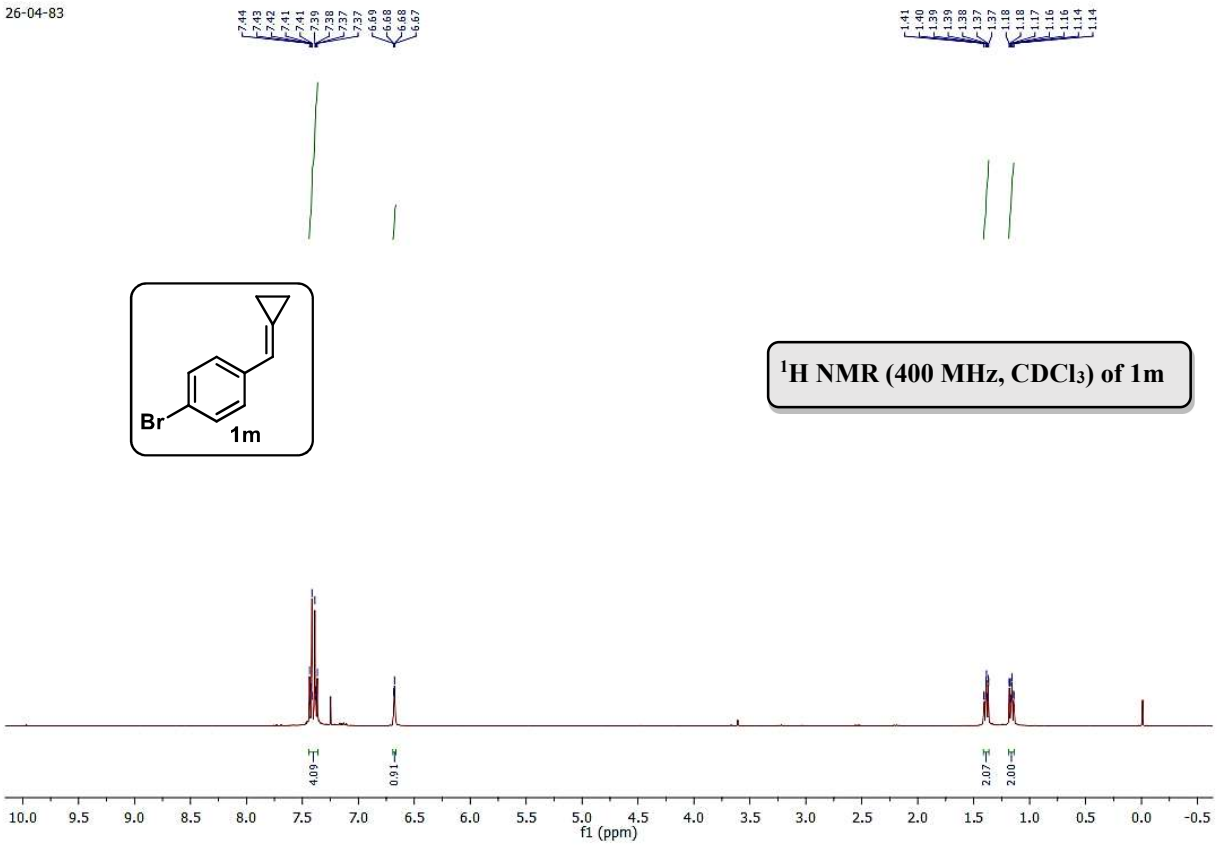

^{1}H NMR (400 MHz, $CDCl_3$) of 1m

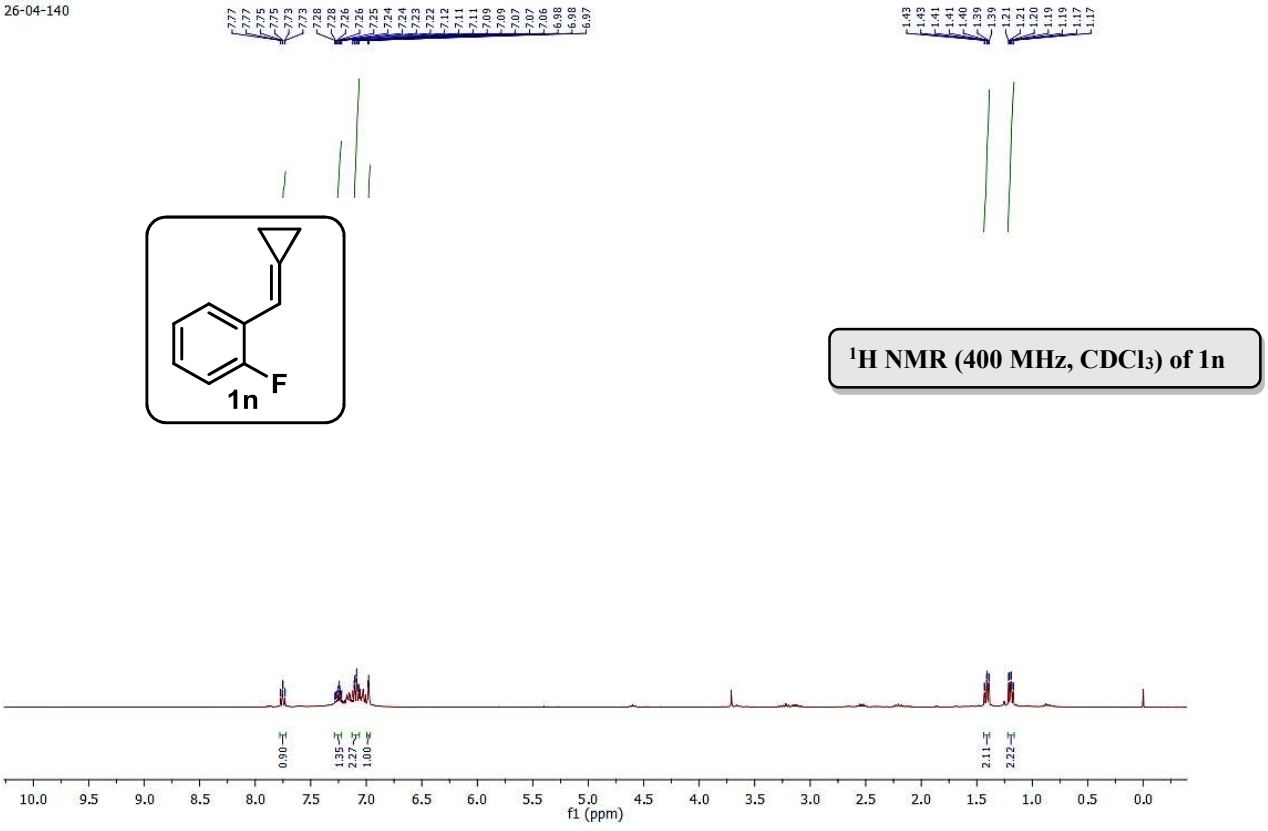

^{1}H NMR (400 MHz, $CDCl_3$) of 1n

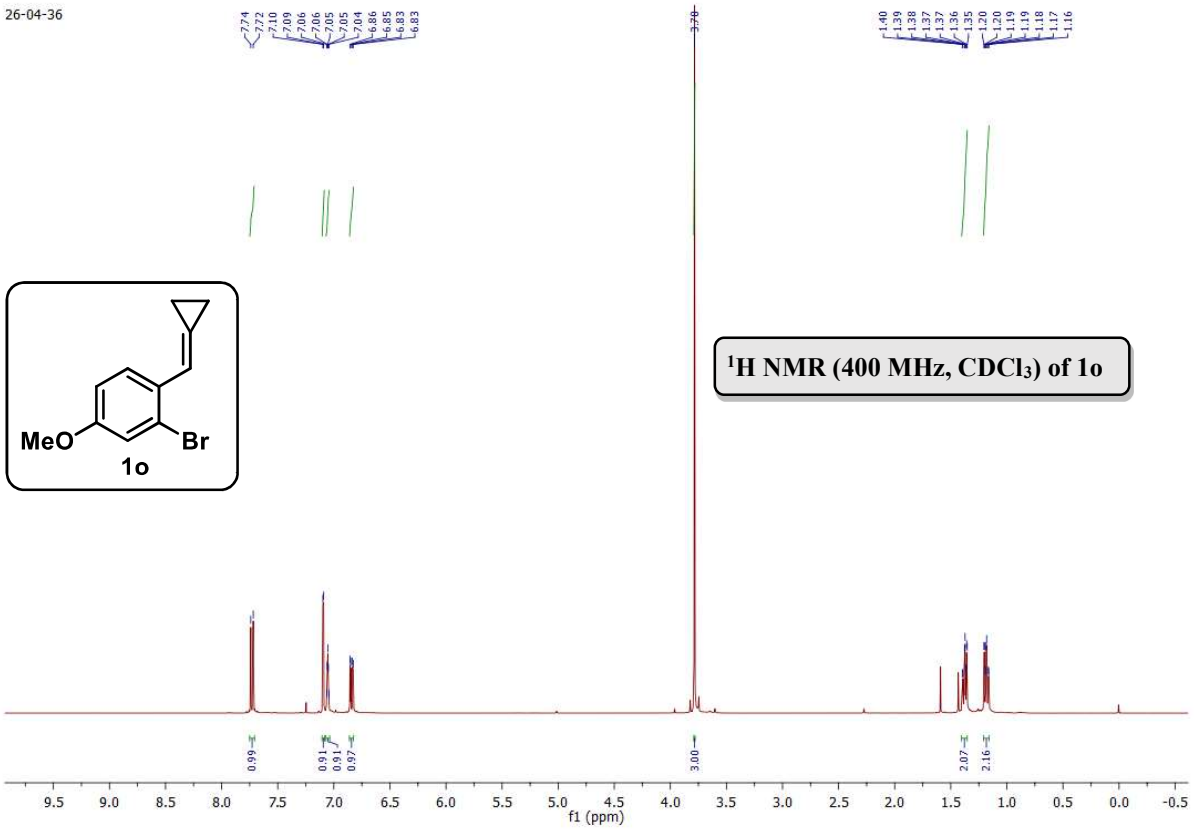

^{1}H NMR (400 MHz, $CDCl_3$) of 1o

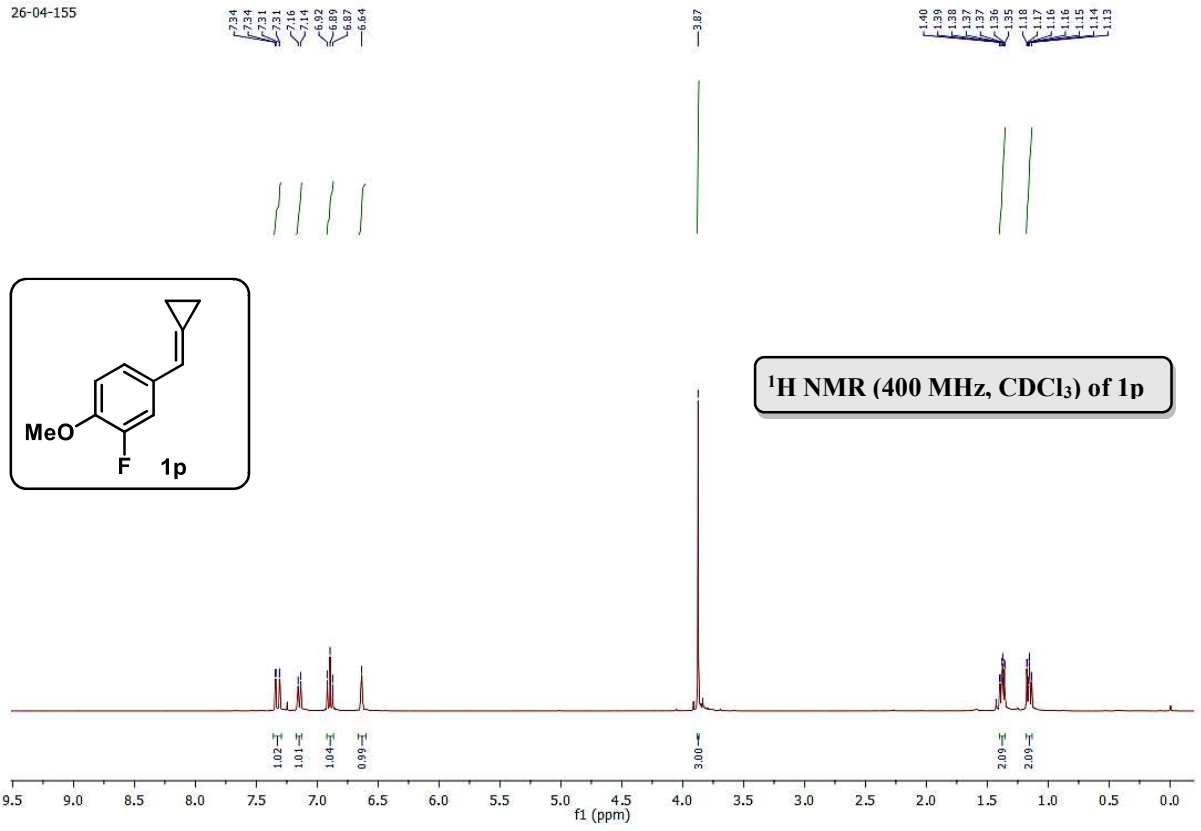

^{1}H NMR (400 MHz, $CDCl_3$) of 1p

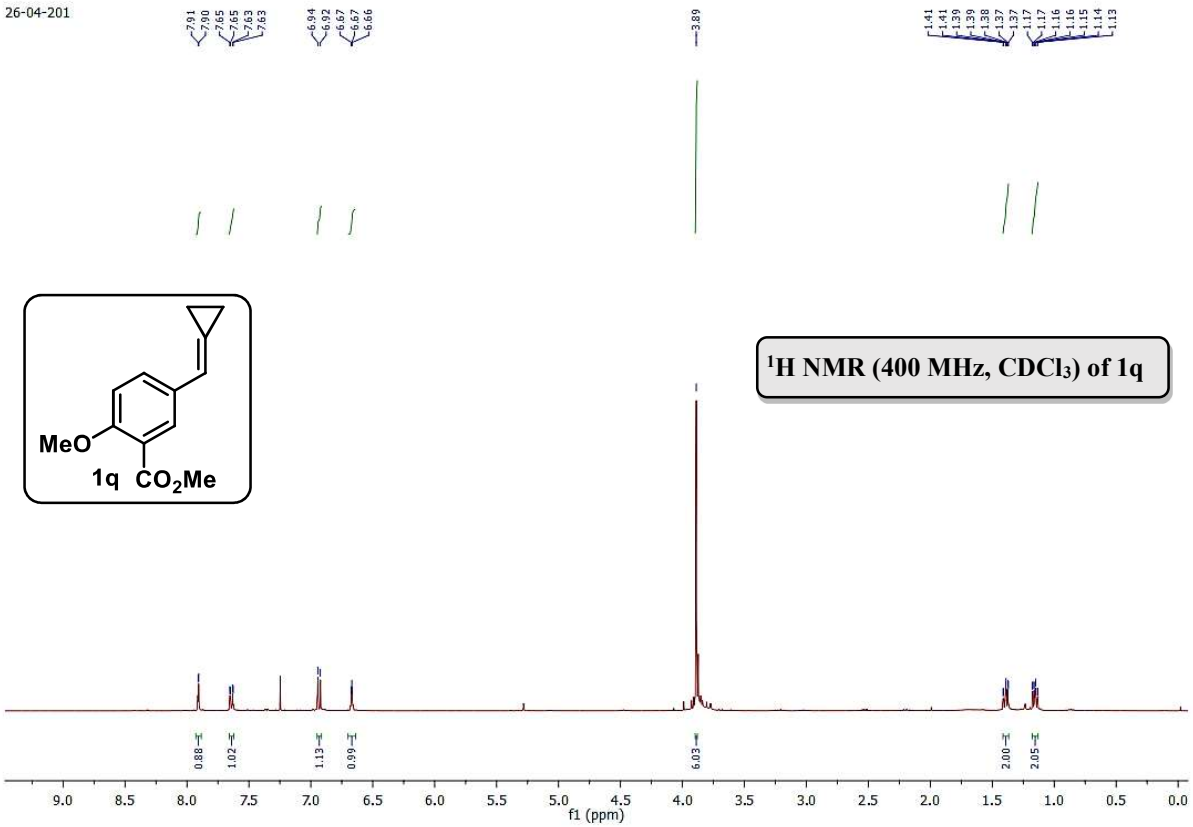

^{1}H NMR (400 MHz, $CDCl_3$) of 1q

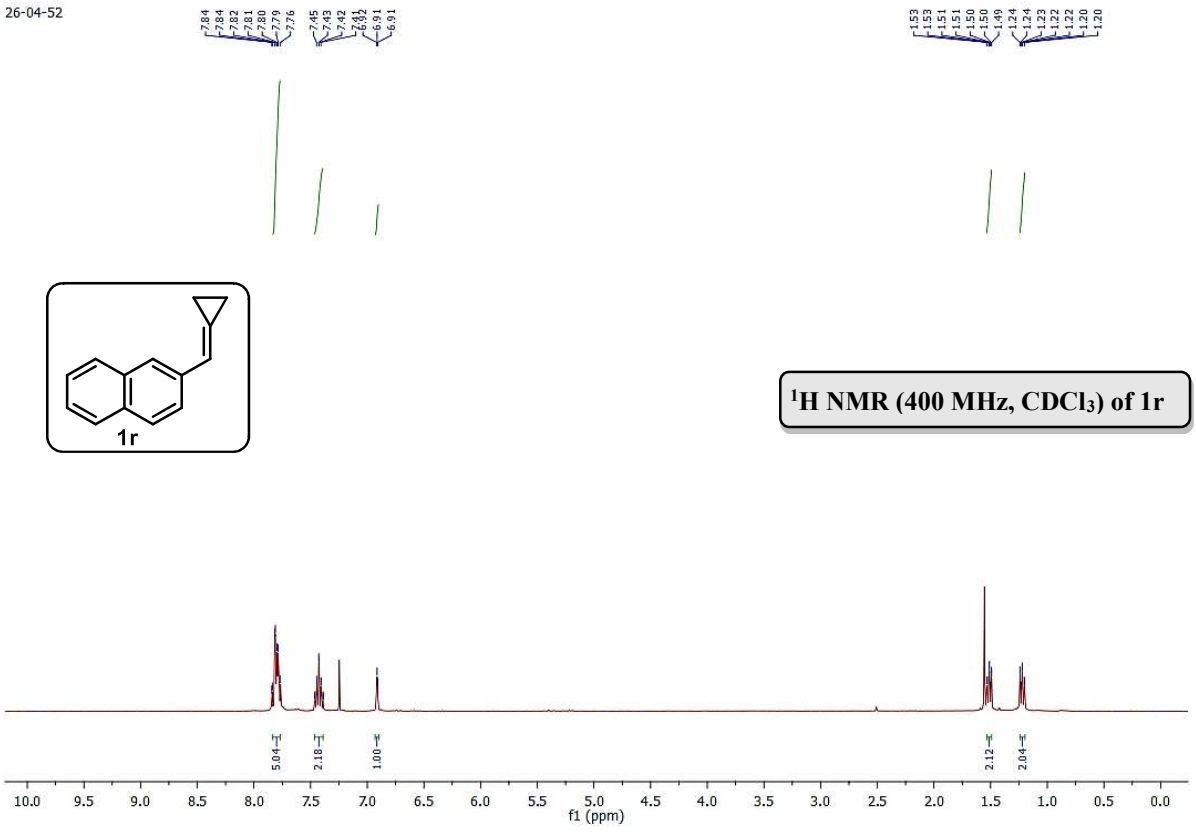

^{1}H NMR (400 MHz, $CDCl_3$) of 1r

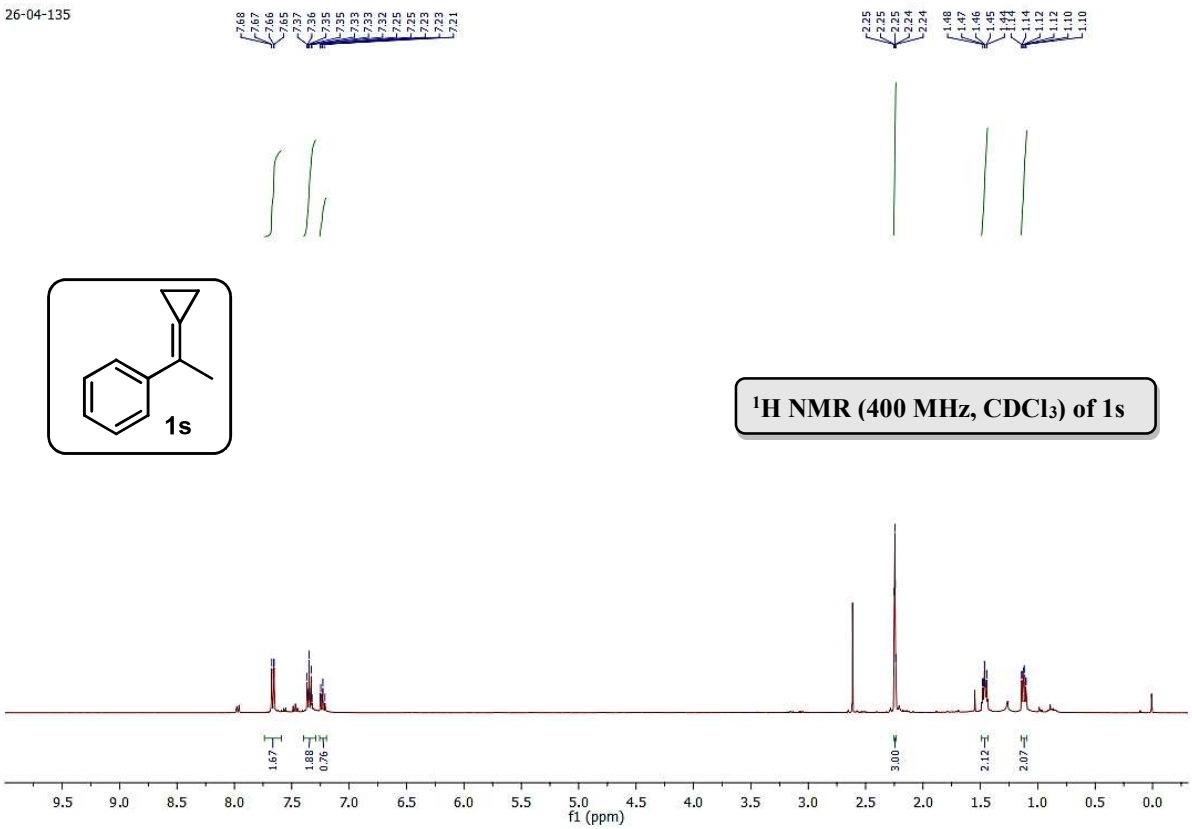

^{1}H NMR (400 MHz, $CDCl_3$) of 1s

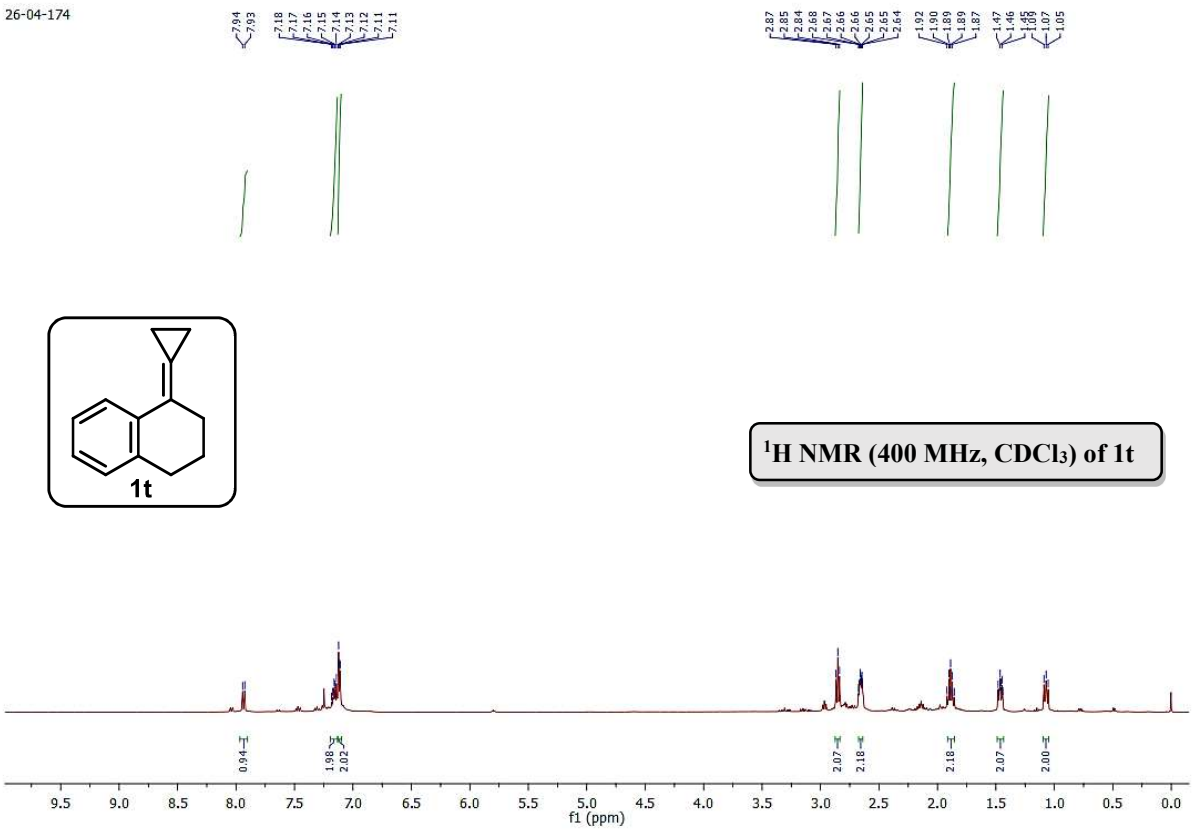

^{1}H NMR (400 MHz, $CDCl_3$) of 1t

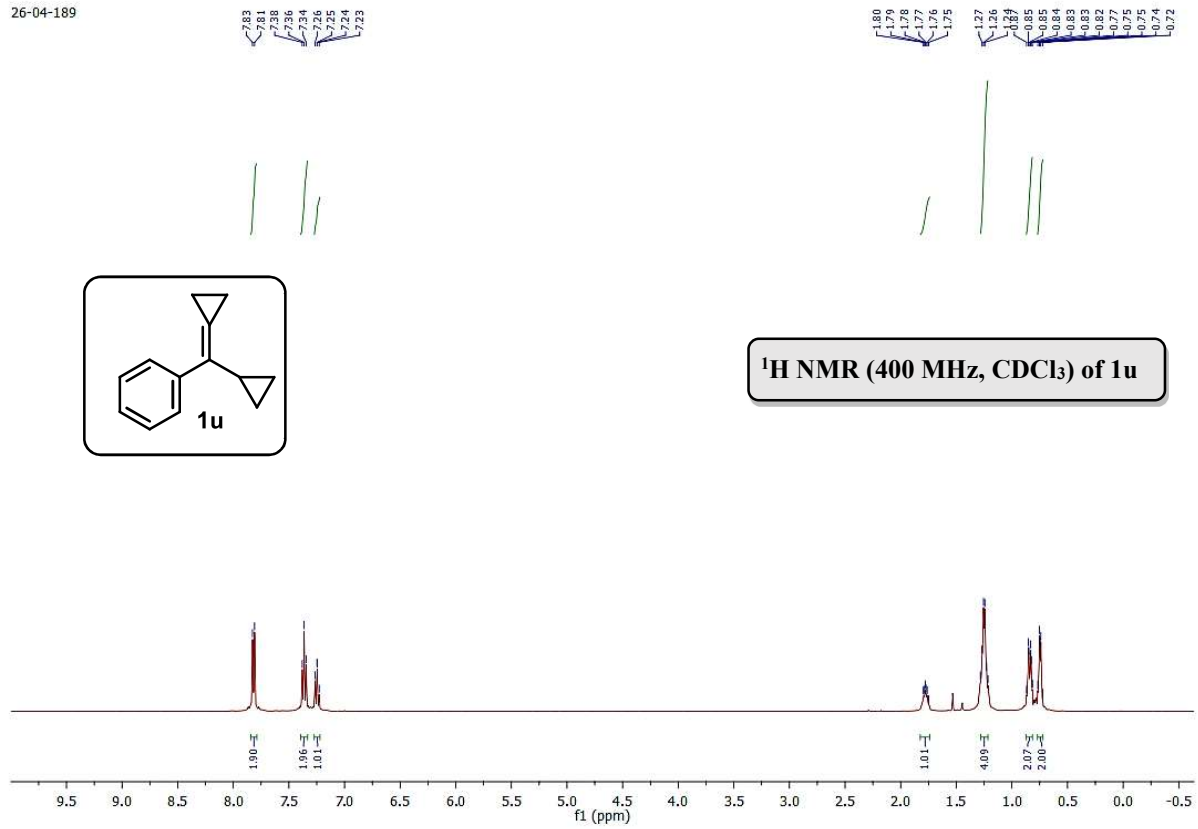
26-04-189
1u
1H NMR (400 MHz, CDCl3) of 1u
f1 (ppm)

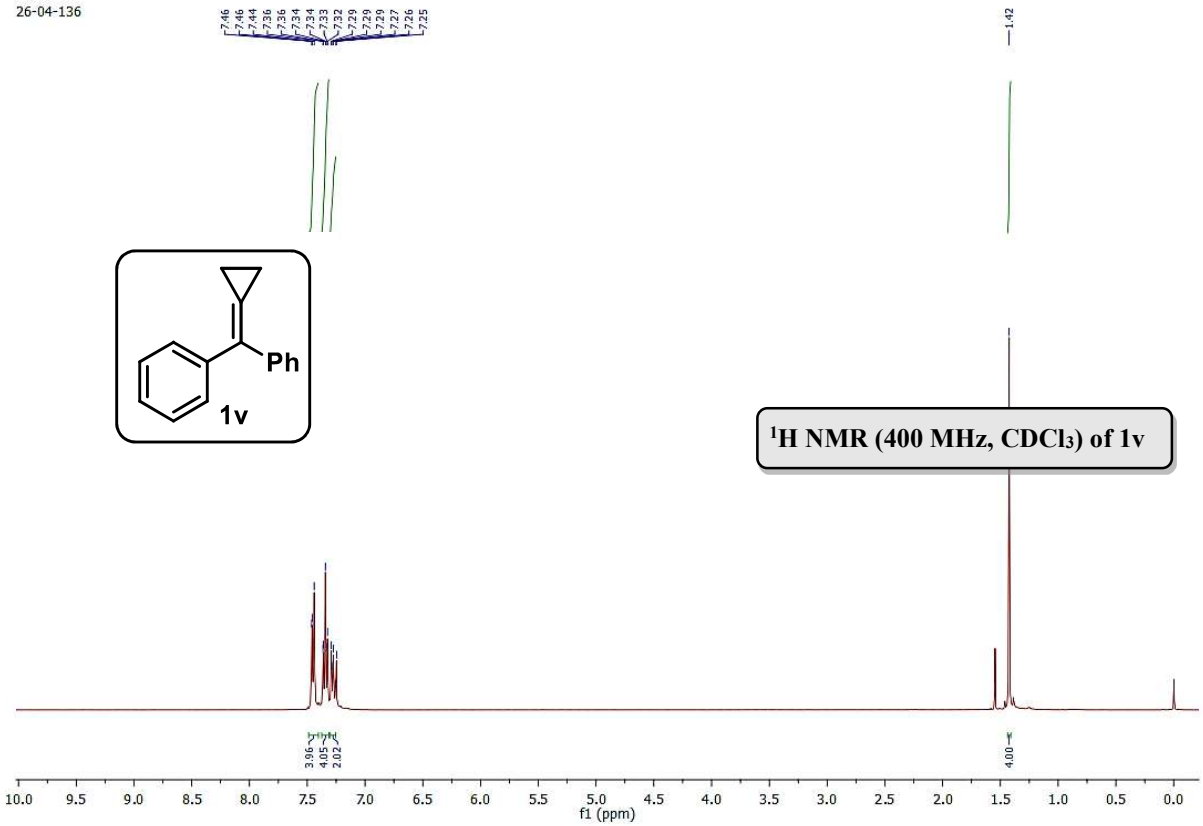
26-04-136
Ph
1v
1H NMR (400 MHz, CDCl3) of 1v
f1 (ppm)

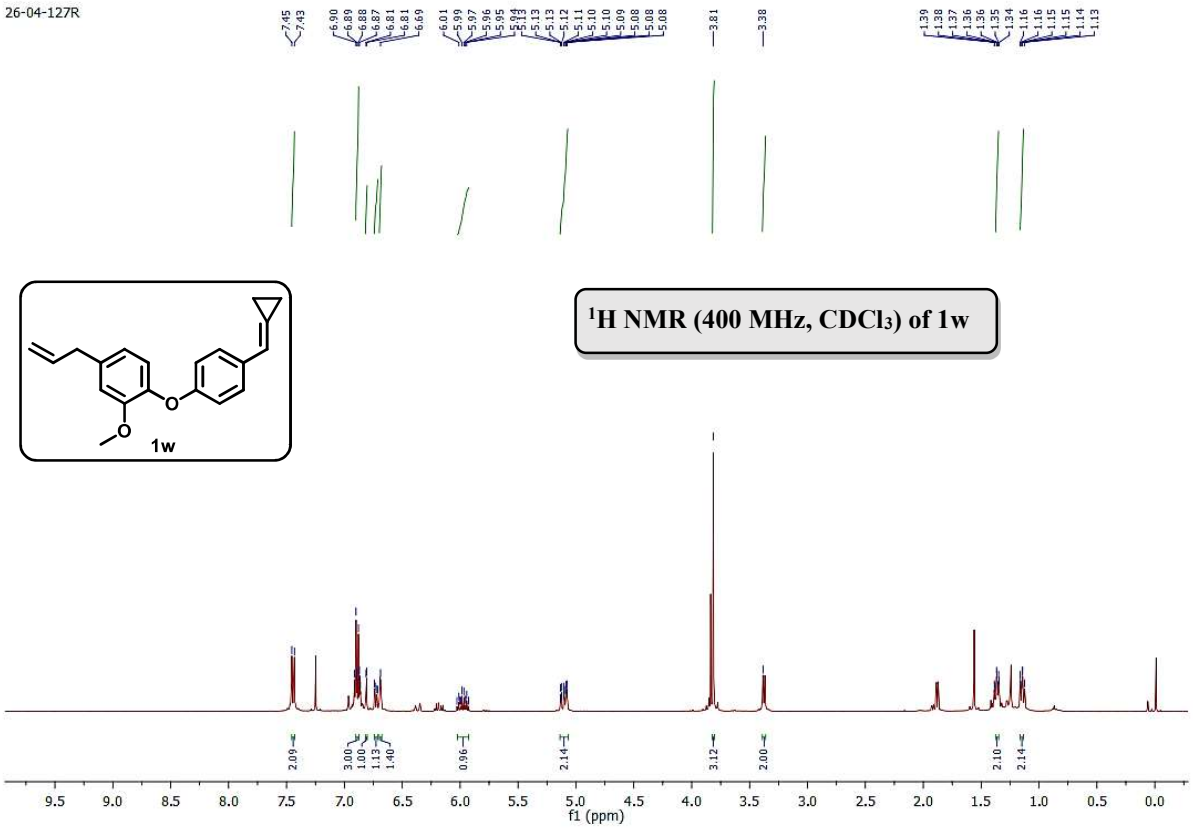

^{1}H NMR (400 MHz, $CDCl_3$) of 1w

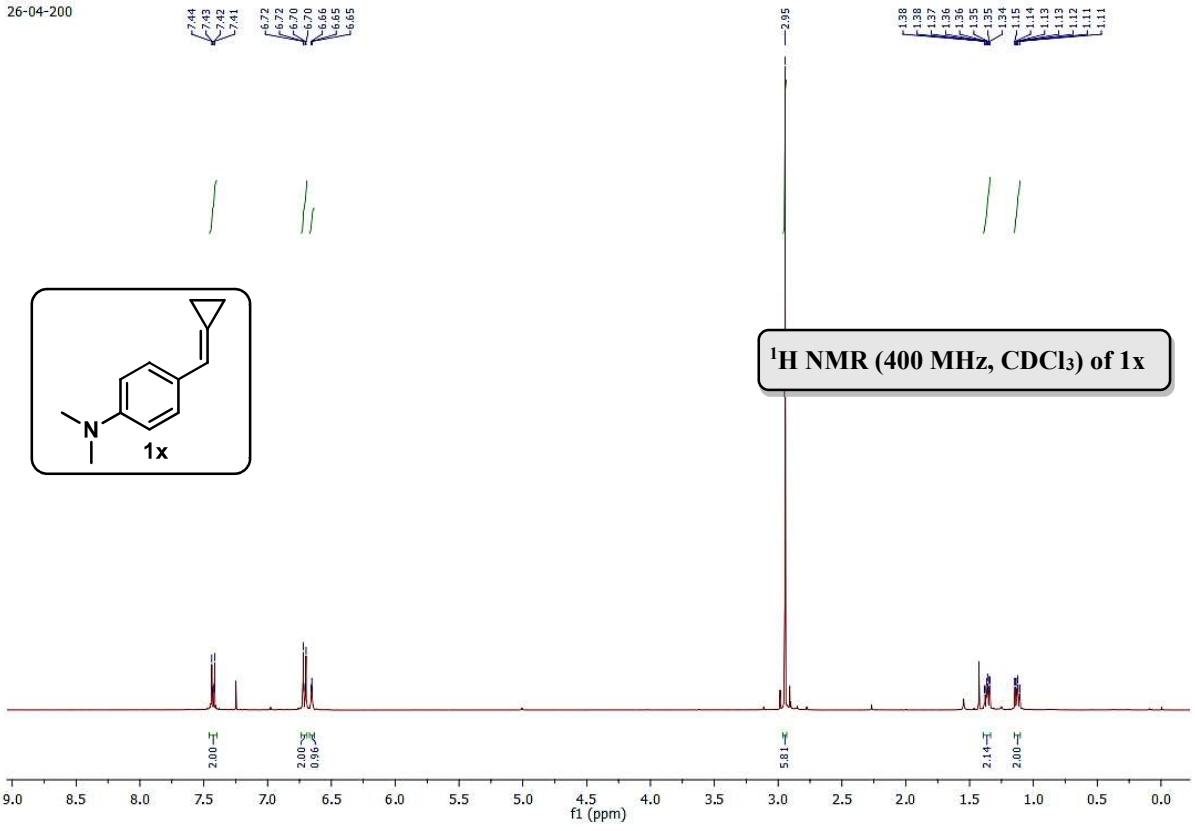

^{1}H NMR (400 MHz, $CDCl_3$) of 1x

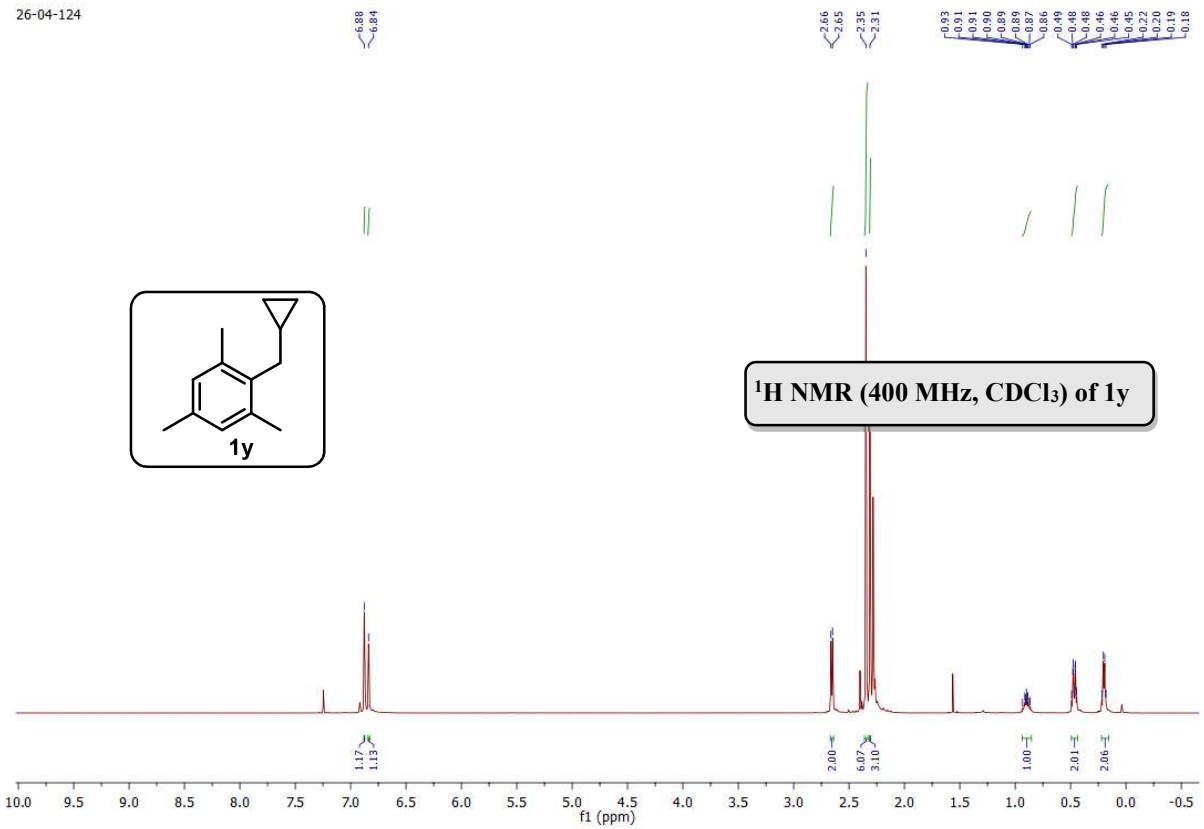

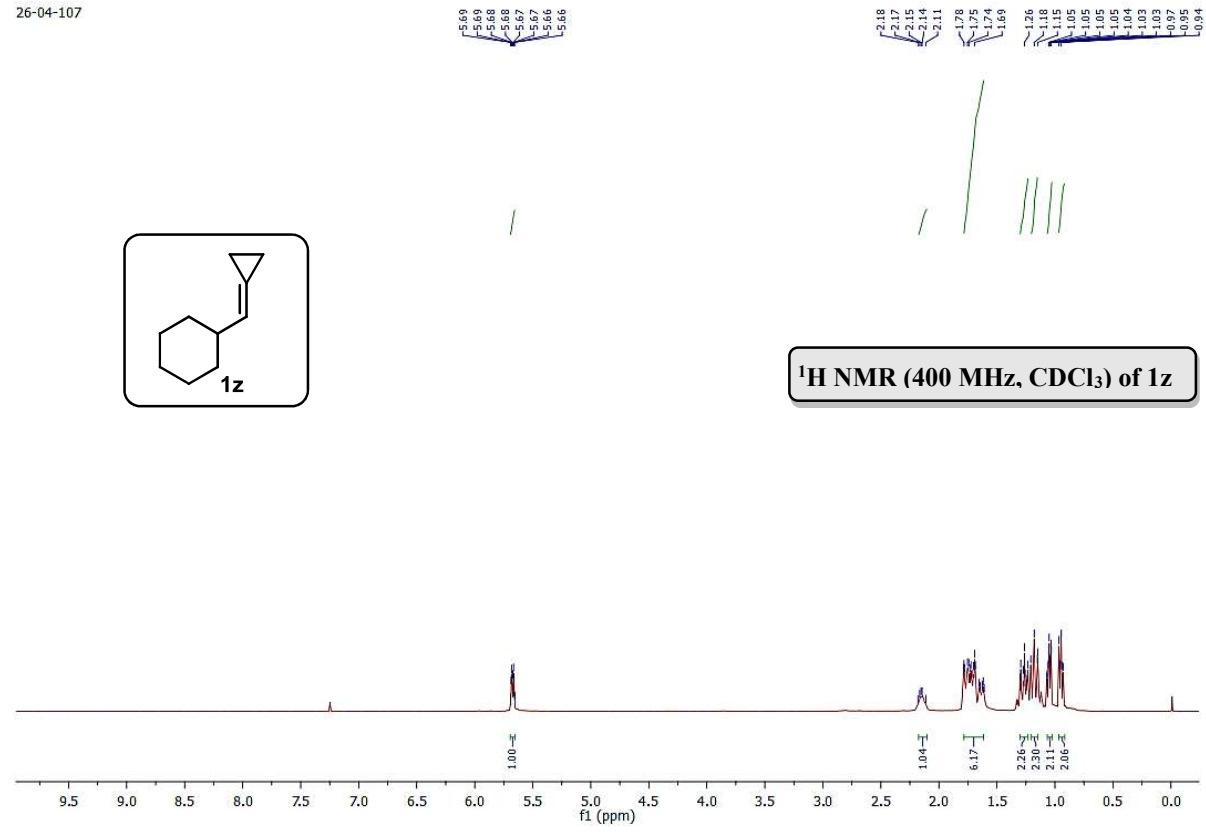

4.7. Spectra of final compounds

^{1}H NMR (400 MHz, $CDCl_3$) of 2a

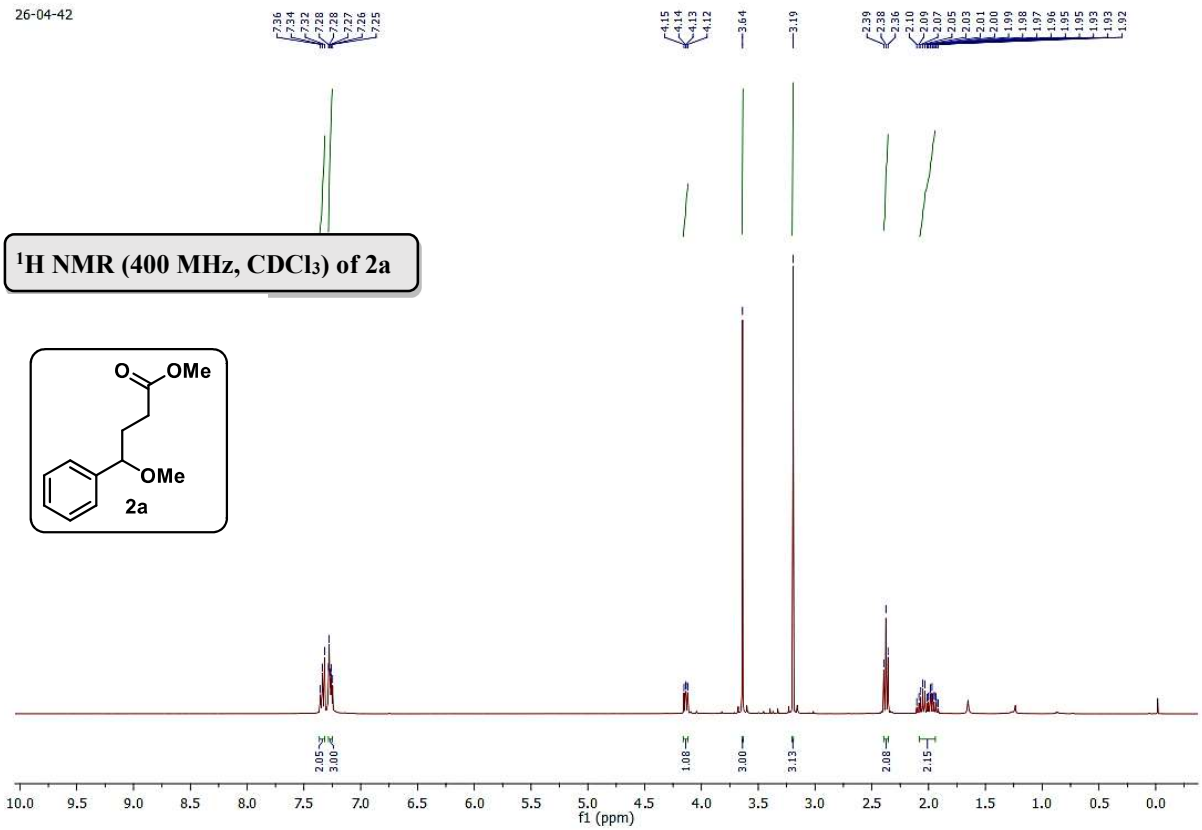

$^{13}C\{^{1}H\}$ NMR (100 MHz, $CDCl_3$) of 2a

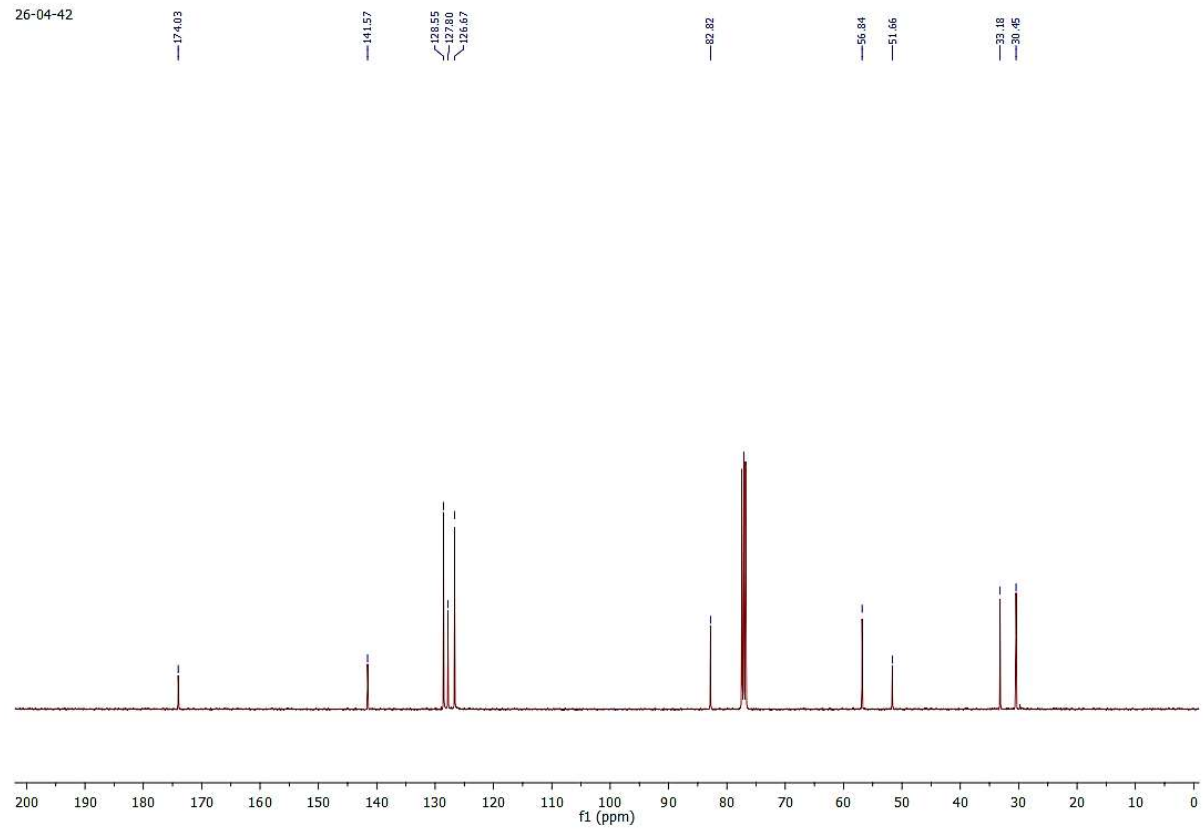

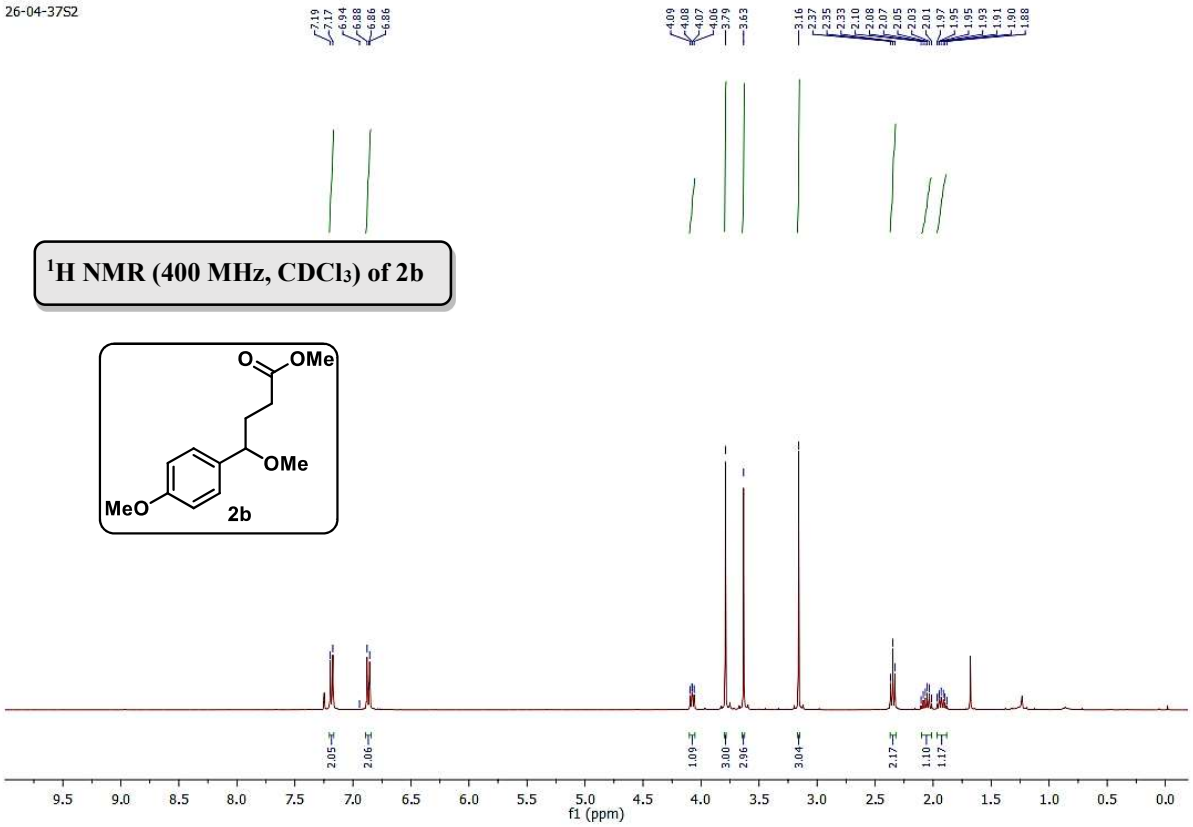

^{1}H NMR (400 MHz, $CDCl_3$) of 2b

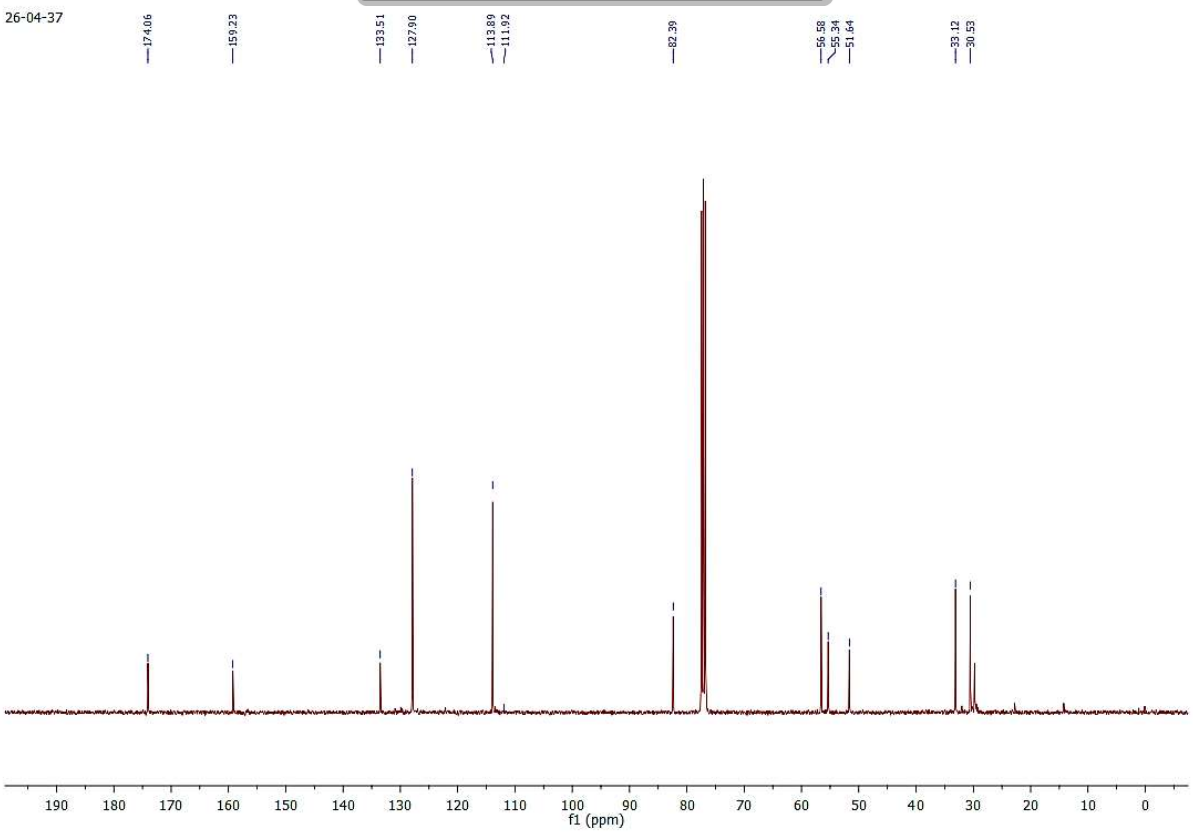

^{13}C{^{1}H} NMR (100 MHz, $CDCl_3$) of 2b

^{1}H NMR (400 MHz, $CDCl_3$) of 2c

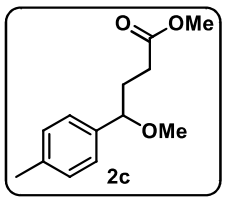

^{13}C{^{1}H} NMR (100 MHz, $CDCl_3$) of 2c

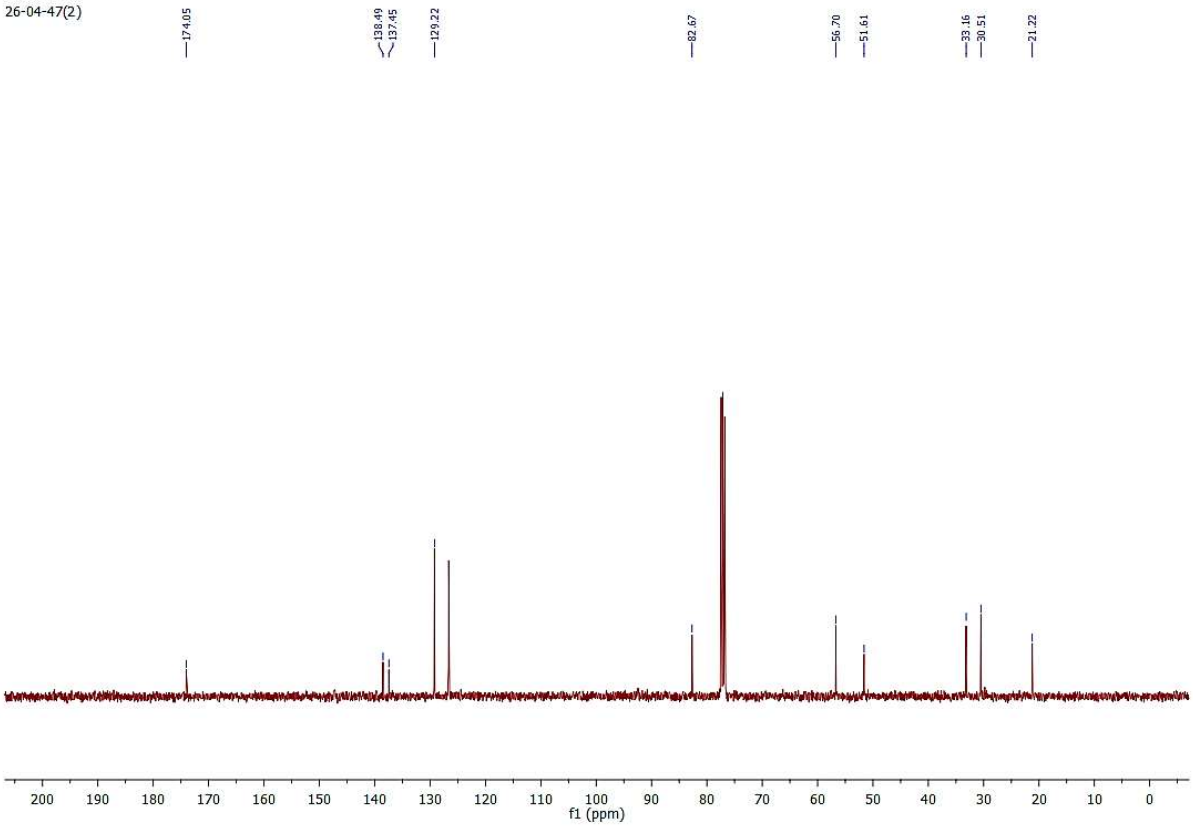

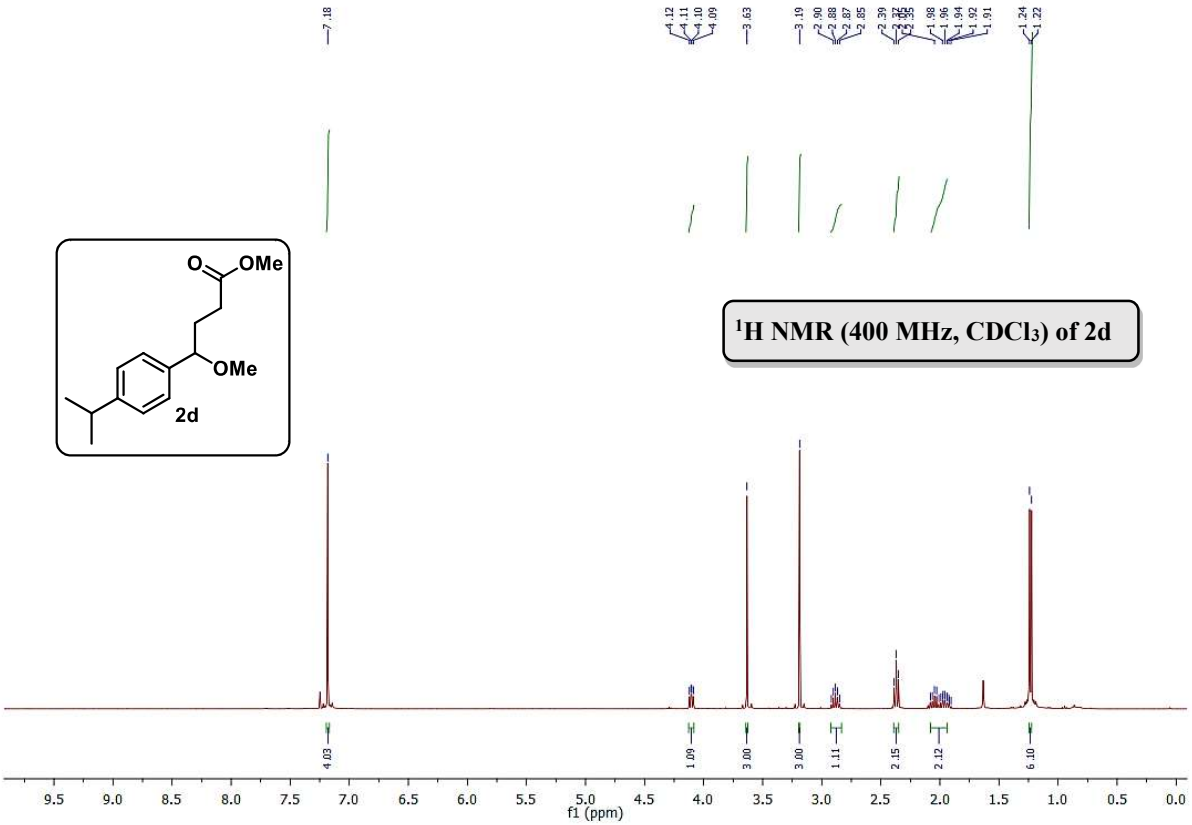

^{1}H NMR (400 MHz, $CDCl_3$) of 2d

$^{13}C\{^{1}H\}$ NMR (100 MHz, $CDCl_3$) of 2d

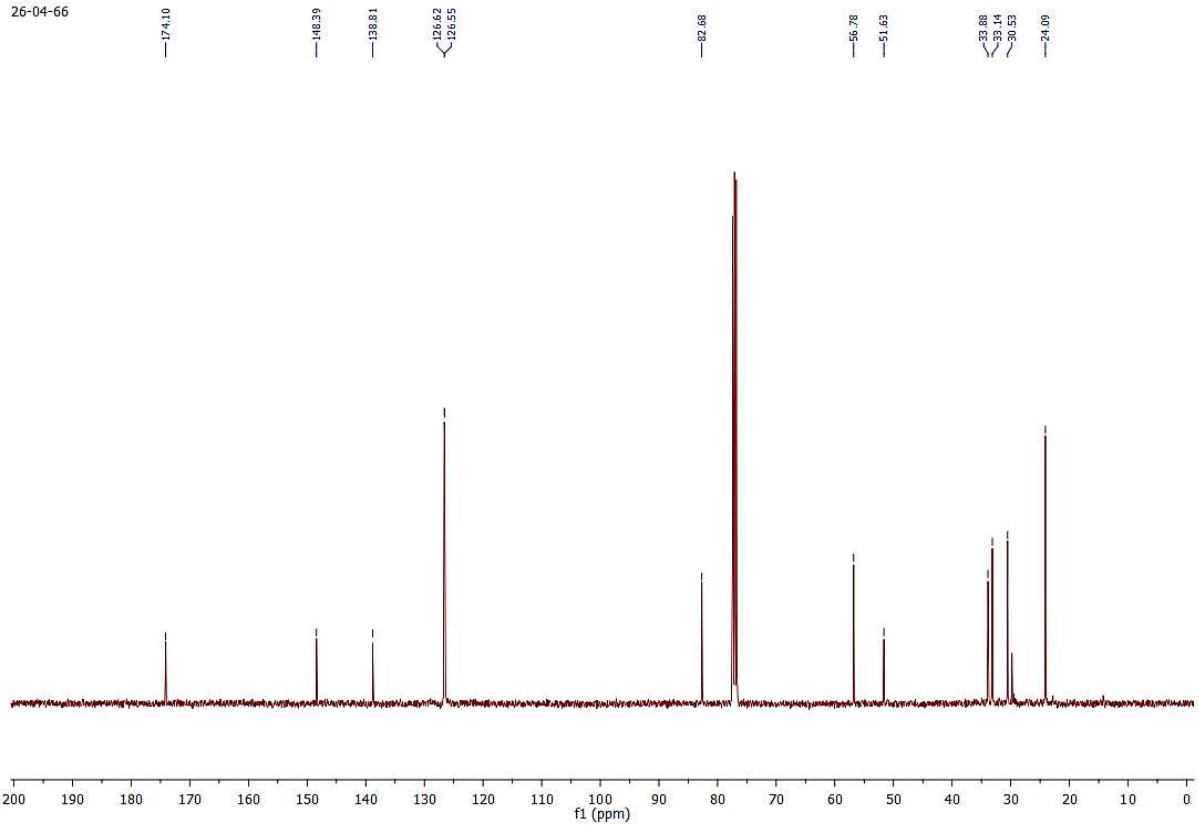

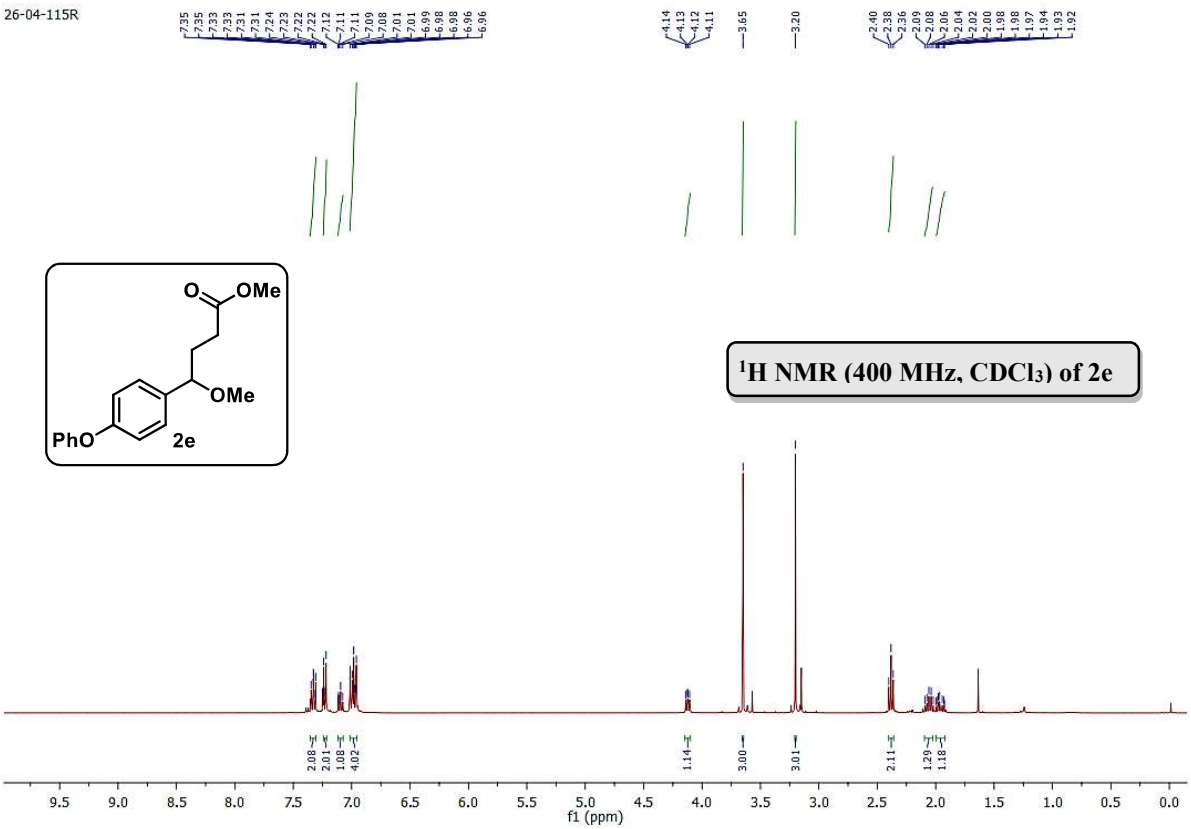

^{1}H NMR (400 MHz, $CDCl_3$) of 2e

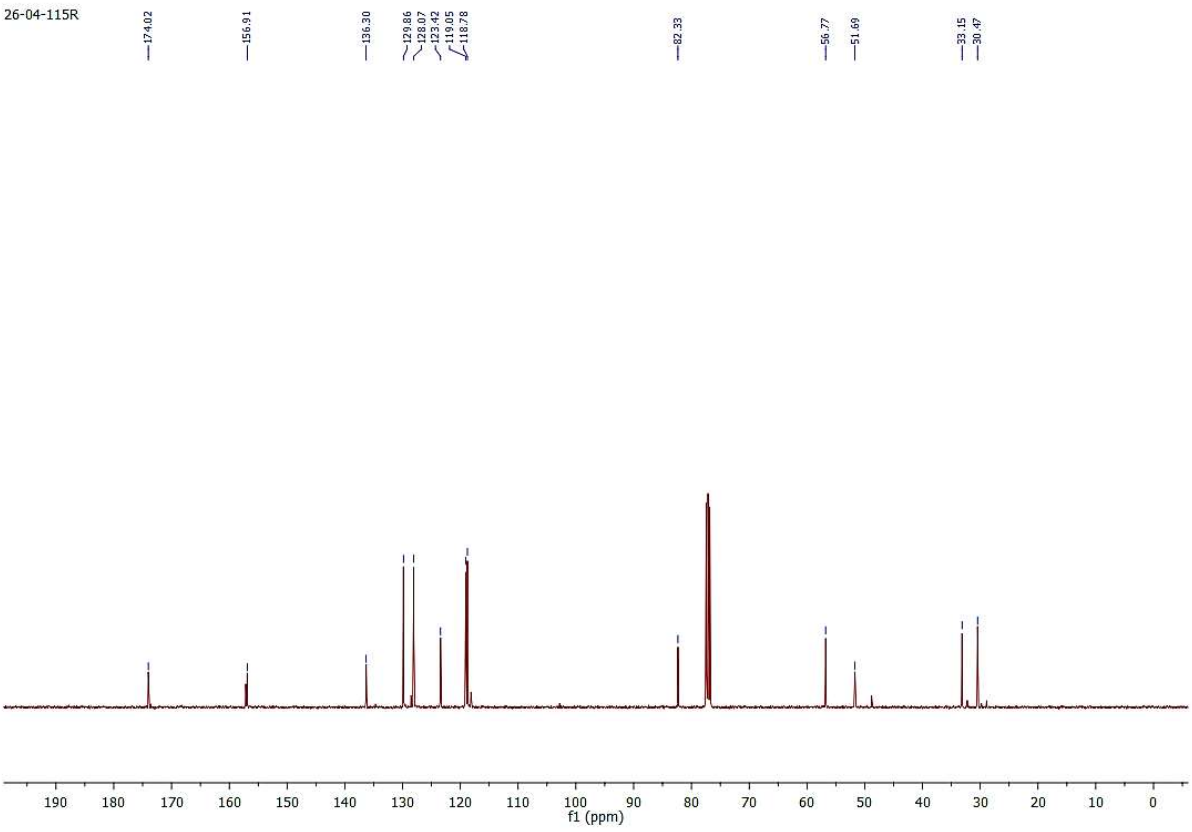

$^{13}C\{^{1}H\}$ NMR (100 MHz, $CDCl_3$) of 2e

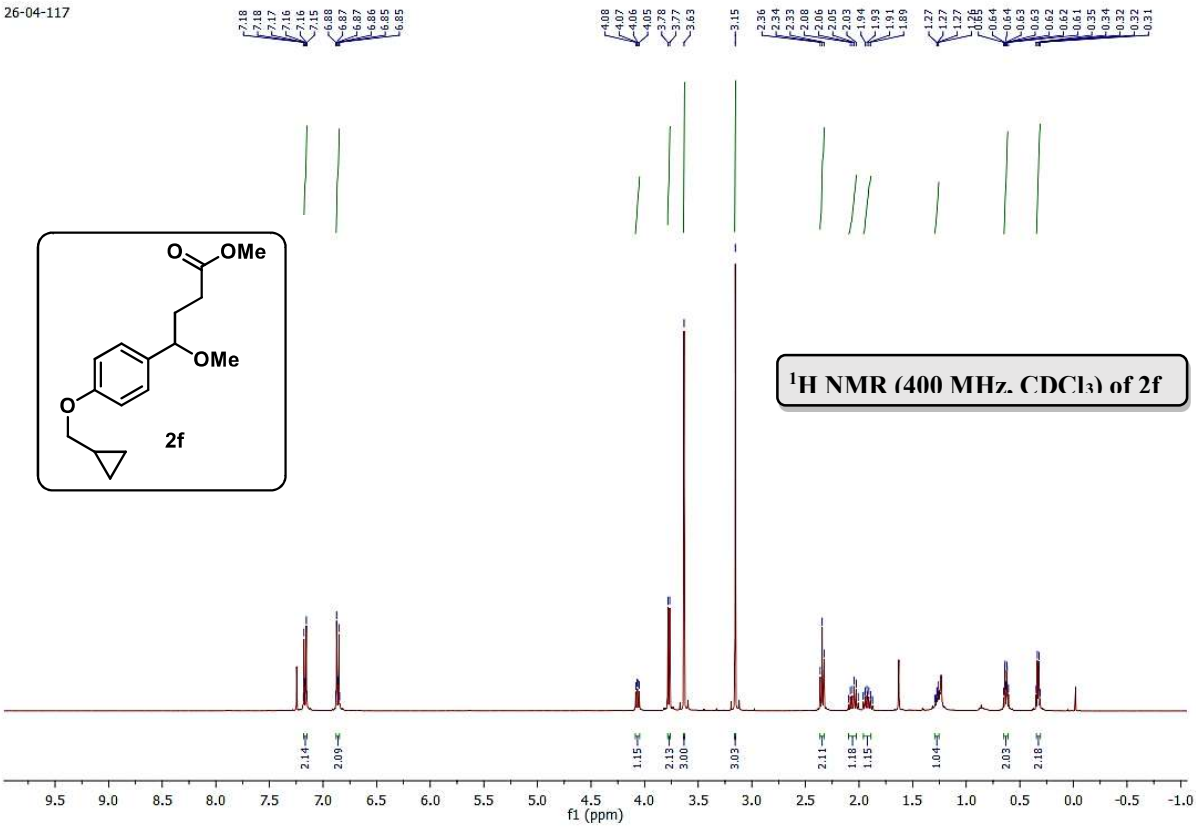

^{1}H NMR (400 MHz, $CDCl_3$) of 2f

$^{13}C\{^{1}H\}$ NMR (100 MHz, $CDCl_3$) of 2f

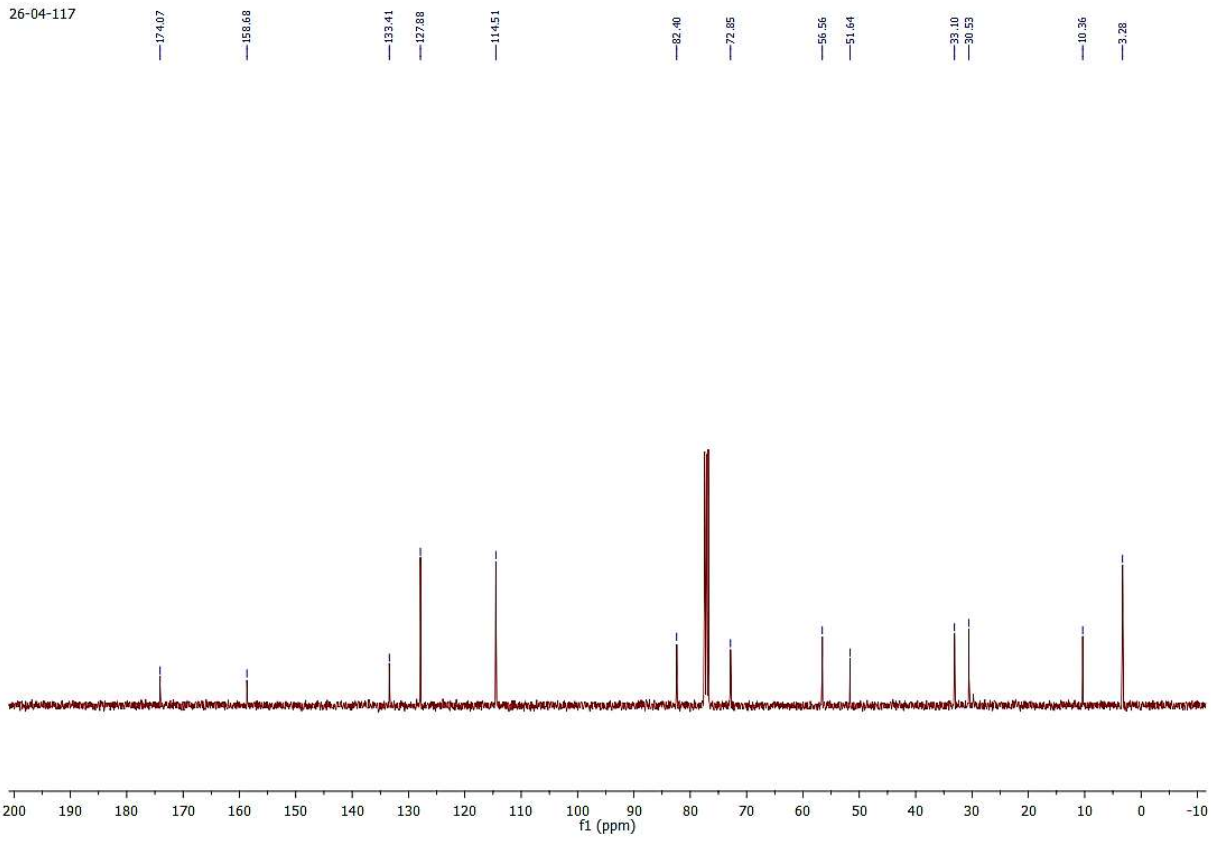

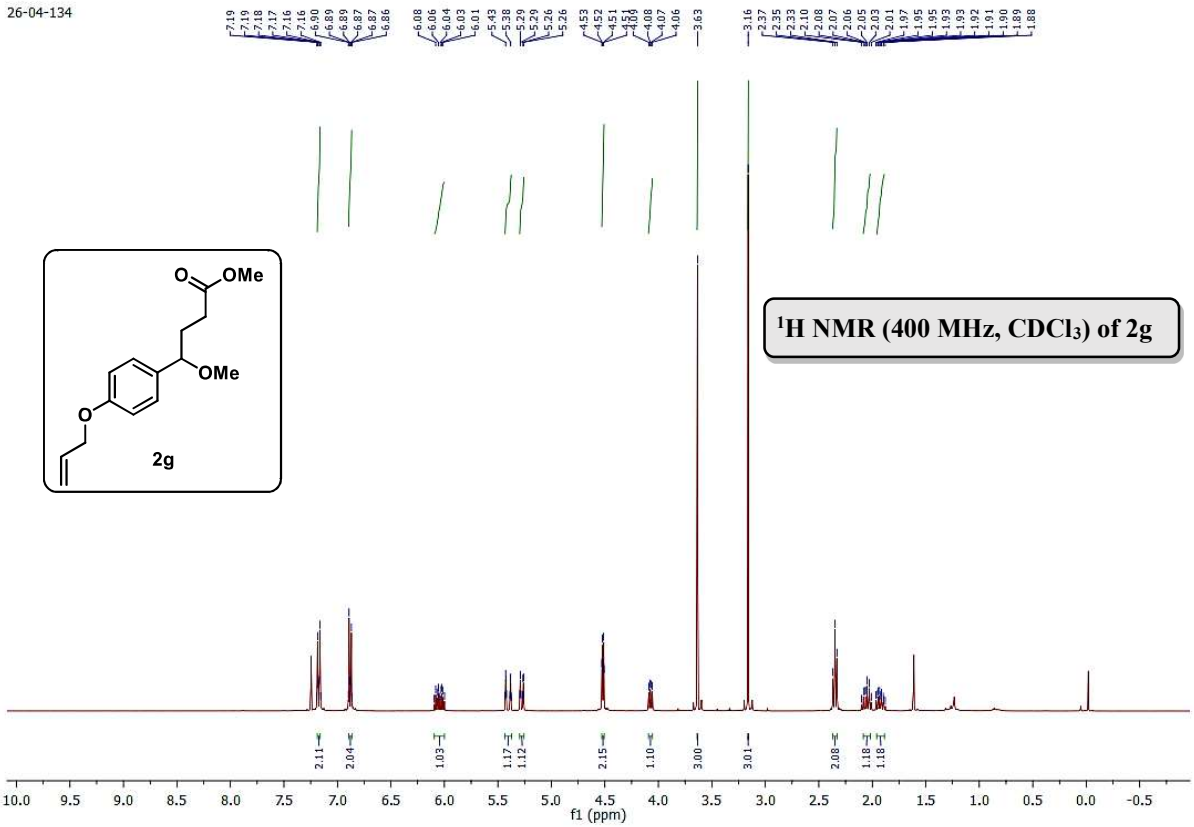

^{1}H NMR (400 MHz, $CDCl_3$) of 2g

$^{13}C\{^{1}H\}$ NMR (100 MHz, $CDCl_3$) of 2g

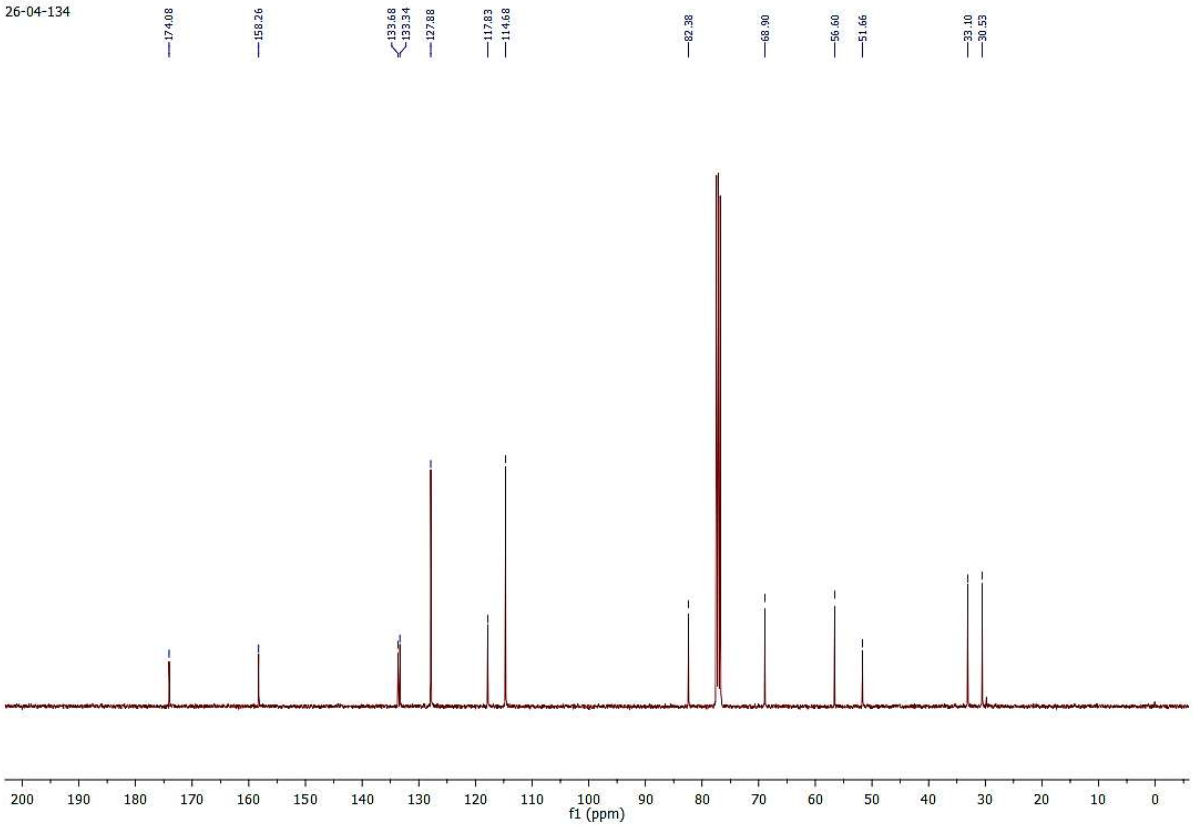

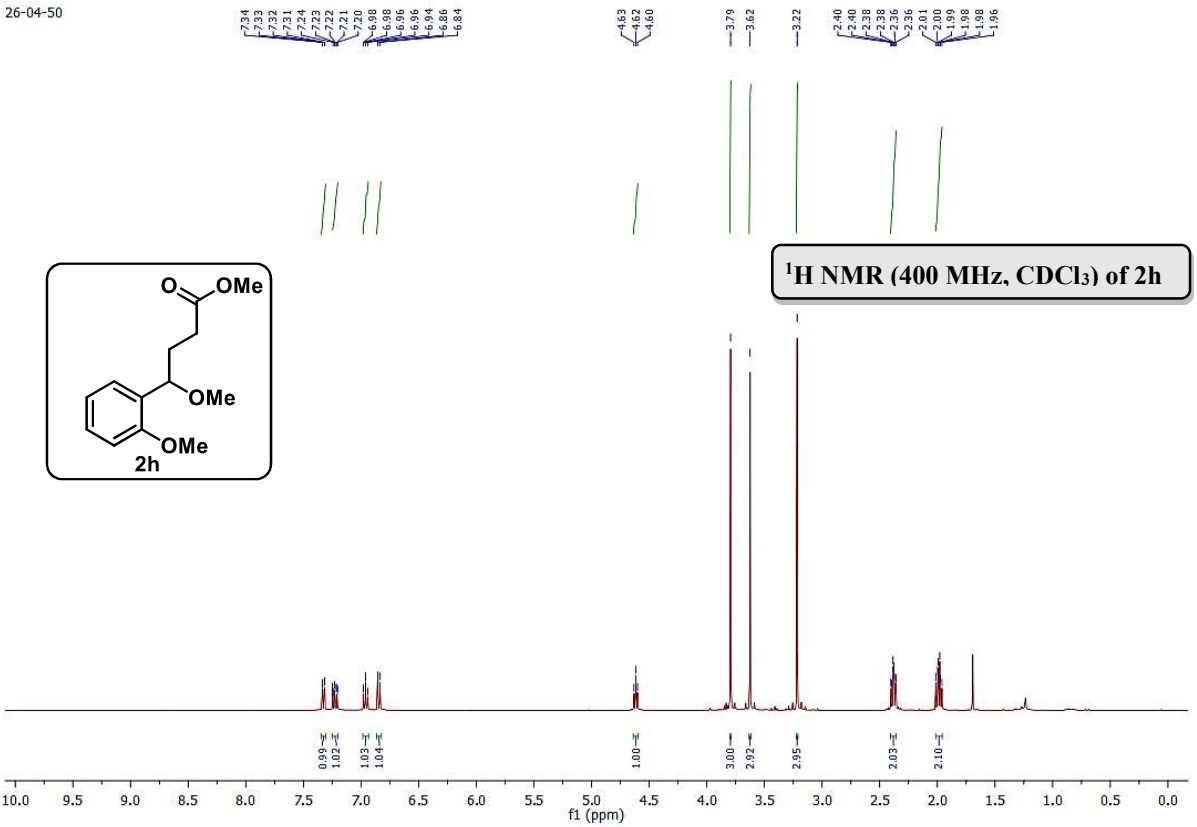

^{1}H NMR (400 MHz, $CDCl_3$) of 2h

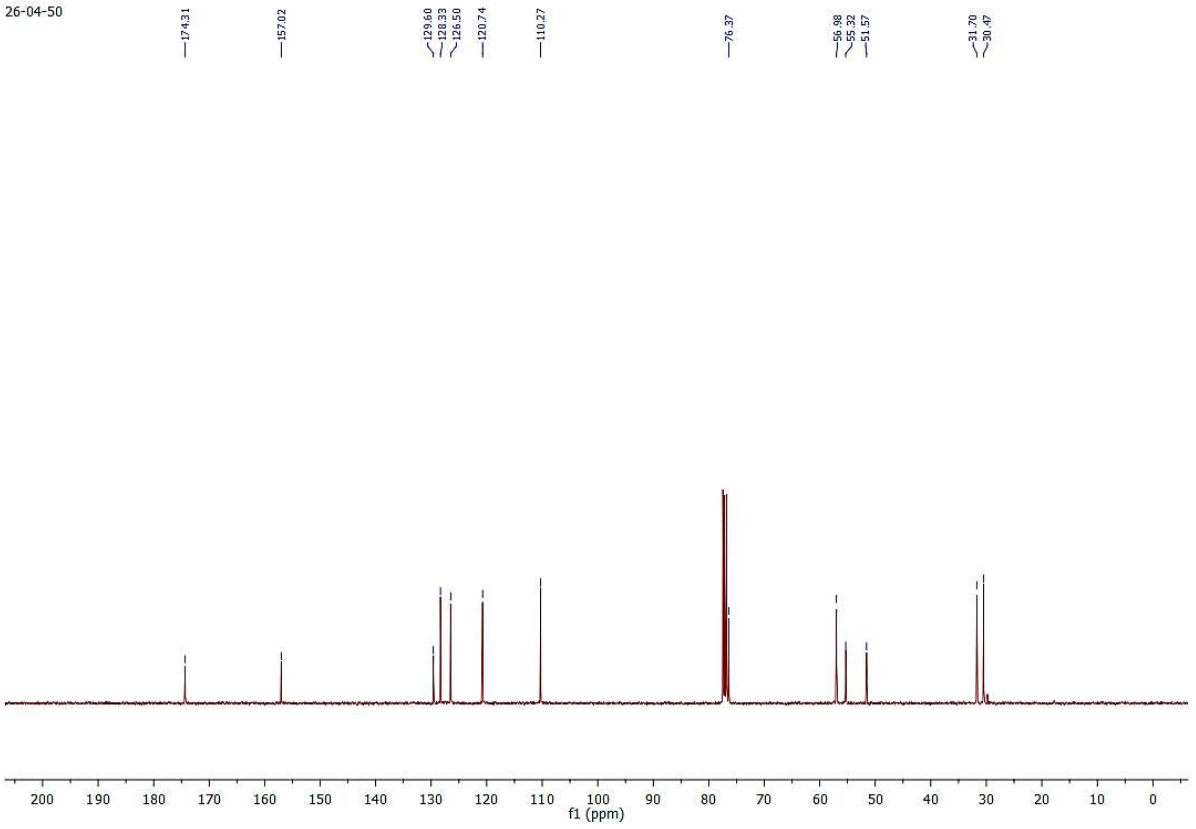

^{13}C{^{1}H} NMR (100 MHz, $CDCl_3$) of 2h

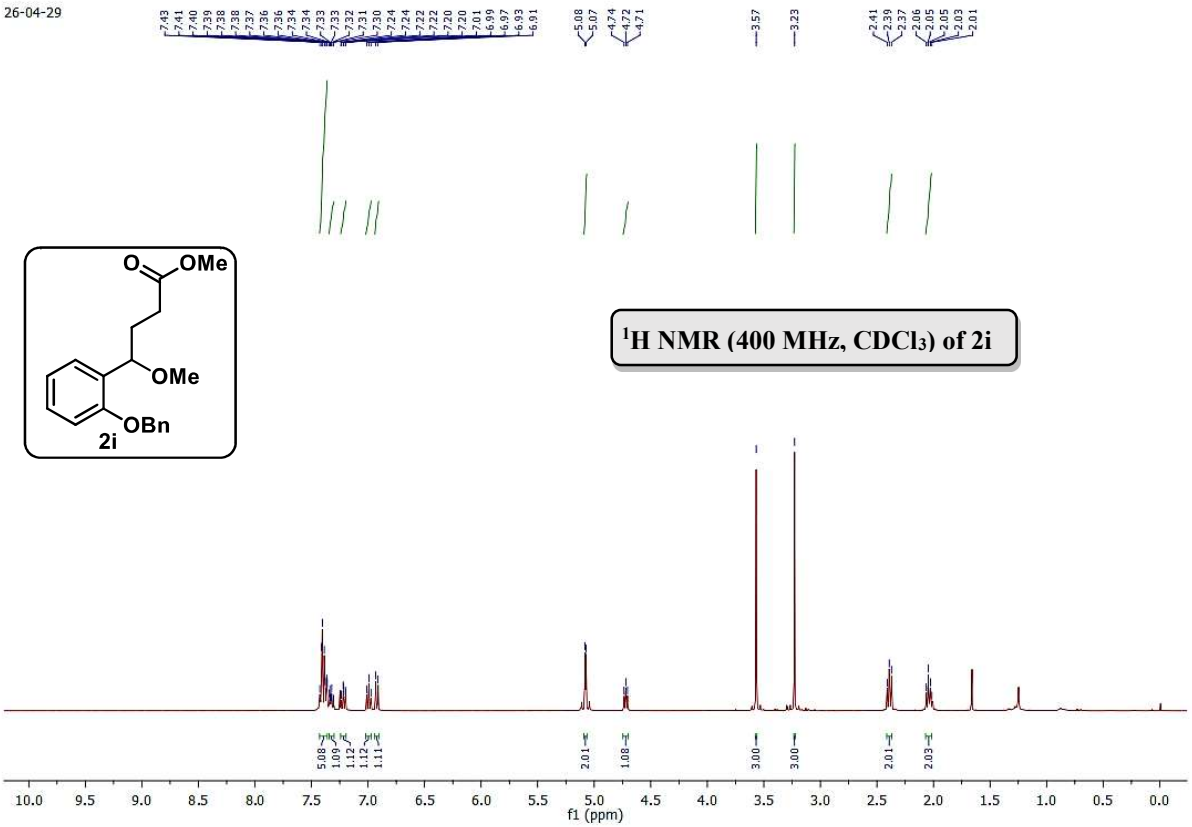

^{1}H NMR (400 MHz, $CDCl_3$) of 2i

$^{13}C\{^{1}H\}$ NMR (100 MHz, $CDCl_3$) of 2i

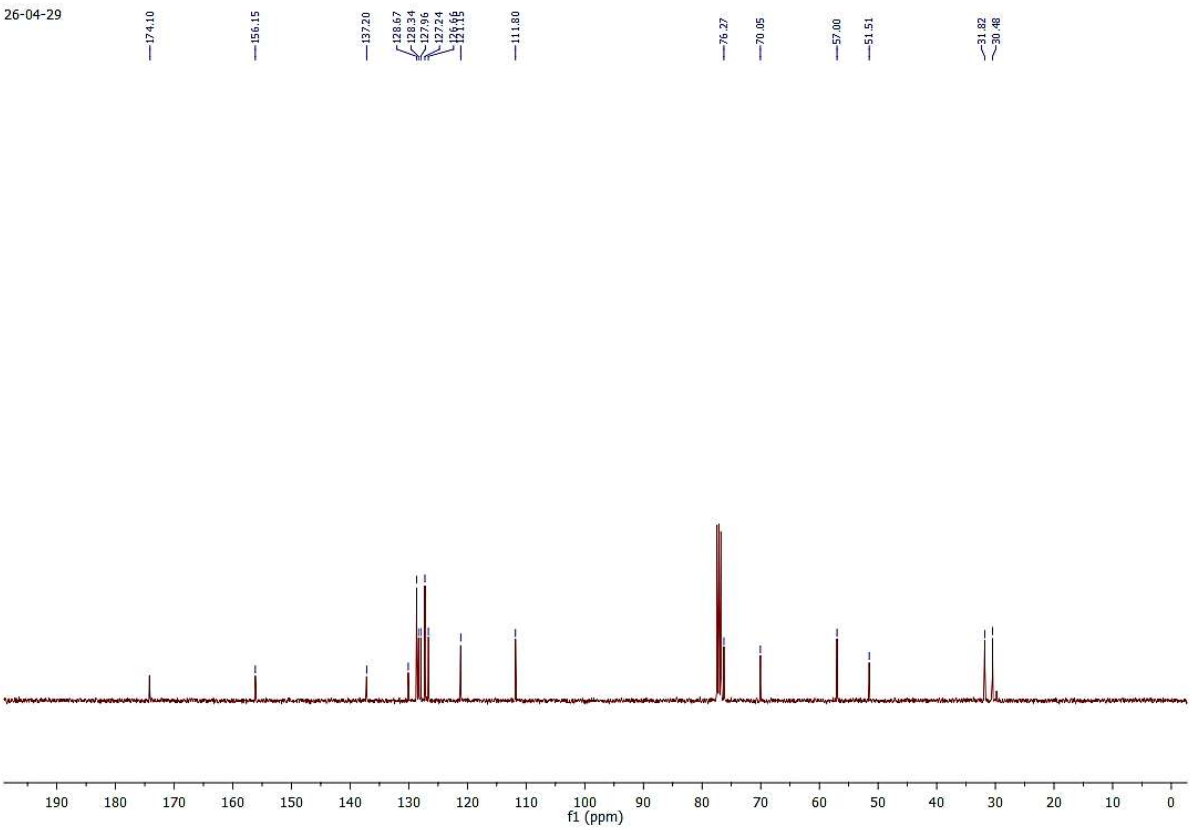

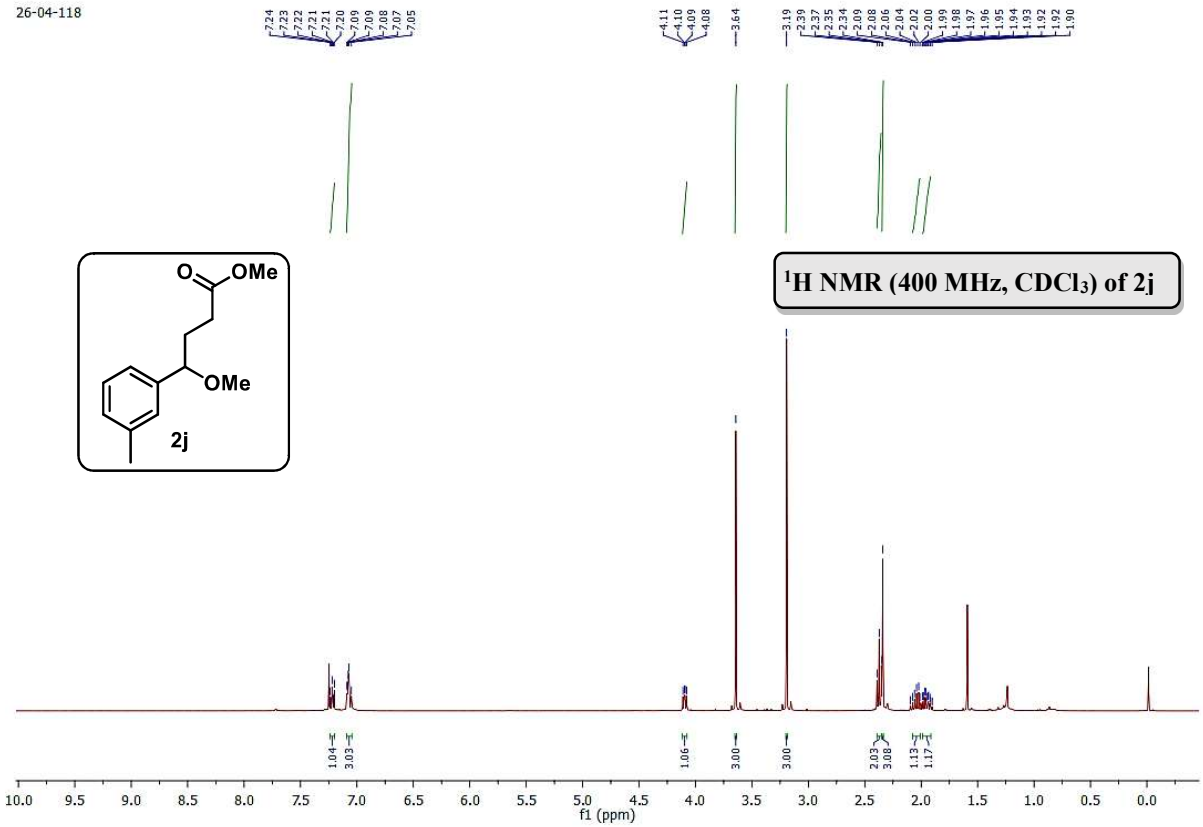

^{1}H NMR (400 MHz, $CDCl_3$) of 2j

$^{13}C\{^{1}H\}$ NMR (100 MHz, $CDCl_3$) of 2j

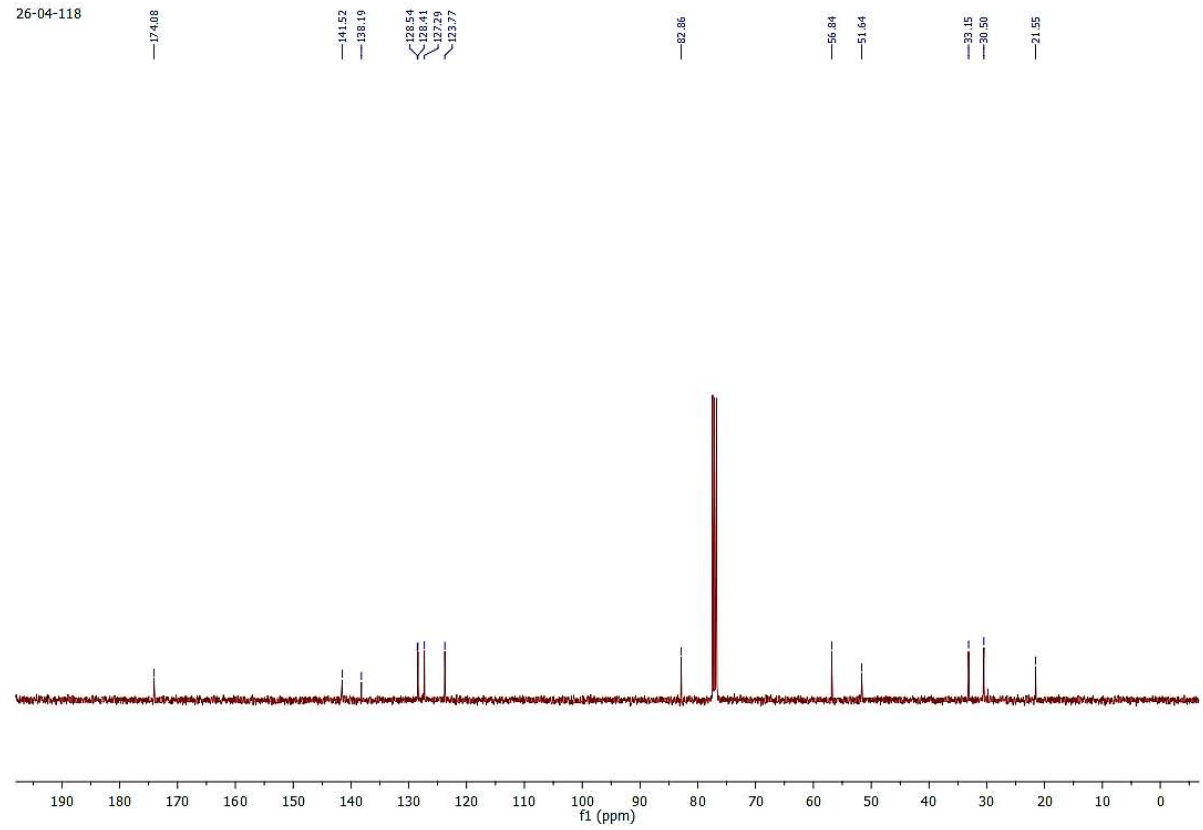

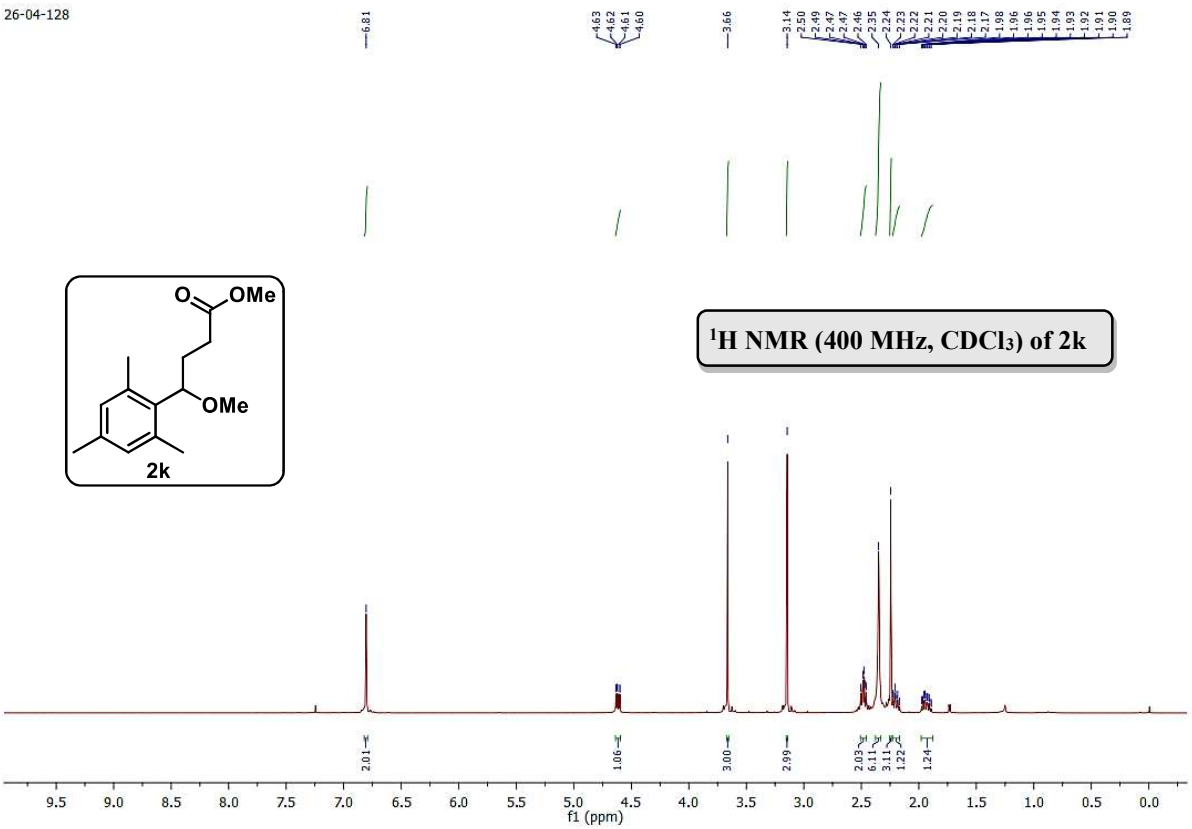

^{1}H NMR (400 MHz, $CDCl_3$) of 2k

$^{13}C\{^{1}H\}$ NMR (100 MHz, $CDCl_3$) of 2k

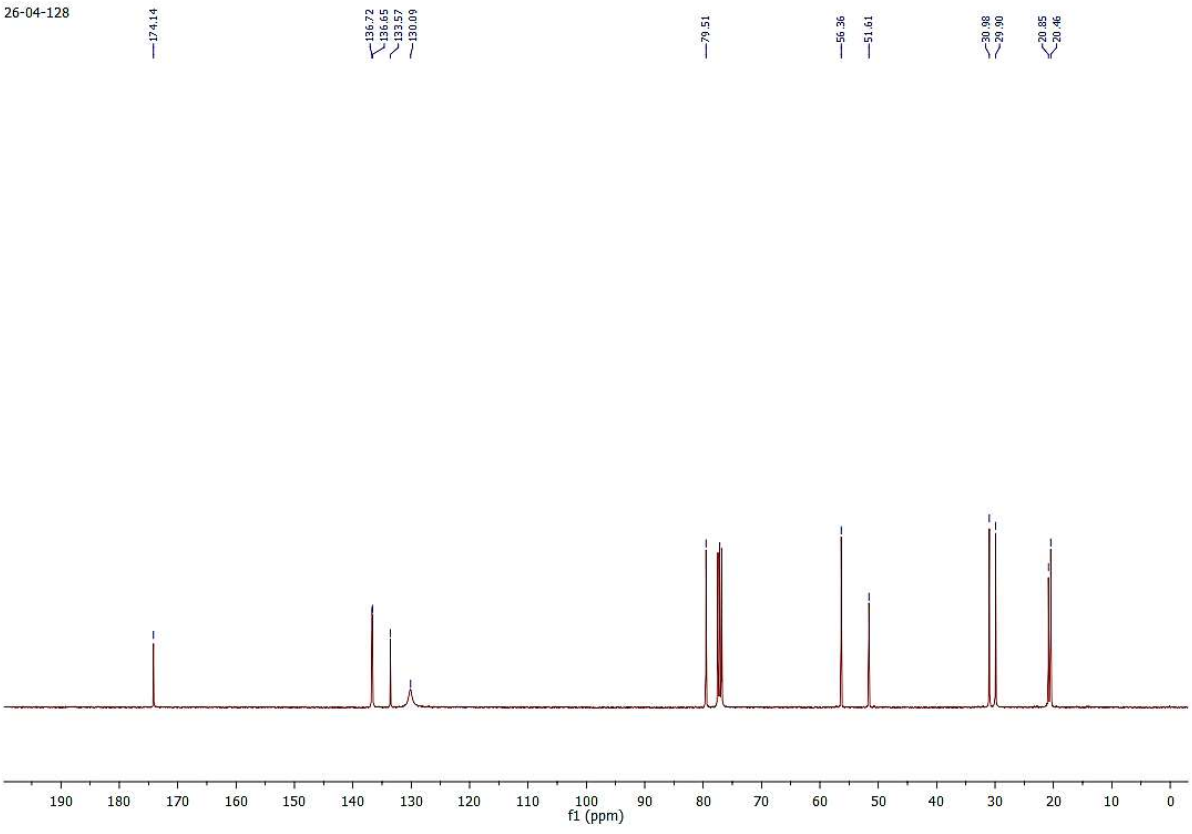

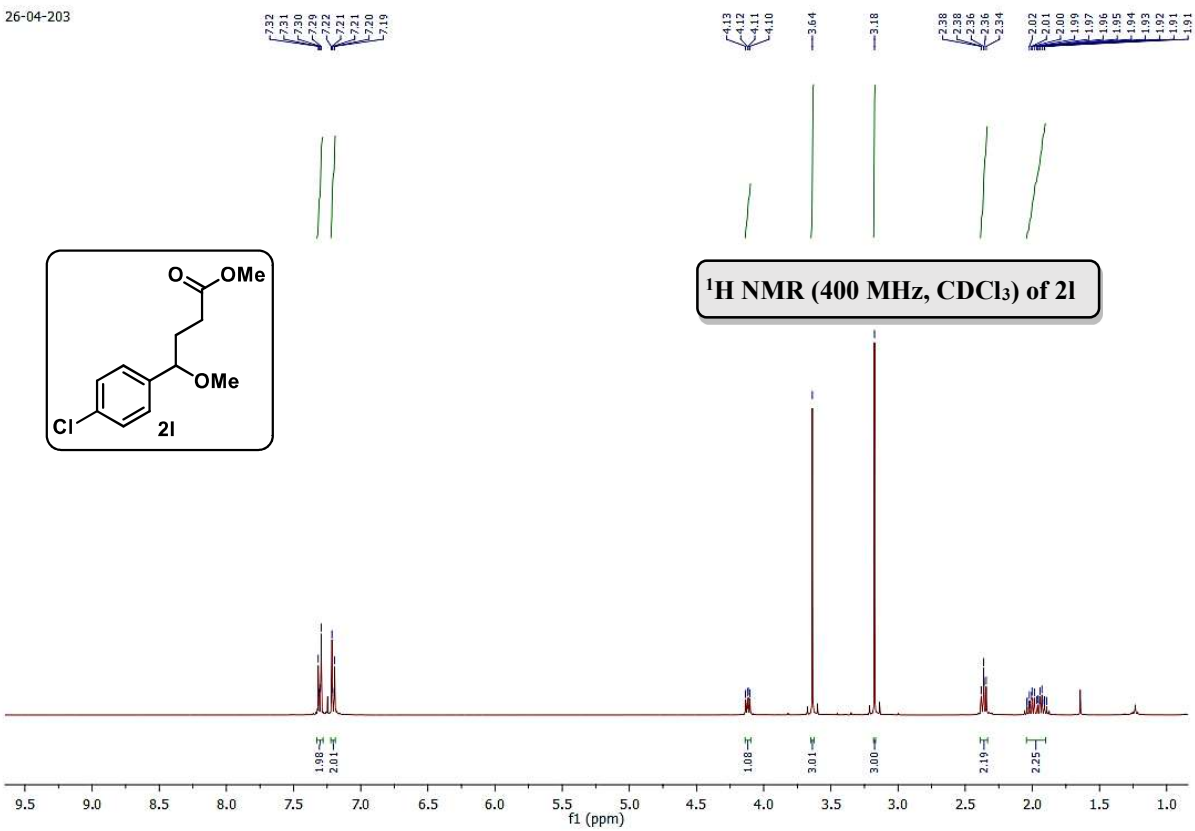

^{1}H NMR (400 MHz, $CDCl_3$) of 2l

$^{13}C\{^{1}H\}$ NMR (100 MHz, $CDCl_3$) of 2l

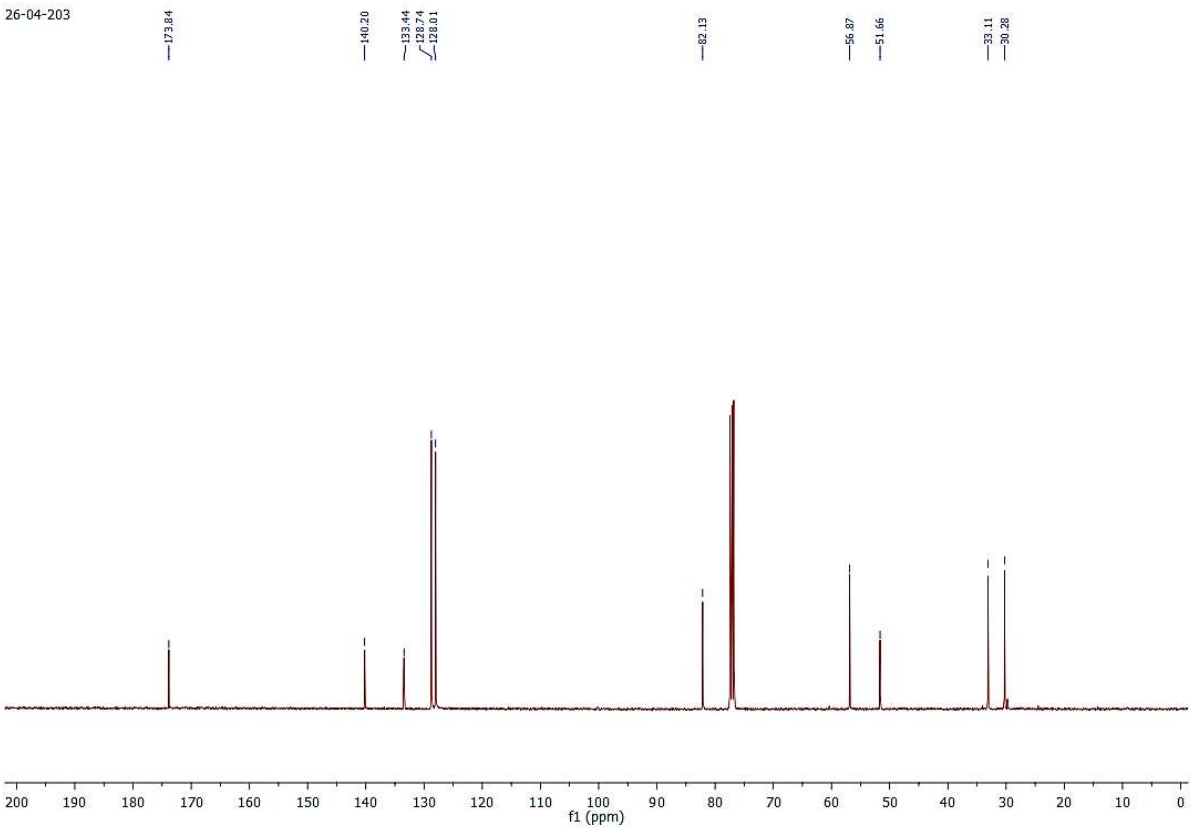

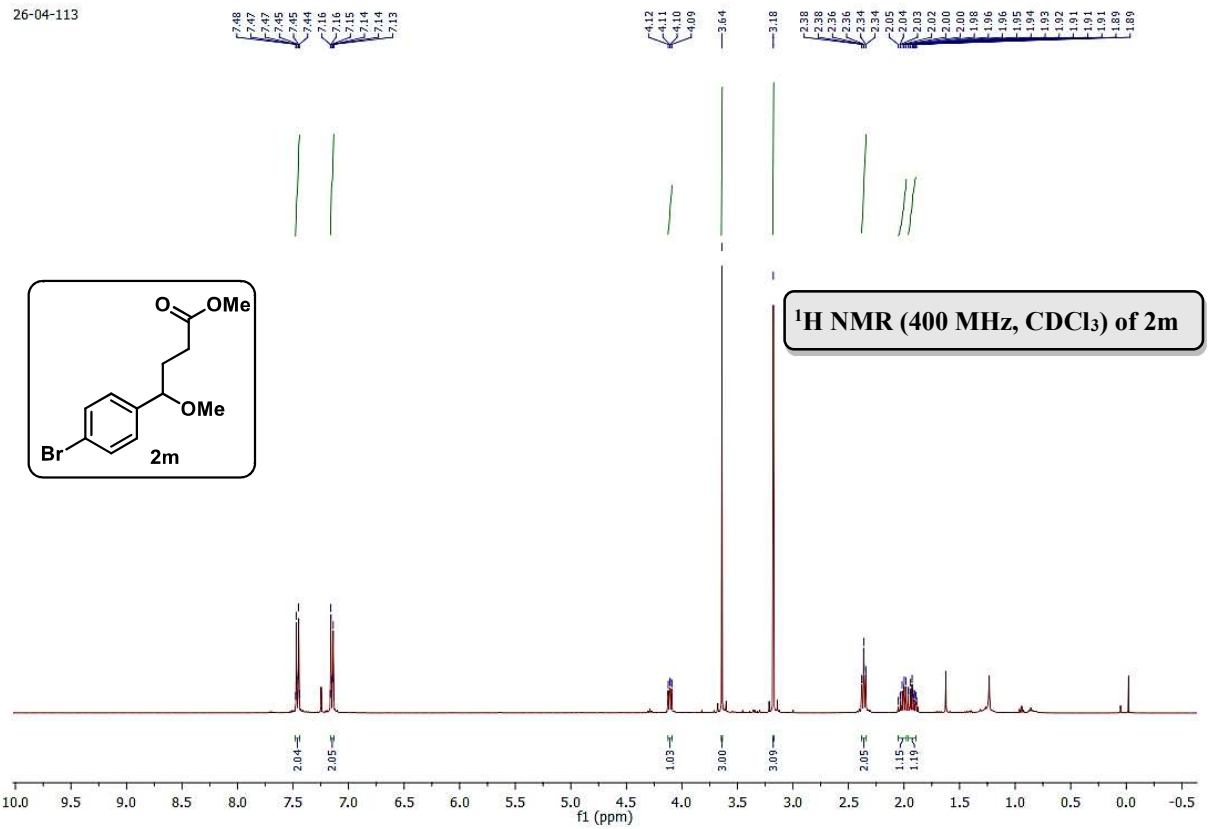

^{1}H NMR (400 MHz, $CDCl_3$) of 2m

$^{13}C\{^{1}H\}$ NMR (100 MHz, $CDCl_3$) of 2m

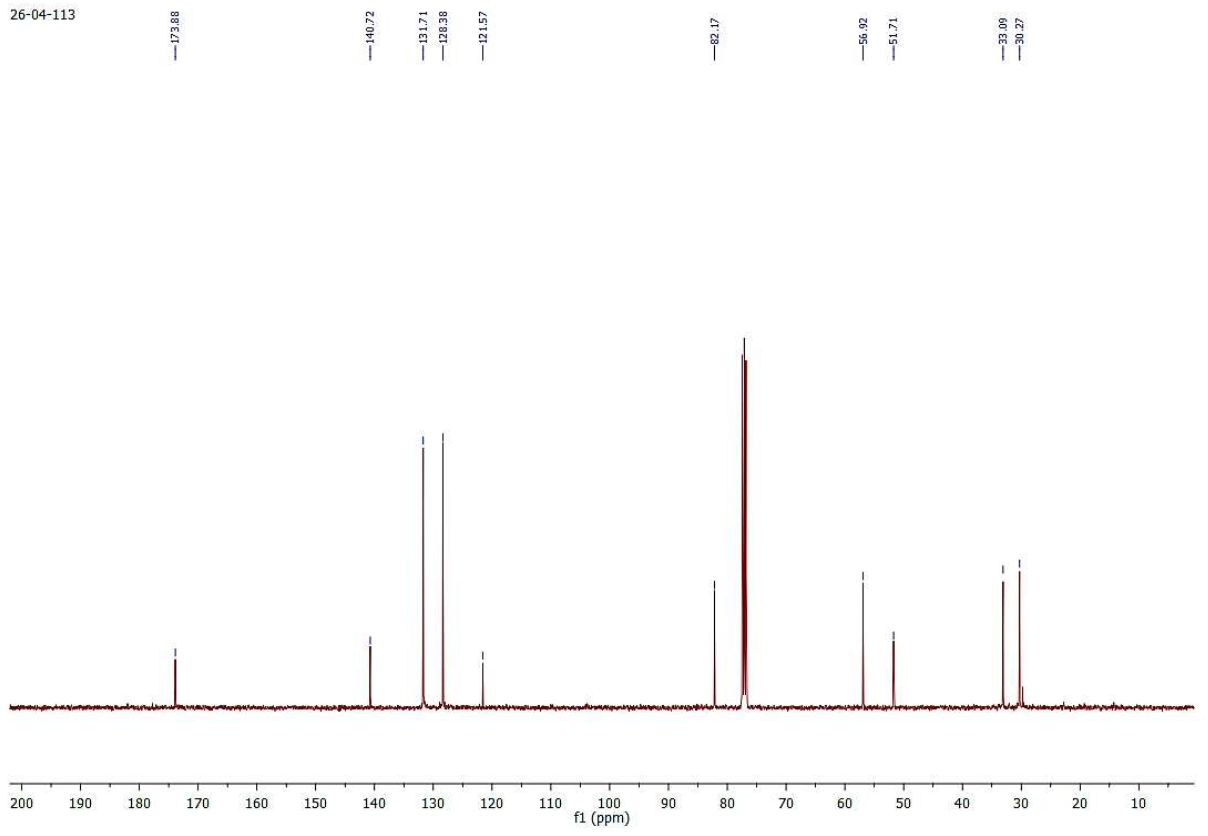

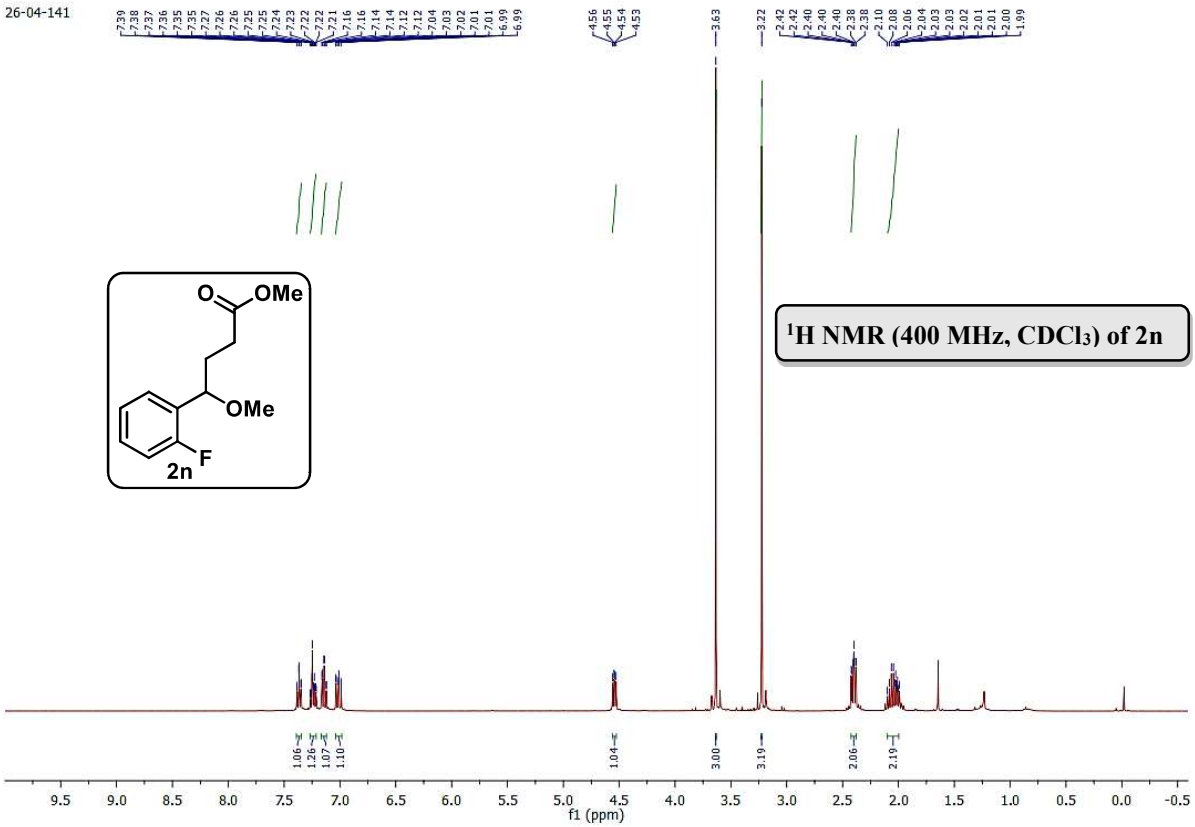

^{1}H NMR (400 MHz, $CDCl_3$) of 2n

$^{13}C\{^{1}H\}$ NMR (100 MHz, $CDCl_3$) of 2n

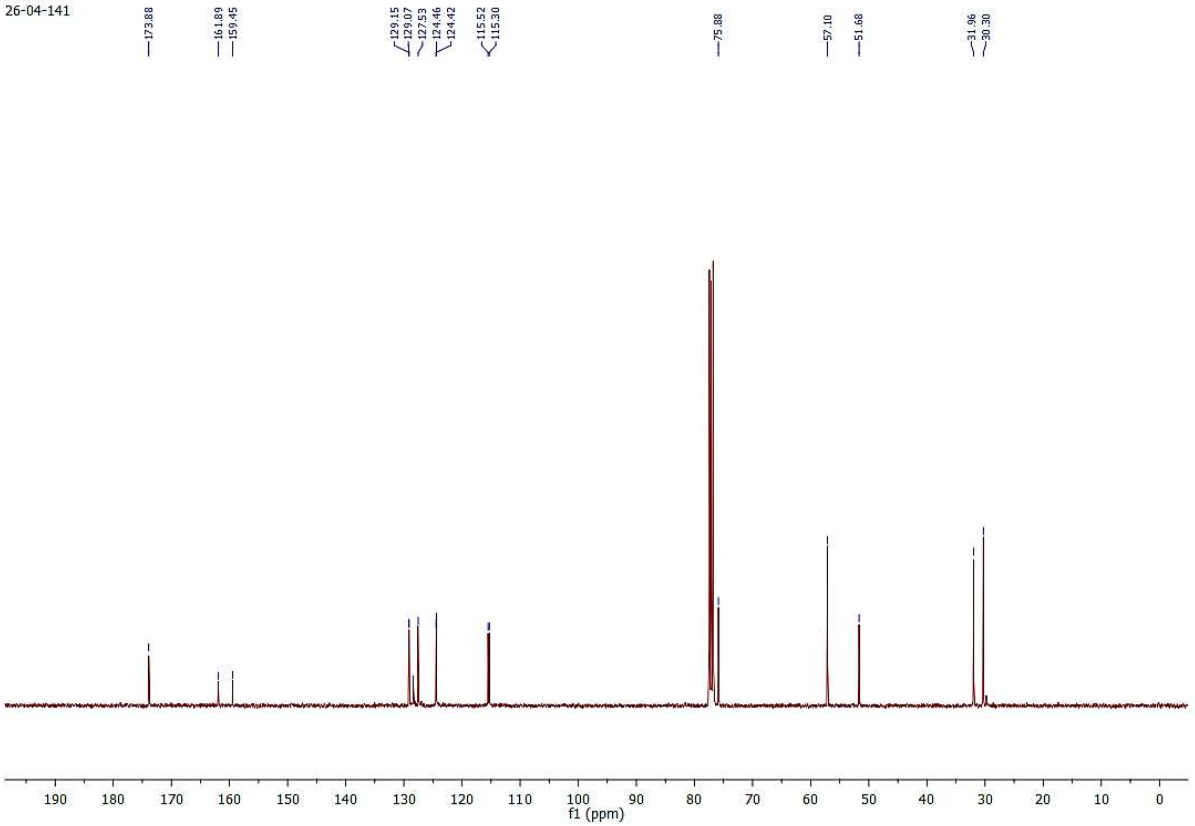

^{19}F NMR (376 MHz, $CDCl_3$) of 2n

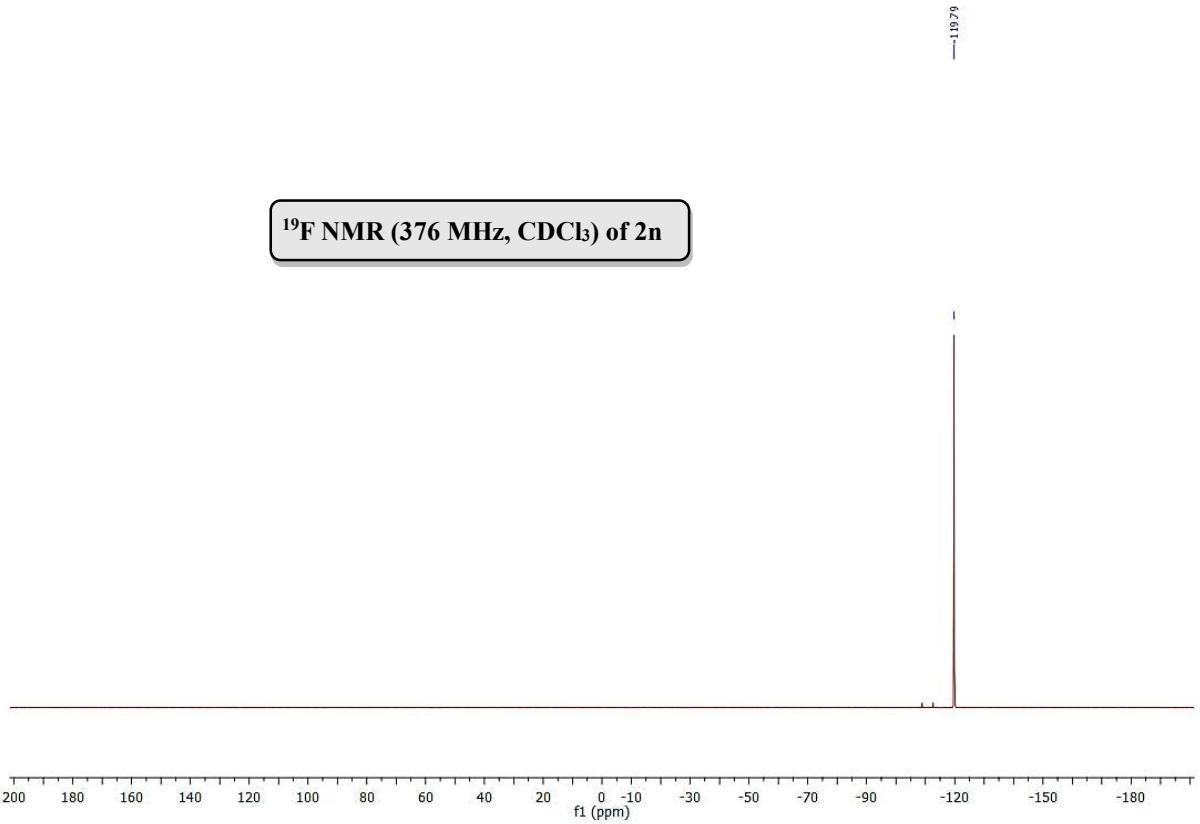

^{1}H NMR (400 MHz, $CDCl_3$) of 2o

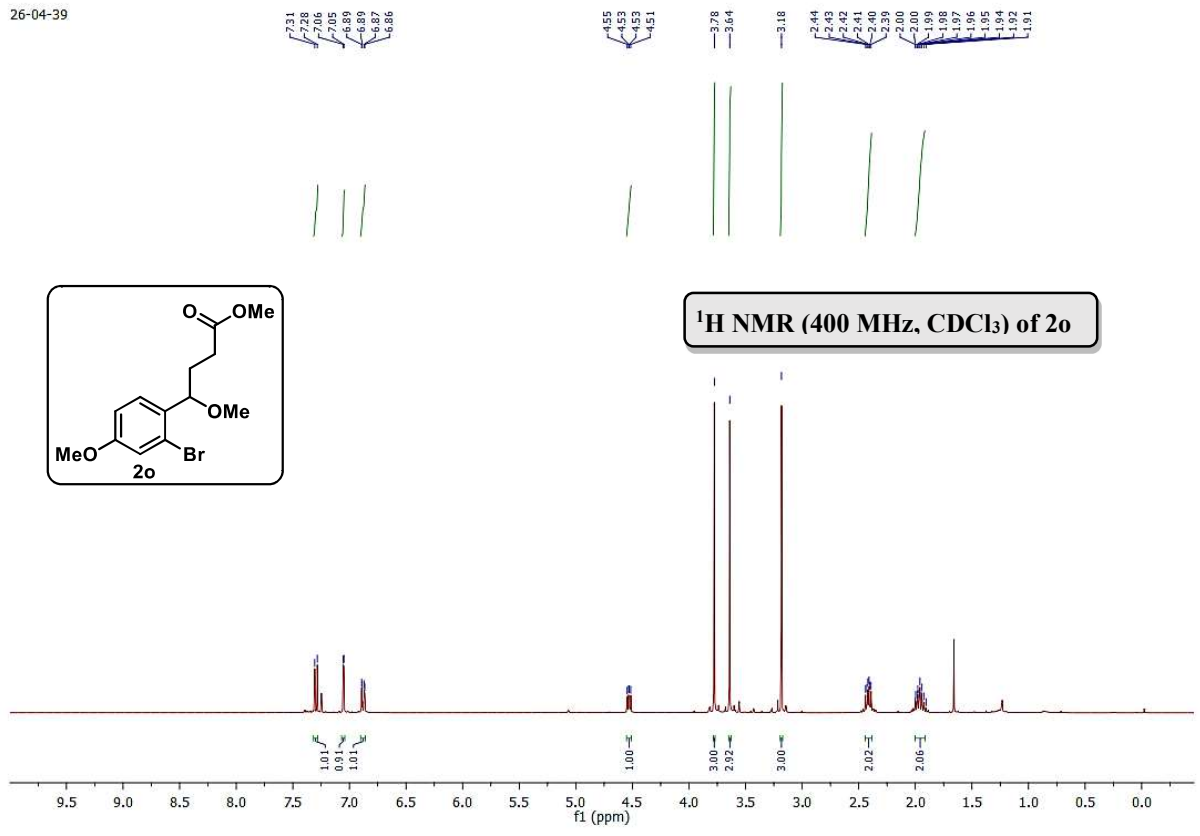

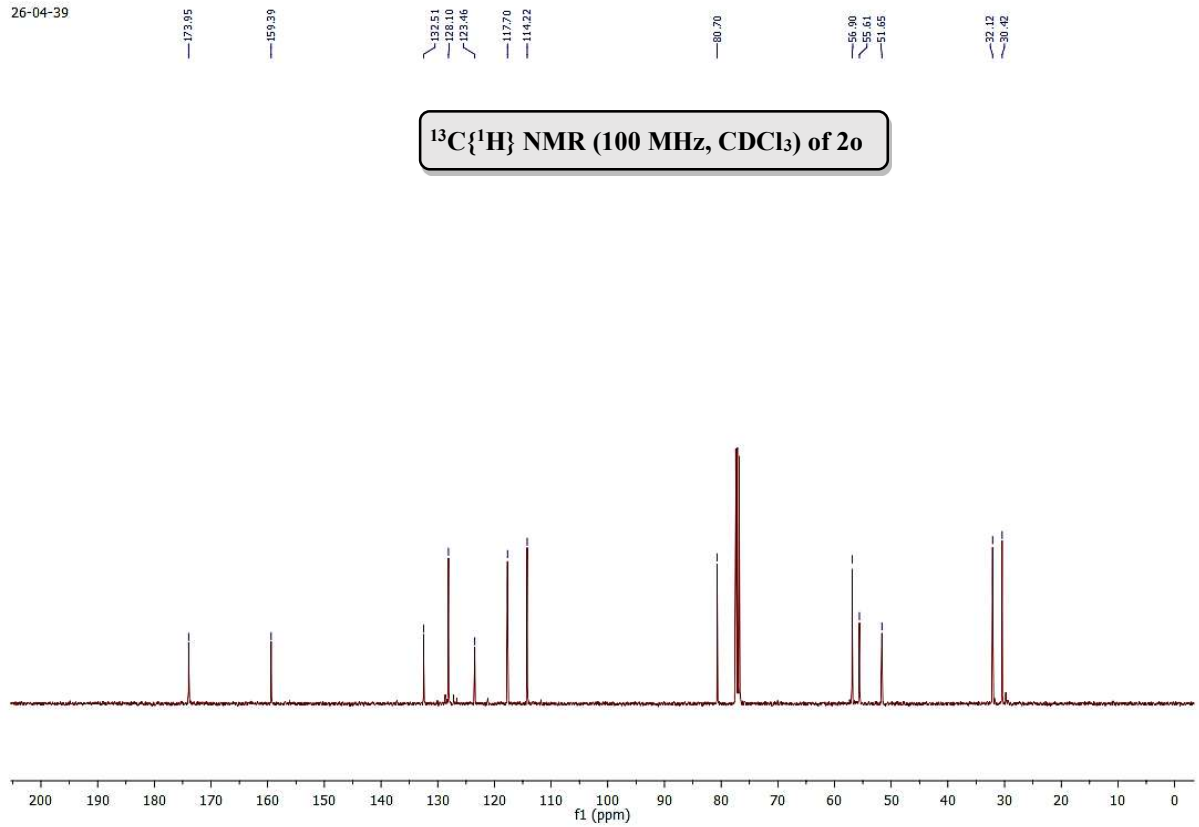

$^{13}C\{^{1}H\}$ NMR (100 MHz, $CDCl_3$) of 2o

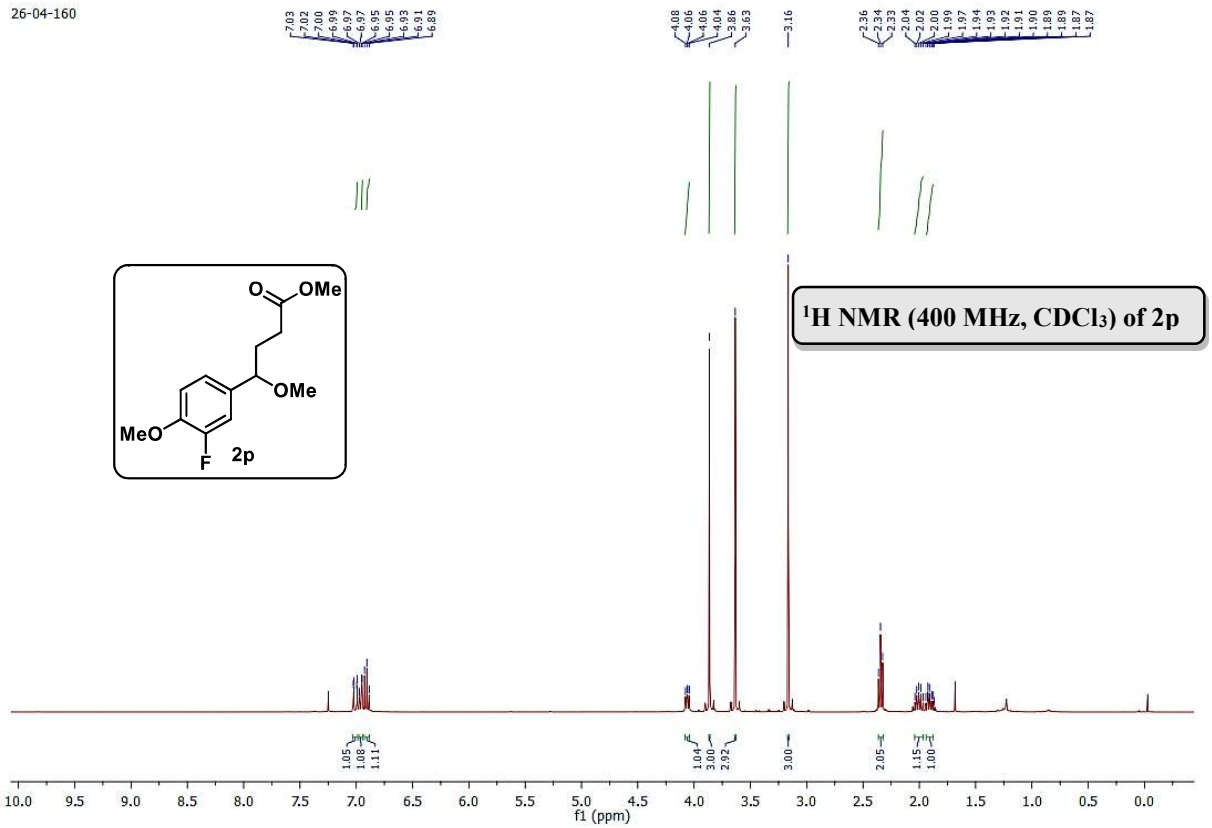

^{1}H NMR (400 MHz, $CDCl_3$) of 2p

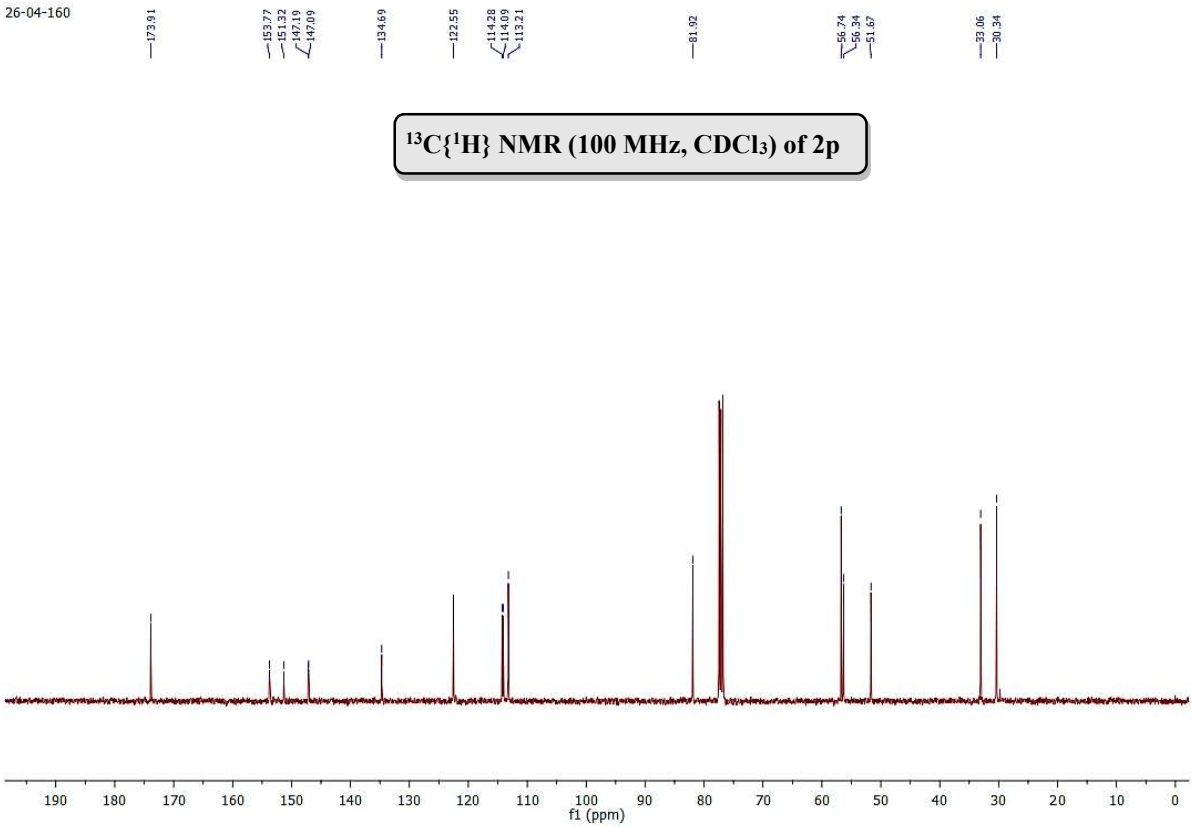

$^{13}C\{^{1}H\}$ NMR (100 MHz, $CDCl_3$) of 2p

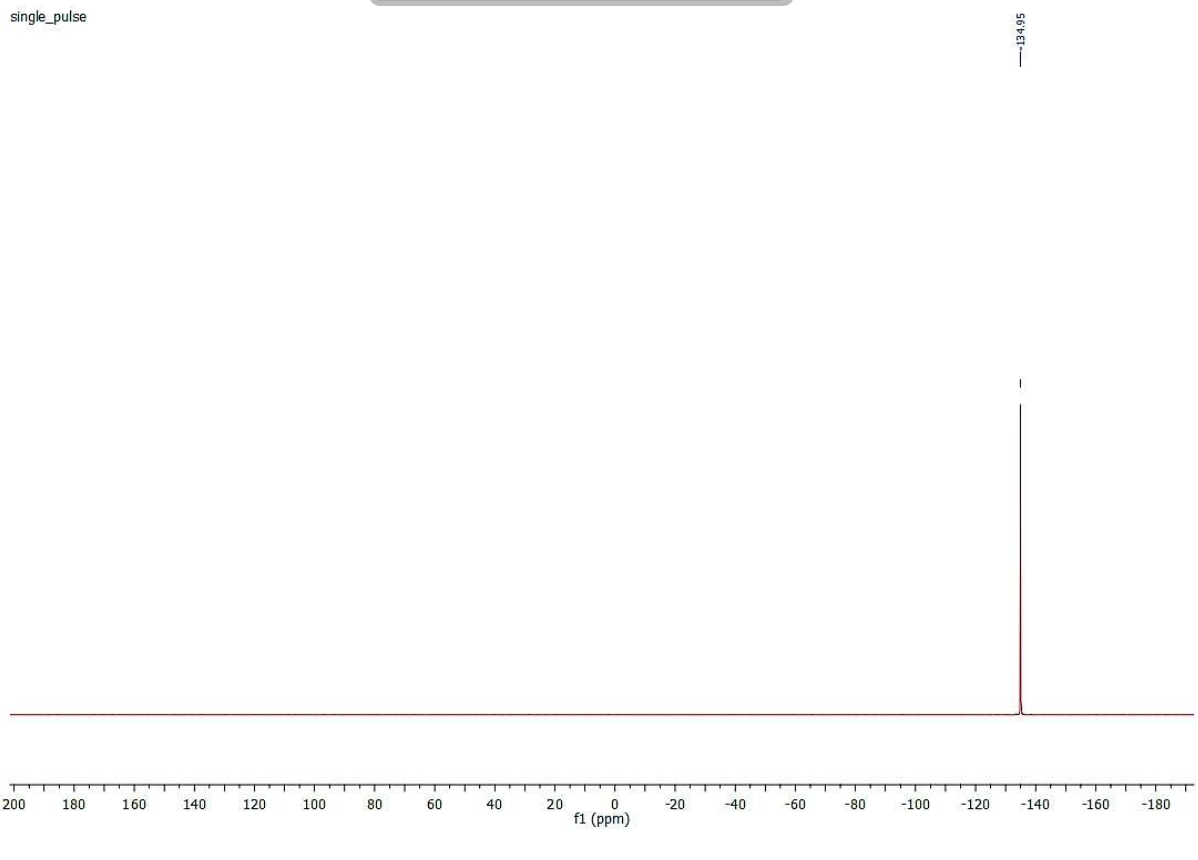

^{19}F NMR (376 MHz, $CDCl_3$) of 2p

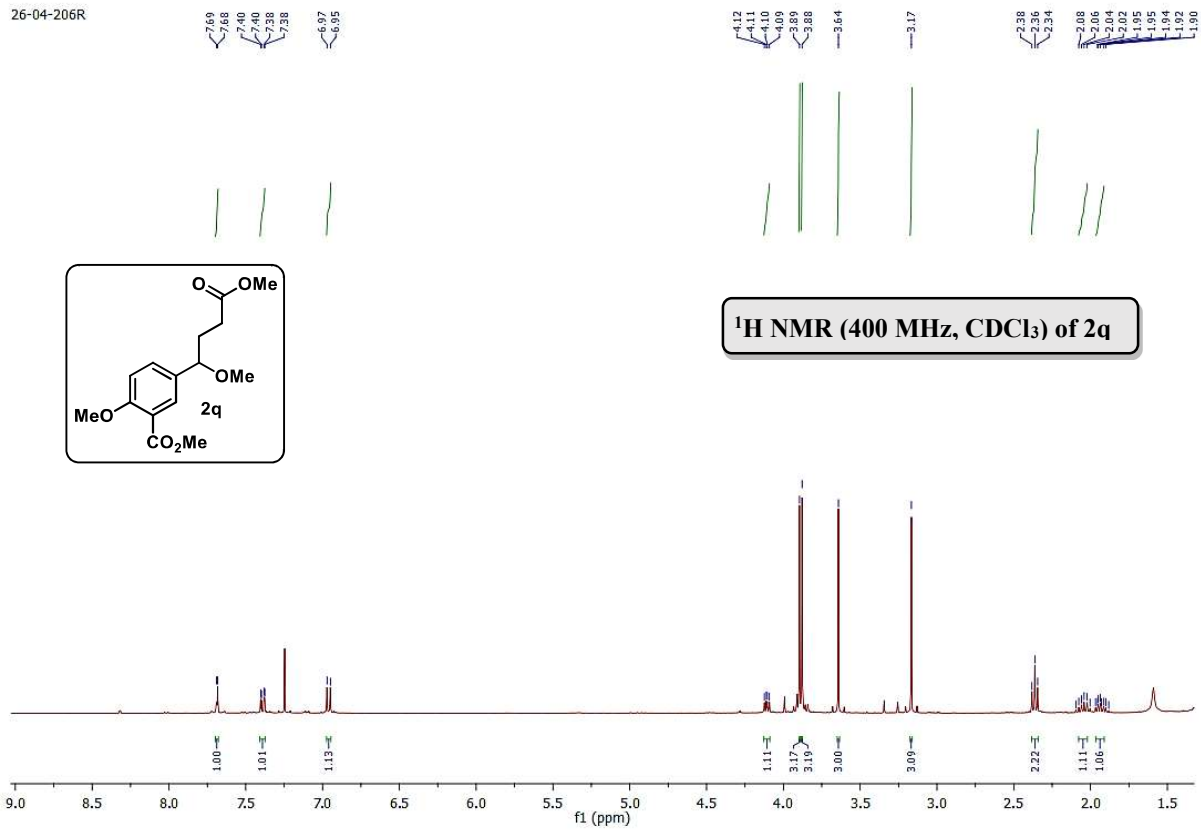

^{1}H NMR (400 MHz, $CDCl_3$) of 2q

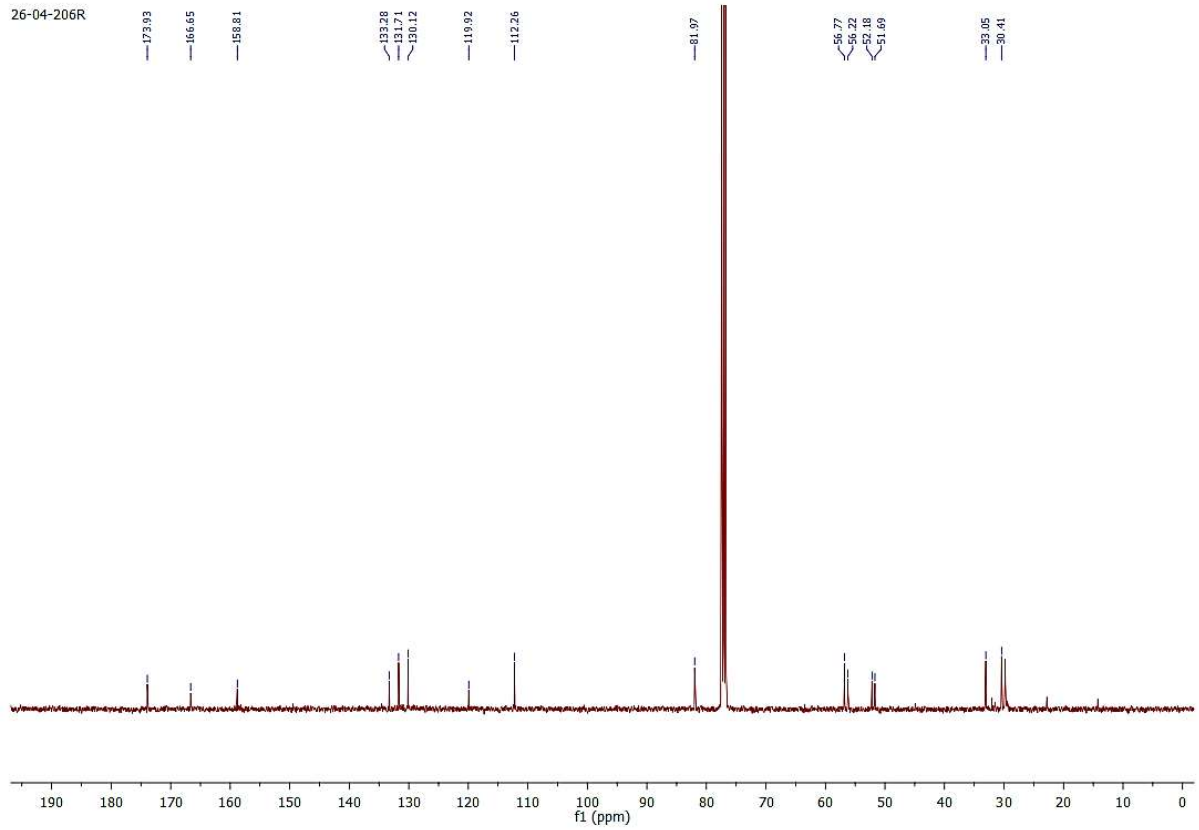

^{13}C{^{1}H} NMR (100 MHz, $CDCl_3$) of 2q

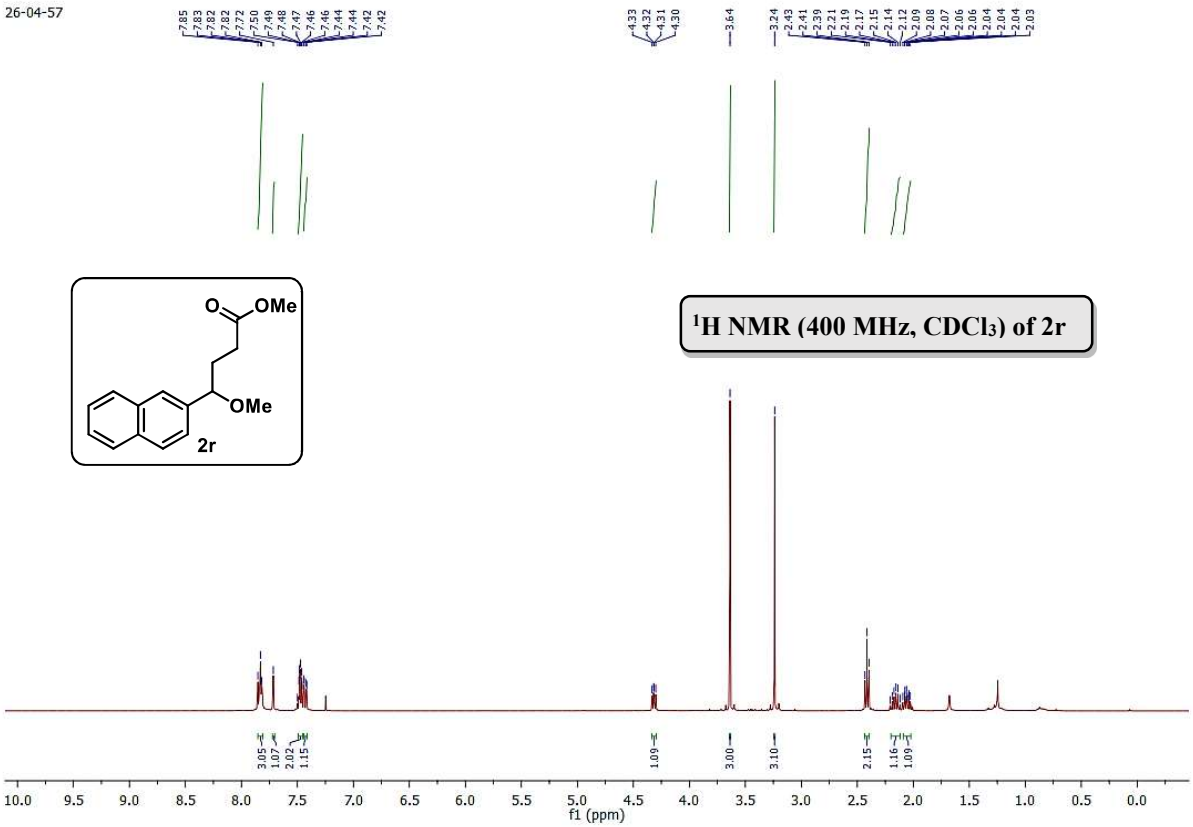

^{1}H NMR (400 MHz, $CDCl_3$) of 2r

$^{13}C\{^{1}H\}$ NMR (100 MHz, $CDCl_3$) of 2r

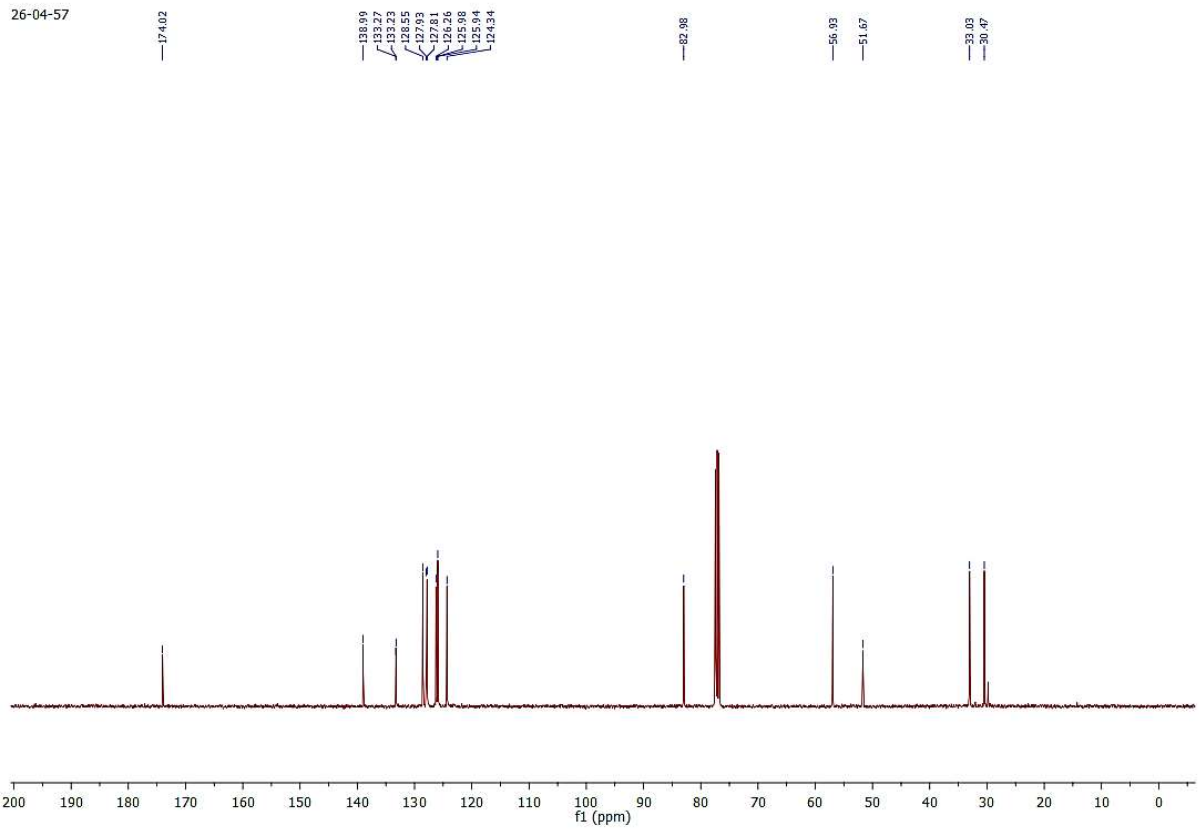

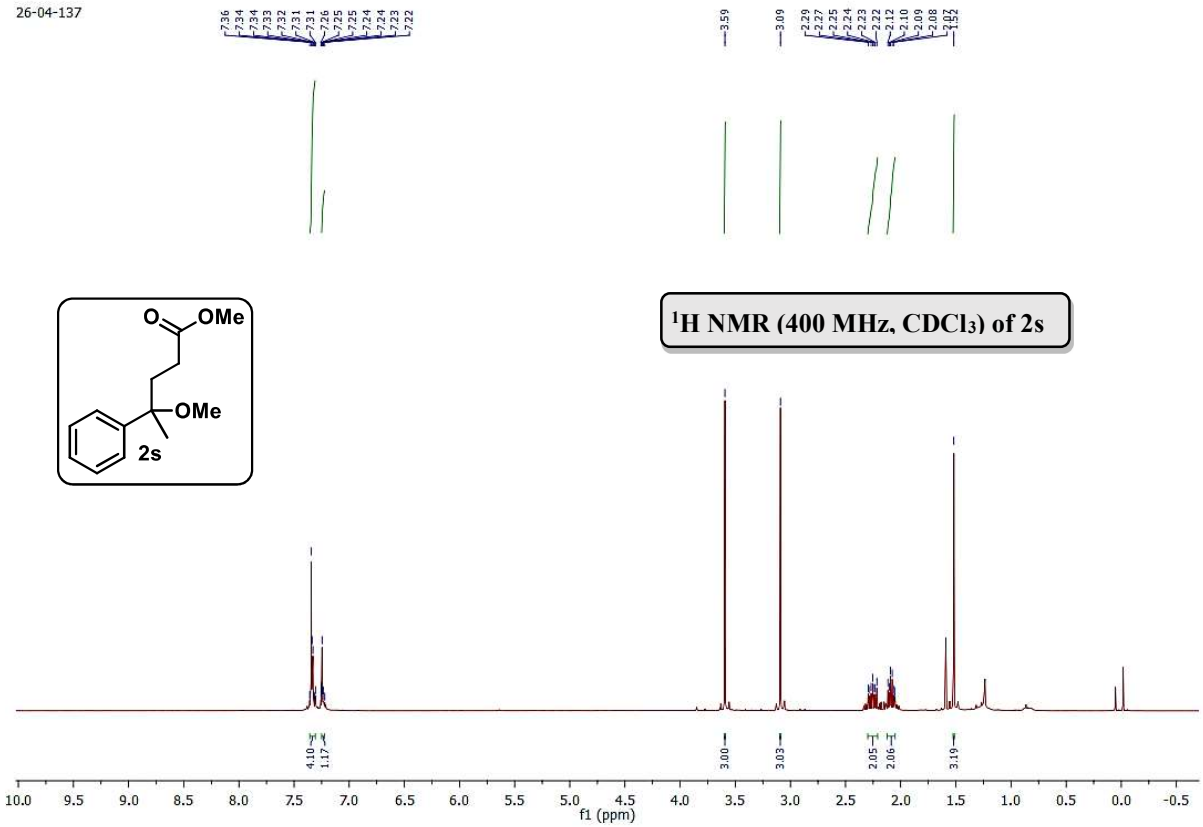

^{1}H NMR (400 MHz, $CDCl_3$) of 2s

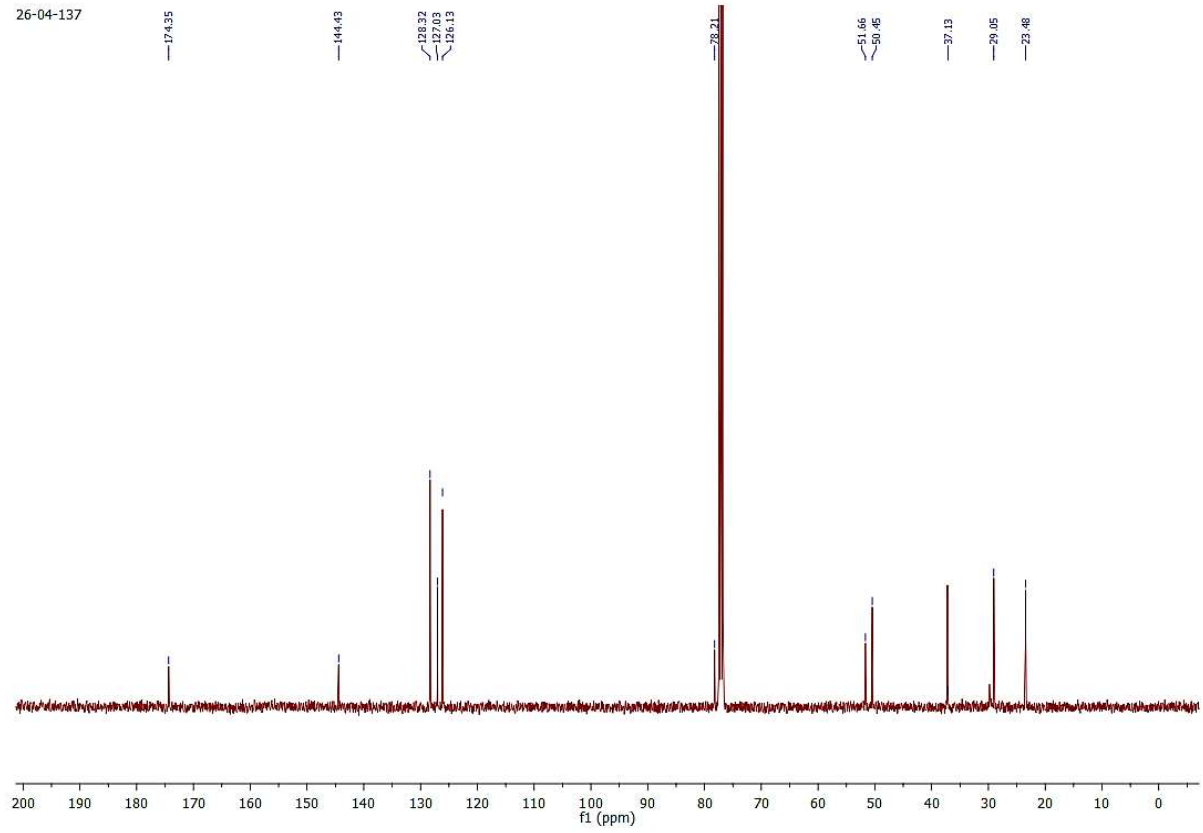

$^{13}C\{^{1}H\}$ NMR (100 MHz, $CDCl_3$) of 2s

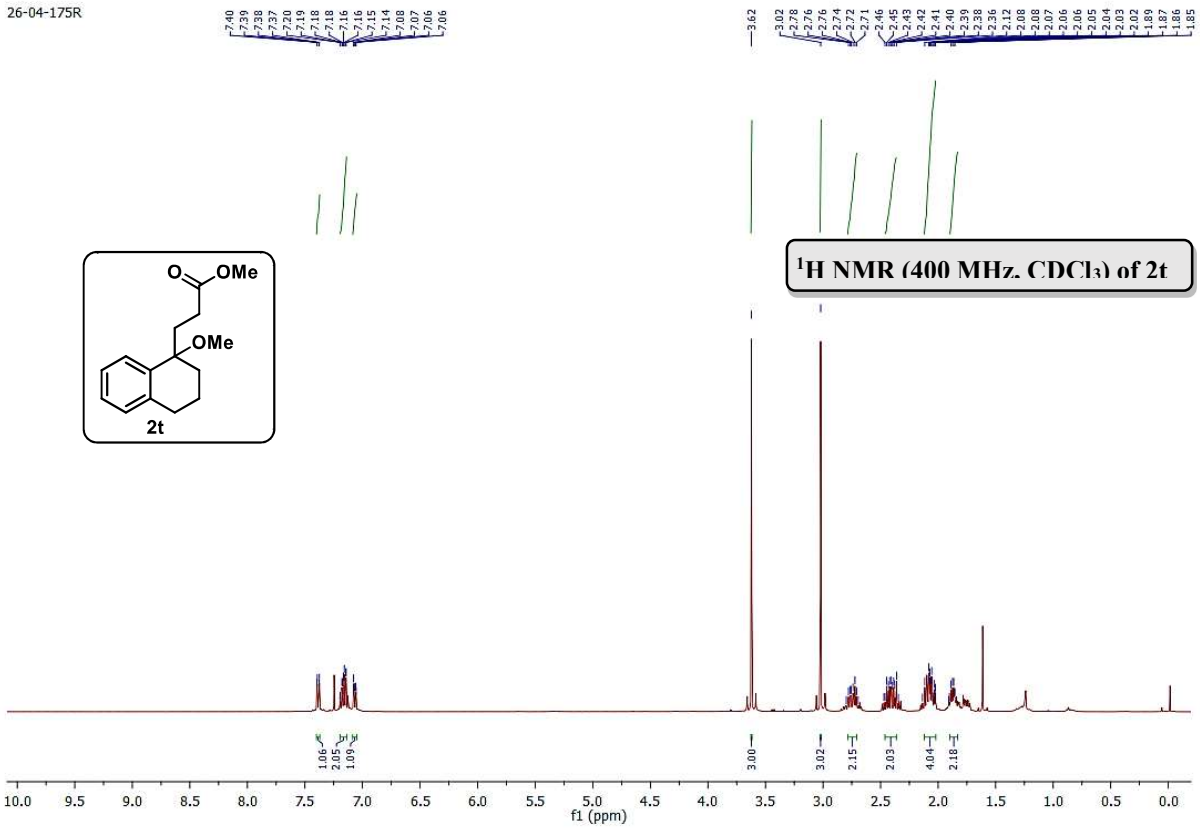

^{1}H NMR (400 MHz, $CDCl_3$) of 2t

$^{13}C\{^{1}H\}$ NMR (100 MHz, $CDCl_3$) of 2t

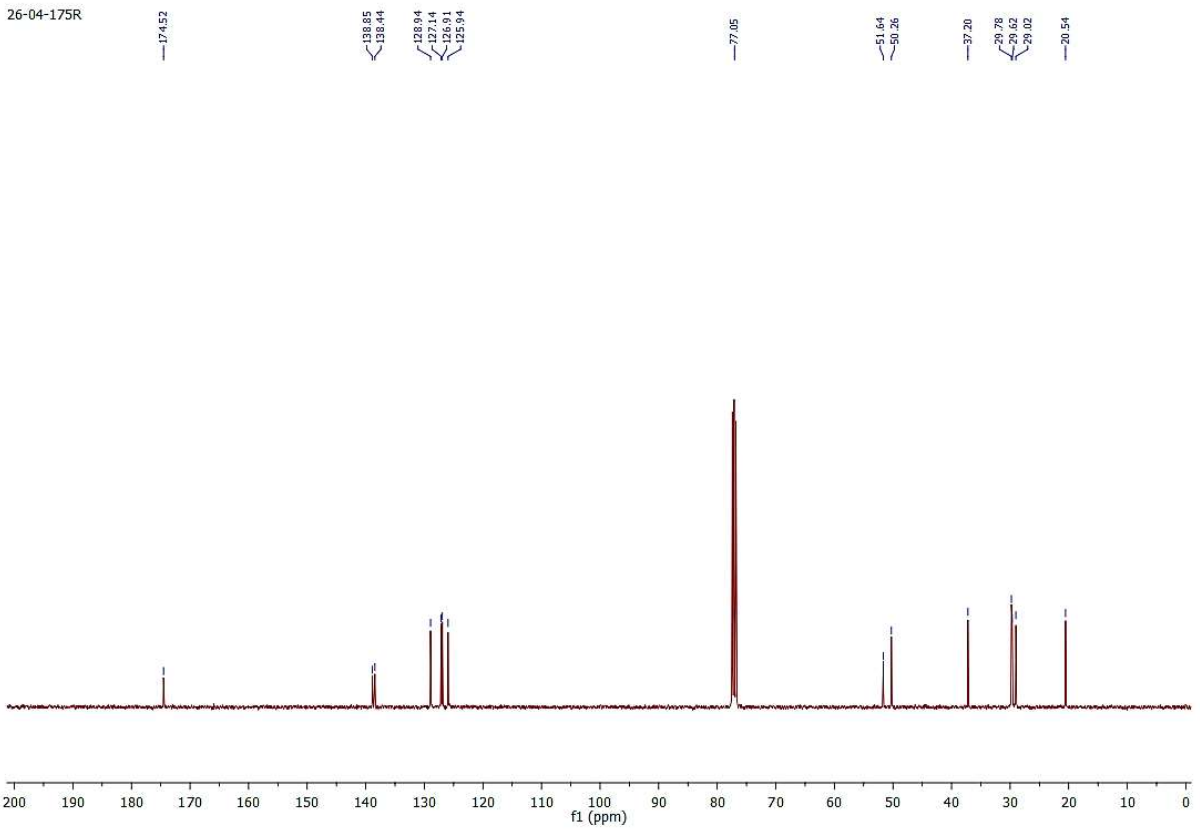

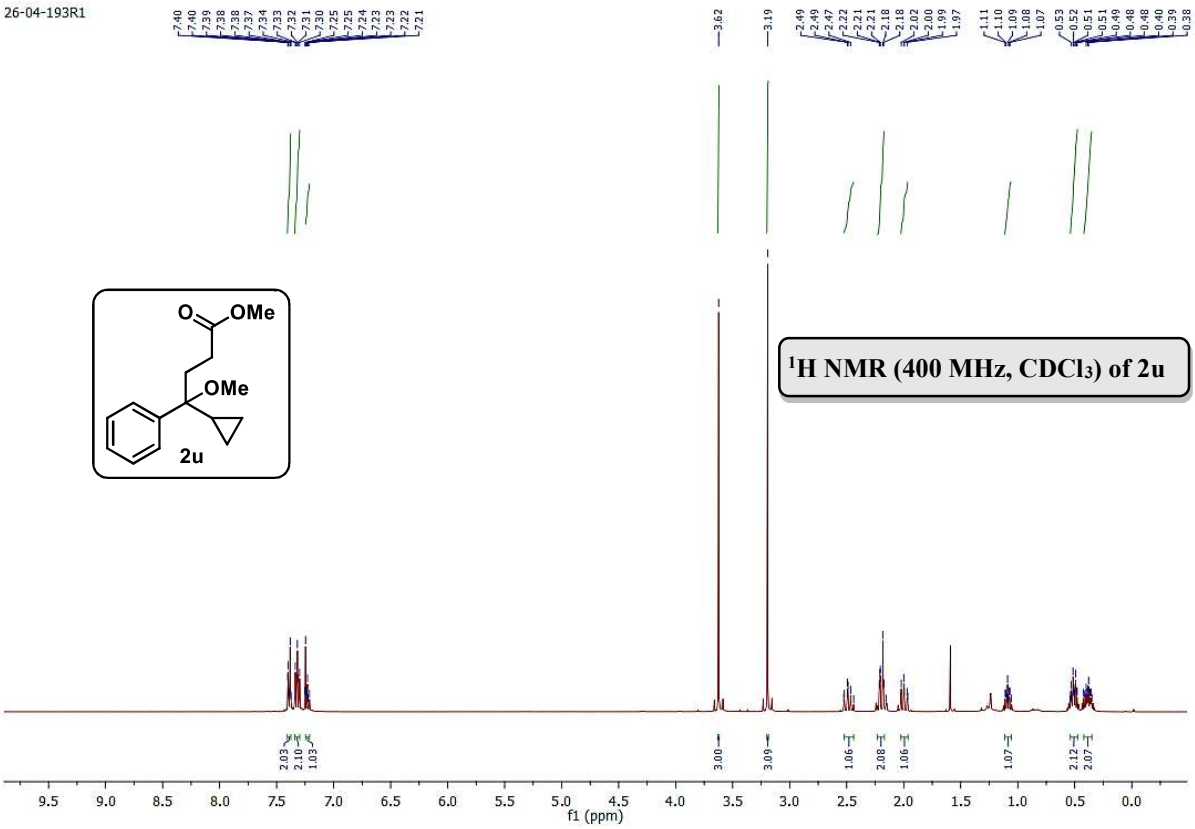

^{1}H NMR (400 MHz, $CDCl_3$) of 2u

$^{13}C\{^{1}H\}$ NMR (100 MHz, $CDCl_3$) of 2u

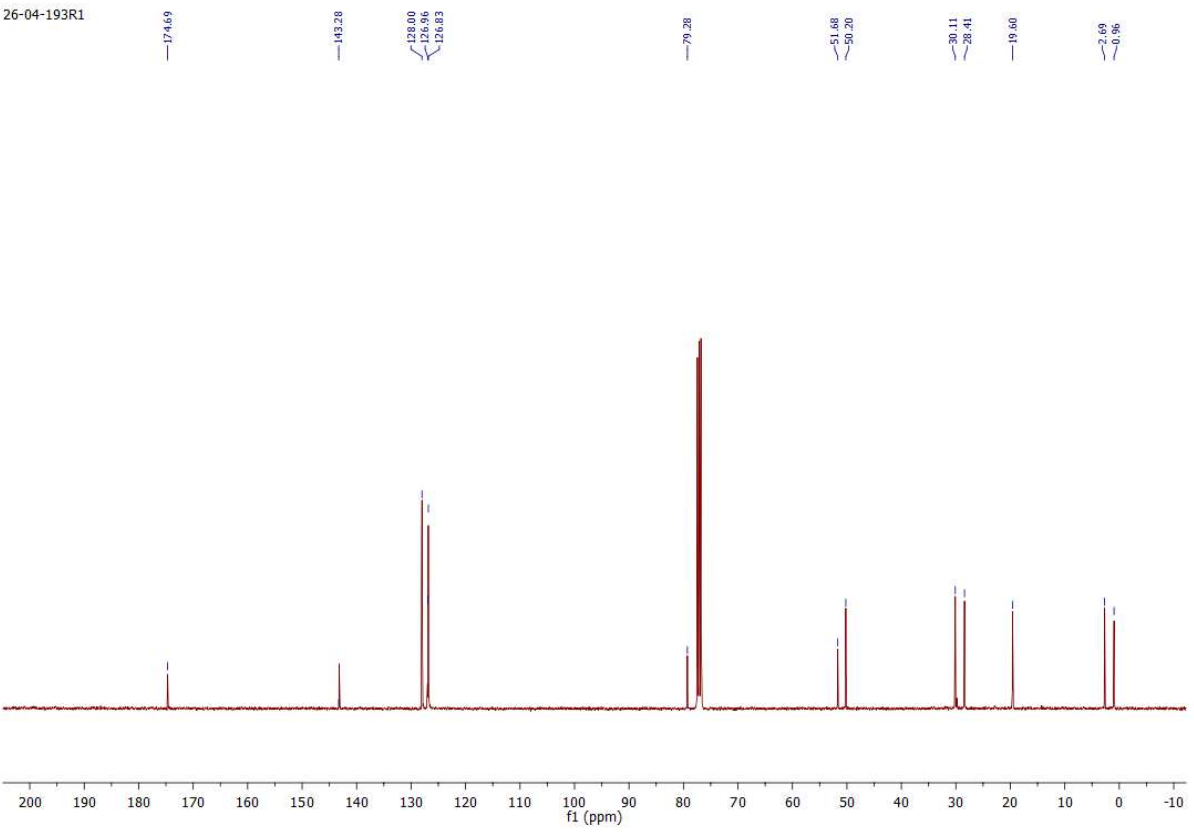

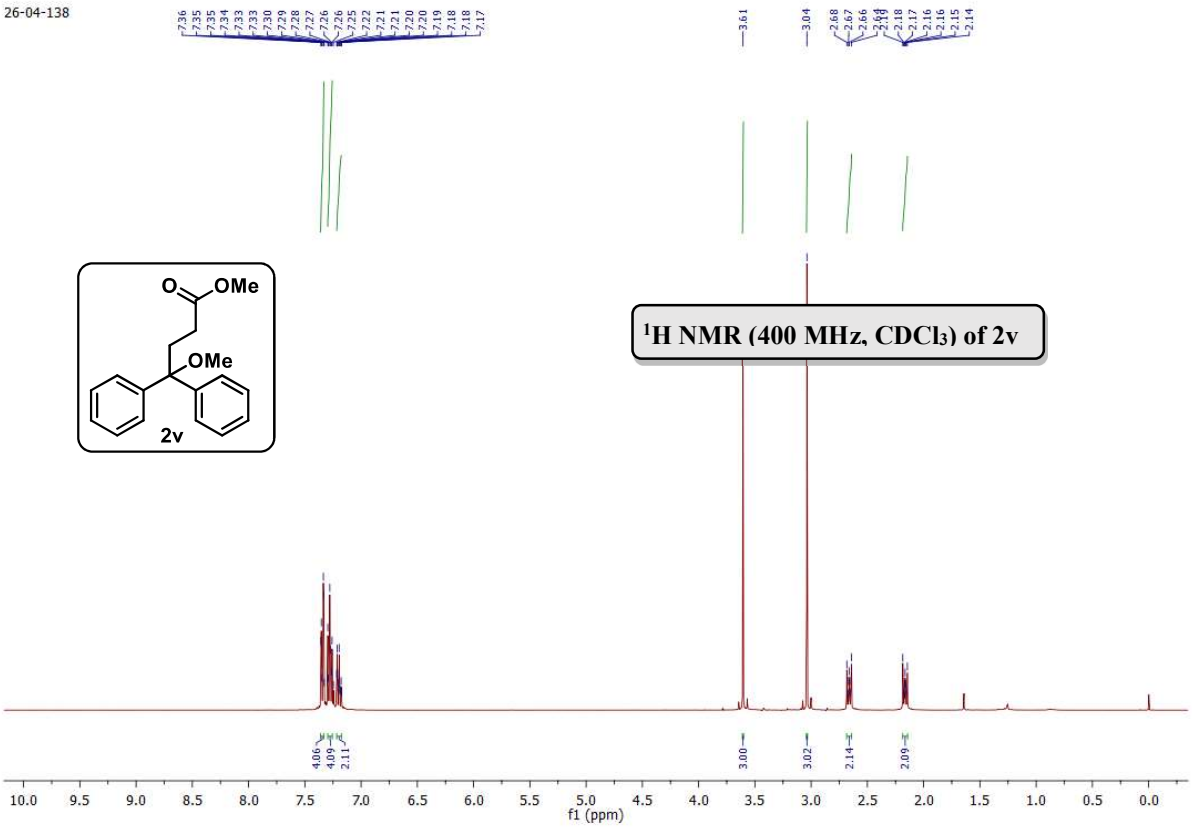

^{1}H NMR (400 MHz, $CDCl_3$) of 2v

$^{13}C\{^{1}H\}$ NMR (100 MHz, $CDCl_3$) of 2v

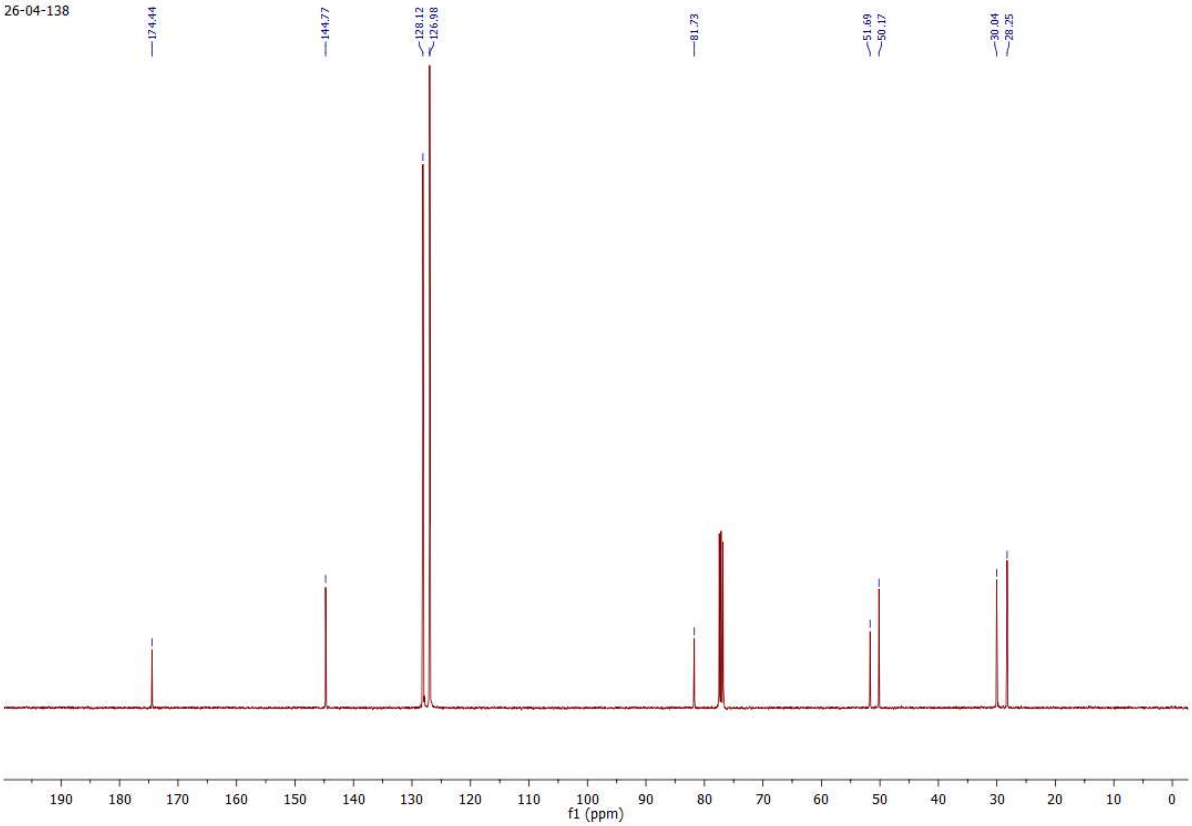

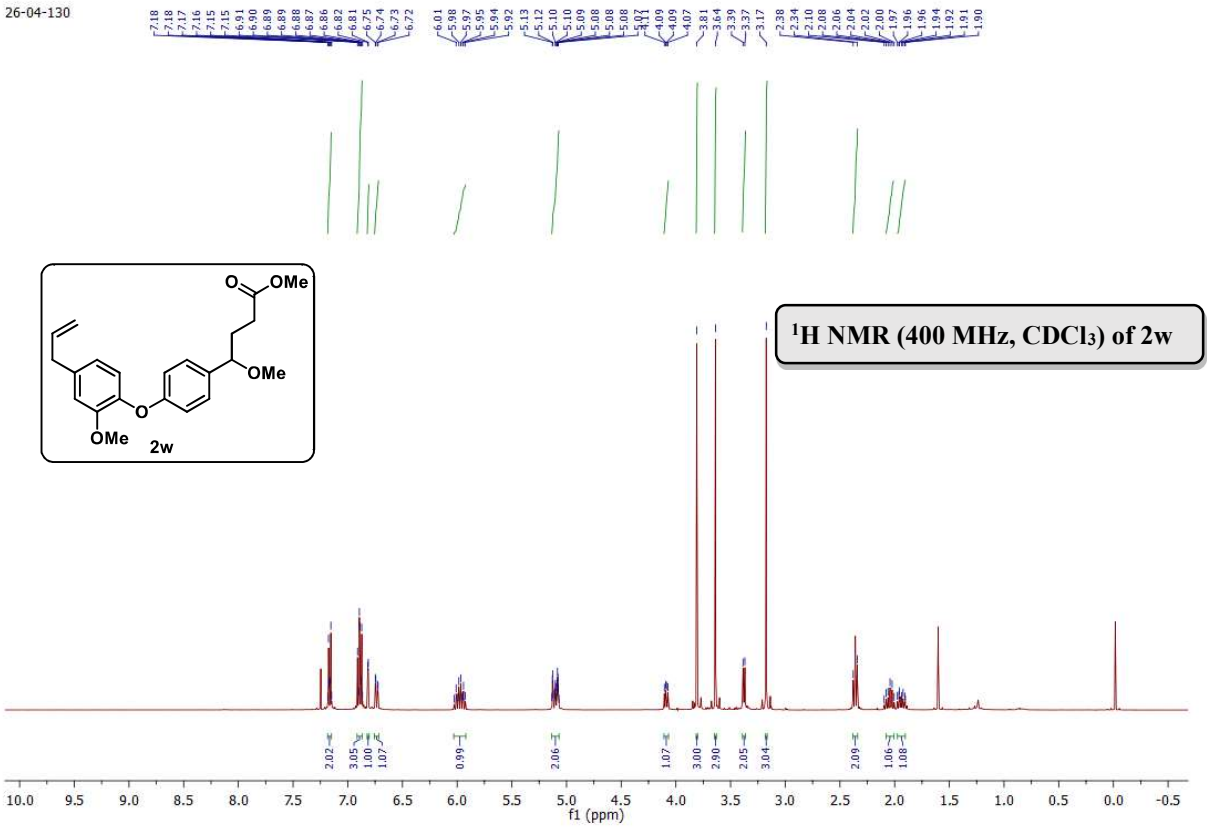

^{1}H NMR (400 MHz, $CDCl_3$) of 2w

$^{13}C\{^{1}H\}$ NMR (100 MHz, $CDCl_3$) of 2w

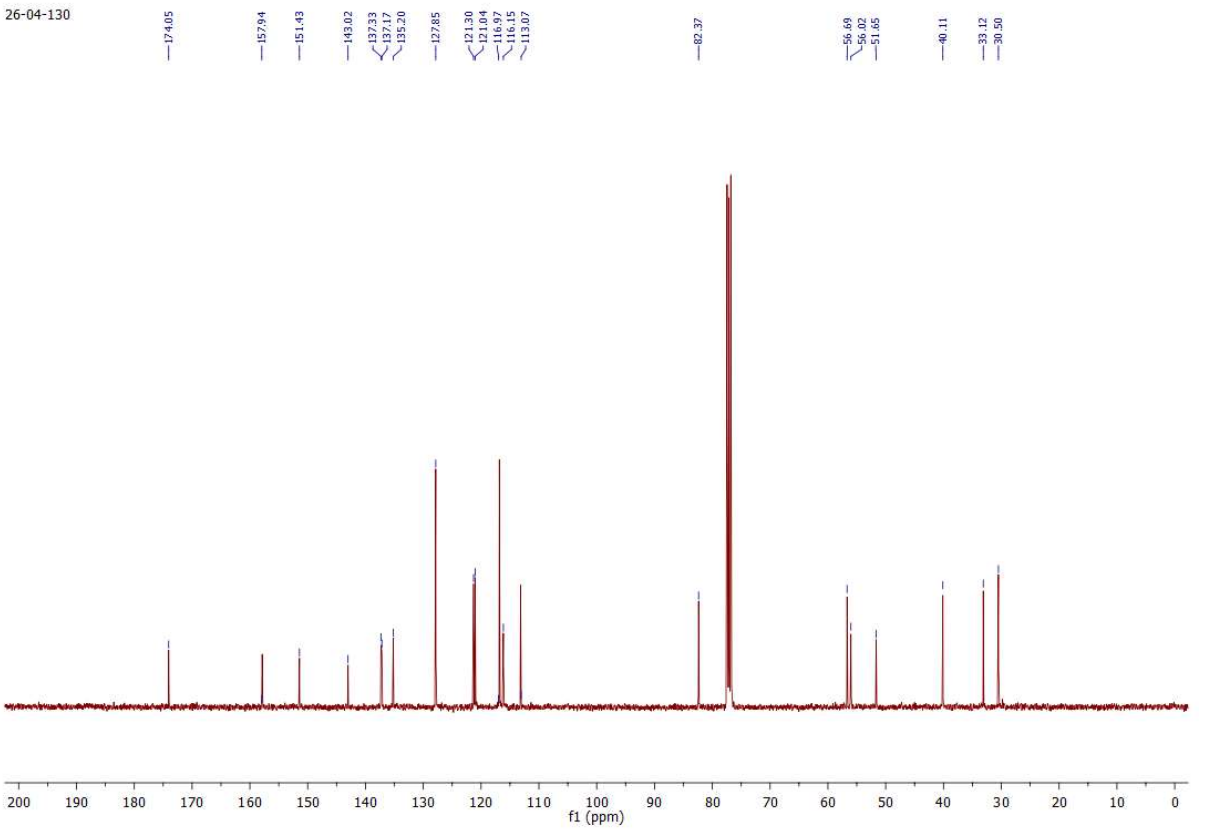

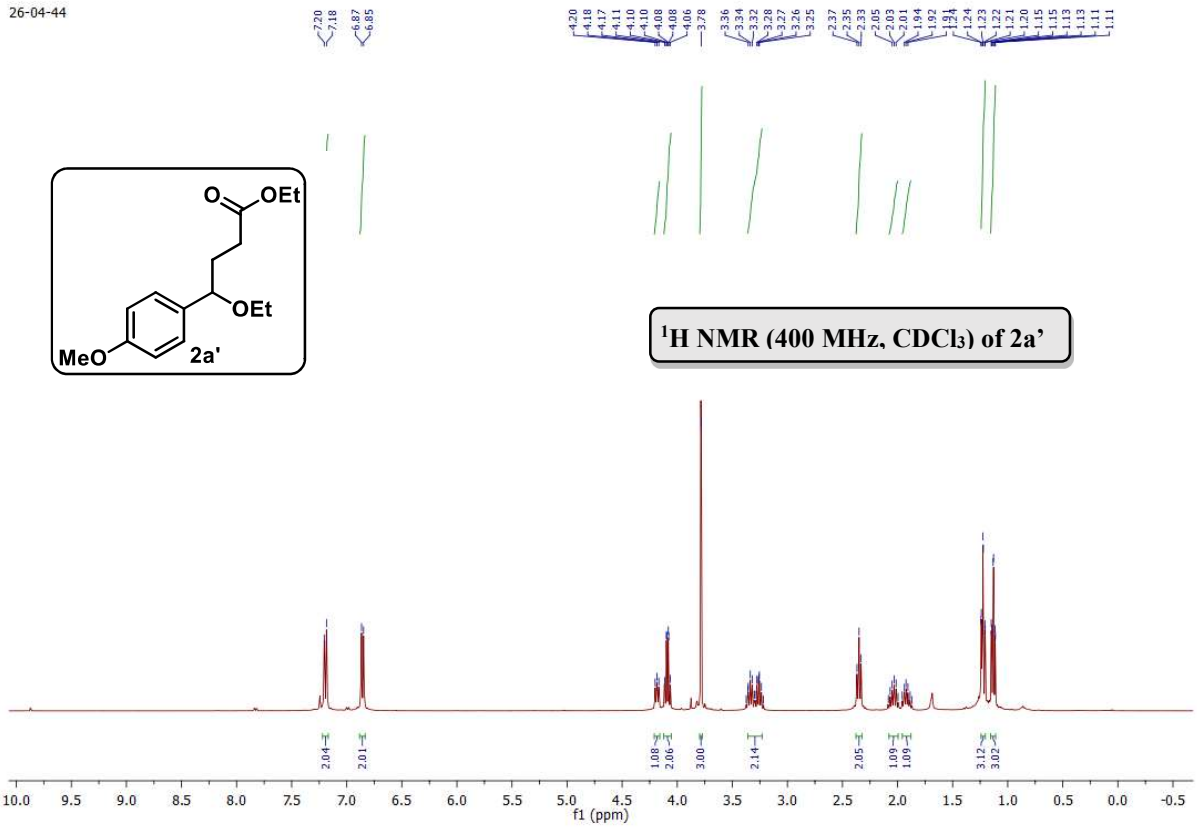

^{1}H NMR (400 MHz, $CDCl_3$) of 2a'

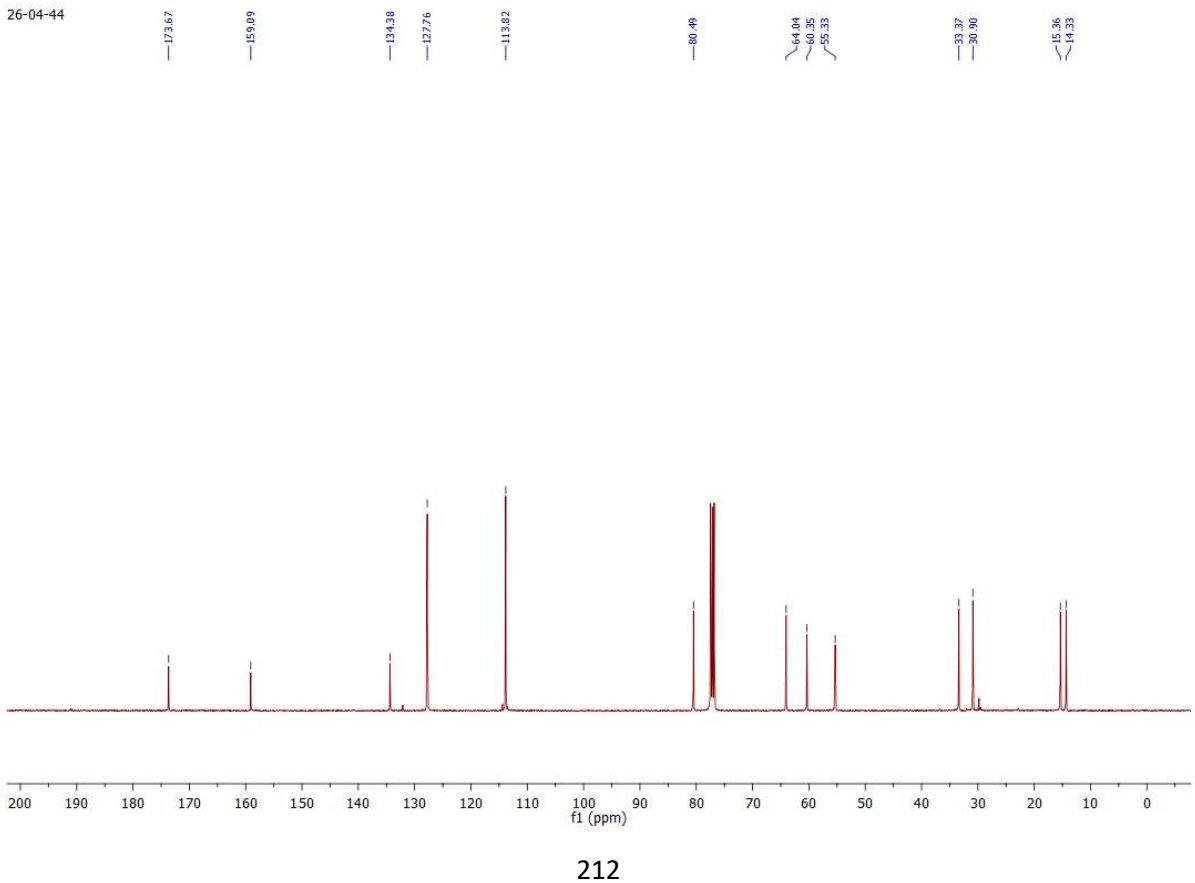

$^{13}C\{^{1}H\}$ NMR (100 MHz, $CDCl_3$) of 2a'

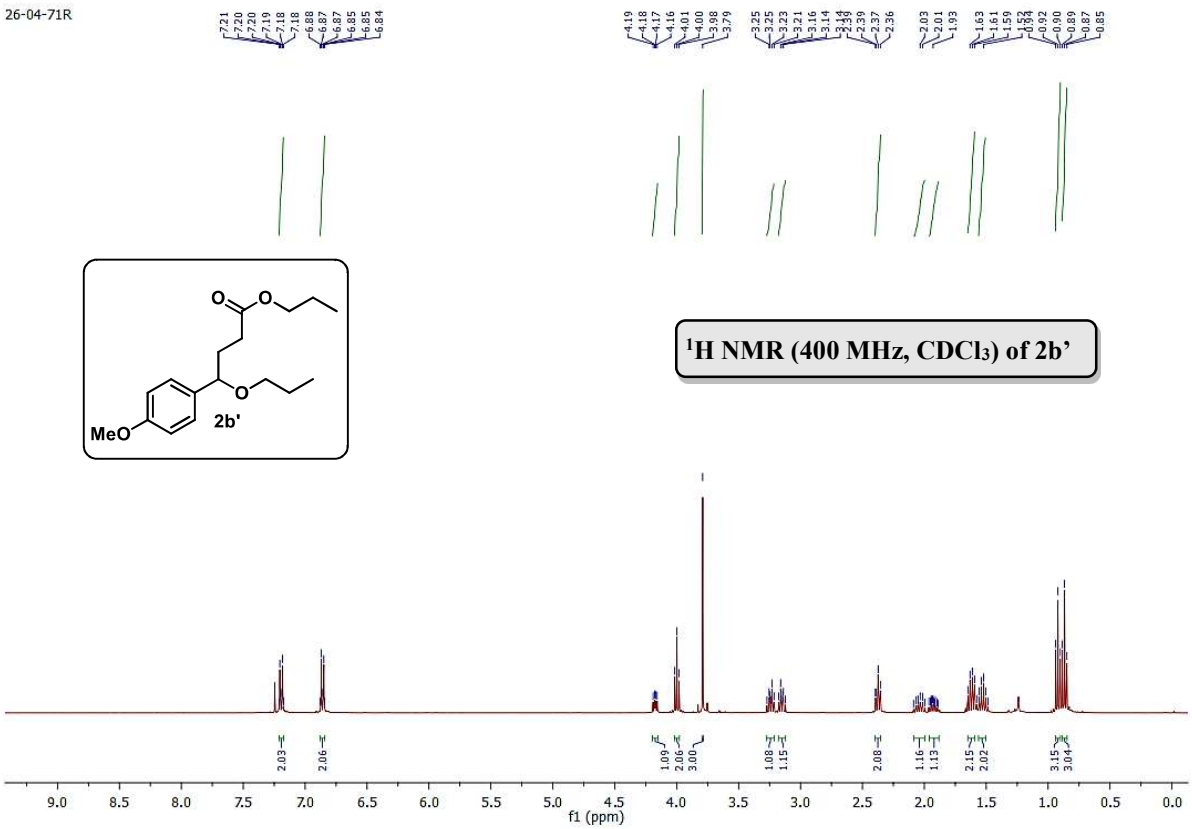

^{1}H NMR (400 MHz, $CDCl_3$) of 2b'

^{1}H NMR (400 MHz, $CDCl_3$) of 2b'

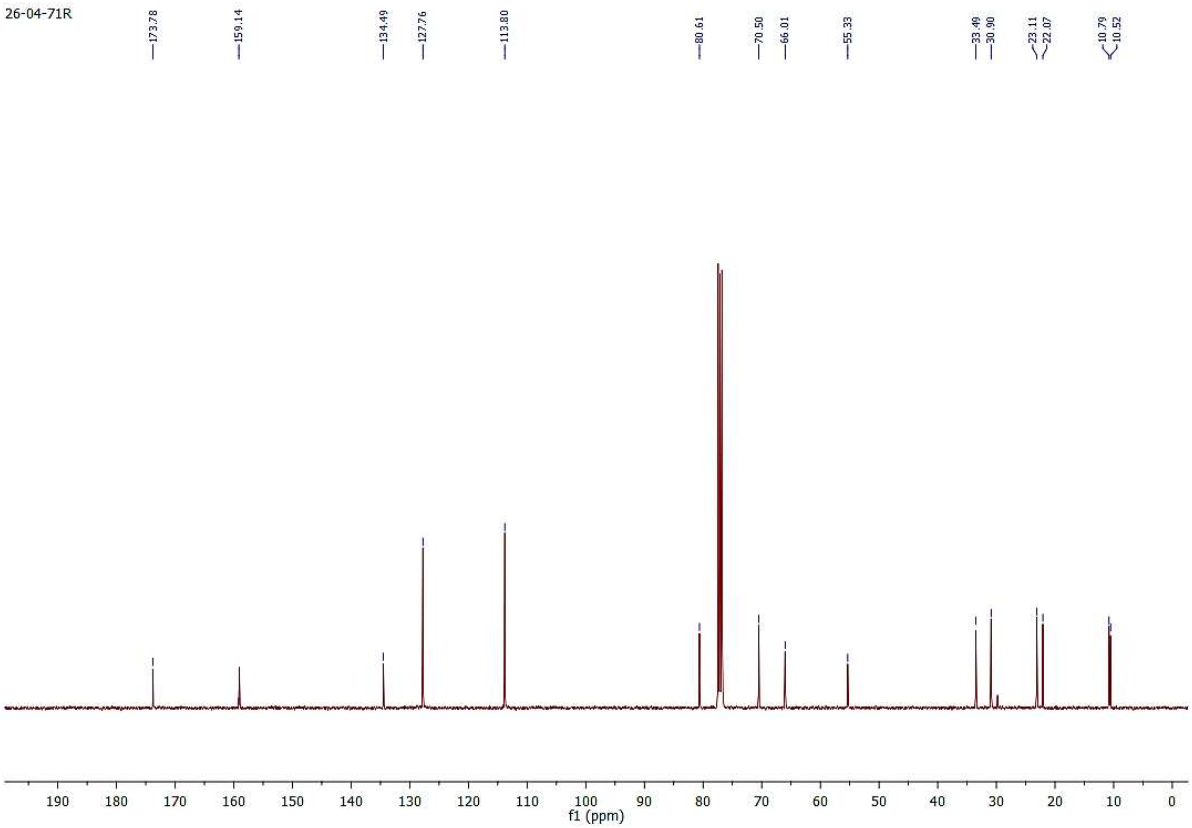

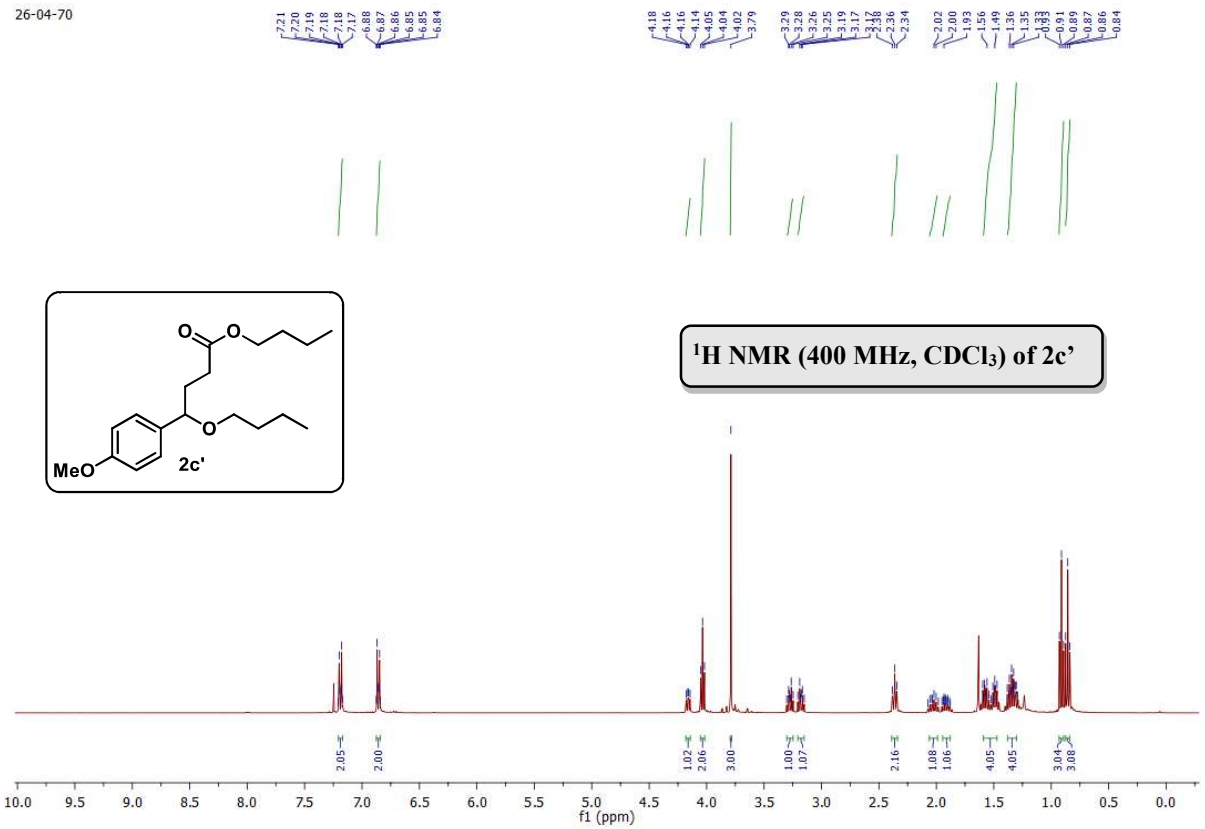

^{1}H NMR (400 MHz, $CDCl_3$) of 2c'

$^{13}C\{^{1}H\}$ NMR (100 MHz, $CDCl_3$) of 2c'

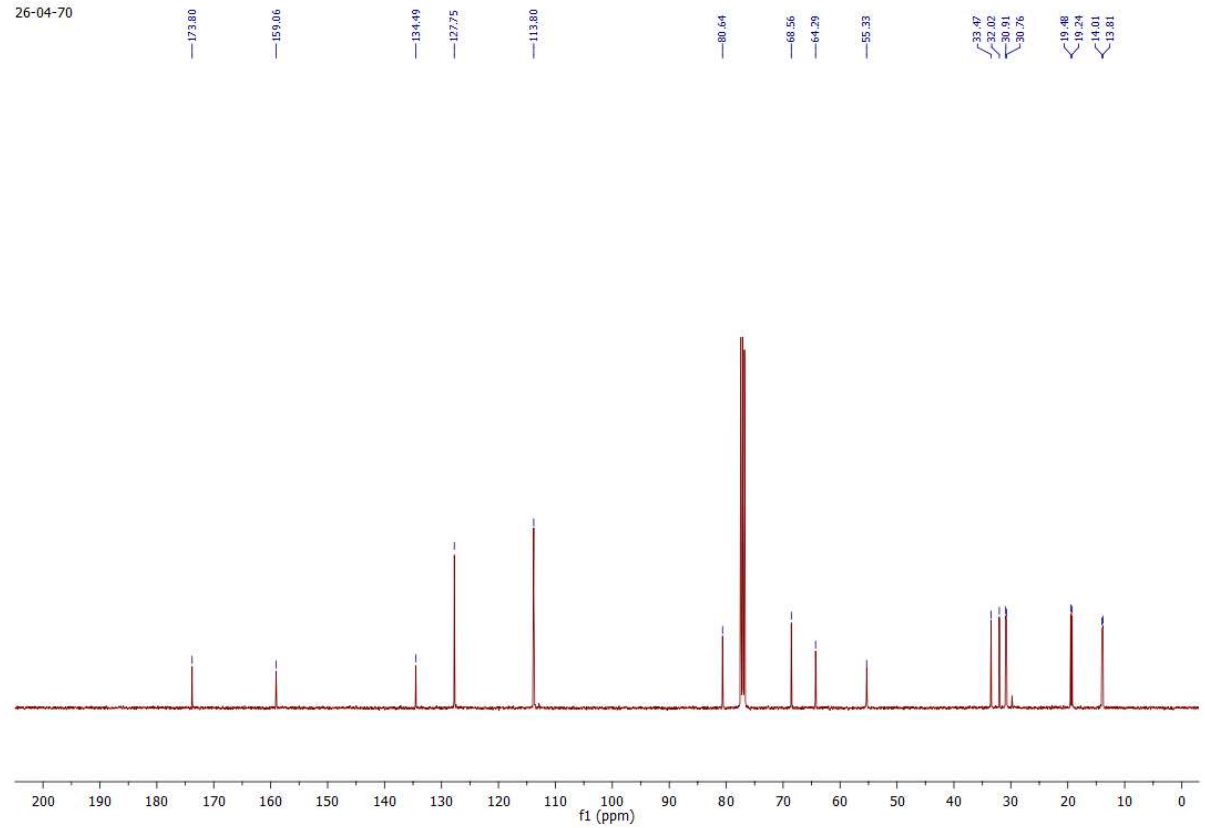

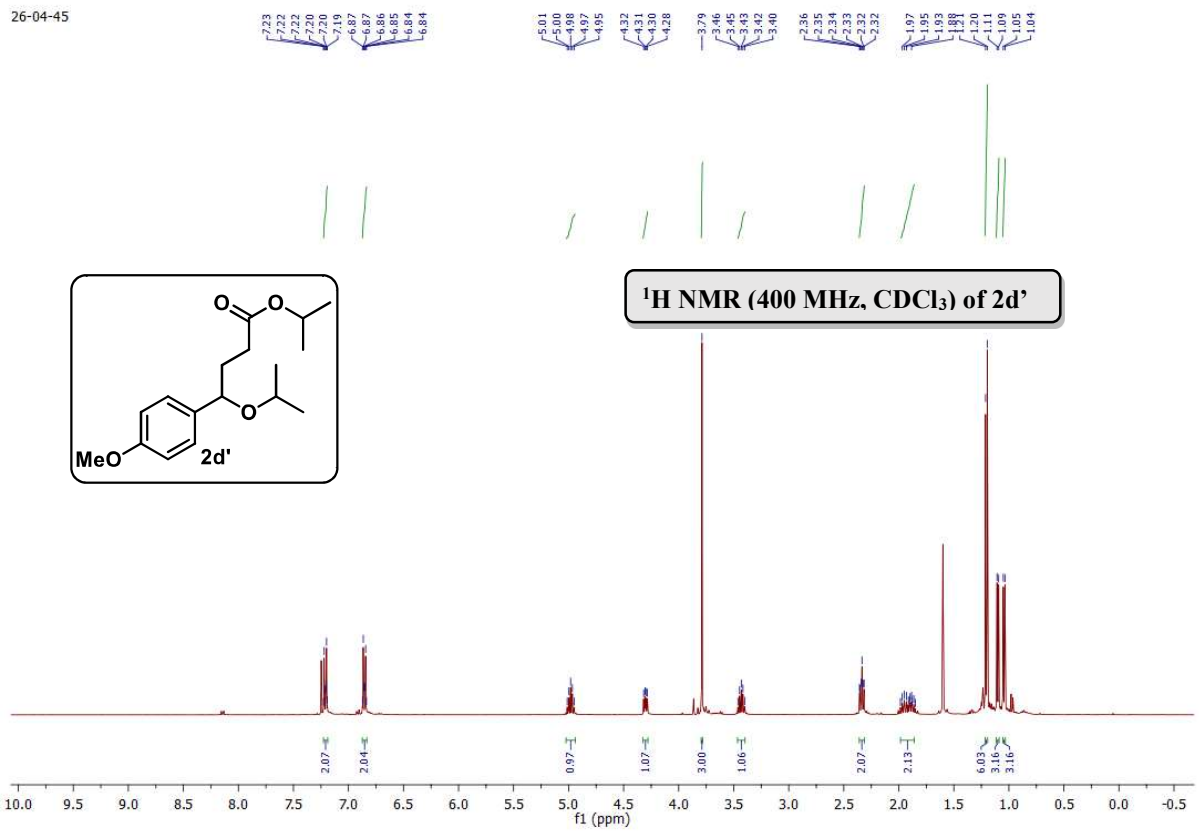

^{1}H NMR (400 MHz, $CDCl_3$) of 2d'

$^{13}C\{^{1}H\}$ NMR (100 MHz, DMSO-d^6) of 2d'

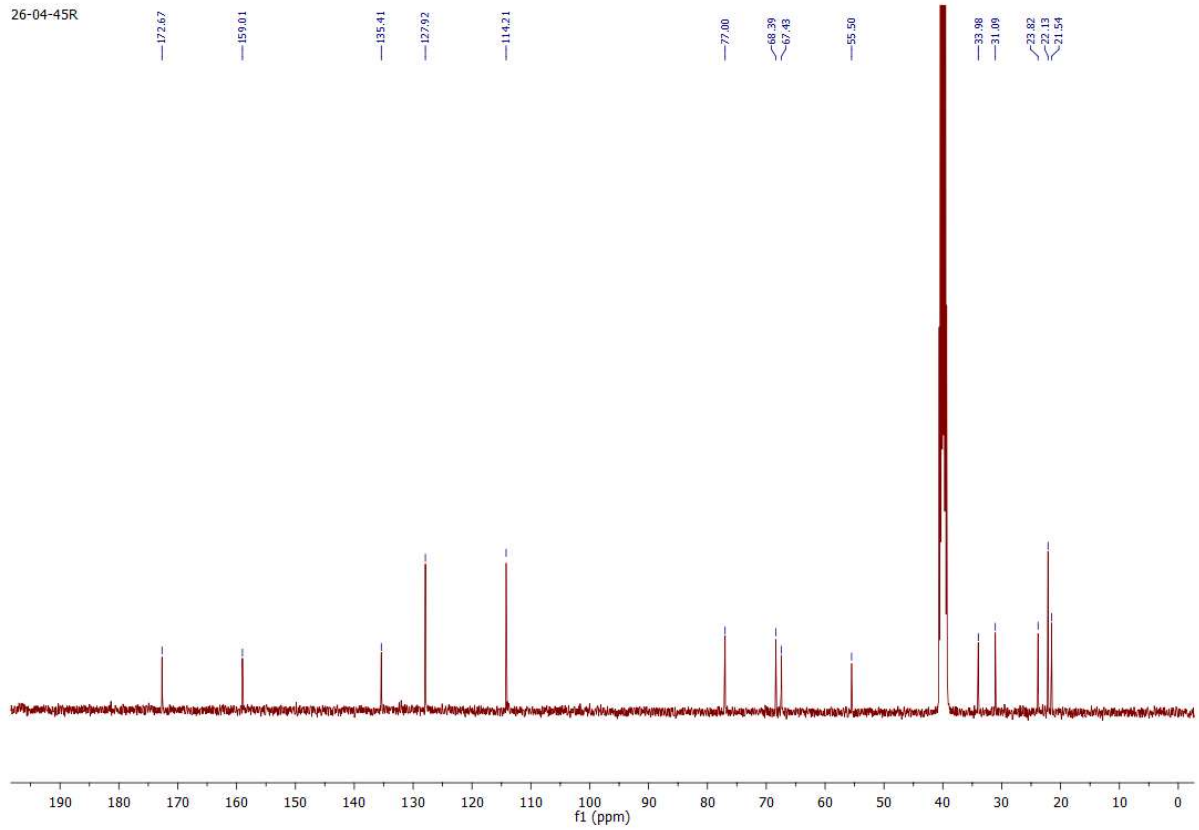

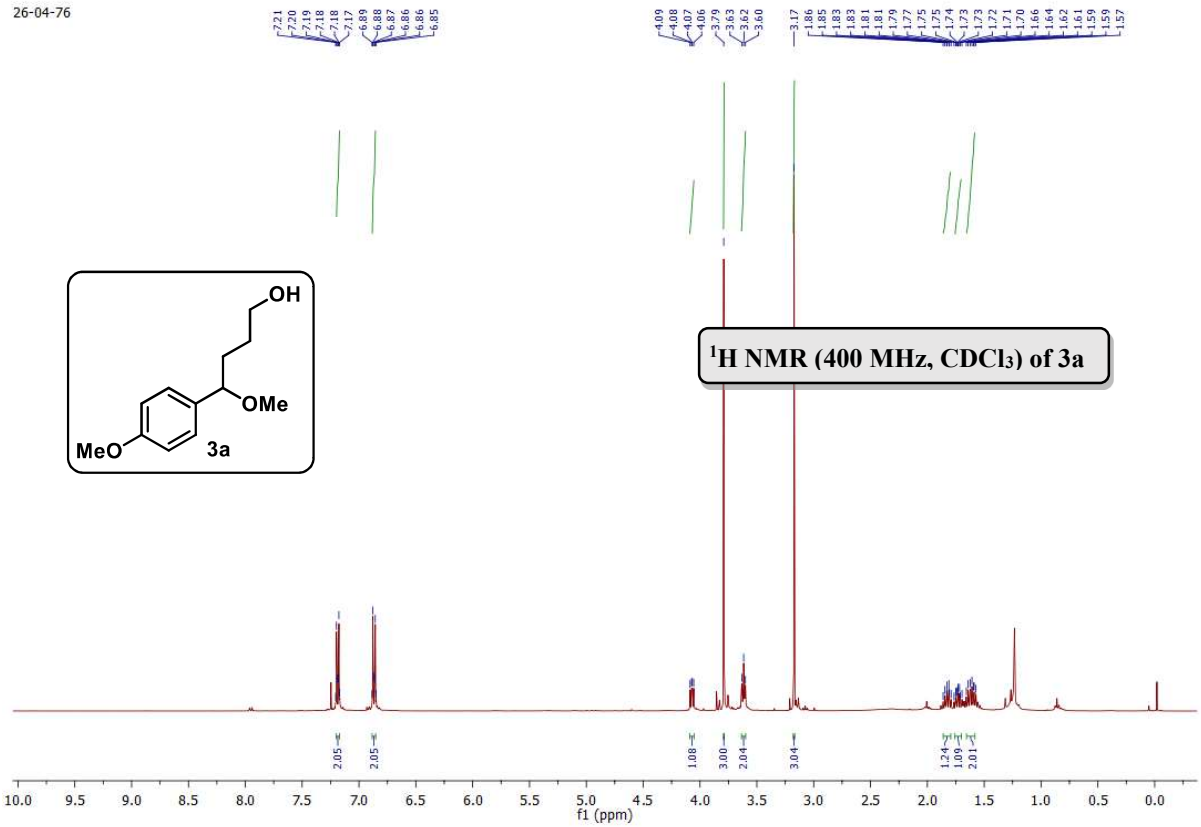

^{1}H NMR (400 MHz, $CDCl_3$) of 3a

$^{13}C\{^{1}H\}$ NMR (100 MHz, $CDCl_3$) of 3a

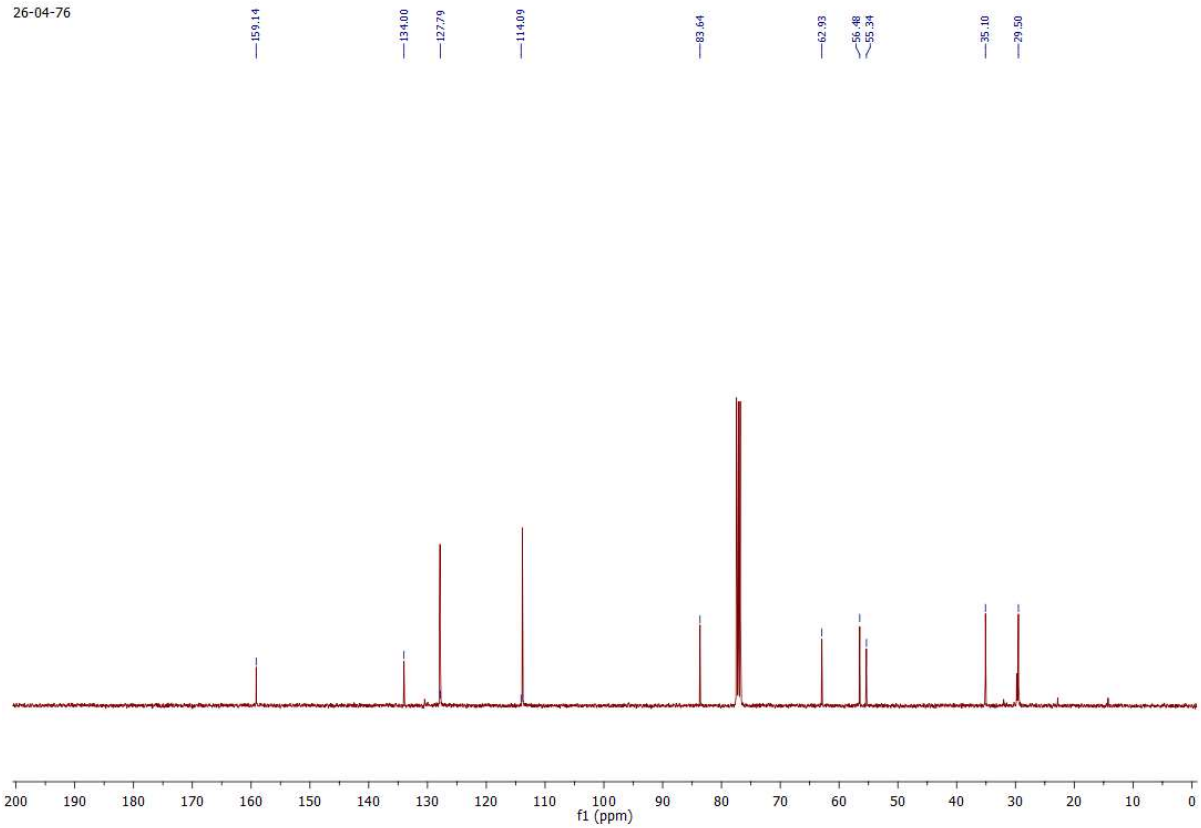

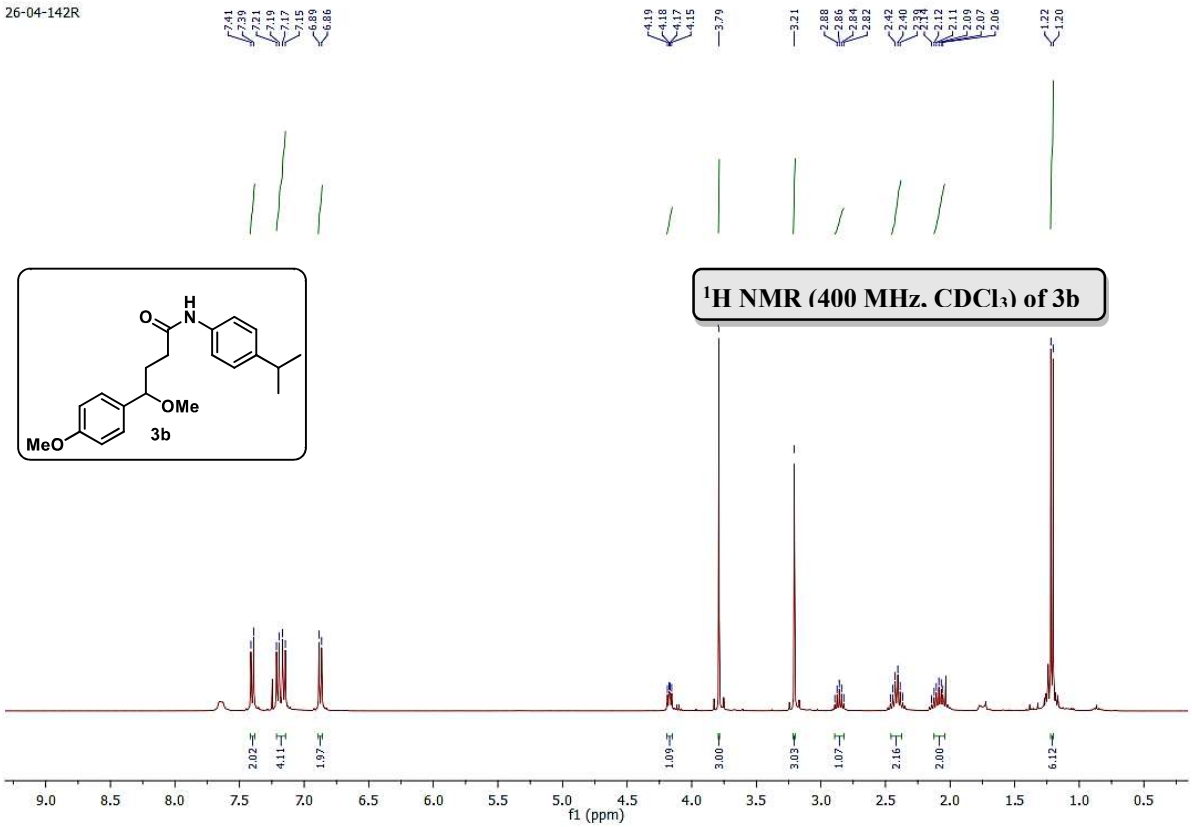

^{1}H NMR (400 MHz. $CDCl_3$) of 3b

$^{13}C\{^{1}H\}$ NMR (100 MHz, $CDCl_3$) of 3b

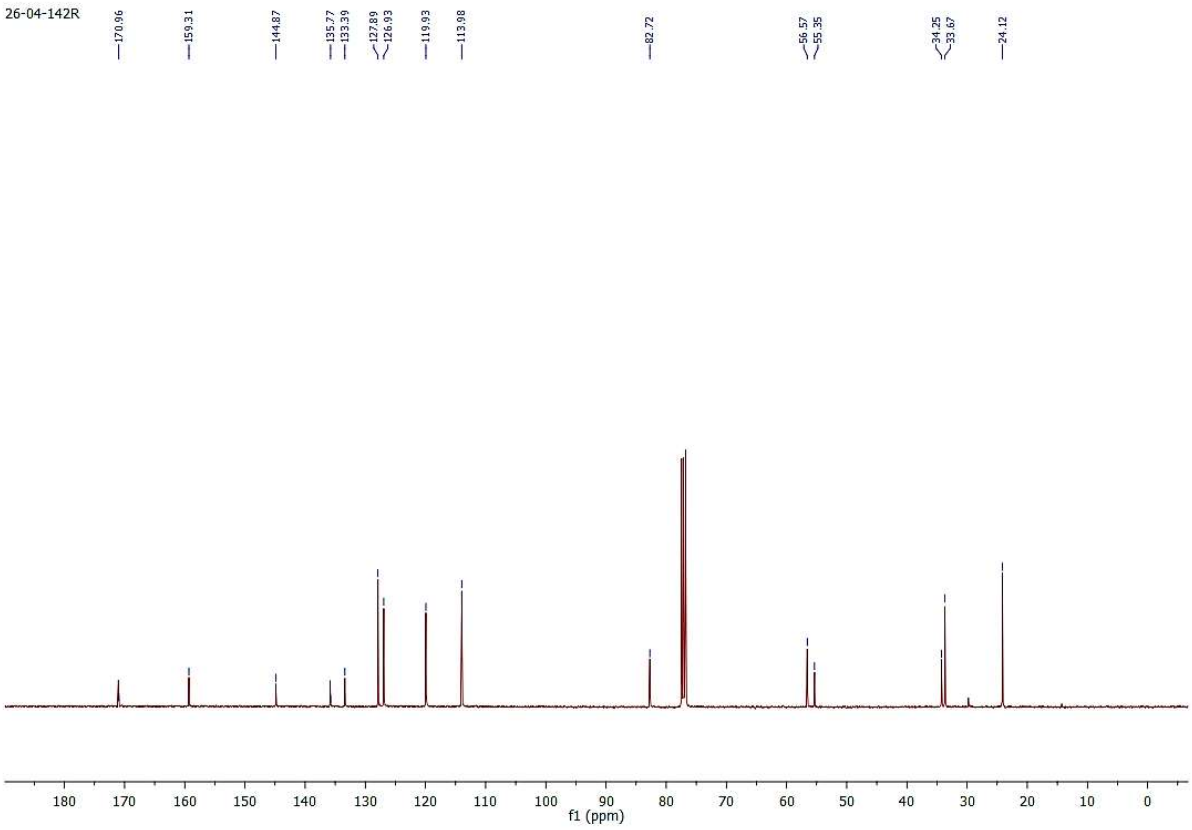

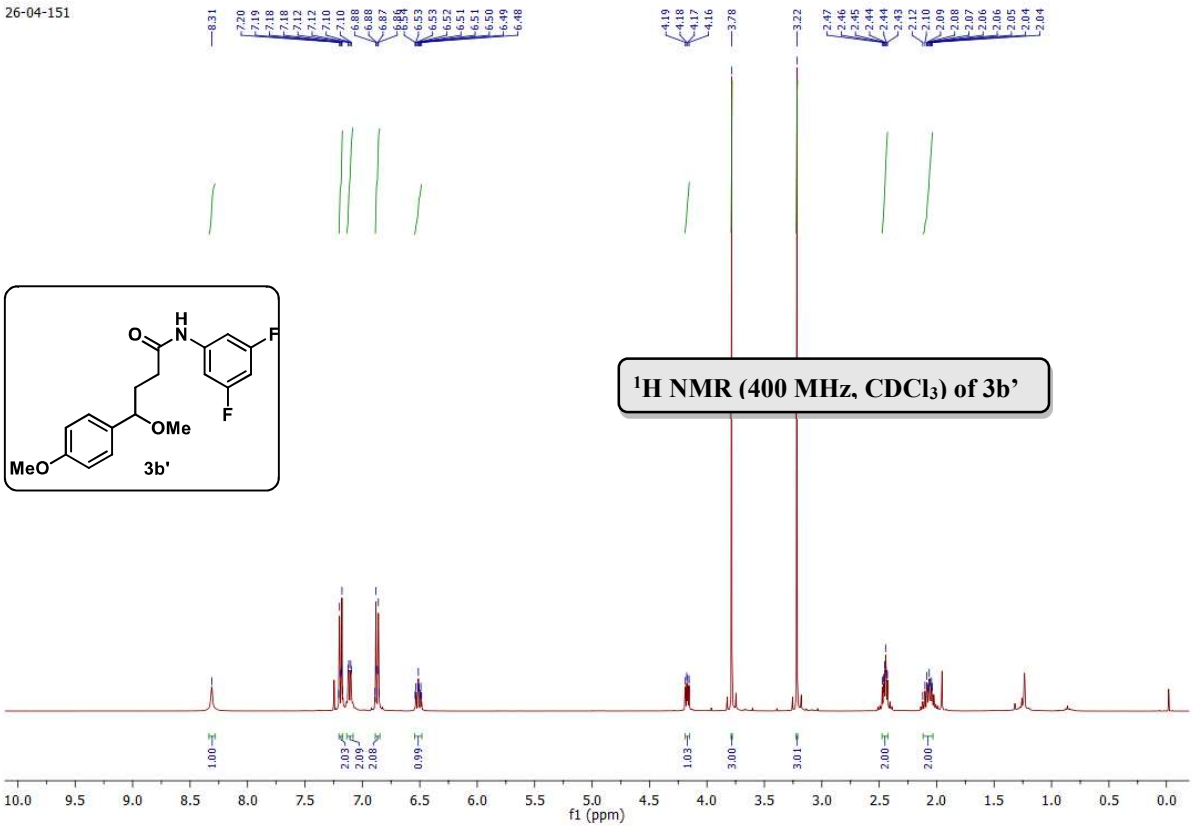

^{1}H NMR (400 MHz, $CDCl_3$) of 3b'

$^{13}C\{^{1}H\}$ NMR (100 MHz, $CDCl_3$) of 3b'

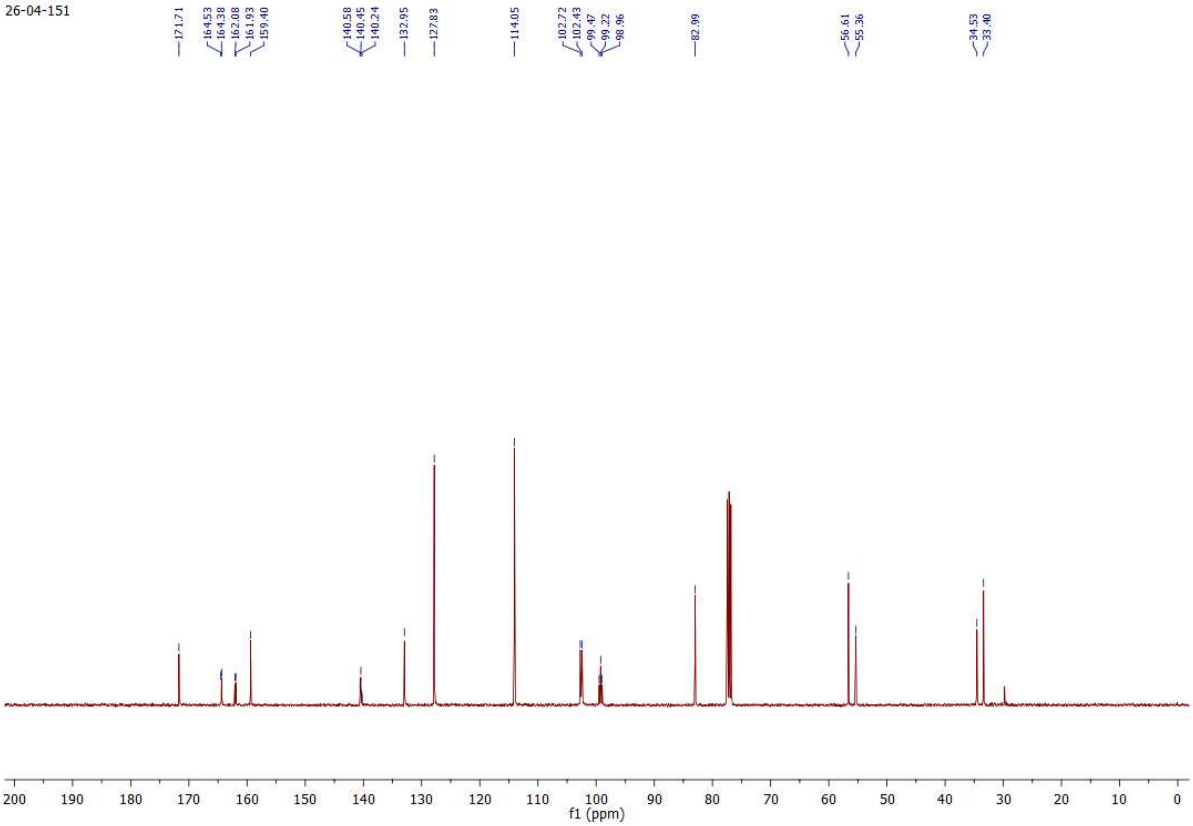

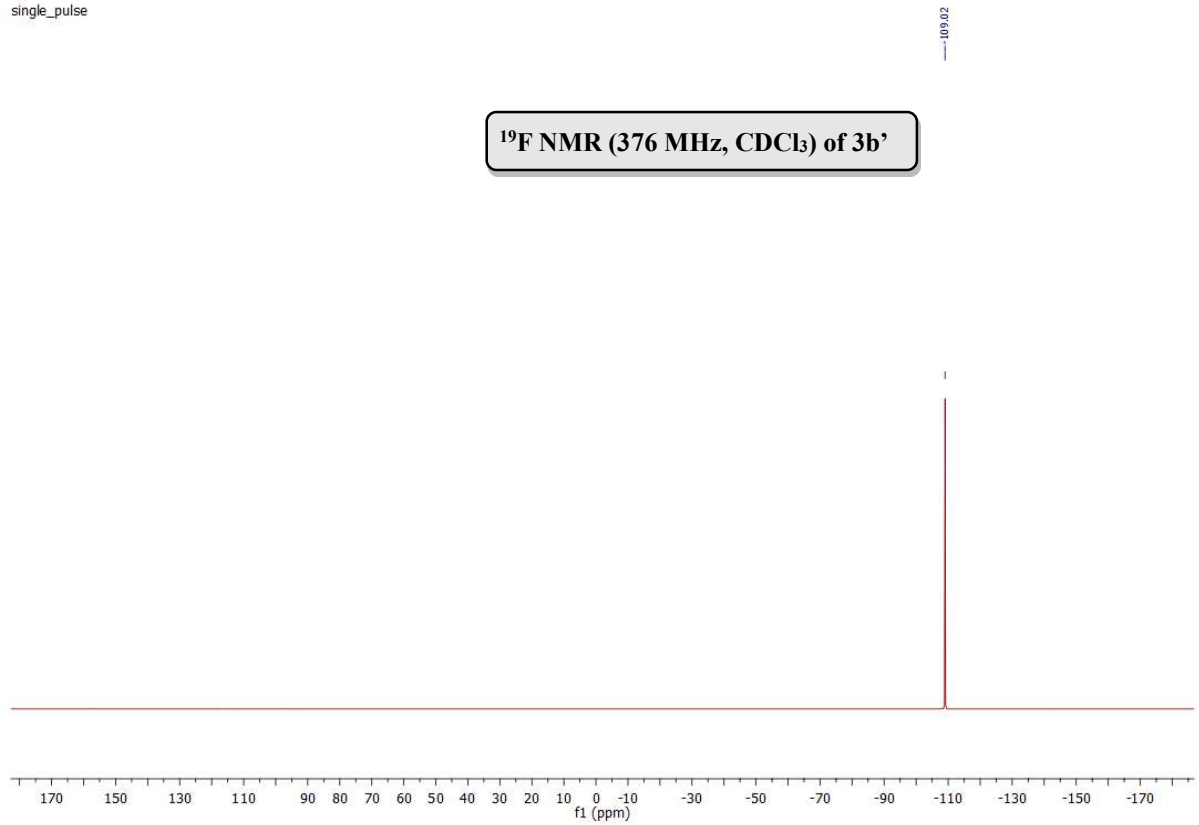

^{19}F NMR (376 MHz, $CDCl_3$) of 3b'

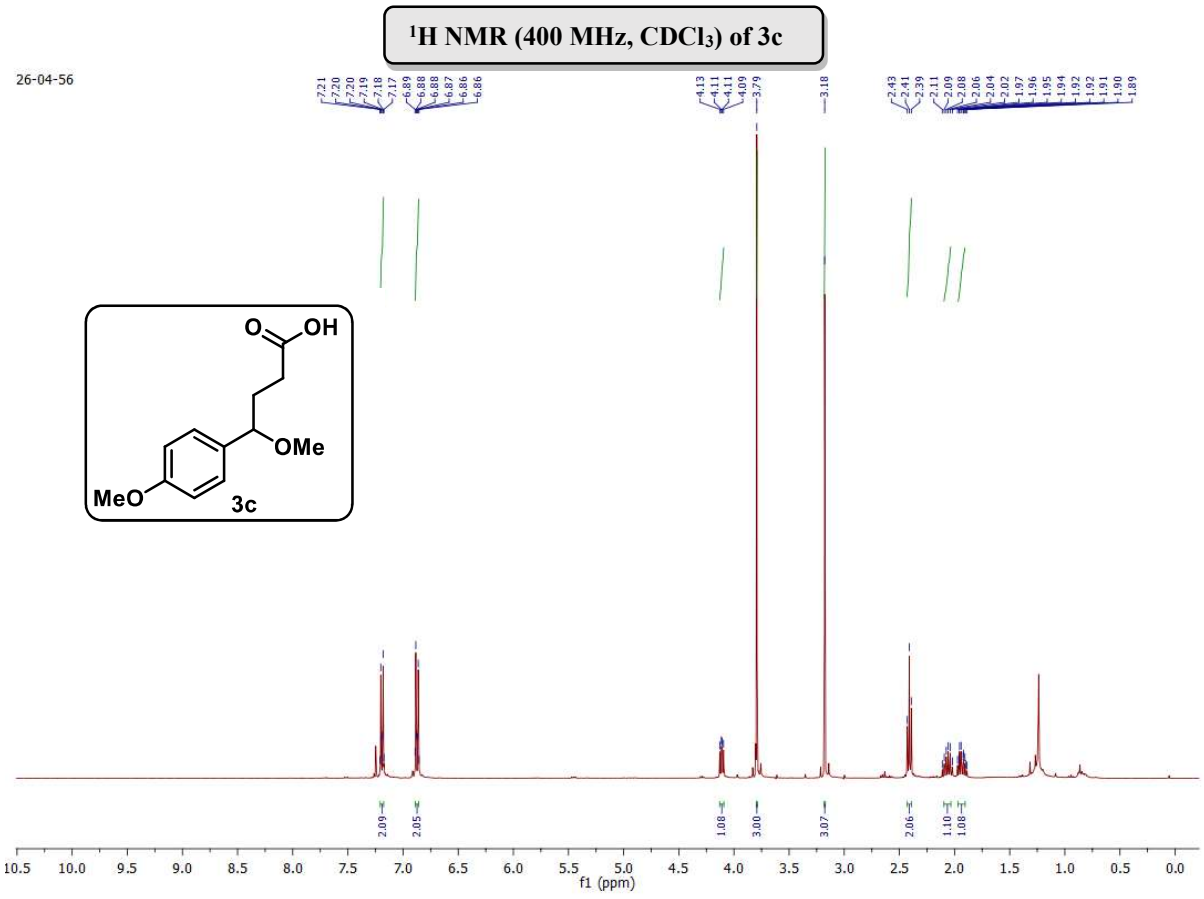

^{1}H NMR (400 MHz, $CDCl_3$) of 3c

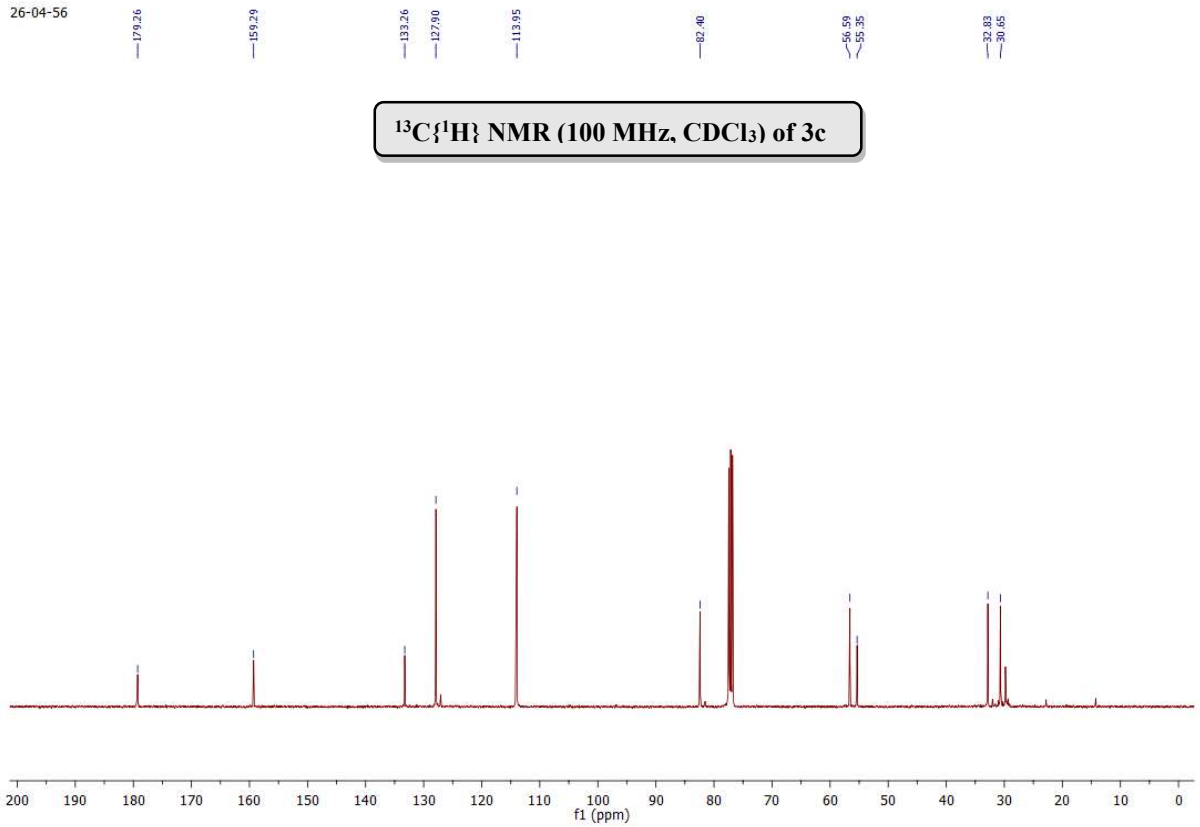

$^{13}C\{^{1}H\}$ NMR (100 MHz, $CDCl_3$) of 3c

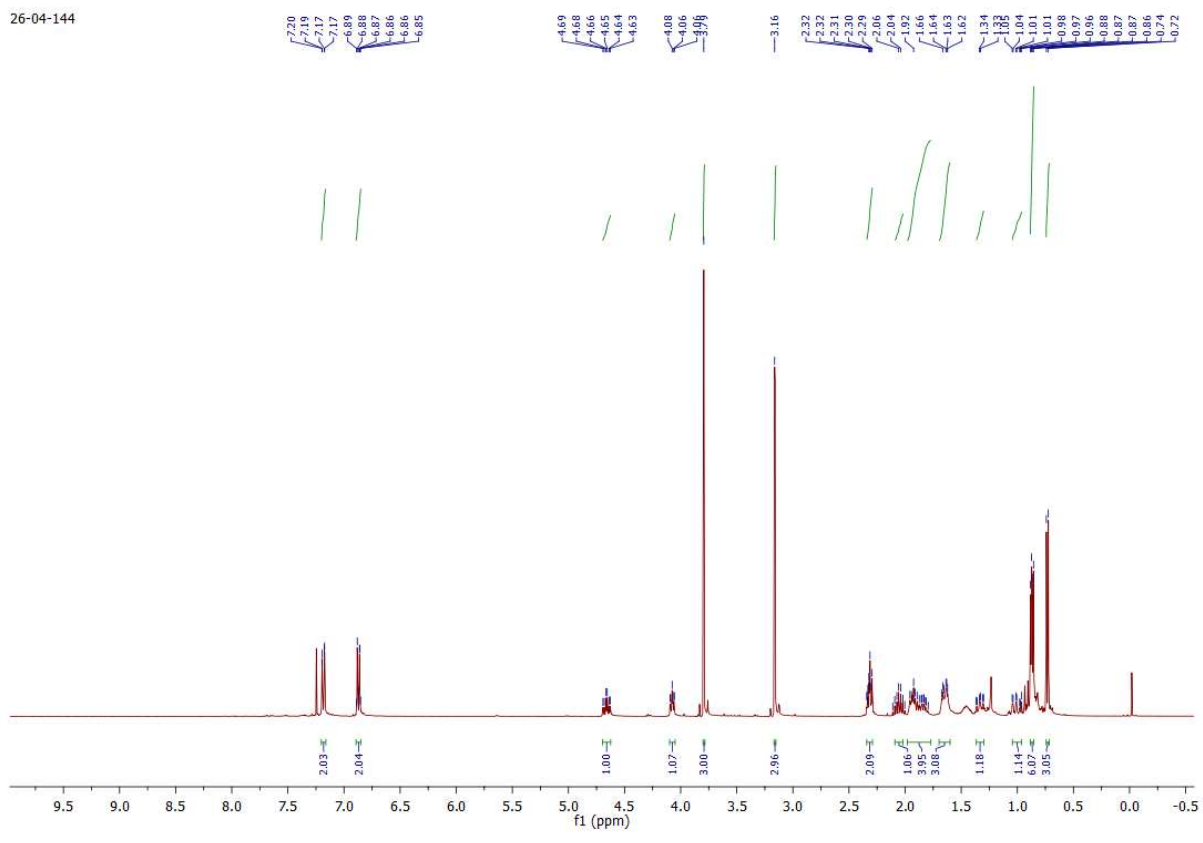

^{1}H NMR (400 MHz, $CDCl_3$) of 4c

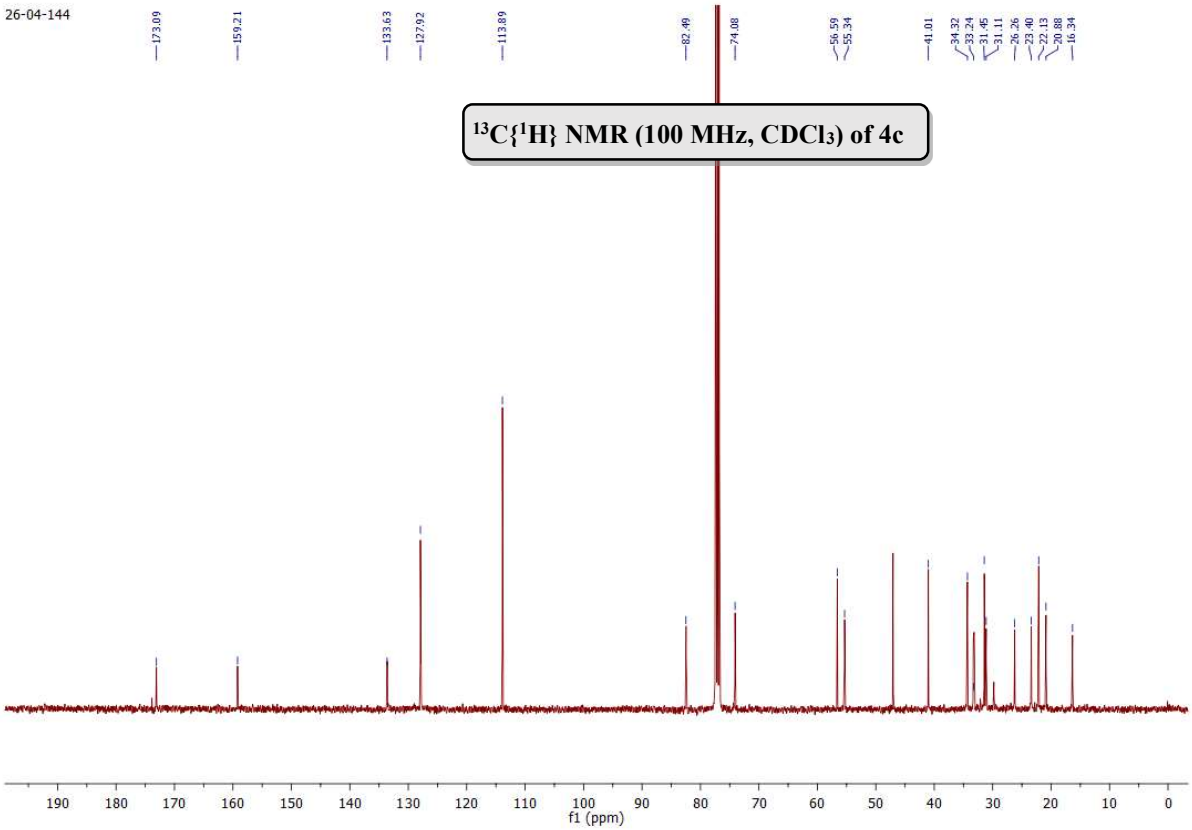

$^{13}C\{^{1}H\}$ NMR (100 MHz, $CDCl_3$) of 4c

HRMS of 2b'

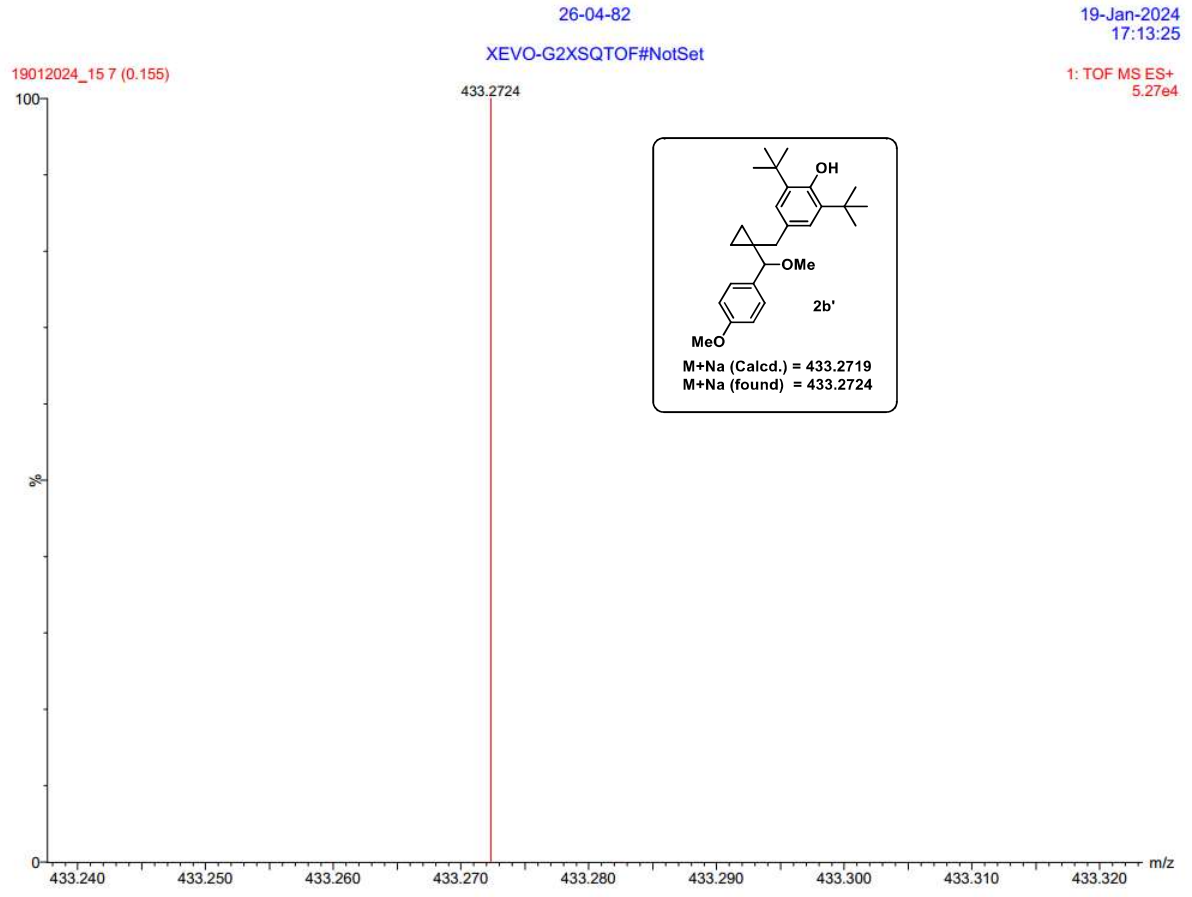

HRMS of intermediate III

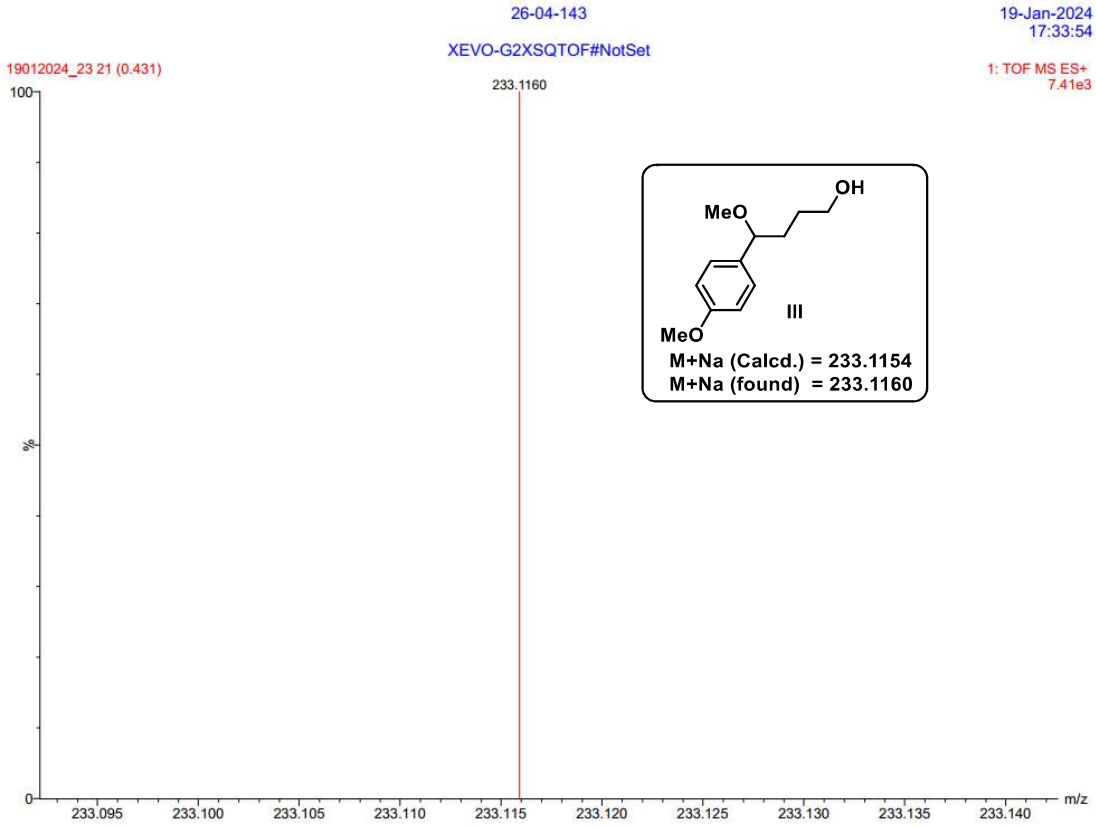

GC-MS of Reaction mixture

Base peak of III-210

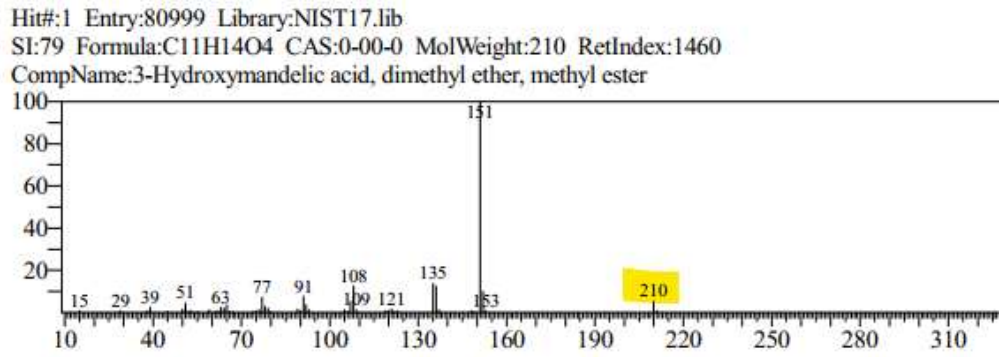

GC-MS of Reaction mixture

Base peak of IV-208

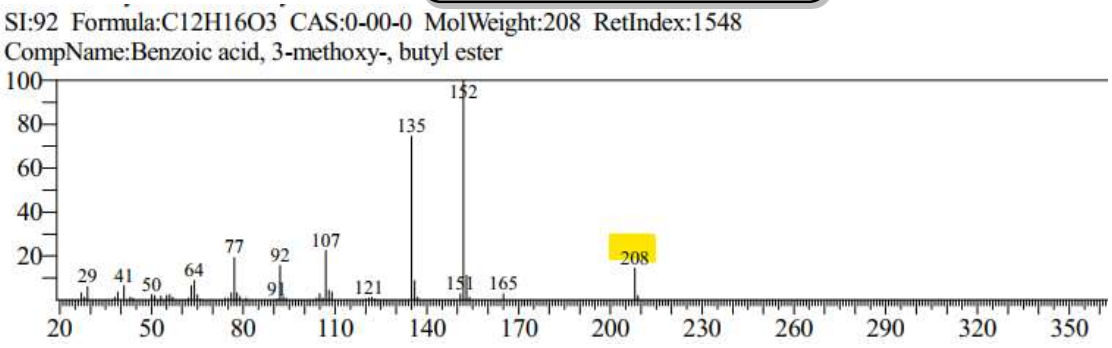

HRMS of intermediate IV

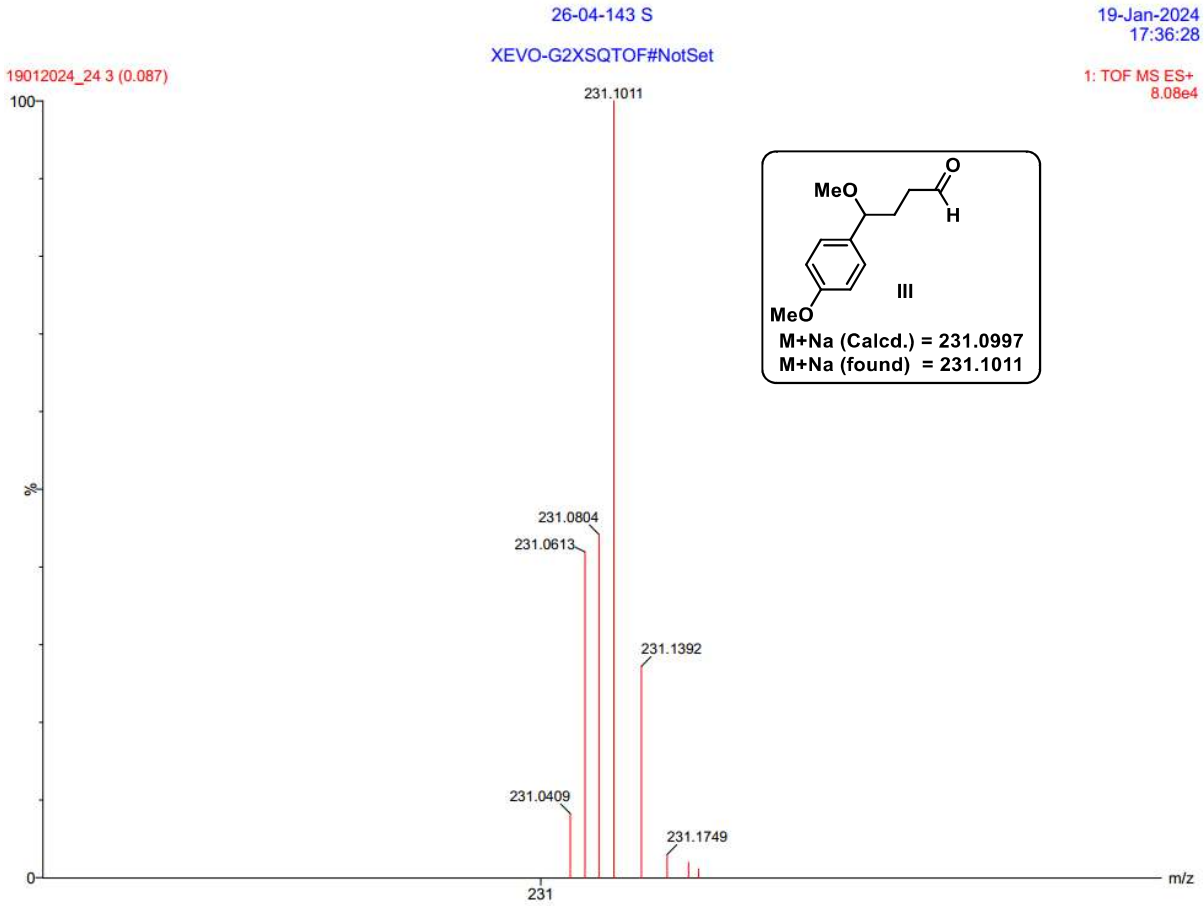

GC-MS of Reaction mixture

Base peak of III'-211

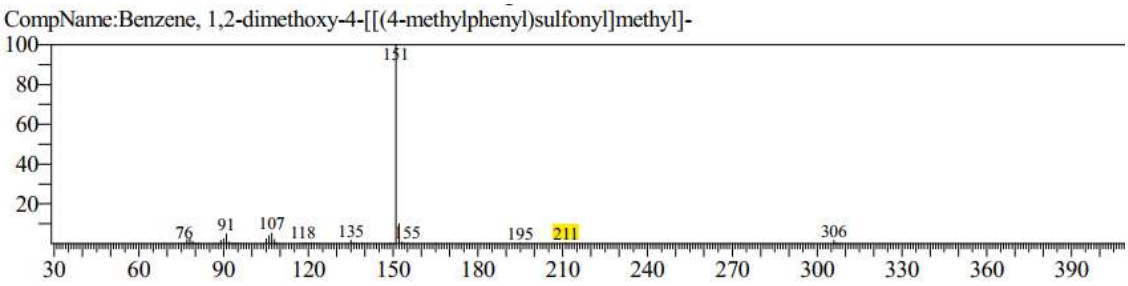

X-ray diffraction:

For the determination of X-ray crystal structures of a single-crystal was selected and mounted with paratone oil on a glass fiber using gum. The data was collected at 298K on a CMOS based Bruker D8 Venture PHOTON 100 diffractometer equipped with a INCOATEC micro-focus source with graphite monochromatic Mo Kα radiation (λ = 0.71073 Å) operation at 50 kV and 30 mA. For the integration of diffraction profiles SAINT program[1] was used. Absorption correction was done applying SADABS HRMS of 4aSI-155 program.[2] The crystal structure was solved by SIR 92[3] and refined by full matrix least square method using SHELXL-97[4] WinGX system, Ver 1.70.01.[5] All the non-hydrogen atoms in the structure were located the Fourier map and refined anisotropically. The hydrogen atoms were fixed by HFIX in their ideal positions and refined using riding model with isotropic thermal parameters. The crystal structure (excluding structure factor) has been deposited to Cambridge Crystallographic Data Centre and allocated deposition number **CCDC 2322098**.[6]

Chapter 4

Single Crystal X-Ray Data of 2v

The CCDC number for the compound **2v** is **2322098**

Crystal structure of Compound 2v

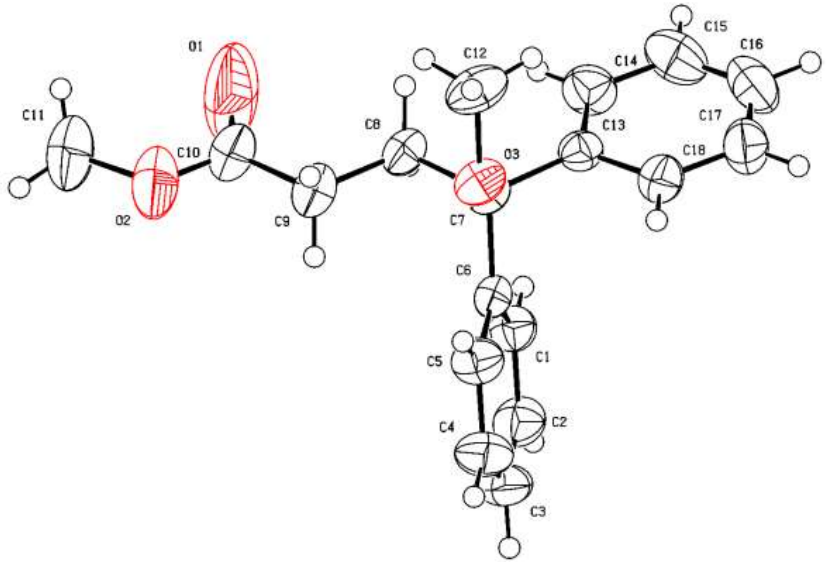

Table 1: Crystal Structure and Structure Refinement of 2a

Ccdc no.	2322098
Empirical formula	$C_{18}H_{20}O_3$
Formula weight	284.34
Temperature/K	298.00
Crystal system	monoclinic
Space group	C2/c

a/Å	33.380(12)
b/Å	5.972(3)
c/Å	18.656(7)
α/°	90
β/°	119.978(11)
γ/°	90
Volume/Å^3	3222(2)
Z	8
ρ_{calc}g/cm^3	1.173
μ/mm^{-1}	0.079
F(000)	1216.0
Crystal size/mm^3	0.215 × 0.123 × 0.045
Radiation	MoKα (λ = 0.71073)
2Θ range for data collection/°	6.898 to 52.862
Index ranges	-41 ≤ h ≤ 41, -7 ≤ k ≤ 7, -23 ≤ l ≤ 22
Reflections collected	17379
Independent reflections	3275 [R_{int} = 0.0606, R_{sigma} = 0.0412]
Data/restraints/parameters	3275/6/194
Goodness-of-fit on F^2	1.041
Final R indexes [I>=2σ (I)]	R_1 = 0.0790, wR_2 = 0.2235
Final R indexes [all data]	R_1 = 0.0978, wR_2 = 0.2399
Largest diff. peak/hole / e Å^{-3}	0.72/-0.44

Table 2 Bond Lengths for 2v

Atom	Atom	Length/Å		Atom	Atom	Length/Å
O3	C7	1.440(3)		C13	C7	1.543(3)
O3	C12	1.424(3)		C7	C6	1.528(3)

Table 2 Bond Lengths for 2v						
Atom	**Atom**	**Length/Å**		**Atom**	**Atom**	**Length/Å**
O1	C10	1.165(5)		C7	C8	1.540(3)
O2	C10	1.335(5)		C6	C5	1.388(3)
O2	C11	1.462(6)		C6	C1	1.391(3)
C18	C17	1.379(4)		C5	C4	1.386(4)
C18	C13	1.397(3)		C4	C3	1.378(4)
C17	C16	1.372(5)		C3	C2	1.375(4)
C16	C15	1.354(5)		C2	C1	1.380(4)
C15	C14	1.399(4)		C8	C9	1.522(4)
C14	C13	1.377(4)		C9	C10	1.481(4)

Table 3 Bond Angles for 2v							
Atom	**Atom**	**Atom**	**Angle/°**	**Atom**	**Atom**	**Atom**	**Angle/°**
C12	O3	C7	115.90(19)	C8	C7	C13	113.44(19)
C10	O2	C11	115.0(4)	C5	C6	C7	122.6(2)
C17	C18	C13	121.4(3)	C5	C6	C1	118.1(2)
C16	C17	C18	119.9(3)	C1	C6	C7	119.3(2)
C15	C16	C17	119.8(3)	C4	C5	C6	120.3(2)
C16	C15	C14	121.0(3)	C3	C4	C5	121.1(3)
C13	C14	C15	120.3(3)	C2	C3	C4	118.9(2)
C18	C13	C7	117.9(2)	C3	C2	C1	120.6(3)
C14	C13	C18	117.6(2)	C2	C1	C6	121.1(2)
C14	C13	C7	124.5(2)	C9	C8	C7	112.5(2)
O3	C7	C13	109.25(17)	C10	C9	C8	113.2(3)
O3	C7	C6	106.04(17)	O1	C10	O2	121.6(3)
O3	C7	C8	110.24(18)	O1	C10	C9	126.7(3)
C6	C7	C13	107.83(17)	O2	C10	C9	110.7(3)
C6	C7	C8	109.75(18)				

References:

(1) Bruker, SAINT V7.68A, Bruker AXS Inc., Madison (WI, USA) 2005.SI-160

(2) Sheldrick, G. M. SADABS 2008/2, Göttingen 2008.

(3) Altomare, A.; Cascarano, G.; Giacovazzo, C.; Guagliardi, A. J. Appl. Cryst. **1993**, *26*, 343.

(4) Sheldrick, G. M. SHELXL-97, Program for Crystal Structure Solution and Refinement, University of Göttingen, Göttingen, Germany **1997**.

(5) Farrugia, L. J. J. *Appl. Cryst*. **1999**, *32*, 837.

(6) CCDC 2322098 contains supplementary crystallographic data for the compound **2v**.

Bio-Data

Rakesh Kumar

Date of Birth: 26th January, 1994

Rakesh.19cyz0012@iitrpr.ac.in

Department of Chemistry

Lab No. 406, SS Bhatnagar Block

Indian Institute of Technology Ropar

Rupnagar, Punjab

India-140001

Educational Qualification:

- **2014: Bachelor of Science** from Vallabh Government College, Mandi, Himachal Pradesh University, India
- **2016: Master of Science** from Department of Chemistry, Shoolini University of Life Sciences and Biotechnology, Solan, Himachal Pradesh, India
    - **Project:** Synthesis of bis quaternary ammonium salt.
- **2019: Bachelor o Education** from Himachal Pradesh University, Shimla, India.

Achievements and Awards:

- Qualified University Grant Commission **UGC(NET)-JRF** in 2018 with All India Rank-67.
- Qualified **Himachal Pradesh State Eligibility Test (HP-SET)** in 2018.

The work described in this thesis highlights the concept of electroorganic chemistry and its utilization in organic synthesis. The electroorganic synthesis has been witnessing a huge upsurge in the past decades, and brought innate growth and recognition to become mainstream in synthetic organic chemistry. Traceless electrons are used as redox agents and participating in various SET processes to generate highly reactive intermediates, which can be further utilized in various organic transformations. In electroorganic synthesis, the electron transfer occurs between electrode and chemical species enabling the chemical transformations in absence of exogenous metal oxidants, hence avoids the generation of chemical waste associated with conventional methods. So, electroorganic synthesis is considered as greener as compare to the traditional chemical methods and supress the environmental burden of chemical processes. Moreover, the methodology has also been employed towards the total synthesis of various biological active molecules like Dixiamycin B, diazonamide drug DZ-2384, Cyclosporine A, and Dragocins A-C etc. These remarkable achievements and the sustainability of this field inspired us to established this technology in our laboratory.

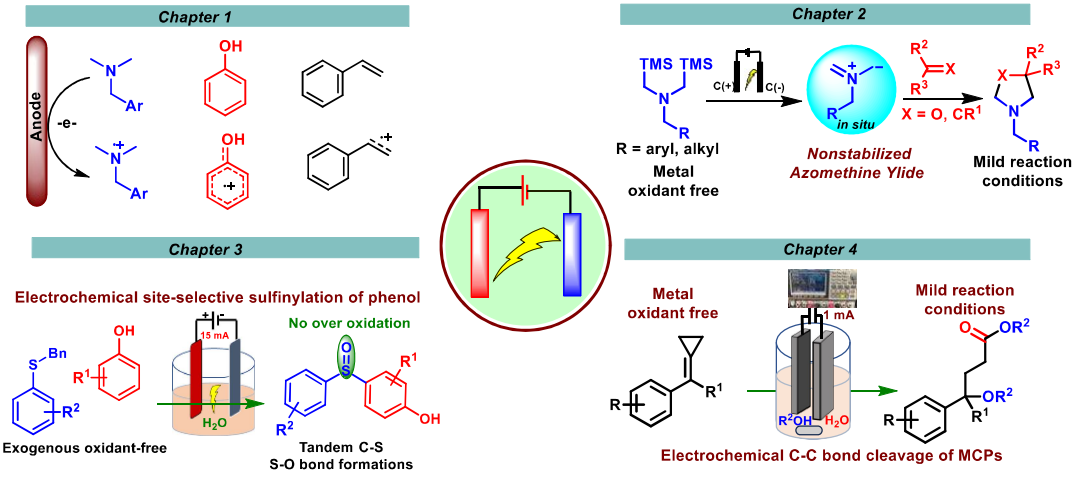

This thesis of majorly classified into four chapters, chapter 1 describes about the brief history of electroorganic chemistry and the requirements related to this field. The several historical developments have been described with some notable achievements in this alluring filed of chemistry. Moreover, this chapter also discloses the electroorganic synthesis of various cyclic and acyclic scaffolds based on direct anodic oxidation of amines, phenols, and alkenes.

Chapter 2 of the thesis discussed an electrochemical protocol towards the *in situ* generation of nonstabilized azomethine ylide and its 3+2 cycloaddition with various dipolarophiles like olefins and aldehydes. This electrosynthetic methodology indulges a straightforward and facile approach for the construction of substituted pyrrolidines and oxazolidines. The mechanistic studies show that the process involves two electron oxidation process and loss of two silyl moieties to generate nonstabilized azomethine ylide. The products were obtained in moderate to good yield and methodology is scalable. In future, the designed methodology can be employed to towards the 3+3 cycloaddition with some other 1,3 dipolar species to give six membered cyclic structure and the dipolarophiles can be extended to imines as well.

Chapter 3 discloses the electrochemical cross coupling reaction of phenols with the sulfide derivatives to access various aromatic sulfoxides. The methodology shows a new arena of CH functionalization of arenes. The two-electron oxidation of phenol generates the phenonium cation which undergoes nucleophilic attack by sulfides followed another oxidation event to deliver sulfoxide product. A diverse class of aromat8ic sulfoxide have been

synthesized in good to moderate yield. The methodology is scalable and the obtained product can be further transformed to sulfone derivative. From the future perspective, the phenol radical or phenonium cation generated in this process can be employed in radical-radical cross coupling reaction or nucleophilic addition reaction with some other reaction partner.

Chapter 4 demonstrates a new handle to towards the ring opening of a methylenecyclopropane. Herein, an electrochemical oxidative C-C bond cleavage of methylenecyclopropanes (MCPs) with alcohols is reported. The designed methodology affords the methyl 4-methoxy-4-phenylbutanoate derivative in presence of alcohol and trace amount of H_2O. The mechanistic studies reveals that the ring opening initiates via anodic oxidation of double bond to generate alkene derived radical cation followed by nucleophilic attack by alcohols to cleave the C-C bond of MCPs. Products were obtained in good to moderated yields and the protocol is scalable. In future, the established concept can be further utilised towards annulation and cycloaddition reaction towards the synthesis of heterocycles and carbocycles.

Overall, the work documented in this thesis utilizes the organic electrochemistry towards the sustainable development of several molecular frameworks with variety of functionalization. All the developed methodology are based on the direct oxidation of substrates on the surface of electrodes and demonstrates the significance of direct electrolysis. In future the concept based on these designed methodologies can be utilized towards the sveral enantioselective transformation. We believe that the protocol devised in this thesis will have significant impact in future generation and motivate them to apply this sustainable technique in future synthesis.